Tris(trimethylsilyl)silyl Stabilized Phosphorus and Lead Clusters

Dissertation

Submitted in Partial Fulfilment of the Requirements for the Degree of
Doctor of Philosophy

In the Institute of Inorganic and Analytical Chemistry

Department of Chemistry and Pharmacy

at

Johannes Gutenberg - University of Mainz

by

Shenglai Yao

from P. R. China

Mainz 2005

Dekan:	Prof. Dr. R. Zentel
Hauptberichter:	Prof. Dr. K. W. Klinkhammer
Mitberichter:	Prof. Dr. J. J. Schneider

Tag der mündlichen Prüfung: 20.05.2005

Abstract

Hypersilyl $(Me_3Si)_3Si$ behaves as a very bulky, electron releasing substituent and can be utilized for stabilizing low oxidation states and unusual structural fragments. By reactions of base-free alkali metal hypersilanides and dihypersilyl plumbylene with various phosphorus containing reagents, a series of hypersilyl stabilized phosphorus and lead clusters have been obtained.

Potassium hypersilanide readily reacts with white phosphorus in toluene at room temperature to yield red-violet potassium bis(hypersilyl)tetraphosphenide $[(Me_3Si)_3Si]_2P_4K_2$ (**1**), a potassium salt of the tetraphosphene $(Me_3Si)_3Si\text{-}PH\text{-}P{=}P\text{-}PH\text{-}Si(SiMe_3)_3$, quantitatively. In toluene or benzene solution there exists an equilibrium between **1** and its dimer, octaphosphanide $[(Me_3Si)_3Si]_4P_8K_4$ (**2**). In toluene **1** decomposes slowly through protolysis to give yellowish pentaphosphanide $[(Me_3Si)_3Si]_3P_5K_2$ (**4**). In benzene, most probably also by partial protolysis of the dimer **2**, another octaphosphanide $[(Me_3Si)_3Si]_3P_8K_3$ (**5**) is obtained. By using coordinating solvents such as diethyl ether, the reaction of potassium hypersilanide with P_4 yields **1** and blue triphosphenide $[(Me_3Si)_3Si]_2P_3K$ (**3**), which comprises a triphosphaallyl anion with a partial P-P double-bond. Replacing potassium for lithium, *i.e.* reacting lithium hypersilanide with white phosphorus in toluene dramatically changes the type of products obtained. Several polyphosphanes such as $[(Me_3Si)_3Si]_2P_4$ (**6**) could be found in the resulting mixture and $[(Me_3Si)_3Si]_2P_4Li_2$ (**7**) could be isolated only in low yield. In the presence of hexahydro-1,3,5-trimethyl-S-triazine, lithium hypersilanide reacts with P_4 to give $[(Me_3Si)_3Si]_2P_3Li$ (**8**) along with considerable amounts of $(Me_3Si)_4Si$, suggesting that cleavage of Si-Si bonds took place during the reaction process. The reaction of sodium hypersilanide with P_4 gives no clean reaction and leads directly to the formation of $[(Me_3Si)_3Si]_3P_5Na_2$ (**9**). The treatment of **1** with $[(Me_3Si)_2Si]_2Sn$ affords the unexpected compounds $[(Me_3Si)_3Si]_3P_4SnK$ (**10**) and $[(Me_3Si)_3Si]_2[(Me_3Si)_2N]P_4SnK$ (**11**), instead of $[(Me_3Si)_3Si]_2P_4Sn$, depending on the solvent used. All the new compounds are identified by NMR spectroscopy and the structures of the phosphenides **1**, **7**, **8**, and the phosphanides **2**, **4**, **5**, **9, 10** are established by X-ray diffraction studies.

When dihypersilyl plumbylene or stannylene is allowed to react with P_4, MPH_2 (M=Li, K), PMe_3, and PH_3 at low temperature, the formal Lewis acid-base adducts are formed, respectively. The adducts $\{[(Me_3Si)_3Si]_2Pb\cdot PH_2\}M$ [M = Li (**15**), K (**18**)], $\{\{[(Me_3Si)_3Si]_2Pb\}_2\cdot PH_2\}M$ [M = Li (**19**), K (**20**)], and $[(Me_3Si)_3Si]_2E\cdot PMe_3$ [E = Pb (**21**), Sn (**22**)] are obtained as pure compounds and were characterized by NMR spectroscopy and X-ray diffraction studies. However, the metastable adducts $\{[(Me_3Si)_3Si]_2E\}_4\cdot P_4$ (E = Pb, Sn) and $[(Me_3Si)_3Si]_2Pb\cdot PH_3$ could only be detected by NMR spectroscopy at low temperature. They undergo ligand exchange at room temperature yielding $[(Me_3Si)_3Si]_4P_4E_4$ [E = Pb (**12**), Sn (**14)**] along with $(Me_3Si)_3SiP{=}PSi(SiMe_3)_3$ (**13**) and $[(Me_3Si)_3SiPbP(H)Si(SiMe_3)_3]_2$ (**17**), respectively. X-ray analyses reveal a heterocubane core for **12** and **14** a monocyclic Pb_2P_2 skeleton for the **17**.

Dihypersilyl plumbylene also reacts very slowly with PH_3 at low temperature in pentane to give the totally unexpected lead cluster compound $[(Me_3Si)_3Si]_6Pb_{12}$ (**23**) in very low yields. It comprises a still centrosymmetric icosahedron Pb_{12} core. It is suggestive that the formation of the lead cluster proceeds via the elusive hydridoplumbylene $HPbSi(SiMe_3)_3$, which has been initially formed by ligand exchange between $Pb[Si(SiMe_3)_3]_2$ and PH_3. Replacing PH_3 by other hydride sources, such as $(Ph_3PCuH)_6$, $(^iBu)_2AlH$, and Me_3NAlH_3, another molecular lead cluster, $[(Me_3Si)_3Si]_6Pb_{10}$ (**24**), is isolated as main product. Both molecular clusters, **23** and **24** match the predictions made by Wade's rules.

Kurzdarstellung

Die Hypersilylgruppe $(Me_3Si)_3Si$ stellt einen sehr sperrigen, Elektronen liefernden Substituenten dar und kann zur Stabilisierung niedriger Oxidationsstufen sowie ungewöhnlicher Strukturelemente dienen. Durch Reaktionen der base-freien Hypersilanide der Alkalimetalle sowie des Dihypersilylplumbandiyls mit unterschiedlichsten phosphorhaltigen Reagenzien konnten eine Reihe hypersilyl-stabilisierter Phosphor- und Bleicluster-Verbindungen erhalten werden.

Kaliumhypersilanid reagiert in Toluol glatt mit weißem Phosphor bei Raumtemperatur in Toluol unter quantitativer Bildung von rotem Kalium-bis(hypersilyl)tetraphosphenid $[(Me_3Si)_3Si]_2P_4K_2$ (**1**), einem Kaliumsalz des Tetraphosphens $(Me_3Si)_3Si\text{-}PH\text{-}P{=}P\text{-}PH\text{-}Si(SiMe_3)_3$. In Benzol oder Toluol steht **1** im Gleichgewicht mit dem dimeren Octaphosphanid $[(Me_3Si)_3Si]_4P_8K_4$ (**2**). Bei längerem Stehen der toluolischen Lösungen zerfällt **1** langsam vermutlich in Folge einer Protolyse zum gelben Pentaphosphanid $[(Me_3Si)_3Si]_3P_5K_2$ (**4**). Aus benzolischer Lösung konnte hingegen ein weiteres Oktaphosphanid, $[(Me_3Si)_3Si]_3P_8K_3$ (**5**), isoliert werden. Führt man die Reaktion Kaliumhypersilanid mit P_4 in stärker koordinierenden Lösungsmitteln wie Diethylether durch, so entstehen neben **1** größere Mengen des Triphosphenids $[(Me_3Si)_3Si]_2P_3K$ (**3**); dieses enthält ein Triphosphaallyl-Anion mit partieller P-P-Doppelbindung. Setzt man Lithiumhypersilanid mit weißem Phosphor um, so beobachtet man eine vollständig andere Produktpallette. Als Hauptprodukte lassen Polyphosphane wie beispielsweise $[(Me_3Si)_3Si]_2P_4$ (**6**) nachweisen, das zu **1** analoge $[(Me_3Si)_3Si]_2P_4Li_2$ (**7**) entsteht nur in vergleichsweise kleinen Mengen. In der Gegenwart von Hexahydro-1,3,5-trimethyl-S-triazin, entsteht aus Lithiumhypersilanid und P_4 hingegen im wesentlichen $[(Me_3Si)_3Si]_2P_3Li$ (**8**) neben beträchtlichen Mengen von $(Me_3Si)_4Si$. Dessen Bildung erfordert eine Si-Si-Bindungsspaltung im Verlauf der Reaktion. Die Reaktion von Natriumhypersilanid mit P_4 verläuft sehr unübersichtlich, das Pentaphosphanid $[(Me_3Si)_3Si]_3P_5Na_2$ (**9**) ist das einzige isolierbare Produkt. Setzt man **1** mit $[(Me_3Si)_2Si]_2Sn$ um, so bilden sich überraschenderweise, je nach verwendetem Solvens $[(Me_3Si)_3Si]_3P_4SnK$ (**10**) oder $[(Me_3Si)_3Si]_2[(Me_3Si)_2N]P_4SnK$ (**11**). Alle neuen Verbindungen wurden NMR-spektroskopisch charakterisiert, die Phosphenide **1**, **7**, **8** sowie die Phosphanide **2**, **4**, **5**, **9, 10** darüber hinaus durch Kristallstrukturanalysen.

Dihypersilylplumbandiyl und -stannandiyl reagieren bei tiefer Temperatur mit P_4, MPH_2 (M=Li, K), PMe_3, and PH_3 zu formalen Lewis-Säure-Base-Addukten. Die Addukte $\{[(Me_3Si)_3Si]_2Pb{\cdot}PH_2\}M$ [M = Li (**15**), K (**18**)], $\{\{[(Me_3Si)_3Si]_2Pb\}_2{\cdot}PH_2\}M$ [M = Li (**19**), K (**20**)], und $[(Me_3Si)_3Si]_2E{\cdot}PMe_3$ [E = Pb (**21**), Sn (**22**)] wurden als kristalline Feststoffe erhalten und konnten vollständig charakterisiert werden. Die metastabilen Addukte $\{[(Me_3Si)_3Si]_2E\}_4{\cdot}P_4$ (E = Pb, Sn) und $[(Me_3Si)_3Si]_2Pb{\cdot}PH_3$ konnten lediglich NMR-spektroskopisch nachgewiesen werden. Bei Raumtemperatur entstehen in Folge von Ligandenaustausch-Prozessen die kristallographisch charakterisierten Heterokubane $[(Me_3Si)_3Si]_4P_4E_4$ [E = Pb (**12**), Sn (**14**)], das Diphosphen $(Me_3Si)_3SiP{=}PSi(SiMe_3)_3$ (**13**) sowie der Pb_2P_2-Heterocyclus $[(Me_3Si)_3SiPbP(H)Si(SiMe_3)_3]_2$ (**17**).

Bei tiefer Temperatur wird aus einer sehr langsamen Reaktion von Dihypersilylplumbandiyl und PH_3 in sehr kleinen Ausbeuten ein weiteres, völlig unerwartetes Produkt gebildet: der Bleicluster $[(Me_3Si)_3Si]_6Pb_{12}$ (**23**). Er weist ein verzerrt ikosaedrisches, zentrosymmetrisches Pb_{12}-Gerüst auf. Nach jetzigen Erkenntnissen läuft seine Bildung über das nicht fassbare Hydridoplumbandiyl $HPbSi(SiMe_3)_3$, das intermediär durch Substituentenaustausch zwischen $Pb[Si(SiMe_3)_3]_2$ and PH_3 entsteht. Der Ersatz des Phosphans durch andere Hydridquellen wie $(Ph_3PCuH)_6$, $(^iBu)_2AlH$, and Me_3NAlH_3 führt ebenfalls zur Bildung von Bleiclustern, allerdings ist jetzt der Cluster $[(Me_3Si)_3Si]_6Pb_{10}$ (**24**) das Hauptprodukt. Beide Cluster, **23** und **24**, gehorchen den Wade-Regeln.

Contents

1 Introduction

Spatially overcrowded substituents play an important role in stabilizing elements in low oxidation states and give way to determine their frequently unusual molecular geometries[1] [2] [3] [4] [5] [6]. Tris(trimethylsilyl)silyl, referred to as “hypersilyl”[7] and abbreviated as “Hyp”, is one of the most frequently used bulky groups. Due to its high steric requirements[8], interesting electronic properties[9] [10], and facile preparation, it has been usually used for the synthesis of several novel compounds which otherwise proofed difficult to isolate such as silenes[11], stannylene, plumbylene[12] and thus has attracted much attention in the last decade.

1.1 Syntheses and Reactivity of Alkali Metal Hypersilanides

Among all of the alkali metal hypersilyl derivatives lithium hypersilanide is a thoroughly studied species and a versatile reagent for the syntheses of other hypersilyl derivatives of both main group elements [13] [14] [15] and transition metal elements[16] [17] [18]. It was first prepared in *situ* by Gilman und Smith in 1967[19] [20] and later isolated and characterized as solvates with tetrahydrofuran (THF)[21] [22] [23], or 1,2-dimethoxyethane (DME)[24] [25] (Scheme 1.1).

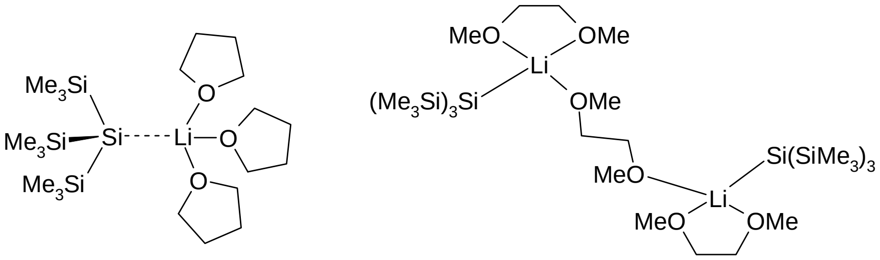

Scheme 1.1

Historically, due to its facile synthesis and high solubility in organic solvents, lithium hypersilanide is usually prepared as the ether solvates and frequently used in the preparation processes. Their applicability may be, however, limited by side reactions, such as deprotonation, cleavage of the coordinating donor ligand, the formation of ate-complexes or other undesirable solvated products as happened for other silyl lithium derivatives[26] [27] [28] .

Accordingly, Klinkhammer investigated in 1990’s the preparation of solvent-free alkali metal hypersilanides. By transmetallation of the dihypersilyl derivatives of the zinc group elements with appropriate alkali metals in n-pentane at room temperature, he obtained solvent-free potassium, rubidium and cesium hypersilanides[29] [30], and solvent-free lithium and sodium hypersilanides at higher temperature by using molten alkali metal in boiling n-heptane[31]. All of solvent-free alkali metal hypersilanides are dimers in solid state.

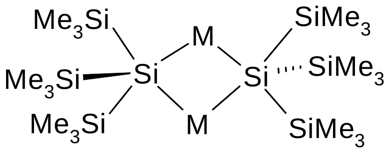

M =Li, Na, K, Rb, Cs

Scheme 1.2

Later a direct synthesis of solvent-free lithium hypersilanide using hypersilyl chloride and lithium was developed by Weidlein's group[3233]. This method became a facile method for preparation of solvent-free lithium hypersilanide.

In 1998 Marschner[34] developed a pratical synthetic route to potassium hypersilanide by treatment of tetrakis(trimethylsilyl)silane with equimolar potassium *tert*-butanolate in THF. Actually, potassium, rubidium as well as cesium hypersilanides can be prepared with this method in good yields and high purity even in the unsolvated form.

The hypersilyl anion exhibits a high tendency for delivering electrons. Consequently, alkali metal hypersilanides act as strong Brönsted bases. However, unlike some other solvent-free alkali metal silanides[35] [36] [37] [38] [39], the applications of which are limited due to the extreme reactivity, *i.e.* deprotonation of hydrocarbon when dissolved in many organic solvents[40], the deprotonation caused by hypersilyl anion are often kinetically hindered. Experiment indeed showed that the solvent-free alkali metal hypersilanides are readily soluble in aromatic hydrocarbons, such as benzene or toluene without deprotonation under ambient conditions. This is probably caused by the extensive steric shielding of the nucleophilic centre in conjunction with an intramolecular stabilization of the alkali metal complexes through $M\cdots CH_3$ agostic interaction.

NBO-analyses using Hartree-Fock densities reveal that the central silicon atom within the hypersilyl group bears a relatively high negative charge, as do the peripheral carbon atoms, whereas in the supersilyl group Si^tBu_3 the negative charge is nearly equally distributed amongst all carbon atoms[31]. Therefore the alkali cation is bonded more tightly to the central silicon in hypersilyl group and alkali metal hypersilanides are much less reactive than the corresponding supersilanides towards weak acids such as benzene or toluene.

The reactivity of hypersilyl anion, however, towards Lewis-acidic substrates such as metal halides, amides, and alcoholates remains high. The impressive application of solvent-free alkali metal hypersilanides is the syntheses of solvent-free hypersilyl derivatives of other elements. For example, aluminium, gallium and indium hypersilanides were synthesized by metatation of lithium hypersilanide with respective metal halides. The dialkyl aluminium chlorides R_2AlCl(R=Me, Et) react with base-free lithium hypersilanide to give the dialkyl aluminiumhyersilanides R_2Al-Hyp[41 42]. Trihypersilylgallium can be prepared in good yield from the reaction of gallium trichloride with base-free lithium hypersilanide[43]. However, not all metatations would result in the expected hypersilyl derivatives. The reaction of the same hypersilanide with $InCl_3$ mainly affords LiCl, metallic indium and "dihypersilyl" Hyp-Hyp; only the unexpected $(Hyp)_2In$-$In(Hyp)_2$ could be obtained in low yield[41]. The reaction of alkali metal hypersilanides with $PbCl_2$ or TlCl quantitatively led to the formation of Hyp-Hyp, neither $PbHyp_2$ nor TlHyp was obtained.[44]. These examples show that the strong nucleophile Hyp^- may also act as strongly reducing agent.

By substituting the halides for the weaker oxidizing amides, the redox-process could be suppressed. Temperature-sensitive hypersilyl derivatives of thallium(I)[45], tin(II) and lead(II)[12] were synthesized by metathesis of base-free potassium or rubidium hypersilanide with bis(trimethylsilyl)amides of thallium(I), tin(II) and lead(II), respectively.

Not only hypersilyl derivatives of main group elements, but also some transition metal complexes could be synthesized by employing solvent-free lithium hypersilanide with CuO^tBu in toluene, such as copper hypersilanide. The compound which was prepared before by an unusual ligand exchange between an copper aryl and dihypersilyllead[46], can be obtained along with $[Li_7(O^tBu)_6][Cu_2Hyp_3]$ by the reation of hypersilyllithium with CuO^tBu[47]. Using the solvent-free heavier alkali metal hypersilanides, the reactions with copper *tert*-butoxide instead lead to formation of novel hypersilyl complexes of Cu^I , the heteroleptic *tert*-butoxy(hypersilyl)cuprates of heavier alkali metals, which have been proved to be valuable starting compounds for other hypersilyl copper complexes [48].

Moreover, treatments of alkali metal hypersilanides with a variety of halosilanes expectedly lead to the formation of polysilanes, which can be further metallated to afford interesting silyl anions with different sterical demand[34 49 50]. Very recently, addition of solvent-free alkali metal hypersilanides to unsaturated system such as guaiazulene has been investigated by our group. Thus number of hypersilyl substituted alkali metal and transition metal guaiazulenides could be synthesized[51].

1.2 Reactivity of Dihypersilyl Stannylene and Plumbylene

Since 1973 Lappert et al. reported the first well-characterized distannene, $[(Me_3Si)_2CH]SnSn[CH(SiMe_3)_2]$[52], especially in the last decade, a great progress has been made in the chemistry of low-coordinate compounds of heavier Group 14 elements. Taking advantage of kinetic stabilization with bulky substituents, a variety of these compounds have been synthesized and many of them have been structurally characterized. These include, among others, 2,2,5,5-tetrakis(trimethylsilyl)stannacyclopentane-1,1-diyl (Scheme1.3)[53 54], $[2,6\text{-}Mes_2C_6H_3]_2Pb$[55], R_2Pb (R=2-t-butyl-4,5,6-Me_3C_6H)[56] as well as dihypersilyl stannylene and plumbylene[12] (Scheme1.3). Since the progress in the chemistry of the reactivity of the heavier tetrylenes, especially that of plumbylenes, is far behind those of its lighter congeners, there are only has been very few reports about their reactivity[57].

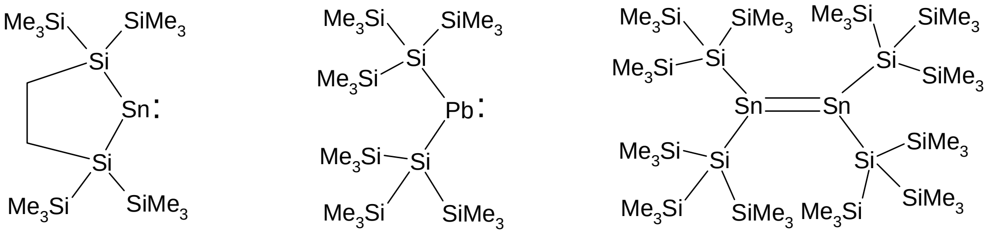

Scheme 1.3

Whereas carbenes which, due to the relatively small energy difference between triplet and singlet, may have a singlet or triplet ground state, stannylenes and plumbylenes as other homologous species of heavier elements exclusively exist in singlet ground states[58]. The energetically high-lying HOMO is predominantly constituted by a lone-pair of high s-character on the tetrel atom and the low-lying LUMO has high contributions of the empty valence p-orbital of the two-valent tetrel atom. The values of singlet-triplet energy difference usually increase with increasing atomic mass of the Group 14 element[59]. As shown by Kutzelnigg both the difference in energy and the radial expansion of s- and p-valence orbitals strongly increase down Group 14, thus leading to a low hybridization tendency and resulting in non-radical singlet species for all heavier carbene congeners[60]. Therefore, all stannylenes and plumbylenes are Lewis-amphoteric compounds and can act as donors (through their lone-pair in 5σ or 6σ orbitals) or as acceptors (through their empty 5p or 6p orbitals) in Lewis-acid/Lewis-base reaction. Because the Lewis-acidic and Lewis-basic behaviour is located at the same tetrel atom in these species, not only the addition of external Lewis-acids or Lewis-bases, but also the oligomerization of these heavier tetrylenes may take place. The bonding within the *dimerization* products –formal alkene homologues- as well as their structural features, spectroscopic and chemical behaviour has been a topic of controversial discussions in the last decade, but is now well understood and widely accepted as a more or less strong double donor-acceptor bond between the two constituting tetrylenes[61 62 63 64 65 66 67 68 69 70]. The typical trans-bent geometry found for these alkene homologues can be understood with a pattern of multiple bonding, which is between the sp^n σ orbital on one atom with a pπ orbital on the other, as shown in Scheme 1.4.

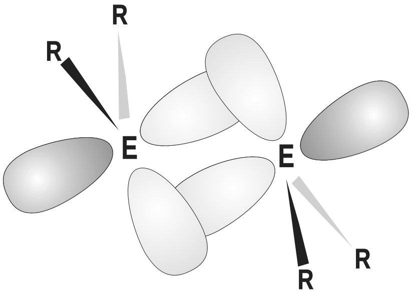

E = Sn, Pb

Scheme 1.4

Quantitative criteria for existence of such double donor-acceptor bonds are based on a simple theoretical approach, the CGMT model[61 67 69 70], which relates the singlet-triplet energy difference ($\Sigma\Delta E_{ST}$) of the constituting tetrylene fragment with the dimerization energy ($E_{\sigma+\pi}$) of the corresponding hypothetical triplet species. Following general rules are provided: classical planar structures are obtained if $\Sigma\Delta E_{ST} < 1/2\ E_{\sigma+\pi}$; trans-bent structures are observed if $1/2\ E_{\sigma+\pi} < \Sigma\Delta E_{ST} < E_{\sigma+\pi}$; in the case of $\Sigma\Delta E_{ST} > E_{\sigma+\pi}$, monomers without E-E bonding will be expected.

Calculations by Apeloig and others[71 72] showed that electropositive substituents should generally lead to a diminished HOMO-LUMO gap for tetrylenes and thus should increase their tendency to form Lewis-acid–Lewis-base adducts and strengthen the bonds within the corresponding dimers. According to calculation by Klinkhammer[73], the substitution of CH_3 for the more electropositive SiH_3 group in $E(CH_3)_2$ (E=Sn, Pb) dramatically increases the dimerization energies. This indicates that the tendency to dimerize of bis(silyl)stannylenes and bis(silyl)plumbylenes is expected to be much higher than that of related diorganyl substituted species.

X-ray structural analysis reveals that dihypersilylstannylene exhibits a dimer molecular structure with double donor-acceptor bond in the solid state, as expected for stannylenes by CGMT-model. Like Lappert's bis[bis(trimethylsilyl)methyl]tin, a monomer-dimer equilibrium already exists in solution for dihypersilylstannene. In contrast, the lead analogue is monomer even in solid state[12].

As expected, both dihypersilyl stannylene and plumbylene react as Lewis-amphoteric carbene homologues with several Lewis-acids and Lewis-bases. In some cases, however, migration of one hypersilyl group from tin or lead may occur. The reactions of dihypersilylstannylene or plumbylene with some diaryltetrylenes yielded quantitatively dimers in the solid state[56 74 75 76 77 78 79]. Unexpectedly, according to Eq. 1.1, a rearrangement took place after the putative initial hetero-dimerisation and homodimers of the heteroleptic tetrylenes were obtained as final products. All heteroleptic dimers synthesized show an undistorted *trans*-bent structure with C_i molecular symmetry. Moreover, several plumbylene dimers diplumbenes with double donor-acceptor bond were finally prepared by this method.

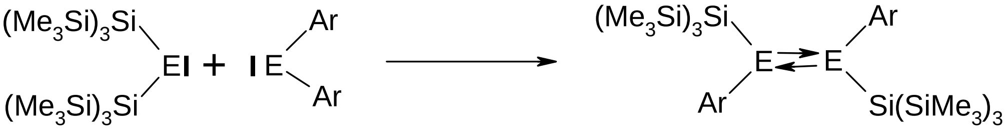

(Eq. 1.1)

E= Sn, Pb

Very recently Schneider et al. showed that the Lappert's stannylene and some diarylstannylenes have high donor capability towards Fe, Co, and Ni atoms in metal organyl compounds and can thus be used to stabilize low-valent transition metal centres[80 81 82 83]. Similarly dihypersilylstannylene and plumbylene can also react as a Lewis-base. With arylcopper complexes, heteroleptic tetrylenes are obtained. Depending on bulkiness of the aryl substituents, they may exist as monomers or dimers in the solid state (Scheme 1.5) [46]. Although the primary adducts of the dihypersilyltetrylene with organylcopper could neither be isolated nor be detected spectroscopically, a rearranged adduct of heteroleptic stannylene with hypersilylcopper was obtained from treatment of dihypersilylstannylene with the extremely congested 2,6,-dimesityl-phenylcopper.

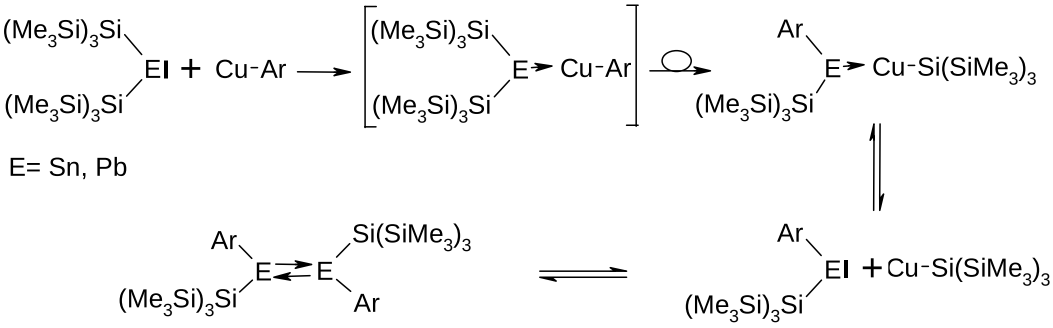

Scheme 1.5

DFT calculations by Klinkhammer on several simple adducts of Lewis-bases with $Pb(CH_3)_2$ and $Pb(SiH_3)_2$ showed that the acidity of the divalent tetrel centre for the latter is stronger than that of the former[73]. Some outcomes of the experiment also showed that dihypersilylstannylene and plumbylene are remarkably strong Lewis-acids compared to the related species bearing more electronegative hydrocarbyl substituents. The reactions with *tert*-butyl isonitrile[84] and cyclohexyl isonitrile[85] quantitatively led to the formation of fairly stable adducts. In contrast to the related isonitrile-stannylene adduct $MesN\equiv C\rightarrow Sn(2,4,6\text{-}(F_3C)_3C_6H_2)_2$, reported by Grützmacher[86], there is no experimental evidence for re-dissociation of these adducts in solution or under reduced pressure.

Dihypersilylplumbylene also reacts with ambident nitrogen/oxygen bases such as azide or isocyanates, but instead of the simple Lewis-adducts, which may be formulated as an initial intermediate, migration of hypersilyl groups leads to heteroleptic Pb(II) derivatives. Spectroscopical and structural data indicate that one hypersilyl group migrates from the lead atom to that heteroatom which bears a formal negative charge[73].

Whereas the reaction of sodium hypersilanide with dihypersilylstannylene in toluene gives sodium tris(hypersilyl)stannanide[31], treatment of these tetrylenes with simple lithium organyls in non-coordinating solvents did not yield any isolable product. Only lithium hypersilanide could be detected spectroscopically. Again ligand exchange reactions probably occurred leading to heteroleptic alkyl(hypersilyl) tetrylene which could not be isolated to date[73]. Recently, experiment shows that the introduction of small amount of coordinating solvents such as diethyl ether changed the reation course and led to the formation of stable stannanides and plumbanides[87].

2 Hypersilyl Stabilized Phosphorus Clusters

2.1 Overview

Alkali metal salts of phosphorus-containing compounds continue to be of considerable interest because of their synthetic value as transfer reagents and structural diversity of their solid-state structures. Among the variety of the alkali metal phosphides, numerous binary metal polyphosphides containing isolated Zintl anion species of the general formula M_4P_6[88], M_3P_7 and M_3P_{11}[89] or derivatives of phosphanides $M[PR_2]$ as well as $M[PR(H)]$[90] have become known and well established since the early seventies. However, only a very limited number of molecular alkali metal polyphosphanides with general formula $R_mP_nM_x$ have been structurally characterized.

According to the double-bond rule, nitrogen hydrides with the formula N_nH_n and their derivatives adopt an acyclic structure with double bonds, whereas phosphanes P_nH_n and their derivatives prefer cyclic structure without a double bond[91] [92] [93]. After deprotonation of the phosphanes, however, the negatively charged phosphides obtained may form unsaturated acyclic structures because the negative charges are probably better stabilized by a π system in a phosphorus chain. It is especially evident that the unsaturated phosphenides $R_2P_3^-$ and $R_2P_4^{2-}$, with sterically overloaded substituents R, are readily formed. For instance, the compounds with the formula $Mes^*{}_2P_2ELi$ (E=P, As; Mes^* = 2,4,6-tri-tert-buthylphenyl) were reported by Jutzi et al[94]. The 2,3,4-triphosphapentadienide $[(Me_3Si)_2CPPPC(SiMe_3)_2]^-$[95] and $[RPPPR]^-$[96] (RR = – CH_2CH_2– and –CHPhCHPh–) containing a P_3 skeleton with a π system were synthesized as alkali metal salts. A lithium salt containing a tetraphosphenide dianion $R_2R'_2P_4^{2-}$ [$R=SiMe_3$, $R'=Cr(CO)_5$] was prepared by Fritz[97].

Sterically overloaded supersilylated phosphane and phosphanide clusters were thoroughly investigated by Wiberg and co-workers[6]. In addition to bis(supersilyl)tetraphosphane $({}^tBu_3Si)_2P_4$, tris(supersilyl)heptaphosphane $({}^tBu_3Si)_3P_7$[98] [99] and tris(supersilyl)nanophosphane $[(Me_3C)_3Si]_3P_9$[100], two unsaturated P=P containing phosphenides $[(Me_3C)_3Si]_2P_3Na$[100] and $[(Me_3C)_3Si]_2P_4Na_2$[101] as well as polyphosphanides $[(Me_3C)_3Si]_4P_8Na_4$[101] and $[(Me_3C)_3Si]_3P_5Na_2$[102] were prepared as ether adducts. In those investigations, supersilyl groups were introduced by reactions of supersilyl radicals with white phosphorus, supersilyl anions with white phosphorus and with phosphorus trichloride, respectively. Very recently, another kind of tetraphosphanides $[(Me_3C)_3Si]_3P_4M_3$ (M=Li, Na) and $[(Me_3C)_2PhSi]_3P_4Na_3$[103] were synthesized by Lerner.

Hypersilyl group, similar to supersilyl group, should also stabilize polyphosphane or polyphosphanide clusters. However, to our best knowledge, no well-characterized hypersilyl stabilized phosphanide has been reported to date. The only hypersilyl stabilized phosphanes ever characterized are $(Me_3Si)_3SiPH_2$, $[(Me_3Si)_3Si]_2PH$[104], and $[(Me_3Si)_3Si]_3P_7$[105].

2.2 $Hyp_2P_4K_2$ (1), $Hyp_4P_8K_4$ (2) and Hyp_2P_3K (3)

2.2.1 Synthesis

Solvent-free potassium hypersilanide readily reacts with white phosphorus in a molar ratio of 2:1 in toluene at room temperature to give a violet solution from which, on cooling to -20°C, violet rhombohedral crystals precipitate in good yield. The NMR spectroscopic data indicate that potassium bis(hypersilyl)tetraphosphenide $[(Me_3Si)_3Si]_2P_4K_2$ (**1**), a potassium salt of $(Me_3Si)_3SiP\text{-}PH\text{-}P{=}P\text{-}PH\text{-}Si(SiMe_3)_3$, is formed nearly quantitatively (Eq. 2.1). The identity of compound **1** is unambiguously derived from the ^{31}P-NMR spectrum and subsequently confirmed by single-crystal X-ray diffraction studies.

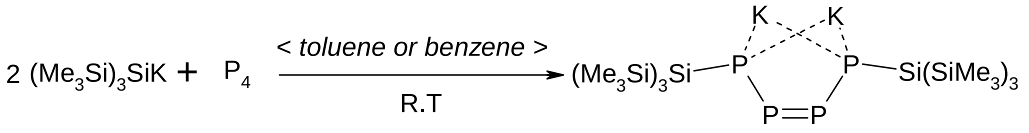

(Eq.2.1)

1

(*as toluene or benzene solvate*)

Under the same conditions, the treatment of potassium hypersilanide with white phosphorus in benzene provides a deep red reaction solution, which contains almost only compound **1** according to the ^{31}P-NMR spectrum. The solubility of **1** in benzene is not as good as in toluene and the product would precipitate as very fine red crystals immediately from the reaction mixture.

The reaction of the same reactants proceeding in diethyl ether at room temperature gives also $[(Me_3Si)_3Si]_2P_4K_2$, but some side reactions take place, *i.e.* bis(hypersilyl)triphosphenide $[(SiMe_3)_3Si]_2P_3K$ (**3**), tris(hypersilyl)pentaphosphanide $[(SiMe_3)_3Si]_3P_5K_2$ (**4**) as well as small amounts of several other phosphorus-containing compounds are formed in the resulting reaction mixture. According to the ^{31}P NMR spectrum, compound **1**, **3**, and **4** were found in the mixture in a molar ratio of 6:9:5. After work-up, compound **3** was isolated as deep blue powder and characterized as a potassium salt of bis(hypersilyl)triphosphene $(Me_3Si)_3SiP{=}P\text{-}PH\text{-}Si(SiMe_3)_3$ by NMR spectroscopy.

The reaction of $KSi(SiMe_3)_3$ with white phosphorus in THF under the same conditions is even more complicated according to the solution ^{31}P NMR spectrum. All attempts to isolate some of the products were unsuccessful. This differs significantly from the reaction of sodium supersilanide with white phosphorus in THF, in which $[(Me_3C)_3Si]_2P_4Na_2$ is isolated as THF solvate quantitatively[101].

Presumably, the insertion of a potassium hypersilanide molecule into a P–P bond of P_4 to form a potassium biscyclotetraphosphanide represents the first step of the reaction. A further combination of the intermediate species with a second molecule of potassium hypersilanide affords thus the final product as shown in Scheme 2.1.

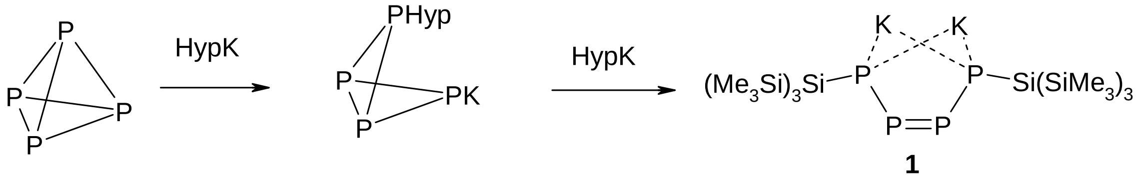

1

Sheme 2.1

Compound **1** in the solid state is thermally quite stable and can be stored under argon indefinitely at room temperature. However, it is extremely air- and moisture-sensitive and ignites spontaneously on contact with air. This compound is well soluble in toluene, but according to the ^{31}P-NMR(10% benzene-d_6 in toluene) spectrum, an equilibrium exists between $[(Me_3Si)_3Si]_2P_4K_2$ and its dimer $[(Me_3Si)_3Si]_4P_8K_4$ (**2**) in toluene solution (Scheme 2.2). In benzene, the dimer is also found according to the ^{31}P-NMR spectrum recorded in benzene-d_6. However, both compound **1** and its dimer **2** can be obtained as solids from benzene solution by controlling the crystallization conditions.

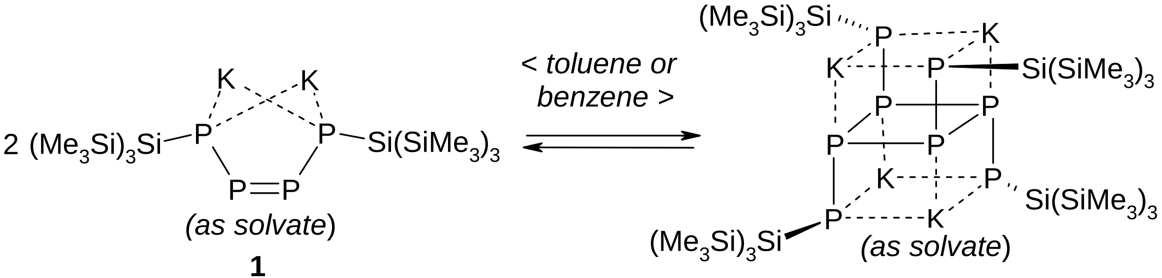

1

2

Scheme 2.2

If the toluene solvate $Hyp_2P_4K_2{\cdot}2C_7H_8$ (**1b**) crystals are dissolved in a small amount of warm benzene and quickly cooled to 5°C, benzene solvate $Hyp_2P_4K_2{\cdot}4C_6H_6$ (**1a**) will be obtained as deep red X-ray diffraction quality crystals. The dimer of this compound, $Hyp_4P_8K_4{\cdot}4C_6H_6$ (**2a)**, could precipitate as light red well shaped X-ray analysis suitable crystals by cooling a clear room-temperature saturated benzene solution of **1b** at 5°C or by simply standing a saturated solution at ambient temperature.

By dissolving the dimer **2a** in toluene or benzene, the equilibrium (Scheme 2.2) may also be established. However, if the deep red violet crystals of **1b** or the light red crystals of **2a** dissolve in benzene in the presence of triazine, the colour of the solution would change immediately from red to green. Yellow-green crystals of benzene and triazine solvate $Hyp_2P_4K_2{\cdot}2C_6H_6{\cdot}2(MeNCH_2)_3$ (**1c**) could precipitate at room temperature.

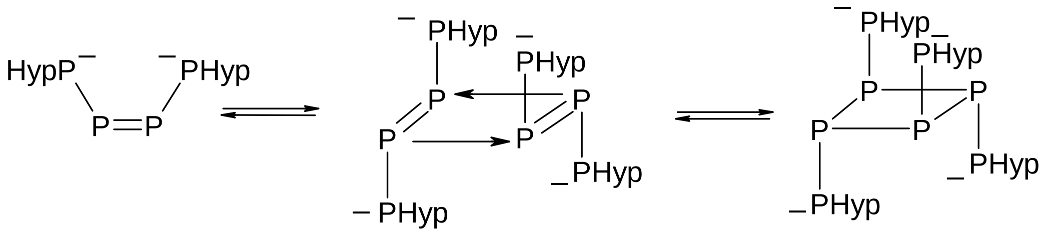

Scheme 2.3

According to the molecular structure determined by X-ray diffraction investigation, $Hyp_4P_8K_4$ might be understood as a [2+2] cycloadduct of $Hyp_2P_4K_2$. Obviously, the cis-configurated phosphorus skeleton has to change to the trans conformation during the $[2_\pi+2_\pi]$–cycloaddition. In addition, the formation tendency of the four membered ring of phosphorus atoms is normally not preferred comparing with that of the three, five or six membered ring of phosphorus atoms[106] [107]. However, the dimerization of $Hyp_2P_4K_2$, taking place even under ambient conditions in toluene or benzene, may be due to the building up of a mixed phosphorus and potassium heterocluster and probably also to solvent effect.

2.2.2 NMR Spectroscopy

The ^{31}P-NMR spectra of $Hyp_2P_4K_2$ recorded in donor solvents such as THF, diethyl ether, TMEDA, toluene or benzene show similar resonance of two multiplets with the classical splitting pattern of an AA'XX' system, however, the chemical shifts depend strongly on the solvent used. The proton decoupled ^{31}P-NMR spectrum recorded in THF consists of two groups of signals centred at -23.6 and 416.3ppm, which lie in the range for a phosphorus atom in phosphenides and for an unsaturated two-coordinate phosphorus atom in diphosphene, respectively [108], [109]. This spectrum is very similar to that of disodium bis(supersilyl)tetraphosphenide, $[(Me_3C)_3Si]_2P_4Na_2$ [101]. In order to determine the four ^{31}P–^{31}P-coupling constants ($^{1}J_{AX}$, $^{2}J_{AX'}$, $^{3}J_{AA'}$, $^{1}J_{XX'}$), a simulation of the spectrum using the parameters published for $[(Me_3C)_3Si]_2P_4Na_2$ as a starting point and a subsequent iteration were performed[110]. The experimental and calculated spectra are shown in Figure 2.1. The chemical shifts and coupling constants are summarized in Table 2.1 and compared with those of its analogues $[(Me_3C)_3Si]_2P_4Na_2$ [101] and $[(Me_3Si)_3Si]_2P_4Li_2$ (**7**, see below).

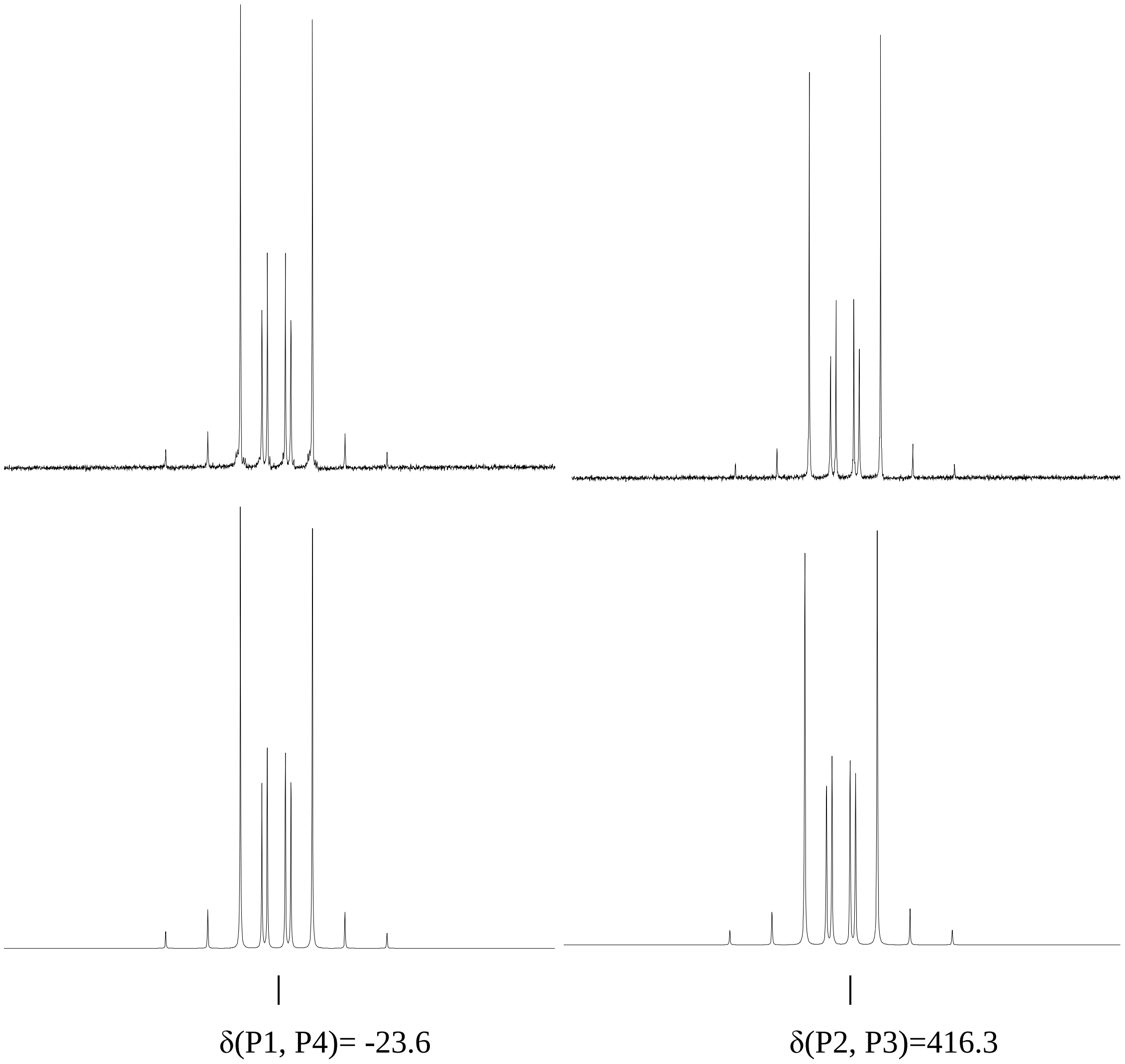

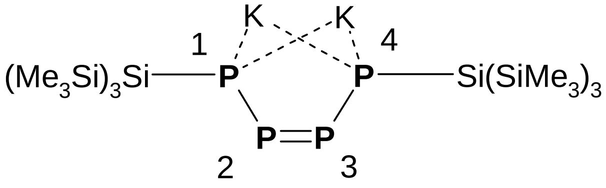

1

Figure 2.1 The ^{31}P{H}-NMR spectrum of **1** in THF + 5% benzene-d6(300K) at 101.256Hz. δ (P1, P4)= -23.6, δ(P2, P3)=416.3. $^{3}J_{p1,p4}$=151.5Hz, $^{1}J_{p1,p2}$ = $^{1}J_{p3,p4}$ =-431.1Hz, $^{2}J_{p1,p3}$=$^{2}J_{p2,p4}$ =-28.5Hz, $^{1}J_{p2,p3}$=-497.1Hz.

Table 2.1 Comparison of ^{31}P-NMR(THF-d8, 300K) chemical shifts and coupling constants

	1 [a]	$[(Me_3Si)_3Si]_2P_4Li_2$(**7**)	$[(Me_3C)_3Si]_2P_4Na_2$ [101]
δ (P1, P4) (ppm)	-23.6	-45.8	-41.1
δ(P2, P3) (ppm)	416.3	398.1	403.0
$^3J_{p1,p4}$ (Hz)	151.5	247.1	184.1
$^1J_{p1,p2}$, $^1J_{p3,p4}$(Hz)	-431.1	-410.3	-432.3
$^2J_{p1,p3,}$ $^2J_{p2,p4}$(Hz)	-28.5	-31.5	-34.7
$^1J_{p2,p3}$ (Hz)	-497.1	-481.0	-502.6

a: recorded in THF + 5% benzene-d6.

Most related coupling constants of the three compounds are similar. Lager difference of up to 96 Hz are found only for the values of $^3J_{p1,p4}$. As can be seen later in the X-ray diffraction studies a correlation to the distances between P1 and P4 in these compounds can be established.

It is worth noting that a trans-P_4 skeleton with a double bond reported by Fritz[97] shows also an AA'XX'-spin pattern at -104ppm and 552ppm in the ^{31}P-NMR spectrum. Here a considerably large $^1J_{XX'}$ value of -640 Hz arises from the two double-bond phosphorus atoms in the middle of the phosphorus chain and no coupling is observed between the trans terminal phosphorus atoms ($^3J_{AA'}$= 0 Hz). By contrast, no resonance for the trans conformer of **1** was found in the ^{31}P-NMR spectrum recorded in toluene solution even over the temperature range from -40°C to 70°C (Scheme 2.4). The adoption of the cis rather than the trans conformation in **1** may be due to the distribution of the two negative charges on all four phosphorus atoms. Thus the two potassium cations could be better coordinated by all four phosphorus atoms from both sides of the phosphorus skeleton plane.

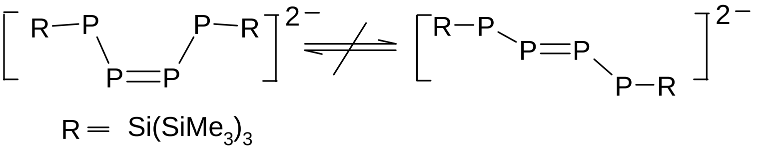

Scheme 2.4

The ^{29}Si-NMR spectrum of **1** displays a broad signal at -12.7ppm for peripheral silicon atoms of the hypersilyl groups and a triplet of triplet originating from the X part of an AA'MM'X spin system for the central silicon atoms at -92.4ppm. Unfortunately, the simulation is impossible because the intensity of the signal is not strong enough to identify all the lines in the spectrum. Only the values of $^1J_{Si,P}$ +$^4J_{Si,P}$ and $^2J_{Si,P}$ +$^3J_{Si,P}$ can be obtained as 46Hz and 14.5Hz, respectively.

As mentioned above, an equilibrium between compound **2** and **1** exists in toluene or benzene solution and the relatively higher concentration of **2** is found in toluene solution. Thus, the best NMR spectrum of compound **2** was obtained in toluene in the presence of a small amount of benzene-d_6. In proton decoupled ^{31}P-NMR spectrum of compound **2**, two groups of signals are observed at 44.8ppm and -207.3 ppm with relative intensities of 1:1 for the cyclotetraphosphane-phosphorus and phosphanide-phosphorus atoms, respectively. The pattern of the signals, as shown in Figure 2.2, reveals multiplets of higher order ($[AX]_4$ spin system). Unfortunately, the comparatively broad signals in this spectrum do not allow an iterative determination of the coupling constants with satisfactory accuracy. Corresponding investigation of a THF-d8 solution is impossible for compound **2**, since only the monomer **1** exists in the THF solution.

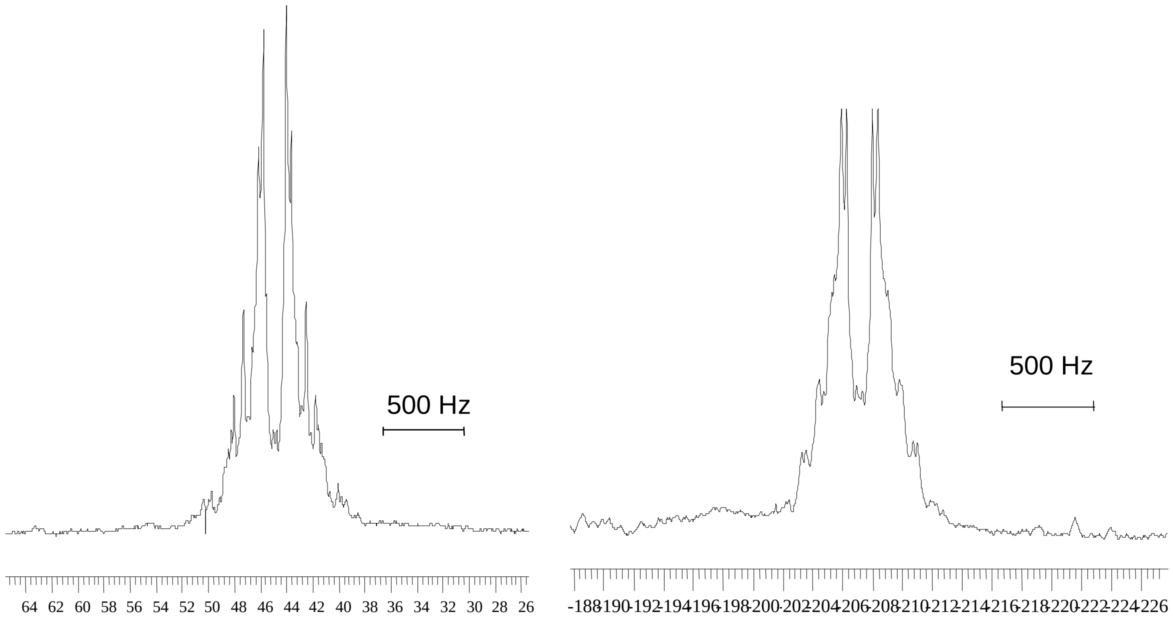

Figure 2.2 The ^{31}P{H}-NMR spectrum of **2** in toluene + 10% C_6D_6 (300K) at 81.015MHz. $\delta =$ 44.8, -207.3 ppm.

Compound **3** was characterized by NMR spectroscopy only. Both ^{1}H and ^{13}C{H} NMR spectra show a singlet for the hypersilyl groups. In the ^{31}P NMR spectrum of **3**, a doublet and a triplet can be observed at 199.8 and 717.2 ppm with relative intensities of 2:1 (Figure.2.3). Obviously, such an AX_2 spin system with a coupling constant of $^{1}J_{p,p}$ = 541Hz found in low field is assignable to a triphosphaallyl anion with partial double bond character and a trans-trans conformation (Figure 2.3). According to the NMR spectrum, no trans-cis isomer is present in solution.

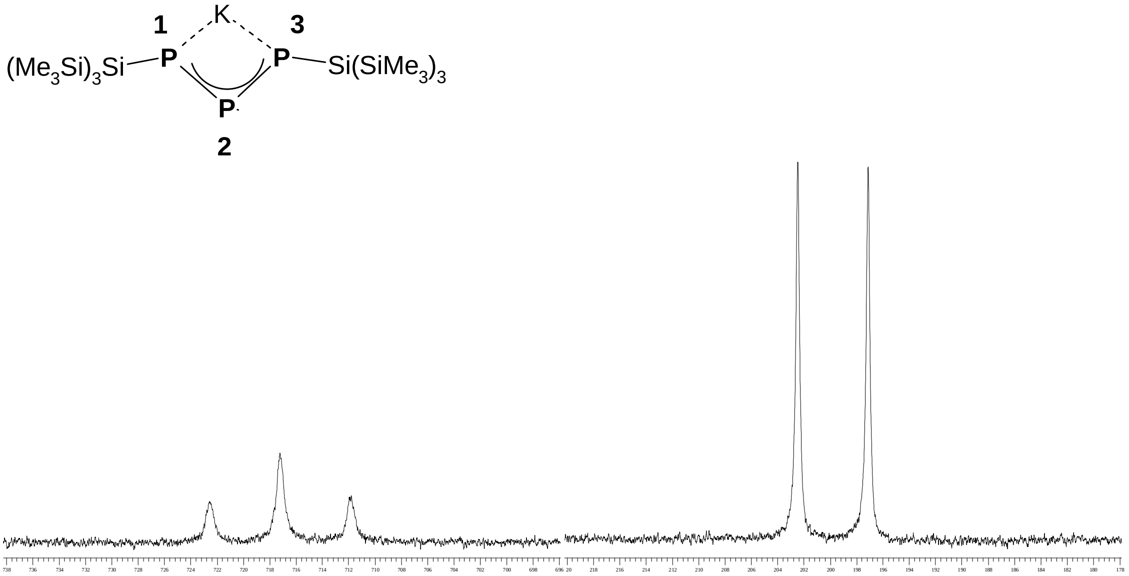

Figure 2.3 The ^{31}P{H}-NMR spectrum of **3** in C_6D_6 (300K) at 101.256MHz. δ(P_2): 717.2 (t, $^1J_{p\text{-}p}$=541Hz)ppm, δ($P_{1,3}$): 199.8(d,$^1J_{p\text{-}p}$=541Hz) ppm.

2.2.3 Crystal Structure

2.2.3.1 $Hyp_2P_4K_2·4C_6H_6$ (1a)

Deep red single crystals of the benzene solvate $Hyp_2P_4K_2$ (**1a**) were grown by quickly cooling a saturated solution of compound **1** in benzene to 5°C. The molecular structure of **1a** was established by X-ray crystallographic analysis (Figure 2.4) and the crystal data for **1a** are summarized in Table 2.2. Selected bond lengths and angles are listed in Table 2.3 and compared with those of the toluene (**1b**) and triazine solvates (**1c**) in Table 2.6**.**

Table 2.2 Crystallographic data of compound **1a**, **1b**, and **1c**.

Compound	**1a**	**1b**	**1c**
Empirical formula	$Hyp_2P_4K_2$·4benzene	$Hyp_2P_4K_2$·2toluene	$Hyp_2P_4K_2·2C_6H_6$·2triazine
Formula weight(g/mol)	1009.84	881.68	1112.05
Temperature(K)	173(2)	173(2)	173(2)
Crystal system	monoclinic	monoclinic	orthorhombic
Space group	P2(1)/n	P2(1)/m	$Cmc2_1$
a(Å)	14.935(2)	10.032(3)	22.156(5)
b(Å)	17.063(2	29.133(15)	18.087(5)
c(Å)	48.800(8)	18.405(7)	16.856(5)
α(°)	90	90	90
β(°)	90.380(12)	92.173(3)	90

γ(°)	90	90	90
Volume($Å^3$)	12436(3)	5375(4)	6754(3)
Formula units	8	4	4
Density(g/cm^3)	1.079	1.089	1.094
μ(Mo-K_α)(mm^{-1})	0.434	0.493	3.728
2Θ range(°)	2.05 to 20.00	2.15 to 24.00	3.15 to 55.29
Refl. collected	14566	8788	2203
Refl. uniqe	11593	8306	2157
R(int)	0.0361	0.1105	0.0558
Ind. Refl. with $F_o > 4\sigma(F_0)$	11593	8306	2157
Parameter	1009	656	277
R1	0.0492	0.0560	0.0778
R1(all refl.)	0.0868	0.2301	0.1101
wR2	0.1227	0.0509	0.1825
wR2(all refl.)	0.1331	0.0747	0.2027
GooF	0.816	0.654	0.95
Larg. Resid. peak(e/$Å^3$)	0.352	0.347	0.778

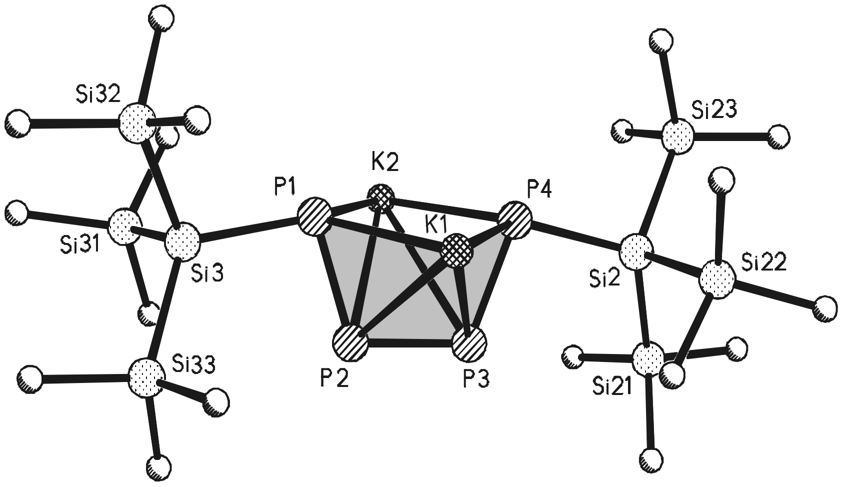

Figure 2.4 Molecular structure of **1a**. Benzene molecules and hydrogen atoms are omitted for clarity. Atoms are represented by spheres of arbitrary radii.

Table 2.3 Selected interatomic distances (pm) and angles(°) for **1a.**

P1-P2	214.0(2)	P2-P1-K2	78.78(7)
P2-P3	208.87(19)	P3-P4-Si2	97.81(9)
P4-P3	214.6(2)	P1-Si3-Si31	107.62(9)
P4-K1	327.4(2)	P1-Si3-Si33	116.22(10)
P3-K1	348.4(2)	P1-Si3-Si32	103.39(9)
P2-K1	348.6(2)	P4-Si2-Si22	108.55(9)

P1-K1	323.1(2)	P4-Si2-Si21	116.84(9)
K2-P1	330.8(2)	P4-Si2-Si23	104.39(10)
K2-P2	357.3(2)	Si3-P1-K1	121.22(8)
K2-P3	357.1(2)	Si3-P1-K2	122.13(8)
K2-P4	326.5(2)	Si2-P4-K2	124.98(8)
Si2-P4	225.4(2)	Si2-P4-K1	118.09(8)
Si3-P1	226.5(2)	Si-Si-Si	107.78(10) to 11.70(10)
Si-Si	234.4(3) to 235.5(3)	P3-P4-K2	79.68(7)
K-$C_{benzene}$	>=316.8(8)	P3-P4-K1	76.89(7)
P3-P2-P1	109.52(9)	K1-P1-K2	114.67(5)
P2-P3-P4	109.65(9)	K1-P3-K2	102.58(6)
P1-K1-P4	65.63(5)	K1-P2-K2	102.49(5)
P4-K2-P1	64.86(5)	K1-P4-K2	114.70(5)
P2-P1-K1	78.04(7)	P2-P1-Si3	98.47(9)

The central moiety of the molecular structure of **1a** exhibits a undistorted C_{2v}-symmetric U-shaped P_4 skeleton with all four P atoms as well as the two central silicon atoms of hypersilyl groups in one plane. The two potassium atoms coordinate from opposite sides of the P_4 plane to all four phosphorus atoms, forming a boat-like P_4K_2 framework with a notably flat rhomboid K_2P_2 ring (folding angle between the plans defined by P1-K1-P4 and P1-K2-P4: 3.2°) as shown in Figure 2.4. Presumably, this cyclobutane-type arrangement of the K_2P_2 ring may partially contribute to the stabilization of the high concentration of negative charges in this molecule. A similar Na_2P_2 ring is observed for the C_2-symmetric disodium 1,2,3,4-tetraphenyltetraphosphane-1,4-diide [$Na_2(P_4Ph_4)(thf)_4(tmu)$] (tmu = tetramethylurea)[111].

Two narrow angles (65.63° and 64.86°) for P-K-P and two wide angles [114.67(5) and 114.70(5)°] for K-P-K can be observed in this K_2P_2 ring. The contacts of K(1,2)-P(1,4) ranging between 323.1(2) and 330.8(2)pm are considerably longer than the sum of covalent radii of phosphorus and potassium, but still comparable to those found in KPH(Mes*)[Mes*=2,4,6-*t*$Bu_3C_6H_2$][327.1(2), 318.1(2), 335.7(2)pm] [112]. The distances of K(1,2)-P(2,3)[ranging between 348.4(2) and 357.(2)pm] are notably longer than those of K(1,2)-P(1,4). The coordination spheres of K atoms are each completed by one η^6-bonded benzene molecule [K···C distances ranging between 316.8(8) and 349.7(9)pm] and one η^2-bonded benzene molecule [K···C distances ≥ 327.5(9)pm] (Figure 2.5). No significant additional K···CH_3 agostic-type interaction with hypersilyl groups is observed in this structure.

The distance between P2 and P3 [208.87(19) pm] is significantly shorter than that between P1 and P2 [214.0(2)pm]or P3 and P4 [214.6(2)pm]. The P2-P3 bond length, however, is significantly longer than the P=P double bond [202.5(1)pm] in [$Li(DME)_3]_2\{(Me_3Si)[Cr(CO)_5]_2P$-P=P-$P[Cr(CO)_5]_2(SiMe_3)\}$[97], in which the P_4 skeleton shows a trans conformation. On the other hand, the other two bond lengths (P1-P2 and P3-P4) in **1a** are in contrast considerably shorter than the single P-P bonds [221.9(1)pm] in the chromium complex. These obviously suggest significant charge delocalizatiion over the whole P_4 chain and are in harmony with the ^{31}P-NMR spectrum described above.

It is worth mentioning that the two hypersilyl groups in the molecule are staggered with respect to each other with a torsion angle Si22-Si2-Si3-Si32 of 64°, as shown in Figure 2.5. In the toluene and triazine solvates of compound **1**, eclipsed arrangements of two hypersilyl groups are found. Therefore, these arrangements may be simply caused by packing effects within thin the crystals.

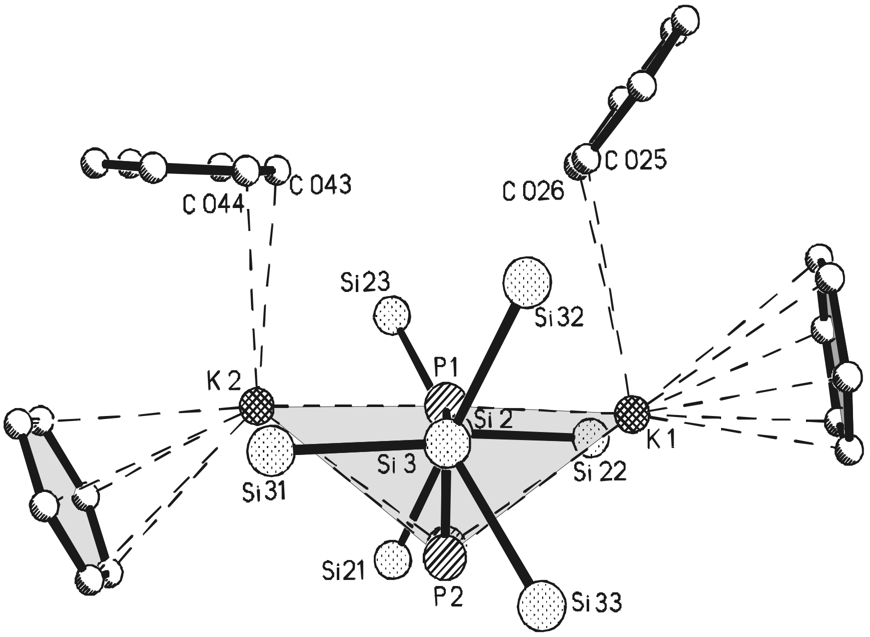

Figure 2.5 Perspective drawings of **1a** in the solid state; atoms are represented by spheres of arbitrary radii; K-P contacts are symbolized as dashed lines; the other dashed lines are used to symbolize interatomic distances markedly smaller than the sum of the corresponding van der Waals radii; methyl groups and hydrogen atoms are omitted for clarity.

2.2.3.2 $Hyp_2P_4K_2 \cdot 2C_7H_8$ (1b)

Violet rhombohedral single crystals of the toluene solvate $Hyp_2P_4K_2$ **(1b)** were obtained by cooling the concentrated reaction mixture in toluene to -20°C for several days. The molecular structure of **1b** was established by X-ray analysis and shown in Figure 2.6. The crystal data are summarized in Table 2.2 along with those of the other two solvates. Selected bond lengths and angles are listed in Table 2.4 and compared with that of **1a** and **1c** in Table 2.6.

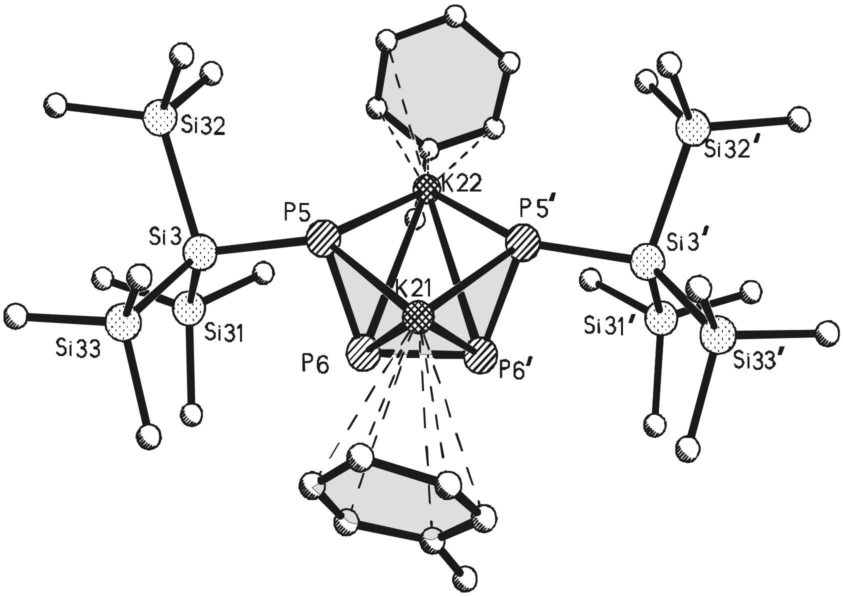

Figure 2.6 Perspective drawing of **1b :** atoms are represented by spheres of arbitrary radii; dashed lines are used to symbolize interatomic distances markedly smaller than the sum of the corresponding van der Waals radii; hydrogen atoms are omitted for clarity. Symmetry operation (′): x, -y+0.5, z

Table 2.4 Selected interatomic distances (pm) and angles (°) for **1b.**

P5-P6	214.2(3)	P5-K22-P6′	61.67(7)
P6-P6′	208.5(5)	P5-K22-P6	37.00(6)
P5-Si3	225.8(3)	P6′-K22-P6	34.71(8)
K21-P5	324.7(3)	Si3-P5-K22	115.01(11)
K22-P5	320.3(3)	Si3-P5-K21	128.03(11)
K22-P6	349.4(3)	K21-P6-K22	103.04(8)
Si3-Si31	234.0(3)	K22-P5-K21	114.46(8)
Si3-Si33	234.6(3)	P6′-P6-P5	109.01(8)
Si3-Si32	235.8(3)	P6-P5-Si3	98.70(12)
K-C	> 314(3)	P5-Si3-Si31	113.44(13)
Si-C	185.2(7) to 196(3)	P5-Si3-Si32	102.20(12)
		P5-Si3-Si33	111.51(13)
		Si31-Si3-Si33	112.00(13)
P5-K21-P5′	64.80(10)	Si31-Si3-Si32	107.45(12)
P5′-K22-P5	65.82(10)	Si33-Si3-Si32	109.67(13)

The conformation of $Si_2P_4K_2$ skeleton in **1b** is almost the same as in **1a**. The main differences between the two structures are found in the coordination spheres of the potassium atoms. As shown in Figure 2.7, two kinds of toluene rings with different coordination modes can be found in this structure. One coordinates only to one of the K atoms in an η^6-bonded fashion, while the other bonds simultaneously to two K atoms from adjacent $Hyp_2P_4K_2$ units, which finally leads to one-dimensional coordination polymers (Figure 2.7). Due to the twofold disordering of the toluene ligands the K···C distances can not be determined to a great accuracy, but the observed values range between 314 and 354pm, thus lying in the expected region. The two hypersilyl groups in $Hyp_2P_4K_2$ adopt an ideal eclipsed conformation.

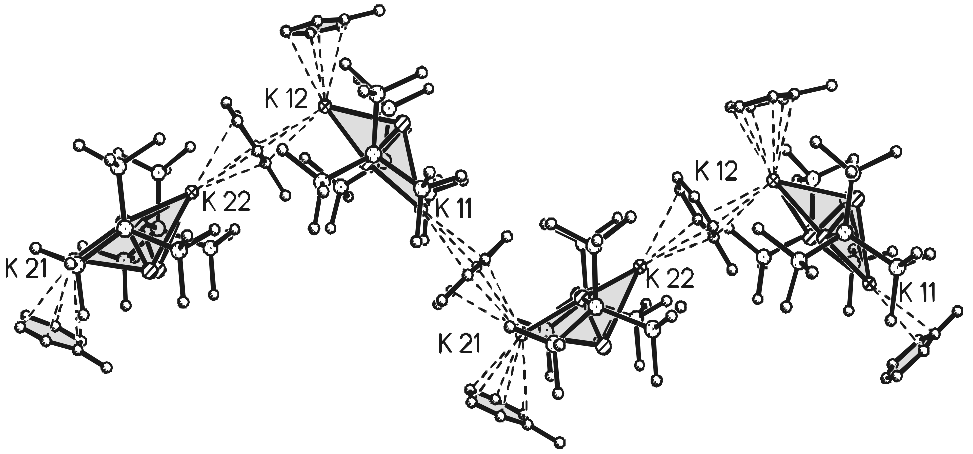

Figure 2.7 View parallel to the crystallographic b axis of the one-dimensional coordination polymer of **1b** in the solid state; dashed lines indicate potassium-toluene contacts; hydrogen atoms are omitted for clarity.

2.2.3.3 $Hyp_2P_4K_2{\cdot}2C_6H_6{\cdot}2(MeNCH_2)_3$ (1c)

The triazine solvate $Hyp_2P_4K_2{\cdot}2C_6H_6{\cdot}2(MeNCH_2)_3$ **(1c)** was obtained as yellowish green well shaped crystals by crystallization of $Hyp_2P_4K_2.4C_6H_6$ from a benzene/triazine mixture (5:1). The X-ray analysis shows **1c** to be monomeric in the solid state. Two triazine and two benzene molecules are found in each unit of $Hyp_2P_4K_2$ (Figure 2.8). The crystal data are summarized in Table 2.2 together with those of the other two solvates. Selected bond lengths and angles are listed in Table 2.5 and compared with those of **1a** and **1b** in Table 2.6.

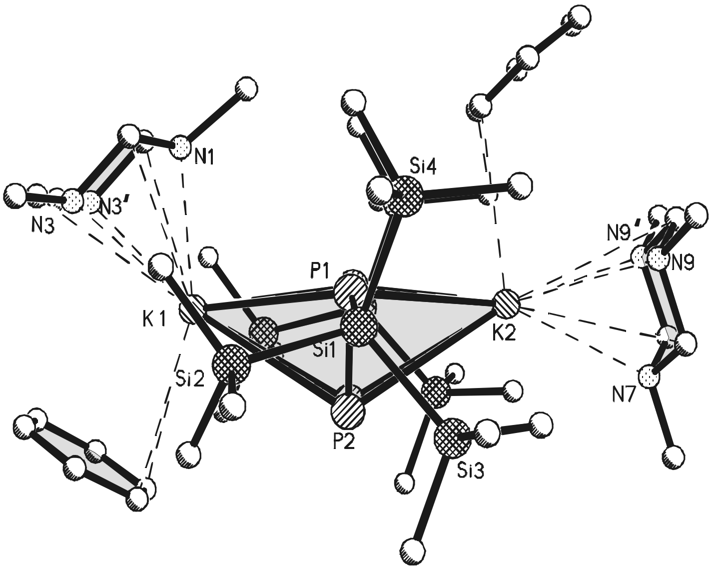

(b)

Figure 2.8 Molecular structure of **1c**: View parallel to the crystallographic axis of c emphasizing the eclipsed conformation; atoms are represented by spheres of arbitrary radii; dashed lines are used to symbolize interatomic distances markedly smaller than the sum of the corresponding van der Walls radii; hydrogen atoms are omitted for clarity. Symmetry operation ('): -x, y, z

Table 2.5 Selected interatomic distances (pm) and angles (°) for **1c**

P1-P2	213.9(5)	P2-P1-Si1	98.0(2)
P1-Si1	223.7(6)	P2′-P2-P1	109.71(16)
P2-P2′	205.8(8)	P1-Si1-Si2	112.8(2)
K-P1	av. 340.4	P1-Si1-Si3	117.0(2)
K-P2	av. 352.6	P1-Si1-Si4	105.1(2)
K-N	av. 293.6		
K-C(triaz.)	av. 342.1		
K-C(benz.)>=	340.7		
Si-Si	av. 234.6		

The $Si_2P_4K_2$ skeleton of **1c** is almost identical with those of **1a** and **1b**. Major differences between the three structures are found only in the coordination environment of potassium. Each potassium atom in **1c** is coordinated by an η^3-N(η^3-C) bonded triazine molecule and an η^2-bonded benzene molecule. The mean distances of K-N of 293.6pm are larger than the sum of the covalent radii of potassium and nitrogen (273pm). Despite different solvent molecules, this coordination environment of potassium atoms is quite similar to that in **1a**. The two hypersilyl groups in this structure, however, are exactly eclipsed with respect to each other as observed in **1b**.

The average distances of K-P(1,4) and K-P(2,3) in **1c**(340.4 and 352.6pm) and in **1a**(326.9 and 352.8pm) are slightly longer than those observed in **1b**(325.0 and 344.7pm). This may be due to the fact that each potassium atom in **1b** is coordinated by only one toluene molecule in average, whereas those in **1a** and **1c** are attached to two (C_6 or N_3C_3 ring).

Table 2.6 Comparison of selected interatomic distances (pm) and angles (°) for **1a**, **1b** ,and **1c**.

Compound	**1a**	**1b**	**1c**
P1-P2	214.4	213.8	213.9
P2-P3	208.9	208.8	205.8
P3-P4	214.6	213.8	213.9
K(1,2)-P(1,4)	326.9	325.0	340.4
K(1,2)-P(2,3)	352.8	344.7	352.6
P-Si	226.0	225.8	223.7
Si-Si	235.1	234.8	234.6
P1-K-P4	65.2	65.0	61.9
Si-P1-P2	98.2	98.5	98.0
P1-P2-P3	109.5	109.2	109.7
P-Si-Si	109.6	109.8	111.6

The numbering of the atoms in **1b** and **1c** has been related to that of **1a**.

2.2.3.4 $Hyp_4P_8K_4 \cdot 4C_6H_6$ (2a)

Bright red well-shaped single crystals of the benzene solvate **2a** were obtained from benzene solution. X-ray diffraction analysis data were collected at 193K under conditions detailed in Table 2.7. The benzene molecules were slightly disordered; however, the P_8K_4

skeleton and hypersilyl groups were ordered and the structure determination gave well-defined structural parameters (Figure 2.9). Selected bond lengths and angles are summarized in Table 2.8.

Table 2.7 Crystallographic data of **2a**.

Empirical formula	$Hyp_4P_8K_4\cdot$7benzene
Formula weight(g/mol)	1941.58
Temperature(K)	193(2)
Crystal system	monoclinic
Space group	P2/n
Lattice constants(Å,°)	a = 15.1356(7) α 90
	b = 14.6526(6) β 99.297(4)
	c = 26.9623(14) γ 90
Volume($Å^3$)	5901(5)
Formula units	2
Density(g/cm^3)	1.093
μ(Mo-K_α)(mm^{-1})	0.455
2Θ range(°)	1.39 to 26.29
Reflections measured	67117
Independent reflections	11884 [R(int) = 0.0621]
Ind. Reflections with $F_o > 4\sigma(F_0)$	11884
Parameter	657
R1,R1(all reflections)	0.0288, 0.0439
wR2,wR2(all reflections)	0.0713, 0.0741
GooF	0.936
Residual electron density($e/Å^3$)	0.272

The molecular structure may be described as a double cube with a shared four membered P_4 ring (the sum of the angles: 355.3°) in the middle, two phosphorus atoms and two potassium atoms in alternating positions on the top and the bottom, in which the four exo-phosphorus atoms each bear a hypersilyl group. The molecule possesses D_{2d} symmetry to a very good approximation. The small deviations are possibly caused by packing effects within the crystal.

The observed P-P bond lengths in the P_4 ring of 226.0± 0.6 pm are slightly longer than the distances between P_{ring} and P_{exo} of 219.0 ± 0.4 pm. However, they all lie in the expected single P-P bond range and resemble the corresponding distances of 226 ± 1 and 219 ± 1 pm observed in $(^tBu_3Si)_4P_8Na_4$.4DME [101], respectively. The rhomboid distortion of the two K_2P_2 planes in K_4P_8 skeleton leads to P-K-P and K-P-K bond angles of approximately 66° and 106°, respectively. The K-P distances ranging from 318.42(7) to 323.05(6)pm are smaller than those (325.0 - 352.8 pm) found for all three $Hyp_2P_4K_2$ solvates described above.

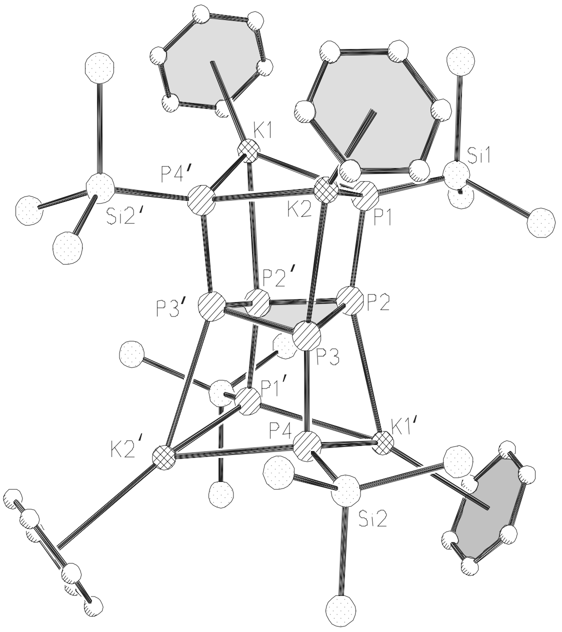

Figure 2.9 Molecular structure of **2a.** Atoms are represented by spheres of arbitrary radii. Methyl groups and hydrogen atoms on benzene are omitted for clarity. Symmetry operation (′):`-x+3/2,y,-z+3/2`

Apart from the coordination by three phosphorus atoms, the coordination environment around each potassium atom is completed by an η^6-bonded benzene molecule. Because of the two fold disordering of benzene molecules in the crystal, the K···C distances could not be determined with great accuracy. Nevertheless, the observed contacts of K and C atoms (327 - 344 pm) lie within the expected range. No significant short agostic interaction between potassium and methyl of hypersilyl group is found in this structure.

According to the symmetry, the hypersilyl groups at each face of the double cube in **2a** are orientated eclipsed with respect to each other. The P-Si bonds (221.45(6) - 221.61(6) pm) are shorter than the sum of the covalent radii of phosphorus and silicon atom (228pm) and even slightly shorter than the P-Si bonds [ranging between 223.7(6) and 226.5(2)pm] observed for the three solvates of $Hyp_2P_4K_2$.

Table 2.8 Selected interatomic distances (pm) and angles (°) for **2a**.

P1-P2	219.36(6)	P2-P3-K2	95.802(19)
P2-P3	225.96(6)	P3′-P3-K2	94.13(2)
P3-P4	218.67(6)	P3-P4-K2′	96.24(2)
P3-P3′	226.59(8)	P3-P4-K1′	95.75(2)
P2-P2′	226.82(9)	P2-P1-K1	95.21(2)
P1-K2	318.51(7)	P2-P1-K2	98.48(2)
P1-K1	320.72(7)	P4′-K1-P1	70.403(15)
P3-K2	323.05(6)	P4′-K1-P2′	66.365(14)
P4-K1′	318.42(7)	P1-K1-P2′	66.341(14)
P4-K2′	321.19(7)	P1-K2-P4′	70.332(15)
	318.42(7)		64.571(13)

K1-P4′	321.69(6)	P1-K2-P3	65.608(14)
K1-P2′	221.61(6)	P4′-K2-P3	105.732(18)
P4-Si2	221.45(6)	K2-P1-K1	105.643(18)
P1-Si1	327.6(7) to 339.5(9)	K1′-P4-K2′	105.35(2)
K-C	233.32(7) to 234.78(6)	P2-P1-Si1	125.33(2)
Si-Si	185.7(3) to 188.0(3)	Si1-P1-K2	119.82(2)
Si-C	103.98(2)	Si1-P1-K1	105.09(2)
P4-P3-P2	103.22(3)	P3-P4-Si2	123.09(2)
P4-P3-P3′	88.863(16)	Si2-P4-K1′	123.30(2)
P2-P3-P3′	100.62(2)	Si2-P4-K2′	114.77(3)
P1-P2-P3	103.94(3)	P1-Si1-Si12	114.51(3)
P1-P2-P2′	88.808(16)	P1-Si1-Si11	99.76(3)
P3-P2-P2′	157.74(2)	P1-Si1-Si13	115.33(3)
P1-P2-K1′	93.40(2)	P4-Si2-Si21	114.99(3)
P3-P2-K1′	93.47(2)	P4-Si2-Si22	99.00(2)
P2′-P2-K1′	153.76(2)	P4-Si2-Si23	107.76(3) to
P4-P3-K2		Si-Si-Si	110.35(3)

2.2.4 Protolysis and Oxidation of $Hyp_2P_4K_2$

The protolysis of $[(Me_3Si)_3Si]_2P_4K_2$ depends strongly on the reaction conditions. When dry hydrochloric gas was bubbled through a toluene solution of **1b** at room temperature, the deep violet colour vanished gradually. According to the ^{31}P-NMR spectrum, the reaction led to the formation of $(Me_3Si)_3SiPH_2$ and tris(hypersilyl)heptaphosphane $[(Me_3Si)_3Si]_3P_7$ (Eq.2.2), which had been synthesized at first from sodium-potassium phosphide and chlorotris(trimethylsilyl)silanide[113].

$$((Me_3Si)_3Si)_2P_4K_2 \xrightarrow{H^+} ((Me_3Si)_3Si)_3P_7 + (Me_3Si)_3SiPH_2 \qquad \text{(Eq.2.2)}$$

Gradual protolysis of **1** with 2,6-di-*tert*-butyl-phenol in benzene at room temperature gave $[(Me_3Si)_3Si]_3P_5K_2$, $[(Me_3Si)_3Si]_2P_3K$, $(Me_3Si)_3SiPH_2$, and further unidentified phosphorus-containing compounds as intermediates. The dominant phosphorus-containing product observed by ^{31}P-NMR spectra was $(Me_3Si)_3SiPH_2$; $[(Me_3Si)_3Si]_3P_7$ was detected in traces only.

Treatment of compound **1** with anhydrous $FeCl_2$ in THF at -20°C led to the oxidation of **1**. According to the ^{31}P-NMR spectrum of the reaction mixture $[(Me_3Si)_3Si]_3P_7$ was found as the main product along with small amounts of $[(Me_3Si)_3Si]_2P_4$, $(Me_3Si)_3SiPH_2$ and other unidentified phosphorus-containing compounds.

2.3 $Hyp_3P_5K_2$ (4) and $Hyp_3P_8K_3$ (5)

2.3.1 Synthesis

Although in the crystalline state $Hyp_2P_4K_2$ had been stored for more than two years without any sign of decomposition under argon, in toluene solution it decomposes slowly at room temperature giving yellowish well-shaped crystals of potassium tris(hypersilyl)pentaphosphanide $Hyp_3P_5K_2$ (**4**) within several weeks. This process beomes even quicker when the solution is warmed to 70°C.

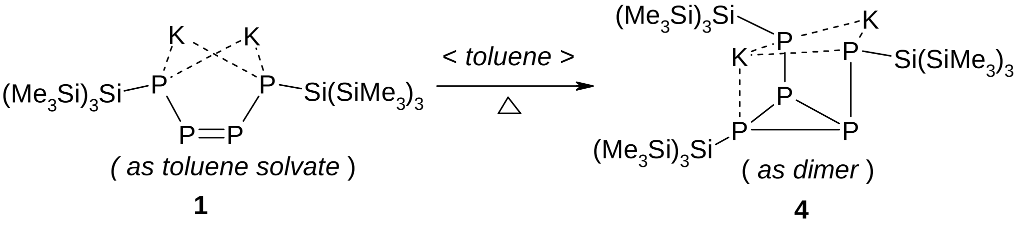

(Eq.2.3)

Compound **4** is also formed as described above by protolysis of $Hyp_2P_4K_2$ with 2,6-di-^{t}Bu-phenol. According to the suggestion made for $[(Me_3C)_3Si]_3P_5Na_2$ by Wiberg[102], the formation of **4** may be understood with Scheme 2.5. Compound **4** is a formal [1+2] addition product of **1** with HypP. Latter might be formed through protolysis of **1**, followed by elimination of “P_2”. Other products detected, such as $HypPH_2$ are further evidence for protolysis and a subsequent cleavage of the phosphorus chain.

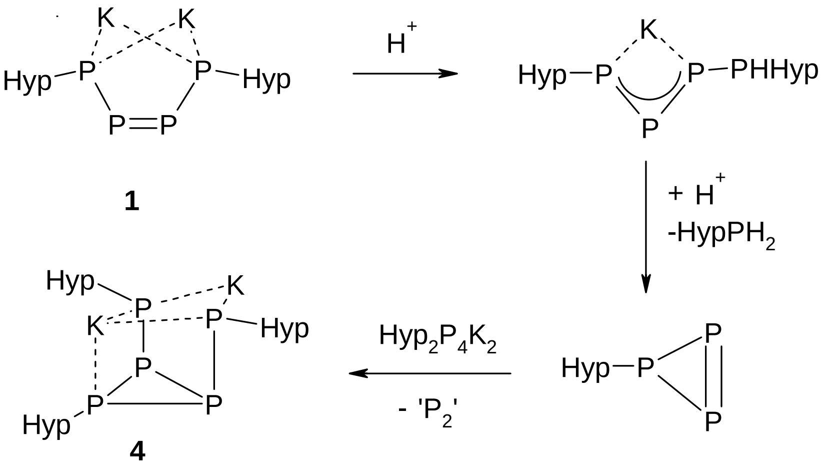

Scheme 2.5

Another polyphosphanide, potassium tris(hypersilyl)octaphosphanide $Hyp_3P_8K_3$ (**5**), is found and isolated as orange cubic shaped X-ray diffraction quality crystals by concentrating a very dilute benzene solution of compound **2** and cooling at 5°C for several days. This compound is formally generated from **2** by elimination of potassium hypersilanide. A possible path to **5** may be a partial protonation of compound **2** by traces of water followed by the elimination of $(Me_3Si)SiH$ and subsequent rearrangement of the phosphorus cage (Eq. 2.4).

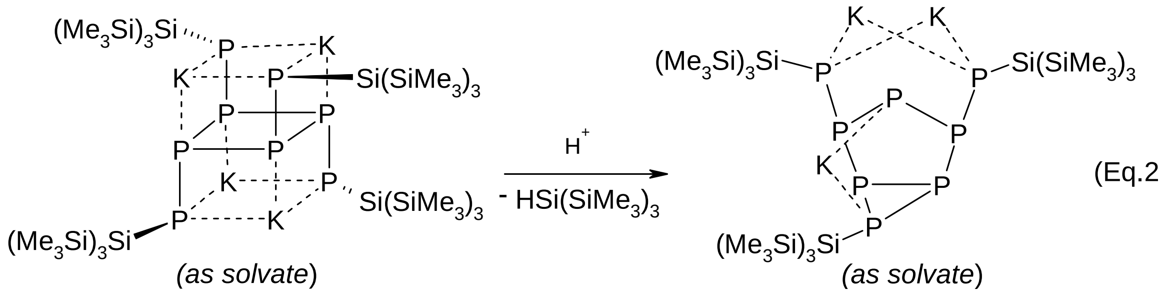

2 **5**

(Eq.2.4)

2.3.2 NMR Spectroscopy

2.3.2.1 $Hyp_3P_5K_2$ (4)

The two inequivalent hypersilyl groups give rise to two singlets with relative intensities of 2:1 in the ^{1}H-NMR spectum and two singlets in the ^{13}C{H}-NMR spectrum. In ^{1}H decoupled ^{31}P-NMR spectrum, three groups of broad signals are observed at -87.4, -197.0 and -242.3ppm with relative intensities of 2:1:2 (Figure 2.10).

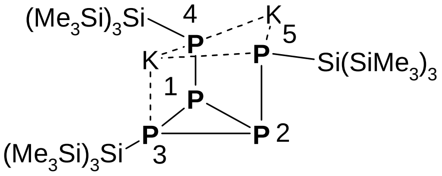

4

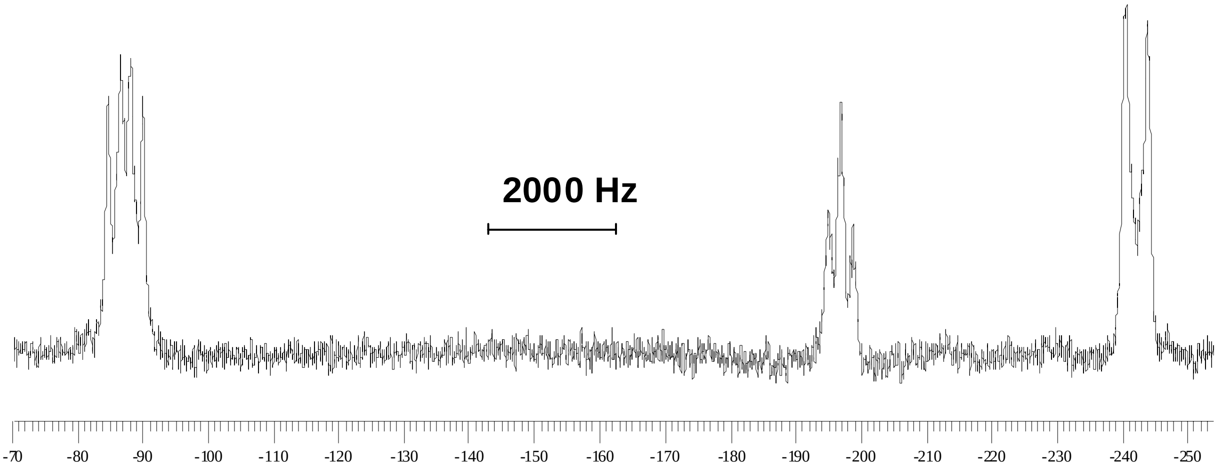

Figure 2.10 The ^{31}P{H}-NMR spectrum of **4** in benzene-d6(300K) at 101.256MHz. δ (P1, P2)= -87.4, δ(P4, P5)=-242.3 . δ (P3)= -197.0 ppm.

In order to get well-resolved signals, a THF-d8 solution of compound **4** was investigated. The ^{31}P{H}-NMR spectrum exhibits three complex multiplets at -81.5, -206.7, and -247ppm in a ratio of 2:1:2 arising from an AA'MM'X spin system, which are verified by simulation using the parameters published for $[(Me_3C)_3Si]_3P_5Na_2$ [102] as a starting point followed by several iterations. The experimental and simulated resonances are shown in Figure 2.11. In order to compare the values of compound **4** with those of its analogues, the corresponding chemical shifts and coupling constants are summarized in Table 2.9. The chemical shifts and the one-bond coupling constants of the three membered ring phosphorus atoms of compound **4**, similar to those of $[(Me_3Si)_3Si]_3P_5Na_2$(**9**, see below) and $[(Me_3C)_3Si]_3P_5Na_2$ [102], are in the typical range of triphosphiranes[114][115]. Compared to the values of $^{1}J_{P1,P2}$, $^{1}J_{P2,P3}$, and $^{1}J_{P1,P3}$, the coupling constants $^{1}J_{P1,P4}$ and $^{1}J_{P2,P5}$ of -347.5Hz are considerably larger.

Table 2.9 Comparison of the ^{31}P-NMR(THF-d8, 300K) spectroscopic data of **4**, **9**, and $[(Me_3C)_3Si]_3P_5Na_2$ [102]

	4	**9**	$[(Me_3C)_3Si]_3P_5Na_2$
δ (P1, P2) (ppm)	-81.5	-94.4	-93.4
δ(P4, P5) (ppm)	-247.2	-249.1	-240.3
δ (P3) (ppm)	-206.7	-193.4	-179.6
$^{3}J_{p4,p5}$ (Hz)	214	302.9	231.8
$^{1}J_{p1,p2}$ (Hz)	-189.8	-195.3	-201.6
$^{2}J_{p1,p5}$, $^{2}J_{p2,p4}$(Hz)	-6.9	-7.3	-5.1
$^{1}J_{p1,p3}$, $^{1}J_{p2,p3}$(Hz)	-178.3	-178.8	-191.9
$^{2}J_{p3,p4}$, $^{2}J_{p3,p5}$(Hz)	61.7	61.4	64.9
$^{1}J_{p1,p4}$, $^{1}J_{p2,p5}$(Hz)	-347.5	-336.6	-348.9

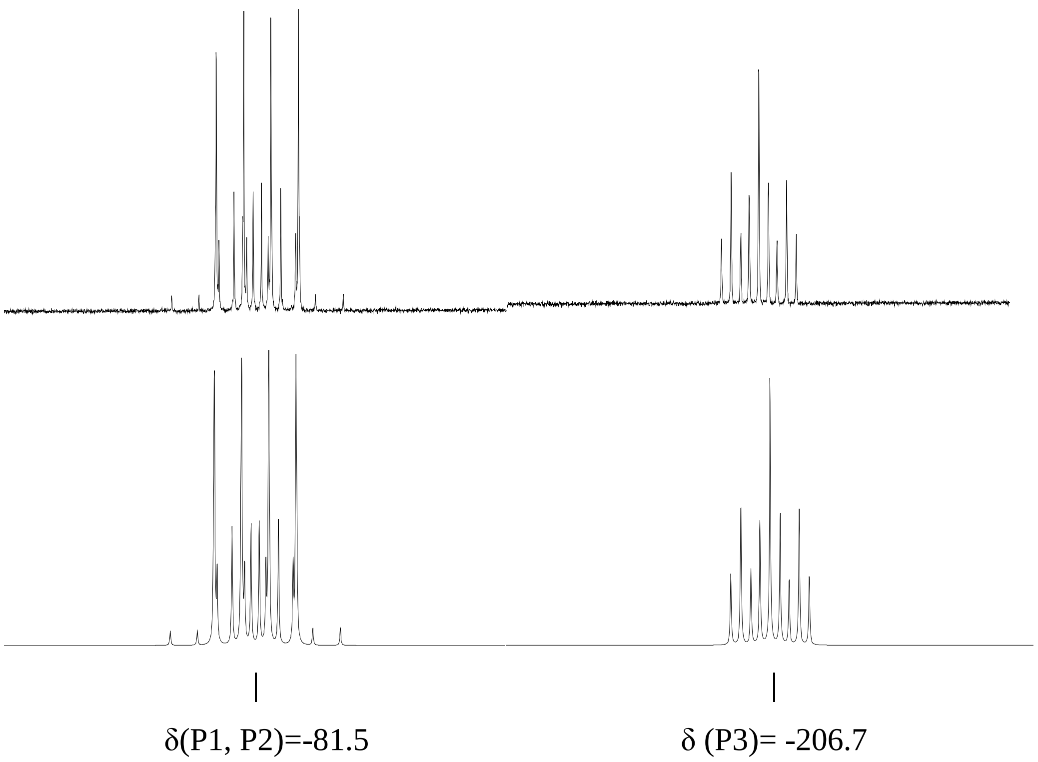

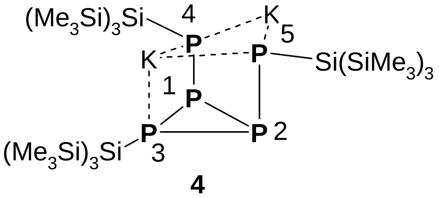

4

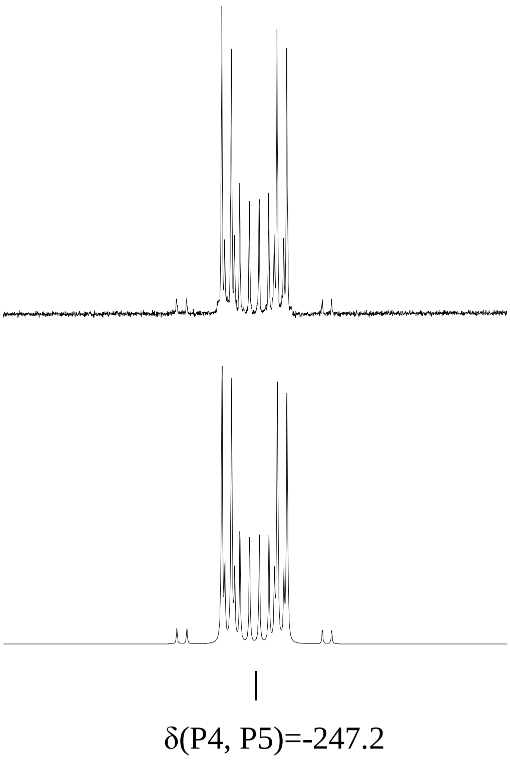

Figure 2.11 The ^{31}P{H}-NMR spectrum of **4** in THF-d8(300K) at 101.256MHz. δ (P1, P2)= -81.5, δ(P4, P5)=-247.2 , δ (P3)= -206.7, $^{1}J_{p1,p4}$=$^{1}J_{p2,p5}$= -347.5Hz, $^{2}J_{p3,p4}$ = $^{2}J_{p3,p5}$ =61.7Hz, $^{1}J_{p1,p3}$=$^{1}J_{p2,p3}$ =-178.3Hz, $^{2}J_{p1,p5}$=$^{2}J_{p2,p4}$ =-6.9Hz, $^{1}J_{p1,p2}$=-189.8Hz, $^{3}J_{p4,p5}$ =214.0Hz. The signs of the coupling constants except for $^{2}J_{p3,p4}$ and $^{2}J_{p3,p5}$ originate from the iteration under setting $^{1}J_{P,P}$ as a negative value[116].

The $^{29}Si\{H\}$-NMR spectrum of compound **4** in THF-d_8 shows two broad signals without fine structure at -9.8 and -12.2ppm for the peripheral silicon atoms of hypersilyl groups in agreement with ^1H- and $^{13}C\{H\}$-NMR spectra, each of which exhibits two singlets. The spectrum also shows two less intense resonances at -90.1 and -91.8 ppm for the two types of the central silicon atoms of hypersilyl groups. The signal at -90.1ppm for Si3, according to a first order interpretation, is a doublet (with a coupling constant of 116Hz split by P3) of triplets (with a two-bond coupling constant of about 6Hz split by P1 and P2). The accuracy of these coupling constants is however reduced to about ±2Hz by peak broadening due to long-range coupling with the other P atoms. The other signal for Si1 and Si2 is a multiplet representing the X part of an AA'MM'RX spin system originating from the two possible isotopomers, each containing one ^{29}Si-nucleus [117]. A simulation using the parameters published for $[(Me_3C)_3Si]_3P_5Na_2$ [102] as a starting point yielded the coupling constents given in Table 2.10. The comparison of the final chemical shifts and coupling constants of **4**, sodium analogues **9** and $[(Me_3C)_3Si]_3P_5Na_2$ are shown in Table 2.21 and will be discussed later.

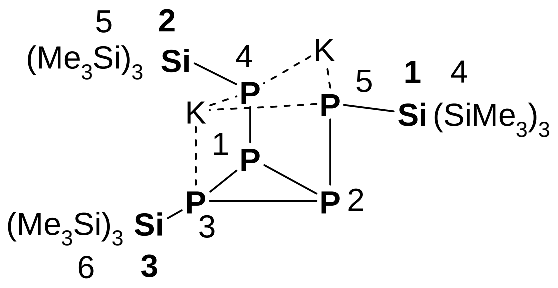

Table 2.10 The calculated silicon-phosphorus coupling constants for compound **4**.

$^1J_{p3,Si3}$ (Hz)	$^2J_{p1,Si3}$ $^2J_{p2,Si3}$ (Hz)	$^1J_{p4,Si2}$, $^1J_{p5,Si1}$ (Hz)	$^2J_{p1,Si2}$, $^2J_{p2,Si1}$ (Hz)	$^3J_{p3,Si2}$, $^3J_{p1,Si1}$ (Hz)	$^4J_{p5,Si2}$, $^4J_{p4,Si1}$ (Hz)
-116.3	7.3	-106.8	-21.4	-17.3	7.6

2.3.2.2 $Hyp_3P_8K_3$ (5)

The $^{31}P\{H\}$-NMR spectrum of **5** in benzene-d6 displays five groups of signals at δ=43.0, -45.7, -56.0 ppm for the formally uncharged phosphorus atoms P3, P4 and P5 and -181.3, -234.5 ppm for phosphanide-phosphorus atoms with relative intensities of 2:1:2:2:1, respectively (Figure 2.12). The signals are all broad, just as those of **4** in benzene (Figure 2.10). Attempts to obtain the coupling constants by simulation are thus unsuccessful. The structure, however, has been unambiguously determined by single crystal X-ray diffraction studies. Approximatively, neglecting the two-bond coupling of the five-membered ring phosphorus atoms, the broad triplet at -234.5ppm for P4 and doublet at -181.3ppm for P1 and P8 as well as the triplet at -

45.7ppm for P7 are consistent with the molecular structure established crystallographically. In the ^{1}H-NMR spectrum, two singlets originating from the two inequivalent hypersilyl groups can be observed at 0.505 and 0.527ppm with relative intensities of 2:1, which are comparable to those found in compound **4** of 0.507 and 0.512 ppm. Moreover, the chemical shifts in the ^{13}C-NMR spectrum of 3.3 and 3.4 ppm for the two types of hypersilyl groups are also similar to those observed for compound **4** (3.1 and 3.8 ppm).

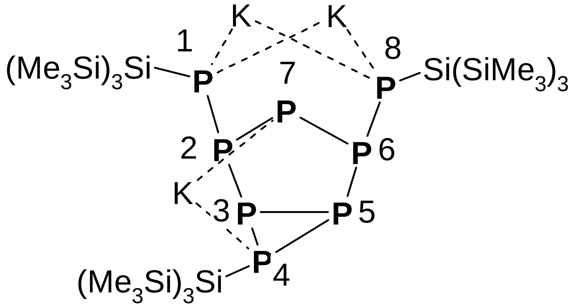

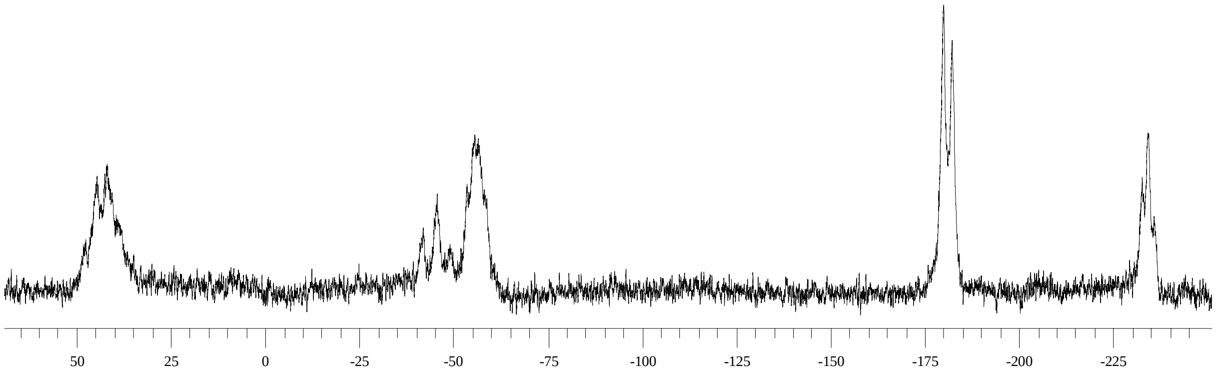

Figure 2.12 The ^{31}P{H}-NMR spectrum of **5** in benzene-d6(300K) at 101.256MHz. δ (P1, P8)= -181.3, δ(P2, 6)=43.0, δ (P3, P5)= -56.0, δ(P4)=-234.5. δ (P7)= -45.7 ppm.

2.3.3 Crystal Structure

2.3.3.1 $(Hyp_3P_5K_2)_2 \cdot 3C_6H_6$ (4a)

The X-ray crystal structure analysis of a yellow well shaped single crystal of compound **4a** obtained from benzene solution shows that **4a** crystallizes as a coordination dimer. The molecule has a C_{2h} symmetry, with the twofold axis running through the two bridging potassium atoms as shown in Figure 2.13. Collection parameters and other crystallographic data are summarized in Table 2.11. Selected bond lengths and angles are listed in Table 2.12.

Table 2.11 Crystallographic data of **4a**.

Empirical formula	$\mathrm{Hyp_3P_3K_2\cdot 1.5}$benzene
Formula weight(g/mol)	1093.21
Temperature(K)	193(2)
Crystal system	triclinic
space group	$P\bar{1}$
Lattice constants(Å,°)	a = 14.7289(14) α 97.292
	b = 17.2007(15) β 93.032(7)
	c = 27.467(2) γ 105.980(7)
Volume(Å^3)	5607.5(10)
Formula units	4
Density(g/cm^3)	1.099
μ(Mo-K$_\alpha$)(mm^{-1})	0.505
2Θ range(°)	1.36 to 26.37
Reflections measured	63967
Independent reflections	26523 [R(int) = 0.0813]
Ind. Reflections with $F_o > 4\sigma(F_0)$	26523
Parameter	1155
R1,R1(all reflections)	0.0573, 0.1050
wR2,wR2(all reflections)	0.1314, 0.1455
GooF	0.904
Residual electron density(e/Å^3)	0.638

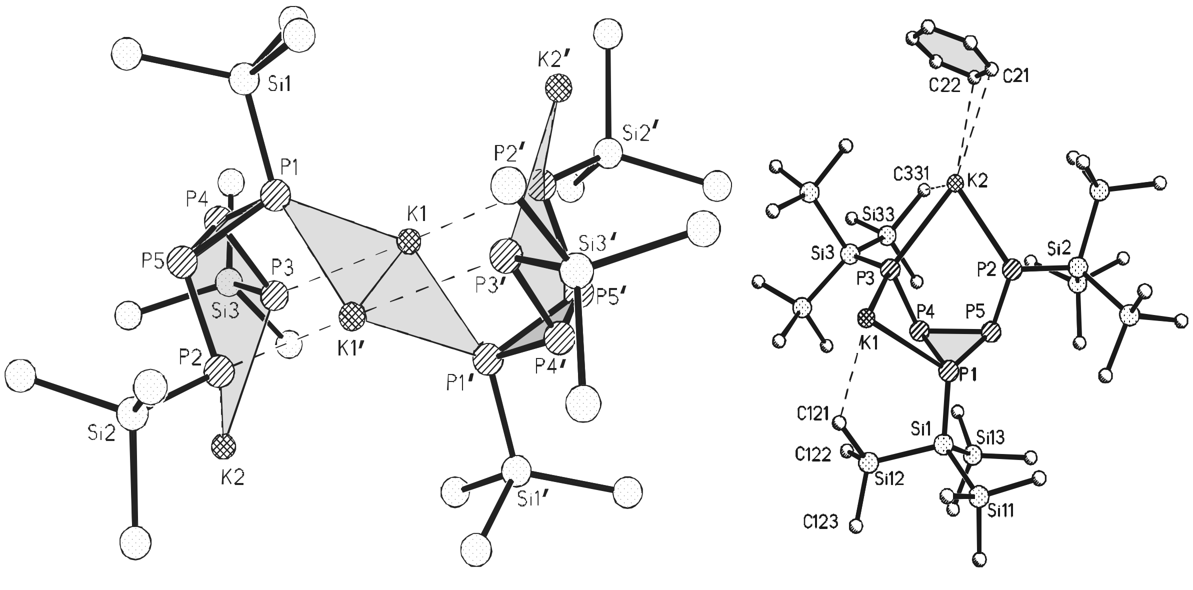

(a) (b)

Figure 2.13 Perspective drawing of **4a**; atoms are represented by spheres of arbitrary radii; dashed lines are used to symbolize interatomic distances markedly smaller than the sum of the corresponding van der Waals radii. (a): Benzene and and methyl groups are omitted. (b): $\mathrm{Hyp_3P_5K_2}$ unit (hydrogen atoms are omitted for clarity). Symmetry operation (′):`-x+1,-y+1,-z`

The $\mathrm{[(Me_3Si)_3Si]_3P_5}$ moiety comprises cyclotriphosphane skeleton with two exocyclic phosphorus atoms attached in a cis fashion. Each of latter links further to a hypersilyl group, while the third P atom in the P_3 ring bears directly a hypersilyl group in trans position to the two P_{exo} atoms. The P_{ring}-P_{ring} distances ranging between 223.03(14) and 225.15(14) pm are significantly longer than the other two P_{ring}-P_{exo} bond lengths [217.57(15), 217.24(14) pm]. All the P-P bond lengths are very similar to those observed in sodium tris(supersilyl)petaphosphanide $[(Me_3C)_3Si]_3P_5Na_2$ [102] (with a mean distance of 224pm for P-P bonds in P_3 ring and 218pm for P_{ring}-P_{exo} bonds), which crystallizes as monomeric THF solvate. A similar difference between endo- and exocyclic bondlengths were found for compound **2a**.

The formally negatively charged atoms P2 and P3 are each linked to two potassium atoms, displaying a distorted tetrahedral coordination environment with K-P-K angles of 126.86(4)° for P2 and 122.30(4)° for P3. With a total coordination number of five (two K atoms, two P atoms and one hypersilyl group), P1 exhibits a distorted square pyramidal environment. The K-P bonds ranging between 316.32(15) and 345.26(14) pm are comparable to those observed for other substituted potassium phosphanides [118] [119] [120]. Apart from the two phosphorus atoms with a P2-K2-P3 angle of 72.22(4)°, the coordination sphere of K2 is completed by disordered η^2-bonded benzene molecule (K···C distances: about 329pm) and agostic interactions to hypersilyl groups with a shortest K···C contact of 317pm. Due to the steric crowding , no short contact to a benzene ring is found for K1. However, agostic-type interactions to methyl groups (K···C ≥ 340 pm) are observed.

Table 2.12 Selected interatomic distances (pm) and angles (°) for **4a**.

P1-P4	223.03(14)	P3-K1-P1	63.61(3)
P1-P5	224.42(14)	P2′-K1-P1	107.02(4)
P2-P5	217.57(15)	P1′-K1-P1	100.92(3)
P3-P4	217.24(14)	K1-P3-K2	122.32(4)
P4-P5	225.15(14)	K2-P2-K11′	126.86(4)
P1-Si1	227.08(15)	K1′-P1-K1	79.08(3)
P2-Si2	224.77(15)	P4-P1-K1	86.51(4)
P3-Si3	224.31(15)	P5-P1-K1	124.62(5)
P2-K2	316.32(15)	P4-P1-K1′	126.21(5)
P1-K1	345.26(14)	P4-P3-K1	93.65(5)
P1-K1′	336.34(15)	P5-P1-K1′	86.48(4)
P2-K1′	322.97(14)	P4-P3-K2	110.42(5)
P3-K1	321.71(14)	P5-P2-K1′	91.05(5)
P3-K2	323.54(16)	P5-P2-K2	112.88(5)
K1-K1′	434.0(2)	P4-P1-Si1	101.43(5)
K2-C111′	317.0(5)	P5-P1-Si1	107.07(5)
K2-C22	338.2(7)	P5-P2-Si2	96.51(6)
K2-C21	347.9(8)	P4-P3-Si3	97.60(6)
Si-Si	234.16(18) to 235.72(16)	Si1-P1-K1′	129.76(5)
		Si1-P1-K1	123.19(5)
P2-P5-P1	104.78(5)	Si2-P2-K2	112.87(5)
P2-P5-P4	109.11(6)	Si2-P2-K1′	110.29(5)
P1-P5-P4	59.48(4)	Si3-P3-K1	131.56(5)
P1-P4-P5	60.09(4)	Si3-P3-K2	97.25(5)
P3-P4-P5	111.81(6)	P3-K1-K1′	85.87(4)
P3-P4-P1	106.19(5)		83.95(4)

P4-P1-P5	60.42(4)	P2′-K1-K1′	51.37(3)
P2-K2-P3	72.22(4)	P1′-K1-K1′	49.55(3)
P3-K1-P2′	169.35(4)	P1-K1-K1′	100.24(6) to 117.95(6)
P3-K1-P1′	111.31(4)	P-Si-Si	105.76(6) to 111.55(6)
P2′-K1-P1′	64.12(3)	Si-Si-Si	

2.3.3.2 $Hyp_3P_8K_3{\cdot}4C_6H_6$ (5a)

An orange cubic-shaped single crystal of **5a** obtained from a benzene solution was investigated by X-ray diffraction analysis. The molecular structure is presented in Figure 2.14. One of the hypersilyl groups is disordered in the crystal (Figure 2.14b); however, the K_3P_8 skeleton is ordered and the structure determination gives well-defined structural parameters. Crystal data for **5a** are summarized in Table 2.13. Selected bond lengths and angles are listed in Table 2.14.

Table 2.13 Crystallographic data of **5a**.

Empirical formula	$Hyp_3P_8K_3{\cdot}$3benzene
Formula weight(g/mol)	1419.48
Temperature(K)	173(2)
Crystal system	triclinic
Space group	$P\bar{1}$
Lattice constants(Å,°)	a = 14.920(3) α 72.961(13)
	b = 16.401(3) β 77.152(12)
	c = 18.743(4) γ 80.088(12)
Volume(Å^3)	4247.2(14)
Formula units	2
Density(g/cm^3)	1.110
μ(Mo-K$_\alpha$)(mm^{-1})	0.509
2Θ range(°)	2.29 to 25.00
Reflections measured	15225
Independent reflections	14620 [R(int) = 0.0396]
Ind. Reflections with $F_o > 4\sigma(F_0)$	14620
Parameter	729
R1,R1(all reflections)	0.0411, 0.0835
wR2,wR2(all reflections)	0.0817, 0.0890
GooF	0.827
Residual electron density(e/Å^3)	0.597

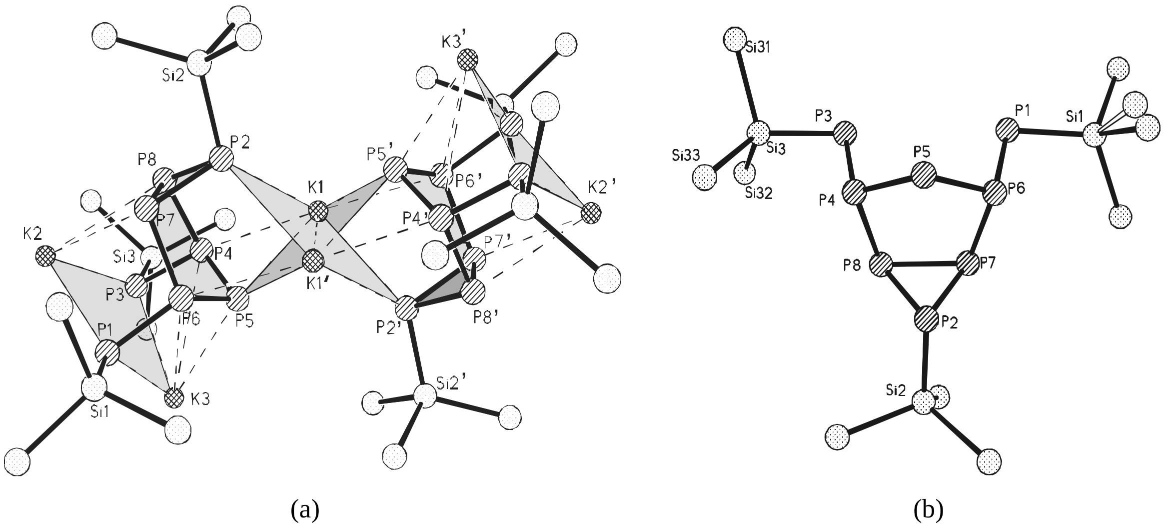

(a) (b)

Figure 2.14 Perspective drawing of **5a**; (a): $Si_{24}P_{16}K_6$ skeleton; (b): $Hyp_3P_8K_3$ skeleton. Atoms are represented by spheres of arbitrary radii; dashed lines are used to symbolize interatomic contacts of potassium and phosphorus atoms. Symmetry operation ($'$):-x, -y, -z

The Hyp_3P_8 moiety displays a boat-like puckered [3,1,0] bicyclohexaphosphane skeleton having local C_s symmetry. Two hypersilylphosphanyl groups (HypP) are located at the five-membered ring and a hypersilyl group at the three-membered ring (Figure 2.14b). Linked by a potassium dumbbell, two Hyp_3P_8 fragments form a C_2 symmetric coordination dimer as shown in Figure 2.14a.

The P-P bond lengths, ranging between 218.03(12) and 225.24(13) pm, are in the P-P single bond region and similar to those observed in **4a**. The formally negatively charged atoms P1, P3 and P5 display slightly shorter P-P distances (ranging from 218.03(12) to 220.33(12) pm). The two exocyclo-phosphorus atoms (P1 and P3) coordinate to two potassium atoms (K2, K3), forming a distorted K_2P_2 rhomboid with P-K-P and K-P-K bond angles of 81.7 and 96°, respectively. Apart from P1 and P3, the coordination environment of K2 is accomplished by two phosphorus atoms (P7, P8) and an η^6-bonded benzene molecule (average K···C distance: 333pm), while that of K3 is completed by other three phosphorus atoms (P4, P5 and P6) and another η^6-bonded benzene molecule (average K···C distance: 329pm). No benzene molecule is found to coordinate to both potassium atoms of the shared dumbbell; only a slight agostic-type interaction (K···C: 365pm) with hypersilyl group is found. The P-K distances, ranging from 317.42(13) to 382.58(14) pm with a shortest value observed for K3-P5 and the longest for P2-K1, are in regions observed previously for related compounds.

Table 2.14 Selected interatomic distances (pm) and angles (°) for **5a**.

P1-P6	220.33(12)	P7-P2-P8	60.92(4)
P2-P7	221.76(12)	P5-P4-P3	115.61(5)
P2-P8	222.57(12)	P5-P4-P8	103.15(5)
P3-P4	219.29(12)	P3-P4-P8	100.58(5)
P4-P5	218.03(12)	P5-P6-P1	114.54(5)
P4-P8	221.36(13)	P5-P6-P7	103.49(5)
P5-P6	218.42(13)	P1-P6-P7	102.05(5)
P6-P7	221.98(12)	P2-P7-P6	100.79(5)
P7-P8	225.24(13)	P2-P7-P8	59.72(4)
P1-K2	326.83(13)	P6-P7-P8	106.33(5)
P1-K3	328.50(14)	P4-P8-P2	103.37(5)
P2-K1′	351.15(13)	P4-P8-P7	106.09(5)
P3-K3	321.73(13)	P2-P8-P7	59.36(4)
P3-K2	322.91(13)	P7-P2-Si2	104.49(5)
P4-K3	371.74(13)	P4-P5-P6	106.27(5)
P5-K3	317.42(13)	P8-P2-Si2	102.09(5)
P5-K1′	320.22(12)	P4-P3-Si3	99.22(5)
P6-K1′	337.80(13)	P6-P1-Si1	96.10(5)
P6-K3	381.30(13)	P4-K1-P6′	167.90(3)
P7-K2	341.95(13)	P3-K2-P1	81.77(3)
P8-K2	353.06(13)	P3-K3-P1	81.69(3)
K1-P2	382.58(14)	K2-P1-K3	95.08(3)
K1-P4	323.23(12)	K3-P3-K2	97.18(3)
K1-P5	337.44(13)	K1′-P2-K1	69.26(3)
K1-K1′	417.75(17)	Si2-P2-K1	127.54(4)
K2-K3	483.46(13)	Si2-P2-K1′	133.35(4)
P1-Si1	225.18(13)	P3-P4-K1	154.97(5)
P2-Si2	229.69(12)	P1-P6-K1′	159.24(4)
P3-Si3	226.21(13)		
Si-Si	234.84(14) to 238.9(3)		
K-C	319.1(4) to 341.6(6)		

2.4 $\mathrm{Hyp_2P_4}$ (6), $\mathrm{Hyp_2P_4Li_2}$ (7), and $\mathrm{Hyp_2P_3Li}$ (8)

2.4.1 Synthesis

Replacing potassium for lithium, i.e. reacting base-free lithium hypersilanide with white phosphorus, dramatically changes the type of products obtained. Under the same conditions *i.e.* a toluene solution of lithium hypersilanide was added to a suspension of white phosphorus in toluene at room temperature, the colour of the solution turned from yellow to brown-red and a pale yellowish precipitate was formed gradually.

The ^{31}P-NMR spectrum of the filtrate of the reaction mixture, showing complicated resonances, indicated that $[(\mathrm{Me_3Si})_3\mathrm{Si}]_3\mathrm{P}_7$, bis(hypersilyl)tetraphosphane $[(\mathrm{Me_3Si})_3\mathrm{Si}]_2\mathrm{P}_4$(**6**), and some other phosphorus-containing compounds were formed in this reaction. Attempt to isolate some of them by crystallization failed. However, several light orange crystals were found in the NMR tube after standing for several months at ambient temperature. According to the X-ray diffraction analysis, these crystals represent the lithium salt:

$[(Me_3Si)_3Si]_3P_5Li_2 \cdot LiP(SiMe_3)Si(SiMe_3)_2Si(SiMe_3)_3$. Unfortunately, the reflection data were of low quality and gave no well-defined structural parameters.

The pale yellowish precipitate isolated by filtration is extremely air- and moisture-sensitive and ignites spontaneously on contact with air. In THF it is solable and give a violet solution. On cooling to -20°C for several days, violet crystals of dilithium bis(hypersilyl)tetraphosphenide $Hyp_2P_4Li_2 \cdot 4THF$ (**7a**) precipitated in low yield (based on P_4). In the solid state compound **7a** is air- and moisture-sensitive, but does not ignite spontaneously in air. In contrast to the potassium analogue, this compound is fairly stable in THF solution at room temperature under argon.

When the pale yellowish precipitate is dissolved in hexahydro-1,3,5-trimethyl-S-triazine, a violet-blue solution is obtained. The ^{31}P-NMR spectrum shows that, instead of the tetraphosphenide **7**, lithium bis(hypersilyl)triphosphenide Hyp_2P_3Li (**8**) is the dominant phosphorus-containing compound (Scheme 2.6).

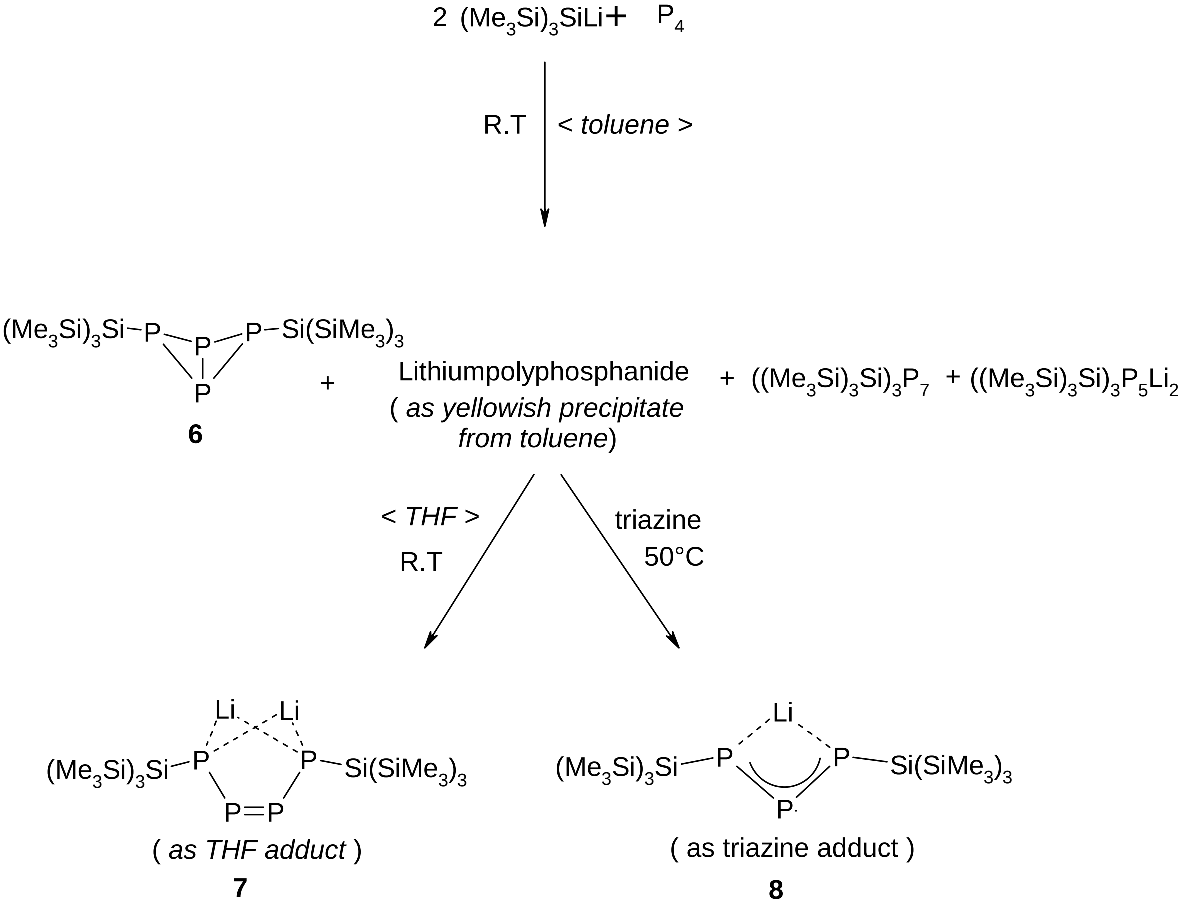

Scheme 2.6

In order to get X-ray diffraction analysis suitable crystals of compound **8**, base-free lithium hypersilanide was allowed to react with white phosphorus in toluene in the presence of hexahydro-1,3,5-trimethyl-S-triazine at room temperature. A violet-blue solution was obtained and no precipitate was found in the reaction mixture this time. The ^{31}P-NMR spectrum of the resulting reaction mixture showed a dominant resonance for lithium bis(hypersilyl)triphosphenide along with some resonances for small amounts of other phosphorus-containing compounds. On cooling to -20°C for several days, violet X-ray diffraction quality crystals of $Hyp_2P_3Li{\cdot}2(MeNCH_2)_3$ (**8a**) were obtained along with a considerable amount of colourless tetrakis(trimethylsilyl)silane crystals.

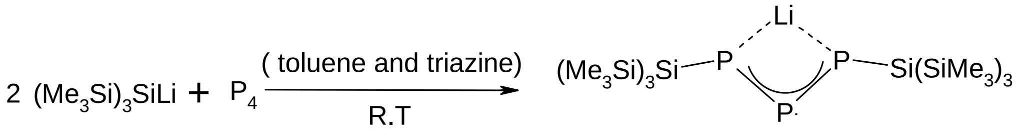

(as triazine adduct)

8

(Eq. 2.5)

The reaction of lithium hypersilanide with white phosphorus in THF under the same conditions was quite complicated. Along with compound **7**, several unknown phosphorus-containing compounds, showing mutually overlapping resonances in the ^{31}P-NMR spectrum, were formed in the resulting solution. In an attempt to isolate some of the products, the reaction mixture was stored at -30°C for several days. Surprisingly, quite large amounts of tetrakis[trimethyl(silyl)]silane precipitated. Obviously, cleavage of Si-Si within the hypersilyl group took place during the reaction process and resulted in the complexity of the reaction.

2.4.2 NMR Spectroscopy

2.4.2.1 $Hyp_2P_4Li_2$ (7)

Compound **7** is characterized by ^{31}P-NMR spectroscopy and a single-crystal X-ray diffraction study. Similar to compound **1**, the ^{31}P{H}-NMR spectrum of **7** exhibits two resonance signals at -45.8 and 398.1 ppm representing an AA'XX' spin system. In spite of the low resolution of the spectrum owing to the relatively poor solubility of $Hyp_2P_4Li_2{\cdot}4THF$ (**7a**) in THF, a simulation of the spectrum has been performed with sufficient accuracy. The simulated and experimental spectra are shown in Figure 2.15. The comparison of the chemical shifts and coupling constants of **7** with its analogues $[(Me_3C)_3Si]_2P_4Na_2$[101] and compound **1** has been shown in Table 2.1.

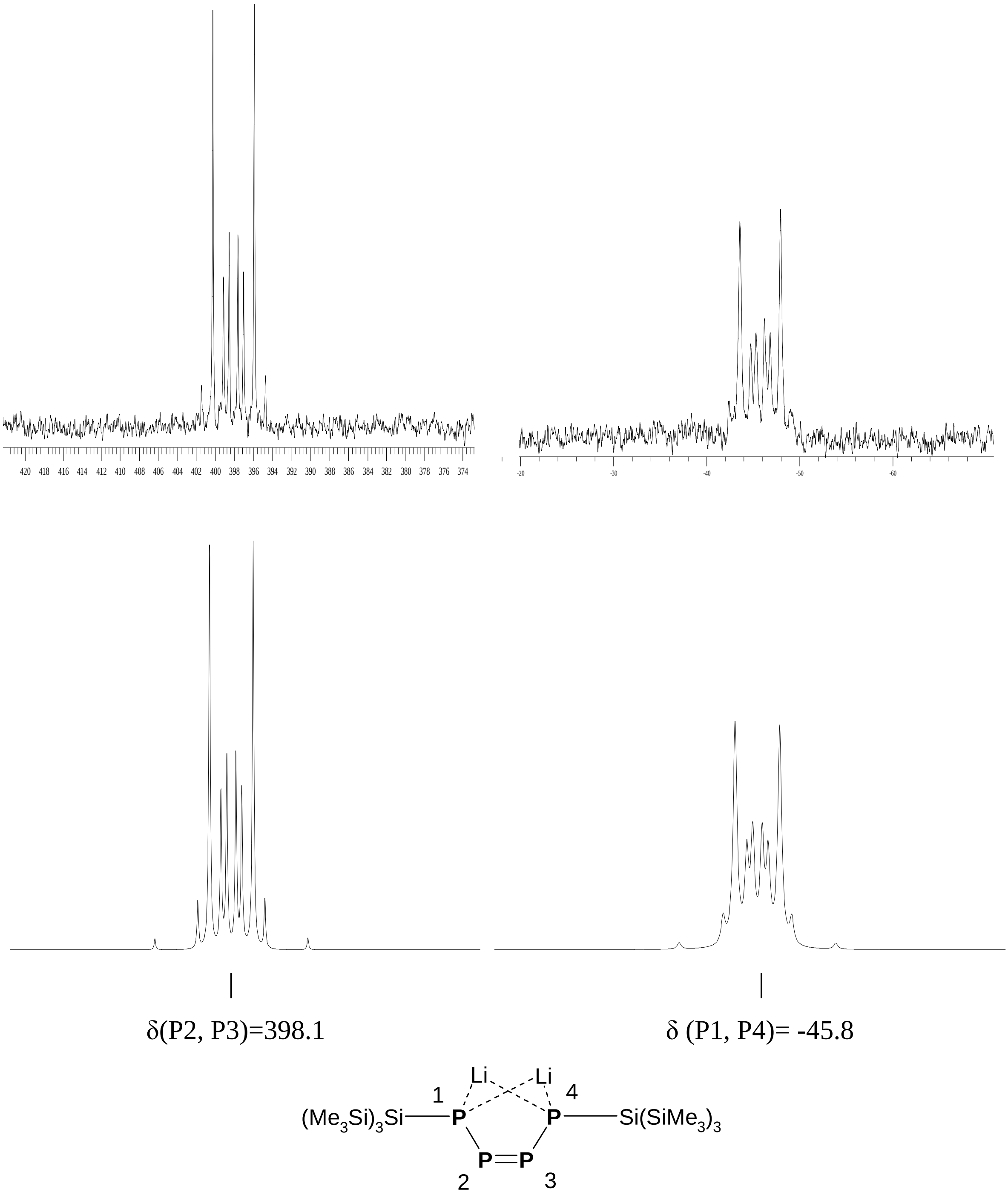

Figure 2.15 The ^{31}P{H}-NMR spectrum of **7** in THF-d8(300K) at 101.256MHz. δ (P1, P4)= -45.8ppm, δ(P2, P3)=398.1ppm. $^{3}J_{p1,p4}$=247.1Hz, $^{1}J_{p1,p2}$ = $^{1}J_{p3,p4}$ =-410.3Hz, $^{2}J_{p1,p3}$=$^{2}J_{p2,p4}$ =-31.5Hz, $^{1}J_{p2,p3}$=-481.0Hz.

2.4.2.2 Hyp$_2$P$_3$Li (8)

In the ^{31}P{H}-NMR spectrum of **8,** a doublet and a triplet of an AX$_2$ spin system are observed at δ=198.2 and 718.4 ppm with relative intensities of 2:1, respectively. The chemical shifts and the coupling constants of this compound as well as those of compound **3** and [(Me$_3$C)$_3$Si]$_2$P$_3$Na[100] are summarized in Table 2.15. With small differences, the chemical shifts of P2 of the three compounds are all in the typical range for the unsaturated two-coordinate phosphorus atom in diphosphene[121], whereas those of P1 and P3 are all in a range expected for unsaturated anionic phosphorus atoms[122 123]. The one-bond coupling constants of a range from 533 to 552.6Hz, without showing any additional coupling constant of $^2J_{P,P}$, suggest a trans-trans configuration of the anions as derived from the X-ray diffraction studies of $[(Me_3Si)_3Si]_2P_3Li$ (see blow) and $[(Me_3C)_3Si]_2P_3Na$[100]. The other isomeric anion with trans-cis configurations, which exists in $Mes^*{}_2P_3Li$ along with the trans-trans isomer[124], haven't been observed in the benzene-d6 solutions according to the ^{31}P-NMR spectroscopy. Presumably this is a consequence of the steric crowding of the supersilyl or hypersilyl groups in these compounds.

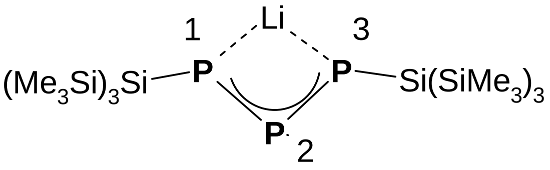

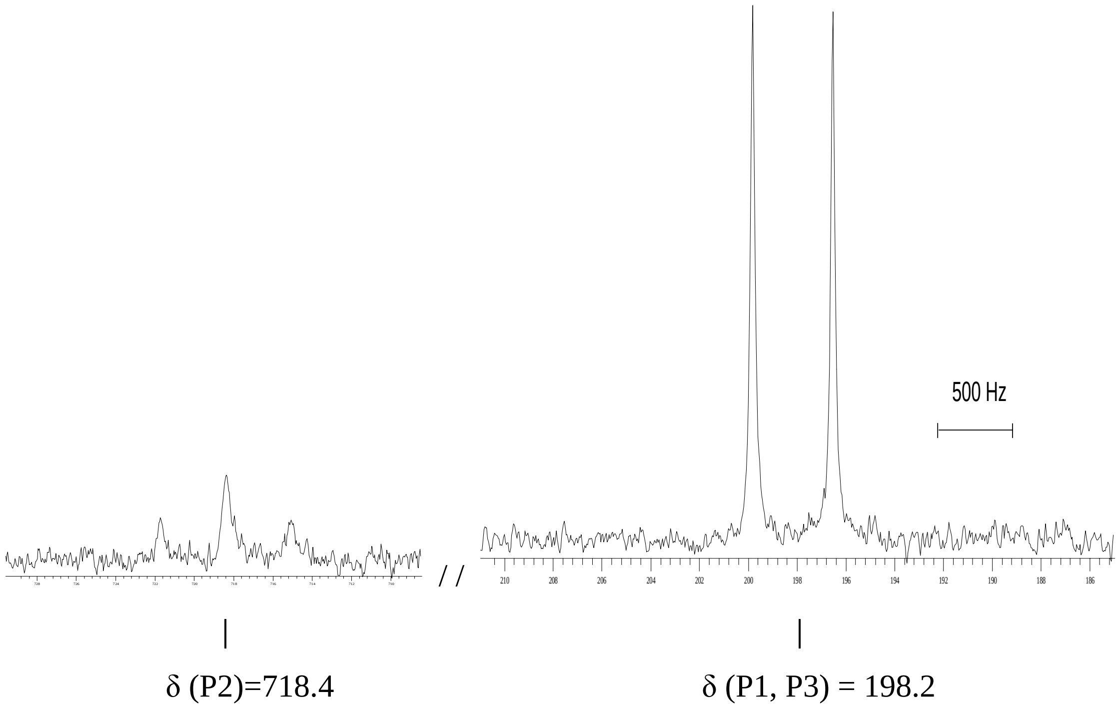

Figure 2.16 The ^{31}P{H}-NMR spectrum of **8** in benzene-d6(300K) at 161.976MHz. $^1J_{p1,p2}$= $^1J_{p2,p3}$ =533 Hz.

Table 2.15 Comparison of the ^{31}P-NMR(benzene-d6) chemical shifts and coupling constants of **8**, **3**, and $[(Me_3C)_3Si]_2P_3Na$[100].

	8 [a]	**3**	$[(Me_3C)_3Si]_2P_3Na$ [b]
δ (P1, P3) (ppm)	198.2	199.8	212.5
δ (P2) (ppm)	718.4	717.2	732.5
$^1J_{p,p}$ (Hz)	533	541	552.6

a: as hexahydro-1,3,5-trimethyl-s-triazin solvate ; b: as THF solvate

2.4.3 Crystal Structure

2.4.3.1 $Hyp_2P_4Li_2\cdot 4THF$ (7a)

After many unsuccessful attempts, a suitable crystal of **7a** could be found and was investigated by X-ray diffraction analysis. The crystal data are summarized in Table 2.16. Selected bond lengths and angles are listed in Table 2.17. Compound **7a** crystallizes in the monoclinic space group P2/c with two symmetry-independent molecules, one of which shows a statistical disordering of the phosphorus atoms. The discussion therefore concentrates on the well-ordered structural unit.

Table 2.16 Crystallographic data of **7a**.

Empirical formula	$Hyp_2P_4Li_2\cdot 4THF$
Formula weight(g/mol)	921.51
Temperature(K)	193(2)
Crystal system	monoclinic
Space group	P2/c
Lattice constants(Å,°)	a = 23.723(3) α 90 b = 9.9065(15) β 92.734(9) c = 24.352(3) γ 90
Volume($Å^3$)	5716.4
Formula units	4
Density(g/cm^3)	1.071
μ(Mo-K_α)(mm^{-1})	0.329
2Θ range(°)	2.06 to 26.54
Reflections measured	56355
Independent reflections	11688 [R(int) = 0.1100]
Ind. Reflections with $F_o > 4\sigma(F_0)$	11688
Parameter	571
R1,R1(all reflections)	0.0419, 0.1552
wR2,wR2(all reflections)	0.0936, 0.1303
GooF	0.650
Residual electron density(e/$Å^3$)	0.136

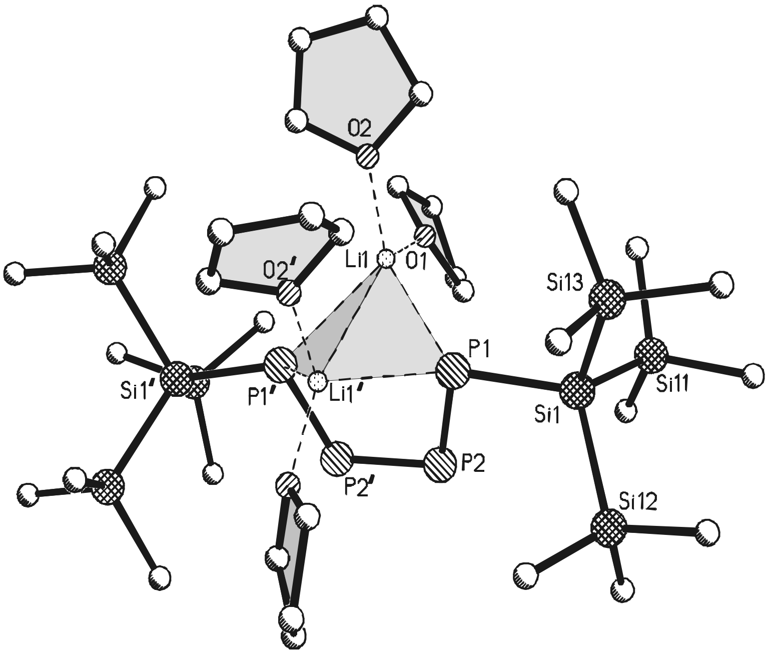

Figure 2.17 Molecular structure of **7a**; atoms are represented by spheres of arbitrary radii; dashed lines are used to symbolize interatomic distances markedly smaller than the sum of the corresponding van der Waals radii; hydrogen atoms are omitted for clarity. Symmetry operation (′):-x,y,-z+3/2

As shown in Figure 2.17, the anionic part of **7a** displays the same Hyp_2P_4 fragment as its potassium analogues, showing a cis-configurated P_4 skeleton with a hypersilyl group attached at each end of the phosphorus chain. In the molecule, each lithium atom is coordinated by two phosphorus and two oxygen atoms from THF, forming a tetrahedral coordination environment with an acute P-Li-P angle [P1-Li1-P1′ =79.25(19)°]. The distance between the two lithium atoms is found to be 349.8(15) pm and no additional short contact – *i.e.* agostic interactions with hypersilyl groups is observed. All of the lithium atoms and oxygen atoms lie in the σ_v mirror plane of the P_4 skeleton (Figure 2.18). Thus, the molecule exhibits a nearly undistorted C_{2v}-symmetric $Si_2P_4Li_2O_4$ framework.

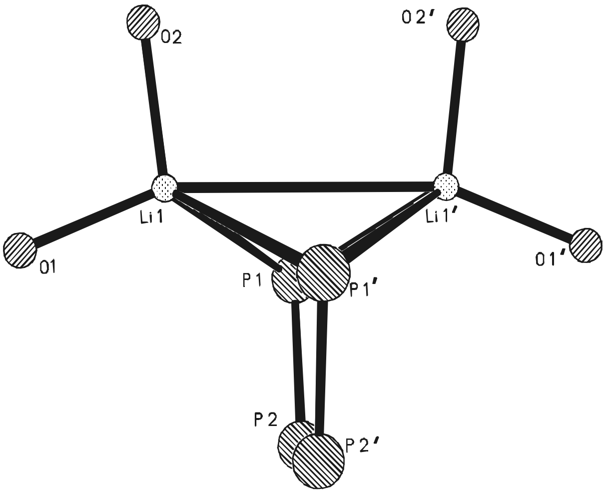

Figure 2.18 View of $P_4O_4Li_2$ skeleton of **7a**; atoms are represented by spheres of arbitrary radii.

As shown in Figure 2.18, unlike the benzene solvate of the potassium analogue, which exhibits an almost planar K_2P_2 ring (folding angle=3.2°), the Li_2P_2 ring is puckered. The Li atoms bent away from the P=P double bond with a folding angle of 61.3° between the planes defined by Li1- P1- P1′ and Li1′-P1- P1′. Thus, considerably long Li-P(2, 2’) distances (about 369pm) are observed, whereas the Li-P(1, 1’) contacts [262.0(7), 265.9(7)pm] lie in the expected Li-P range and close to the value of 262(2)pm found for Li-P in dimeric $Li(thf)_2P(SiMe_3)_2$[125].

As far as the P_4 skeleton is concerned, notable structural differences compound **7a** and **1a** are the less obtuse narrow P-P-P angle in **7a** (107.7 vs 109.5° on average, Table 2.18) and the shorter distance between P1 and P1’ (337.7 pm for **7a** vs 352.5 pm for **1a**). This is consistent with the different coupling between P1 and P1′. As shown in Table 2.1, the three-bond coupling constant of 247.1Hz for **7a** is considerable larger than that of 151.5Hz for **1a**.

Table 2.17 Selected interatomic distances (pm) and angles (°) of **7a**.

P1-P2	213.89(15)	Si1-P1-Li1	131.99(16)
P2-P2′	206.5(2)	P2-P1-Li1′	99.99(16)
P1-Si1	224.56(15)	Si1-P1-Li1′	135.56(17)
P1-Li1	262.0(7)	Li1-P1-Li1′	83.0(3)
P1-Li1′	265.9(7)	P1-Li1-P1′	79.25(19)
Li1-Li1′	349.8(15)	O1-Li1-O2	104.3(4)
O1-Li1	189.9(9)	O1-Li1-P1	117.1(3)
O2-Li1	193.2(7)	O1-Li1-P1′	119.0(4)
Si2-P3	225.05(15)	O2-Li1-P1′	117.5(3)
Si1-Si11	233.92(15)	O2-Li1-P1	119.3(4)
Si1-Si13	234.73(15)	P1-Si1-Si11	112.84(6)
Si1-Si12	235.13(15)	P1-Si1-Si12	113.83(6)
P2′-P2-P1	107.72(4)	P1-Si1-Si13	104.59(6)
P2-P1-Si1	98.62(6)	Si11-Si1-Si13	108.66(6)
P2-P1-Li1	100.74(17)	Si11-Si1-Si12	109.79(6)
		Si13-Si1-Si12	106.69(6)

Table 2.18 Comparison of selected interatomic distances (pm) for **7a** and **1.**

Compound		**7a**	**1a**	**1b**	**1c**
P1-P1′	(av. pm)	337.7	352.5	349.1	350.1
P1-P2-P2′	(av. deg)	107.7	109.5	109.2	109.7
Folding angle(K-P-P-K) or (Li-P-P-Li)	(av. deg)	61.3	3.2	8.3	11.6

2.4.3.2 $Hyp_2P_3Li\cdot 2(MeNCH_2)_3$

Violet single crystals of the triazine solvate **8a** were obtained from toluene in the presence of triazine at -30°C and investigated by X-ray diffraction analysis. The crystal data are summarized in Table 2.19. Selected bond lengths and angles are listed in Table 2.20.

Table 2.19: Crystallographic data of **8a**.

Empirical formula	Hyp$_2$P$_3$Li·3triazine(toluene)
Formula weight(g/mol)	945.74
Temperature(K)	173(2)
Crystal system	monoclinic
Space group	P2(1)/n
Lattice constants(Å,°)	a = 15.3307(10) α 90
	b = 16.4357(10) β 98.311(3)
	c = 24.0715(15) γ 90
Volume(Å^3)	6001.6(7)
Formula units	4
Density(g/cm^3)	1.047
μ(Mo-K$_\alpha$)(mm^{-1})	0.287
2Θ range(°)	2.37 to 28.46
Reflections measured	106062
Independent reflections	14990 [R(int) = 0.0983]
Ind. Reflections with $F_o > 4\sigma(F_0)$	14990
Parameter	596
R1,R1(all reflections)	0.0459, 0.1065
wR2,wR2(all reflections)	0.1004, 0.1243
GooF	1.006
Residual electron density(e/Å^3)	0.363

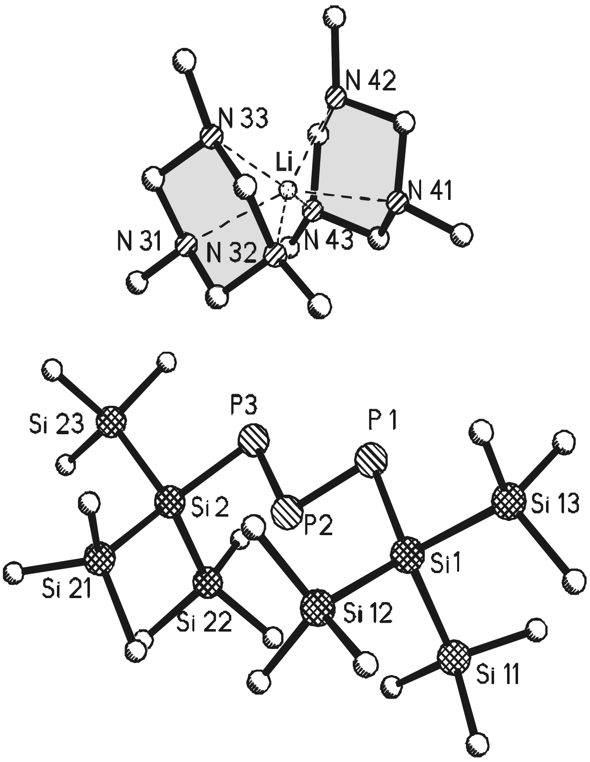

Figure 2.19 Structure of **8a**; atoms are represented by spheres of arbitrary radii; dashed lines are used to symbolize interatomic distances markedly smaller than the sum of the corresponding van der Waals radii; hydrogen atoms are omitted for clarity.

As shown in Figure 2.19, the structure of **8a** exhibits a salt composed of solvated Li^+ cations $[Li(N,N',N''\text{-trimethyltriazinane})_2]^+$ and $[Hyp_2P_3]^-$ anions. No unusually short Li-P contacts are observed from the complex cation to the corresponding anion. The structure of the anion displays a nearly undistorted C_{2v}-symmetric W-shape Si_2P_3 skeleton with two similar P-P bond lengths [P1-P2= 207.74(8), P2-P3= 207.30(8) pm]. Analogous to $[(Me_3C)_3Si]_2P_3Na(THF)_4$ (av 210pm) [100], these P-P distances lie in between those for P-P single (about 220pm) and P=P double bonds (about 200pm)[91 126 127 107], suggesting that both P-P bonds have partial double-bond character (Scheme 2.7). The P-P-P angle of 105.52(3)° is close to those found in $[(Me_3C)_3Si]_2P_3Na(THF)_4$ [ranging between 101.3(7) and 106.6(9)°][100]. The P-Si bond lengths with a value of 224.59(9)pm are comparable to those found in $Hyp_2P_4Li_2$ [225.05(15)pm].

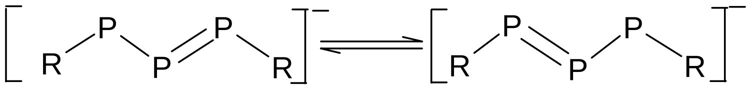

$R = Si(SiMe_3)_3$

Scheme 2.7

As shown in Figure 2.20, the lithium cation in $[Li(N,N',N''\text{-trimethyltriazinane})_2]^+$ is coordinated to two $(MeNCH_2)_3$ molecules, which are eclipsed with respect to each other with only slight distortion (torsion angel: C413-N43-N31-C311=-6.7°), forming a sandwich structure. The Li-N distances ranging between 215.3(4) and 234.0(4)pm are comparable to those found for the same cation in $[(\mu\text{-}NO_3\text{-}O,O')R_2AlCH_2AlR_2]^-$ $[Li(N,N',N''\text{-trimethyltriazinane})_2]^+$ (between 215.7 and 234.0pm) [128], in which the two triazine molecules are staggered with respect to each other.

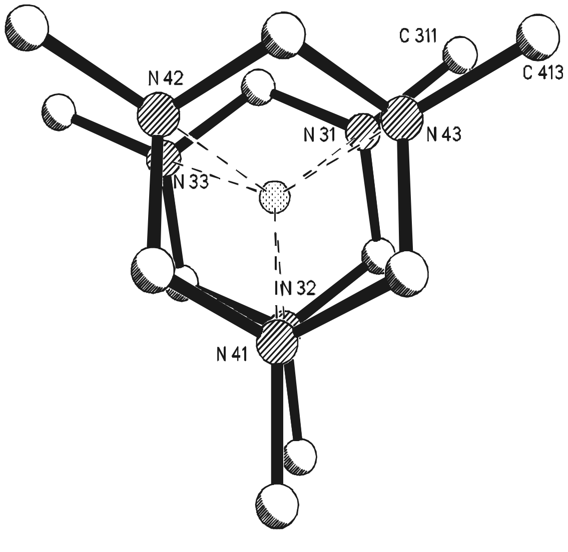

Figure 2.20 Structure of $[Li((MeNCH_2)_3)_2]^+$ cation in solid state of **8a**; atoms are represented by spheres of arbitrary radii; dashed lines are used to symbolize interatomic distances markedly smaller than the sum of the corresponding van der Waals radii; hydrogen atoms are omitted for clarity.

Table 2.20: Selected interatomic distances (pm) and angles (°) for **8a**.

P2-P3	207.30(8)	P3-P2-P1	105.52(3)
P2-P1	207.74(8)	P2-P3-Si2	100.20(3)
Si13-Si1	235.09(9)	P2-P1-Si1	99.10(3)
P3-Si2	224.59(8)	P1-Si1-Si11	112.82(3)
P1-Si1	224.54(9)	P1-Si1-Si12	116.39(4)
Si-Si	233.85(10) to 234.46(10)	P1-Si1-Si13	104.46(3)
N-Li	215.3(4) to 234.0(4)	P3-Si2-Si21	112.76(3)
C-Li	261.7(5) to 275.2(5)	P3-Si2-Si22	111.68(3)
Li·····P1	505.9	P3-Si2-Si23	105.65(3)
Li·····P2	588.9	Si21-Si2-Si23	106.79(4) to 110.01(3)
Li·····P3	525.0		

2.5 $Hyp_3P_5Na_2$ (9)

2.5.1 Synthesis

The reaction of white phosphorus with base-free sodium hypersilanide in toluene again strongly differs from those with potassium and lithium hypersilanide under the same reaction conditions. In this reaction, no tetraphosphenide $Hyp_2P_4Na_2$ was found in the resulting reaction mixture according to ^{31}P-NMR spectroscopy. Instead, $Hyp_3P_5Na_2$ (**9**) could be evidently identified among the complicated products from a ^{31}P NMR spectrum. After exchanging the solvent to n-pentane and storing the extract at -20°C for several weeks, a small amount of compound **9** was isolated as well-shaped yellow crystals (Eq.2.6).

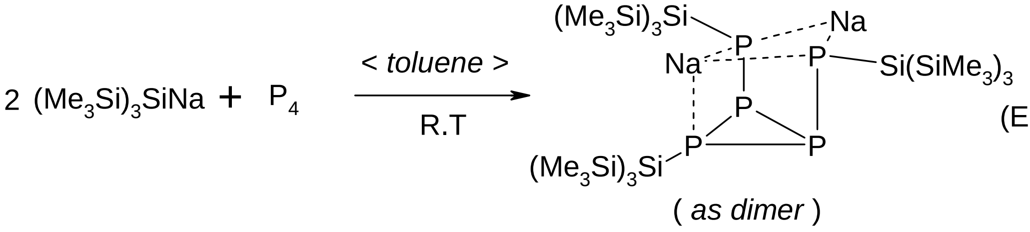

(Eq. 2.6)

9

Compound $Hyp_3P_5Na_2$ is fairly stable in n-pentane or benzene at room temperature and the C_6D_6 solution in a NMR tube can be stored more than six months without decomposition. However, it is sensitive towards air and moisture even in the solid state.

2.5.2 NMR Spectroscopy

The ^{1}H- and 13C{H}-NMR spectra of **9** recorded in benzene-d6 or THF-d8 show two singlets for the two kinds of hypersilyl groups with relative intensities of 2:1. In the ^{31}P{H}-NMR spectrum recorded in THF-d8 solution, three multiplets representing an AA'MM'X spin system are observed at -94.4, -193.4, and -249.1ppm with an integral ratio of 2:1:2. The spectrum can be solved by iterative fitting [110], starting from the values of compound **4.** The experimental and simulated spectra are presented in Figure 2.20.

In this spectrum, the signal of P-4 and P-5 are relatively broad, similar to the resonances observed for supersilyl analogue $[(Me_3C)_3Si]_3P_5Na_2$ [102] but differing from that of its potassium analogue **4**, presumably owing to the quadrupolar moment broadening caused by sodium. The chemical shifts and coupling constants, along with those of its analogues, are summarized in Table 2.9 and have been compared previously.

The ^{29}Si{H}-NMR spectrum of **9** (Figure 2.21), similar to that of the potassium analogue **4**, exhibits two broad resonance signals with different intensities at -9.6 and -11.7ppm for the peripheral silicon of the two kinds of hypersilyl groups, consistent with the ^{1}H- and ^{13}C{H}-NMR spectra, each of which displays two singlets, respectively. In addition, two less intense signals at -87.9 and -92.7ppm are found for the two types of central silicon atoms. The former, which is less intense than the latter and may be assignable to Si-3, is a broad doublet with a coupling constant of 113.8Hz split by P-3. The accuracy is reduced to about ±5Hz by peak broadening due to the long-rang coupling with other ^{31}P atoms within the molecule. The latter signal for Si-1 and Si-2 is a multiplet exhibiting the X part of the classical splitting pattern of an AA'MM'RX spin system similar to that observed for compound **4**. A simulation using the parameters calculated for **4** as a starting point was performed and the spectrum could be solved by iterative fitting (Figure 2.21)[110]. In Table 2.21, the final chemical shifts and coupling constants are compared with those of **4** and $[(Me_3C)_3Si]_3P_5Na_2$ [102].

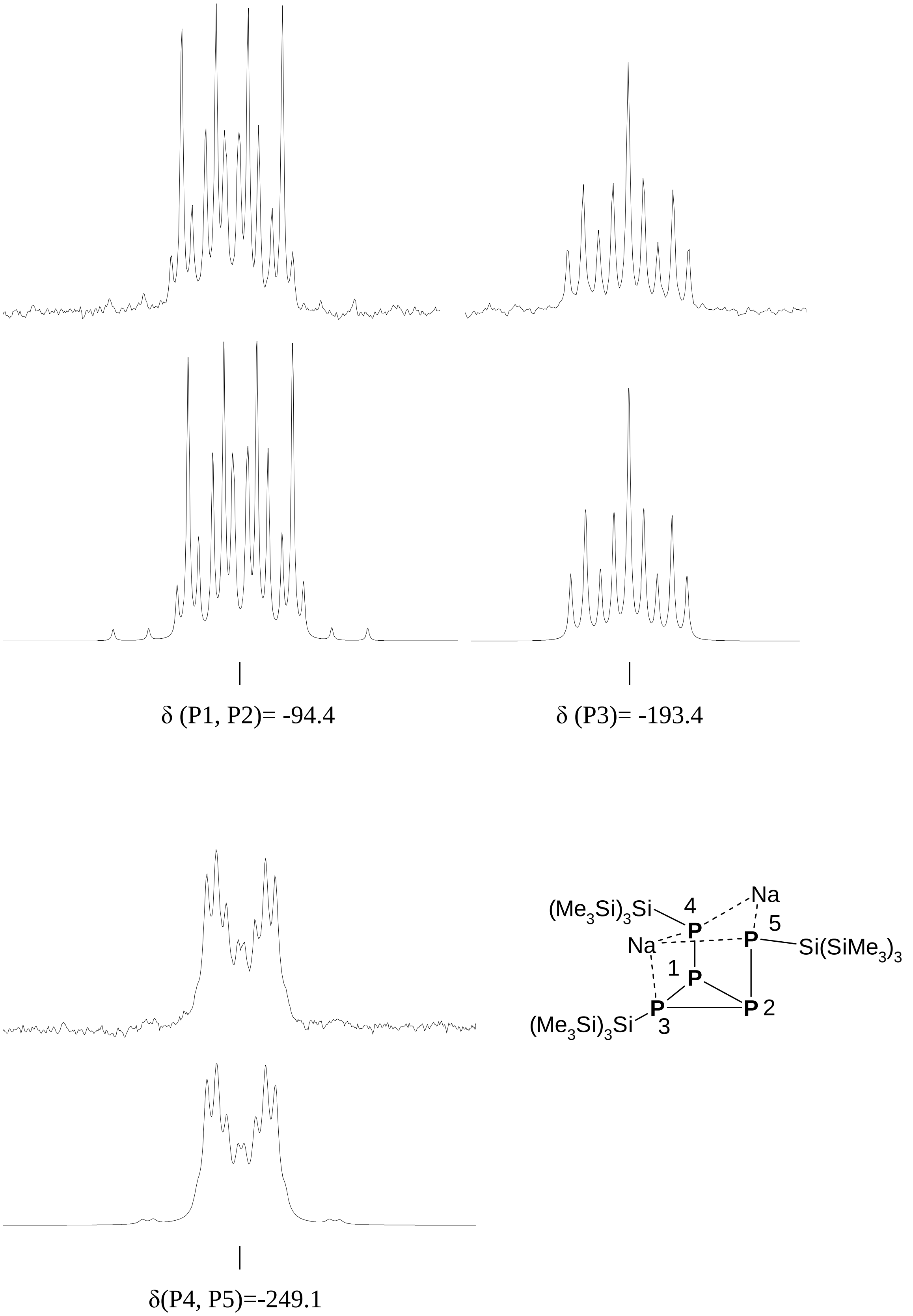

Figure 2.20 The ^{31}P{H}-NMR spectrum of **9** in THF-d8(300K) at 161.976MHz. δ (P1, P2)= -94.4, δ(P4, P5)=-249.1 . δ (P3)= -193.4. $^1J_{p1,p4}$=$^1J_{p2,p5}$= -336.6Hz, $^2J_{p3,p4}$ = $^2J_{p3,p5}$ =61.4Hz, $^1J_{p1,p3}$=$^1J_{p2,p3}$ =-178.8Hz, $^2J_{p1,p5}$=$^2J_{p2,p4}$ =-7.3Hz, $^1J_{p1,p2}$=-195.3Hz, $^3J_{p4,p5}$ =302.9Hz. The signs of the coupling constants except for $^2J_{p3,p4}$and $^2J_{p3,p5}$ originate from the iteration under setting $^1J_{P,P}$ as a negative value[129].

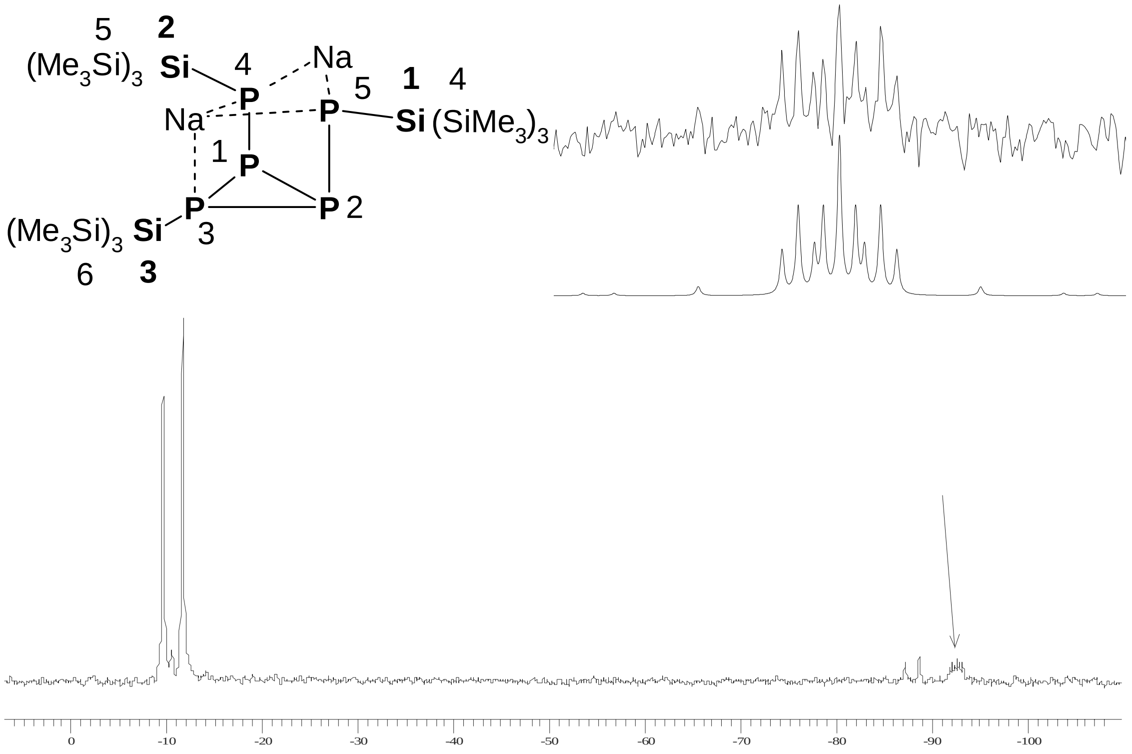

Figure 2.21 The ^{29}Si{H}-DEPT-NMR spectrum of **9** in THF-d8(300K) at 79.495MHz. δ (Si1, Si2)= -92.7, δ(Si3)=-87.9. δ (Si4,Si5)= -11.7, δ(Si6)=-9.6 ppm. $^{1}J_{P3,Si3}$=-113.8Hz, $^{1}J_{P4,Si2}$=$^{1}J_{P5,Si1}$=-98.8Hz, $^{2}J_{P1,Si2}$=$^{2}J_{P2,Si1}$=-18.4Hz, $^{3}J_{P3,Si2}$=$^{3}J_{P1,Si1}$=-14.3Hz, $^{4}J_{P5,Si2}$=$^{4}J_{P4,Si1}$=15.6Hz. The signs of the coupling constants concerned Si1 and Si2 originate from the iteration under setting $^{1}J_{P,Si}$ and $^{2}J_{P,Si}$ as negative values[129].

Table 2.21. The ^{29}Si-NMR(THF-d8, 300K) chemical shifts and some coupling constants of **4**, **9**, and $[(Me_3C)_3Si]_3P_5Na_2$[102].

Compound	**4**	**9**	$[(Me_3C)_3Si]_3P_5Na_2$
δ (Si1, Si2) (ppm)	-91.8	-92.7	31.3
δ (Si3) (ppm)	-90.1	-87.9	18.0
$^{1}J_{p3,Si3}$ (Hz)	-116.3	-113.8	-106.9
$^{1}J_{p4,Si2}$, $^{1}J_{p5,Si1}$(Hz)	-106.8	-98.8	-90.8
$^{2}J_{p1,Si2}$, $^{2}J_{p2,Si1}$(Hz)	-21.4	-18.4	-15.6
$^{3}J_{p3,Si2}$, $^{3}J_{p1,Si1}$(Hz)	-17.3	-14.3	-2.1
$^{4}J_{p5,Si2}$, $^{4}J_{p4,Si1}$(Hz)	7.6	15.6	21.4

The chemical shifts of the central silicon of the two hypersilyl derivatives **4** and **9** are almost identical. They differ considerably from those of the supersilyl compound, indicating the significant influence of peripheral trimethylsilyl and *tert*-butyl groups, respectively. The phosphorus-silicon coupling constants in these three compounds, however, are comparable to one another. A closer inspection of the coupling constants in Table 2.21 reveals that all the values for **9** lie in between those of **4** and $[(Me_3C)_3Si]_3P_5Na_2$[102]. Obviously, the small deviation of **9** from **4** is derived from the replacement of sodium for the more electropositive potassium atoms, while the difference between **9** and $[(Me_3C)_3Si]_3P_5Na_2$ is caused by the replacement of the peripheral silicon for the more electronegative carbon atoms.

2.5.3 Crystal Structure

Compound **9** was obtained as yellowish well shaped single crystals from n-pentane. As shown by X-ray diffraction analysis (Figure 2.22), **9** crystallizes as a coordination dimer, again linked by a dumbbell of two sodium cations as its potassium analogue described above. Pentane molecules cocrystallize as free molecules along with compound **9**. Some of the hypersilyl groups are disordered in the crystal and the structure determination gave only moderate-defined structural parameters. Crystal data for **9** are summarized in Table 2.22.

Table 2.22 Crystallographic data of **9**.

Empirical formula	$Hyp_3P_5Na_2 \cdot 1/3C_5H_{12}$
Formula weight(g/mol)	967.88
Temperature(K)	193(2)
Crystal system	monoclinic
Space group	P2(1)/n
Lattice constants(Å,°)	a = 45.543(2) α 90
	b = 25.3055(9) β 106.608(3)
	c = 48.6244(19) γ 90
Volume(Å^3)	53701(4)
Formula units	36
Density(g/cm^3)	1.077
μ(Mo-K$_\alpha$)(mm^{-1})	0.48
2Θ range(°)	1.56 to 21.00
Reflections measured	55236
Independent reflections	55236 [R(int) = 0.0000]
Ind. Reflections with $F_o > 4\sigma(F_0)$	55236
Parameter	3925
R1,R1(all reflections)	0.0722, 0.1679
wR2,wR2(all reflections)	0.1602, 0.1830
GooF	0.688
Residual electron density(e/Å^3)	0.753

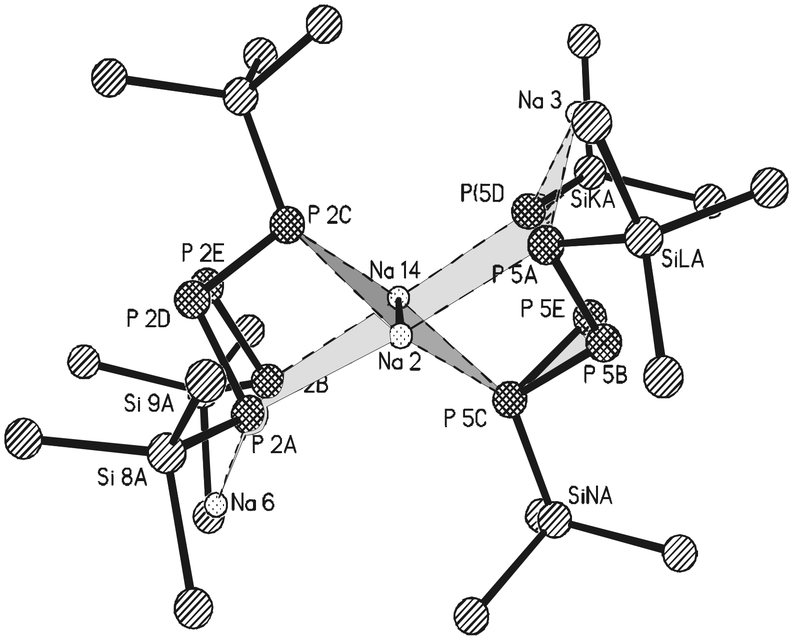

Figure 2.22 Perspective drawing of **9**; atoms are represented by spheres of arbitrary radii; dashed lines are used to symbolize interatomic distances between potassium and phosphorus atoms; methyl groups are omitted for clarity.

As shown in Figure 2.23, strong agostic-type interactions are found between Na2 and hypersilyl groups(Na···C: 288pm), whereas no significant agostic interaction is found for the bridging sodium Na1. The parameters of the P_5 skeleton in **9** are comparable to those observed for **4a**, but differ from those of its sodium supersilyl analogue. The selected bond lengths and angles are summarized in Table 2.23 and compared with its potassium analogue **4a** and a supersilyl derivative in Table 2.24. The angles P3-P4-P5 and P2-P5-P4 of 111.13°, for instance, are about 6° larger than those found in $[(Me_3C)_3Si]_3P_5Na_2(THF)_4$ and the distance between Na2 and P(2,3) of 275.8pm (mean value) is considerably shorter than the corresponding values found in $[(Me_3C)_3Si]_3P_5Na_2(THF)_4$ [287.8(5) , 282.6(5)pm], although, the P1-Na1 distance of 314.9pm (mean value) in **9** lies close to that observed in $[(Me_3C)_3Si]_3P_5Na_2(THF)_4$ [316.7(5)pm] [102]. The differences between the two sodium species are probably not only because of the different substituents, but also due to the solvent. In $[(Me_3C)_3Si]_3P_5Na_2(THF)_4$, THF molecules strongly coordinate to the Na atoms, thus leading to a monomers in the solid state.

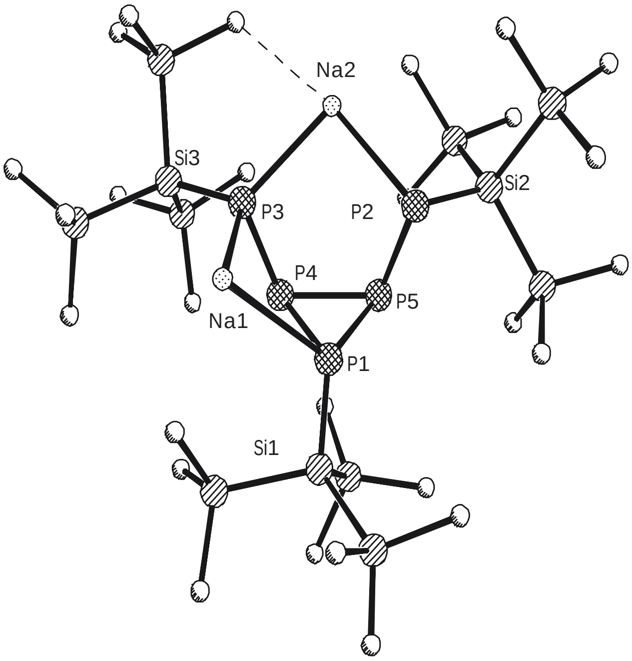

Figure 2.23 Perspective drawing of $Hyp_3P_5Na_2$ unit in the solid state of **9** with the numbering referring to that of compound **3a** depicted above; atoms are represented by spheres of arbitrary radii; dashed lines are used to symbolize interatomic distances markedly smaller than the sum of the corresponding van der Waals radii; hydrogen atoms are omitted for clarity.

Table 2.23 Selected interatomic distances (pm) and angles (°) for **9**[*].

P1-P4, P1-P5	av. 222.9	Na1-P1	av. 314.9
P3-P4, P2-P5	av. 218.1	Na1-P3	av. 283.4
P4-P5	av. 225.3	Na2-P2,P3	av. 275.8
P2-Si2,P3-Si3	av. 225.3	P2-P5-P1,P3-P4-P1	av.105.09
P1-Si	av. 227.6	P4-P4-P5,P2-P5-P4	av.111.13
Si-Si	av. 234.6	P5-P2-Si2,P4-P3-Si3	av. 98.15
Na1-Na1′ **	av. 385.7	P5-P1-Si1,P4-P1-Si1	av. 103.75

[*] The numbering is shown is Figure 2.23. ** Na1′ : the other bridging Na atom within the dimer molecule.

Table 2.24 Comparison of selected interatomic distances (pm) and angles (°) of **9**, **4a** and $[(Me_3C)_3Si]_3P_5Na_2$[102].

Compound	**4a**	**9**	$[(Me_3C)_3Si]_3P_5Na_2$
P1-P4, P1-P5	223.72	av. 222.9	224.3
P3-P4, P2-P5	217.40	av. 218.1	218.1
P4-P5	225.15	av. 225.3	224.4
P2-Si2,P3-Si3	224.54	av. 225.3	223.6
P1-Si	227.08	av. 227.6	230.7
P2-P5-P1,P3-P4-P1	105.48	av.105.09	106.8
P3-P4-P5,P2-P5-P4	110.46	av.111.13	106.0
P5-P2-Si2,P4-P3-Si3	97.05	av. 98.15	107.1
P5-P1-Si1,P4-P1-Si1	104.25	av. 103.75	109.9

2.6 *Hyp$_3$P$_4$SnK (10) and [(Me$_3$Si)$_2$N] Hyp$_2$P$_4$SnK (11)*

2.6.1 Synthesis of Hyp$_3$P$_4$SnK

The treatment of $[(Me_3Si)_3Si]_2P_4K_2$ with bis[bis(trimethylsilyl)amino]stannylene in toluene at room temperature, accompanied by a colour change from deep red to orange, leads to the formation of the unexpected compounds $[(Me_3Si)_3Si]_3P_4SnK$ (**10**) and $[(Me_3Si)_3Si]_2[(Me_3Si)_2N]P_4SnK$ (**11**) instead of $[(Me_3Si)_3Si]_2P_4Sn$, which is expected from a simple metathesis reaction .

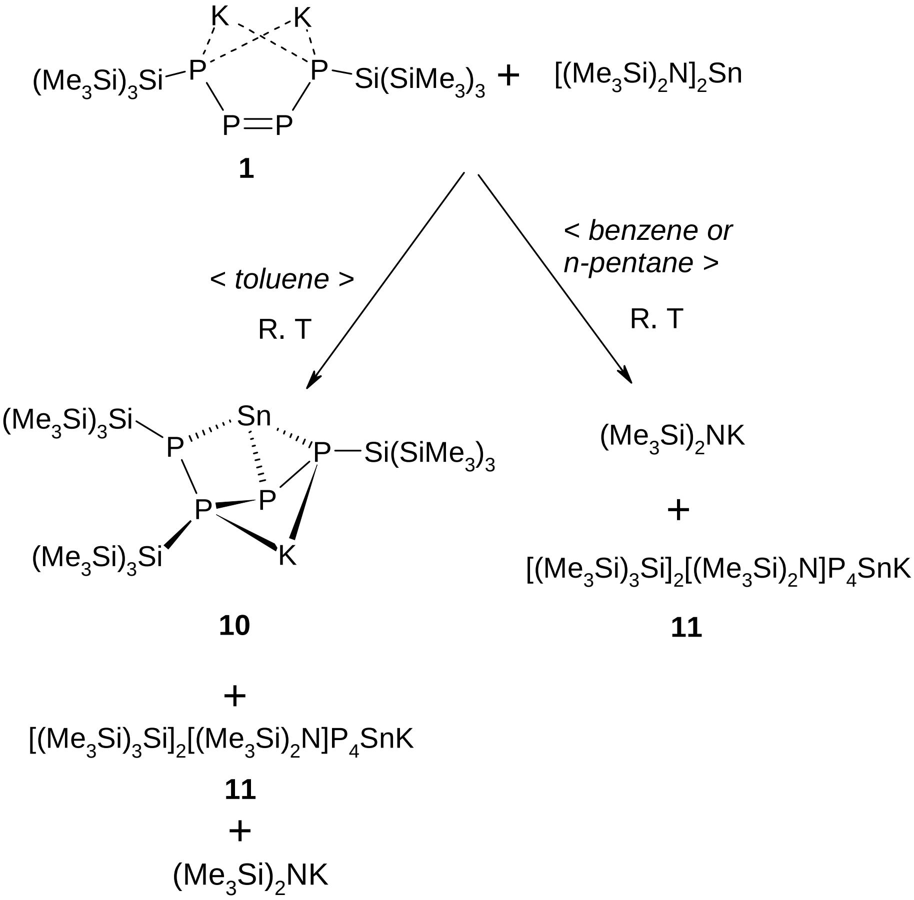

Scheme 2.6

Compound **10** was isolated as orange crystals and was characterized by NMR spectroscopy and X-ray crystallography. The other product, $[(Me_3Si)_3Si]_2[(Me_3Si)_2N]P_4SnK$ (**11**) , which has a similar solubility as the by-product $(Me_3Si)_2NK$ in the resulting mixture solution, has not been isolated as pure substance. However, from its ^{31}P-NMR spectrum a four phosphorus skeleton similar to that of compound **10** could be concluded. The satellites of ^{119}Sn and ^{117}Sn in the ^{31}P-NMR spectrum imply the existence of Sn atoms in this compound. Three signals observed in the ^{1}H-NMR spectrum with a intensity ratio of 27:27:18 indicate that two hypersilyl groups and a bis(trimethylsilyl)amino group may be included in this compound. Unfortunately, the molecular structure remains unknown.

The same reactants were allowed to react in benzene and n-pentane respectively, both giving only compound **11** and $(Me_3Si)_2NK$ as main products. But again the compound **11** has not yet been isolated in its pure state.

In these reactions the expected metathesis product Hyp_2P_4Sn, which is putatively formed primarily, could neither be isolated nor detected spectroscopically. Once formed it immediately undergoes an addition reaction with the other product $(Me_3Si)_2NK$ to form compound **11** (Scheme 2.7). In the presence of potassium hypersilanide, presumably formed according to Eq. 2.7, compound **10** is obtained.

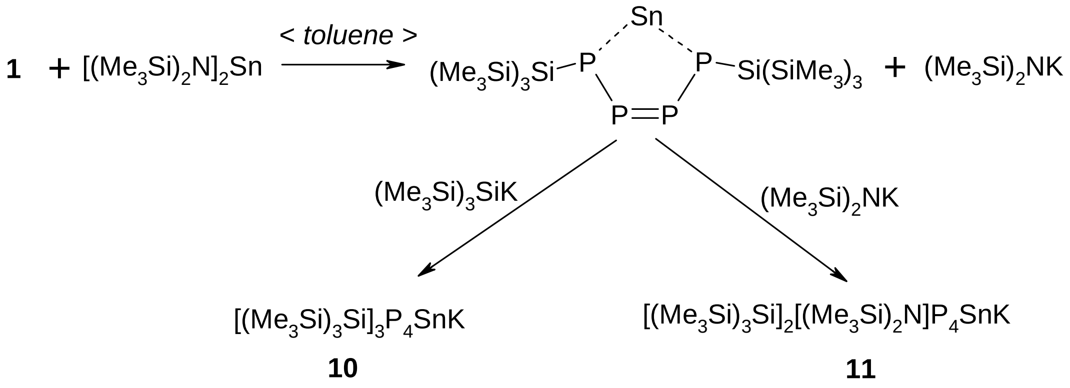

Scheme 2.7

$$2\,[(Me_3Si)_3Si]_2P_4K_2 \rightleftharpoons [(Me_3Si)_3Si]_4P_8K_4 \longrightarrow [(Me_3Si)_3Si]_3P_8K_3 + (Me_3Si)_3SiK \quad \text{(Eq. 2.7)}$$

1 **2** **4**

2.6.2 NMR Spectroscopy

2.6.2.1 Hyp_3P_4SnK (10)

The $^{31}P\{H\}$-NMR spectrum of **10** displays four multiplets at -58.5, -192.4, -231.3, and -256.1ppm with the same intensity and can be understood according to a first-order interpretation (Figure 2.24). The ^{119}Sn and ^{117}Sn satellites are found in signals of P-1, P-3 and P-4. Three inequivalent hypersilyl groups are observed in the ^{1}H- and $^{13}C\{H\}$-NMR spectra with the same intensity, respectively. This resonance information suggests a molecule with low symmetry, which is confirmed later by X-ray diffraction studies.

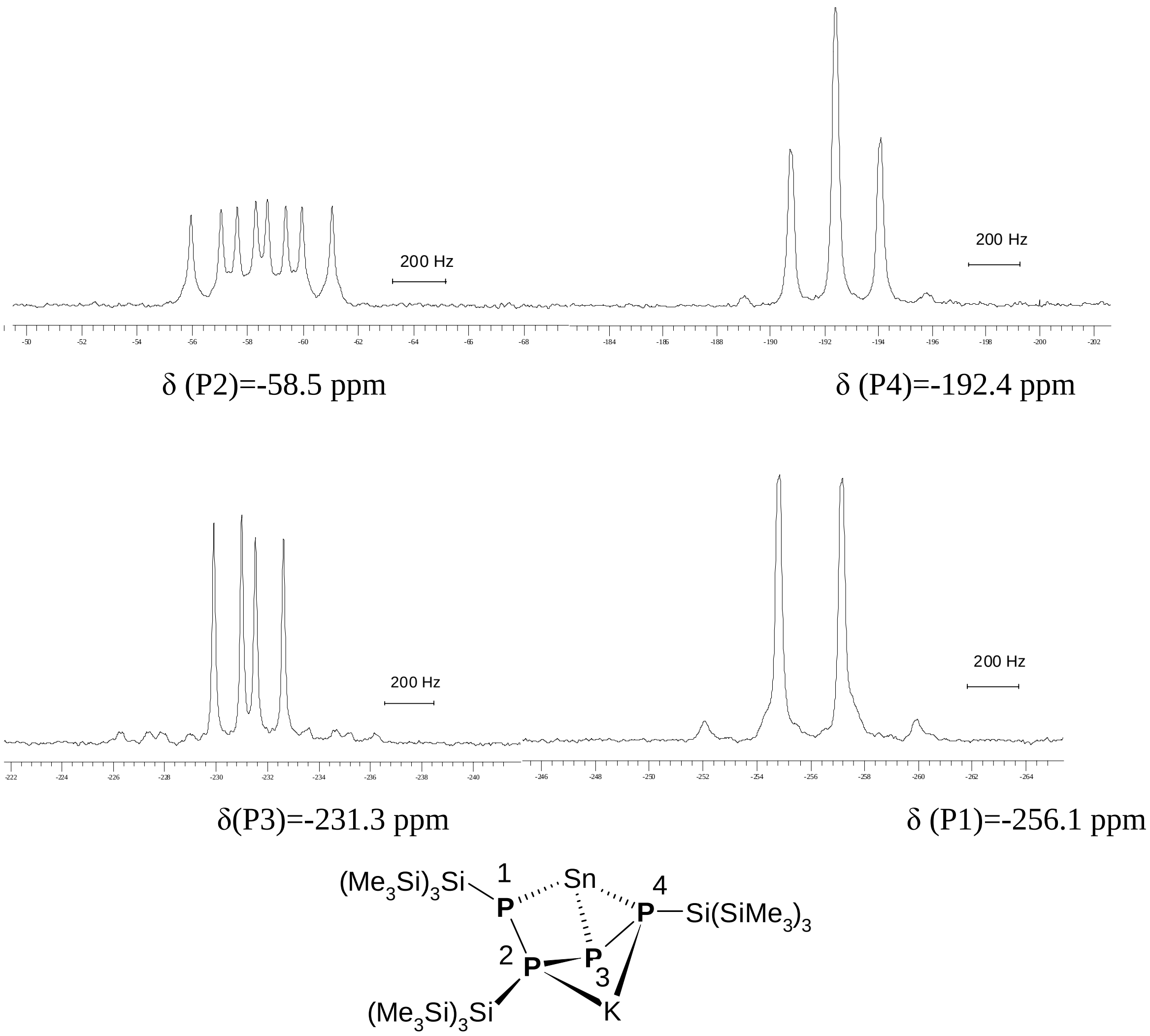

Figure 2.24 The ^{31}P{H}-NMR spectrum of **10** in benzene-d6(300K) at 101.256MHz. δ (P1)=-256.1, δ (P2)=-58.5, δ(P3)=-231.3, δ (P4)=-192.4ppm. $^{1}J_{p1,p2}$=-239Hz, $^{3}J_{p1,p4}$= -11Hz, $^{1}J_{p2,p3}$ =-109Hz, $^{2}J_{p2,p4}$ =-169Hz, $^{1}J_{p3,p4}$=-163Hz.

2.6.2.2 Hyp$_2$[(Me$_3$Si)$_2$N]P$_4$SnK (11)

The ^{31}P{H}-NMR spectrum of **11** exhibits four multiplets with the same intensity at -211.0, -128.2, -234.4, and -184.6 ppm, which are comparable to those of compound **10**. This spectrum can be solved as a first-order spectrum and the resulting coupling constants are shown in Figure 2.25. With a closer inspection of this spectrum, ^{119}Sn and ^{117}Sn satellites are found in the signals arising from P-1 and P-4, indicating that at least one tin atom coordinates with phosphorus in this compound.

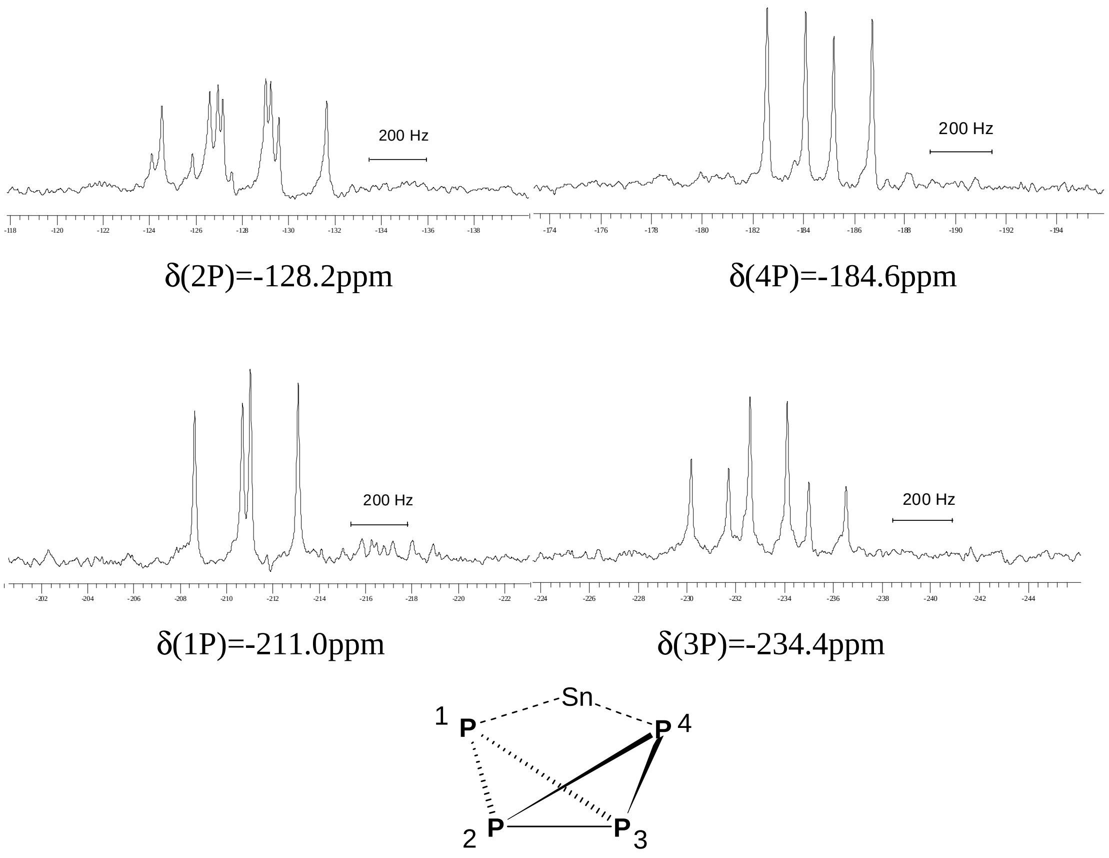

δ(2P)=-128.2ppm δ(4P)=-184.6ppm

δ(1P)=-211.0ppm δ(3P)=-234.4ppm

(two hypersilyl and one $(Me_3Si)_2N$ group
as well as the K atom are omited)

Figure 2.25 The $^{31}P\{H\}$-NMR spectrum of **11** in benzene-d6(300K) at 101.256MHz. δ (P1)=-211.0, δ (P2)=-128.2, δ(P3)=-234.4, δ (P4)=-184.6 ppm. $^1J_{p1,p2}$=-167Hz, $^1J_{p1,p3}$= -195Hz, $^1J_{p2,p3}$ =-196Hz, $^1J_{p2,p4}$ =-213Hz, $^1J_{p3,p4}$=-124Hz.

The ^{1}H-NMR spectrum of a mixture of **11** and $(Me_3Si)_2NK$ shows three singlets at 0.58, 0.43, 0.24ppm with relative intensities of 27:27:18, and one singlet at 0.09ppm for $(Me_3Si)_2NK$, respectively, implying that two magnetically inequivalent hypersilyl groups and one bis(trimethylsilyl)amino group should be attached to the phosphorus skeleton.

2.6.3 Crystal Structure

Figure 2.26 shows the structure and numbering scheme of **10**. Discrete molecules weakly interlinked by K···Sn and agostic-type interactions are formed in the crystal (Figure 2.27). Each asymmetric unit contains one tin, one potassium, four phosphorus atoms, and three hypersilyl groups.

Table 2.25 Crystallographic data of **10**.

Empirical formula	Hyp$_3$P$_4$SnK
Formula weight(g/mol)	1024.67
Temperature(K)	173(2)
Crystal system	monoclinic
Space group	P2(1)/c
Lattice constants(Å,°)	a = 14.057(3) α 90
	b = 24.037(4) β 103.135(13)
	c = 17.628(3) γ 90
Volume(Å^3)	5800.3(18)
Formula units	4
Density(g/cm^3)	1.173
μ(Mo-K$_\alpha$)(mm^{-1})	0.888
2Θ range(°)	2.27 to 30.00
Reflections measured	13722
Independent reflections	13302 [R(int) = 0.0287]
Ind. Reflections with $F_o > 4\sigma(F_0)$	13302
Parameter	433
R1,R1(all reflections)	0.0475, 0.0763
wR2,wR2(all reflections)	0.1110, 0.1210
GooF	1.161
Residual electron density(e/Å^3)	1.765

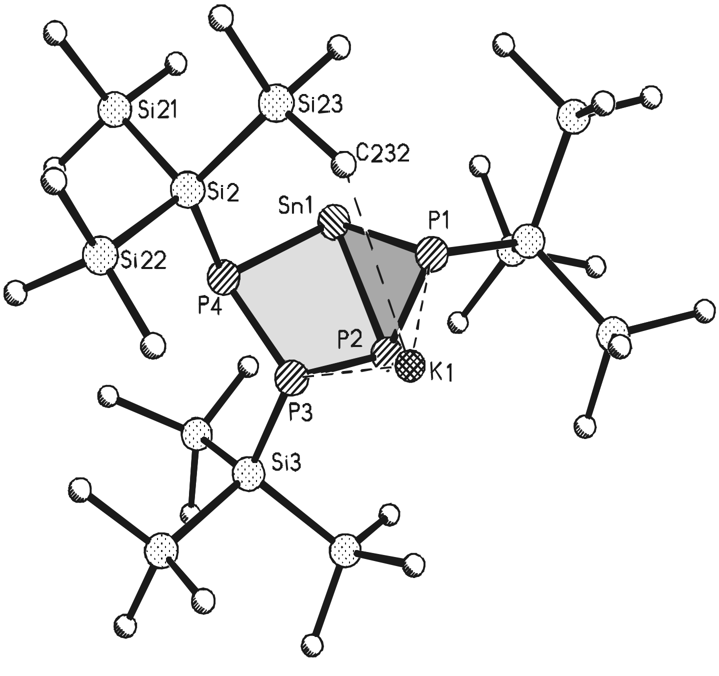

Figure 2.26 Molecular structure of **10**; atoms are represented by spheres of arbitrary radii; dashed lines are used to symbolize interatomic distances markedly smaller than the sum of the corresponding van der Waals radii; hydrogen atoms are omitted for clarity.

The central moiety of this structure is a P$_4$SnK framework, in which the tin atom is connected to three phosphorus atoms and to the potassium cation from the neighbouring unit. The phosphorus chain, showing a torsion angle of 73.5° (P1- P2-P3-P4), is no longer coplanar as in its precursor $Hyp_2P_4K_2$. The P-P bond lengths in this compound, with a narrow range between 222.33(13) and 223.80(12)pm are clearly single bonds and are comparable to those found in **2a, 4a** and **5a**. Two short K···P distances of 335.5 and 330.9pm are slightly longer than those found in **1a** and **2a**, but lie in the range of those observed for **4a**, **5a** and compare well with the K-P distances observed in $[K(thf)P(SiMe_3)_2]_\infty$[331.69(7) to 342.73(8)pm][130]. The coordination sphere of potassium is completed by a K···Sn interaction of 384.7pm between the neighbouring units as well as K···CH_3 agostic interactions to one hypersilyl group within the molecular unit (K···C: 341.8pm) and to the neighbouring unit (K···C: 346.6, 348.6, 353.5pm), which finally results in one-dimensional coordination polymers (Figure 2.27). The Sn-P distances [257.95(10), 262.86(10), and 264.92(10) pm] are only slightly longer than the sum of covalent radii. The three P-Si bond lengths, with two similar values to P1 and P4 [228.43(13), 228.05(12)pm] and a slightly longer value to P3 [230.27(13) pm], are in good agreement with the sum of the covalent radii of phosphorus and silicon.

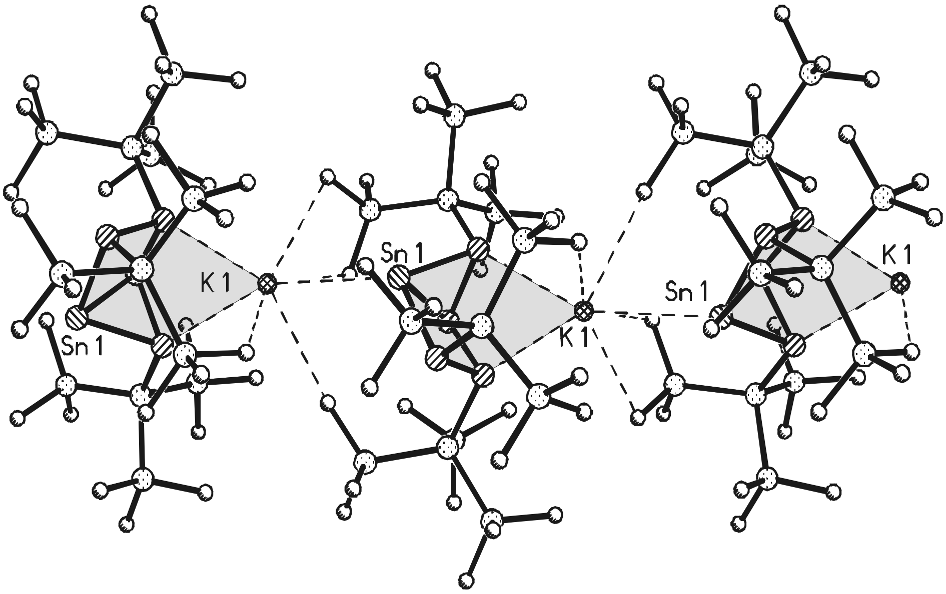

Figure 2.27 Plot of the structure of **10** in the crystal in a view along the a axes. Atoms are represented by spheres of arbitrary radii; dashed lines are used to symbolize interatomic distances markedly smaller than the sum of the corresponding van der Waals radii; hydrogen atoms are omitted for clarity.

Table 2.26 Selected interatomic distances (pm) and angles (°) for **10**.

P3-P2	223.49(12)	P1-Sn1-P2	50.31(3)
P1-P2	222.33(13)	P4-Sn1-P2	80.05(3)
P4-P3	223.80(12)	P2-P1-Sn1	66.47(3)
Sn1-P1	257.95(10)	P1-P2-Sn1	63.22(3)
Sn1-P4	262.86(10)	P3-P2-Sn1	89.55(4)

Sn1-P2	264.92(10)	P3-P4-Sn1	90.01(4)
K1-P3	330.9(2)	Si1-P1-Sn1	100.10(4)
K1-P1	335.5(2)	Si2-P4-Sn1	107.93(4)
P4-Si2	228.43(13)	P1-Si1-Si13	104.78(5)
P1-Si1	228.05(12)	P1-Si1-Si11	105.92(5)
P3-Si3	230.27(13)	P1-Si1-Si12	120.26(5)
Si2-Si22	235.08(15) to 238.37(14)	P3-Si3-Si31	108.24(5)
P2-P3-P4	98.72(5)	P3-Si3-Si32	116.86(5)
P1-P2-P3	96.56(5)	P3-Si3-Si33	107.33(5)
P4-P3-Si3	102.65(5)	P4-Si2-Si22	109.14(6)
P2-P1-Si1	96.21(5)	P4-Si2-Si21	97.62(5)
P3-P4-Si2	114.13(5)	P4-Si2-Si23	123.33(5)
P2-P3-Si3	95.46(5)	Si-Si-Si	. 80(5) to 109.97(6)
P1-Sn1-P4	96.06(3)		

3 Hypersilyl Stabilized Lead (Tin) and Phosphorus Clusters

3.1 Overview

Since du Mont and Kroth[131] in 1977 published synthetic pathways to bis(di-*tert*-butylphosphanyl)stannylene, which were shown to be dimers by NMR-spectroscopy, only few further homoleptic tin(II) and lead(II) phosphido complexes had been reported. X-ray diffraction experiments showed them to have one of the structural motifs A-D (Scheme 3.1) unless multidental phosphanes are utilized.

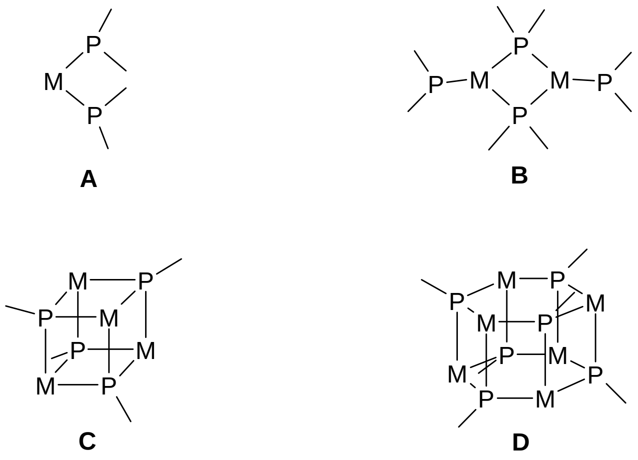

M=Sn or Pb

Scheme 3. 1

The first structurally characterized lead(II) and tin(II) phosphido complexes with central M_2P_2 (M= Sn, Pb) ring (Scheme3.1 **B**) were published by Cowley and Jones[132], Buhro and co-workers[133] in 1980’s, respectively. Several years later, using bulkier substituents, Driess et al. successfully synthesized and structurally characterized the first monomeric bis(phosphanyl)stannylene and plumbylene[134] with the expected V-shaped molecular structure (Scheme3.1 **A**) as well as the first example of a formal tin(II) phosphandiide[135], which crystallizes as a hexamer with a hexagonal prismatic P_6Sn_6 core (Scheme3.1 **D**). A related tetramer with a P_4Sn_4 heterocubane structure (Scheme3.1 **C**) was synthesized by Westerhausen et al. using the extremely bulky tri(*tert*-butyl)silyl substituent[136]. Very recently, the first structurally characterized homologous compound with chemical bonds between lead and arsenic atoms, $[i\mathrm{Pr}_3\mathrm{SiAsPb}]_6$, was prepared by Hänisch, exhibiting a hexagonal prismatic As_6Pb_6 core (Scheme3.1 **D**)[137]. However, no similar cage-like lead-phosphorus cluster with molecular structure **C** or **D** (Scheme3.1) has been reported to date.

As mentioned above, previous work in our group showed that dihypersilyl plumbylene and stannylene with several Lewis-acids and Lewis-bases react as Lewis-amphoteric carbene homologues. However, the initial formation of the simple adducts is sometimes followed by subsequent ligand exchange reactions, especially if the initial adduct still provides a Lewis-acidic centre. Such rearrangement reactions allowed for the preparation of several novel compounds, such as a neutral copper(I) silanide, a stannylene complex of Cu(I) as well as heteroleptic distannenes and diplumbenes with very short M=M bonds[46].

White phosphorus, phosphanes (PH_3 and PMe_3) as well phosphanides ($LiPH_2$ and KPH_2) provide lone-pairs which should allow for an initial formation of Lewis-acid-base adducts with tetrylenes. White phosphorus is expected to be a very weak base and to our knowledge no adduct to a heavier tetrylene has been reported.

3.2 $Hyp_4P_4Pb_4$ (12), Hyp_2P_2 (13) and $Hyp_4P_4Sn_4$ (14)

3.2.1 Synthesis

3.2.1.1 Reaction of dihypersilylplumbylene and stannylene with white phosphorus

When dihypersilyl plumbylene is allowed to react with white phosphorus at room temperature in toluene, after a few seconds the colour of the solution changes from blue to violet and on further warming to 50°C again changes to brown. A colour change from deep brown to brown can also be observed for the reaction of dihypersilyl stannylene with P_4 under the same reaction conditions.

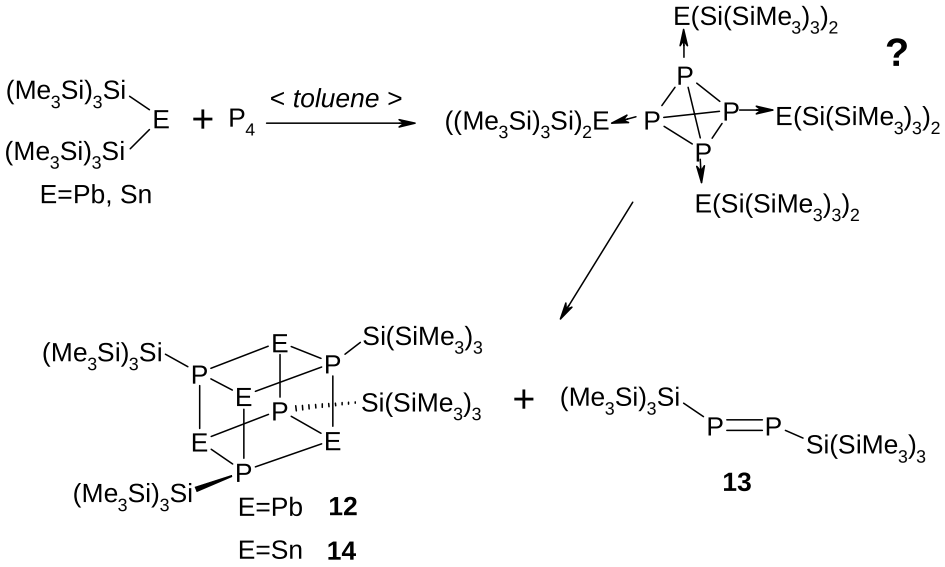

Scheme 3.2

According to the ^{31}P NMR spectra, several products containing phosphorus are present in the resulting solutions, but two dominant species for both reactions giving rise to resonances in the very low field region, at +735 ppm, and in the very high field region, at -506.2 (E=Pb) and -463.6 ppm (E=Sn), respectively. The former gives just a singlet with ^{29}Si satellites ($^{1}J_{P,Si}$ = 46.2 Hz) and can unambiguously be attributed to dihypersilyldiphosphene, $(Me_3Si)_3SiP{=}PSi(SiMe_3)_3$ (**13**). It is very soluble and can be isolated as bright green crystals in small amounts only by fractional crystallization at a temperature below -60°C. Unfortunately those are not suitable for X-ray structure analysis. The latter resonances exhibit an intense central line with a complicated satellite structure, indicating the presence of four coupling Pb or Sn atoms, respectively. Fortunately, these species are not well soluble in toluene. Therefore they could be almost quantitatively isolated as dark brown crystals from toluene. By X-ray diffraction they were identified as tetrameric lead(II) (**12**) and tin(II) (**14**) hypersilylphosphandiide, respectively. Both are fairly stable in hydrocarbon solution at room temperature as far as air is excluded.

When dihypersilyl plumbylene is treated with P_4 at -30°C in toluene, again a colour change from deep blue to violet within several minutes indicates that a reaction took place. The ^{31}P NMR spectrum of the reaction mixture now in addition to the signals mentioned above showing a strong signal at -350 ($^{1}J_{P,Pb}$ = 510 Hz) ppm, suggests that a third compound is formed under these conditions. The ^{207}Pb satellites in the ^{31}P NMR spectrum exhibit intensities consistent with four Pb atoms which are equivalent on the NMR time scale and show no fine structure, indicating a rapid exchange process. We suggest the initial formation of a 1:4 Lewis-acid-base adduct between P_4 with dihypersilylplumbylene. Such an adduct would be a very probable intermediate for the formation of the mentioned products (Scheme 3.2), since it allows for the low energy approach of both reactants.

According to the ^{31}P NMR data of the reaction mixture further products are formed to a smaller extent, most of them giving complicated multiplet signals and showing no ^{207}Pb satellites. At least two of those are polycyclic hypersilyl substituted phosphanes. By their coupling pattern they could be unambiguously identified as dihypersilyltetraphosphane Hyp_2P_4 (**6**) with a butterfly structure and the trihypersilylheptaphosphane Hyp_3P_7 with a nortricyclene-P_7 core.

3.2.1.2 Reaction of bis[bis(trimethylsilyl)amino]-stannylene and plumbylene with hypersilylphosphane

Similar to Westerhausen's method to get tin (II) tri(*tert*-butyl)silylphosphandiide[136], the metallation of $HypPH_2$ with bis[bis(trimethylsilyl)amino]-substituted stannylene or plumbylene affords also compound **12** and **14**. The reactions are almost quantitatively carried out in toluene at 50°C and the products are again isolated by crystallization at low temperature (Eq. 3.1).

$$4\,[(Me_3Si)_2N]_2E + 4\,(Me_3Si)_3SiPH_2 \rightarrow [(Me_3Si)_3SiPE]_4 + 8\,(Me_3Si)_2NH \qquad \text{(Eq. 3.1)}$$

E=Pb, **12**; E=Sn, **14**

3.2.2 NMR Spectroscopy

The ^{1}H-NMR spectrum of compound **12** shows only one singlet at 0.42 ppm in benzene-d6, while the $^{13}C\{^{1}H\}$-NMR spectrum displays one singlet at 2.7 ppm. Both are consistent with the heterocubane molecular structure and lie in the expected chemical shift range for hypersilyl groups. Since compound **12** does not dissolve very well in benzene-d6, only the signal of the peripheral silicon atoms can be observed as a singlet at 7.4 ppm in the $^{29}Si\{^{1}H\}$-NMR spectrum, the signal of the central silicon should be split into a multiplet and may hardly be found due to its poor intensity. The $^{31}P\{^{1}H\}$-NMR spectrum recorded in benzene solution, as described above, displays a signal with high order ^{207}Pb satellites at -506.2 ppm, as shown in Figure 3.1. Unfortunately, again owing to the poor intensity of the ^{207}Pb satellites, corresponding simulation has not been successful.

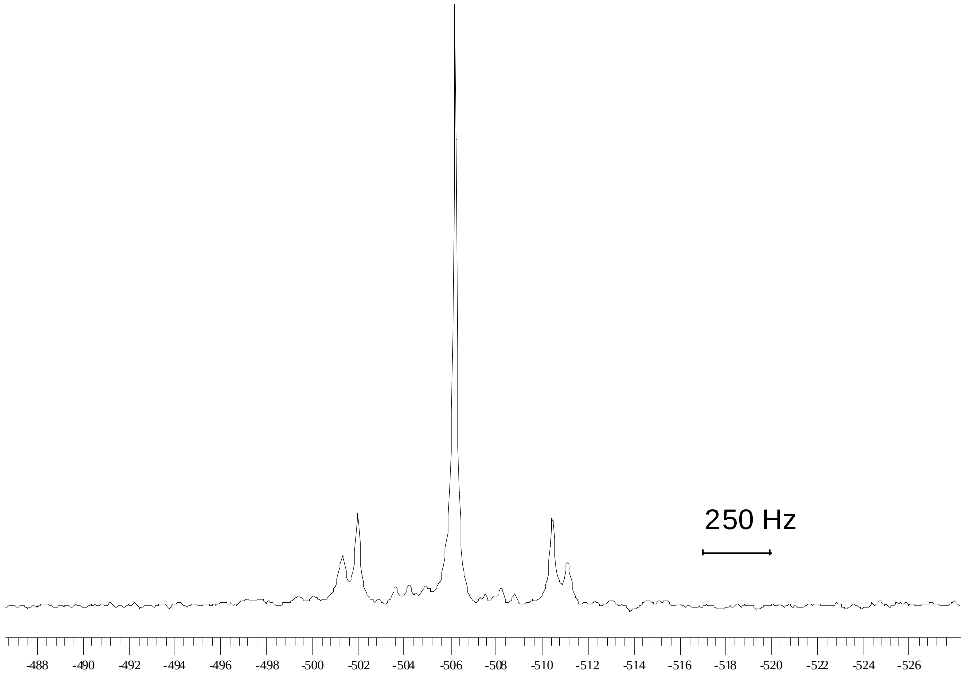

Figure 3.1 Observed ^{31}P-NMR spectrum of **12** at 81.015MHz in benzene-d6(300K):δ=-506.2ppm.

The ^{1}H-NMR spectrum of compound **14** recorded in deuterated benzene solution shows a singlet at δ = 0.43 and the $^{13}C\{^{1}H\}$-NMR spectrum exhibits a singlet at δ = 2.6 for the hypersilyl groups. The $^{31}P\{^{1}H\}$-NMR spectrum displays at -463.6ppm a singlet with high order ^{117}Sn /^{119}Sn satellites(Figure 3.2), which is close to that for the carbon analogue tetrameric tin(II)tri-tert-butylsilylphosphandiide(-452.1ppm)[136] (Table 3.1). Remarkably, the phosphorus atoms in another tin-phosphorus cluster, hexatin(II)-hexakis-[μ_3-tri(iso-propyl)silylphosphandiide], resonate at -475.2ppm showing an even more unordinary up-field shift.

Table 3.1 Comparison of $^{31}P\{^{1}H\}$- and $^{119}Sn\{^{1}H\}$- NMR(benzene-d6, 300K) shifts and some coupling constants.

Compound	**14**	**$Sn_6P_6[Si(CHMe_2)_3]_6$**[135]	**$Sn_4P_4[Si(CMe_3)_3]_4$**[136]
δ(^{31}P NMR, ppm)	-463.6	-475.2	-452.1 [b]
δ(^{119}Sn NMR,ppm)	1515.7	–	1234.3 [b]
$^{1}J_{P,Sn}$(Hz)	741	708	766 [b]
$^{3}J_{P,Sn}$(Hz)	138	–	84 [b]

[b]: recorded in toluene-d_8.

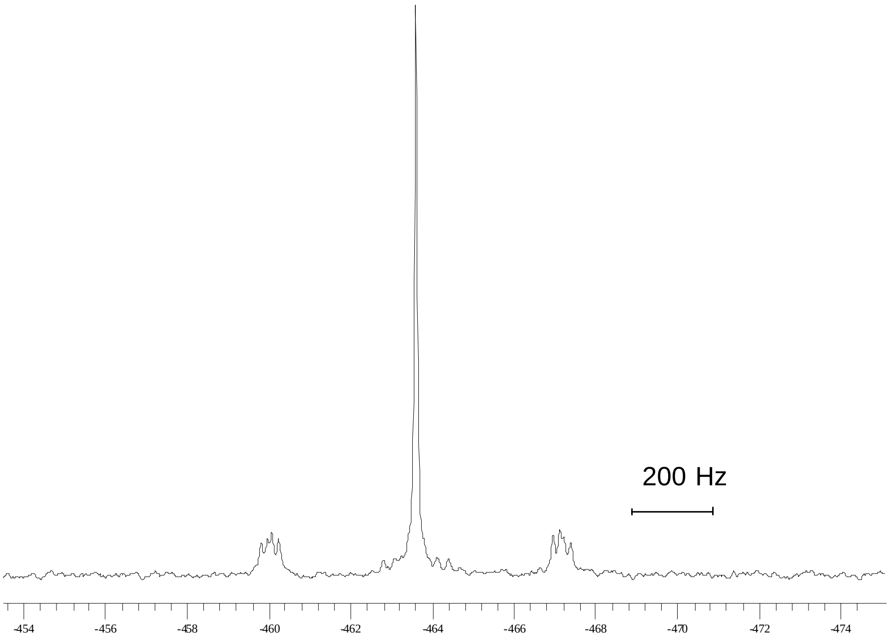

Figure 3.2 Observed $^{31}P\{^{1}H\}$-NMR spectrum of **14** at 101.256MHz in benzene-d6(300K):δ=-463.6ppm.

The $^{119}Sn\{^{1}H\}$-NMR spectrum recorded in deuterated benzene exhibits a quartet of doublets pattern at 1515.7ppm with a one-bond coupling constant of $^{1}J_{Sn,P}$ = 741Hz and a three-bond coupling constant of $^{3}J_{Sn,P}$ = 138Hz (Figure 3.3). The $^{31}P\{^{1}H\}$- and $^{119}Sn\{^{1}H\}$-NMR shifts and some coupling constants are summarized in Table 3.1 and compared with the values reported for the analogue $^{t}Bu_3Si$-substituted heterocubane[136] and the $^{i}Pr_3Si$-substituted hexagonal Sn_6P_6-prism[135]. As found for the $^{t}Bu_3Si$-substituted heterocubane and contrasting the high-field shift of the resonance found in the $^{31}P\{^1H\}$-NMR spectrum, the signal of compound **14** in the $^{119}Sn\{^1H\}$-NMR spectrum is strongly shifted to low field.

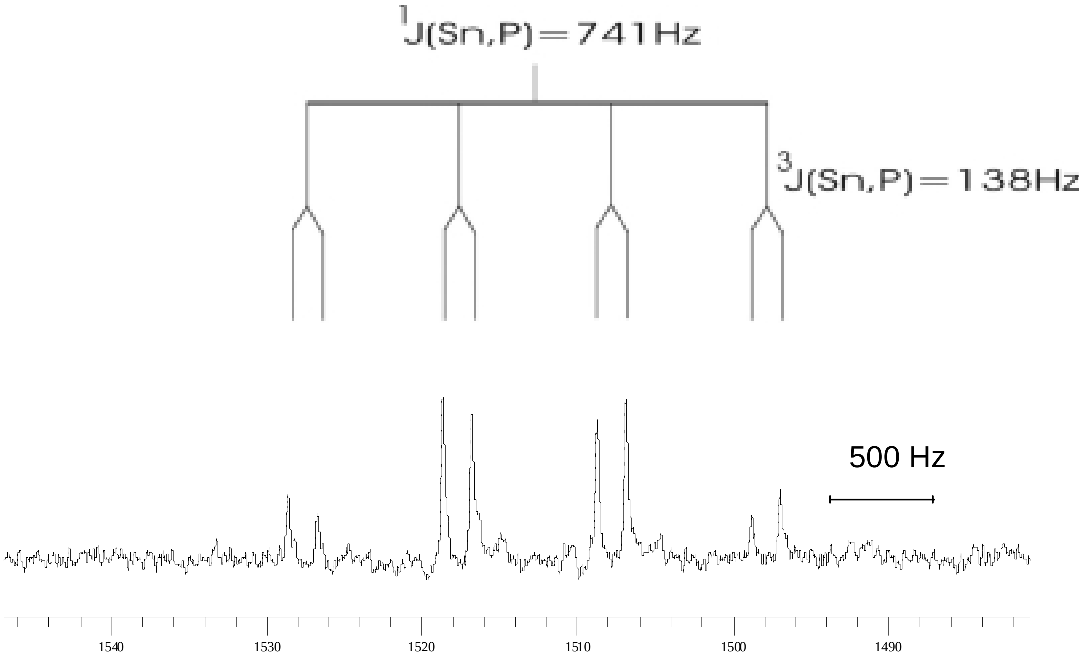

Figure 3.3 Observed $^{119}Sn\{^1H\}$-NMR spectrum of **14** at 74.631MHz in benzene-d6(300K): δ=1515.7ppm, $^1J_{PSn}$= 741Hz, $^3J_{PSn}$= 138Hz.

3.2.3 Crystal Structure

3.2.3.1 $Hyp_4P_4Pb_4$ (12)

The dark brown single crystals of $Hyp_4P_4Pb_4$ suitable for X-ray diffraction analysis were grown from cyclo-pentane at -20°C. Space group $P\overline{3}c1$ was suggested and later confirmed by a successful structure solution. The molecular structure of **12** and its numbering scheme are illustrated in Figure 3.4. The methyl groups are neglected for clarity. The disordered cyclo-pentane molecules originating from the recrystallization solution are not shown. Selected crystallographic data are summarized in Table 3.2. Selected interatomic distances and angles are listed in Table 3.3:

Table 3.2 Selected crystallographic data of **12**.

Empirical formula	$Hyp_4P_4Pb_4 \cdot 1.5Cyp$*
Formula weight [g/mol]	2048.50
Temperature[K]	173(2)K
Crystal system	hexagonal
Space group	$P\bar{3}c1$
a[Å]	16.201(2)
b[Å]	16.201(2)
c[Å]	37.756(8)
α[°]	90
β[°]	90
γ[°]	120
Volume[Å^3]	8582(2)
Formula units	4
Density[g/cm^3]	1.585
μ(Mo-K$_\alpha$)[mm^{-1}]	8.146
2Θ range[°]	2.16 to 22.50
Reflections measured	7522
Independent reflections	3770 [R(int) = 0.1147]
Ind. Reflections with $F_o > 4\sigma(F_0)$	3770
Parameter	213
R1 [$I > 2\sigma(I)$]	0.0718
R1(all reflections)	0.1397
wR2	0.1449
wR2(all reflections)	0.1709
GooF	1.101
Residual electron density[e/Å^3]	2.565, -1.452

* Cyp: cyclo-pentane.

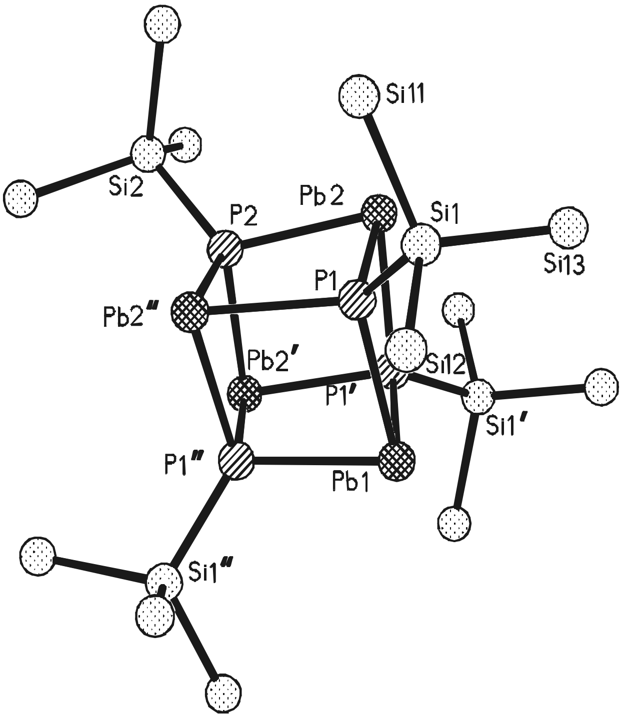

Figure 3.4 Molecular structure of **12**; atoms are represented by spheres of arbitrary radii; methyl groups are omitted for clarity. Symmetry operation (′):`-x+y,-x+1,z;` (″):`-y+1,x-y+1,z`

The tetrameric lead hypersilylphosphandiide **12** is the first isolated lead- and phosphorus-containing compound with a heterocubane molecular unit. As shown in Figure 3.4, the lead atoms possess no exocyclic ligands and consequently have a trigonal pyramidal coordination sphere. The phosphorus atoms each bear a hypersilyl group and display a distorted tetrahedral coordination environment. The rhomboid distortion of the Pb_2P_2 planes of the Pb_4P_4 heterocubane arrangement leads to P-Pb-P and Pb-P-Pb angles of approximately 81° and 97°, respectively. The Pb-P-Si angles range between 118.3(2) and 119.71(16)°. The Pb-P bond lengths in this molecule, ranging between 272.0(5) and 274.6(5)pm, are significantly longer than the mean value of 265.4pm for the Pb-P bond lengths in bis{[(*tert*-butyl(2,4,6-tri-isopropylphenyl)fluorosilanyl](tri-isopropylsilanyl)phosphanyl)}-lead[134], in which the lead atom is coordinated only to two three-coordinate phosphorus atoms. The P-Si bond lengths [226.1(7) and 228.2(12)pm] are significantly longer than those observed in **2a** [221.61(6) and 221.45(6)pm].

Table 3.3 Selected interatomic distances (pm) and angles (°) for **12**.

Pb1-P1	272.9(5)	Si-Si	233.0(8) to 236.4(8)
Pb2-P1´	272.0(5)	P-Pb-P	80.3(2) to 82.01(16)
Pb2-P2	273.4(4)	Pb-P-Pb	97.5(2) to 99.29(16)
Pb2-P1	274.6(5)	Si-P-Pb	118.3(2) to 119.72(16)
P1-Si1	226.1(7)	P-Si-Si	106.3(3) to 111.5(3)
P2-Si2	228.2(12)	Si-Si-Si	110.2(3) to 110.6(3)

3.2.3.2 $Hyp_4P_4Sn_4$ (14)

A dark brown well shaped single crystal of $Hyp_4P_4Sn_4$ obtained from a benzene solution was investigated by X-ray diffraction analysis. The molecular structure of **14** and its numbering scheme are depicted in Figure 3.5. The methyl groups are neglected for clarity. One of the hypersilyl groups in the molecule was disordered in the crystal (Figure 3.6), however, the structure determination gave well-defined structural parameters. Selected crystallographic data are summarized in Table 3.4. Selected interatomic distances and angles are listed in Table 3.5:

Table 3.4 Crystallographic data of **14**.

Empirical formula	$\mathrm{Hyp_4P_4Sn_4}\cdot$1.5benzene
Formula weight(g/mol)	1706.47
Temperature(K)	173(2)K
Crystal system	hexagonal
Space group	$P32_1$
Lattice constants(Å,°)	a = 16.2775(3) α 90
	b = 16.2775(3) β 90
	c = 18.5675(4) γ 120
Volume(Å^3)	4260.49(14)
Formula units	2
Density(g/cm^3)	1.330
μ(Mo-K$_\alpha$)(mm^{-1})	1.485
2Θ range(°)	2.50 to 28.31
Reflections measured	31724
Independent reflections	7064 [R(int) = 0.0328]
Ind. Reflections with $F_o > 4\sigma(F_0)$	7064
Parameter	230
R1,R1(all reflections)	0.0213, 0.0327
wR2,wR2(all reflections)	0.0541, 0.0561
GooF	1.100
Residual electron density(e/Å^3)	0.735

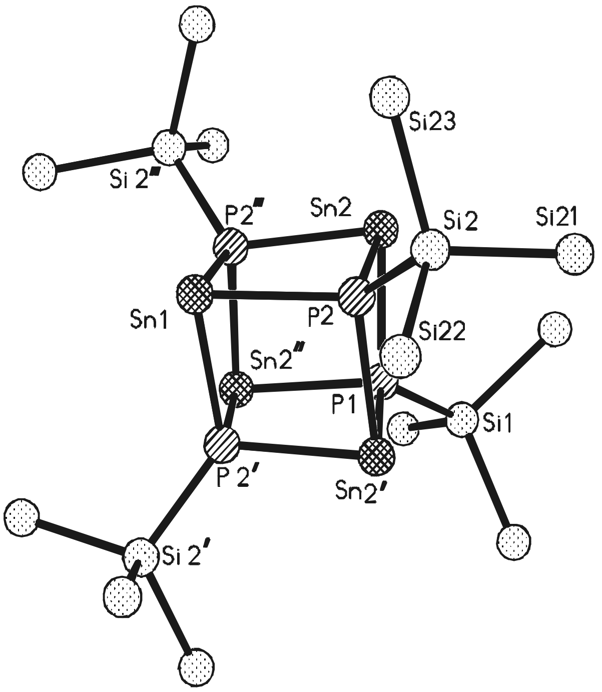

Figure 3.5 Molecular structure of **14**; atoms are represented by spheres of arbitrary radii; methyl groups are omitted for clarity. Symmetry operation ('):-x+y,-x+1,z; (''):-y+1,x-y+1,z

Similar to the molecular structure of **12**, the central moiety of molecular structure of **14** is a slightly distorted cubane-like P_4Sn_4 core with trigonal pyramidal coordinated tin atoms. The rhomboid distortion of the P_2Sn_2 planes of the P_4Sn_4 heterocubane arrangement again leads to a difference of 16° between the angles of P-Sn-P and Sn-P-Sn. Distorted tetrahedral coordination environment with Sn-P-Si angles ranging between 117.45(3) and 120.973(16) was found for the phosphorus atoms in this compound. The Sn-P distances with an average length of 265.4pm lie very close to the mean value of 265.1pm found in its supersilyl analogue $[(Me_3C)_3SiPSn]_4$ [136], which exhibits the same $Si_4P_4Sn_4$ core in the molecular structure. Similar distances were also observed for another tin-phosphorus cluster, hexatin(II)-hexakis-[μ_3-tri(*iso*-propyl)silylphosphandiide], $[(Me_2CH)_3SiPSn]_6$[135], with a distorted hexagonal P_6Sn_6-prism, showing 262.6(3) pm for Sn-P bond distances within the P_3Sn_3 planes and 266.5(3)pm for those between the two planes. The P-Si bond lengths vary in a narrow range between 225.65(8) and 226.76(12) pm are also similar to those observed in $[(Me_3C)_3SiPSn]_4$[136] and $[(Me_2CH)_3SiPSn]_6$[135].

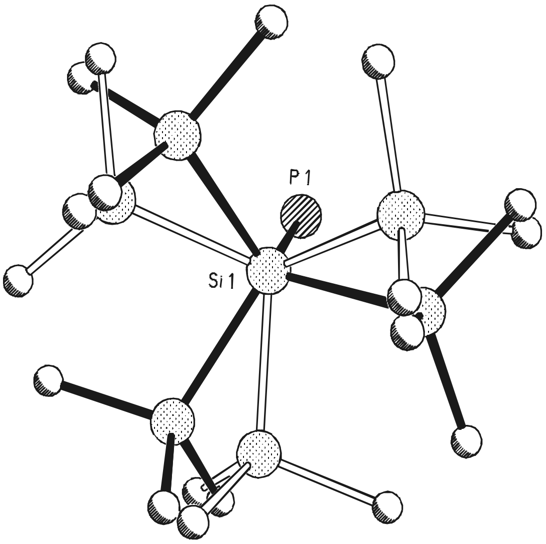

Figure 3.6 Representation of the disordering of the hypersilyl group in the crystal of **14**. The population ratio amounts to 0.904(solid bonds)/0.006(empty bonds).

Table 3.5 Selected interatomic distances (pm) and angles (°) for **14**.

Sn1-P2	265.65(6)	Si-Si	234.79(9) to 235.00(9)
Sn2-P2	264.46(6)	P-Sn-P	81.427(18) to 83.487(17)
Sn2-P2'	265.08(6)	Sn-P-Sn	95.90(2) to 97.993(19)
Sn2-P1	265.76(5)	Sn-P-Si	117.45(3) to 121.51(3)
P1-Si1	226.76(12)	P-Si-Si	106.28(4) to 110.13(4)
P2-Si2	225.65(8)	Si-Si-Si	110.30(4) to 110.90(4)

3.3 Li[$Hyp_2Pb{\cdot}PH_2$] (15), Li[$Hyp_2Pb{\cdot}P(H)Hyp$] (16) and K[$Hyp_2Pb{\cdot}PH_2$] (18)

3.3.1 Synthesis

3.3.1.1 Li[$Hyp_2Pb{\cdot}PH_2$] (15)

The adduct Li[$Hyp_2Pb{\cdot}PH_2$] (**15**) is prepared by reaction of dihypersilylplumbylene with an equimolar amount of lithium phosphanide at -20°C in diethyl ether(Eq 3.2).

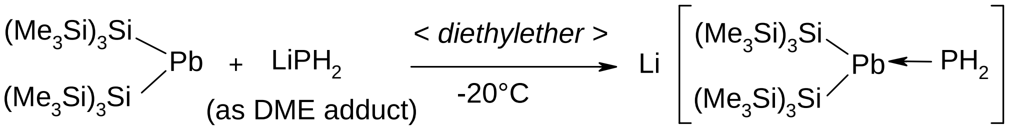

(Eq.3.2)

15
(as DME and Et_2O adduct)

The reaction mixture immediately changes its colour from deep blue to orange-red when the dihypersilylplumbylene solution is dropwise added to the suspension of lithium phosphanide in diethyl ether, indicating a rapid reaction. The ^{31}P-NMR spectrum of the resulting mixture reveals that almost only one phosphorus-containing product (compound **15**) is formed. After work-up, orange-brown crystals of Li[$Hyp_2Pb{\cdot}PH_2$]$\cdot Et_2O \cdot$DME (**15a**) are isolated in good yield. Compound **15a** is air- and moisture-sensitive, but stable enough to be stored under argon over a period of one year.

3.3.1.2 Li[$Hyp_2Pb{\cdot}P(H)Hyp$] (16)

When dihypersilylplumbylene was reacted with equimolar amounts of $LiPH_2$(as DME adduct) in DME at -20°C, the immediate colour change from blue to violet-red indicates a fast reaction occurred. According to the ^{31}P-NMR spectrum of the resulting mixture, the expected 1:1 adduct of compound **15** was obtained in good yield. As mentioned above, solid **15a** is fairly stable at room temperature as long as air and moisture is excluded. In solution, however, this compound is unstable and may slowly decompose to give some metallic lead and some other lead- and phosphorus-containing compounds. One of these decomposition products, Li[$Hyp_2Pb{\cdot}P(H)Hyp$] (**16**), has been isolated as red crystals and identified by X-ray diffraction analysis (Scheme 3.2). Unfortunately, the diffraction data are not good enough to give good structure parameters mainly due to the strong disordering within the coordinating ether. However, the anionic [Hyp$_2$Pb·P(H)Hyp]$^-$ fragment can be readily identified.

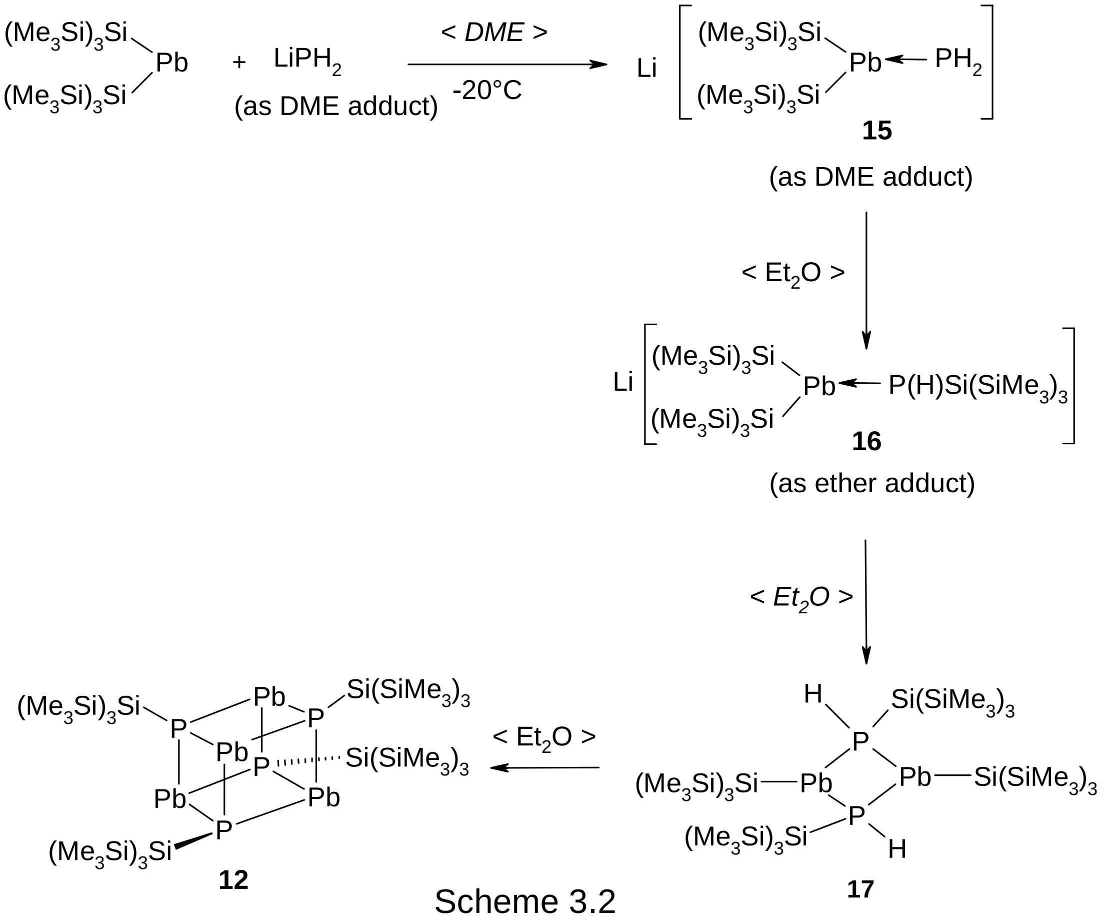

Scheme 3.2

Just as many other adducts of dihypersilylplumbylene, compound **16** is unstable in ether solution and decomposes further under formation of [HypPbP(H)Hyp]$_2$ **17** over a period of several months even at -60°C. Compound **17** is also unstable at room temperature in ether or benzene-d6 solution. On standing at ambient temperature it undergoes decomposition finally leading to the heterocucane cluster **12** along with small amounts of [(Me$_3$Si)$_3$Si]$_2$PH, HSi(SiMe$_3$)$_3$, and Si$_2$(SiMe$_3$)$_6$.

3.3.1.3 K[Hyp$_2$Pb·PH$_2$] (18)

Treatment of a diethyl ether solution of Hyp$_2$Pb with equimolar amounts of KPH$_2$ in diethyl ether at -20°C immediately gives a reaction, indicated by a colour change from deep blue to orange-brown (Eq.3.3). This reaction proceeds nearly quantitative, giving compound

$K[Hyp_2Pb \cdot PH_2]$ (**18)** as the only product. After adding small amounts of triazine, the expected adduct **18** can be obtained in good yield as orange-brown crystals at -60°C.

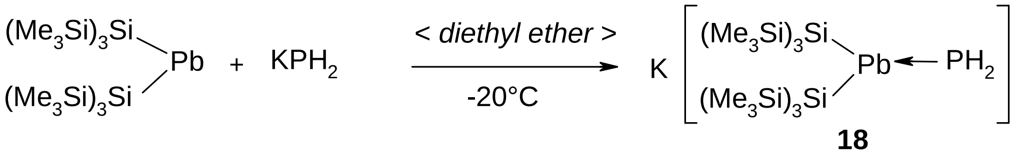

18

(Eq. 3.3)

In the solid state, compound **18** is fairly stable at room temperature under argon, but decomposes slowly to precipitate elementary lead in diethyl ether solution when stored under ambient light at ambient temperature for several days.

3.3.2 NMR Spectroscopy

The $^{31}P\{^1H\}$-NMR spectrum of **15** recorded in Et_2O/10%THF-d8 at 253K shows a singlet at -278.8ppm with satellites of ^{207}Pb ($^1J_{P,Pb}$= 653Hz), while the ^{31}P-NMR(THF-d8, 253K) spectrum of **15** displays a triplet ($^1J_{P,H}$= 155Hz) at -280.9ppm with satellites of ^{207}Pb, indicating that there are two hydrogen atoms bonded to phosphorus atom within the molecule(Figure 3.7). The room temperature ^{31}P-NMR spectrum of this compound, however, gives only a very broad signal with the same chemical shift, reflecting probably the presence of a rapid ligand exchange under these conditions.

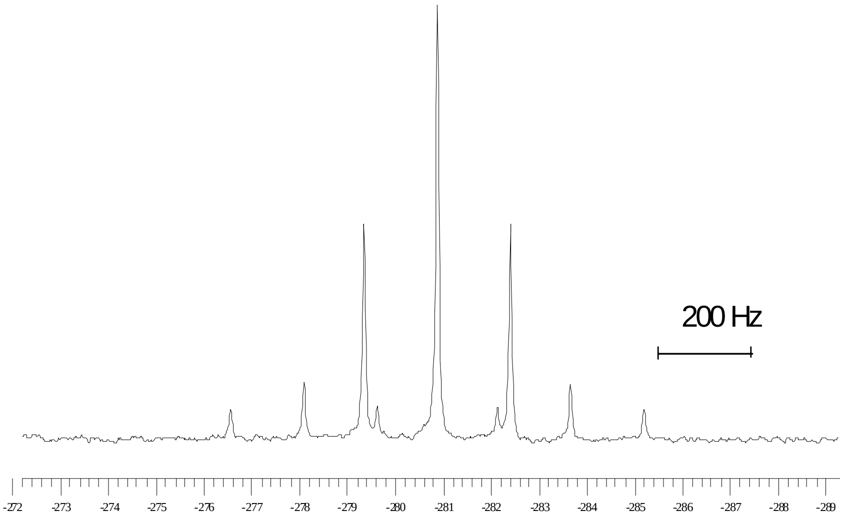

Figure 3.7 Observed ^{31}P-NMR spectrum of **15a** in THF-d8 at 101.256MMHz(253K); δ=-280.9ppm, $^1J_{PH}$=155Hz.$^1J_{PPb}$=653Hz.

The ^{1}H-NMR(THF-d8, 253K) spectrum of **15** shows two small peaks at 0.66ppm and 1.05ppm, which should be considered as a doublet derived from the coupling of phosphorus with a $^{1}J_{P,H}$ coupling constant of 155Hz. The same spectrum shows also an intense singlet at 0.17ppm for the two equivalent hypersilyl groups. The integral ratio of the former ($-PH_2$) to the latter (hypersilyl) protons amounts to 2:54. The presences of the signals at 1.10ppm(triplet) and 3.35ppm(quartet) for Et_2O , 3.25ppm(singlet) and 3.42ppm(singlet) for DME, reflect that these donors strongly coordinate to lithium cation, yielding a large cation moiety for the stabilization of the huge anionic part of $[Hyp_2PbPH_2]^-$.

The ^{29}Si{^{1}H}-NMR(THF-d8, 253K) spectrum exhibits an intense singlet at -3.6ppm for the peripheral silicon atoms (Figure 3.8a) and a small doublet with a coupling constant $^{2}J_{Si,P}$ of 10Hz for the central silicon atom**(**Figure 3.8b). Interestingly, satellites of ^{207}Pb can be observed for the signal of the central silicon with a one-bond coupling constant $^{1}J_{Si,Pb}$ of 1555Hz.

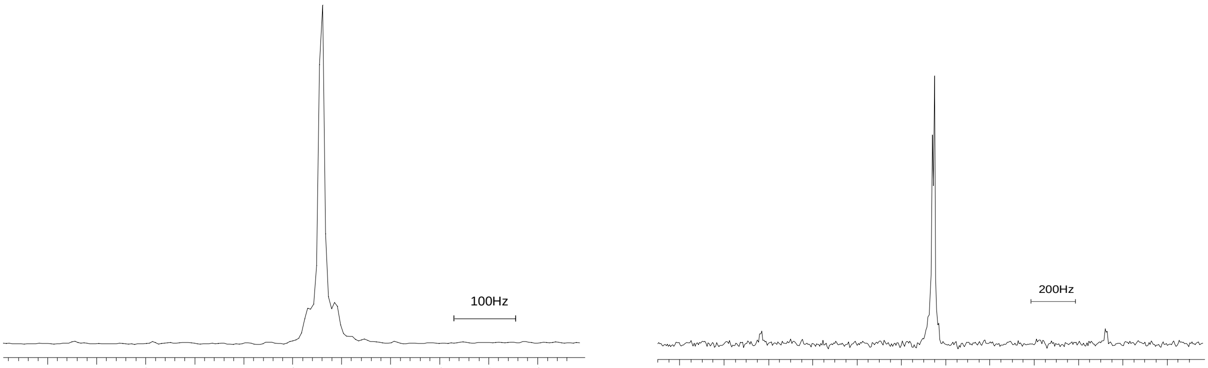

(a) (b)

Figure 3.8 Observed ^{29}Si{^{1}H}-NMR spectrum of **15a** in THF-d8 at 79.495MHz(253K): (a):δ=-3.66 for the peripheral silicon; (b): δ=-135.2 for the central silicon, $^{1}J_{Si,Pb}$=1555Hz. $^{2}J_{Si,P}$ =10Hz. Note: The figure (b) has been arbitrarily enlarged

The ^{31}P{H}-NMR spectrum of $K[Hyp_2Pb \cdot PH_2]$ (**18**) displays a singlet at -281.7ppm with satellites of ^{207}Pb, which is similar to that of compound **15** described above. The ^{1}H coupled ^{31}P-NMR spectrum, showing a triplet with $^{1}J_{P,H}$ coupling constant of 156 Hz as well as ^{207}Pb ($^{1}J_{Pb,P}$=590 Hz) satellites, is shown in Figure 3.9. In the ^{1}H-NMR spectrum, a doublet at 0.95 ppm with a coupling constant of $^{1}J_{P,H}$ =156Hz and an intense singlet at 0.21 ppm derived from hypersilyl groups are found in an integral ratio of about 2: 54, suggesting the formulated simple 1:1 adduct of KPH_2 and dihypersilylplumbylene.

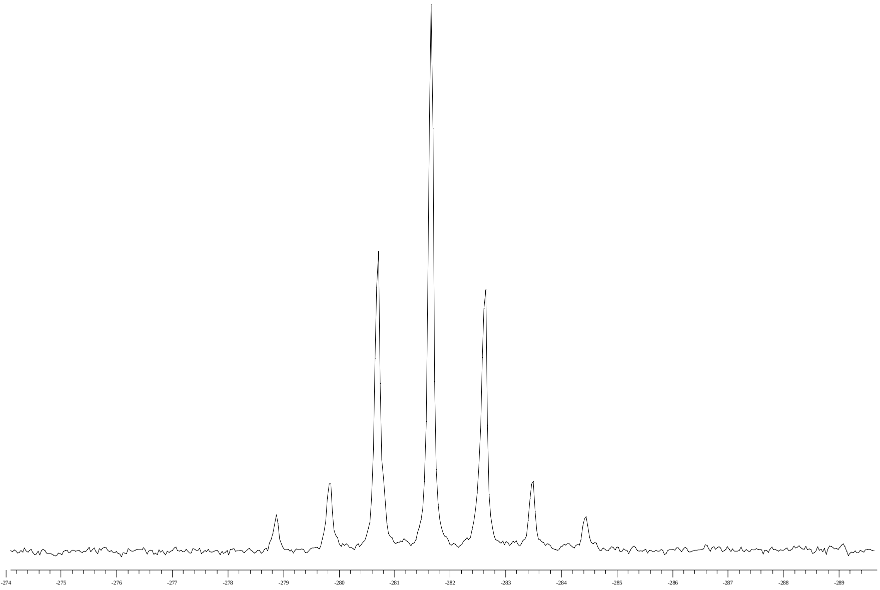

Figure 3.9 Observed ^{31}P-NMR spectrum of **18** at 161.976 MHz in D_8-THF (253K):δ=-281.7 ppm, $^1J_{PH}$= 156 Hz, $^1J_{P,Pb}$= 590 Hz

3.3.3 Crystal Structure

3.3.3.1 [$Et_2O(DME)Li$] [$Hyp_2Pb{\cdot}PH_2$] (15a)

A brown crystal of **15a** was investigated by X-ray diffraction analysis. The diethyl ether solvate molecule is twofold disordered in the crystal, however, the structure determination gave well-defined structural parameters. Selected crystallographic data are given in Table 3.6. Selected interatomic distances and angles are shown in Table 3.7. The molecular structure of **15a**, showing the numbering scheme, is depicted in Figure 3.10.

Table 3.6 Crystallographic data of **15a**.

Empirical formula	$Hyp_2PbP(H_2)Li{\cdot}Et_2O(DME)$	
Formula weight(g/mol)	906.69	
Temperature(K)	173(2)	
Crystal system	triclinic	
Space group	$P\bar{1}$	
Lattice constants(Å,°)	a = 13.084(2)	α 88.150(17)
	b = 13.334(3)	β 79.516(12)
	c = 15.404(3)	γ 68.553(15)
Volume(Å^3)	2457.8(9)	
Formula units	2	
Density(g/cm^3)	1.225	
μ(Mo-K_α)(mm^{-1})	3.681	
2Θ range(°)	2.08 to 25.00	
Reflections measured	8968	
Independent reflections	8565 [R(int) = 0.0532]	
Ind. Reflections with $F_o > 4\sigma(F_0)$	8565	
Parameter	409	
R1,R1(all reflections)	0.0333, 0.0594	

wR2,wR2(all reflections)	0.0587, 0.0624
GooF	0.733
Residual electron density(e/Å^3)	0.865

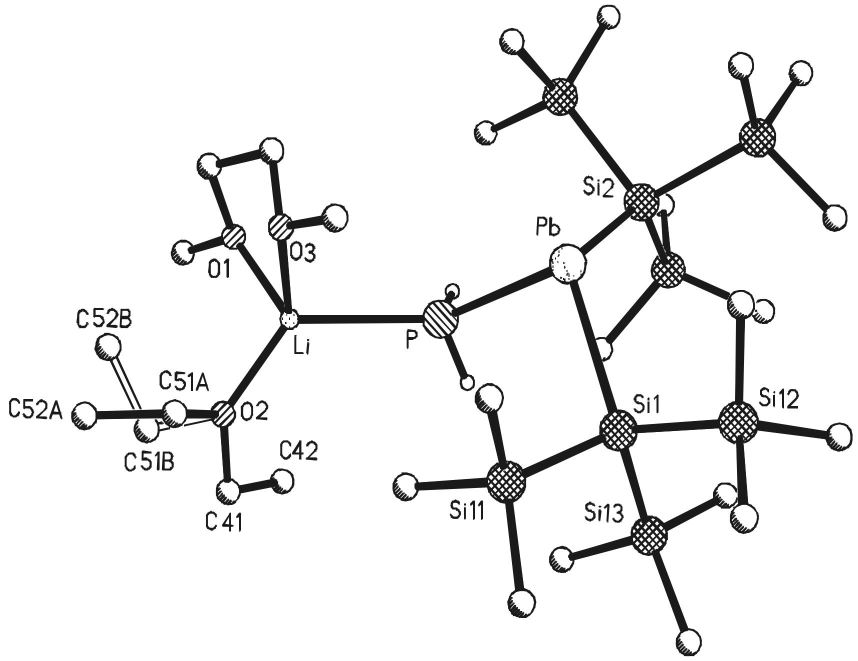

Figure 3.10 Molecular structure of **15a** with the disordered arrangement of the coordinated diethyl ether[the minor components(24%) are depicted as empty bonds]. Atoms are represented by spheres of arbitrary radii; hydrogen atoms except for the two bonded to phosphorus are omitted for clarity.

The molecular structure is best described as an intimate ion-pair with a predominantly ionic binding mode between the Li$^+$ cation and the phosphanide anion. The Li–P distance of 262.2(11) pm lies in the range observed for **7a** [between 262.0(7) and 265.9(7)pm]. The coordination sphere of lithium cation is accomplished by one DME and one diethyl ether molecule. Thus the lithium atom has a distorted tetrahedral coordination (three O atoms and one P atom). The Li-O bond lengths, with a value of 188.6(11)pm for Li-O2(Et$_2$O) and two longer values [198.8(11), 201.0(10) pm] for Li-O(DME), are still within the normal range. Two hydrogen atoms can be found near the phosphorus atom, showing P-H distances of 126(7) and 118(7)pm, respectively. A distorted tetrahedral coordination environment of P atom is completed by the coordination to the Pb atom of a dihypersilylplumbylene with a large Li-P-Pb angle of 128.3(2)°. The phosphorus-lead bond of 275.73(17) pm is only slightly longer than those observed for **12** [ranging from 271.9(5) to 274.6(5)], and lies in the range found in bis[bis(diphenylphosphino)-trimethylsilylmethanide-P,P’]-lead(II) (271.5-297.1ppm)[138]. With this coordinated phosphorus atom, the lead atom is found to be three coordinate with P-Pb-Si angles of 94.37(5) and 94.75(5)°, respectively. The Si-Pb-Si angle with a value of 114.79(4)°, however, is only slightly wider than that in the precursor dihypersilylplumbylene[113.55(10)°]. Due to the increase in coordination number at Pb atom, elongated Pb-Si bond lengths [276.60(15) and 275.66(15) vs 270.0(3) and 270.4pm in dihypersilylplumbylene] are observed. The other parameters of plumbylene fragment in this structure including Si-Si bond lengths ranging between 233.7(2) and 236.4(2) pm are comparable to those found in dihypersilylplumbylene.

Table 3.7 Selected interatomic distances (pm) and angles (°) for **15a**.

Pb-P	275.73(17)	Si12-Si1-Pb	108.29(6)
P-Li	262.2(11)	Si23-Si2-Pb	104.74(7)
P-H1	126(7)	Si21-Si2-Pb	128.31(7)
P-H2	118(7)	Si22-Si2-Pb	101.94(7)
Li-O3	201.0(10)	Li-P-Pb	128.3(2)
Li-O1	198.8(11)	Li-P-H1	117(3)
Li-O2	188.6(11)	Pb-P-H1	102(3)
Li-C71	274.3(11)	Li-P-H2	112(3)
Li-C51A	277.9(14)	Pb-P-H2	104(3)
Pb-Si1	276.60(15)	H1-P-H2	83(4)
Pb-Si2	275.66(15)	O2-Li-O1	109.2(5)
Si-Si	233.7(2) to 236.4(2)	O2-Li-O3	114.1(5)
		O1-Li-O3	83.5(4)
Si2-Pb-P	94.37(5)	O2-Li-P	127.3(4)
P-Pb-Si1	94.75(5)	O1-Li-P	113.4(5)
Si2-Pb-Si1	114.79(4)	O3-Li-P	100.3(4)
Si13-Si1-Pb	125.98(7)	Si-Si-Si	103.50(8) to 109.37(8)
Si11-Si1-Pb	101.19(6)		

3.3.3.2 [{$(MeNCH_2)_3$}$_2$K] [$Hyp_2Pb\cdot PH_2$] (18a)

Crystallization of **18** from diethyl ether in the presence of triazine yielded large orange-brown crystals of [{$(MeNCH_2)_3$}$_2$K] [$Hyp_2Pb\cdot PH_2$] (18a), which were suitable for X-ray structural analysis. The anion [$Hyp_2Pb\cdot PH_2$]$^-$ was disordered in a ratio of 0.87/0.13. In the following discussion only the structural parameters of the major component are considered. Selected data collection parameters and other crystallographic data are summarized in Table 3.8. Selected bond lengths and angles are listed in Table 3.9.

Table 3.8 Crystallographic data of **18a**.

Empirical formula	$Hyp_2PbP(H_2)K\cdot$2triazine	
Formula weight(g/mol)	1020.93	
Temperature(K)	193(2)	
Crystal system	triclinic	
Space group	$P\bar{1}$	
Lattice constants(Å,°)	a = 12.5404(10)	α 86.5800(10)
	b = 13.0367(11)	β 82.5140(10)
	c = 17.4872(14)	γ 76.9430(10)
Volume($Å^3$)	2759.9(4)	
Formula units	2	
Density(g/cm^3)	1.229	
μ(Mo-K_α)(mm^{-1})	3.359	
2Θ range(°)	1.60 to 28.33	
Reflections measured	32172	
Independent reflections	12902 [R(int) = 0.0844]	
Ind. Reflections with $F_o > 4\sigma(F_0)$	12902	
Parameter	750	
R1,R1(all reflections)	0.0400, 0.0635	
wR2,wR2(all reflections)	0.0810, 0.0881	
GooF	0.942	
Residual electron density($e/Å^3$)	0.900	

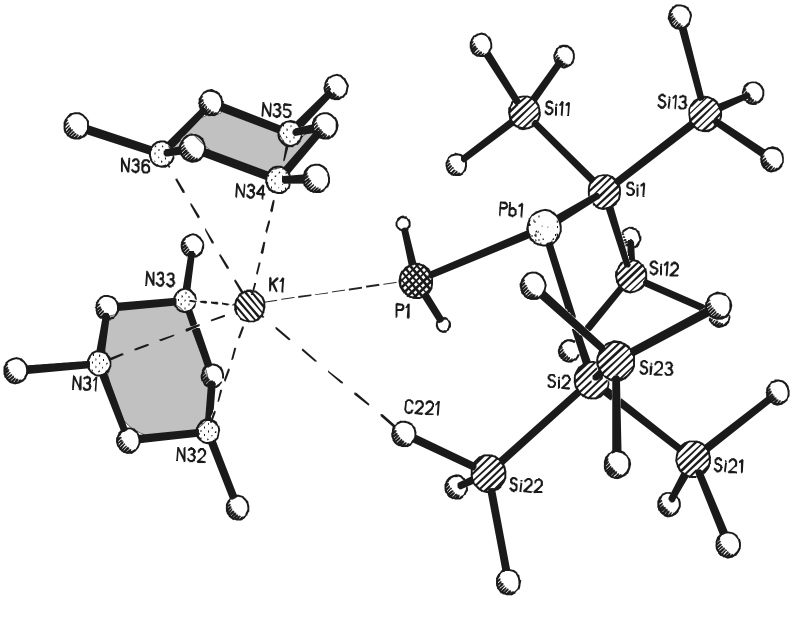

Figure 3.11 Molecular structure of **18a**. Atoms are represented by spheres of arbitrary radii; dashed lines are used to symbolize interatomic distances markedly smaller than the sum of the corresponding van der Waals radii; hydrogen atoms except for the two bonded to phosphorus are omitted for clarity.

The result of the structure determination of **18a** is shown in Figure 3.11. The molecule comprises an intimate ion-pair of $[Hyp_2Pb\cdot PH_2]^-$ and $[\{(MeNCH_2)_3\}_2K]^+$ with a K···P distance of 401.0 pm. In addition to the phosphorus atom, the K atom is coordinated to two η^3-N bonded triazine molecules (K···N distances: 284.2 to 296.8 pm) and the coordination sphere is completed by agostic-type interactions between K and hypersilyl groups.

Similar to **15a**, in the anion part the lead atom of the plumbylene is coordinated to the phosphanide with two slightly different P-Pb-Si angles of 93.9 and 97.6°. The Pb-P distance of 269.15(19) pm is 5 pm shorter than that observed in the lithium analogue **15a**. The Pb-Si bond lengths (276.1 and 277.4 pm), however, lie very close to those found in **15a** and are longer than those found in the precursor dihypersilylplumbylene (about 270 pm) again due to the increase in coordination number at Pb atom. In contrast to the observation in **15a**, the Si-Pb-Si angle of 111.2° observed in **18a** is slightly smaller than that in the precursor [113.55(10)°].

Table 3.9 Selected interatomic distances (pm) and angles (°) for **18a**.

Pb1-Si1	276.1	Pb1-P1	269.15(19)
Pb1-Si2	277.4	Si1-Si12	233.1(3)
P1-Pb1-Si1	97.6	Si1-Si11	234.29(17)
P1-Pb1-Si2	93.9	Si1-Si13	235.23(19)
Si1-Pb1-Si2	111.2	Si2-Si23	233.4(15)
K1-N	284.2 to 296.8	Si2-Si21	235.8(12)
K1-C221	333.7	Si2-Si22	237.9(15)
K1…P1	401.0	Si-Si-Si	102.0(5) to 109.47(11)

3.4 Li[(Hyp$_2$Pb)$_2$·PH$_2$] (19) and K[(Hyp$_2$Pb)$_2$·PH$_2$](20)

3.4.1 Synthesis

3.4.1.1 Li[(Hyp$_2$Pb)$_2$·PH$_2$] (19)

Li[(Hyp$_2$Pb)$_2$·PH$_2$] (**19)** with two dihypersilylplumbylene molecules bonded to the same phosphorus atom in phosphanide, is readily synthesized either by reaction of PbHyp$_2$ with LiPH$_2$ in a molar ratio of 2:1 or by reaction of Li[Hyp$_2$Pb·PH$_2$] with an equimolar amount of PbHyp$_2$.

Reaction of LiPH$_2$ (as DME adduct) with two equiv of PbHyp$_2$ at -20°C in DME or in a diethyl ether/12-crown-4 ether mixture affords dark brown crystals of **19** in good yield (Scheme 3.3). The ^{31}P-NMR spectrum of the reaction mixture shows that a small amount of **15** may be found as side product along with the main product of **19**. Although compound **19** can be isolated as a pure product by fractional crystallization, a small excess of dihypersilylplumbylene may improve the yield and facilitate the purification.

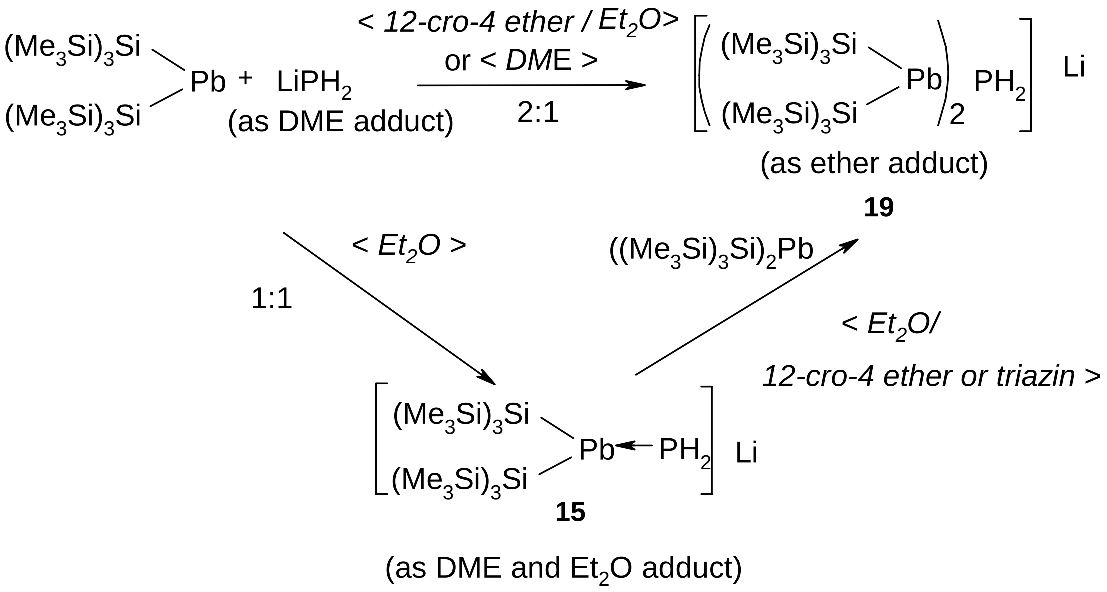

Scheme 3.3

Treatment of solution of **15a** (as DME and Et_2O adduct) in a 12-crown-4 ether/diethyl ether mixture (or a hexahydro-1,3,5-trimethyl-S-triazine/diethyl ether mixture) with a solution of equimolar dihypersilylplumbylene in diethyl ether at -20°C also produces **19** according to Scheme 3.3. The reaction mixture changes colour from orange-brown to deep violet-red immediately when the reactants are combined. After work-up, dark brown crystals of **19** were obtained in good yield. The crystals of this compound are air- and moisture-sensitive, but stable to be stored under argon up to one year at -20°C. They are insoluble in common hydrocarbons such as pentane or toluene, thus could be purified by washing with these solvents. However, they dissolve very well in diethyl ether or THF. At ambient temperature, the THF-d8 solution of **19** decomposes completely during a period of several days.

3.4.1.2 K[(Hyp$_2$Pb)$_2$·PH$_2$] (20)

Compound $K[(Hyp_2Pb)_2 \cdot PH_2]$ (**20**) was first found as one of the products from reaction of PH_3 with dihypersilylplumbylene in the presence of some $KN(SiMe_3)_2$ (formed during the preparation of dihypersilylplumbylene). As shown in Scheme 3.4, $KN(SiMe_3)_2$ might first react with PH_3 to give KPH_2. The so-formed KPH_2 combined dihypersilylplumbylene, which was excess in the reaction solution, to yield compound **20** as a black precipitate in n-pentane. This assumption has been verified by a direct reaction of dihypersilylplumbylene with KPH_2, which is prepared and isolated from the reaction of $KN(SiMe_3)_2$ with PH_3 in DME.

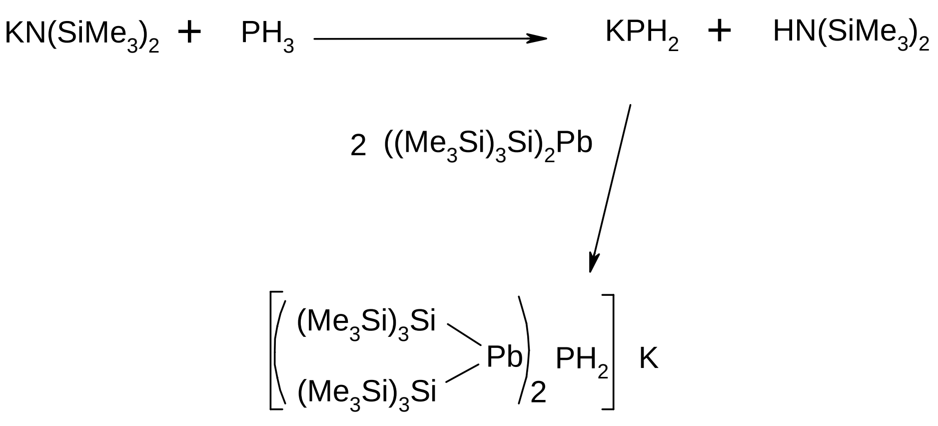

20

Scheme 3.4

The precipitate of **20** could be dissolved in diethyl ether, but the crystals obtained from the solution cooled at -60°C were not suitable for X-ray diffraction analysis. Recrystallization with a diethyl ether/triazine mixture finally afforded X-ray diffraction quality crystals of $[(Hyp_2Pb)_2{\cdot}PH_2]K{\cdot}3$triazine (**20a**). Compound **20a** is air- and moisture-sensitive, but stable enough to be stored at -20°C under argon over one year.

3.4.2 NMR Spectroscopy

3.4.2.1 Li[(Hyp$_2$Pb)$_2$·PH$_2$] (19)

The ^{31}P-NMR spectrum of the 12-crown-4 ether solvate of $Li[(Hyp_2Pb)_2{\cdot}PH_2]$ **(19a)**, like that of compound **15**, gives only a broad flat signal at room temperature. At lower temperature, the $^{31}P\{^1H\}$-NMR(THF-d8, 243K) spectrum shows a singlet at -352.0ppm with ^{207}Pb satellites. The coupling constant $^1J_{P,Pb}$ of 1420Hz is even two times larger than that observed for compound **15**(Table 3.10). The ^{31}P NMR(Et_2O+10%THF-d8, 243K) spectrum, showing a triplet at -352.0ppm with coupling constants of $^1J_{P,H}$ = 222Hz, indicates that two hydrogen atoms are bonded to the phosphorus atom within the molecule(Figure 3.12). The presence of 1.11ppm(triplet) and 3.37ppm(quartet) for Et_2O, 3.26ppm(singlet) and 3.42ppm(singlet) for DME, 3.70ppm(singlet) for 12-crown-4 ether in the ^{1}H-NMR spectrum suggests that these ethers coordinate to the lithium atom as donor ligands, forming a large cation to stabilize the huge phosphanide anion with two dihypersilylplumbylene molecules attached.

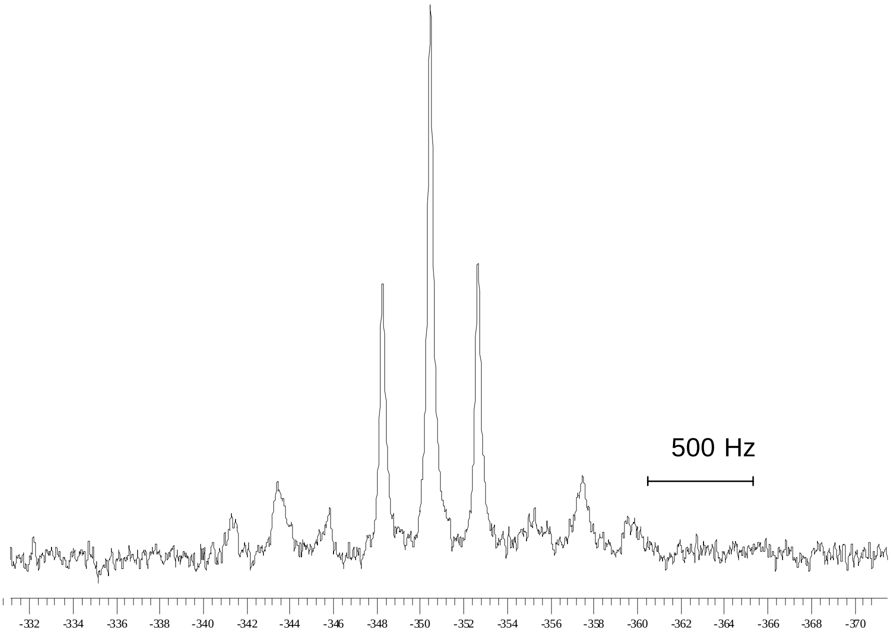

Figure 3.12 Observed ^{31}P-NMR spectrum of **19a** in THF-d8 at 101.256MHz(243K): δ=-352.0ppm, $^{1}J_{PH}$=222Hz, $^{1}J_{PPb}$=1428Hz.

The ^{31}P-NMR spectra of the DME solvate (**19b**) and triazine solvate (**19c)** recorded in THF-d8 show virtually identical signals as that of **19a**, so do the signals for the hypersilyl group observed in the ^{1}H- and ^{13}C-NMR spectra. Temperature-dependent ^{1}H-NMR spectra of **19c** in THF-D8 were recorded over a temperature range of -50°C to 25°C. A broad doublet with a coupling constant $^{1}J_{P,H}$ of 218Hz at 2.67ppm derived from the hydrogen atoms bonded to phosphorus, along with an intense singlet for the hypersilyl group, could be found at the spectrum recorded at room temperature. Lowering the temperature led to broadening of the latter and sharpening of the former. At the temperature below -20°C, the resonance of the hypersilyl group began to split into two singlets. On cooling, the resonance of the hypersilyl group shifted slightly to higher field, while the resonance of the hydrogen bonded to phosphorus atoms, in contrast, shifted to lower field, accompanying a slight increasing of the coupling constant ^{1}J(P,H). In accordance with the ^{1}H-NMR spectra, the ^{29}Si{^{1}H}-NMR spectrum of **19c** recorded at room temperature shows a singlet assignable to the peripheral silicon at -2.36ppm, which splits into two single resonances(-2.05, -2.56ppm) at -50°C.

3.4.2.2 K[(Hyp$_2$Pb)$_2$·PH$_2$] (20)

The ^{1}H-, ^{13}C-, ^{29}Si, and ^{31}P-NMR spectra of K[(Hyp$_2$Pb)$_2$·PH$_2$] (**20**) are very similar to those of the Lithium analogue **19**, implying their ionic properties. The similar thermodynamic effect has also been observed from the temperature-dependent ^{31}P-, ^{1}H-, and ^{29}Si-NMR spectra. The ^{31}P-NMR spectrum recorded at -20°C exhibits a sharp triplet with broad ^{207}Pb satellites at -350.9ppm while that measured at 25°C shows no signal (Figure 3.13). The ^{1}H-NMR spectrum shows a singlet assignable to the hypersilyl group at room temperature; but it splits into two single resonances if the temperature is lower than -30°C. The ^{29}Si-NMR spectrum recorded at room temperature again exhibits a singlet at -2.4ppm for the peripheral silicon atoms, which splits into two peaks at -2.1 and -2.6 ppm when the sample is measured at -50°C. Further measurements show that no resonance can be observed in the temperature range of -30°C to 0°C.

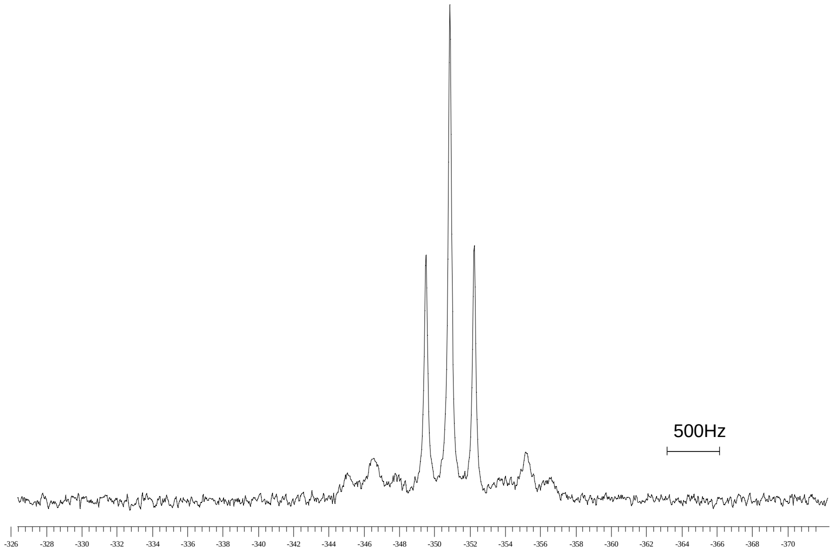

Figure 3.13 Observed ^{31}P-NMR spectrum of **20** at 161.976MHz in THF-d8 (253K):δ=-350.9ppm, $^{1}J_{P,H}$= 222Hz, $^{1}J_{P,Pb}$= 1420Hz.

Selected chemical shifts and coupling constants of **20a** are summarized in Table 3.10 and compared with the values for **15a** and **19c**. All data for **20a** are similar to those for **19c**, but significantly differ from those for **15a**. In addition to the chemical shift difference in the ^{31}P-NMR spectra (about 70 ppm), the one-bond phosphorus-hydrogen coupling constants of **20a** and **19c** are 67 Hz larger than that observed for **15a**. Moreover, the one-bond phosphorus-lead coupling constants of the formers are even more than two times as large as that of the latter.

Table 3.10 Selected ^{1}H-, ^{13}C-, ^{31}P-, ^{29}Si- ,and ^{7}Li-NMR spectra data of **20a**, **15a**, and **19c.**

Compound	**20a**	**19c**	**15a**
δ(^{1}H NMR, SiMe$_3$ ppm)	0.24	0.24	0.17
δ(^{1}H NMR, PH$_2$, ppm)	2.79	2.78	0.86
δ(^{13}C NMR, ppm)	6.5	6.4[a]	5.6

$\delta(^{31}P$ NMR, ppm)	-350.9	-352.0 [a]	-280.9
$^1J_{P,H}$(Hz)	222	222 [a]	155
$^1J_{P,Pb}$(Hz)	1420	1428 [a]	653
$\delta(^{29}Si$ NMR, $SiMe_3$,ppm)	-2.4 [b]	-2.36 [b]	-3.6
$\delta(^7Li$ NMR, ppm)	-	0.95 [a]	2.1

All recorded in THF-d8 at 253K except [a]: at 243K, [b]: 300K

3.4.3 Crystal Structure

Dark brown X-ray diffraction quality crystals of $[\{(MeNCH_2)_3\}_3K][(Hyp_2Pb)_2\cdot PH_2]$ (**20a**) were obtained from diethyl ether in the presence of triazine at -60°C. The compound crystallizes together with one free molecule of diethyl ether as triclinic, P-1, with two formula units in the unit cell. Crystal data for **20a** are summarized in Table 3.11. Selected bond length and angles are listed in Table 3.12. Several atoms are disordered in the crystal, however, the structure determination gives defined structural parameters.

Table 3.11 Crystallographic data of **20a**.

Empirical formula	$Hyp_4Pb_2PK\cdot$3triazine(Et_2O)
Formula weight(g/mol)	1936.86
Temperature(K)	173(2)K
Crystal system	triclinic
Space group	$P\bar{1}$
Lattice constants(Å,°)	a = 16.460(5) α 95.48(3) b = 16.906(6) β 100.81(3) c = 19.253(6) γ 100.62(3)
Volume(Å^3)	5125(3)
Formula units	2
Density(g/cm^3)	1.255
μ(Mo-K_α)(mm^{-1})	8.881
2Θ range(°)	2.68 to 73.89
Reflections measured	21220
Independent reflections	20580 [R(int) = 0.0906]
Ind. Reflections with $F_o > 4\sigma(F_0)$	20580
Parameter	914
R1,R1(all reflections)	0.0743, 0.0945
wR2,wR2(all reflections)	0.1928, 0.2081
GooF	1.021
Residual electron density(e/Å^3)	4.631

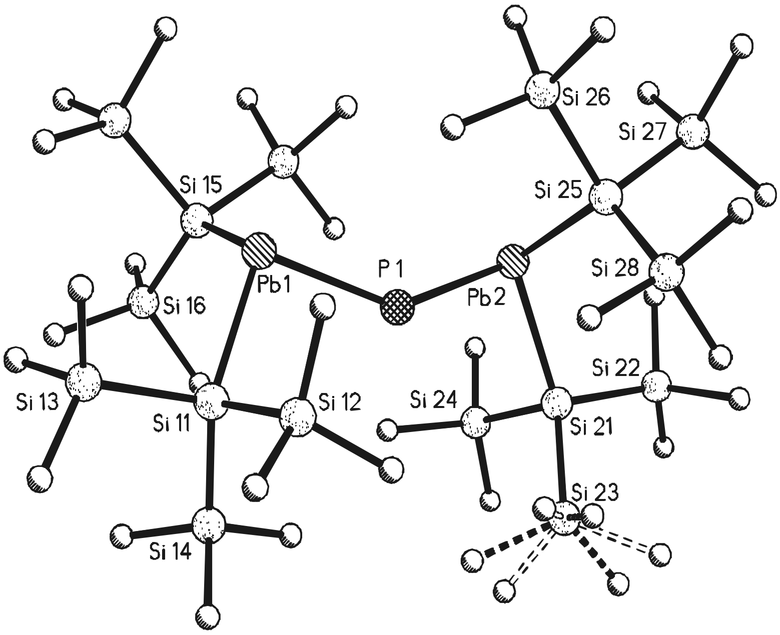

Figure 3.14: The structure of the anion part of **20a.** Atoms are represented by spheres of arbitrary radii; hydrogen atoms are omitted for clarity. Dashed bonds are used to symbolize the disordered orientations. One of the trimethylsilyl groups is two-fold disordered in a ratio of 0.41/0.59.

As revealed by X-ray diffraction analysis, the structure of **20a** displays a salt composed of separated solvated potassium cations, $[\{(MeNCH_2)_3\}_3K]^+$, and $[(Hyp_2Pb)_2{\cdot}PH_2]^-$ anions. No short K···P contacts are found.

In the anionic part(Figure 3.14), one of the lead atoms is disordered in a ratio of 0.87 (Pb1) to 0.13 (Pb1A) as stereoscopically displayed in Figure 3.15. Although the two hydrogen atoms bonded to phosphorus, which could be unambiguously deduced from NMR data, can not be observed in the structure, the angle of Pb-P-Pb of 142.00(9) implies already the distorted tetrahedral coordination environment of phosphorus. Both lead atoms of the dihypersilylplumbylene molecules, coordinated to the same phosphorus atom, have coordination number three and each display a trigonal pyramidal environment. The Pb-P bond lengths with a mean value of 283.2pm are approximately 8 pm longer than in compound **15a**, probably owing to the steric demand of hypersilyl groups. Additionally, the average angle of P-Pb-Si of 97.42° is also wider than those observed in **15a** (av. 94.55°). As a consequence of the higher coordination number of the Pb atoms, the Pb-Si bond lengths in this anion ranging between 273.5(2) and 279.2(2)pm are significantly longer than the corresponding contacts in dihypersilylplumbylene [270.0(3), 270.4(3)pm]. The elongation of the Pb-Si bond lengths are comparable to that observed for compound **15a**.

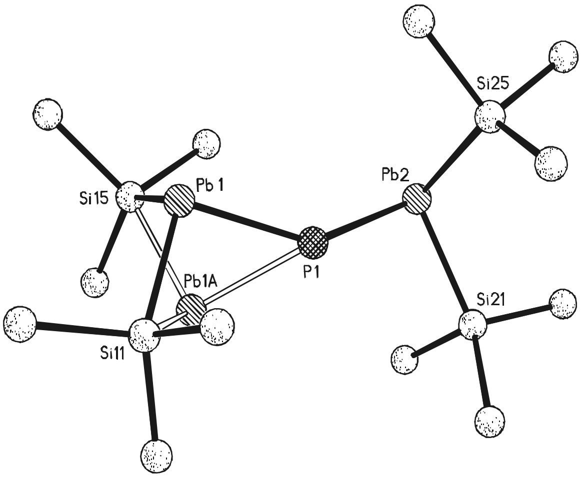

Figure 3.15 Stereoscopic representation of the disordering of the lead atom in the anion part of compound **20a** with the same orientation as shown in Figure 3.13. Empty bonds are used to symbolize the arrangement of the minor component.

At first glance, the unusual structural feature of the cation part of compound **20a** is that the potassium center is coordinated to three triazine molecules with mearly ideal C_{3h} symmetry. The threefold axis runs through the K atom and is oriented perpendicular to the plane defined by the three centroids of the triazine molecules. As Figure 3.16(a) reveals, the potassium atom is approximately coplanar with the centers of the three triazine molecules, however, the whole cation part does not possess a C_{3h} symmetry due to the orientation of methyl groups in triazine.One of the triazine molecules is two-fold disordered as shown in Figure 3.16(b). The K⋯N distances, ranging from 278.9(18) to 318(2)pm are considerably longer than the sum of the covalent radii of potassium and nitrogen(273pm) and comparable to those found in the structure of compound **1c**.

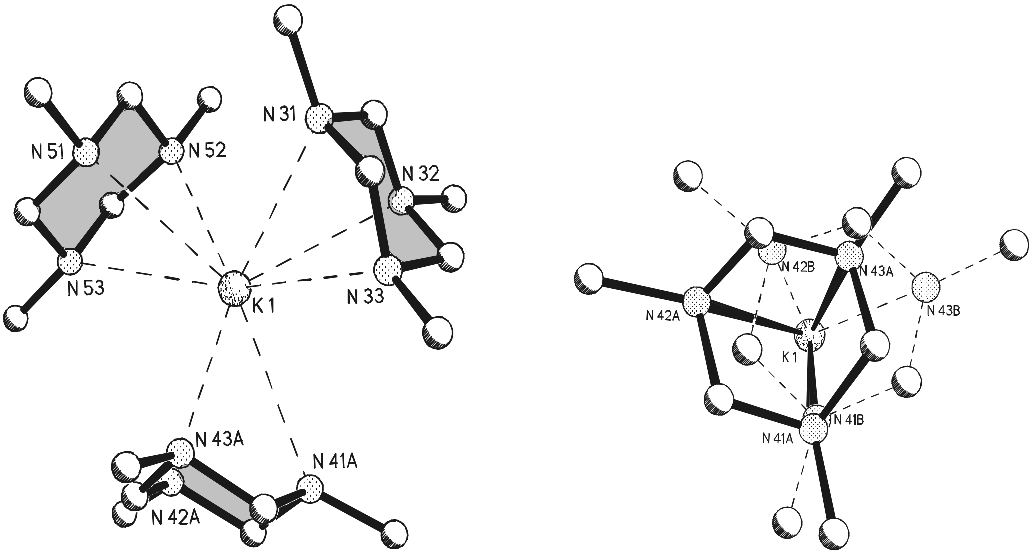

(a) (b)

Figure 3.16 (a). Structure of the cation part of compound **20a** (one of the disordered conformation of triazine is omitted). (b). The arrangement of the disordered triazine (dashed lines are used to symbolize the disordered orientations). The population ratio of the two conformations amounts to 0.58/0.42. Atoms are represented by spheres of arbitrary radii; hydrogen atoms are omitted for clarity.

Table 3.12 Selected interatomic distances (pm) and angles (°) of **20a**.

Pb1-Si15	273.5(2)	K1-N53	306.8(11)
Pb1-Si11	277.7(3)	K1-N41A	308.6(18)
Pb1-P1	283.6(2)	K1-N42A	310(2)
Pb1A-Si15	277.6(4)	K1-N31	316(2)
Pb1A-Si11	284.4(4)	K1-N33	318(2)
Pb1A-P1	286.4(3)	Pb2-P1-Pb1A	133.69(10)
Pb1A-Si16	326.4(4)	Pb2-P1-Pb1	142.00(9)
P1-Pb2	282.8(2)	Si15-Pb1-Si11	112.24(8)
Pb2-Si25	276.3(2)	Si15-Pb1A-Si11	109.05(12)
Pb2-Si21	279.2(2)	Si11-Pb1A-Si16	121.88(12)
Si-Si	av. 234.2	Si25-Pb2-Si21	101.8(7)
K1-N43A	278.9(18)	Si15-Pb1A-P1	98.40(12)
K1-N32	284.8(15)	Si11-Pb1A-P1	92.72(10)
K1-N41B	282(3)	P1-Pb1A-Si16	133.80(13)
K1-N42B	280(3)	Si15-Pb1-P1	100.03(8)
K1-N52	293.2(8)	Si11-Pb1-P1	94.75(7)
K1-N51	299.3(11)	Si25-Pb2-P1	98.28(7)
K1-N43B	306(3)	Si21-Pb2-P1	96.62(7)

3.5 Hyp$_2$Sn·PMe$_3$(21) and Hyp$_2$Pb·PMe$_3$(22)

3.5.1 Synthesis

If both dihypersilylstannylene and plumbylene are treated with trimethylphosphane in n-pentane or toluene at -20°C, an immediate colour change from brown to yellow and blue to red will be observed, respectively. The ^{31}P-NMR spectra, showing only one signal for each of the reaction solutions, indicate that the reactions of Eq. 3.4 quantitatively occurred.

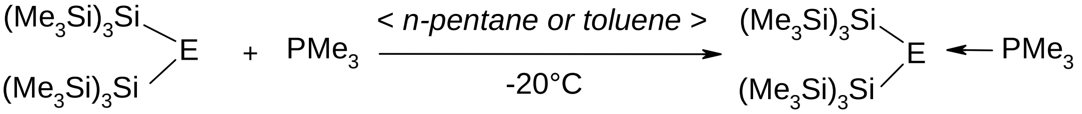

(Eq. 3.4)

E=Sn **21**
E=Pb **22**

The expected phosphane adducts **21**, **22** are obtained in high yields as orange-yellow and red crystalline compounds. No re-dissociation is detectable in solution under reduced pressure. These compounds are air- and moisture-sensitive, although they can be stored in the solid state for a long time under argon. Attempt to grow single crystals from n-pentane, cyclopentane, or toluene unfortunately failed. The formulated forms, however, have been proved unambiguously by NMR spectroscopy.

3.5.2 NMR Spectroscopy

The $^{31}P\{^1H\}$-NMR(cyclopentane+10%C_6D_6, 243K) spectrum of phosphane adduct **21** exhibits a broad singlet flanked by $^{117/119}Sn$ satellites, showing a $^1J_{119Sn,P}$ coupling constant of 1960Hz and a $^1J_{117Sn,P}$ coupling constant of 1881Hz (Figure 3.17). The chemical shift of the resonance (-60.1ppm), however, is similar to that of free PMe_3(-62ppm).

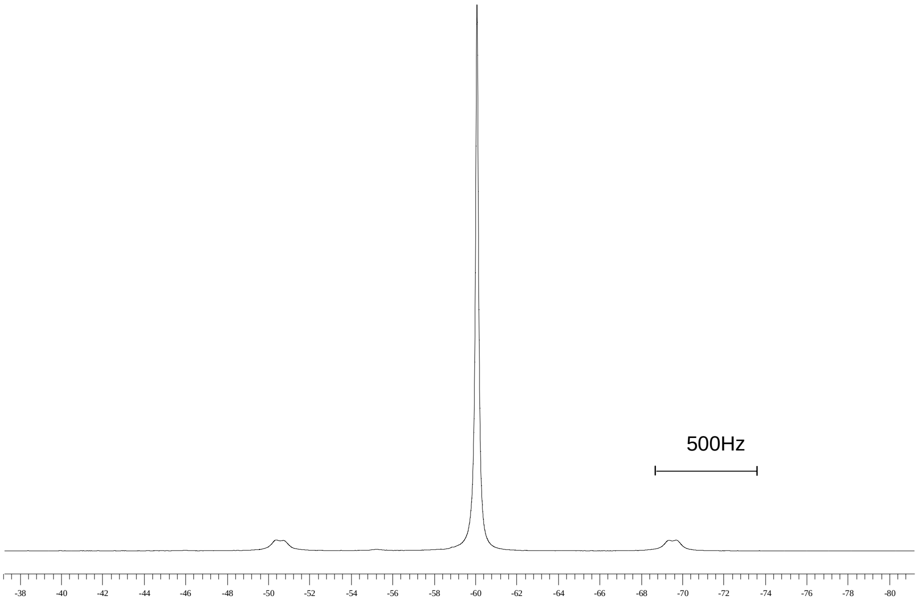

Figure 3.17 Observed $^{31}P\{^1H\}$-NMR spectrum of **21** at 101.256MHz in 10%benzene-d6+cyclopentane(243K):δ=-60.1ppm, $^1J_{P119Sn}$= 1960Hz, $^1J_{P117Sn}$= 1881Hz.

In accordance with the ^{119}Sn satellites observed in the $^{31}P\{^1H\}$-NMR spectrum, the ^{119}Sn-NMR(C_6D_6, 300K) spectrum exhibits a doublet at -37ppm with a coupling constant $^1J_{119Sn,P}$ of 1930Hz, which is considerably greater than $^1J_{117/119Sn,P}$ of 1580Hz observed in $(PMe_3)Sn[TeSi(SiMe_3)_3]_2$[139]. From the ^1H-NMR(C_6D_6, 300K) spectrum of **21**, which shows a singlet at 0.44ppm(54H) derived from the hypersilyl group and a doublet with a two-bond phosphorus-hydrogen coupling constant $^2J_{P,H}$ of 7.5Hz at 1.07ppm(9H) assignable to the methyl groups of trimethylphosphane, the formulated simple 1:1 adduct of dihypersilylstannylene and trimethylphosphane can be concluded directly.

The ^{31}P NMR(C_6D_6,300K) spectrum of **22** exhibits also a broad singlet at -111.8ppm, shielded strongly compared to that of uncoordinated PMe_3. No satellites of ^{207}Pb can be observed in the spectrum, just as no satellites of $^{117/119}Sn$ found in the $^{31}P\{^1H\}$-NMR spectrum of **21** recorded at 300K, implying the existence of dynamic behaviour in benzene-d_6 solution at room temperature. The ^{1}H NMR(C_6D_6, 300K) spectrum of **22** is similar to that of **21** and shows a singlet at 0.48ppm (54H) for the hypersilyl group and a doublet with $^2J_{P,H}$= 7.5Hz at 1.17ppm (9H) for trimethylphosphane. These reflect again the composition of the Lewis acid-base adduct, the formulated 1:1 adduct of dihypersilylplumbylene and trimethylphosphane.

3.6 [HypP(H)PbHyp]$_2$ (17)

3.6.1 Synthesis

When phosphane (PH_3), generated from the reaction of $LiPH_2$ with 2,6-di-tert-butylphenol in DME, is allowed to bubble through a solution of dihypersilylplumbylene in n-pentane at room temperature, an immediate reaction takes place, indicated by a colour change from deep blue to dark red. On cooling at -60°C black crystals are isolated which were identified by its NMR and X-ray diffraction data as dimeric hypersilyl lead(II) hypersilylphosphanide (**17**). The yields are good, however, according to the NMR spectra of the reaction mixture, $(Me_3Si)_3SiH$ as well as small amounts of dihypersilylphosphane and **12** were formed along with the main product **17.** After standing the sealed NMR tube of a C_6D_6 solution of **17** for 24h at ambient temperature, the resonance of **17** disappears completely, and dihypersilylphosphane and **12** are formed quantitatively.

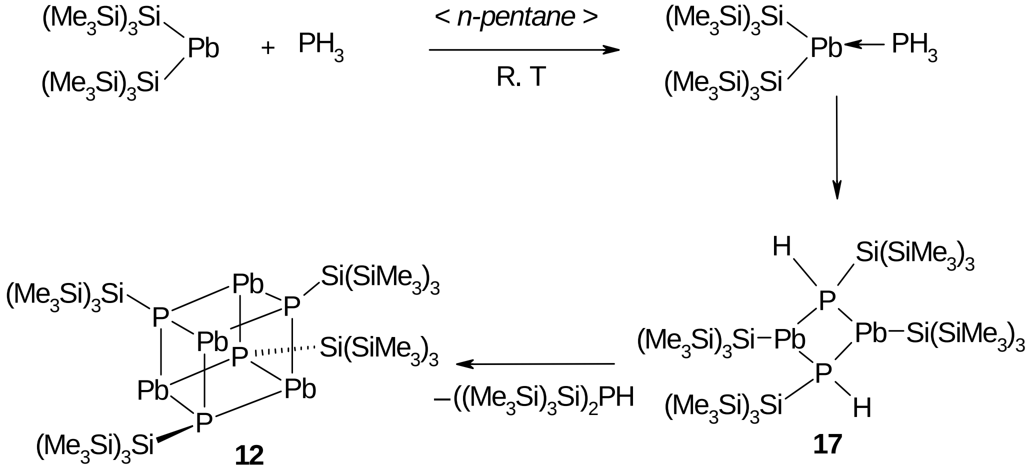

Scheme 3.5

We assumed that compound **17** has been formed via a Lewis adduct of dihypersilylplumbylene and PH_3 followed by hypersilyl group migration and $(Me_3Si)_3SiH$ elimination. In an attempt to find some experimental evidences, PH_3 was allowed to bubble through a cooled (-30°C) n-pentane solution of dihypersilylplumbylene. The ^{1}H-coupled ^{31}P

NMR spectrum of the resulting solution recorded at -20°C shows only a quartet at -286.5ppm ($^1J_{P,H}$ = 236Hz) and a triplet at -224.2ppm ($^1J_{P,H}$ = 236Hz). In spite of showing no ^{207}Pb satellites, because of the observed high-field shift of more than 40 ppm when compared with uncoordinated PH_3 (δ = -242.5ppm, $^1J_{P,H}$ = 187Hz) we think that the quartet originates from the primary Lewis-acid-base adduct of PH_3 and dihypersilylplumbylene. The triplet at -224.2ppm indeed shows ^{207}Pb satellites and can be ascribed to either $HypPb(H)\leftarrow PH_2Hyp$ or to $(HypPbPH_2)_x$, both being most probable intermediates in the reaction to **17**[*].

Compound **17** can also be synthesized by treating $HypPH_2$ (prepared from protolysis of compound **1**) with dihypersilylplumbylene in benzene at room temperature (Eq. 3.4). The reaction is completed in about 30 minutes, further standing at ambient temperature would lead to decomposition of **17** as decribed above. According to the ^{31}P-NMR spectrum of the reaction mixture, compound **17** could be obatined in about 70% yield.

$$2\ Hyp_2Pb + 2\ HypPH_2 \rightarrow \underset{\mathbf{17}}{[HypPbP(H)Hyp]_2} + 2\ (Me_3Si)_3SiH \qquad \text{(Eq. 3.4)}$$

3.6.2 NMR Spectroscopy

Compound **17** was unambiguously identified by ^{31}P NMR data and confirmed by X-ray structure analysis. The ^{31}P{H} NMR(C_6D_6, 300K) spectrum displays a sharp singlet flanked by ^{207}Pb satellites at characteristic high field (δ=-367.4). The considerably large one-bond coupling constant of $^1J_{p,pb}$=1622Hz lies very close to those observed for the bridging phosphorus atoms in the cis- and trans-isomer of $\{Pb[P(SiMe_3)_2]_2\}_2$[133] (598Hz and 1658Hz). The ^{1}H-coupled ^{31}P-NMR spectrum of the same sample exhibits a multiplet of higher order flanked by ^{207}Pb satellites, the A part of a AA'XX' spin system (A, A'=^{31}P; X, X'=^{1}H). The X part of this spin system is also observed at 3.4 ppm in the ^{1}H NMR spectrum. Approximate values for $J_{P,P}$ and $J_{P,H}$ can be estimated by simple examination of the experimental spectrum. Starting from these values the spectrum can be solved by iterative fitting[110]. The experimental and the calculated spectra are summarized in Figure 3.18. These resonances pertain obviously to the structure observed in the solid state (see blow), in which the hypersilyl groups are all trans to one another. On cooling, the signals in the ^{1}H, ^{31}P, and ^{29}Si NMR spectra of **17** shift

---

[*] As mentioned above, if the dihypersilylplumbylene is not pure enough, *i.e.*, containing $KN(SiMe_3)_2$ from the preparation, PH_3 may react with the potassium amide and compound **20** may precipitate as a black solid from the reaction mixture according to Scheme 3.4.

only slightly. Even at our low-temperature limit (-60°C), no significant change can be observed. It is remarkable, cis and trans isomers of the model complex [Pb(μ-H)H]$_2$ was found to be nearly isoenergetic[140]. The existence of only one isomer of **17** in the solid state as well as in solution may be owing to the steric demands of the hypersilyl groups.

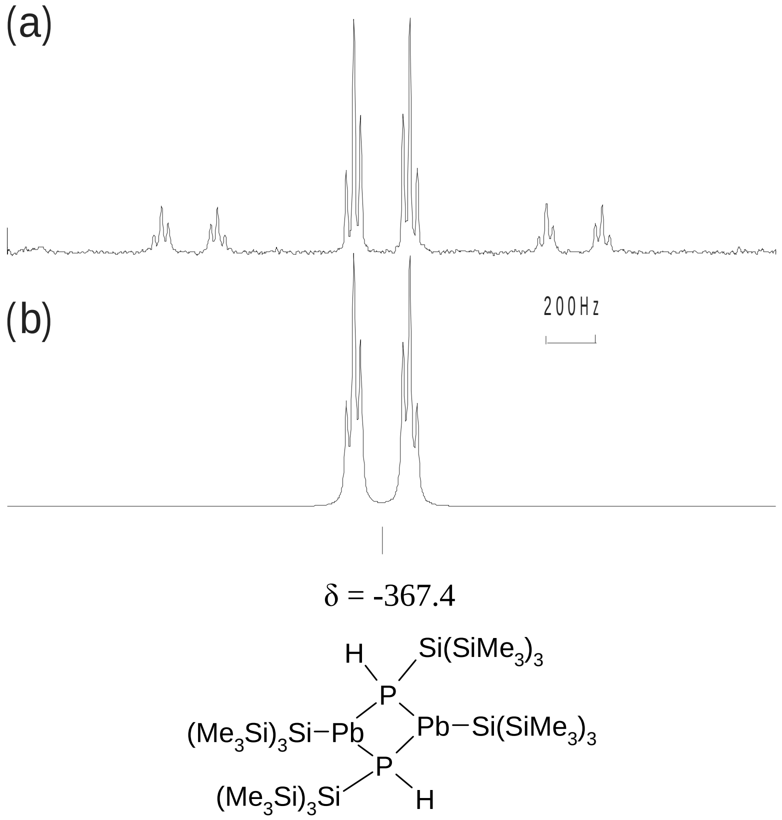

17

Figure 3.18 Observed (a) and calculated (b) ^{31}P NMR spectrum of **17** at 101.256MHz in C_6D_6 (300K): δ=-367.4ppm, $^1J_{P,H}$= 233.2Hz, $^3J_{P,H}$= 2.3Hz, $^4J_{H,H}$= 0 Hz, $^2J_{P,P}$= 59.8Hz, $^1J_{P,Pb}$=1622Hz.

3.6.3 Crystal Structure

Dark crystals of compound **17** suitable for X-ray diffraction analysis were obtained from diethyl ether. Figure 3.19 shows the molecular structure and the numbering scheme of dimeric **17**. The diethyl ether molecule originating from the recrystallization is not shown. The crystal data are summarized in Table 3.13. Selected bond lengths and angles are listed in Table 3.14.

Table 3.13 Crystallographic data of **17**.

Empirical formula	$Hyp_4P_2(H)_2Pb_2{\cdot}Et_2O$
Formula weight(g/mol)	1541.10
Temperature(K)	188(2)K
Crystal system	monoclinic
Space group	P2(1)/n

Lattice constants(Å,°)	a = 14.4402(4) α 90 b = 24.4936(6) β 94.287(2) c = 22.2942(6) γ 90
Volume(Å^3)	7863.2(4)
Formula units	4
Density(g/cm^3)	1.302
μ(Mo-K$_\alpha$)(mm^{-1})	4.585
2Θ range(°)	3.43 to 28.31
Reflections measured	71278
Independent reflections	19355 [R(int) = 0.0738]
Ind. Reflections with $F_o > 4\sigma(F_0)$	19355
Parameter	745
R1,R1(all reflections)	0.0460, 0.0835
wR2,wR2(all reflections)	0.0995, 0.1197
GooF	1.036
Residual electron density(e/Å^3)	1.917

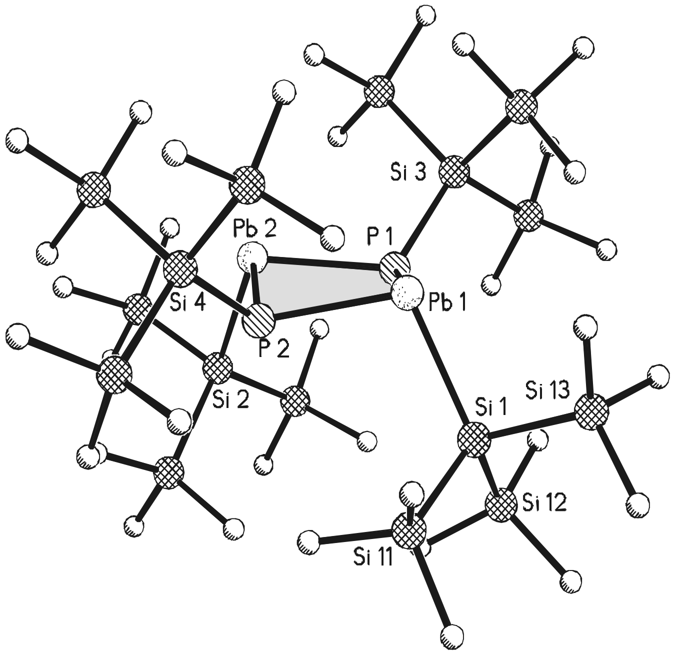

Figure 3.19. Molecular structure of compound **17**. Atoms are represented by spheres of arbitrary radii; hydrogen atoms are omitted for clarity.

The whole molecule was disordered in a ratio of 0.91/0.09 (Figure 3.20). In the solid state, compound **17** adopts a dimeric molecular structure with the central moiety of a slightly distorted Pb_2P_2 ring shielded by the sterically bulky hypersilyl substituents which are all trans to one another and stretch away from the Pb_2P_2 ring. According to the NMR investigation, both phosphorus atoms each bear an additional hydrogen atom. Unfortunately, these hydrogen atoms could hardly be identified by crystallography because the disordered Pb atoms are found almost right at the position where the hydrogen atoms may locate. The central Pb_2P_2 ring with a puckered rather than a planar geometry (folding angles are approximately 20°) also implys the existence of stereochemically active lone pairs on the three-coordinate lead atoms. It is remarkable that $\{Pb[P(SiMe_3)_2]_2\}_2$[133] displays a cis-isomer conformation with a similarly puckered Pb_2P_2 ring, whereas $\{Pb[P\text{-}tert\text{-}Bu_2]_2\}_2$[132] shows a trans-isomer structure with a planar central Pb_2P_2 ring. The Pb-P bond lengths of **17**, ranging from 277.62(17) to 279.65(17) pm, lie very close to those observed in $\{Pb[P(SiMe_3)_2]_2\}_2$[133] [274.7(7) to 279.6(7)pm], but slightly longer than those observed in compound **12** [272.0 to 274.6(5)pm]. With the three-coordinate lead atoms, the two Pb-Si distances [277.1(3) and 278.5(2)pm] are expectedly longer than those found in its precursor dihypersilylplumbylene (about 270pm).

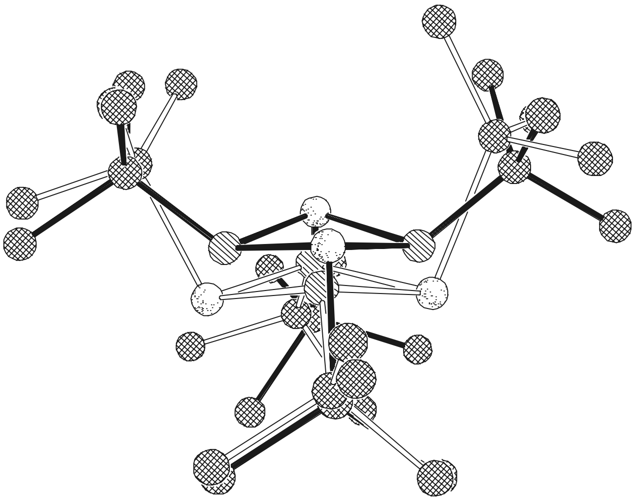

Figure 3.20 Representation of the disordering model of **17**. The population ratio amounts to 0.91 (solid bonds) / 0.09 (empty bonds).

Table 3.14 Selected interatomic distances (pm) and angles (°) for **17**.

Pb1-P1	277.62 (17)	P2-Si4	228.2 (2)
Pb1-P2	279.43 (16)	Si-Si	233.0(3) to 237.1(3)
Pb2-P1	279.21 (17)	P1-Pb1-P2	79.56 (5)
Pb2-P2	279.65 (17)	P1-Pb2-P2	79.25 (5)
Pb1-Si1	278.5(2)	Pb1-P2-Pb	98.46 (5)
Pb2-Si2	277.1(3)	Pb1-P1-Pb2	98.99 (5)
P1-Si3	228.6(3)		

4 Hypersilyl Stabilized Lead Clusters

4.1 Overview

Several anionic cluster compounds of lead have been synthesized during the last decades[141 142 143]. The first species $NaPb_4$ and KPb_2 had already been obtained in 1891 by Joanis from the reaction of alkali metals with lead in liquid ammonia[144 145]. Extensive exploration of this chemistry was done by Kraus, Zintl and others during the first decades of the 20th century[146 147]. Addition of cryptants finally allowed for the isolation of macrocrystalline material and the structural characterization of several anionic species such as Pb_5^{2-}, Pb_9^{4-} and Pb_9^{3-}[148 149]. The structures observed may all be understood using Wade's electron counting rules.

Molecular species bearing hydrocarbyl or related organoelement substituents at the lead skeleton are, however, very scarce. Very recently, Power et al. reported the first lead analogue of a substituted acetylene molecule, 2,6-$Trip_2H_3C_6PbPbC_6H_3$-2,6-$Trip_2$ (Trip = 2,4,6-triisopropylphenyl)[150]. Using the smaller substituent (Trip) Weidenbruch et al. synthesized Pb_2Trip_4 as the first example of a molecule with a lead / lead double bond[151]. Later they prepared the cyclotriplumbane Pb_3R_6 by utilizing a less bulky substituent 2,4,6-triethylphenyl[152]. All attempts to transform the Pb_x^{y-} salts to such derivatives by the reaction with electrophiles failed and no organically substituted lead deltahedron species with naked lead atoms reported to date. There are some reports however for transition-metal carbonyl complexes of lead clusters[153]. Only for the lighter congeners germanium and tin hydrocarbyl or organoelement substituted species became available very recently: $[Sn_8(2,6\text{-}Mes_2C_6H_3)_4]$(Mes=2,4,6-$Me_3C_6H_2$)[154], $[Sn_8\{Si(CMe_3)_2\}_6]$[155], $[Ge_9\{Si(SiMe_3)_3\}_3]^-$[156] and $[Ge_8\{N(SiMe_3)_2\}_6]$[157]. Their synthesis had not used anionic clusters, however, but proceeded through cluster formation from smaller units. It became evident that for those examples as for cluster of the neighbouring elements of the group 13 Wade's rules are sometimes, but not generally obeyed.

4.2 Hyp_6Pb_{12} (23)

4.2.1 Synthesis

As mentioned above, when phosphane was bubbled through a dihypersilylplumbylene solution at a temperature below -30°C, compound **12** and **17** were not found in the resulting solution; instead, the primary Lewis-acid-base adduct between PH_3 and dihypersilylplumbylene as well as either $HypPb(H)\leftarrow P(H)_2Hyp$ or $(HypPbPH_2)_x$ were formed according to the ^{31}P spectrum of the reaction mixture recorded at -20°C. In an attempt to isolate one of these metastable species, the supernatant solution of the resulting mixture was stored at -60°C for several weeks. A few dark brown well shaped crystals were found in a matrix of unconsumed red dihypersilylplumbylene crystals. Astonishingly, the structure analysis revealed that the dark brown crystals contained no phosphorus. Instead, the molecular lead cluster $[(Me_3Si)_3Si]_6Pb_{12}$ (**23**) was found (Scheme 4.1).

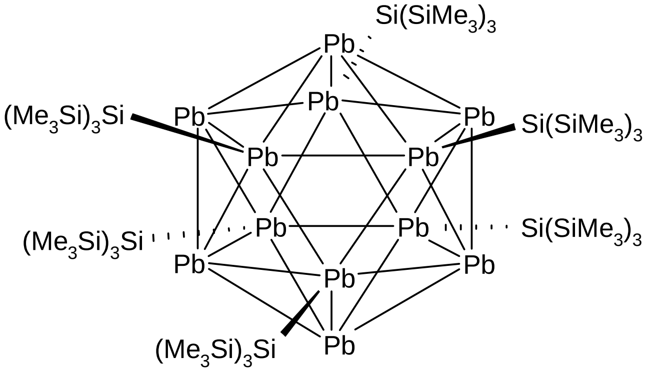

23

Scheme 4.1

Other products detected in the supernatant liquid, such as the monocyclic compound **17**, the heterocubane **12** and $[(Me_3Si)_3Si]_2PH$, indicate that during the reaction hypersilyl groups are transferred from Pb to P. In turn, hydrogen may be transferred from P to Pb to give the presumably unstable hydrido(hypersilyl)plumbylene $(Me_3Si)_3Si\,PbH$ (Scheme 4.2). It is well known that the Pb-H bond is very weak and labile. Compounds bearing this structural fragment easily loose hydrogen or decompose otherwise. Recently a hydridoplumbylene with a very bulky meta-terphenyl substituent was postulated by Power et al as the key intermediate in the formation of the appropriate "diplumbyne" – the first alkyne homologue of lead[150]. Other than this diplumbyne, the analogue $[(Me_3Si)_3Si]_2Pb_2$ would not be stable under normal conditions. It may associate to oligomers, or due to its bis(plumbylene) nature may give self-insertion reactions. By loosing hydrogen or hypersilane such compounds could be possible intermediates in the formation of lead clusters.

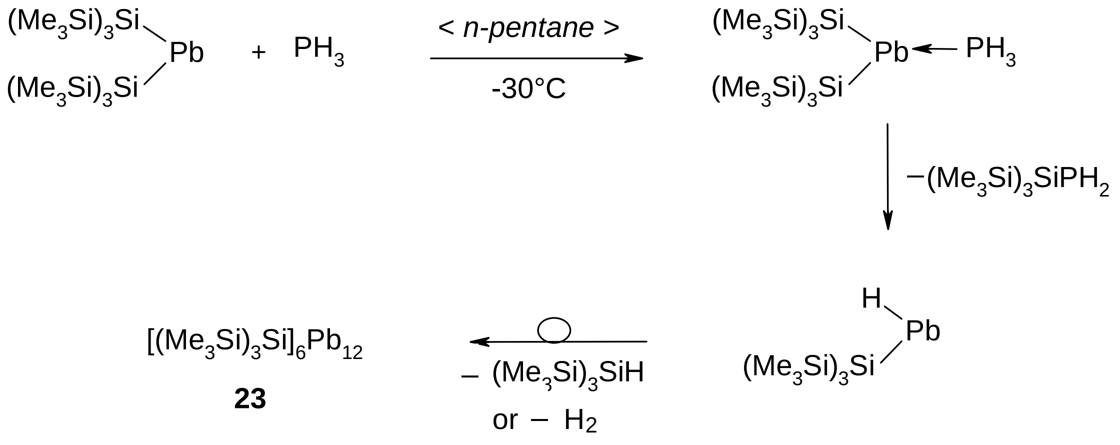

Scheme 4.2

4.2.2 Crystal Structure

A suitable crystal of compound **23** selected from matrix of unconsumed reactant dihypersilylplumbylene was investigated by X-ray diffraction analysis. The view of the molecule in the crystal is shown in Figure 4.1. The crystal data are summarized in Table 4.1. Selected bond lengths and angles are listed in Table 4.2.

Table 4.1 Crystallographic data of **23**.

Empirical formula	Hyp_6Pb_{12}·pentane
Formula weight(g/mol)	4044.42
Temperature(K)	173(2)K
Crystal system	hexagonal
Space group	$R\bar{3}$
Lattice constants(Å,°)	a = 16.1051(3) α 90 b = 16.1051(3) β 90 c = 41.6827(10) γ 120
Volume($Å^3$)	9363.0(3)
Formula units	3
Density(g/cm^3)	2.152
μ(Mo-K_α)(mm^{-1})	16.374
2Θ range(°)	2.44 to 28.31
Reflections measured	23561
Independent reflections	5183 [R(int) = 0.0798]
Ind. Reflections with $F_o > 4\sigma(F_0)$	5183
Parameter	192
R1,R1(all reflections)	0.0459, 0.0756
wR2,wR2(all reflections)	0.1093, 0.1242
GooF	1.044
Residual electron density(e/$Å^3$)	1.332

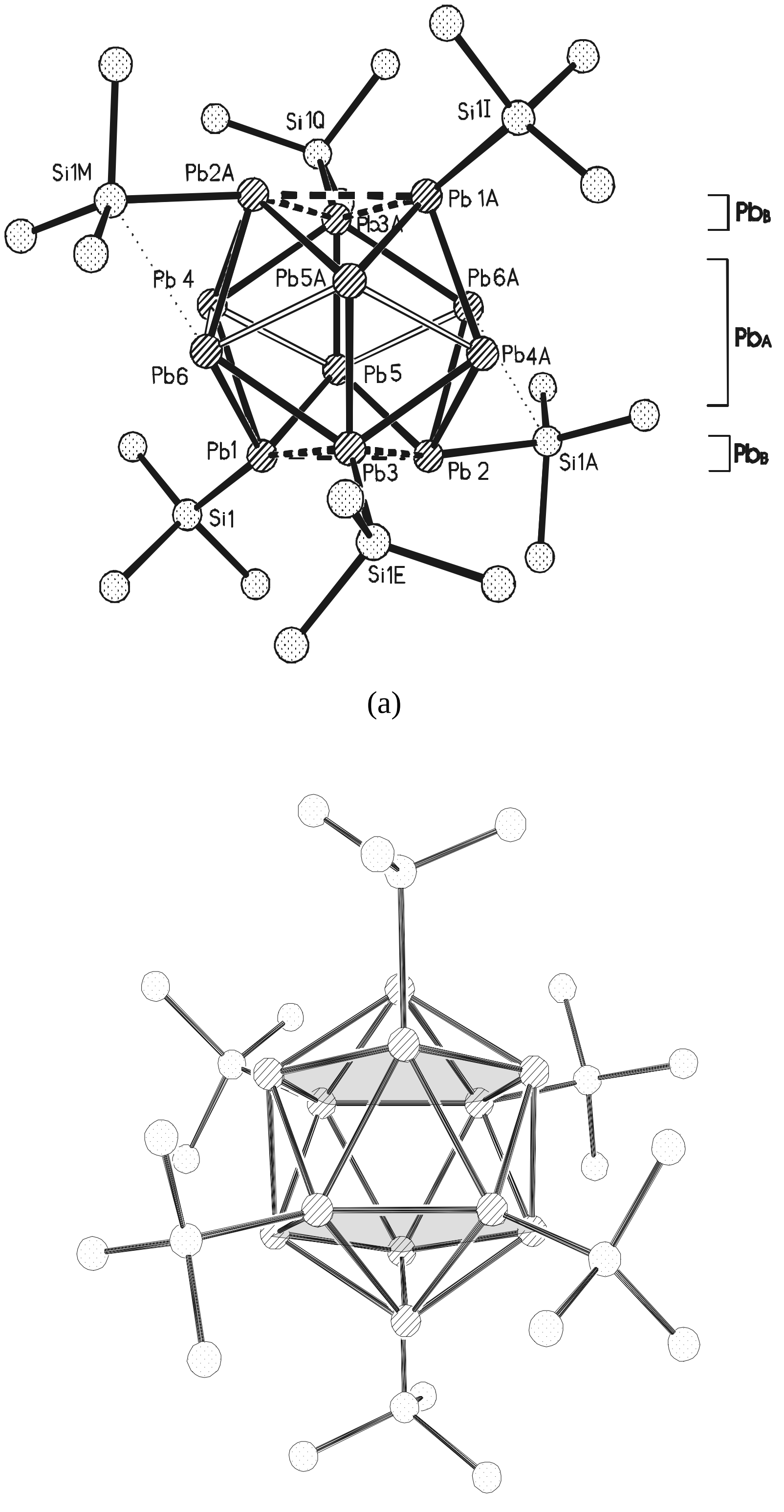

Figure 4.1 $Pb_{12}Si_{24}$ skeleton of the lead cluster **23** as found in the crystal structure. Differing orientations have been chosen for better illustrating the structure details. Methyl groups are omitted for clarity. (a): Pb-Pb contacts within the open faces of the icosahedron are indicated by dashes, short intramolecular Pb-Si contacts are indicated by dots. Atom groups belonging to the "belt" are denoted as Pb_A, those of the capping triangles as Pb_B.

Despite of disordering of the lead atoms about the crystallographic three-fold axis, the structure parameters could be refined with great accuracy. The twelve lead atoms constitute a distorted but still centrosymmetric icosahedron. It can be seen from the space filling model (Figure 4.2) that the sterically crowding hypersilyl groups effectively surround the Pb_{12} moiety thereby ensuring its stability against decomposition. As shown in Figure 4.1a, six atoms (Pb_A) bear no substituent and form a puckered ring with chair conformation (the belt). The remaining six atoms (Pb_B) each bearing a hypersilyl group form two three-membered rings above and below the central Pb_6 belt. The Pb-Pb distances between neighbouring lead atoms range from 307.6(1) to 338.9(1)pm. The longest distances are found between the lead atoms of type Pb_B the shortest between Pb_A and Pb_B, giving rise to the description of the polyhedron as an icosahedron with two open faces. This finding is in line with the expectations according to Wade's rules. Having 30 electrons for the Pb_{12} skeleton (2 from each naked Pb and 3 from each lead bearing a substituent) an *arachno*-type cluster is expected. One structural peculiarity of compound **23** remains worth mentioning and is not understood. Whereas four hypersilyl groups are bonded in the expected end-on fashion (Pb-Si 263.8(2) – 269.6(2) pm), two substituents show a bridging functionality [Pb(2A)-Si1M 3 308.5(2), Pb6-Si1M 328.2(2) pm and their symmetry equivalents].

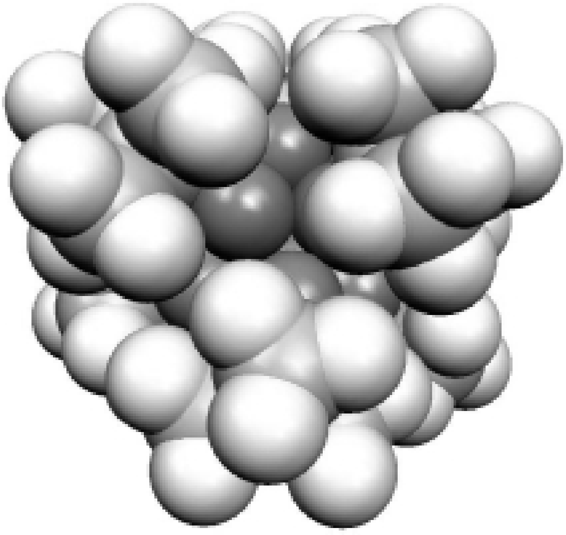

Figure 4.2 Space filling model of **23** illustrating the high steric protection of the Pb_{12} moiety (hydrogen atoms are omitted).

Table 4.2 Selected interatomic distances (pm) for **23**.

Pb1-Pb4	311.0(5)	Pb3-Pb4A	311.0(9)
Pb1-Pb5	311.18(13)	Pb3-Pb6	323.35(13)
Pb1-Pb3	332.41(10)	Pb4-Pb6	323.3(9)
Pb1-Pb6	334.92(12)	Pb4-Pb5	326.7(6)
Pb1-Pb2	336.82(11)	Pb5-Pb6A	324.52(11)
Pb2-Pb6A	305.58(14)	Pb3-Si1E	263.8(2)
Pb2-Pb5	319.88(11)	Pb2-Si1A	308.5(2)
Pb2-Pb4A	321.7(2)	Pb4A-Si1A	328.2(2)
Pb3-Pb5A	310.13(13)	Si-Si	234.3(3) to 234.7(3)

4.3 Hyp_6Pb_{10} (24)

4.3.1 Synthesis

In order to prove our assumption of the formation of Hyp_6Pb_{12}(**23**) and find a rational route to synthesize Pb(H)Hyp, some efforts have been made. The reactions of dihypersilylplumbylene with several hydride sources, such as B_2H_6 and $NaBH_4$ at various conditions, however, lead only to the nearly quantitative formation of elementary lead and hypersilane $(Me_3Si)_3SiH$ or the reversible formation of adducts (Eq. 4.1, 4.2).

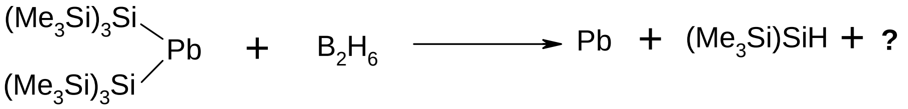

(Eq. 4.1)

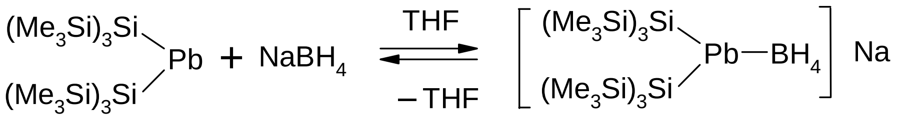

(Eq. 4.2)

(as THF adduct)

Finally, by using the strategy of synthesis of unsymmetrical substituted plumbylenes aryl(hypersilyl)plumbylene[46], dihypersilylplumbylene is allowed to react with the triphenylphospine adduct of copper hydride at -20°C and indeed a spontaneous but slow reaction is found. The deep blue suspension turns to a dark brown solution from which, on cooling to -60°C, appreciable amounts (ca. 30% yield) of dark brown crystals are isolated.

The structural analysis shows them not to consist of the expected $[(Me_3Si)_3Si]_6\ Pb_{12}$ but another molecular lead cluster compound: $[(Me_3Si)_3Si]_6Pb_{10}$(**24**).

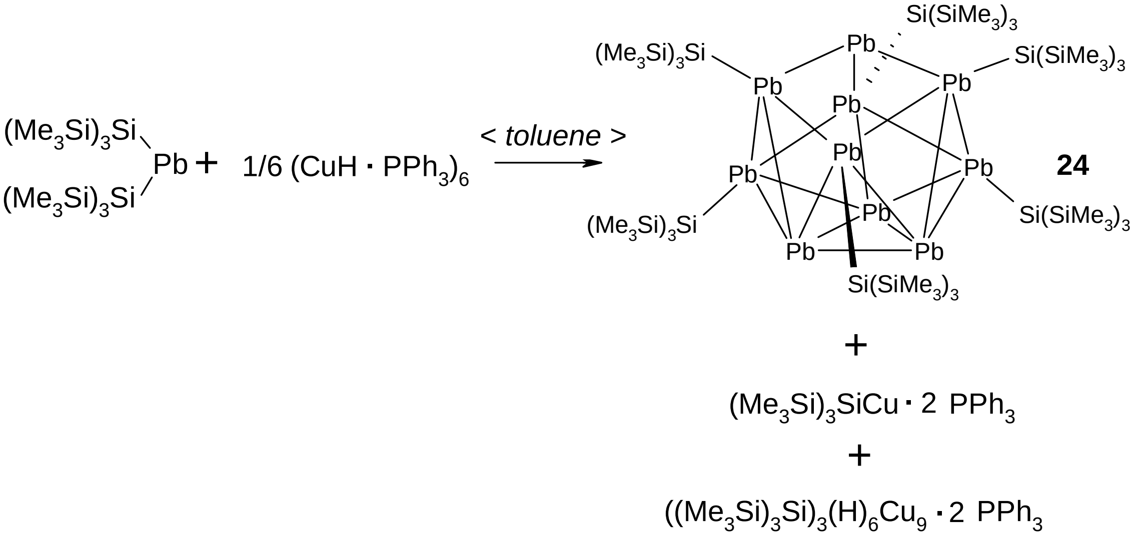

Scheme 4.3

The inspection of the NMR data obtained from pure **24** and from the crude reaction mixture revealed that ligand exchange took place, since the main products besides cluster compound **24** comprise $(Me_3Si)_3SiH$, $(Me_3Si)_3SiCu(PPh_3)$, and $[(Me_3Si)_3Si]_3Cu_9(H)_6(PPh_3)_2$. Further products are present, however, giving unusual high field ^{1}H-NMR signals between 0.6 and 0.8 ppm as does compound **24** (0.64 ppm). Moreover, a small singlet observed at 0.51 ppm, which could also be found at the ^{1}H NMR spectrum of the reaction mixture of dihypersilylplumbylene with PH_3, might be assignable to compound **23**. It is therefore assumable that a mixture of several cluster compounds is produced, from which only the predominant and less soluble species crystallizes easily.

Similar experiments have been carried out with two aluminium hydrides. According to the NMR spectra, the reactions lead to the formation of compound **24** (Eq. 4.3; Eq. 4.4). No resonance at 0.51 ppm or between 0.6 and 0.8 ppm except for the signal assignable to **24** is observed in ^{1}H NMR spectrum of the resulting mixture for these reactions, indicating that compound **24** is the only lead cluster formed under these conditions. However, because of the reactivity of these aluminium hydrides, the expected product of compound **24** isolated from the resulting mixtures always contaminates with small amounts of elementary lead. Therefore, the most suitable route to cluster compound **24** is still the reaction with copper hydride, which can provide pure product as crystals.

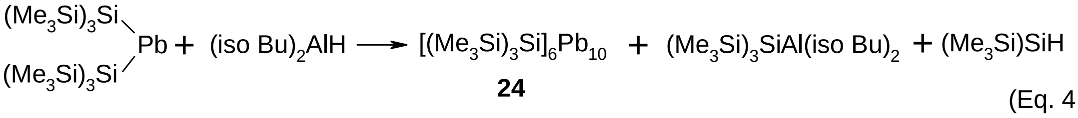

$$\begin{array}{l}(Me_3Si)_3Si\diagdown\\ \qquad\qquad\quad Pb\\ (Me_3Si)_3Si\diagup\end{array} + (iso\ Bu)_2AlH \longrightarrow \underset{\mathbf{24}}{[(Me_3Si)_3Si]_6Pb_{10}} + (Me_3Si)_3SiAl(iso\ Bu)_2 + (Me_3Si)SiH$$

(Eq. 4.3)

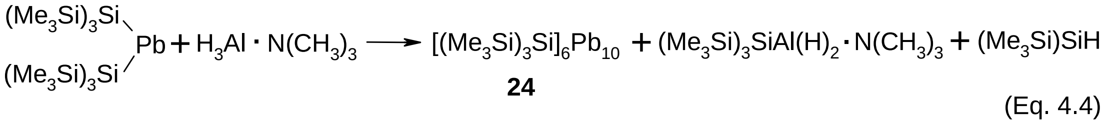

$$\begin{array}{l}(Me_3Si)_3Si\diagdown\\ \qquad\qquad\quad Pb\\ (Me_3Si)_3Si\diagup\end{array} + H_3Al\cdot N(CH_3)_3 \longrightarrow \underset{\mathbf{24}}{[(Me_3Si)_3Si]_6Pb_{10}} + (Me_3Si)_3SiAl(H)_2\cdot N(CH_3)_3 + (Me_3Si)SiH$$

(Eq. 4.4)

At ambient temperature solid **24** is indefinitely stable as long as light is excluded. In solution the cluster slowly undergoes first-order decomposition, yielding the octasilane $(Me_3Si)_3SiSi(SiMe_3)_3$ and a black powder (presumably elementary lead). Further investigation shows that the decomposition of **24** first leads to the formation of dihypersilylplumbylene, which decomposes further to give octasilane and lead as final products. Obviously, disproportionation of compound **24** occurs as the first stage of the decomposition, producing the more stable dihypersilylplumbylene and elementary lead.

4.3.2 NMR Spectroscopy

The ^{1}H-NMR spectrum of **24** recorded at room temperature exhibits only one peak for the protons of hypersilyl groups at 0.64 ppm (in benzene-d_6) or at 0.59ppm (in toluene-d_8). On cooling, the peak at 0.59ppm in toluene-d_8 vanishes. This finding indicates a dynamic behaviour of compound **24** in the solution. The coalescence point is reached at 240K. At 213K, two signals of equal intensity at 0.60 and 0.64 ppm can be observed, giving an approximate activation barrier of 50KJ/mol (Figure 4.2).

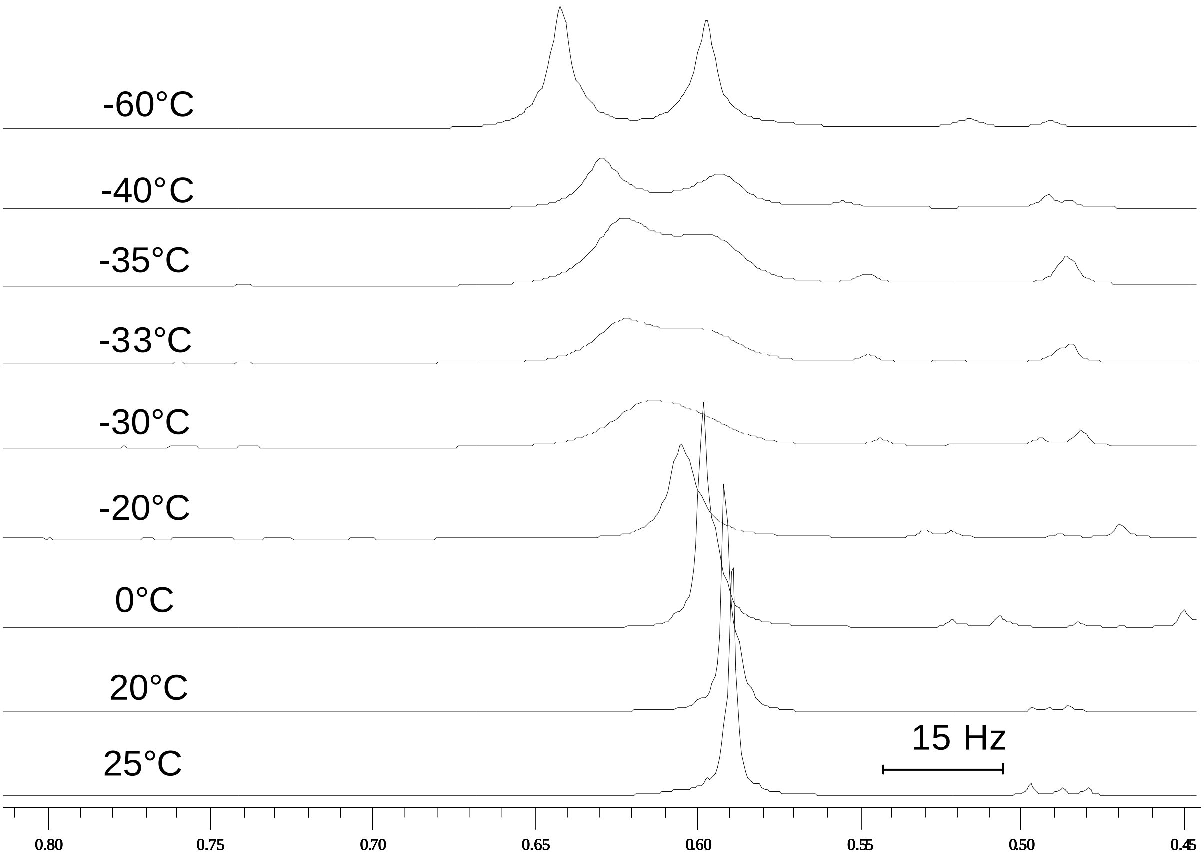

Figure 4.2 Observed temperature dependent ^{1}H-NMR spectrum of **24** at 400.130MHz in toluene-d8.

4.3.3 Mass Spectroscopy

The mass spectrum recorded in Et_2O/MeCN is shown in Figure 4.3. Although the molecular ion of **24** has not been observed in the spectrum, the major ion at mass-to-charge (m/z) 3311 could be unambiguously assigned to $[Hyp_5Pb_{10}]^+$, an ion originating from **24** by losing a hypersilyl group. In addition, the ion at 2815 might be assignable to $[Hyp_3Pb_{10}]^+$.

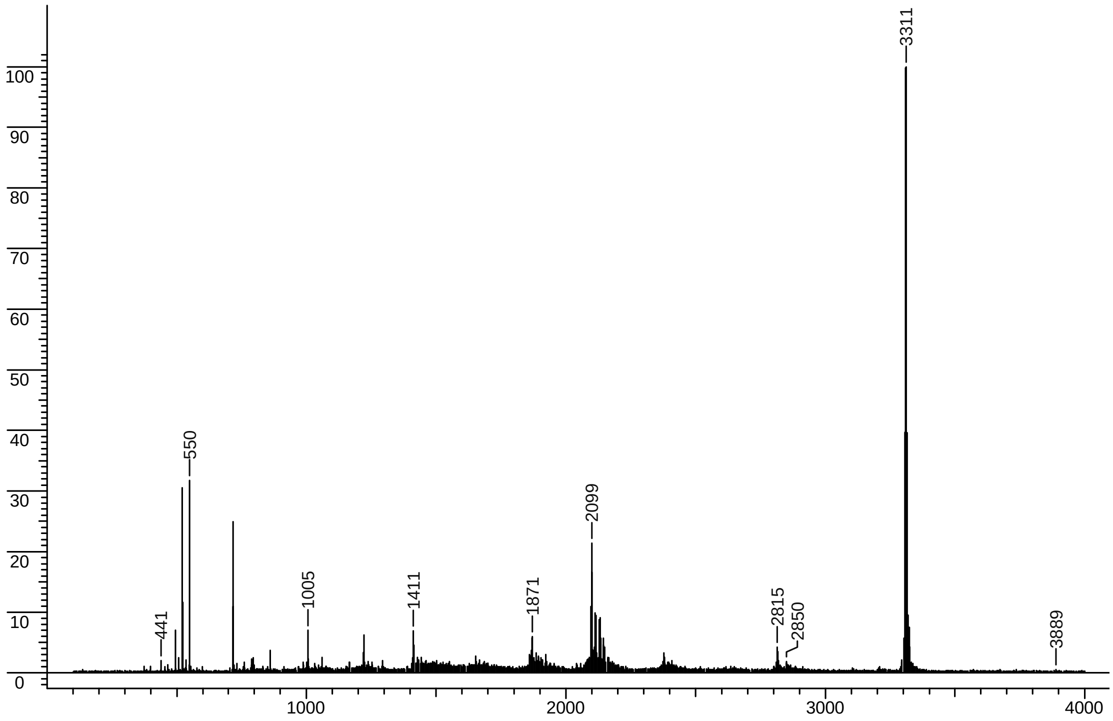

Figure 4.3 Mass spectrum of **24**.

4.3.4 Crystal Structure

Different crystalline phases of **24** were obtained from different solvents. The structure analysis was hampered by twinning. However, from benzene solutions very small single-crystals had been isolated which finally gave structural parameters of sufficient accuracy. Selected data collection parameters and other crystallographic data are summarized in Table 4.3. Selected bond lengths and angles are listed in Table 4.4.

Table 4.3 Crystallographic data of **24**.

Empirical formula	$Hyp_6Pb_{10}\cdot 2$benzene
Formula weight(g/mol)	3714.11
Temperature(K)	186(2)K
Crystal system	orthorhombic
Space group	$P\overline{3}c1$
Lattice constants(Å,°)	a = 15.597(2) α 90
	b = 24.943(4) β 90
	c = 33.873(5) γ 90
Volume(Å^3)	13178(2)
Formula units	4
Density(g/cm^3)	1.872
μ(Mo-K_α)(mm^{-1})	12.971
2Θ range(°)	2.76 to 25.00
Reflections measured	62117
Independent reflections	22869 [R(int) = 0.3679]
Ind. Reflections with $F_o > 4\sigma(F_0)$	22869
Parameter	609

R1,R1(all reflections)	0.0783, 0.2867
wR2,wR2(all reflections)	0.1639, 0.2781
GooF	0.932
Residual electron density(e/Å^3)	2.289

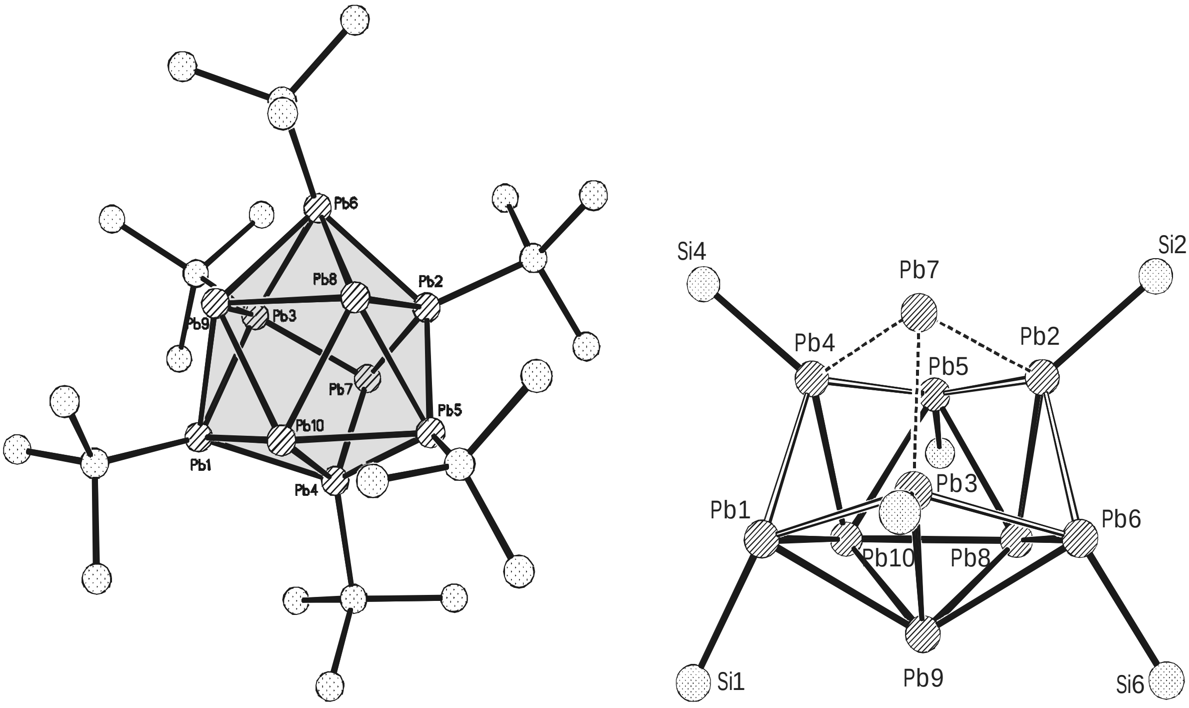

(a) (b)

Figure 4.4 (a) Molecular structure of **24**; atoms are represented by spheres of arbitrary radii; methyl groups are omitted for clarity (b): $Pb_{10}Si_6$ skeleton of the lead cluster **24** as found in the crystal structure. Pb-Pb between the *hypo*-type cluster and the capping atom Pb7 are indicated by dashes.

The Pb_{10} skeleton of **24** has approximate C_{3v} symmetry(Figure 4.4) and is best derived from Pb_{12} icosahedron by replacing one trigonal face by a single lead atom (Scheme 4.4). This picture also matches the prediction made by Wade’s rules. These only hold for cluster compound **24** if it is formally composed from a $[(Me_3Si)_3Si]_6$ Pb_9 *hypho*-type cluster dianion (26 skeleton electrons) and a model compound with hypersilyl groups replaced by SiH_3 groups indeed revealed a charge distribution according to the proposed model. The negative charge (derived from NBO analyses) is mainly concentrated at the open face (Pb2, Pb3, Pb4), whereas Pb7 bears the highest positive charge within the Pb_{10} skeleton. This uneven charge distribution should result in a significant dipole moment. It was calculated to be 2.7 D for the model compound.

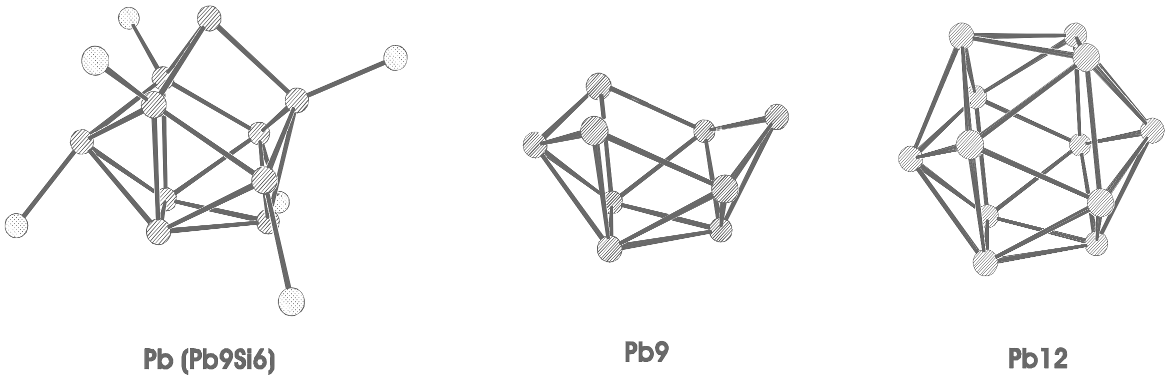

Scheme 4.4

The Pb-Pb distances within the Pb_9 fragment (except for Pb7) of **24** differ only slightly [310.3(3)-319.84(17)pm] and are all within the range found for compound **23** and the known lead clusters anions[158] [159] [160], whereas the three bonds to the capping atom (Pb7) are significantly shorter [298.3(4)-299.33(16)pm]. Other than in **23** all six hypersilyl groups are located at the puckered six-membered ring (Pb1, Pb4, Pb5, Pb2, Pb6, Pb3) and the capping Pb_3 triangle (Pb8, Pb9, Pb10) only consists of naked Pb atoms. The hypersilyl groups are bonded in an end-on fashion. The three Pb-Si bonds directed to the naked lead triangle – perhaps for steric reasons – are significantly longer [276.0(5) ppm] than the remaining [267.3(5) ppm]. Therefore, as shown by the space filling model in Figure 4.5, the Pb_{10} core is also well-shielded by the six hypersilyl groups, which may account for the stability of the species.

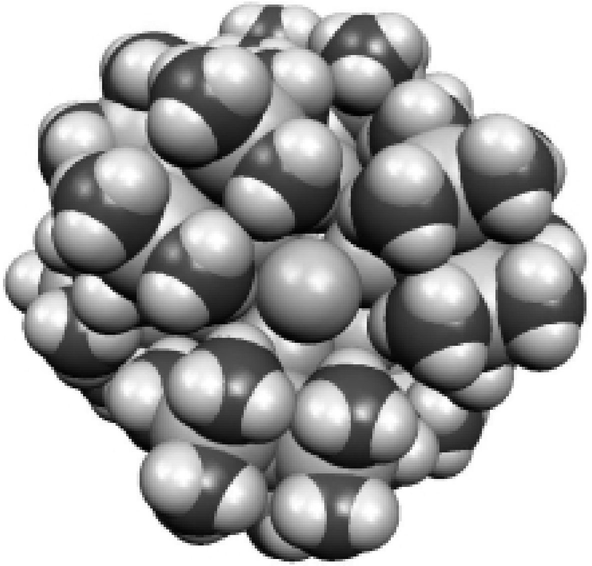

Figure 4.5 Space filling model of **24** (view almost along the C_3 axis)

Table 4.4 Selected interatomic distances (pm) and angles (°) for **24.**

Pb1-Pb3	313.9(4)	Pb6-Pb9	317.9(3)
Pb1-Pb4	314.5(4)	Pb6-Pb8	319.3(5)
Pb1-Pb9	318.1(3)	Pb8-Pb10	318.2(4)
Pb1-Pb10	318.5(4)	Pb8-Pb9	319.0(4)
Pb2-Pb7	299.33(16)	Pb9-Pb10	319.84(17)
Pb2-Pb8	312.20(18)	Pb1-Si1	276.8(7)
Pb2-Pb5	313.4(5)	Pb2-Si2	267.0(7)
Pb2-Pb6	314.3(5)	Pb3-Si3	269.4(7)
Pb3-Pb7	298.3(4)	Pb4-Si4	265.7(7)
Pb3-Pb9	310.3(3)	Pb5-Si5	275.2(7)
Pb3-Pb6	314.1(3)	Pb6-Si6	275.9(4)
Pb4-Pb7	298.6(4)	Si-Si	231.6(5) to 235.0(8)
Pb4-Pb10	310.8(4)	Pb3-Pb7-Pb4	86.43(5)
Pb4-Pb5	314.3(3)	Pb3-Pb7-Pb2	87.14(10)
Pb5-Pb10	318.0(3)	Pb4-Pb7-Pb2	86.90(11)
Pb5-Pb8	318.6(5)		

5 Experiment Section

5.1 General Comments

All experiments were performed under inert gas atmosphere of purified dry argon(BTS-Katalysator[161], P_4O_{10}) with standard Schlenk techniques. Toluene, benzene, triazine, and tetrahydrofuran were dried over sodium and potassium (Na/K) alloy, n-pentane, cyclo-pentane, diethyl ether, and DME over lithiumaluminiumtetrahydride ($LiAlH_4$), and freshly distilled prior to use. All glassware was oven-dried at 130°C over night.

5.2 Characterization

5.2.1 Elemental Analyses

Carbon- and hydrogen-contents were determined using combustions analysis with an instrument from Perkin Elmer Company, model PE 2400. Because of the existence of the silicon element in these compounds, which would combine with carbon to SiC instead of CO_2, the carbon contents obtained by using this method were often lower than the actual values[162].

5.2.2 Melting Points and Decomposition Temperatures Measurement

The determination of melting point (MP) and decomposition temperature (DT) was done in sealed glass-capillary with a melting point determination apparatus from Büchi Company. The data measured are uncorrected.

5.2.3 NMR Spectroscopy

^{1}H, ^{13}C, ^{31}P, ^{27}Al, ^{11}B, ^{29}Si, ^{119}Sn, and ^{7}Li NMR spectra were recorded with Brucker Spectrometers AM 200, AC250, and AM 400, respectively. Chemical shifts of the deuterated solvents in ^{1}H NMR data: benzene-d_6: $\delta(C_6D_5H) = 7.15$ ppm, toluene-d_8: $\delta(CD_2H) = 2.08$ ppm, THF-d_8: $\delta(\beta\text{-CDH}) = 1.72$ ppm. Chemical shifts of the deuterated solvents in ^{13}C NMR data: benzene-d_6: $\delta = 128.02$ ppm, toluene-d_8: $\delta(CD_3) = 20.4$ ppm, THF-d_8: $\delta(\beta\text{-C}) = 25.3$ ppm. ^{29}Si NMR data: $SiMe_4$ (external, $\delta = 0$ ppm); ^{7}Li NMR data: 14.4M LiCl in D_2O (external, $\delta = 0$ ppm); ^{11}B NMR data: BF_3-diethylether adduct (external, $\delta = 0$ ppm); ^{31}P NMR data: 85% H_3PO_4 (external, $\delta = 0$ ppm); ^{27}Al NMR data: $AlCl_3$ (external, $\delta = 0$ ppm); ^{119}Sn NMR data: $SnMe_4$ (external, $\delta = 0$ ppm). The signal types are assigned as follows: s = singlet, d = doublet, t = triplet, q = quartet, m = multiplet. The solvent for NMR measurement were dried over potassium and trap-to-trap distilled before use.

5.3.4 Uv-Spectroscopy

UV-vis spectra were measured on a JASCO V-530 UV/VIS Spectrophotometer at 25 °C using a 0.5 cm path-length cell for the 190-1100 nm region.

5.2.5 Mass Spectroscopy

Mass spectra were measured with Micro Mass Q-TOF Ultima 3 from Micro Mass by ESI technique

5.2.6 X-ray Analysis

Crystals were removed from Schlenk tubes and immediately covered with a layer of viscous hydrocarbon oil (Paratone N, or Nujol). A suitable crystal was selected, attached to a glass fiber, and immediately mounted on the diffractometer under a stream of cold nitrogen gas[163]. All data were collected with either a Siemens SMART CCD or a Siemens P4 four-circle diffractometer using monochromated Mo-K_α radiation (λ=0.71073 Å). The cell dimensions were determined from the positions of 35-52 selected reflections ($20 < 2\theta < 25°$). Calculations were carried out with the SHELXTL-PC 5.03[164] and SHLXL-97[165] program system installed on a local PC. The phase problem was solved by direct methods and the structures were refined on F_o^2 by full-matrix least-squares refinement. Absorption corrections were applied by the use of semiempirical ψ scans. The data with $F_o^2 \geq -3\sigma(F_o^2)$ were used. The residuals R-factor were calculated with formula $R1=\sum||F_o|-|F_c|| / \sum|F_o|$, where F_o means the measured (observed) structure factor, and F_c the theoretical (calculated) structure factor. The weighted R-factor were calculated with $wR_2=\{\sum[w(F_o^2-F_c^2)^2]/\sum w(F_o^2)^2\}^{1/2}$, in which $w=1/(\sigma^2(F_o^2)+(a\cdot P)^2+bP)$ and $P=[\max(0, F_o^2)+2F_c^2] /3$. Goodness of fit on S were calculated with $S=\{\sum[w(F_o^2-F_c^2)^2]/N_o-N_p\}^{1/2}$, where N_o is the number of reflections, and N_p is the number of parameters. Anisotropic thermal parameters were included for all non-hydrogen atoms. Hydrogen atoms were placed geometrically and refined with riding model, including free rotation of methyl groups. Their isotropic thermal parameters were either allowed to refine or were constrained to 1.2(aryl-H) or 1.5(methyl groups) times the U_{eq} of the bonded carbon.

5.3 Syntheses and Reactions

$[CuH(PPh_3)]_6$ was purchased from Fluka; Hexahydro-1,3,5-trimethyl-S-triazine, $LiN(SiMe_3)_2$, KO^tBut, $HSiCl_3$, Me_3SiCl, $ClSi(SiMe_3)_3$, 2,6-di-^{t}Bu-phenol, PMe_3, $NaBH_4$, $F_3B\cdot Et_2O$, 12-crown-4 ether and diisobutylaluminiumhydride from Aldrich. $LiPH_2\cdot 0.86DME$

was friendly given by Manfried. All anhydrous metal salts and elemental metals were commercially obtained. $HSiCl_3$ and Me_3SiCl were heated with CaH_2 under reflux and then distilled. $Pb[N(SiMe_3)_2]_2$[166], $Sn[N(SiMe_3)_2]_2$[167], and $H_3Al{\cdot}NMe_3$[168] were prepared as described in the literature.

5.3.1 Syntheses of Reactants

1. Tetrakis(trimethylsilyl)silane [169]

32.3mL of $HSiCl_3$ (0.320mol, d=1.342g/mL) and 179.0mL of Me_3SiCl (1.410mol, d=0.856 g/mL) in 200mL of THF was dropwise added to a suspension of 25.0g (3.57mol) of lithium in 500mL of THF with stark stirring at 0°C (ice bath). The dripping period was controlled for about 4h and the reaction mixture turned gradually from pale yellow to dark brown. After the addition of $HSiCl_3$ and Me_3SiCl, the reaction mixture was slowly allowed to come to room temperature and stirred overnight. The resulting mixture was filtered through a porosity fritted glass filter(G3). The THF in the filtrate and all other volatile were then removed under reduced pressure and the residue was dried in vacuum (1×10^{-3} torr) at room temperature for 24h. Sublimation of the brown residue at 80°C in vacuum (1.0×10^{-3} torr) gave white wax-like crystals in 44.8% yield (based on $HSiCl_3$). Formula: $Si(SiMe_3)_4$, M=320.84g/mol. : ^1H NMR(250.133MHz, C_6D_6, 298K): δ 0.26(s, $^2J_{Si,H}$=6.4Hz, $SiMe_3$); $^{13}C\{H\}$ NMR (62.896Hz, C_6D_6, 298K): δ2.85(s, $SiMe_3$); $^{29}Si\{H\}$ NMR(39.761Hz, C_6D_6, 298K): δ -9.8(s, $\underline{Si}Me_3$), -134.3(s, $\underline{Si}Si_3$) .

2. Solvent free potassium tris(trimethylsilyl)silanide[34]

The synthesis of $KSi(SiMe_3)_3$ is mainly according to Marschner´s method. 73.4g (0.229mol) of tetrakis(trimethylsilyl)silane $Si(SiMe_3)_4$ in 250mL of THF was added to a solution of potassium *tert*-butanolate(25.7g, 0.229mmol) in 250mL of THF at room temperature. After 24 hours, the ^1H-NMR spectrum showed that the reaction had quantitatively taken place. The solvent THF as well as the volatile by-product Me_3SiO^tBu were removed at 40°C under reduced pressure and the resulting solid was dried in vacuum(1.0×10^{-3} torr) overnight. After washing the solid with 3×30mL of n-pentane and drying the residue in vacuum for 5h, a white solid of pure $KSi(SiMe_3)_3$ was obtained in 85% yield. Formula: $KSi(SiMe_3)_3$, M=286.75g/mol. ^1H NMR(250.133MHz, C_6D_6, 298K): δ 0.54(s,

$SiMe_3$); $^{13}C\{H\}$ NMR (62.896MHz, C_6D_6, 298K): δ7.40(s, $SiMe_3$); $^{29}Si\{H\}$ NMR(39.761, C_6D_6, 298K): δ -5.8(s, $\underline{Si}Me_3$), -185.7(s, $\underline{Si}Si_3$).

3. Solvent free lithium tris(trimethylsilyl)silanide[170]

$LiSi(SiMe_3)_3$ was synthesized mainly according to R.E. Wochele´s dissertation. A solution of $ClSi(SiMe_3)_3$ (25.00g, 88.30mmol) in 50mL of toluene was added to a suspension of lithium(4.3g, 619.6mmol) and sodium(0.20g, 8.70mmol) in 200mL of toluene at room temperature. The reaction mixture was then heated to about 85°C and stirred for 3.5 hours. The surplus solid lithium, sodium as well as the produced LiCl and NaCl were then separated away from the solution with a G3 porosity fritted glass filter. To the filtrate was added 2.0 g of lithium and the reaction mixture was again heated to 85°C for 2 h in order to convert $NaSi(SiMe_3)_3$ formed at the first step to $LiSi(SiMe_3)_3$. After the filtration through a G4 porosity fritted glass filter, the volatile in the filtrate was carefully distilled under reduced pressure at 50°C and the residue was extracted with n-pentane. The resulting n-pentane solution was concentrated under reduced pressure and cooled at -20°C for 24h to afford colourless crystals of pure product, solvent free $LiSi(SiMe_3)_3$, in 85.4% yield (based on $ClSi(SiMe_3)_3$). Formula: $LiSi(SiMe_3)_3$. M=254.60g/mol. ^1H NMR(250.133MHz, C_6D_6, 298K): δ 0.36(s, $SiMe_3$); $^{13}C\{H\}$ NMR (62.896MHz, C_6D_6, 298K): δ5.7(s, $SiMe_3$); $^{29}Si\{H\}$ NMR(39.761, C_6D_6, 298K): δ -7.2(s,$\underline{Si}Me_3$), -181.9(s, $\underline{Si}Si_3$).

4. Dihypersilylplumbylene[12]

A yellow solution of $Pb[N(SiMe_3)_2]_2$ (8.20g, 15.5mmol) in 100mL of n-pentane was added to a stirred suspension of $KSi(SiMe_3)_3$ (8.91g, 31.0mmol) in 100mL of n-pentane at a temperature below -30°C. About 1h later the mixture was allowed to come to room temperature, whereupon it was stirred for a further 10 minutes. Filtration, followed by concentration of the deep blue reaction mixture to ca. 16mL and cooling to -60°C for 24 h, gave 9.0g (12.8mmol) black well shaped crystals of the title compound. Yield: 83%. Formula: $Pb[Si(SiMe_3)_3]_2$, M=702.51/mol. ^1H NMR(400.132MHz, C_6D_6, 298K): δ 0.54(s, $SiMe_3$); $^{13}C\{H\}$ NMR (100.620MHz, C_6D_6, 298K): δ8.5(s, $SiMe_3$).

5. Dihypersilylstannylene[12]

A orange solution of $Sn[N(SiMe_3)_2]_2$ (6.70g, 15.2mmol) in 100mL of n-pentane was added to a stirred suspension of $KSi(SiMe_3)_3$ **(**8.74g, 30.4mmol) in 80 mL of n-pentane at a temperature below -50°C. About 1h later the mixture was allowed to come to room temperature and was stirred for a further 10 minutes. The dark brown reaction mixture was filtered through a G4 frit and the filtrate was concentrated under reduced pressure. On cooling to -60°C for 24 h, 7.28g black crystals of the title compound was obtained in 78% yield. Formula: $Sn[Si(SiMe_3)_3]_2$, M=614.0g/mol. ^{1}H NMR(400.132MHz, C_6D_6, 298K): δ 0.44(s, $SiMe_3$); ^{13}C{H} NMR (100.620MHz, C_6D_6, 298K): δ4.9(s, $SiMe_3$).

5.3.2 Synthesis of $Hyp_2P_4K_2$ (1) and Hyp_2P_3K (3)

a). Reaction of potassium hypersilanide with white phosphorus in toluene

A solution of $KSi(SiMe_3)_3$ (6.5g, 22.6mmol) in 50mL of toluene was added to a suspension of white phosphorus(P_4, 1.4g, 11.3mmol) in 30 mL of toluene with intense stirring at room temperature. The colour of the solution turned rapidly from pale yellow to deep violet-red. After stirring 2 hours at room temperature until the white phosphorus was consumed, about 65mL of solvent was removed under reduced pressure and the remaining solution was cooled at -20°C for 24 h to give deep violet-red rhombohedral crystals of $Hyp_2P_4K_2{\cdot}2C_7H_8$, which was suitable for X-ray diffraction analysis.

Yield: 79% (7.87g, 8.93mmol), violet, extremely air- and moisture-sensitive crystals.

Formula: $[(Me_3Si)_3Si]_2P_4K_2 \cdot 2C_7H_8$

^{1}H NMR(250.133MHz, C_6D_6, 298K): $Si(Si(C\underline{H}_3)_3)_3$: δ= +0.52 ppm (s), $^2J_{Si,H}$=6.4Hz.

^{13}C{H} NMR (62.896MHz, C_6D_6, 298K): $Si(Si(\underline{C}H_3)_3)_3$: δ= +2.6ppm(s) .

^{31}P{H} NMR(101.256MHz, C_6D_6, 298K): δ (P1, P4) = -9.6 ppm, δ (P2, P3) = +423.2 ppm. $^3J_{p1,p4}$=139.3Hz, $^1J_{p1,p2}$ = $^1J_{p3,p4}$ =-434.5Hz, $^2J_{p1,p3}$=$^2J_{p2,p4}$ =-32.2Hz, $^1J_{p2,p3}$=-492.8Hz.

^{31}P{H} NMR(101.256MHz, THF+5%C_6D_6, 298K): (P1, P4) = -23.6 ppm, δ (P2, P3) = +416.3 ppm; $^3J_{p1,p4}$=151.5Hz, $^1J_{p1,p2}$ = $^1J_{p3,p4}$ =-431.1Hz, $^2J_{p1,p3}$=$^2J_{p2,p4}$ =-28.5Hz, $^1J_{p2,p3}$=-497.1Hz.

^{29}Si{H} NMR(79.490MHz, THF-D_8, 298K): $Si(\underline{Si}(CH_3)_3)_3$: δ = -12.7ppm (m), $\underline{Si}(Si(CH_3)_3)_3$: δ = -92.4ppm (m). $^1J_{Si,p}$ + $^4J_{Si,p}$ = 46 Hz, $^2J_{Si,p}$ + $^3J_{Si,p}$ = 14.5 Hz.

b). Reaction of potassium hypersilanide with white phosphorus in benzene

A solution of $K(Si(SiMe_3)_3$ (0.98g, 3.4 mmol) in 12mL of benzene was added to a stirred suspension of white phosphorus(P_4, 0.21g, 1.7 mmol) in 4mL of benzene at room temperature.

The reaction led almost quantitatively to a deep red solution of desired compound of $Hyp_2P_4K_2$ after 2 hours according to ^{31}P NMR spectrum of a sample of the resulting solution. The volume of the solution was then reduced to about 5 mL under reduced pressure and the resulting saturated solution was cooled at 5°C for 24 h. A deep red crystalline product of $Hyp_2P_4K_2 \cdot 4C_6H_6$ was obtained.

Yield: 79% (1.34mmol, 1.36g), deep-red, extremely air- and moisture-sensitive crystals.

Formula: : $[(Me_3Si)_3Si]_2P_4K_2 \cdot 4C_6H_6$

^{1}H NMR(250.133MHz, C_6D_6, 298K): $Si(Si(C\underline{H}_3)_3)_3$: δ= +0.52 ppm (s), $^2J_{Si,H}$=6.4Hz.

^{13}C{H} NMR (62.896MHz, C_6D_6, 298K): $Si(Si(\underline{C}H_3)_3)_3$: δ= +2.6ppm(s).

^{31}P{H} NMR(101.256MHz, C_6D_6, 298K): δ (P1, P4) = -9.6 ppm, δ (P2, P3) = +423.2 ppm. $^3J_{p1,p4}$=139.3Hz, $^1J_{p1,p2} = {}^1J_{p3,p4}$ =-434.5Hz, $^2J_{p1,p3}={}^2J_{p2,p4}$ =-32.2Hz, $^1J_{p2,p3}$=-492.8Hz.

^{29}Si{H} NMR(79.490MHz, THF-D_8, 298K): $Si(\underline{Si}(CH_3)_3)_3$: δ = -12.7ppm (m), $\underline{Si}(Si(CH_3)_3)_3$: δ = -92.4ppm (m). $^1J_{Si,p} + {}^4J_{Si,p}$ = 46 Hz, $^2J_{Si,p} + {}^3J_{Si,p}$ = 14.5 Hz.

Note: Dissolved $Hyp_2P_4K_2 \cdot 2C_7H_8$ crystals in benzene at room temperature and cooled the deep red saturated solution at 5°C for 24h, $Hyp_2P_4K_2 \cdot 4C_6H_6$ was also obtained as the deep red X-ray diffraction quality crystals.

c). Synthesis of potassium bis(hypersilyl)octaphosphenide ($Hyp_2P_4K_2$) as benzene and triazine solvate

Dissolved 0.82g(0.81mmol) of deep red crystals of $Hyp_2P_4K_2 \cdot 4C_6H_6$ in 4 mL of a mixture of benzene (2 mL) and triazine (2 mL), the colour of the solution turned immediately from red to green. Yellowish green crystals of monomeric $Hyp_2P_4K_2$ as benzene and triazine solvate were obtained at ambient temperature after several days.

Yield: 76% (0.62mmol, 0.68g), yellowish green, extremely air- and moisture-sensitive crystals.

Formula: $[(Me_3Si)_3Si]_2P_4K_2 \cdot 2C_6H_6 \cdot 2(MeNCH_2)_3$

d). Reaction of potassium hypersilanide with white phosphorus in diethyl ether

A solution of $K(Si(SiMe_3)_3$ (1.47g, 5.2 mmol) in 15mL of diethyl ether was added to a stirred suspension of white phosphorus (P_4, 0.32g, 2.6 mmol) in 5mL of diethyl ether at ambient temperature. The colour of the solution turned to violet immediately. After stirring for 1h, ^{31}P NMR analysis(in C_6D_6) of a sample of this resulting mixture indicated that $Hyp_2P_4K_2$, $Hyp_3P_5K_2$, Hyp_2P_3K, and small amounts of several other phosphor-containing compounds were formed. In order to isolate Hyp_2P_3K, diethyl ether was distilled off and the residue was extracted with 20 mL of cyclo-hexane and the undissolvable $Hyp_2P_4K_2$ and $Hyp_3P_5K_2$ were filtered off. Concentration of the violetish blue cyclo-hexane solution to a volume of 5 mL and cooling at 5°C furnished a small amount of thermally stable dark blue solid of Hyp_2P_3K. Attempts of recrystallization in n-pentane and benzene failed.

^{31}**P NMR** (101.256MHz, C_6D_6, 298K) of the resulting reaction mixture:

Products	Chemical shifts and coupling constants	Percentage
$Hyp_2P_4K_2$	δ 423.2(m, 2P), δ -9.6(m, 2P) ; $^1J_{p1,p2}$ = $^1J_{p3,p4}$ =-434.5Hz, $^2J_{p1,p3}$=$^2J_{p2,p4}$ =-32.2Hz, $^1J_{p2,p3}$=-492.8Hz,$^3J_{p1,p4}$=139.3Hz	30%
$Hyp_2P_3K_3$	δ 717.2(t, 1P, ^{1}Jp,p=541Hz), δ 199.8(d, 2P, ^{1}Jp,p=541Hz)	45%
$Hyp_3P_5K_2$	δ -87.4(q, broad, 2P), δ -197.0(t, broad, 1P), δ -242.3(d, broad, 2P)	25%

NMR spectra of Hyp_2P_3K:

^{1}**H NMR**(250.133MHz, C_6D_6, 298K): $Si(Si(C\underline{H}_3)_3)_3$: δ= +0.47 ppm (s).

^{13}**C{H} NMR** (62.896MHz, C_6D_6, 298K): $Si(Si(\underline{C}H_3)_3)_3$: δ= +2.3ppm(s).

^{31}**P{H} NMR**(101.256MHz, C_6D_6, 298K): δ (P2) = 717.2 ppm (t), $^1J_{p,p}$ = 541Hz, δ (P1,P3) = 199.8 ppm (d), $^1J_{p,p}$ = 541Hz.

e). Reaction of potassium hypersilanide with white phosphorus in THF

To a suspension of white phosphorus (P_4, 0.22g, 1.77mmol) in 3mL of THF was added dropwise a solution of potassium hypersilanide (1.02g, 3.55mmol) in 7mL of THF at room temperature with stirring. The colour of the solution turned to violetish red immediately. After stirring for 1h, ^{31}P- NMR spectrum of the reaction mixture with 10% d_6-benzene showed that a number of products were formed. Attempts of isolating some of the products failed.

^{31}**P NMR** (101.256MHz, 10%C_6D_6, 298K) of resulting reaction mixture:

Products	Chemical shifts and coupling constants	Percentage
$Hyp_2P_4K_2$	δ (P1, P4) = -23.6 ppm(m), δ (P2, P3) = +416.3 ppm(m); $^3J_{p1,p4}$=151.5Hz, $^1J_{p1,p2}$ = $^1J_{p3,p4}$ =-431.1Hz, $^2J_{p1,p3}$=$^2J_{p2,p4}$ =-28.5Hz, $^1J_{p2,p3}$=-497.1Hz.	8%
$Hyp_2P_3K_3$	δ 717(t, 1P), δ 200(d, 2P, ^{1}Jp,p=540Hz)	15%
$Hyp_3P_5K_2$	δ -81.5(m), δ -206.9(m), δ -247.8(m).	7%
unknown phosphorus-containing compounds	δ -56.7(t, br), δ -103.4(m,br), δ -108.0(m, br), δ -117.0(m,br).	70%

5.3.3 Synthesis of $Hyp_4P_8K_4$ (2)

1.36g (1.5mmol) of crystalline $Hyp_2P_4K_2{\cdot}2C_7H_8$ was slowly dissolved in 25mL of benzene at room temperature with stirring. The deep red solution was then concentrated under reduced pressure gradually to a volume of about 8mL and cooled at 5°C in refrigerator for several days. Light-red well shaped X-ray diffraction quality crystals of $[(Me_3Si)_3Si]_4P_8K_4$ as benzene solvate were obtained.

Yield: 0.93g (0.47mmol, 62%), light-red, extremely air- and moisture-sensitive crystals.

Formula: $[(Me_3Si)_3Si]_4P_8K_4 \cdot 8C_6H_6$

^{13}C{H}-NMR (50.323MHz, 10%C_6D_6 +toluene, 298K): $Si(Si(\underline{C}H_3)_3)_3$: δ= +3.0ppm(s).

^{31}P{H}-NMR(81.015MHz, 10%C_6D_6 +toluene, 298K): 40% (intensity) at δ = 44.8 ppm(m, 4P, P_{ring}), δ = -207.3 ppm(m, 4P, P_{exo}) originated from $Hyp_4P_8K_4$; 60% (intensity) at δ (m,P1, P4) = -9.6 ppm, δ (m,P2, P3) = +423.2 ppm originated from $Hyp_2P_4K_2$.

^{29}Si{H}-NMR(39.761MHz, 10%C_6D_6 +toluene, 298K): $Si(\underline{Si}(CH_3)_3)_3$: δ = -12.8ppm (m).

^{31}P{H}-NMR (101.256MHz, 298K) of $[(Me_3Si)_3Si]_4P_8K_4 \cdot 8C_6H_6$ in benzene-d6:

Products	Chemical shifts and coupling constants	Percentage
$Hyp_2P_4K_2$	δ (P1, P4) = -9.6 ppm, δ (P2, P3) = +423.2 ppm. $^1J_{p1,p2} = {}^1J_{p3,p4}$ =-434.5Hz, $^2J_{p1,p3}={}^2J_{p2,p4}$ =-32.2Hz, $^3J_{p1,p4}$=139.3Hz, $^1J_{p2,p3}$=-492.8Hz.	95%
$Hyp_4P_8K_4$	δ = 43.2 ppm(m, 4P, P_{ring}), δ = -208.1 ppm(m, 4P, P_{exo}).	5%

5.3.4 Oxidation of $Hyp_2P_4K_2$

A solution of $[(Me_3Si)_3Si]_2P_4K_2{\cdot}4C_6H_6$(1.12g, 1.1mmol) in 8mL of THF was added to a suspension of anhydrous $FeCl_2$ (0.14g, 1.1mmol) in 4 mL of THF with stirring at -20°C. The colour of the reaction mixture turned from violet to dark-brown immediately. After stirring about 1 hour, the resulting mixture, from which a NMR sample was taken, was stored in -20°C refrigerator. A layer of a fine black precipitate, presumably metallic iron, was found at the bottom of the flask the next day.

^{31}P{H}-NMR(101.256MHz, C_6D_6, 298K):

Products	Chemical shifts and coupling constants	Percentage
Hyp_3P_7	δ = -7.3 ppm(m, 3P), δ = -101.0 ppm(m, 1P), δ = -162.2 ppm(m, 3P)	63%
Hyp_2P_4	δ = -153.2 ppm(t, 2P), δ = -329.6 ppm(t, 2P), $^1J_{p,H}$ =161.0Hz	15%
$HypPH_2$	δ = -265.5 ppm(s)	12%
unknown phosphorus-containing compounds	δ = -71.1 ppm(t, br), δ = -116.4 ppm(m,br), δ = -201.5ppm(s), δ = -211.6ppm(s), δ = -256.3 ppm(s), δ = -299.8 ppm(s).	10%

5.3.5 Protolysis of $Hyp_2P_4K_2$

a). Reaction of potassium bis(hypersilyl)tetraphosphenide with HCl

To a solution of $[(Me_3Si)_3Si]_2P_4K_2 \cdot 4C_6H_6$(2.28g, 2.26mmol) in 20mL of toluene was bubbled a HCl gas (8mmol, excess, generated from reaction of $CaCl_2$ and concentrated sulphuric acid) at room temperature. The colour of the reaction mixture turned from deep-red to light yellow gradually. The toluene and all volatile compounds were removed under reduced pressure and residue was extracted with 50 mL of n-pentane in portions. After filtration, the filtrate was dried under reduced pressure to afford an oil-like liquid.

^{31}P{H}-NMR(101.256MHz, C_6D_6, 298K):

Products	Chemical shifts and coupling constants	Percentage
Hyp_3P_7	δ = -7.3 ppm(m, 3P), δ = -101.0 ppm(m, 1P), δ = -162.2 ppm(m, 3P)	28%
$HypPH_2$	δ = -265.5 ppm(s)	49%
unknown phosphorus-containing compounds	δ = -188.3 ppm(d, $^1J_{p,p}$ =-137Hz), δ = -229.6 ppm(d, $^1J_{p,p}$ =-137Hz)	23%

From this liquid, $(Me_3Si)_3SiPH_2$ was separated by sublimation(100°C/10^{-3} mbar) as colourless wax-like crystals.

Yield: 0.26g(41%, based on $Hyp_2P_4K_2$).

^{1}H-NMR(250.133MHz, C_6D_6, 298K): $Si(Si(C\underline{H}_3)_3)_3$: δ= +0.21ppm (s, 27H). PH_2: δ= +1.34ppm (d, 2H), $^1J_{p,H}$ = 179.2 Hz.

^{13}C{H}-NMR (62.896MHz, C_6D_6, 298K): $Si(Si(\underline{C}H_3)_3)_3$: δ= +0.7ppm(s) , $^1J_{C,Si}$ = 45.1 Hz.

^{31}P{H}-NMR(101.256MHz, C_6D_6, 298K): δ = -265.5 ppm (s).

^{31}P-NMR(101.256MHz, C_6D_6, 298K): δ = -265.5 ppm (t), $^1J_{p,H}$ = 179.2 Hz.

b). Reaction of potassium bis(hypersilyl)tetraphosphenide with 2,6-di-^{t}Bu-phenol

1). A solution of 2,6-di-^{t}Bu-phenol(0.21g, 1.0mmol) in 5 mL of benzene was added to a solution of $[(Me_3Si)_3Si]_2P_4K_2{\cdot}4C_6H_6$ [1.02g, 1.0mmol (1:1)] in 12mL of benzene with stirring at room temperature. The solution changed colour from deep red to violet gradually. According to the ^{31}P-NMR spectrum (C_6D_6) the reaction solution contained, in addition to unconsumed starting material, $HypPH_2$, Hyp_2P_3K, and $Hyp_3P_5K_2$ (identified by comparison with authentical samples) in a molar ratio of 6:3:1, as well as small amounts of unidentified phosphorus-containing compounds.

2). A solution of 2,6-di-^{t}Bu-phenol(0.33g, 1.62mmol) in 5 mL of benzene was added to a solution of $[(Me_3Si)_3Si]_2P_4K_2{\cdot}4C_6H_6$ [0.82g, 0.81mmol (2:1)] in 10mL of benzene with stirring at room temperature. The deep red colour of the reaction mixture vanished immediately. According to the ^{31}P-NMR spectrum (C_6D_6), the starting material was completely consumed and the reaction solution contained $HypPH_2$ as the main product along with small amounts of Hyp_3P_7 and unidentified phosphorus-containing compounds(presumably, oligophosphane).

5.3.6 Synthesis of $Hyp_3P_5K_2$ (4)

A solution of $K(Si(SiMe_3)_3$ (1.74g, 6.1mmol) in 15mL of toluene was added to a stirred suspension of white phosphorus(P_4, 0.38g, 3.05mmol) in 5mL of toluene at room temperature. The colour of the reaction mixture turned to violet immediately. The mixture was stirred for about 2h until the white phosphorus completely disappeared. The volume of the resulting mixture was reduced to 10mL under vacuum. On standing for about several weeks at room temperature, the deep violet solution turned gradually to yellowish brown and a few large yellow rhombohedral X-ray diffraction quality crystals of title compound was obtained. $Hyp_3P_5K_2$ can also be recrystallized from benzene solution as benzene solvate.

Yield**:** 0.82g. yellow rhombohedral, air- and moisture-sensitive crystals.

Formula: $[(Me_3Si)_3Si]_6P_{10}K_4{\cdot}3C_6H_6$

Mp(decomp.): crystals turned dark >410°C.

^{1}H-NMR(400.132MHz,C_6D_6, 300K): δ = 0.507ppm (s, 54H, $Si(Si(C\underline{H}_3)_3)_3$), δ = 0.512ppm (s, 27H, $Si(Si(C\underline{H}_3)_3)_3$).

^{13}C{H}-NMR (100.620MHz, C_6D_6, 300K): δ = 3.1ppm (s, $Si(Si(\underline{C}H_3)_3)_3$), δ = 3.8ppm(s, $Si(Si(\underline{C}H_3)_3)_3$).

^{31}P{H}- NMR(162.048MHz, C_6D_6, 300K): δ = -87.4ppm (q, broad, 2P), δ= -197.0ppm (t, broad, 1P), δ = -242.3ppm (d, broad, 2P). **^{31}P{H}-NMR**(101.256MHz, D_8-THF, 300K): δ (P1, P2)= -81.5 ppm, δ(P4, P5)=-247.2ppm. δ (P3)= -206.7ppm. $^1J_{p1,p4}$=$^1J_{p2,p5}$= -347.5Hz, $^2J_{p3,p4}$ = $^2J_{p3,p5}$ =61.7Hz, $^1J_{p1,p3}$=$^1J_{p2,p3}$ =-178.3Hz, $^2J_{p1,p5}$=$^2J_{p2,p4}$ =-6.9Hz, $^1J_{p1,p2}$=-189.8Hz, $^3J_{p4,p5}$ =214.0Hz.

^{29}Si{H}-DEPT-NMR(79.495MHz, THF-d8, 300K): δ = -9.8ppm (m, broad, Si6, $Si(\underline{Si}(CH_3)_3)_3$), -12.2ppm (s, broad, Si4, Si5, $Si(\underline{Si}(CH_3)_3)_3$)), -90.1ppm(dt, Si3, $\underline{Si}(Si(CH_3)_3)_3$), $^1J_{P3,Si3}$=-116.3Hz, $^2J_{P1,Si3}$= $^2J_{P2,Si3}$=-7.3Hz), -91.8 ppm(m, Si1,Si2, $\underline{Si}Si_3$, $^1J_{P4,Si2}$=$^1J_{P5,Si1}$=-106.8Hz, $^2J_{P1,Si2}$=$^2J_{P2,Si1}$=-21.4Hz, $^3J_{P3,Si2}$=$^3J_{P1,Si1}$=-17.3Hz, $^4J_{P5,Si2}$=$^4J_{P4,Si1}$=7.6Hz)**.**

5.3.7 Synthesis of $Hyp_3P_8K_3$ (5)

Some crystals of potassium tetrakis(hypersilyl)octaphosphanide ($Hyp_4P_8K_4 \cdot 4C_6H_6$) was dissolved in D_6-benzene and stored at a refrigerator (5°C) for several days. Cubic orange X-ray diffraction quality crystal was obtained.

Formula: $[(Me_3Si)_3Si]_6P_{16}K_6 \cdot 4C_6H_6$

^{1}H-NMR(250.133MHz, toluene-d_8, 300K): δ = 0.51ppm (s, 54H, $Si(Si(C\underline{H}_3)_3)_3$), δ = 0.53ppm (s, 27H, $Si(Si(C\underline{H}_3)_3)_3$).

^{13}C{H}-NMR (62.896MHz, toluene-d_8, 300K): δ = 3.3ppm (s, $Si(Si(\underline{C}H_3)_3)_3$), δ = 3.4ppm(s, $Si(Si(\underline{C}H_3)_3)_3$).

^{31}P{H}- NMR(101.256MHz, toluene-d_8, 300K): δ = 43.0ppm (q, broad, 2P), δ = -45.7ppm (t, broad, 1P), δ= -56.0ppm (q, broad, 2P), δ = -181.3ppm (d, broad, 2P), δ = -234.5ppm (t, broad, 2P).

5.3.8 Synthesis of Hyp_2P_4 (6) and $Hyp_2P_4Li_2$ (7)

a) Reaction of lithium hypersilanide with white phosphorus in toluene

To a suspension of white phosphorus (P_4, 0.70g, 5.6mmol) in 8mL of toluene was added a solution of $LiSi(SiMe_3)_3$(2.85g, 11.2mmol) in 12mL of toluene with stirring at room temperature. Immediately, the reaction mixture became deep red and a light yellow precipitate appeared. Stirring continued for about 1.5h followed by filtration, the ^{31}P NMR spectrum of the filtrate indicated that it consisted of $P_7(Si(SiMe_3)_3)_3$ (^{31}P NMR(101.256, C_6D_6, 300K):δ=-8.6(m,3P), -102.0(m,1P), -163.0(m,3P)), $P_4(Si(SiMe_3)_3)_2$ (δ= -153.6(t, 2P), -329.8(t,

^{1}Jp,p=161Hz,2P)), and some other phosphorus-containing compounds. Attempts of separating them by crystallization failed.

The light yellow residue of the filtration mentioned above was washed with 2×5mL of toluene and extracted with 15mL of tetrahydrofuran to give a violet solution. The volume of the solution was then reduced under dynamic vacuum at room temperature until a few violet crystals appeared. The resulting solution was cooled at -20°C for 3d to afford deep violet X-ray diffraction quality crystals of $Li_2P_4[Si(SiMe_3)_3]_2 \cdot 4THF$.

Yield: 0.4g(9.2%).

Formula: $[(Me_3Si)_3Si]_2P_4Li_2 \cdot 4THF$

^{1}H-NMR(400.132MHz, THF-D_8, 300K): δ = 0.21ppm (s, 54H, $Si(Si(C\underline{H}_3)_3)_3$).

^{13}C{H}-NMR (100.613MHz, THF-D_8, 300K): δ = 1.34ppm (s, $Si(Si(\underline{C}H_3)_3)_3$).

^{31}P{H}-NMR(101.256MHz, THF-D_8, 300K): δ (P2, P3)= 406.3 ppm(m, 2P), δ(P1, P4)=-60.1ppm(m, 2P); $^3J_{p1,p4}$=247.1Hz, $^1J_{p1,p2}$ = $^1J_{p3,p4}$ =-410.3Hz, $^2J_{p1,p3}$=$^2J_{p2,p4}$ =-31.5Hz, $^1J_{p2,p3}$=-481.0Hz.

^{29}Si{H}-NMR(79.495MHz, THF-D8, 300K): δ = -11.3ppm (m, broad, $Si(\underline{Si}(CH_3)_3)_3$).

b) Reaction of lithium hypersilanide with white phosphorus in THF

To a suspension of white phosphorus(P_4, 0.58g, 4.8mmol) in 5 mL of THF was added dropwise a solution of $LiSi(SiMe_3)_3$ (2.42g, 9.5mmol) in 20mL of THF with stirring at room temperature in 0.5h. The colour turned to red-brown gradually and no precipitate formed. The reaction mixture was stirred for an additional 1.5h until the white phosphorus was consumed. According to ^{31}P-NMR spectrum, the reaction solution contained, in addition to $Li_2P_4[Si(SiMe_3)_3]_2$ and $LiP_3[Si(SiMe_3)_3]_2$, some other phosphorus-containing products, which could not be identified owing to superposition of the signals. Attempts of isolating some of them failed.

5.3.9 Synthesis of Hyp_2P_3Li (8)

a) A solution of $LiSi(SiMe_3)_3$(6.63g, 26.0mmol) in 30mL of toluene was added to a suspension of white phosphorus(P_4, 1.61g, 13.0mmol) in 10mL of toluene with stirring at room temperature. A pale yellow precipitate formed gradually. After stirring for about 1.5h, the reaction mixture was filtered through a porosity fritted glass filter and the residue was washed with 15mL of toluene in portions. Dissolved some of this light yellow powder-like solid in a mixture of benzene and hexahydro-1,3,5-trimethyl-S-triazine, an intense violet-blue solution was obtained. According to the ^{31}P-NMR spectrum, Hyp_2P_3Li was the dominant phosphorus-containing product. But attempts of crystallization of this compound from n-pentane, benzene, or toluene failed.

b) A solution of $LiSi(SiMe_3)_3$ (1.73g, 6.80mmol) in 10mL toluene was added dropwise to a suspension of white phosphorus(P_4, 0.42g, 3.40mmol) and 2.0mL of hexahydro-1,3,5-trimethyl-S-triazine(13.8mmol, d=0.89g/ml) in 5 mL of toluene with stirring at room temperature in 0.5h. The reaction mixture was then stirred for an additional 1.5h until the white phosphorus was consumed. The ^{31}P NMR spectrum indicated that more than 70% of the white phosphorus had been changed to the title compound. The resulting deep violet mixture was filtered through a porosity fritted glass filter and concentrated under reduced pressure to ca. 4 mL. Adding 2mL of n-pentane and cooling to -30°C for 2d, the solution furnished the title compound as deep violet rod-like crystals, along with some colourless crystals of $Si(SiMe_3)_4$.

Formula: $[(Me_3Si)_3Si]_2P_3Li\cdot 2(MeNCH_2)_3$

^{1}H-NMR(400.132MHz, C_6D_6, 300K): δ = 0.49ppm (s, 54H, $Si(Si(C\underline{H}_3)_3)_3$), δ = 2.03ppm(s,18H, $NC\underline{H}_3$);

^{13}C{H}-NMR (100.613MHz, C_6D_6, 300K): δ = 2.17ppm (s, $Si(Si(\underline{C}H_3)_3)_3$), δ = 77.3ppm (s,$N\underline{C}H_2N$), δ = 39.5ppm(s,NCH_3);

^{31}P{H}-NMR(162.048MHz, C_6D_6, 300K): δ = 198.2 ppm(d,2P**,** ^{1}Jp,p=533Hz), δ = 718.4 ppm(t, 1P**,** ^{1}Jp,p=533Hz),

^{29}Si{H}-NMR(79.495MHz, C_6D_6, 300K): δ = -11.0ppm (d, broad, $Si(\underline{Si}(CH_3)_3)_3$, ^{2}Jsi,p=10Hz).

^{7}Li{^{1}H}- NMR(155.506MHz, C_6D_6, 300K): δ = 0.41ppm(s).

5.3.10 Synthesis of $Hyp_3P_5Na_2$ (9)

A solution of $NaSi(SiMe_3)_3$ (0.49g, 3.7mmol) in 10mL of toluene was added to a stirred suspension of white phosphorus(P_4, 0.23g, 1.85mmol**)** in 3mL of toluene at room temperature. The reaction mixture was stirred for about 1h until the white phosphorus completely was consumed and the colour of the mixture turned from pale yellow to brown. After filtration through a G3 porosity fritted glass filter, the dark brown filtrate was concentrated under reduced pressure and cooled at -20 °C for several days, no crystal precipitated. All volatile compounds in the solution were then removed under vacuum and the residue was extracted with 15 mL of n-pentane. After concentration, the resulting solution was cooled at 5°C for several weeks to provide a small amount of X-ray diffraction quality yellow crystals.

Yield: 0.21g (15.8%). Air- and moisture-sensitive yellow crystals.

Formula: $[(Me_3Si)_3Si]_6P_{10}Na_4$

^{1}**H-NMR**(400.132MHz,C_6D_6, 300K): δ = 0.46ppm (s, 54H, $Si(Si(C\underline{H}_3)_3)_3$), δ = 0.47ppm (s, 27H, $Si(Si(C\underline{H}_3)_3)_3$);^{1}**H-NMR**(400.132MHz, THF-D_8, 300K): δ = 0.28ppm (s, 54H, $Si(Si(C\underline{H}_3)_3)_3$), δ = 0.27ppm (s, 27H, $Si(Si(C\underline{H}_3)_3)_3$).

^{13}**C{H}-NMR** (100.613MHz, C_6D_6, 300K): δ = 2.91ppm (s, $Si(Si(\underline{C}H_3)_3)_3$), δ = 3.40ppm(s, $Si(Si(\underline{C}H_3)_3)_3$);^{13}**C{H}-NMR** (100.613MHz, THF-D_8, 300K): δ = 3.94ppm (s, $Si(Si(\underline{C}H_3)_3)_3$), δ = 2.82ppm(s, $Si(Si(\underline{C}H_3)_3)_3$).

^{31}**P{H}- NMR**(162.048MHz, C_6D_6, 300K): δ = -65.4ppm (m, broad, 2P), δ= -202.0ppm (m, broad, 1P), δ = -281.5ppm (m, broad, 2P). ^{31}**P{H}-NMR**(101.256MHz, D_8-THF, 300K): δ (P1, P2)= -94.3 ppm(m,2P), δ(P4, P5)=-249.1ppm(m,2P). δ (P3)= -193.4ppm(m, 1P). $^1J_{p1,p4}$=$^1J_{p2,p5}$= -336.6Hz, $^2J_{p3,p4}$ = $^2J_{p3,p5}$ =61.4Hz, $^1J_{p1,p3}$=$^1J_{p2,p3}$ =-178.8Hz, $^2J_{p1,p5}$=$^2J_{p2,p4}$ =-7.3Hz, $^1J_{p1,p2}$=-195.3Hz, $^3J_{p4,p5}$ =302.9Hz.

^{29}**Si{H}-DEPT-NMR**(79.495MHz, THF-d8, 300K): δ = -9.6ppm (m, broad, Si6, $Si(\underline{Si}(CH_3)_3)_3)$), -11.7ppm (s, broad, Si4, Si5, $Si(\underline{Si}(CH_3)_3)_3)$), -87.9ppm(dt, Si3, $\underline{Si}(Si(CH_3)_3)_3$), $^1J_{P3,Si3}$=-113.8Hz, $^2J_{P1,Si3}$= $^2J_{P2,Si3}$=-7.3Hz), -92.6ppm(m, Si1,Si2, $\underline{Si}Si_3$, $^1J_{P4,Si2}$=$^1J_{P5,Si1}$=-98.8Hz, $^2J_{P1,Si2}$=$^2J_{P2,Si1}$=-18.4Hz, $^3J_{P3,Si2}$=$^3J_{P1,Si1}$=-14.3Hz, $^4J_{P5,Si2}$=$^4J_{P4,Si1}$=15.6Hz).

5.3.11 Synthesis of Hyp_3P_4SnK (10)

To a solution of $Sn(N(SiMe_3)_2)_2$ (0.43g, 0.99mmol) in 5mL of toluene was added a solution of $K_2P_4(Si(SiMe_3)_3)_2 \cdot 2C_7H_8$ (0.87g, 0.99mmol) in 8 mL of toluene with stirring at -20°C . The reaction solution changed colour gradually from deep red to yellow-brown. After 30min, the mixture was allowed to warm to room temperature and stirred for another 1h. The ^{31}P-NMR(C_6D_6) spectrum of a sample of the reaction mixture indicated that compound **10** (δ -58.5(o, 1P), -192.4(t, 1P), -231.3(q, 1P), -256.1(d, 1P)) and $KSnP_4(Si(SiMe_3)_3)_2N(SiMe_3)_2$ (δ -128.2(o, 1P), -184.6(q, 1P), -211.0(q, 1P), -234.4(h, 1P)) formed in a molar ratio of 2:3. Toluene was removed in vacuo and the residue was extracted with 15mL of n-pentane followed by filtration through a porosity fritted glass filter. The filtrate was cooled at -20°C for 24h and fine yellow-orange crystalline solid precipitated. After decanting the supernatant liquid, the residue was washed with 10mL of n-pentane in portions and extracted with benzene-d6. The ^{31}P-NMR spectrum of this residue showed that it contained almost only compound **10**. On standing for several weeks at 5°C, a large well shaped orange X-ray diffraction quality crystal formed in the NMR tube.

Formula: $[(Me_3Si)_3Si]_3P_4SnK$

Mp(decomp.): crystal turned dark > 168°C.

^{1}H-NMR(250.133MHz, C_6D_6, 300K): δ = 0.60ppm (s, $^2J_{Si,H}$= 6.4Hz, 27H, $Si(Si(C\underline{H}_3)_3)_3$), δ = 0.47ppm (s, $^2J_{Si,H}$= 6.4Hz ,27H, $Si(Si(C\underline{H}_3)_3)_3$), δ = 0.39ppm (s, $^2J_{Si,H}$= 6.4Hz, 27H, $Si(Si(C\underline{H}_3)_3)_3$);

^{13}C{H}-NMR (62.896MHz, C_6D_6, 300K): δ = 4.1ppm (s, $Si(Si(\underline{C}H_3)_3)_3$), δ = 4.0ppm (s, $Si(Si(\underline{C}H_3)_3)_3$), δ = 3.3ppm (s, $Si(Si(\underline{C}H_3)_3)_3$);

^{31}P{H}-NMR(101.256MHz, C_6D_6, 300K): δ (P2)= -58.5 ppm(o,1P), δ (P4) = -192.4 ppm(t, 1P), δ(P3) = -231.3 ppm(q,1P), δ(P1) = -256.1 ppm(d, 1P); $^1J_{p1,p2}$=-239Hz, $^3J_{p1,p4}$= -11Hz, $^1J_{p2,p3}$ =-109Hz, $^2J_{p2,p4}$ =-169Hz, $^1J_{p3,p4}$=-163Hz.

5.3.12 Synthesis of $(Me_3Si)_2N(Hyp)_2P_4K_2$ (11)

To a suspension of $K_2P_4(Si(SiMe_3)_3)_2 \cdot 4C_6H_6$ (0.82g, 0.81mmol) in 10mL of n-pentane was added a solution of $Sn(N(SiMe_3)_2)_2$ (0.36g, 0.81mmol) in 15mL of n-pentane with stirring at -20°C. The reaction solution changed colour gradually from red to yellow-orange and a yellow precipitate formed. The mixture was allowed to come to room temperature after 30 min and stirred for another 1h. The ^{31}P NMR(C_6D_6) spectrum of a sample of the reaction mixture indicated that the starting material was almost all converted into $KSnP_4(Si(SiMe_3)_3)_2N(SiMe_3)_2$ and $KN(SiMe_3)_2$. After filtration through a porosity fritted glass filter, the filtrate was concentrated under dynamic vacuum at room temperature until a few yellow-orange crystals appeared and then placed at -60°C for 24h. A mixture of $KSnP_4(Si(SiMe_3)_3)_2N(SiMe_3)_2$ and $KN(SiMe_3)_2$ was precipitated as a yellow-orange crystalline solid. Attempts of isolating $KSnP_4(Si(SiMe_3)_3)_2N(SiMe_3)_2$ failed.

^{1}H-NMR(400.132MHz, C_6D_6, 300K): δ = 0.58ppm (s, 27H, $Si(Si(C\underline{H}_3)_3)_3$), δ = 0.43ppm (s, 27H, $Si(Si(C\underline{H}_3)_3)_3$), δ = 0.24ppm (s, 18H, $N(Si(C\underline{H}_3)_3)_2$).

^{31}P{H}-NMR(101.256MHz, C_6D_6, 300K): δ(P2) = -128.2 ppm(o,1P), δ(P4) = -184.6 ppm(q, 1P), δ(P1) = -211.0 ppm(q,1P), δ(P3) = -234.4 ppm(h, 1P); $^1J_{p1,p2}$=-167Hz, $^1J_{p1,p3}$= -195Hz, $^1J_{p2,p3}$ =-196Hz, $^1J_{p2,p4}$ =-213Hz, $^1J_{p3,p4}$=-124Hz.

5.3.13 Synthesis of $Hyp_4P_4Pb_4$ (12) and Hyp_2P_2 (13)

a) Reaction of dihypersilylplumbylene with white phosphorus

A solution of $Pb(Si(SiMe_3)_3)_2$ (1.0g, 1.4mmol) in 10mL of toluene was added to a stirred suspension of white phosphorus(P_4, 0.086g, 0.7mmol) in 5mL of toluene at room temperature. The reaction mixture was heated to about 50°C for 20 min until white phosphorus was completely consumed. The resulting dark brown solution was then concentrated in vacuo to incipient crystallization and cooled at -60°C for 2d. Decanting of the supernatant liquid gave a dark brown crystalline solid. Recrystallization of this solid with cyclopentane and subsequent cooling at -20°C for several days afforded dark brown hexagonal shaped X-ray analysis suitable crystals of $Pb_4P_4(Si(SiMe_3)_3)_4$.

Yield: 0.38g(0.20mmol, 57%, based on plumbylene), dark brown hexagonal platelets.

Formula: $Pb_4P_4(Si(SiMe_3)_3)_4$

Mp(decomp.): crystals turned dark >280.3°.

^{1}H-NMR(250.133MHz, C_6D_6, 300K): $\delta = 0.42$ppm (s, 54H, $Si(Si(C\underline{H}_3)_3)_3$).

^{13}C{H}-NMR (50.323MHz, C_6D_6, 300K): $\delta = 2.7$ppm (s, $Si(Si(\underline{C}H_3)_3)_3$).

^{31}P{H}-NMR(81.015MHz, C_6D_6, 300K): $\delta = -506.2$ ppm(s, with ^{207}Pb satellites, $Pb_4\underline{P}_4$).

^{29}Si{H}-NMR(39.761MHz, C_6D_6, 300K): $\delta = 7.4$ppm (s, $Si(\underline{Si}(CH_3)_3)_3$).

Elemental analysis:			
	Cal:	C: 22.25%;	H: 5.60%
	Exp:	C: 22.47%;	H: 6.27%

Further concentrating the supernatant liquid of the crystals of $Pb_4P_4(Si(SiMe_3)_3)_4$ mentioned above and cooling at -60°C for several days yielded light green crystals, which were not suitable for X-ray analysis, but identified unambiguously as $(SiMe_3)_3SiP{=}PSi(SiMe_3)_3$ according to the ^{31}P NMR spectrum: ^{1}H-NMR(250.133MHz, C_6D_6, 300K): δ 0.36(s, $^{2}J_{Si,H}$= 6.65Hz, $SiMe_3$); ^{13}C{H}-NMR (62.896MHz, C_6D_6, 300K): δ 1.87(s,$SiMe_3$); ^{31}P{H}-NMR(101.256MHz, C_6D_6, 300K): δ 735.2(s, $^{1}J_{Si,P}$=46.2Hz). The final supernatant liquid contained then $P_7(Si(SiMe_3)_3)_3$(^{31}P{H}-NMR(101.256MHz, C_6D_6, 300K):-8.6(m,3P), -102.0(m,1P), -163.0(m,3P)), $P_4(Si(SiMe_3)_3)_2$ (^{31}P{H}-NMR(101.256MHz, C_6D_6, 300K):-153.6(t, $^{1}J_{P,P}$=161Hz,2P), -329.8(t, 2P)) as well as some other phosphorus-containing compounds according to ^{31}P NMR spectrum.

b) Reaction of lead bis[bis(trimethylsilyl)amide] with hypersilylphosphane

0.16g(0.30mmol) of $[(Me_3Si)_2N]_2Pb$ and 0.085g(0.30mmol) $(Me_3Si)_3SiPH_2$ were solved in 2 mL of toluene at room temperature. The reaction mixture was allowed to warm up to about 50°C for 20 min and the colour of the solution turned to brown. According to ^{31}P NMR spectrum of the resulting mixture, $(Me_3Si)_3SiPH_2$ were converted to **12** quantitatively. The solution was then concentrated under reduced pressure and cooled at -60°C. After 12h, dark brown hexagonal shaped crystals of $[(Me_3Si)_3SiPPb]_4$ formed. Yield: 82%.

5.3.14 Synthesis of $Hyp_4P_4Sn_4$ (14)

a). Reaction of dihypersilylstannylene with white phosphorus

A solution of $Sn(Si(SiMe_3)_3)_2$ (1.4g, 2.3mmol) in 15mL of toluene was added to a suspension of white phosphorus(P_4, 0.14g, 1.15mmol) in 5mL of toluene with stirring at room temperature. The reaction mixture was then heated to about 50°C for 20 min until white phosphorus was completely consumed. The ^{31}P-NMR(C_6D_6) spectrum of this reaction mixture indicated that along with $Sn_4P_4(Si(SiMe_3)_3)_4$ some $(SiMe_3)_3SiP{=}PSi(SiMe_3)_3$ (δ 735.2(s, $^1J_{Si,P}$=46.2Hz)) formed. Removal of all volatile compounds in vacuo gave a dark brown residue. Extracting the residue with toluene and cooling the brown saturated extract at 5°C for several days afforded hexagonal-shaped dark brown X-ray diffraction quality crystals of $Sn_4P_4(Si(SiMe_3)_3)_4$. Recrystallization with cyclohexane or benzene gave also X-ray diffraction quality crystals.

Yield: 0.47g (0.30mmol, 52%, based on stannylene), hexagonal-shaped dark brown crystals.

Formula: $Sn_4P_4(Si(SiMe_3)_3)_4$

^{1}H-NMR(250.133MHz, C_6D_6, 300K): δ= 0.43ppm(s, $^2J_{Si,H}$= 6.4Hz, $Si(Si(C\underline{H}_3)_3)_3$).

^{13}C{H}-NMR (50.323MHz, C_6D_6, 300K): δ = 2.6ppm (s, $Si(Si(\underline{C}H_3)_3)_3$).

^{31}P{H}-NMR(81.015MHz, C_6D_6, 300K): δ = -463.6 ppm(s, $^{117/119}$Sn satellites, $Sn_4\underline{P}_4$).

^{119}Sn{^{1}H}- NMR(74.631MHz, C_6D_6, 300K) :δ=1515.7ppm(qd, $^1J_{Sn,P}$= 741Hz, $^3J_{Sn,P}$= 138Hz, $\underline{Sn}_4P_4$).

b) Reaction of tin bis[bis(trimethylsilyl)amide] with hypersilylphosphane

0.19g(0.44mmol) of $[(Me_3Si)_2N]_2Sn$ and 0.12g(0.44mmol) $(Me_3Si)_3SiPH_2$ were solved in 3 mL of toluene at room temperature. The reaction mixture was heated to about 50°C for 20 min and the colour of the solution turned to red-brown. According to ^{31}P NMR spectrum of the resulting mixture, **14** was quantitatively formed. The solution was concentrated under reduced pressure and cooled at -60°C. After 24h, brown crystals of $[(Me_3Si)_3SiPSn]_4$ precipitated. Yield: 79%.

5.3.15 Synthesis of $Li[Hyp_2Pb{\cdot}PH_2]$ (15)

a). Reaction of dihypersilylplumbylene with lithium phosphanide in diethyl ether

To a precooled (-20°C) stirred suspension of $LiPH_2{\cdot}0.86DME$ (0.23g, 2.0mmol) in 22mL of diethyl ether was added dropwise a solution of $Pb(Si(SiMe_3)_3)_2$ (1.37g, 2.0mmol) in 8mL of diethyl ether. The deep blue reaction mixture turned gradually to orange-red. After stirring for about 1h, the reaction mixture was allowed to come to room temperature and stirred for an additional 10min. The resulting mixture was then filtered through a porosity fritted glass filter and the filtrate was concentrated under reduced pressure. Cooling of the saturated orange-red solution at -60°C for 24h provided yellow-brown X-ray diffraction quality crystals of $Pb(Si(SiMe_3)_3){\cdot}LiPH_2{\cdot}DME{\cdot}Et_2O$, which turned to dark brown by immerging in nujol in the air.

Yield: 1.61g(1.8mmol, 91%), air- and moisture-sensitive yellow-brown crystals.

Formula: $((Me_3Si)_3Si)_2Pb\ {\cdot}LiPH_2\ {\cdot}DME{\cdot}Et_2O$.

Mp (decomp.): crystals turned dark >108 °C.

^{1}H-NMR(400.130MHz, THF-d8, 253K): δ =0.17ppm(s, 54H, $Si(Si(C\underline{H}_3)_3)_3$), δ =0.86ppm(d, $^1J_{P,H}$= 155Hz, 2H, $P\underline{H}_2$); δ =1.10ppm(t, $(C\underline{H}_3CH_2)_2O$), δ =3.35 ppm (q, $(CH_3C\underline{H}_2)_2O$); δ =3.25 ppm (s, $C\underline{H}_3O(CH_2)_2OC\underline{H}_3$), δ =3.42 ppm (s, $CH_3O(C\underline{H}_2)_2OCH_3$).

^{13}C{^{1}H }- NMR (62.896MHz, THF-d8, 253K): δ =5.6ppm(s, $Si(Si(\underline{C}H_3)_3)_3$), δ =15.8ppm(s, $(\underline{C}H_3CH_2)_2O$), δ =66.4ppm(s, $(CH_3\underline{C}H_2)_2O$); δ =58.9ppm(s, $\underline{C}H_3O(CH_2)_2O\underline{C}H_3$), δ =72.7ppm(s, $CH_3O(\underline{C}H_2)_2OCH_3$).

^{31}P-NMR(101.256MHz, THF-d8, 253K): δ= -280.9ppm(t, $^1J_{P,H}$= 155Hz, $\underline{P}H_2$);

^{31}P{^{1}H }-NMR(81.015MHz, Et_2O+10%THF-d8, 253K) :δ= -278.8ppm(s, $^1J_{P,Pb}$= 653Hz, $\underline{P}H_2$).

^{7}Li{^{1}H}- NMR(77.779MHz, Et_2O+10%THF-d8, 253K): δ= 2.1ppm.

^{29}Si{^{1}H }-NMR(79.495MHz, THF-d8, 253K): δ= -3.6ppm (s, $Si(\underline{Si}(CH_3)_3)_3$), δ=-135.2ppm (d, $\underline{Si}(Si(CH_3)_3)_3$,, $^1J_{Si,Pb}$= 1555Hz).

b) Reaction of dihypersilylplumbylene with lithium phosphanide in DME(1:1)

A solution of $Pb(Si(SiMe_3)_3)_2$ (1.10g, 1.56mmol) in 5mL of DME was added to a precooled(-20°C) suspension of $LiPH_2 \cdot 0.86DME$ (0.184g, 1.56mmol) in 5mL of DME with stirring. Immediately, the reaction mixture changed colour to violet-red. After stirring for 1h at -20°C, the mixture was allowed to come to room temperature and filtered through a porosity fritted glass filter. The ^{31}P-NMR (THF-d8) spectrum of the filtrate indicated that an adduct $Hyp_2Pb \cdot LiPH_2$ was almost quantitatively formed.

^{31}P{^{1}H}-NMR(101.256MHz, DME +10%THF-d8, 253K) :δ= -279.7ppm(s, $^1J_{P,Pb}$= 563Hz, $\underline{P}H_2$);

^{31}P-NMR (101.256MHz, DME +10%THF-d8, 253K): δ= -279.7ppm(t, $^1J_{P,H}$= 155.1Hz, $^1J_{P,Pb}$= 564Hz, $\underline{P}H_2$).

5.3.16 Synthesis of Li[$Hyp_2Pb \cdot P(H)Hyp$] (16)

To a precooled (-20°C) suspension of $LiPH_2 \cdot 0.86DME$ (0.16g, 1.4mmol) in 6mL of DME was added a solution of $Pb(Si(SiMe_3)_3\,)_2$ (1.0g, 1.4mmol) in 6mL of DME with stirring. The reaction mixture changed colour gradually to deep violet-red. After stirring about 1h at -20°C, the mixture was allowed to warm to room temperature and stirred for an additional 10min, followed by filtration through a G4 porosity fritted glass filter, the deep violet-red filtrate was concentrated to about 4mL under vacuum. Cooling of the resulting solution to -60°C for several weeks, didn’t afforded crystals. Removal of the solvent(DME) under vacuum and crystallization of the dark brown residue with THF at -60°C for several days afforded dark brown crystals, which were not suitable for single-crystal X-ray analysis. After removal of the supernatant liquid, the crystals were washed with n-pentane and extracted with diethyl ether. On cooling to -60°C for several weeks, dark red crystals of title compound precipitated, which was investigated by X-ray diffraction analysis. Unfortunately, the cation moieties were disordered in the crystal and the structure determination gave bad-defined structural parameters; however, the anion $[Hyp_2Pb \cdot P(H)Hyp]^-$ was ordered and could be unambiguously identified.

5.3.17 Synthesis of $[HypP(H)PbHyp]_2$ (17)

a) Reaction of $[(Me_3Si)_3Si]_2Pb$ with PH_3

Dry PH_3 gas [generated from reaction of $LiPH_2{\cdot}0.86DME$ (0.33g, 2.8mmol) with 2,6-di-^{t}Bu-phenol (0.58g, 2.8mmol) in 16 mL of diethyl ether] was bubbled through a solution of $[(Me_3Si)_3Si]_2Pb$ (0.91g, 1.3mmol) in 10mL of n-pentane at room temperature. After 20 minutes the dark blue solution changed colour to red-brown. The resulting solution was concentrated in dynamic vacuum at ambient temperature until a few dark brown crystals appeared then placed at -60°C for several days. The compound **17** was obtained as black crystals in 54% yield (based on $PbHyp_2$). X-ray diffraction-quality crystals of **17** was crystallized from diethyl ether for several weeks at -60°C.

^{1}H NMR (400.132MHz, toluene-d_8): **298K**: δ= 0.34(s, 54H, $^2J_{Si,H}$=6.2Hz, $SiMe_3$), 0.52(s, 54H, $^2J_{Si,H}$=6.5Hz, $SiMe_3$), 3.40(m, 2H, $^1J_{P,H}$=232.8Hz, $^3J_{P,H}$= 1.4Hz , $^4J_{H,H}$= 0 Hz , $^2J_{P,P}$= 60.7Hz, P*H*) ppm; **253K**: δ= 0.35 (s, 54H, $^2J_{Si,H}$=6.2Hz, $SiMe_3$), 0.59(s, 54H, $^2J_{Si,H}$=6.5Hz, $SiMe_3$), 3.59(m, 2H, $^1J_{P,H}$=233.9Hz, $^3J_{P,H}$= 1.9Hz , $^4J_{H,H}$= 0 Hz , $^2J_{P,P}$= 63.4Hz, P$\underline{H}$)ppm.

^{13}C{^{1}H} NMR(100.613MHz, toluene-d_8): **298K**: δ= 3.3(s, $SiMe_3$), 6.9(s, $SiMe_3$) ppm; **253K**: δ= 3.0(s, $SiMe_3$), 6.6(s, $SiMe_3$)ppm.

^{31}P NMR(101.256MHz, benzene-d6, 300K): -367.4(m, $^1J_{P,H}$= 233.2Hz, $^3J_{P,H}$= 2.3Hz , $^4J_{H,H}$= 0 Hz , $^2J_{P,P}$= 59.8Hz, ^{207}Pb satellites: $^1J_{P,Pb}$=1622Hz) ppm.

^{31}P NMR(161.975MHz, touluene-d_8, 298K): δ= -367.0(m, 2H, $^1J_{P,H}$=232.8Hz, $^3J_{P,H}$= 1.4Hz , $^4J_{H,H}$= 0 Hz , $^2J_{P,P}$= 60.7Hz, ^{207}Pb satellites: $^1J_{P,Pb}$=1620Hz) ppm.

^{31}P{H} NMR(161.975MHz, touluene-d_8, 298K):δ= -367.0(s, ^{207}Pb satellites: $^1J_{P,Pb}$=1620Hz) ppm.

^{31}P NMR(161.975MHz, toluene-d_8, 253K):δ= -370.0(m, 2H, $^1J_{P,H}$=233.9Hz, $^3J_{P,H}$= 1.9Hz , $^4J_{H,H}$= 0 Hz , $^2J_{P,P}$= 63.4Hz, ^{207}Pb satellites: $^1J_{P,Pb}$=1622Hz)ppm.

^{29}Si{H} NMR(79.490MHz, toluene- d_8, 298K): δ = -0.2 (s, Si(*Si*$Me_3)_3$), -4.9 (s, $Si(SiMe_3)_3$) ppm.

^{29}Si{H} NMR(79.490MHz, toluene-d_8, 253K): δ = -0.2 (s, Si(*Si*$Me_3)_3$), -5.0 (s, *Si*$(SiMe_3)_3$).

b) Reaction of $[(Me_3Si)_3Si]_2Pb$ with $(Me_3Si)_3SiPH_2$

0.093g(0.13mmol) of $[(Me_3Si)_3Si]_2Pb$ and 0.037g(0.13mmol) $(Me_3Si)_3SiPH_2$ were solved in 1 mL of benzene-d_6 and sealed in a 5mm i. d. NMR tube at room temperature. After 30min, the **^{31}P{H} NMR** (161.975MHz, C_6D_6, 298K) spectrum of the resulting mixture showed that more than 70% phosphorus was converted to **17** (identified by comparison with an authentic sample prepared above), which then decomposed gradually on standing at ambient temperature.

Note: After a solution of **17** in toluene- *d*$_8$ had been stored for 24h at ambient temperature in a sealed NMR tube, the resonance of **17** was no longer observable in the ^{31}P NMR and ^{1}H NMR spectra, new signals appeared instead, which could be assigned to the compounds **12**, $(Me_3Si)_3SiPH_2$ (identified by comparison with authentic sample), and $(Me_3Si)_3SiH$.

5.3.18 Synthesis of K[Hyp$_2$Pb·PH$_2$] (18)

To a precooled (-20°C) suspension of KPH_2 (0.073g, 1.01 mmol) in 10mL of diethyl ether was added a solution of $Pb(Si(SiMe_3)_3)_2$ (0.71 g, 1.01 mmol) in 10mL of diethyl ether with stirring. The deep blue reaction mixture developed immediately a orange-brown colour. After stirring for approximately 1h, the mixture was allowed to come to room temperature and continued stirring for about 10min. The mixture then filtered through a porosity fritted glass filter and the filtrate was concentrated under reduced pressure. After adding 0.5 mL triazine, the resulting solution was cooled in a -60°C refrigerator for several days to afford the orange-brown crystals of $Hyp_2Pb{\cdot}KPH_2$ (as triazine adduct).

Yield: 0.95g.

Formula: $[(Me_3Si)_3Si]_2Pb\cdot KPH_2\cdot 2[(MeNCH_2)_3]$

^{1}H-NMR (400.132 MHz, THF-d8 + 50% toluene, 253K): δ =0.21 ppm(s, Si(Si(C$\underline{H}_3$)$_3$)$_3$); δ = 0.95 ppm,(d, $^{1}J_{P,H}$ =156Hz, P$\underline{H}_2$); δ =1.99 ppm(t, (NC$\underline{H}_3$), δ =2.36 (s), 2.38 (s) ppm (NCH$_2$N).

^{13}C{H}-NMR(100.613 MHz, THF-d8 + 50% toluene, 253K): δ =5.5 ppm(s, Si(Si($\underline{C}$H$_3$)$_3$)$_3$), δ =40.2 ppm (s, N$\underline{C}$H$_3$), δ = 77.9 ppm(s, NCH$_2$N).

^{31}P{H}-NMR(161.976 MHz, THF-d8 + 50% toluene, 253K): δ = -281.7ppm (s, $^{1}J_{Pb,P}$= 590 Hz).

^{31}P-NMR(161.976 MHz, THF-d8 + 50% toluene, 253K): δ = -281.7ppm (t, $^{1}J_{P,H}$ =156Hz, $^{1}J_{Pb,P}$= 590 Hz).

^{29}Si{^{1}H}- NMR (79.495 MHz, THF-d8 + 50% toluene, 253K): δ = -3.46 ppm (s, Si$\underline{Si}_3$); -133.94 ppm (s, $\underline{Si}$Si$_3$).

5.3.19 Synthesis of Li[(Hyp$_2$Pb)$_2$·PH$_2$] (19)

a) Reaction of dihypersilylplumbylene with lithium phosphanide in DME(2:1)

A solution of $Pb(Si(SiMe_3)_3)_2$ (2.41g, 3.43mmol) in 15mL of DME was added to a precooled(-20°C) suspension of $LiPH_2{\cdot}0.86DME$ (0.20g, 1.72mmol) in 10mL of DME with stirring. The reaction mixture changed colour immediately to dark violet-red. After stirring for

1h, the mixture was allowed to come to room temperature and filtered through a porosity fritted glass filter. The ^{31}P-NMR(THF-d8) spectrum of the filtrate indicated that along with some of $LiPH_2 \cdot Pb(Si(SiMe_3)_3)_2$ and small amounts of some other phosphorus- and lead-containing compounds, adduct $LiPH_2 \cdot 2Pb(Si(SiMe_3)_3)_2$ was formed as the main product . The resulting reaction mixture was filtered through a porosity fritted glass filter and the solvent was removed in vacuo. The residue was then washed with 15mL of pentane in portions and extracted with 20mL of diethyl ether. Reduction of the volume of the extract to approximately 4mL and cooling at -60°C for several days led to the deposition of dark brown crystals of $Hyp_2Pb{\cdot}LiPH_2$(as DME solvate). Due to the strong disordering of the cation moiety, the single-crystal X-ray diffraction analysis revealed only a structure of the anion moiety $[(Hyp_2Pb)_2PH_2]^-$ for this compound.

Yield: 1.23g

Formula: $(((Me_3Si)_3Si)_2Pb)_2 \cdot LiPH_2 \cdot x$DME.

^{1}H-NMR(250.133MHz, THF-d8, 253K): δ=0.24ppm(s, $Si(Si(C\underline{H}_3)_3)_3$), δ=3.26 ppm (s, $C\underline{H}_3O(CH_2)_2OC\underline{H}_3$), δ=3.42ppm(s, $CH_3O(C\underline{H}_2)_2OCH_3$).

^{13}C{^{1}H}-NMR (62.896MHz, THF-d8, 253K): δ=6.4ppm(s, $Si(Si(\underline{C}H_3)_3)_3$), δ=58.9ppm(s, $\underline{C}H_3O(CH_2)_2O\underline{C}H_3$), δ=72.6ppm(s, $CH_3O(\underline{C}H_2)_2OCH_3$).

^{31}P-NMR(101.256MHz, THF-d8, 253K):δ= -350.5ppm(t, $^1J_{P,H}$= 222Hz, $\underline{P}H_2$);

^{31}P{^{1}H}-NMR (101.256MHz, THF-d8, 253K) :δ= -350.5ppm(s, $^1J_{P,Pb}$= 1411Hz, $\underline{P}H_2$).

b) Reaction of dihypersilylplumbylene with lithium phosphanide (2:1) in 12-crown-4 ether

A diethyl ether (10mL) solution of $Pb(Si(SiMe_3)_3)_2$ (1.20g, 1.7mmol) was slowly added to a diethyl ether (10mL) suspension of $LiPH_2{\cdot}0.86$DME (0.10g, 0.85mmol) and 12-crown-4 ether (0.30g, 1.7mmol) with stirring at -25°C. Gradually, the reaction mixture became dark violet-red. After 1h, the mixture was allowed to warm up to room temperature and stirred for an additional 10min. After filtration through a G3 porosity fritted glass filter, the filtrate was dried under vacuo. The residue was washed with 10mL of n-pentane in portions and extracted with in 8mL of diethyl ether. The volume of the solution was then reduced to about 4mL under reduced pressure. Cooling of the solution to -60°C for several days led to recrystallization of $2Hyp_2Pb{\cdot}LiPH_2$ as ether solvate. Again, due to the strong disordering of the cation moiety, the single-crystal X-ray diffraction analysis revealed only a structure of the anion moiety $[(Hyp_2Pb)_2PH_2]^-$ for this compound.

Yield: 1.02g, dark brown, air- and moisture-sensitive crystals.

Formula: $2Pb(Si(SiMe_3)_3)_2 \cdot LiPH_2 \cdot x12\text{-crown-}4 \cdot yDME \cdot zEt_2O$.

^{1}H-NMR(250.133MHz, THF-d8, 253K): δ= 0.25ppm(s, 54H, $Si(Si(C\underline{H}_3)_3)_3$); δ= 1.11ppm(t, $C\underline{H}_3CH_2)_2O$), δ=3.37ppm(q, $CH_3C\underline{H}_2)_2O$); δ=3.26ppm(s, $C\underline{H}_3O(CH_2)_2OC\underline{H}_3$), δ=3.42ppm(s, $CH_3O(C\underline{H}_2)_2OCH_3$); δ=3.70ppm(s, 12-crown-4 ether);

^{13}C{^{1}H}-NMR(62.896MHz, THF-d8, 253K): δ 6.4ppm(s, $Si(Si(\underline{C}H_3)_3)_3$); δ=15.7ppm(s, $\underline{C}H_3CH_2)_2O$), δ=66.4ppm(s, $CH_3\underline{C}H_2)_2O$); δ=58.8ppm(s, $\underline{C}H_3O(CH_2)_2O\underline{C}H_3$), δ=72.6ppm(s, $CH_3O(\underline{C}H_2)_2OCH_3$); δ=68.9ppm(s, 12-crown-4 ether);

^{31}P-NMR(101.256MHz, THF-d8, 253K) :δ= -350.5ppm(s, $^{1}J_{P,Pb}$= 1420Hz);

^{31}P{^{1}H}-NMR(81.015MHz, Et_2O+10%THF-d8, 253K) :δ= -350.5ppm(t, $^{1}J_{P,H}$= 222Hz);

^{7}Li{^{1}H}-NMR(77.779MHz, Et_2O+10%THF-d8, 253K): δ= 2.2ppm(s);

^{29}Si{^{1}H}-NMR((49.694MHz, Et_2O+10%THF-d8, 253K)): δ= 3.4 ppm(s, $Si(\underline{Si}(CH_3)_3)_3$).

c) Reaction of dihypersilylplumbylene with 15a (2:1) in diethyl ether in presence of triazine

A solution of $Pb(Si(SiMe_3)_3)_2$ (0.56g, 0.80mmol) in 6mL of diethyl ether was added to a stirred solution of $Hyp_2Pb \cdot LiPH_2 \cdot DME \cdot Et_2O$ (0.69g, 0.80mmol) in 9mL of diethyl ether and 1mL of triazine at -20°C. The reaction led almost quantitatively to a deep violet-red solution of expected adduct $2PbHyp_2 \cdot LiPH_2$ after 1 hour according to the ^{31}P-NMR spectrum of a sample of the resulting solution. The volume of the solution was then reduced to about 4 mL under reduced pressure and the resulting saturated solution was cooled to -60°C for several days to give dark brown crystals of $2PbHyp_2 \cdot LiPH_2$ as triazine solvate. Attempts to grow single crystals suitable for X-ray diffraction investigation failed.

Yield: 0.97g, dark brown, air- and moisture-sensitive crystals.

Formula: $2Pb(Si(SiMe_3)_3)_2 \cdot LiPH_2 \cdot x$ triazine$\cdot yEt_2O$.

^{1}H-NMR(400.13MHz, THF-d8, δ: ppm)

temp.	-50°C	-30°C	-20°C	-10°C	0°C	25°C
$P\underline{H}_2$	d 2.53 3.09 (223Hz)	d 2.52 3.08 (223Hz)	d (br) 2.50 3.05 (222Hz)	d (br) 2.48 3.03 (221Hz)	d (br) 2.45 3.01 (220Hz)	d (br) 2.39 2.94 (218Hz)
$C\underline{H}_3$ (Hyp)	d 0.223 0.238	d 0.227 0.242	s 0.243	s 0.247	s 0.252	s 0.259
$C\underline{H}_3$ (triazine)	s 2.154	s 2.158	s 2.165	s 2.17	s 2.17	s 2.18
$C\underline{H}_2$ (triazine)	d 2.56(10.0Hz) d	d 2.57(10.0Hz) d	d(br) 2.59(9.1Hz) d(br)	s (br) 2.60 s(br)	s (br) 2.61 s(br)	s (very br) 3.1

	3.54(10.3Hz)	3.54(10.3Hz)	3.53(9.4Hz)	3.52	3.51	
C$\underline{H}_3$ (Et_2O)	t 1.10(7.0Hz)	t 1.10(7.0Hz)	t 1.10(7.0Hz)	t 1.10(7.0Hz)	t 1.10(7.0Hz)	t 1.10(7.0Hz)
C$\underline{H}_2$ (Et_2O)	q 3.35(7.0Hz)	q 3.35(7.0Hz)	q 3.36(7.0Hz)	q 3.36(7.0Hz)	q 3.36(7.0Hz)	q 3.37(7.0Hz)

^{13}C-NMR(100.613MHz, THF-d8, 243K): δ= 6.4ppm(s, $^1J_{Si,C}$=42Hz, $Si(Si(\underline{C}H_3)_3)_3$); δ= 15.8ppm(s, $\underline{C}H_3CH_2)_2O$), δ= 66.5 ppm (s, $CH_3\underline{C}H_2)_2O$); δ= 40.5 ppm (s, N-$\underline{C}H_3$), δ= 78.2 ppm (s, N-$\underline{C}H_2$-N)(triazine).

^{31}P{H}-NMR(161.93MHz, THF-d8, 243K): δ= -352.0ppm (s, ^{207}Pb satellites: ^{1}Jp,pb=1420Hz);

^{31}P-NMR(161.93MHz, THF-d8, 243K): δ= -352.0ppm (t, $^1J_{p,H}$=222Hz, with ^{207}Pb satellites).

^{7}Li{H}-NMR(155.51MHz, THF-d8, 243K): δ= 0.95ppm(s).

^{29}Si{H}-NMR(79.50MHz, THF-d8, 298K): δ= -2.36ppm (s, $Si(\underline{Si}(CH_3)_3)_3$).

^{29}Si{H}-NMR(79.50MHz, THF-d8, 223K): δ= -2.05ppm, δ=-2.56ppm (d, $Si(\underline{Si}(CH_3)_3)_3$).

5.3.20 Synthesis of $K[(Hyp_2Pb)_2{\cdot}PH_2]$ (20)

a) Reaction of dihypersilylplumbylene(excess) with potassium phosphanide

$LiPH_2{\cdot}0.86DME$ (1.0g, 8.53mmol) and 2,6-di-^{t}Bu-phenol (1.76g, 8.53mmol) were brought together at -70°C in 25mL of DME. The mixture was slowly warmed to room temperature, and the liberated gas PH_3 was then bubbled through a solution of $Pb[Si(SiMe_3)_3]_2$ (1.60g, with a small amount of $KN(SiMe_3)_2$ as by product from the preparation) in 25mL of n-pentane at a temperature below -30°C. After 30 minutes the dark blue solution changed colour to violet-red and a dark brown precipitate formed. This precipitate was then separated by filtration and extracted with a 5 mL of diethyl ether. Cooling to -60°C led to the crystallization of $KPH_2{\cdot}2Pb[Si(SiMe_3)_3]_2$ as ether solvate.

Yield: 0.18g.

Formula: $KPH_2{\cdot}2Pb[Si(SiMe_3)_3]_2{\cdot}xDME{\cdot}yEt_2O$.

^{1}H-NMR(400.13MHz, THF-d8, δ:ppm):

temp.	-70°C	-60°C	-30°C	-20°C	25°C
PH_2	d 2.55 3.11 (224Hz)	d 2.54 3.10 (224Hz)	d 2.51 3.07 (222Hz)	d (br) 2.51 3.06 (222Hz)	d(br) 2.25 2.77 (215Hz)
$SiMe_3$	d 0.22 0.24	d 0.23 0.24	s 0.238	s 0.243	s 0.26

CH_3 (DME)	s 3.25	s 3.25	s 3.25	s 3.25	s 3.26
CH_2 (DME)	s 3.41	s 3.41	s 3.41	s 3.41	s 3.42
CH_3 (Et_2O)	t 1.10(7.0Hz)	t 1.10(7.0Hz)	t 1.10(7.0Hz)	t 1.10(7.0Hz)	t 1.11(7.0Hz)
CH_2 (Et_2O)	q 3.35(7.0Hz)	q 3.35(7.0Hz)	q 3.36(7.0Hz)	q 3.36(7.0Hz)	q 3.37(7.0Hz)

^{13}C-NMR(100.613MHz, THF-d8, 253K): δ= 6.5ppm(s, $^1J_{Si,C}$=43Hz, $Si(Si(C\underline{H}_3)_3)_3$); δ= 15.8ppm(s, $\underline{C}H_3CH_2)_2O$), δ= 66.5ppm(s, $CH_3\underline{C}H_2)_2O$); δ= 58.9ppm(s, $\underline{C}H_3O(CH_2)_2O\underline{C}H_3$), 72.7(s, $CH_3O(\underline{C}H_2)_2OCH_3$).

^{29}Si{H}-NMR(79.495MHz, THF-d8, 300K): δ= -2.4ppm(s, $Si(\underline{Si}(CH_3)_3)_3$);

^{29}Si{H}-NMR(79.495MHz, THF-d8, 223K): δ= -2.0ppm(s, $Si(\underline{Si}(CH_3)_3)_3$), δ= -2.6ppm(s, $Si(\underline{Si}(CH_3)_3)_3$), -82.0(m, $\underline{Si}(Si(CH_3)_3)_3$).

^{31}P{H}-NMR(161.976MHz, THF-d8, 253K): δ =-350.9ppm(s, ^{207}Pb satellites: $^1J_{P,Pb}$=1420Hz).

^{31}P-NMR(161.976MHz, THF-d8, 253K): δ= -350.9ppm(t, $^1J_{P,H=}$222Hz, with ^{207}Pb satellites).

Note: Single-crystal X-ray diffraction analysis suitable crystals were recrystallized from a mixture of diethyl ether and triazine at -60°C.

b) Reaction of dihypersilylplumbylene with potassium phosphanide

To a precooled(-20°C) suspension of KPH_2 (0.04g, 0.55mmol) in 5mL of diethyl ether was added a solution of $Pb(Si(SiMe_3)_3)_2$ (0.78g, 1.1mmol) in 15mL of diethyl ether and 1mL of triazine(6.9mmol) with stirring. The reaction mixture turned to deep violet-red immediately. After stirring for about 30min at -20°C, the mixture was allowed to warm to room temperature and stirred for an additional 10min. The volume of the resulting solution was reduced to about 5 mL under vacuum. On cooling to -60°C for several days, dark red crystals of title compound precipitated.

Yield: 0.91g(92%).

Formula: $KPH_2 \cdot 2Pb[Si(SiMe_3)_3]_2 \cdot 3(MeNCH_2)_3$.

^{13}C-NMR(100.613MHz, THF-d8, 253K): δ= 6.6ppm(s,$Si(Si(\underline{C}H_3)_3)_3$); δ= 40.6 ppm (s, N-$\underline{C}H_3$), δ= 78.5 ppm (s, N-$\underline{C}H_2$-N)(triazine).

^{31}P{H}-NMR(161.93MHz, THF-d8, 253K): δ= -350.91ppm (s, ^{207}Pb satellites: ^{1}Jp,pb=1400Hz);

^{31}P-NMR(161.93MHz, THF-d8, 253K): δ= -350.9ppm (t, $^{1}J_{P,H}$=222Hz, with ^{207}Pb satellites).

5.3.21 Synthesis of Hyp$_2$Sn·PMe$_3$ (21)

To a precooled(-20°C) solution of $Sn(Si(SiMe_3)_3)_2$ (0.82g, 1.3mmol) in 5mL of n-pentane was added dropwise a solution of trimethylphosphane (0.10g, 1.3mmol) in 3mL of n-pentane with stirring at -20°C. Immediately the reaction solution changed colour from dark brown to yellow-brown. After stirring for about 1h, the resulting solution was allowed to come to room temperature and concentrated under reduced pressure. The yellow-brown saturated solution was cooled at -60°C for 2 days to afford orange crystals of Hyp$_2$Sn·PMe$_3$ in good yield. Attempts to obtain X-ray diffraction suitable single crystal by recrystallization with n-pentane , cyclopentane, or toluene failed.

Yield: 0.79g(1.1mmol, 88%), air- and moisture-sensitive yellow-orange crystals.

Formula: $Sn(Si(SiMe_3)_3)_2 \cdot P(CH_3)_3$

^{1}H-NMR(250.133MHz, C_6D_6, 300K): δ= 0.44ppm(s, $^{2}J_{Si,H}$= 6.3Hz, 54H, $Si(Si(C\underline{H}_3)_3)_3$), δ= 1.07ppm(d, $^{2}J_{P,H}$= 7.5Hz, 9H, $P(C\underline{H}_3)_3$).

^{13}C{H}-NMR (62.896MHz, C_6D_6, 300K): δ = 5.3ppm (s, $Si(Si(\underline{C}H_3)_3)_3$). δ= 18.7ppm(d, $^{1}J_{P,C}$= 7.8Hz, $P(\underline{C}H_3)_3$).

^{31}P{H}-NMR(101.256MHz, C_6D_6, 300K): δ = -61.0 ppm(s, $\underline{P}(CH_3)_3$).

^{31}P{H}-NMR(101.256MHz, cyclopentane+10%C_6D_6, 243K): δ= -60.1ppm(s, $^{1}J_{119Sn,P}$=1960 Hz, $^{1}J_{117Sn,P}$=1881 Hz, $\underline{P}(CH_3)_3$).

^{29}Si-NMR(39.761MHz, C_6D_6, 300K): δ= -6.9ppm(s, $Si(\underline{Si}(CH_3)_3)_3$), δ=-126ppm(s, $\underline{Si}(Si(CH_3)_3)_3$).

^{119}Sn{^{1}H}-NMR(74.631MHz, C_6D_6, 300K): δ=-37ppm(d, $^{1}J_{119Sn,P}$= 1930Hz).

5.3.22 Synthesis of Hyp$_2$Pb·PMe$_3$ (22)

To a precooled(-20°C) solution of $Pb(Si(SiMe_3)_3)_2$ (0.80g, 1.1mmol) in 5mL of n-pentane was added a solution of trimethylphosphane (0.086g, 1.1mmol) in 3mL of n-pentane with stirring at -20°C. The reaction mixture turned immediately from deep blue to deep red. After stirring for about 1h, the resulting solution was allowed to come to room temperature and concentrated under reduced pressure. The deep red saturated solution was cooled at -60°C for 2 days to provide dark red crystals of $Hyp_2Pb{\cdot}P(CH_3)_3$. Attempts to obtain X-ray diffraction analysis suitable single crystal by recrystallization with n-pentane, cyclopentane, or toluene failed.

Yield: 0.79g(0.99 mmol, 90%). air- and moisture-sensitive dark red crystals.

Formula: $Pb(Si(SiMe_3)_3)_2{\cdot}P(CH_3)_3$.

^{1}H-NMR(250.133MHz, C_6D_6, 300K): δ= 0.48ppm(s, 54H, $Si(Si(C\underline{H}_3)_3)_3$), δ= 1.17ppm(d, $^2J_{P,H}$= 5.7Hz, 9H, $P(C\underline{H}_3)_3$).

^{13}C{H}-NMR (62.896MHz, C_6D_6, 300K): δ = 6.5ppm (s, $Si(Si(\underline{C}H_3)_3)_3$). δ= 19.8ppm(d, $^1J_{P,C}$= 5.0Hz, $P(\underline{C}H_3)_3$).

^{31}P{H}-NMR(101.256MHz, C_6D_6, 300K): δ = -111.8 ppm(s, $\underline{P}(CH_3)_3$).

5.3.23 Synthesis of Hyp_6Pb_{12} (23)

Reaction of dihypersilylplumbylene with PH_3

Dry PH_3 gas (generated from the reaction of $LiPH_2{\cdot}0.86DME$ (1.0g, 8.53mmol) with 2,6-di-^{t}Bu-phenol (1.76g, 8.53mmol) in 25 mL of DME) was bubbled through a solution of $Pb[Si(SiMe_3)_3]_2$ (1.60g, 2.2mmol) in 25mL of n-pentane at a temperature below -30°C. After 30 minutes the dark blue solution changed colour to deep violet-red. The **^{31}P NMR**(161.975MHz, toluene-d_8, 253K) spectrum of the reaction solution showed two resonances at δ=-286.5(q, br, $^1J_{P,H}$= 236Hz), -224.2(t, $^1J_{P,H}$= 163.5Hz, ^{207}Pb satellites: $^1J_{Pb,P}$= 733.9Hz) ppm. The **^{31}P{H} NMR**(161.975MHz, toluene-d_8, 253K) of the same sample showed two singlets at -286.5 (s, br) and -224.2(s, ^{207}Pb satellites: $^1J_{Pb,P}$= 736Hz) ppm.

After filtration, the volume of the filtrate was reduced in vacuo to 2~3mL. Cooling at -60°C for two weeks, nearby unconsumed crystals of $Pb[Si(SiMe_3)_3]_2$ several dark brown rhombohedral crystals of $Pb_{12}[Si(SiMe_3)_3]_6$ formed, which is suitable for single-crystal X-ray diffraction analysis.

Note a) Reaction of dihypersilylplumbylene with $(BH_3)_2$

Dry $(BH_3)_2$ gas (generated from $NaBH_4$ (0.34g, 9.0mmol) and $BF_3{\cdot}Et_2O$ (1.52mL, 12.0mmol, d=1.12g/mL) in DME) was bubbled through a deep blue solution of $Pb[Si(SiMe_3)_3]_2$(1.0g, 1.4mmol) in 15mL of n-pentane at -40°C. After 30 minutes the reaction mixture changed colour to light blue and a black precipitate of metal lead formed. The NMR spectra of the resulting mixture indicated that along with some of the unconsumed plumbylene almost only $HSi(SiMe_3)_3$ was formed:

Note b) Reaction of dihypersilylplumbylene with $NaBH_4$

A solution of $Pb[Si(SiMe_3)_3]_2$ (1.36g, 1.9mmol) in 8mL of THF was added to a suspension of $NaBH_4$(0.073g, 1.9mmol) in 7mL of THF with stirring at room temperature. The reaction mixture changed colour gradually to brown-red. After stirring for about 30 min, the resulting solution was then concentrated and cooled to -60°C to give red crystals of adduct of dihypersilylplumbylene and $NaBH_4$ in good yield. X-ray diffraction quality crystals was obtained by recrystallization from a mixture of diethyl ether(4mL) and triazine(1mL) at -60°C.

Yield: 1.12g.

^{1}H-NMR(400.613MHz, THF-d8, 253K): δ= 0.26ppm(s, $Si(Si(C\underline{H}_3)_3)_3$); δ= 2.17 ppm (s, $N\text{-}C\underline{H}_3$), δ= 2.54ppm(d, $^2J_{H,H}$=8.3Hz), δ= 3.56ppm(d, $^2J_{H,H}$ =8.3Hz)($N\text{-}C\underline{H}_2\text{-}N$), δ= 1.77ppm(m), δ= 3.61(m)(THF), δ= -1.5ppm(s,br)(BH_4).

^{13}C{H}-NMR(100.613MHz, THF-d8, 253K): δ= 5.9ppm(s, $^1J_{C,Si}$=42.3Hz, $Si(Si(\underline{C}H_3)_3)_3$); δ= 26.4ppm(s), δ= 68.2ppm(s, THF); δ= 40.4ppm(s, $N\text{-}\underline{C}H_3$), δ= 78.3ppm(s, $N\text{-}\underline{C}H_2\text{-}N$).

^{29}Si{H}-NMR(79.495MHz, THF-d8, 253K): δ= -1.8ppm(s, $Si(\underline{Si}(CH_3)_3)_3$), δ= 36.9ppm(s, $\underline{Si}(Si(CH_3)_3)_3$).

^{11}B{H}-NMR(128.378MHz, THF-d8, 253K): δ= -49.5ppm(s, br);

^{11}B-NMR(128.378MHz, THF-d8, 253K): δ= -49.5ppm(quintet, br).

5.3.24 Synthesis of Hyp_6Pb_{10} (24)

a) Reaction of dihypersilylplumbylene with $(CuHPPh_3)_6$

A solution of $Pb[Si(SiMe_3)_3]_2$ (3.01g, 4.28mmol) in 20mL of toluene was added to a stirred suspension of triphenylphosphane-copper(I)-hydride hexamer (90%) (1.55g, 4.28mmol) in 30mL of toluene at -20°C. After 25 min the mixture was allowed to come to room temperature and stirred for an additional 20 min. The brown resulting mixture was filtered through a porosity fritted glass filter and the volume of the filtrate was reduced to about 9mL in vacuo. On cooling to -60°C for 48h, dark brown rhombohedral crystals of $Pb_{10}[Si(SiMe_3)_3]_6$ precipitated.

Yield: 0.51g (32.7%, 0.14mmol), dark brown, air- and moisture-sensitive crystals.

Formula: $Pb_{10}[Si(SiMe_3)_3]_6$

^{1}H-NMR(400.133MHz, C_6D_6,298K): δ=0.63ppm(s, $^2J_{Si,H}$=6.2Hz, $Si(Si(C\underline{H}_3)_3)_3$);

^{1}H-NMR(400.133MHz, toluene-d8, 298K):

Temp.	25°C	0°C	-20°C	-30°C	-35°C	-40°C	-60°C
δ (ppm)	0.591 (s)	0.598 (s)	0.604 (s)	0.613 (s)	0.622 0.598 (d)	0.629 0.593 (d)	0.642 0.597 (d)

^{13}**C-NMR**(100.620MHz, C_6D_6, 298K): δ = 9.07ppm (s, $Si(Si(\underline{C}H_3)_3)_3$).

^{13}**C-NMR**(100.620MHz, toluene-d8, 298K): δ= 9.0ppm (s, $Si(Si(\underline{C}H_3)_3)_3$).

The supernatant liquid was dried in vacuo and extracted with two portions of 15mL of n-pentane. The extract was then concentrated to incipient crystallization under reduced pressure and cooled to -60°C for 12 h to afford 1.69g(47%, based on $CuHPPh_3$) of $CuSi(SiMe_3)_3{\cdot}2PPh_3$ as colourless X-ray diffraction quality crystals:

^{1}**H-NMR**(400.133MHz, C_6D_6, 298K): δ=0.53ppm(s, 27H, $^{2}J_{Si,H}$=6.5Hz, $Si(Si(C\underline{H}_3)_3)_3$); δ=6.98ppm(m,18H), δ=7.37ppm(m,12H) (PPh_3).

^{13}**C-NMR**(100.620MHz, C_6D_6, 298K) δ=5.6ppm(s, $Si(Si(\underline{C}H_3)_3)_3$), δ=133.8ppm(d, $^{2}J_{c,p}$ = 16.7Hz), δ=129.4ppm(s), δ=128.6ppm (d, $^{3}J_{c,p}$ = 8.4Hz)(PPh_3).

^{31}**P-NMR**(162.048MHz, C_6D_6,298K) δ=-7.3ppm(s, PPh_3).

^{29}**Si-NMR**(79.490MHz, C_6D_6,298K) δ=-6.8ppm(s,$Si(\underline{Si}(CH_3)_3)_3$,).

Further crystallization of the pentane supernate by cooling at -60°C for a week provided a few orange well shaped X-ray diffraction quality crystals: $Cu_9H_6(Si(SiMe_3)_3)_3{\cdot}2PPh_3$.

^{1}**H-NMR**(400.133MHz, C_6D_6, 298K): δ=0.48ppm(s, $^{2}J_{Si,H}$=6.2Hz, $Si(Si(C\underline{H}_3)_3)_3$); δ=2.5ppm(s, 6H, br, $Cu\underline{H}$); δ=7.1 ppm (m,6H), δ=7.2 ppm (m,12H), δ=7.8 ppm (m, 12H)(PPh_3).

^{13}**C-NMR**(100.620MHz, C_6D_6, 298K): δ=6.0ppm(s, $Si(Si(\underline{C}H_3)_3)_3$); δ= 128.9 ppm (d, $^{3}J_{c,p}$ = 8.8Hz), δ=130.0 ppm (s), δ=133.2 ppm (d, $^{1}J_{c,p}$ = 33.2Hz), δ=134.8ppm(d, $^{2}J_{c,p}$ = 14.4Hz)(PPh_3).

^{31}**P-NMR**(162.048MHz, C_6D_6, 298K): δ= 9.7ppm (s, br, $\underline{P}Ph_3$).

^{29}**Si-NMR**(79.490MHz, C_6D_6, 298K): δ=-8.1ppm (s, $Si(\underline{Si}(CH_3)_3)_3$).

b) Reaction of dihypersilylplumbylene with diisobutylaluminiumhydride

To a precooled (-20°C) solution of $Pb(Si(SiMe_3)_3)_2$ (2.61g, 3.72mmol) in 15mL of n-pentane was added a hexane solution of diisobutylaluminiumhydride(5.58mL, 1M, 5.58mmol). After stirring at -20°C for 4h, the resulting solution was allowed to come to room temperature and stirred for an additional 30 minutes. During this period the colour of the mixture turned gradually from deep blue to brown. Reduction of the mixture to a volume of approximately 6mL under reduced pressure and storage at -60°C for 24 h led to the deposition of black crystalline solid, which consisted of $Pb_{10}[Si(SiMe_3)_3]_6$ (67%) and $Pb(Si(SiMe_3)_3)_2$(33%) according to ^{1}H-NMR spectrum. Recrystallization from n-pentane furnished black crystals of $Pb_{10}[Si(SiMe_3)_3]_6$.

Yield of compound **24**: 0.74g (56%, based on Pb in dihypersilylplumbylene).

NMR of $(i\text{-bu})_2AlSi(SiMe_3)_3$:

^{1}H-NMR(400.132MHz, C_6D_6, 300K): δ= 0.33ppm(s, 27H, $Si(Si(C\underline{H}_3)_3)_3$).1.05ppm(d, $CH_2CH(C\underline{H}_3)_2$, 12H, $^3J_{C,H}$=6.75Hz)).

^{13}C{H}-NMR (100.613MHz, C_6D_6, 300K): δ = 4.2 ppm (s, $Si(Si(\underline{C}H_3)_3)_3$).

MS[ESI; Et_2O/MeCN (4:1)]: m/z (%): 3311 (100, M^+-Hyp), 2815 (8, $[Pb_{10}Hyp_3]^+$), 2113 (25, $[Pb_{10}Hyp]^+$), 2099 (43, $[Pb_9$ Hyp-H-$CH_3]^+$), 717 (51, $[Hyp_2MePb]^+$).

c) Reaction of plumbylene with trihydrido(trimethylamine)aluminium

At -30°C a solution of $Pb(Si(SiMe_3)_3)_2$ (2.79g, 3.97mmol) in 15mL of n-pentane was added to a suspension of trihydrido(trimethylamine)aluminium(0.35g, 3.97mmol) in 5 mL of n-pentane. The colour of the mixture turned from deep blue to brown immediately. After stirring about 1.5h, the reaction mixture was allowed to come to room temperature. The volatile components were removed in vacuo and the residue was extracted with 15mL toluene. Concentration and storage of the resulting solution at -60°C for 24 h afforded black crystals of $Pb_{10}[Si(SiMe_3)_3]_6$.

Yield of compound **24**: 0.89g (63%, based on Pb in dihypersilylplzumbylene).

NMR of $(Me_3Si)_3SiAlH_2{\cdot}NMe_3$:

^{1}H-NMR(400.132MHz, C_6D_6, 300K): δ= 0.43ppm(s, 27H, $Si(Si(C\underline{H}_3)_3)_3$), 1.92ppm(s, 9H, $C\underline{H}_3$).

^{13}C{H}-NMR (100.613MHz, C_6D_6, 300K): δ = 4.1 ppm (s, $Si(Si(\underline{C}H_3)_3)_3$), 48.9 ppm (s, $N(\underline{C}H_3)_3$).

^{29}Si{H}-NMR (79.495MHz, C_6D_6, 300K): δ = -7.9 ppm (s, $Si(\underline{Si}(CH_3)_3)_3$).

^{27}Al{H}-NMR (104.261MHz, C_6D_6, 300K): δ = -31.7ppm (s, br).

6 Summary

Hypersilyl $(Me_3Si)_3Si$ behaves as a very bulky, electron delivering substituent and can be utilized for stabilizing elements in low oxidation states and unusual geometries. By reactions of base-free alkali metal hypersilanides and dihypersilyl plumbylene with various phosphorus sources, a series of hypersilyl stabilized phosphorus and lead clusters have been obtained. The syntheses and structural characterization of these novel compounds represent the main theme of this thesis.

Solvent-free potassium hypersilanide readily reacts with white phosphorus in a molar ratio of 2:1 in toluene or benzene at room temperature to give potassium bis(hypersilyl)tetraphosphenide $[(Me_3Si)_3Si]_2P_4K_2$ (**I**), a potassium salt of $(Me_3Si)_3Si$-PH-P=P-PH-$Si(SiMe_3)_3$, quantitatively. The ^{31}P-NMR spectrum shows two multiplets with the classical splitting pattern of an AA'XX' system in the range for a phosphorus atom in phosphenide and for an unsaturated phosphorus atom in diphosphene, respectively. Toluene, benzene, and hexahydro-1,3,5-trimethyl-S-triazine solvates of $[(Me_3Si)_3Si]_2P_4K_2$ are investigated by X-ray crystallography. The central moiety of the molecular structures exhibits an undistorted C_{2v}-symmetric U-shaped P_4 skeleton featuring two hypersilyl groups either staggered or eclipsed with respect to each other at each end of the P chain. The P-P distance between both middle P atoms (about 209 pm) is only about 5 pm shorter than the other two P-P bonds and all three display partial P=P double-bond character, suggesting significant charge delocalization over the whole P_4 chain. The two potassium atoms each coordinate from one side of the P_4 plane to all four phosphorus atoms and the coordination sphere of K is completed by the corresponding solvent molecules.

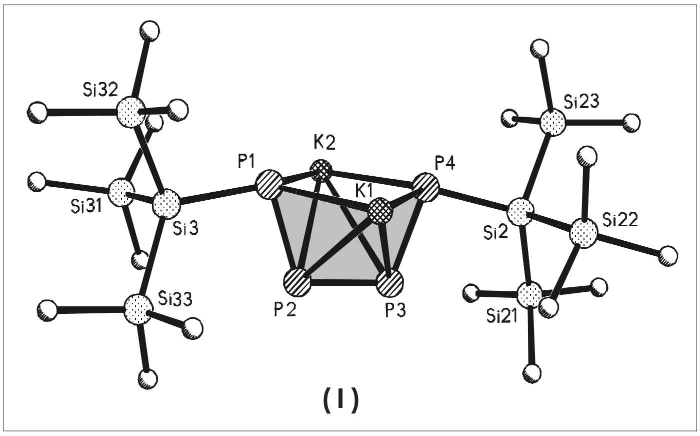

(I)

There exists an equilibrium between $[(Me_3Si)_3Si]_2P_4K_2$ and its dimer tetrakis(hypersilyl)octaphosphanide $[(Me_3Si)_3Si]_4P_8K_4$ (**II**) in toluene or benzene solution. Both monomer and dimer, however, can be obtained from benzene by crystallization, respectively. According to the molecular structure determined by X-ray diffraction analysis, the P_8K_8–core of $[(Me_3Si)_3Si]_4P_8K_4$ may be described as a double cube with a four membered P_4 ring in the middle, two phosphorus atoms and two potassium atoms in alternating positions on the top and the bottom, in which the four exo-phosphorus atoms each bear a hypersilyl group and the potassium atoms are each coordinated to a η^6-bonded benzene molecule. The P-P bond lengths of 219 pm within the P_4 ring are 7 pm longer than the other P-P contacts, but they all lie in the P-P single bond range**.** Obviously, $[(Me_3Si)_3Si]_4P_8K_4$ may be understood as a [2+2] cycloadduct of $[(Me_3Si)_3Si]_2P_4K_2$, in which the cis-configurated phosphorus skeleton has to change to the trans-configurated conformation during the $[2_\pi+2_\pi]$–cycloaddition.

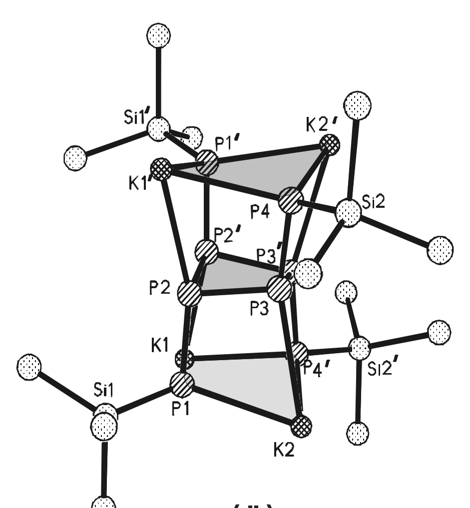

(II)

In toluene potassium bis(hypersilyl)tetraphosphenide decomposes slowly at room temperature to give yellowish well-shaped crystals of potassium tris(hypersilyl)pentaphosphanide $[(Me_3Si)_3Si]_3P_5K_2$ (**III**) within several weeks. This process becomes even quicker on heating to about 70°C. Other products detected, such as $(Me_3Si)_3SiPH_2$, indicate that protolysis has played an important role in this reaction and cleavage of phosphorus chain should be involved in the course of formation of $[(Me_3Si)_3Si]_3P_5K_2$. Its $^{31}P\{H\}$-NMR spectrum exhibits three multiplets arising from an AA'MM'X spin system in the expected range. The X-ray crystal structure analysis of a single crystal obtained from benzene solution shows that $[(Me_3Si)_3Si]_3P_5K_2$ crystallizes as a coordination dimer with a K_4P_{10} skeleton linked by two potassium atoms. The molecule exhibits C_{2h} symmetry, with the twofold axis running through the two central potassium atoms. The $[(Me_3Si)_3Si]_3P_5$ moiety comprises a three-membered phosphorus ring featuring two exocyclo-phosphorus atoms in a cis orientation, each of which

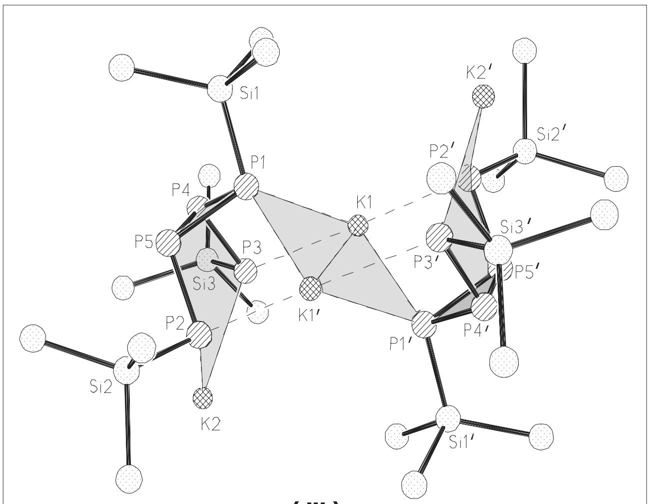

(III)

links further to a hypersilyl group, while the third P atom in the P3 ring bears directly a hypersilyl group in trans position to the two P_{exo} atoms. The P-P bond lengths range between 217.24(14) pm and 225.15(14) pm with the three longer contacts in the P_3 ring, however, all falling within the single bond range. The terminal K atoms are each coordinated by a benzene molecule in addition to the agostic interaction to methyl groups, while the bridging K atoms have only the agostic interaction with methyl groups aside from the coordination of P atoms.

Most probably by partial hydrolysis another potassium octaphosphanide $[(Me_3Si)_3Si]_3P_8K_3$ (**IV**) may be generated. It is isolated as orange cubic shaped crystals by concentrating a very dilute benzene solution of $[(Me_3Si)_3Si]_4P_8K_4$ and cooling to 5°C for several days. Similar to $[(Me_3Si)_3Si]_3P_5K_2$, in the solid state $[(Me_3Si)_3Si]_3P_8K_3$ exists as a coordination dimer with a twofold axis running through the two potassium atoms in the center of the two $[(Me_3Si)_3Si]_3P_8$ fragments. The P_8 skeleton comprises a five-membered and a three-membered ring with a shared edge. The cyclo-pentaphosphorus ring features two exocyclo-phosphorus atoms, each of which links further to a hypersilyl group, while one of the cyclo-triphosphorus binds directly to a hypersilyl group. The P-P contacts range from 218.03(12) to 225.24(13) pm also lying in the typical single bond range. The coordination spheres of the terminal K atoms in this molecule are each completed by a η^6-bonded benzene molecule, whereas the bridging K atoms join the two K_3P_8 fragments together by coordination to phosphorus atoms in both fragments, showing only a slight agostic-type interaction with hypersilyl groups.

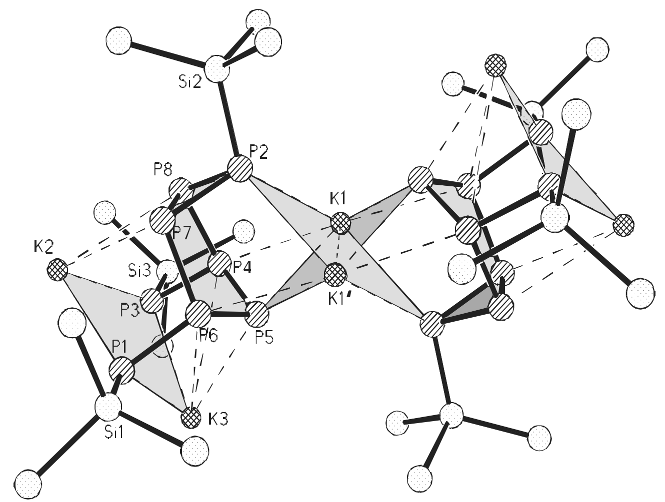

(IV)

The reaction of the same reactants, namely solvent-free potassium hypersilanide with white phosphorus, but now using coordinating solvents such as diethyl ether at room temperature yields bis(hypersilyl)triphosphenide $[(Me_3Si)_3Si]_2P_3K$ (**V**) in addition to $[(Me_3Si)_3Si]_2P_4K_2$ as well as small amounts of several other phosphorus-containing compounds. $[(Me_3Si)_3Si]_2P_3K$ is isolated as deep blue powder and characterized as a potassium salt of bis(hypersilyl)triphosphene $(Me_3Si)_3Si\text{-}P\text{=}P\text{-}PH\text{-}Si(SiMe_3)_3$ by NMR spectroscopy. An AX_2 spin pattern with a coupling constant of $^1J_{p,p}$ = 541Hz observed at low field in the ^{31}P NMR spectrum is assignable to a triphosphaallyl anion with partial double-bond character and a trans-trans structure can be concluded.

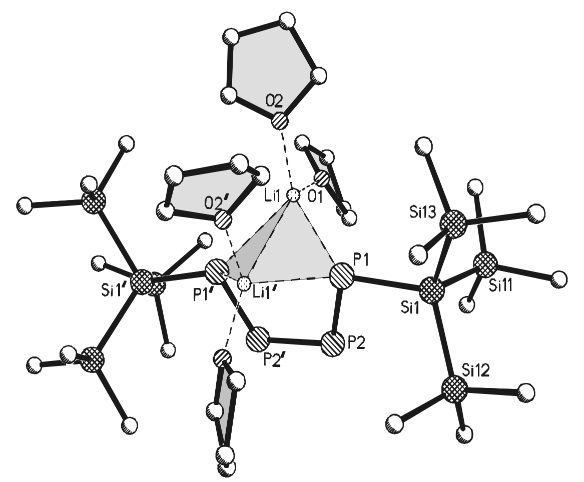

(VI)

Replacing potassium for lithium, *i.e.* reacting base-free lithium hypersilanide with white phosphorus, dramatically changes the type of products obtained. Under the same reaction conditions, a pale yellowish precipitate was formed along with $[(Me_3Si)_3Si]_3P_7$, $[(Me_3Si)_3Si]_2P_4$, and $[(Me_3Si)_3Si]_3P_5Li_2$ according to NMR data. The pale yellowish precipitate isolated by filtration was dissolved in THF, giving red violet $[(Me_3Si)_3Si]_2P_4Li_2$. X-ray structure analysis of $[(Me_3Si)_3Si]_2P_4Li_2{\cdot}4THF$ (**VI**) displays a $[(Me_3Si)_3Si]_2P_4$ moiety similar to that in its potassium analogue. In this molecule the lithium atoms, however, are each only coordinated by two phosphorus in addition to two oxygen atoms of THF, showing a Li···Li separation of 349.48(15) pm.

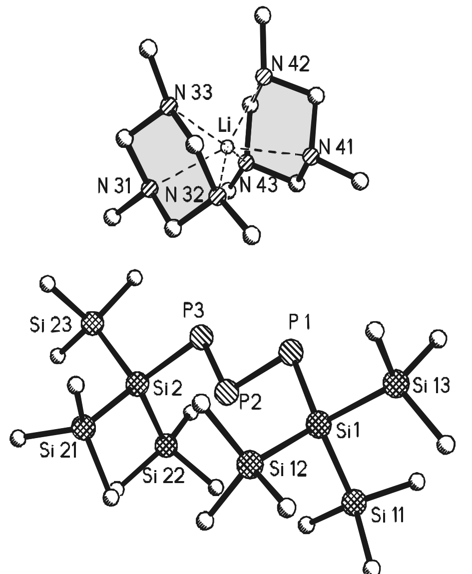

(VII)

When base-free lithium hypersilanide was allowed to react with white phosphorus in toluene in the presence of hexahydro-1,3,5-trimethyl-S-triazine at room temperature, the main phosphorus-containing product turned out to be $[(Me_3Si)_3Si]_2P_3Li$ (**VII**). It precipitated as violet crystals along with a considerable amount of colourless $(Me_3Si)_4Si$ crystals, suggesting that cleavage of Si-Si within hypersilyl group took place during the reaction process and led to the complexity of the reaction. The structure of the triazine solvate may be described as a salt composed of a sandwiched Li^+ cation $\{Li[(MeNCH_2)_3]_2\}^+$ and an triphosphaallyl anion $\{[(Me_3Si)_3Si]_2P_3\}^-$ without short Li···P contact. The structure of the anion thus displays a nearly undistorted C_{2v}-symmetric W-shape Si_2P_3 skeleton with a P-P-P angle of 105.52(3)° and two similar P-P bond lengths (about 207 pm) again with partial P=P double-bond character.

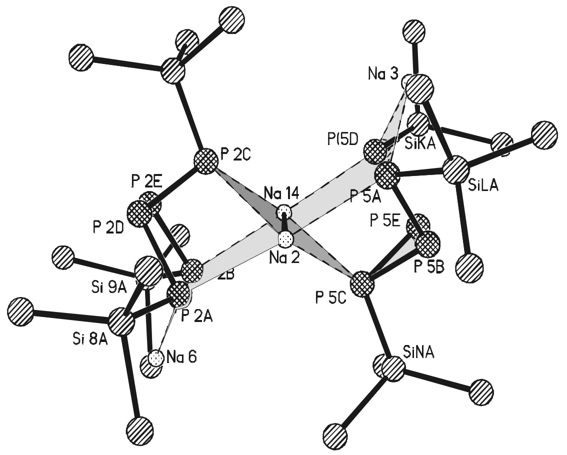

(VIII)

The reaction of white phosphorus with base-free sodium hypersilanide in toluene does not lead to the formation of tetraphosphenide, instead, $[(Me_3Si)_3Si]_3P_5Na_2$ (**VIII**) is isolated as yellow crystals. As shown by X-ray diffraction analysis, it crystallizes as a dimer similar to its potassium analogue described above despite of the lack of benzene molecule in this crystal. However, strong agostic-type interaction is found between the terminal sodium atoms and hypersilyl groups, whereas no significant agostic interaction is found for the bridging sodium atoms in this structure.

The treatment of $[(Me_3Si)_3Si]_2P_4K_2$ with bis[bis(trimethylsilyl)amino]stannylene in toluene at room temperature affords the unexpected compounds $[(Me_3Si)_3Si]_3P_4SnK$ (**IX**) and $[(Me_3Si)_3Si]_2[(Me_3Si)_2N]P_4SnK$ (**X**) instead of $[(Me_3Si)_3Si]_2P_4Sn$, which may be expected from the metathesis reaction. $[(Me_3Si)_3Si]_3P_4SnK$ was isolated as orange crystals and was characterized by NMR spectroscopy and X-ray crystallography, while $[(Me_3Si)_3Si]_2[(Me_3Si)_2N]P_4SnK$, being mixed with the by-product $(Me_3Si)_2NK$, has not yet been isolated as pure substance. $[(Me_3Si)_3Si]_3P_4SnK$ crystallizes as discrete molecules weakly interlinked by K···Sn (384.7 pm) and agostic-type interactions between K atoms and hypersilyl groups of neighbouring molecule units. The phosphorus chain, showing a torsion angle of 73.5° and an average bond length of 223 pm, is no longer coplanar and has no P=P bouble bond character.

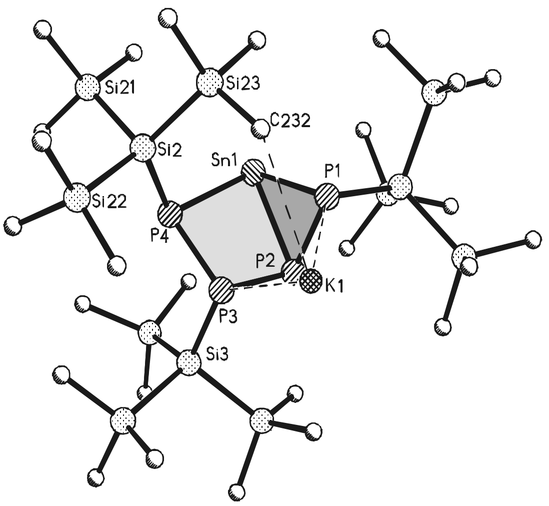

(IX)

When dihypersilyl plumbylene is allowed to react with white phosphorus at room temperature in toluene, the tetrameric lead(II) hypersilylphosphandiide $[(Me_3Si)_3Si]_4P_4Pb_4$ (**XI**) and dihypersilylphosphene $[(Me_3Si)_3Si]_2P_2$ are formed as the main products along with small amounts of dihypersilyltetraphosphane $[(Me_3Si)_3Si]_2P_4$ as well as the trihypersilylheptaphosphane $[(Me_3Si)_3Si]_3P_7$. A 1:4 Lewis-acid-base adduct between P_4 with dihypersilylplumbylene, which could be trapped at -30°C and resonances at -350ppm with ^{207}Pb satellites in ^{31}P NMR spectrum, would be a very probable intermediate for the formation of the mentioned products, since it allows for the low energy approach of both reactants. Analogously, reaction of dihypersilylstannylene with P_4 forms $[(Me_3Si)_3Si]_4P_4Sn_4$ (**XII**) in good yields under the same conditions. Both $[(Me_3Si)_3Si]_4P_4Sn_4$ and $[(Me_3Si)_3Si]_4P_4Pb_4$ can also be synthesized and isolated in almost quantitative yields by the metallation of $(Me_3Si)_3SiPH_2$ with bis[bis(trimethylsilyl)amino]-substituted stannylene or plumbylene in toluene.

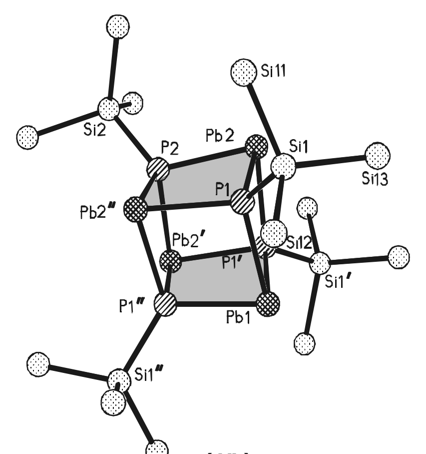

(XI)

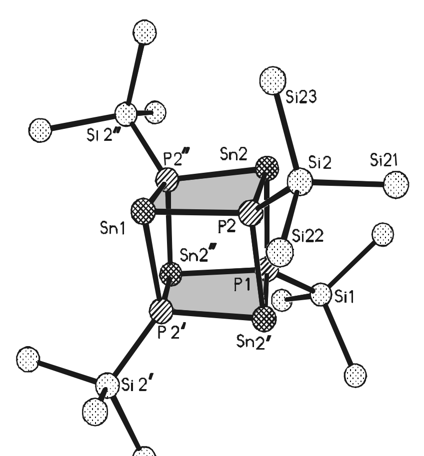

(XII)

Lead(II) and tin(II) hypersilylphosphandiide form tetrameric aggregates containing a P_4Pb_4 or P_4Sn_4 heterocubane core. The lead and tin atoms possess no exocyclic ligands and consequently have a trigonal pyramidal coordination sphere, while the phosphorus atoms each bear a hypersilyl group and display a distorted tetrahedral coordination environment. The interatomic distances of Pb-P range from 272.0(5) to 274.6(5) pm and those between tin and phosphorus atoms range between 264.46(6) and 265.76(5) pm in the heterocubane cores, respectively.

The reactions of dihypersilylplumbylene with MPH_2 (M = Li, K) in a ratio of 1:1 in diethyl ether at -20°C quantitatively yield ate-complexes $M\{[(Me_3Si)_3Si]_2Pb\cdot PH_2\}$ (M = Li, K) as ether solvates, respectively. The structures of both products are established by NMR spectroscopy and confirmed by X-ray crystallography.

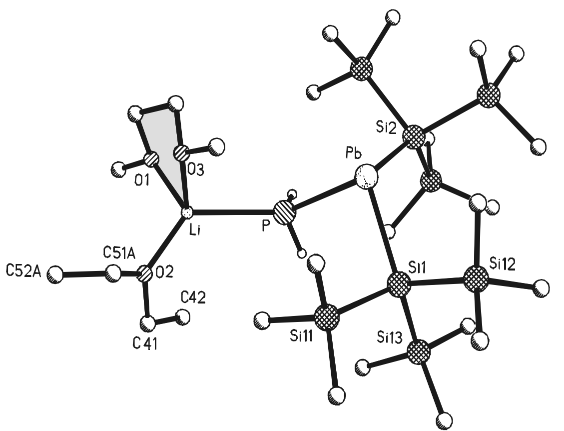

(XIII)

The molecular structure of [LiEt$_2$O(DME)]{[(Me$_3$Si)$_3$Si]$_2$Pb·PH$_2$} (**XIII**) is best described as an intimate ion-pair with predominantly ionic binding between the Li$^+$ cation and the phosphanide [Li···P distance: 262.2(11) pm]. The lead atom is found to be three-coordinate with two P-Pb-Si angles of 94.37(5) and 94.75(5)°.

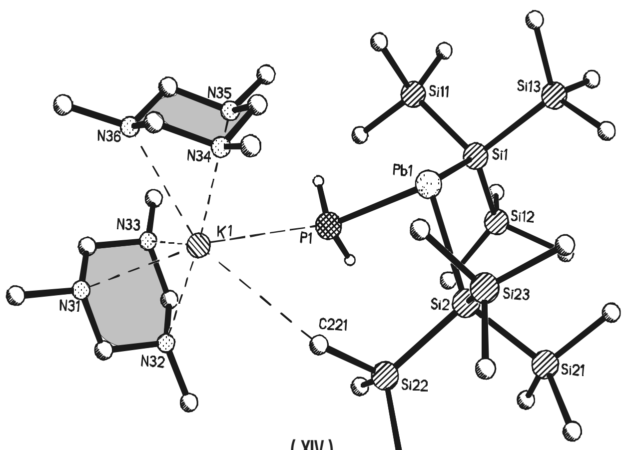

(XIV)

The X-ray analysis shows that {K[(MeNCH$_2$)$_3$]$_2$}{[(Me$_3$Si)$_3$Si]$_2$Pb·PH$_2$} (**XIV**) comprises an contact ion-pair of {[(Me$_3$Si)$_3$Si]$_2$Pb·PH$_2$}$^-$ and {K[(MeNCH$_2$)$_3$]$_2$}$^+$ with a K···P distance of 401.0 pm. In addition to the phosphorus atom, the K atom is coordinated to two hexahydro-1,3,5-trimethyl-S-triazine molecules and the coordination sphere is completed by intra- and inter-molecular agostic-type K···CH$_3$ interactions leading to a one-dimensional coordination polymer chain. The lead atom of the anion shows a trigonal pyramidal coordination environment with Pb-P bond of 269.15(19) pm.

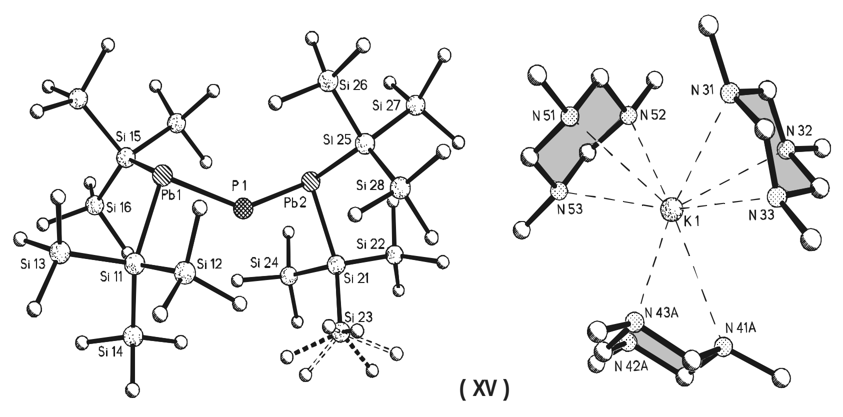

(XV)

In the presence of a stronger donor ligand, such as DME, crown ether, or triazine, MPH$_2$ (M = Li, K) can even add to two dihypersilyl plumbylene moieties to produce the 1:2 adducts M{{[(Me$_3$Si)$_3$Si]$_2$Pb}$_2$·PH$_2$} (M = Li, K) in good yields. X-ray diffraction analysis of [K((MeNCH$_2$)$_3$)$_3$]{{[(Me$_3$Si)$_3$Si]$_2$Pb}$_2$·PH$_2$} (**XV**) reveals a salt composed of a solvated potassium cation,

$[K((MeNCH_2)_3)_3]^+$, and an anion, $\{\{[(Me_3Si)_3Si]_2Pb\}_2\cdot PH_2\}^-$, which separate from each other and no unusually short K···P contact is observed. Both lead atoms of the dihypersilylplumbylene moieties, coordinated to the same phosphorus atom, have coordination number three and each display a pyramidal environment with Pb-P contacts approximately 14 pm longer than that observed for $\{K[(MeNCH_2)_3]_2\}\{[(Me_3Si)_3Si]_2Pb\cdot PH_2\}$.

If dihypersilylstannylene and plumbylene are treated with trimethylphosphane in pentane or toluene at -20°C, simple 1:1 adducts with PMe_3 are formed quantitatively. Unfortunately, the orange and red crystals isolated from these reaction mixtures were not suitable for structure analysis by X-ray diffraction. Their constitutions, however, have been proved unambiguously by NMR spectroscopy. The ^{31}P NMR spectrum of $[(Me_3Si)_3Si]_2Sn\cdot PMe_3$ (**XVI**) exhibits a broad singlet at -60.1 ppm flanked by $^{117/119}$Sn satellites with a coupling constant $^1J_{119/117Sn,P}$ = 1900Hz. In the ^{31}P NMR spectrum of $[(Me_3Si)_3Si]_2Pb\cdot PMe_3$ (**XVII**), no ^{207}Pb satellites could be found. However, an up-field shift of about 40 ppm when compared with uncoordinated PMe_3 (-62 ppm) indicates that adduct **XVII** is also present in solution, but most probably in equilibrium with its components.

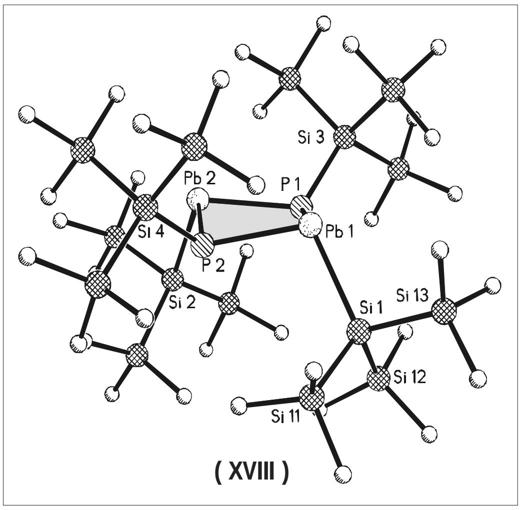

(XVIII)

When phosphane (PH_3) was allowed to bubble through a solution of dihypersilylplumbylene in n-pentane at room temperature, an immediate reaction took place, yielding the dimeric hypersilyl lead(II) hypersilylphosphanide $[(Me_3Si)_3SiPbP(H)Si(SiMe_3)_3]_2$ (**XVIII**). This compound can also be synthesized in good yields by treating $(Me_3Si)_3SiPH_2$ with dihypersilylplumbylene in benzene at room temperature. On standing at ambient temperature, however, $[(Me_3Si)_3SiPbP(H)Si(SiMe_3)_3]_2$ in solution undergoes further condensation to give finally $[(Me_3Si)_3Si]_4P_4Pb_4$ (**XI**). The existence of hydrogen atoms bound to phosphorus atoms could be concluded from the AA'XX' spin pattern observed in both ^{1}H- and ^{31}P-NMR spectra. In the solid state, a puckered Pb_2P_2 ring shielded by four hypersilyl substituents mutually trans to one another is observed. The three-coordinate lead atoms possess a trigonal pyramidal coordination geometry with Pb-P bond lengths of about 279 pm.

When phosphane was bubbled through a dihypersilylplumbylene solution at a temperature below -30°C, the primary Lewis-acid-base adduct between PH_3 and dihypersilylplumbylene as well as either $(Me_3Si)_3SiPb(H){\leftarrow}P(H)_2Si(SiMe_3)_3$ or $[(Me_3Si)_3SiPbPH_2]_x$ were formed according to the ^{31}P spectrum of the reaction mixture recorded at -20°C. After keeping the resulting mixture at -60°C for several weeks, dark brown crystals of molecular lead cluster $[(Me_3Si)_3Si]_6Pb_{12}$ (**XIX**) were astonishingly found. According to the X-ray diffraction studies, the twelve lead atoms of this species constitute a distorted but still centrosymmetric icosahedron. Six atoms (Pb_A) bear no substituent and form a puckered ring with chair conformation (the belt). The remaining six atoms (Pb_B) each bearing a hypersilyl group form two three-membered rings above and below the central Pb_6 belt. The Pb-Pb distances between neighbouring lead atoms range from 307.6(1) to 338.9(1)pm. The longest distances are found between the lead atoms of type Pb_B, the shortest between Pb_A and Pb_B, giving rise to the description of the polyhedron as an icosahedron with two open faces. This finding is in line with the expectations of a *arachno*-type cluster according to Wade's rules.

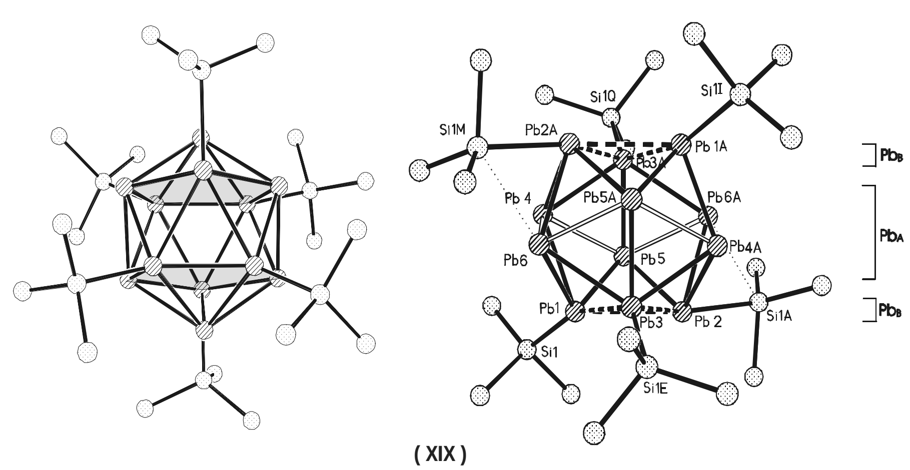

(XIX)

We suppose that the formation of the lead cluster proceeds via the elusive hydridoplumbylene $HPbSi(SiMe_3)_3$ which has been initially formed by ligand exchange between PH_3 and $Pb[Si(SiMe_3)_3]_2$. The intermediate species may associate to oligomers, or due to its bis(plumbylene) nature may give self-insertion reactions. By loosing hydrogen or hypersilane this could possibly lead to the formation of lead clusters. This particular reaction, however, is not suitable for giving access to larger quantities of lead clusters, since the thermodynamically favored process is the competitive formation of hypersilyl substituted lead phosphanides. We therefore looked for hydride sources other than PH_3.

By using a strategy which was already successful in synthesizing other unsymmetrically substituted plumbylenes, dihypersilylplumbylene is allowed to react with the triphenylphospine adduct of copper hydride. Surprisingly, in addition of $[(Me_3Si)_3Si]_6Pb_{12}$ another molecular lead cluster $[(Me_3Si)_3Si]_6Pb_{10}$ (**XX**) is formed and isolated. Similar results had been obtained by treatment of dihypersilylplumbylene with two aluminium hydrides. At ambient temperature solid $[(Me_3Si)_3Si]_6Pb_{10}$ is indefinitely stable as long as light is excluded. In solution the cluster slowly undergoes first-order decomposition, *i.e.* a disproportionation yielding dihypersilyl plumbylene and finally giving $(Me_3Si)_3SiSi(SiMe_3)_3$ as well as elementary lead.

$[(Me_3Si)_3Si]_6Pb_{10}$ is characterized by NMR spectroscopy, mass spectroscopy, and X-ray crystallography. The Pb_{10} skeleton has approximate C_{3v} symmetry and is best derived from Pb_{12} icosahedron by replacing one trigonal face by a single lead atom. This picture also matches the prediction made by Wade’s rules. However, these only hold for cluster $[(Me_3Si)_3Si]_6Pb_{10}$ if it is formally composed from a $[(Me_3Si)_3Si]_6Pb_9$ *hypho*-type cluster dianion and Pb^{2+}. A model compound with hypersilyl groups replaced by SiH_3 groups indeed revealed a charge distribution according to the proposed model. The negative charge derived from NBO analyses is mainly concentrated at the open face, while Pb7 bears the highest positive charge within the Pb_{10} skeleton. This uneven charge distribution should result in a significant dipole moment, which was calculated to be 2.7 D for the model compound. The Pb-Pb distances within the Pb_9 fragment differ only slightly [310.3(3)-319.84(17)pm] and are all within the range found for $[(Me_3Si)_3Si]_6Pb_{12}$ and the known lead clusters anions, whereas the three bonds to the capping atom P7 are significantly shorter [298.3(4)-299.33(16)pm].

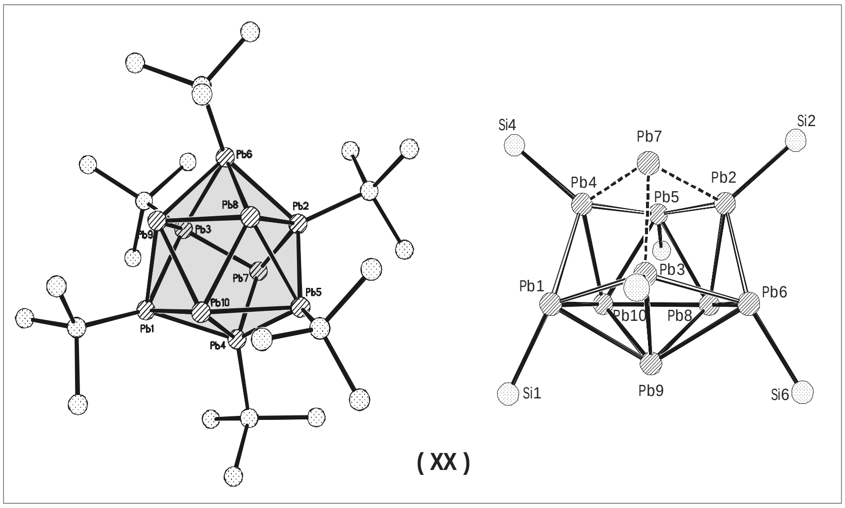

(XX)

7 Appendix

7.1 Crystallographic data for $Hyp_2P_4K_2\cdot 4C_6H_6$

7.1.1 Crystal data and structure refinement

Empirical formula	$Hyp_2P_4K_2$·4benzene
Formula weight	1009.84
Temperature	293(2) K
Wavelength	0.71073 Å
Crystal system, space group	Monoclinic, P2(1)/n
Unit cell dimensions	a = 14.935(2) Å alpha = 90 deg. b = 17.063(2) Å beta = 90.380(12) deg. c = 48.800(8) Å gamma = 90 deg.
Volume	12436(3) $Å^3$
Z, Calculated density	8, 1.079 g/cm^3
Absorption coefficient	0.434 mm^{-1}
F(000)	4320
Theta range for data collection	2.05 to 20.00 deg.
Limiting indices	-2<=h<=14, -1<=k<=16, -46<=l<=46
Reflections collected / unique	14566 / 11593 [R(int) = 0.0361]
Completeness to theta = 20.00	99.9 %
Refinement method	Full-matrix least-squares on F^2
Data / restraints / parameters	11593 / 0 / 1009
Goodness-of-fit on F^2	0.816
Final R indices [I>2sigma(I)]	R1 = 0.0492, wR2 = 0.1227
R indices (all data)	R1 = 0.0868, wR2 = 0.1331
Largest diff. peak and hole	0.352 and -0.291 e.$Å^{-3}$

7.1.2 Atomic coordinates (x 10^4), equivalent isotropic displacement parameters ($Å^2$ x 10^3) and Anisotropic displacement parameters ($Å^2$ x 10^3). U(eq) is defined as one third of the trace of the orthogonalized Uij tensor. The anisotropic displacement factor exponent takes the form: $-2\pi^2[h^2a^{*2}U11 + ... + 2hka^*b^*U12]$

Atom	x	y	z	U(eq)	U11	U22	U33	U23	U13	U12
Si(4)	2477(1)	-4572(1)	4526(1)	39(1)	44(1)	35(1)	37(1)	0(1)	1(1)	-2(1)
Si(3)	7582(1)	466(1)	2979(1)	38(1)	40(1)	37(1)	37(1)	1(1)	-1(1)	-1(1)
P(1)	7448(1)	450(1)	3441(1)	44(1)	46(1)	49(1)	38(1)	5(1)	2(1)	3(1)
P(5)	2573(1)	-4558(1)	4063(1)	44(1)	48(1)	47(1)	38(1)	-3(1)	1(1)	-3(1)
Si(32)	6393(1)	1275(1)	2836(1)	46(1)	46(1)	44(1)	47(1)	4(1)	-4(1)	4(1)
Si(1)	2440(1)	-5390(1)	2921(1)	36(1)	40(1)	33(1)	37(1)	2(1)	-1(1)	-1(1)
K(4)	893(1)	-4017(1)	3659(1)	70(1)	51(1)	92(1)	66(1)	-9(1)	-1(1)	14(1)
Si(42)	3667(1)	-3757(1)	4667(1)	48(1)	53(1)	42(1)	49(1)	0(1)	-6(1)	-8(1)
Si(2)	7507(1)	-432(1)	4578(1)	37(1)	36(1)	38(1)	37(1)	0(1)	2(1)	1(1)
K(2)	9104(1)	991(1)	3854(1)	67(1)	47(1)	87(1)	67(1)	9(1)	-3(1)	-11(1)
Si(11)	2301(1)	-4258(1)	2649(1)	47(1)	53(1)	40(1)	49(1)	6(1)	-6(1)	-2(1)
Si(21)	8726(1)	-1254(1)	4682(1)	42(1)	42(1)	41(1)	43(1)	4(1)	-1(1)	3(1)

Atom	x	y	z	U(eq)	U11	U22	U33	U23	U13	U12
Si(43)	2662(1)	-5801(1)	4739(1)	61(1)	69(1)	46(1)	69(1)	15(1)	-11(1)	-6(1)
Si(12)	1230(1)	-6230(1)	2820(1)	45(1)	44(1)	39(1)	50(1)	-1(1)	-5(1)	-2(1)
P(8)	2526(1)	-4916(1)	3352(1)	45(1)	49(1)	44(1)	40(1)	-4(1)	4(1)	-6(1)
Si(33)	7465(1)	-755(1)	2757(1)	61(1)	75(1)	43(1)	65(1)	-14(1)	-12(1)	2(1)
P(4)	7454(1)	79(1)	4152(1)	43(1)	45(1)	44(1)	40(1)	5(1)	1(1)	5(1)
P(7)	1922(1)	-5883(1)	3563(1)	53(1)	74(1)	46(1)	40(1)	-3(1)	3(1)	-19(1)
P(3)	8072(1)	-880(1)	3941(1)	52(1)	68(1)	50(1)	38(1)	4(1)	0(1)	15(1)
Si(23)	7556(1)	668(1)	4869(1)	47(1)	48(1)	46(1)	45(1)	-10(1)	-8(1)	4(1)
K(1)	5870(1)	-525(1)	3736(1)	77(1)	54(1)	113(2)	66(1)	21(1)	-7(1)	-23(1)
P(2)	8086(1)	-651(1)	3520(1)	53(1)	66(1)	57(1)	36(1)	2(1)	2(1)	18(1)
K(3)	4134(1)	-5530(1)	3759(1)	80(1)	58(1)	110(2)	71(1)	-18(1)	-6(1)	21(1)
Si(13)	3764(1)	-6065(1)	2821(1)	44(1)	44(1)	45(1)	45(1)	-2(1)	4(1)	3(1)
P(6)	1932(1)	-5661(1)	3984(1)	55(1)	73(1)	55(1)	37(1)	0(1)	3(1)	-20(1)
Si(31)	8931(1)	1100(1)	2875(1)	51(1)	47(1)	57(2)	51(1)	-2(1)	12(1)	-4(1)
Si(22)	6188(1)	-1145(1)	4652(1)	45(1)	40(1)	50(1)	46(1)	2(1)	2(1)	-4(1)
Si(41)	1137(1)	-3970(1)	4657(1)	57(1)	51(1)	57(2)	62(1)	-6(1)	13(1)	-1(1)
C(221)	6136(5)	-1625(5)	5003(1)	74(2)	75(5)	89(6)	59(4)	21(4)	8(4)	-16(5)
C(321)	5304(4)	848(5)	2952(1)	64(2)	55(4)	73(6)	63(4)	12(4)	0(3)	0(5)
C(044)	8177(8)	2724(7)	3800(2)	97(3)	97(7)	104(8)	89(8)	-25(6)	-26(6)	20(7)
C(311)	9013(5)	1444(5)	2510(1)	75(2)	65(5)	82(5)	78(5)	18(4)	20(4)	-3(4)
C(211)	9782(4)	-865(4)	4527(1)	55(2)	46(4)	63(6)	57(4)	8(4)	2(3)	5(4)
C(121)	1016(5)	-6265(4)	2437(1)	64(2)	78(5)	58(5)	56(4)	0(4)	-15(4)	-17(4)
C(322)	6335(4)	1416(5)	2454(1)	67(2)	66(5)	74(5)	60(4)	27(4)	-8(3)	11(4)
C(031)	4197(5)	-1514(5)	3533(2)	88(3)	84(6)	65(6)	115(8)	2(6)	3(6)	-19(5)
C(122)	173(4)	-5872(5)	2988(1)	71(2)	46(4)	65(6)	103(5)	-3(5)	11(4)	-5(5)
C(083)	-1201(6)	-3173(6)	3734(3)	100(3)	86(7)	93(9)	122(8)	-23(7)	6(6)	13(6)
C(421)	3746(5)	-3626(5)	5047(1)	78(2)	109(6)	60(5)	64(4)	5(4)	-23(4)	-14(5)
C(212)	8882(4)	-1303(4)	5066(1)	55(2)	47(4)	56(5)	60(4)	-2(4)	-8(3)	0(4)
C(086)	-1155(5)	-4663(6)	3532(2)	84(3)	82(6)	89(8)	83(6)	-38(7)	-4(5)	3(6)
C(013)	11185(5)	1848(5)	3773(2)	92(3)	91(6)	67(7)	119(8)	15(6)	-14(6)	-17(5)
C(015)	11219(5)	498(6)	3688(2)	73(2)	61(5)	83(8)	76(7)	-11(5)	6(4)	-3(5)
C(431)	2816(6)	-5682(5)	5121(1)	115(3)	176(9)	86(6)	80(5)	43(5)	-65(6)	-48(7)
C(051)	6338(6)	-5180(7)	3993(3)	97(3)	90(7)	85(8)	114(9)	-18(7)	-21(6)	-2(6)
C(032)	4048(6)	-1487(6)	3809(2)	83(3)	83(6)	78(8)	88(8)	32(6)	1(5)	-23(6)
C(411)	1061(6)	-3769(8)	5025(2)	189(7)	103(7)	390(20)	79(6)	-85(9)	38(5)	24(10)
C(034)	3565(5)	-183(6)	3773(2)	90(3)	73(6)	101(8)	95(7)	-8(6)	7(5)	-17(6)
C(123)	1463(5)	-7254(4)	2932(1)	55(2)	64(5)	43(5)	57(4)	2(3)	-2(3)	-9(4)
C(064)	1799(7)	-2312(5)	3760(2)	93(3)	114(8)	85(7)	78(7)	14(5)	-26(5)	-13(6)
C(011)	11116(6)	905(8)	4138(2)	81(3)	70(6)	109(9)	63(6)	17(7)	-11(4)	2(7)
C(213)	8538(5)	-2283(4)	4561(1)	57(2)	61(5)	41(5)	69(4)	-4(4)	1(4)	8(4)
C(012)	11128(5)	1690(7)	4055(2)	98(3)	73(6)	115(10)	107(8)	-46(7)	-14(5)	-3(6)
C(084)	-1141(6)	-3292(7)	3455(3)	110(4)	81(7)	97(9)	152(11)	62(8)	-4(7)	6(7)
C(085)	-1130(6)	-4063(9)	3350(2)	97(4)	77(6)	151(12)	65(6)	8(8)	-13(5)	17(8)
C(016)	11167(5)	329(6)	3956(2)	79(3)	80(6)	71(7)	87(7)	8(6)	2(5)	12(5)
C(082)	-1227(6)	-3798(7)	3904(2)	84(3)	71(6)	105(9)	75(6)	-6(7)	5(4)	7(6)
C(042)	8443(12)	2766(7)	4264(2)	128(5)	208(15)	104(9)	72(7)	-1(6)	9(9)	56(10)
C(323)	6522(5)	2279(4)	2997(1)	75(2)	69(5)	49(5)	108(6)	-3(4)	-12(4)	14(5)
C(014)	11222(6)	1240(7)	3595(2)	81(3)	73(6)	91(8)	80(6)	27(7)	-3(5)	-22(6)
C(036)	4006(6)	-863(8)	3375(2)	86(3)	85(7)	112(9)	61(5)	-3(7)	-7(5)	-33(7)
C(422)	3544(5)	-2761(4)	4506(1)	72(2)	86(6)	44(5)	86(5)	15(4)	-20(4)	-18(5)
C(033)	3727(6)	-828(8)	3928(2)	86(3)	68(6)	138(10)	52(5)	4(7)	4(4)	-45(7)
C(432)	1693(5)	-6473(5)	4694(1)	80(2)	111(6)	63(5)	68(4)	17(4)	-13(4)	-27(5)
C(222)	6097(5)	-1948(4)	4384(1)	76(2)	68(5)	64(6)	96(5)	-19(4)	6(4)	-22(5)
C(035)	3702(6)	-189(6)	3501(2)	84(3)	77(6)	88(8)	88(7)	34(6)	-14(5)	-5(6)
C(312)	9042(5)	1989(4)	3104(1)	71(2)	63(5)	75(6)	76(5)	-14(4)	13(4)	-23(5)
C(025)	5203(5)	1476(4)	3781(2)	76(2)	75(6)	72(5)	82(6)	10(4)	21(4)	14(5)
C(072)	4766(5)	-3547(4)	3696(2)	78(2)	81(6)	51(5)	101(7)	-12(4)	17(5)	-7(4)
C(111)	1158(4)	-3822(4)	2710(1)	65(2)	61(4)	45(4)	89(5)	7(4)	-20(4)	5(4)
C(231)	8673(4)	1154(4)	4822(1)	71(2)	77(5)	62(5)	75(4)	-12(4)	-18(4)	-10(4)
C(232)	6655(5)	1384(5)	4769(1)	72(2)	82(5)	58(5)	75(5)	-18(4)	-11(4)	18(4)
C(423)	4760(5)	-4178(5)	4553(2)	83(3)	56(5)	78(7)	113(6)	-16(5)	-1(4)	-8(5)

Atom	x	y	z	U(eq)	U11	U22	U33	U23	U13	U12
C(112)	2425(5)	-4441(4)	2269(1)	76(2)	96(5)	78(5)	54(4)	23(4)	1(4)	-14(5)
C(113)	3166(4)	-3519(4)	2755(1)	60(2)	65(5)	49(5)	66(4)	10(4)	-11(3)	-16(4)
C(331)	8480(5)	-1379(4)	2794(1)	78(2)	102(6)	55(5)	77(5)	-13(4)	0(4)	26(5)
C(332)	7300(6)	-610(5)	2378(1)	120(4)	195(10)	81(6)	83(6)	-30(5)	-51(6)	45(7)
C(131)	3782(5)	-6493(4)	2466(1)	61(2)	72(5)	45(4)	66(4)	-10(3)	8(3)	1(4)
C(233)	7422(4)	448(4)	5243(1)	66(2)	81(5)	72(5)	46(4)	-12(4)	-2(3)	15(4)
C(132)	3924(5)	-6881(4)	3079(1)	63(2)	58(5)	66(5)	64(4)	11(4)	-3(3)	20(4)
C(412)	1013(6)	-3025(6)	4469(2)	176(6)	103(8)	88(8)	339(16)	90(9)	108(9)	56(7)
C(313)	9909(4)	444(5)	2956(1)	75(2)	50(4)	91(6)	82(5)	-7(4)	-1(4)	3(5)
C(056)	6035(6)	-5860(8)	4120(2)	92(3)	84(7)	124(10)	67(6)	-3(8)	-11(5)	42(7)
C(433)	3673(5)	-6297(5)	4592(2)	130(3)	116(7)	70(6)	204(9)	47(6)	35(7)	45(6)
C(133)	4769(4)	-5404(4)	2855(1)	64(2)	53(4)	66(5)	74(4)	-10(4)	4(3)	-4(4)
C(413)	154(5)	-4569(6)	4549(2)	118(4)	51(5)	129(9)	174(9)	-41(7)	-16(5)	1(6)
C(333)	6492(5)	-1305(4)	2902(2)	121(3)	109(7)	61(6)	192(9)	-22(6)	2(6)	-31(5)
C(043)	7933(6)	2554(5)	4054(4)	112(3)	97(8)	81(7)	160(10)	-6(8)	61(9)	-2(6)
C(054)	5940(6)	-6487(6)	3689(2)	92(3)	96(7)	86(9)	95(8)	-18(6)	-1(6)	36(7)
C(052)	6449(6)	-5178(6)	3714(3)	94(3)	67(6)	83(8)	132(9)	14(7)	1(6)	-6(5)
C(223)	5177(4)	-502(5)	4608(1)	65(2)	41(4)	85(6)	70(4)	0(4)	5(3)	-8(4)
C(055)	5829(6)	-6492(6)	3961(2)	95(3)	93(7)	92(8)	100(8)	10(7)	5(6)	23(6)
C(053)	6252(6)	-5835(8)	3560(2)	92(3)	56(5)	137(11)	83(6)	2(8)	9(5)	34(7)
C(073)	4778(6)	-3637(4)	3418(2)	90(2)	97(7)	71(6)	100(7)	-25(5)	-38(6)	0(5)
C(022)	3769(7)	1943(6)	4082(2)	110(3)	87(8)	133(9)	111(8)	-19(7)	41(6)	8(7)
C(026)	5220(5)	1361(4)	4053(2)	75(2)	71(5)	74(5)	80(6)	16(4)	-9(5)	10(5)
C(076)	6218(7)	-2983(6)	3684(2)	96(3)	77(7)	95(8)	115(8)	1(6)	-7(6)	-33(6)
C(066)	1558(8)	-2206(6)	3282(2)	106(3)	126(9)	112(8)	82(6)	4(6)	-6(7)	-15(7)
C(063)	1021(9)	-1909(6)	3804(2)	95(3)	131(10)	61(6)	94(7)	-13(5)	20(7)	0(7)
C(046)	9470(6)	3345(5)	3958(4)	117(4)	83(7)	89(7)	180(11)	-58(8)	47(9)	-30(6)
C(045)	8942(11)	3115(6)	3747(2)	102(4)	172(12)	48(6)	86(7)	10(5)	48(8)	11(7)
C(065)	2062(5)	-2447(4)	3498(2)	91(2)	67(5)	67(6)	138(8)	7(6)	11(6)	9(5)
C(024)	4477(7)	1815(5)	3657(2)	88(3)	117(8)	76(6)	70(5)	7(5)	-16(6)	14(6)
C(081)	-1209(5)	-4520(6)	3802(2)	83(3)	74(6)	60(7)	115(9)	-2(5)	9(5)	-2(5)
C(062)	508(6)	-1662(5)	3587(3)	107(3)	76(7)	70(6)	177(10)	27(7)	31(8)	23(5)
C(075)	6234(7)	-3059(6)	3401(3)	110(3)	80(7)	105(8)	146(10)	22(7)	48(7)	-11(6)
C(074)	5506(8)	-3405(6)	3270(2)	102(3)	130(9)	114(8)	63(5)	-9(5)	13(6)	-3(7)
C(041)	9234(9)	3170(9)	4220(3)	130(5)	92(8)	163(13)	135(12)	-71(9)	-33(7)	14(9)
C(071)	5502(7)	-3225(5)	3826(2)	91(3)	128(8)	77(6)	68(5)	-14(5)	-14(6)	-8(6)
C(061)	798(8)	-1814(7)	3331(2)	114(4)	84(8)	129(10)	127(10)	31(8)	-34(7)	15(8)
C(023)	3764(7)	2060(6)	3804(2)	104(3)	83(7)	104(8)	125(9)	1(7)	-14(6)	28(6)
C(021)	4486(8)	1601(7)	4211(2)	103(3)	121(8)	137(9)	51(5)	7(5)	-1(6)	-7(7)

7.1.3 Bond lengths [Å]

Atoms	Bond length	Atoms	Bond length	Atoms	Bond length
Si(4)-P(5)	2.264(2)	P(8)-K(3)	3.277(2)	Si(41)-C(413)	1.861(8)
Si(4)-Si(41)	2.342(3)	Si(11)-C(113)	1.876(6)	Si(41)-C(412)	1.862(9)
Si(4)-Si(43)	2.356(3)	Si(11)-C(111)	1.888(6)	C(044)-C(043)	1.323(11)
Si(4)-Si(42)	2.358(3)	Si(11)-C(112)	1.890(6)	C(044)-C(045)	1.350(12)
Si(3)-P(1)	2.265(2)	Si(21)-C(213)	1.872(7)	C(031)-C(032)	1.370(10)
Si(3)-Si(31)	2.344(3)	Si(21)-C(211)	1.874(6)	C(031)-C(036)	1.381(11)
Si(3)-Si(32)	2.352(3)	Si(21)-C(212)	1.892(6)	C(083)-C(082)	1.352(12)
Si(3)-Si(33)	2.355(3)	Si(43)-C(432)	1.857(7)	C(083)-C(084)	1.383(12)
P(1)-P(2)	2.140(2)	Si(43)-C(433)	1.878(8)	C(086)-C(081)	1.346(10)
P(1)-K(1)	3.231(2)	Si(43)-C(431)	1.887(6)	C(086)-C(085)	1.355(12)
P(1)-K(2)	3.308(2)	Si(12)-C(123)	1.863(7)	C(013)-C(014)	1.355(11)
P(5)-P(6)	2.147(2)	Si(12)-C(122)	1.884(7)	C(013)-C(012)	1.403(11)
P(5)-K(3)	3.229(2)	Si(12)-C(121)	1.896(6)	C(015)-C(016)	1.340(10)
P(5)-K(4)	3.312(2)	Si(33)-C(331)	1.860(7)	C(015)-C(014)	1.345(11)

Atoms	Bond length	Atoms	Bond length	Atoms	Bond length
Si(32)-C(321)	1.872(7)	Si(33)-C(333)	1.874(8)	C(051)-C(052)	1.374(11)
Si(32)-C(322)	1.882(6)	Si(33)-C(332)	1.879(7)	C(051)-C(056)	1.394(12)
Si(32)-C(323)	1.895(7)	P(4)-P(3)	2.146(2)	C(032)-C(033)	1.355(12)
Si(1)-P(8)	2.258(2)	P(4)-K(1)	3.274(2)	C(034)-C(035)	1.348(10)
Si(1)-Si(13)	2.343(3)	P(7)-P(6)	2.0885(19)	C(034)-C(033)	1.355(12)
Si(1)-Si(11)	2.353(3)	P(7)-K(3)	3.485(2)	C(064)-C(065)	1.358(10)
Si(1)-Si(12)	2.355(3)	P(3)-P(2)	2.0887(19)	C(064)-C(063)	1.369(11)
K(4)-C(064)	3.245(8)	P(3)-K(1)	3.484(2)	C(011)-C(016)	1.327(11)
K(4)-P(8)	3.254(2)	Si(23)-C(233)	1.877(5)	C(011)-C(012)	1.400(12)
K(4)-C(065)	3.297(8)	Si(23)-C(231)	1.878(6)	C(084)-C(085)	1.410(13)
K(4)-C(086)	3.305(8)	Si(23)-C(232)	1.879(7)	C(082)-C(081)	1.328(11)
K(4)-C(081)	3.332(8)	K(1)-C(031)	3.168(8)	C(042)-C(043)	1.324(12)
K(4)-C(085)	3.368(9)	K(1)-C(032)	3.200(8)	C(042)-C(041)	1.384(14)
K(4)-C(082)	3.413(9)	K(1)-C(036)	3.335(8)	C(036)-C(035)	1.382(12)
K(4)-C(084)	3.423(9)	K(1)-C(033)	3.380(8)	C(025)-C(026)	1.345(8)
K(4)-C(083)	3.465(8)	K(1)-C(035)	3.475(8)	C(025)-C(024)	1.366(9)
K(4)-P(7)	3.568(2)	K(1)-P(2)	3.486(2)	C(072)-C(073)	1.366(9)
K(4)-P(6)	3.572(2)	K(1)-C(034)	3.497(9)	C(072)-C(071)	1.380(10)
Si(42)-C(421)	1.869(6)	K(3)-C(055)	3.169(8)	C(056)-C(055)	1.364(12)
Si(42)-C(423)	1.872(7)	K(3)-C(054)	3.174(8)	C(054)-C(055)	1.339(10)
Si(42)-C(422)	1.883(7)	K(3)-C(053)	3.356(8)	C(054)-C(053)	1.361(12)
Si(2)-P(4)	2.254(2)	K(3)-C(056)	3.379(8)	C(052)-C(053)	1.378(12)
Si(2)-Si(22)	2.345(3)	K(3)-P(6)	3.481(2)	C(073)-C(074)	1.366(11)
Si(2)-Si(21)	2.352(3)	K(3)-C(052)	3.518(8)	C(022)-C(021)	1.367(11)
Si(2)-Si(23)	2.355(3)	K(3)-C(051)	3.527(9)	C(022)-C(023)	1.375(11)
K(2)-P(4)	3.265(2)	K(3)-C(072)	3.528(7)	C(026)-C(021)	1.404(11)
K(2)-C(044)	3.275(9)	Si(13)-C(131)	1.877(6)	C(076)-C(071)	1.342(11)
K(2)-C(011)	3.305(8)	Si(13)-C(133)	1.883(7)	C(076)-C(075)	1.389(11)
K(2)-C(016)	3.316(8)	Si(13)-C(132)	1.892(6)	C(066)-C(061)	1.341(12)
K(2)-C(043)	3.338(8)	Si(31)-C(313)	1.880(7)	C(066)-C(065)	1.355(10)
K(2)-C(015)	3.372(8)	Si(31)-C(311)	1.883(6)	C(063)-C(062)	1.367(12)
K(2)-C(012)	3.390(8)	Si(31)-C(312)	1.892(7)	C(046)-C(045)	1.352(12)
K(2)-C(014)	3.441(9)	Si(22)-C(223)	1.877(7)	C(046)-C(041)	1.365(13)
K(2)-C(013)	3.460(8)	Si(22)-C(222)	1.896(7)	C(024)-C(023)	1.353(11)
K(2)-P(3)	3.571(2)	Si(22)-C(221)	1.900(6)	C(062)-C(061)	1.350(12)
K(2)-P(2)	3.573(2)	Si(41)-C(411)	1.834(7)	C(075)-C(074)	1.387(12)
P(8)-P(7)	2.147(2)				

7.1.4 Angles [deg]

Atoms	Angle	Atoms	Angle
P(5)-Si(4)-Si(41)	109.08(9)	C(321)-Si(32)-C(322)	108.3(3)
P(5)-Si(4)-Si(43)	116.26(10)	C(321)-Si(32)-C(323)	108.2(3)
Si(41)-Si(4)-Si(43)	111.61(10)	C(322)-Si(32)-C(323)	107.5(3)
P(5)-Si(4)-Si(42)	103.47(9)	C(321)-Si(32)-Si(3)	109.7(2)
Si(41)-Si(4)-Si(42)	107.74(10)	C(322)-Si(32)-Si(3)	113.6(2)
Si(43)-Si(4)-Si(42)	108.07(9)	C(323)-Si(32)-Si(3)	109.5(2)
P(1)-Si(3)-Si(31)	107.62(9)	P(8)-Si(1)-Si(13)	109.14(9)
P(1)-Si(3)-Si(32)	103.39(9)	P(8)-Si(1)-Si(11)	103.67(10)
Si(31)-Si(3)-Si(32)	108.21(10)	Si(13)-Si(1)-Si(11)	110.91(9)
P(1)-Si(3)-Si(33)	116.22(10)	P(8)-Si(1)-Si(12)	116.80(9)
Si(31)-Si(3)-Si(33)	111.70(10)	Si(13)-Si(1)-Si(12)	107.78(10)
Si(32)-Si(3)-Si(33)	109.16(9)	Si(11)-Si(1)-Si(12)	108.50(9)
P(2)-P(1)-Si(3)	98.47(9)	C(064)-K(4)-P(8)	100.3(2)
P(2)-P(1)-K(1)	78.04(7)	C(064)-K(4)-C(065)	23.95(17)
Si(3)-P(1)-K(1)	121.22(8)	P(8)-K(4)-C(065)	82.74(15)
P(2)-P(1)-K(2)	78.78(7)	C(064)-K(4)-C(086)	135.4(3)
Si(3)-P(1)-K(2)	122.13(8)	P(8)-K(4)-C(086)	116.86(16)
K(1)-P(1)-K(2)	114.67(5)	C(065)-K(4)-C(086)	135.8(3)

Atoms	Angle	Atoms	Angle
P(6)-P(5)-Si(4)	97.96(9)	C(064)-K(4)-P(5)	81.14(16)
P(6)-P(5)-K(3)	77.84(7)	P(8)-K(4)-P(5)	64.88(5)
Si(4)-P(5)-K(3)	120.22(8)	C(065)-K(4)-P(5)	88.15(18)
P(6)-P(5)-K(4)	78.56(7)	C(086)-K(4)-P(5)	135.7(2)
Si(4)-P(5)-K(4)	122.95(8)	C(064)-K(4)-C(081)	126.3(3)
K(3)-P(5)-K(4)	114.57(6)	P(8)-K(4)-C(081)	133.24(19)
P(5)-K(4)-C(085)	159.0(3)	C(065)-K(4)-C(081)	139.5(2)
C(081)-K(4)-C(085)	41.0(2)	C(086)-K(4)-C(081)	23.39(18)
C(064)-K(4)-C(082)	103.6(3)	P(5)-K(4)-C(081)	120.95(17)
P(8)-K(4)-C(082)	155.9(2)	C(064)-K(4)-C(085)	117.4(3)
C(065)-K(4)-C(082)	119.3(2)	P(8)-K(4)-C(085)	117.14(19)
C(086)-K(4)-C(082)	40.8(2)	C(065)-K(4)-C(085)	112.8(3)
P(5)-K(4)-C(082)	121.52(16)	C(086)-K(4)-C(085)	23.4(2)
C(081)-K(4)-C(082)	22.67(19)	C(081)-K(4)-P(7)	101.83(18)
C(085)-K(4)-C(082)	47.8(2)	C(085)-K(4)-P(7)	107.9(3)
C(064)-K(4)-C(084)	95.1(3)	C(082)-K(4)-P(7)	123.0(2)
P(8)-K(4)-C(084)	134.7(3)	C(084)-K(4)-P(7)	131.8(3)
C(065)-K(4)-C(084)	96.2(2)	C(083)-K(4)-P(7)	140.81(18)
C(086)-K(4)-C(084)	41.2(2)	C(064)-K(4)-P(6)	117.23(16)
P(5)-K(4)-C(084)	160.3(3)	P(8)-K(4)-P(6)	60.63(5)
C(081)-K(4)-C(084)	47.0(2)	C(065)-K(4)-P(6)	121.00(16)
C(085)-K(4)-C(084)	24.0(2)	C(086)-K(4)-P(6)	102.7(2)
C(082)-K(4)-C(084)	40.4(2)	P(5)-K(4)-P(6)	36.09(4)
C(064)-K(4)-C(083)	89.2(3)	C(081)-K(4)-P(6)	96.40(16)
P(8)-K(4)-C(083)	157.60(19)	C(085)-K(4)-P(6)	124.5(3)
C(065)-K(4)-C(083)	99.6(2)	C(082)-K(4)-P(6)	109.37(19)
C(086)-K(4)-C(083)	47.5(2)	C(084)-K(4)-P(6)	142.67(17)
P(5)-K(4)-C(083)	137.2(2)	C(083)-K(4)-P(6)	132.0(2)
C(081)-K(4)-C(083)	39.9(2)	P(7)-K(4)-P(6)	34.02(4)
C(085)-K(4)-C(083)	41.4(2)	C(421)-Si(42)-C(423)	107.0(3)
C(082)-K(4)-C(083)	22.66(19)	C(421)-Si(42)-C(422)	108.3(3)
C(084)-K(4)-C(083)	23.2(2)	C(423)-Si(42)-C(422)	107.7(4)
C(064)-K(4)-P(7)	129.8(2)	C(421)-Si(42)-Si(4)	113.8(3)
P(8)-K(4)-P(7)	36.31(4)	C(423)-Si(42)-Si(4)	110.1(3)
C(065)-K(4)-P(7)	117.70(14)	C(422)-Si(42)-Si(4)	109.8(2)
C(086)-K(4)-P(7)	94.41(18)	P(1)-K(2)-C(015)	118.81(15)
P(5)-K(4)-P(7)	60.28(4)	C(016)-K(2)-C(015)	23.09(17)
P(4)-Si(2)-Si(22)	108.55(9)	C(043)-K(2)-C(015)	139.7(2)
P(4)-Si(2)-Si(21)	116.84(9)	P(4)-K(2)-C(012)	135.5(2)
Si(22)-Si(2)-Si(21)	107.93(10)	C(044)-K(2)-C(012)	94.6(3)
P(4)-Si(2)-Si(23)	104.39(10)	C(011)-K(2)-C(012)	24.1(2)
Si(22)-Si(2)-Si(23)	110.10(9)	P(1)-K(2)-C(012)	159.3(2)
Si(21)-Si(2)-Si(23)	108.93(9)	C(016)-K(2)-C(012)	41.4(2)
P(4)-K(2)-C(044)	98.4(3)	C(043)-K(2)-C(012)	95.9(3)
P(4)-K(2)-C(011)	118.62(17)	C(015)-K(2)-C(012)	47.3(2)
C(044)-K(2)-C(011)	117.1(3)	P(4)-K(2)-C(014)	157.07(19)
P(4)-K(2)-P(1)	64.86(5)	C(044)-K(2)-C(014)	104.4(3)
C(044)-K(2)-P(1)	83.67(16)	C(011)-K(2)-C(014)	47.4(2)
C(011)-K(2)-P(1)	156.4(2)	P(1)-K(2)-C(014)	119.76(16)
P(4)-K(2)-C(016)	118.30(17)	C(016)-K(2)-C(014)	40.7(2)
C(044)-K(2)-C(016)	135.3(3)	C(043)-K(2)-C(014)	119.5(2)
C(011)-K(2)-C(016)	23.13(19)	C(015)-K(2)-C(014)	22.75(19)
P(1)-K(2)-C(016)	133.3(2)	C(012)-K(2)-C(014)	40.7(2)
P(4)-K(2)-C(043)	81.52(16)	P(4)-K(2)-C(013)	158.99(18)
C(044)-K(2)-C(043)	23.06(19)	C(044)-K(2)-C(013)	89.3(3)
C(011)-K(2)-C(043)	112.9(3)	C(011)-K(2)-C(013)	41.5(2)
P(1)-K(2)-C(043)	90.6(3)	P(1)-K(2)-C(013)	135.78(18)
C(016)-K(2)-C(043)	135.7(3)	C(016)-K(2)-C(013)	47.7(2)
P(4)-K(2)-C(015)	134.33(19)	C(043)-K(2)-C(013)	99.7(2)
C(044)-K(2)-C(015)	127.0(3)	C(015)-K(2)-C(013)	40.1(2)
C(011)-K(2)-C(015)	40.42(19)	C(012)-K(2)-C(013)	23.61(18)

Atoms	Angle	Atoms	Angle
P(4)-K(2)-P(3)	36.24(4)	C(014)-K(2)-C(013)	22.64(18)
C(044)-K(2)-P(3)	129.4(3)	C(113)-Si(11)-C(111)	108.3(3)
C(011)-K(2)-P(3)	107.6(2)	C(113)-Si(11)-C(112)	108.1(3)
P(1)-K(2)-P(3)	60.12(4)	C(111)-Si(11)-C(112)	108.4(3)
C(016)-K(2)-P(3)	94.53(17)	C(113)-Si(11)-Si(1)	109.7(2)
C(043)-K(2)-P(3)	116.90(16)	C(111)-Si(11)-Si(1)	108.1(2)
C(015)-K(2)-P(3)	102.18(18)	C(112)-Si(11)-Si(1)	114.1(3)
C(012)-K(2)-P(3)	131.7(2)	C(213)-Si(21)-C(211)	109.3(3)
C(014)-K(2)-P(3)	123.5(2)	C(213)-Si(21)-C(212)	106.7(3)
C(013)-K(2)-P(3)	141.26(16)	C(211)-Si(21)-C(212)	108.5(3)
P(4)-K(2)-P(2)	60.62(5)	C(213)-Si(21)-Si(2)	112.2(2)
C(044)-K(2)-P(2)	119.56(17)	C(211)-Si(21)-Si(2)	110.7(2)
C(011)-K(2)-P(2)	122.6(2)	C(212)-Si(21)-Si(2)	109.3(2)
P(1)-K(2)-P(2)	35.97(4)	C(432)-Si(43)-C(433)	107.7(4)
C(016)-K(2)-P(2)	101.15(19)	C(432)-Si(43)-C(431)	105.9(3)
C(043)-K(2)-P(2)	122.5(2)	C(433)-Si(43)-C(431)	109.4(4)
C(015)-K(2)-P(2)	95.25(15)	C(432)-Si(43)-Si(4)	114.1(3)
C(012)-K(2)-P(2)	141.59(17)	C(433)-Si(43)-Si(4)	108.9(3)
C(014)-K(2)-P(2)	108.60(19)	C(431)-Si(43)-Si(4)	110.7(3)
C(013)-K(2)-P(2)	131.23(19)	C(123)-Si(12)-C(122)	109.4(3)
P(3)-K(2)-P(2)	34.00(3)	C(123)-Si(12)-C(121)	106.8(3)
C(122)-Si(12)-C(121)	107.6(3)	C(233)-Si(23)-C(231)	107.9(3)
C(123)-Si(12)-Si(1)	111.6(2)	C(233)-Si(23)-C(232)	107.6(3)
C(122)-Si(12)-Si(1)	110.9(2)	C(231)-Si(23)-C(232)	108.5(3)
C(121)-Si(12)-Si(1)	110.4(2)	C(233)-Si(23)-Si(2)	115.1(2)
P(7)-P(8)-Si(1)	98.62(9)	C(231)-Si(23)-Si(2)	107.6(2)
P(7)-P(8)-K(4)	79.82(7)	C(232)-Si(23)-Si(2)	110.0(2)
Si(1)-P(8)-K(4)	124.01(8)	C(031)-K(1)-C(032)	24.84(19)
P(7)-P(8)-K(3)	76.83(7)	C(031)-K(1)-P(1)	135.4(2)
Si(1)-P(8)-K(3)	119.18(8)	C(032)-K(1)-P(1)	159.66(18)
K(4)-P(8)-K(3)	114.83(6)	C(031)-K(1)-P(4)	157.9(2)
C(331)-Si(33)-C(333)	108.1(4)	C(032)-K(1)-P(4)	134.70(18)
C(331)-Si(33)-C(332)	105.8(4)	P(1)-K(1)-P(4)	65.63(5)
C(333)-Si(33)-C(332)	110.0(4)	C(031)-K(1)-C(036)	24.4(2)
C(331)-Si(33)-Si(3)	113.8(2)	C(032)-K(1)-C(036)	42.5(2)
C(333)-Si(33)-Si(3)	108.9(3)	P(1)-K(1)-C(036)	117.58(17)
C(332)-Si(33)-Si(3)	110.2(3)	P(4)-K(1)-C(036)	168.3(2)
P(3)-P(4)-Si(2)	97.81(9)	C(031)-K(1)-C(033)	42.2(2)
P(3)-P(4)-K(2)	79.68(7)	C(032)-K(1)-C(033)	23.6(2)
Si(2)-P(4)-K(2)	124.98(8)	P(1)-K(1)-C(033)	153.8(2)
P(3)-P(4)-K(1)	76.89(7)	P(4)-K(1)-C(033)	123.87(15)
Si(2)-P(4)-K(1)	118.09(8)	C(036)-K(1)-C(033)	48.07(19)
K(2)-P(4)-K(1)	114.70(5)	C(031)-K(1)-C(035)	41.7(2)
P(6)-P(7)-P(8)	109.39(9)	C(032)-K(1)-C(035)	48.0(2)
P(6)-P(7)-K(3)	72.44(7)	P(1)-K(1)-C(035)	116.67(15)
P(8)-P(7)-K(3)	66.31(7)	P(4)-K(1)-C(035)	145.1(2)
P(6)-P(7)-K(4)	73.10(7)	C(036)-K(1)-C(035)	23.3(2)
P(8)-P(7)-K(4)	63.87(6)	C(033)-K(1)-C(035)	40.1(2)
K(3)-P(7)-K(4)	102.59(6)	C(031)-K(1)-P(3)	137.57(19)
P(2)-P(3)-P(4)	109.65(9)	C(032)-K(1)-P(3)	132.89(17)
P(2)-P(3)-K(1)	72.62(7)	C(055)-K(3)-C(054)	24.37(19)
P(4)-P(3)-K(1)	66.24(6)	C(055)-K(3)-P(5)	134.5(2)
P(2)-P(3)-K(2)	73.06(7)	C(054)-K(3)-P(5)	158.52(19)
P(4)-P(3)-K(2)	64.08(6)	C(055)-K(3)-P(8)	159.1(2)
K(1)-P(3)-K(2)	102.58(6)	C(054)-K(3)-P(8)	135.9(2)
P(1)-K(1)-P(3)	61.77(5)	P(5)-K(3)-P(8)	65.56(5)
P(4)-K(1)-P(3)	36.87(4)	C(055)-K(3)-C(053)	42.0(2)
C(036)-K(1)-P(3)	154.8(2)	C(054)-K(3)-C(053)	23.8(2)
C(033)-K(1)-P(3)	141.95(18)	P(5)-K(3)-C(053)	153.8(2)
C(035)-K(1)-P(3)	177.4(2)	P(8)-K(3)-C(053)	124.23(17)
C(031)-K(1)-P(2)	128.41(18)	C(055)-K(3)-C(056)	23.8(2)

Atoms	Angle	Atoms	Angle
C(032)-K(1)-P(2)	144.3(2)	C(054)-K(3)-C(056)	42.2(2)
P(1)-K(1)-P(2)	36.90(4)	P(5)-K(3)-C(056)	116.93(17)
P(4)-K(1)-P(2)	61.51(4)	P(8)-K(3)-C(056)	168.2(2)
C(036)-K(1)-P(2)	128.37(17)	C(053)-K(3)-C(056)	48.3(2)
C(033)-K(1)-P(2)	167.6(2)	C(055)-K(3)-P(6)	128.56(18)
C(035)-K(1)-P(2)	142.62(18)	C(054)-K(3)-P(6)	143.7(2)
P(3)-K(1)-P(2)	34.88(4)	P(5)-K(3)-P(6)	37.08(4)
C(031)-K(1)-C(034)	48.0(2)	P(8)-K(3)-P(6)	61.43(5)
C(032)-K(1)-C(034)	40.7(2)	C(053)-K(3)-P(6)	167.3(2)
P(1)-K(1)-C(034)	131.2(2)	C(056)-K(3)-P(6)	128.13(18)
P(4)-K(1)-C(034)	128.48(17)	C(055)-K(3)-P(7)	138.5(2)
C(036)-K(1)-C(034)	40.4(2)	C(054)-K(3)-P(7)	133.3(2)
C(033)-K(1)-C(034)	22.65(19)	P(5)-K(3)-P(7)	61.94(5)
C(035)-K(1)-C(034)	22.28(17)	P(8)-K(3)-P(7)	36.86(4)
P(3)-K(1)-C(034)	160.32(19)	C(053)-K(3)-P(7)	141.9(2)
P(2)-K(1)-C(034)	164.3(2)	C(056)-K(3)-P(7)	154.9(2)
P(3)-P(2)-P(1)	109.52(9)	P(6)-K(3)-P(7)	34.90(4)
P(3)-P(2)-K(1)	72.50(7)	C(055)-K(3)-C(052)	47.5(2)
P(1)-P(2)-K(1)	65.06(6)	C(054)-K(3)-C(052)	40.9(2)
P(3)-P(2)-K(2)	72.95(7)	P(5)-K(3)-C(052)	130.9(2)
P(1)-P(2)-K(2)	65.25(6)	P(8)-K(3)-C(052)	128.56(19)
K(1)-P(2)-K(2)	102.49(5)	C(053)-K(3)-C(052)	23.0(2)
P(5)-K(3)-C(051)	116.09(18)	C(056)-K(3)-C(052)	40.4(2)
P(8)-K(3)-C(051)	145.1(2)	P(6)-K(3)-C(052)	164.2(2)
C(053)-K(3)-C(051)	40.5(2)	P(7)-K(3)-C(052)	160.4(2)
C(056)-K(3)-C(051)	23.2(2)	C(055)-K(3)-C(051)	41.0(2)
P(6)-K(3)-C(051)	142.3(2)	C(054)-K(3)-C(051)	47.9(2)
P(7)-K(3)-C(051)	177.1(2)	C(313)-Si(31)-C(311)	109.1(3)
C(052)-K(3)-C(051)	22.49(18)	C(313)-Si(31)-C(312)	106.8(3)
C(055)-K(3)-C(072)	108.1(2)	C(311)-Si(31)-C(312)	107.6(3)
C(054)-K(3)-C(072)	104.8(3)	C(313)-Si(31)-Si(3)	110.4(3)
P(5)-K(3)-C(072)	75.05(12)	C(311)-Si(31)-Si(3)	114.3(2)
P(8)-K(3)-C(072)	80.53(15)	C(312)-Si(31)-Si(3)	108.3(2)
C(053)-K(3)-C(072)	82.5(3)	C(223)-Si(22)-C(222)	106.9(3)
C(056)-K(3)-C(072)	88.9(3)	C(223)-Si(22)-C(221)	108.5(3)
P(6)-K(3)-C(072)	110.10(13)	C(222)-Si(22)-C(221)	107.8(3)
P(7)-K(3)-C(072)	113.30(14)	C(223)-Si(22)-Si(2)	110.8(2)
C(052)-K(3)-C(072)	64.4(2)	C(222)-Si(22)-Si(2)	108.9(2)
C(051)-K(3)-C(072)	67.4(2)	C(221)-Si(22)-Si(2)	113.7(2)
C(131)-Si(13)-C(133)	107.4(3)	C(411)-Si(41)-C(413)	109.0(4)
C(131)-Si(13)-C(132)	108.9(3)	C(411)-Si(41)-C(412)	108.3(6)
C(133)-Si(13)-C(132)	106.6(3)	C(413)-Si(41)-C(412)	105.1(5)
C(131)-Si(13)-Si(1)	113.6(2)	C(411)-Si(41)-Si(4)	114.0(3)
C(133)-Si(13)-Si(1)	111.1(2)	C(413)-Si(41)-Si(4)	110.8(3)
C(132)-Si(13)-Si(1)	109.0(2)	C(412)-Si(41)-Si(4)	109.2(3)
P(7)-P(6)-P(5)	109.63(9)	C(043)-C(044)-C(045)	121.9(9)
P(7)-P(6)-K(3)	72.66(7)	C(043)-C(044)-K(2)	81.1(6)
P(5)-P(6)-K(3)	65.08(6)	C(045)-C(044)-K(2)	95.9(6)
P(7)-P(6)-K(4)	72.88(7)	C(032)-C(031)-C(036)	119.3(9)
P(5)-P(6)-K(4)	65.35(6)	C(032)-C(031)-K(1)	78.9(5)
K(3)-P(6)-K(4)	102.59(5)	C(036)-C(031)-K(1)	84.6(5)
C(014)-C(013)-C(012)	119.0(9)	C(082)-C(083)-C(084)	119.3(10)
C(014)-C(013)-K(2)	77.9(5)	C(082)-C(083)-K(4)	76.5(6)
C(012)-C(013)-K(2)	75.4(5)	C(084)-C(083)-K(4)	76.7(5)
C(016)-C(015)-C(014)	122.2(8)	C(081)-C(086)-C(085)	120.4(9)
C(016)-C(015)-K(2)	76.1(5)	C(081)-C(086)-K(4)	79.4(5)
C(014)-C(015)-K(2)	81.5(5)	C(085)-C(086)-K(4)	80.9(6)
C(052)-C(051)-C(056)	119.1(10)	C(083)-C(084)-C(085)	119.7(9)
C(052)-C(051)-K(3)	78.4(5)	C(083)-C(084)-K(4)	80.1(5)
C(056)-C(051)-K(3)	72.4(6)	C(085)-C(084)-K(4)	75.8(6)
C(033)-C(032)-C(031)	120.6(9)	C(086)-C(085)-C(084)	117.9(9)

Atoms	Angle	Atoms	Angle
C(033)-C(032)-K(1)	85.7(5)	C(086)-C(085)-K(4)	75.7(5)
C(031)-C(032)-K(1)	76.2(5)	C(084)-C(085)-K(4)	80.2(6)
C(035)-C(034)-C(033)	121.1(10)	C(011)-C(016)-C(015)	119.8(9)
C(035)-C(034)-K(1)	77.9(5)	C(011)-C(016)-K(2)	78.0(5)
C(033)-C(034)-K(1)	73.8(5)	C(015)-C(016)-K(2)	80.8(5)
C(065)-C(064)-C(063)	118.9(8)	C(081)-C(082)-C(083)	120.1(9)
C(065)-C(064)-K(4)	80.2(5)	C(081)-C(082)-K(4)	75.3(6)
C(063)-C(064)-K(4)	96.9(5)	C(083)-C(082)-K(4)	80.8(5)
C(016)-C(011)-C(012)	120.9(8)	C(043)-C(042)-C(041)	120.4(11)
C(016)-C(011)-K(2)	78.9(5)	C(015)-C(014)-C(013)	120.3(8)
C(012)-C(011)-K(2)	81.3(5)	C(015)-C(014)-K(2)	75.7(5)
C(011)-C(012)-C(013)	117.9(8)	C(013)-C(014)-K(2)	79.5(5)
C(011)-C(012)-K(2)	74.5(5)	C(055)-C(056)-C(051)	118.5(9)
C(013)-C(012)-K(2)	81.0(5)	C(055)-C(056)-K(3)	69.5(5)
C(031)-C(036)-C(035)	119.2(8)	C(051)-C(056)-K(3)	84.4(6)
C(031)-C(036)-K(1)	71.0(5)	C(044)-C(043)-C(042)	120.1(10)
C(035)-C(036)-K(1)	84.1(5)	C(044)-C(043)-K(2)	75.8(5)
C(032)-C(033)-C(034)	119.9(8)	C(042)-C(043)-K(2)	98.3(6)
C(032)-C(033)-K(1)	70.7(5)	C(055)-C(054)-C(053)	120.4(10)
C(034)-C(033)-K(1)	83.5(5)	C(055)-C(054)-K(3)	77.6(5)
C(034)-C(035)-C(036)	119.9(9)	C(053)-C(054)-K(3)	85.6(5)
C(034)-C(035)-K(1)	79.8(5)	C(051)-C(052)-C(053)	120.6(10)
C(036)-C(035)-K(1)	72.6(5)	C(051)-C(052)-K(3)	79.1(5)
C(026)-C(025)-C(024)	120.5(7)	C(053)-C(052)-K(3)	71.9(5)
C(073)-C(072)-C(071)	119.1(7)	C(054)-C(055)-C(056)	122.1(10)
C(073)-C(072)-K(3)	89.1(5)	C(054)-C(055)-K(3)	78.0(5)
C(071)-C(072)-K(3)	123.6(6)	C(056)-C(055)-K(3)	86.8(5)
C(062)-C(063)-C(064)	120.4(9)	C(054)-C(053)-C(052)	119.2(9)
C(045)-C(046)-C(041)	119.9(10)	C(054)-C(053)-K(3)	70.6(5)
C(044)-C(045)-C(046)	119.0(9)	C(052)-C(053)-K(3)	85.1(5)
C(066)-C(065)-C(064)	121.1(8)	C(074)-C(073)-C(072)	120.3(7)
C(066)-C(065)-K(4)	98.0(5)	C(021)-C(022)-C(023)	121.0(9)
C(064)-C(065)-K(4)	75.9(5)	C(025)-C(026)-C(021)	119.4(7)
C(023)-C(024)-C(025)	121.6(8)	C(071)-C(076)-C(075)	120.1(9)
C(082)-C(081)-C(086)	122.5(9)	C(061)-C(066)-C(065)	118.6(9)
C(082)-C(081)-K(4)	82.1(6)	C(046)-C(041)-C(042)	118.6(10)
C(086)-C(081)-K(4)	77.2(5)	C(076)-C(071)-C(072)	121.4(8)
C(061)-C(062)-C(063)	118.4(9)	C(066)-C(061)-C(062)	122.5(9)
C(074)-C(075)-C(076)	118.6(8)	C(024)-C(023)-C(022)	118.6(9)
C(073)-C(074)-C(075)	120.4(8)	C(022)-C(021)-C(026)	119.0(8)

7.2 Crystallographic data for $Hyp_4P_8K_4\cdot4C_6H_6$

7.2.1 Crystal data and structure refinement

Empirical formula	$Hyp_4P_8K_4\cdot$7benzene
Formula weight	1941.58
Temperature	193(2) K
Wavelength	0.71073 Å
Crystal system, space group	monoclinic; P2/n
Unit cell dimensions	a = 15.1356(7) Å alpha = 90 deg. b = 14.6526(6) Å beta = 99.297(4) deg. c = 26.9623(14) Å gamma = 90 deg.
Volume	5901.0(5) $Å^3$

Z, Calculated density	2, 1.093 g/cm^3
Absorption coefficient	0.455 mm^{-1}
F(000)	2076
Theta range for data collection	1.39 to 26.29 deg.
Limiting indices	-18<=h<=18, -18<=k<=18, -33<=l<=33
Reflections collected / unique	67117 / 11884 [R(int) = 0.0621]
Completeness to theta = 26.29	99.3 %
Refinement method	Full-matrix least-squares on F^2
Data / restraints / parameters	11884 / 440 / 657
Goodness-of-fit on F^2	0.936
Final R indices [I>2sigma(I)]	R1 = 0.0288, wR2 = 0.0713
R indices (all data)	R1 = 0.0439, wR2 = 0.0741
Extinction coefficient	0.00134(14)
Largest diff. peak and hole	0.272 and -0.257 e.Å^{-3}

7.2.2 Atomic coordinates (x 10^4), equivalent isotropic displacement parameters (Å^2 x 10^3) and Anisotropic displacement parameters (Å^2 x 10^3). U(eq) is defined as one third of the trace of the orthogonalized Uij tensor. The anisotropic displacement factor exponent takes the form: $-2\pi^2[h^2a^{*2}U11 + ... + 2hka^*b^*U12]$

Atom	x	y	z	U(eq)	U11	U22	U33	U23	U13	U12
P(1)	8803(1)	4980(1)	6924(1)	46(1)	39(1)	51(1)	51(1)	14(1)	13(1)	1(1)
P(2)	7422(1)	4916(1)	7075(1)	42(1)	38(1)	47(1)	42(1)	5(1)	11(1)	-2(1)
P(3)	7213(1)	3390(1)	7085(1)	41(1)	34(1)	47(1)	41(1)	-3(1)	3(1)	-5(1)
P(4)	5774(1)	3239(1)	7080(1)	48(1)	35(1)	60(1)	51(1)	-16(1)	6(1)	-9(1)
K(1)	9687(1)	5351(1)	8069(1)	69(1)	54(1)	78(1)	71(1)	-12(1)	-1(1)	-20(1)
K(2)	9093(1)	2863(1)	6737(1)	66(1)	69(1)	68(1)	66(1)	-13(1)	27(1)	11(1)
Si(1)	8801(1)	6071(1)	6356(1)	42(1)	42(1)	44(1)	43(1)	6(1)	11(1)	0(1)
Si(11)	8415(1)	7515(1)	6620(1)	67(1)	64(1)	45(1)	96(1)	2(1)	22(1)	5(1)
C(111)	7178(2)	7718(2)	6439(1)	97(1)	77(1)	79(2)	135(2)	4(1)	22(1)	26(1)
C(112)	9012(2)	8470(2)	6352(1)	117(1)	114(2)	52(1)	193(3)	25(2)	47(2)	-2(1)
C(113)	8704(2)	7578(2)	7320(1)	97(1)	96(2)	91(2)	106(2)	-42(2)	23(1)	4(1)
Si(12)	7986(1)	5734(1)	5567(1)	67(1)	64(1)	91(1)	45(1)	6(1)	1(1)	4(1)
C(121)	6798(1)	5465(2)	5628(1)	84(1)	63(1)	107(2)	73(1)	1(1)	-12(1)	-2(1)
C(122)	8463(2)	4702(2)	5297(1)	108(1)	94(2)	149(2)	76(2)	-47(2)	3(1)	12(2)
C(123)	7977(2)	6700(2)	5107(1)	121(1)	117(2)	168(3)	73(2)	58(2)	-3(1)	-8(2)
Si(13)	10330(1)	6098(1)	6295(1)	56(1)	48(1)	59(1)	68(1)	-1(1)	25(1)	-8(1)
C(131)	10977(1)	6596(2)	6881(1)	101(1)	52(1)	133(2)	119(2)	-46(2)	20(1)	-19(1)
C(132)	10578(2)	6760(2)	5742(1)	112(1)	107(2)	113(2)	135(2)	39(2)	77(2)	-1(2)
C(133)	10757(1)	4916(2)	6229(1)	84(1)	54(1)	77(1)	124(2)	-10(1)	28(1)	4(1)
Si(2)	5332(1)	2196(1)	6498(1)	39(1)	32(1)	46(1)	39(1)	-4(1)	3(1)	-2(1)
Si(21)	5942(1)	744(1)	6664(1)	61(1)	50(1)	48(1)	85(1)	4(1)	13(1)	3(1)
C(211)	7089(1)	679(2)	6502(1)	100(1)	68(1)	82(2)	156(2)	22(2)	38(2)	26(1)
C(212)	5262(2)	-186(2)	6316(2)	153(2)	102(2)	57(2)	283(5)	-40(2)	-22(2)	6(1)
C(213)	6034(2)	489(2)	7346(1)	144(1)	180(3)	139(3)	129(2)	81(2)	72(2)	80(2)
Si(22)	5468(1)	2623(1)	5679(1)	57(1)	52(1)	80(1)	40(1)	1(1)	8(1)	4(1)
C(221)	4939(2)	1773(2)	5200(1)	104(1)	104(2)	158(3)	52(1)	-26(1)	16(1)	-35(2)
C(222)	6672(1)	2764(2)	5608(1)	71(1)	66(1)	84(1)	66(1)	8(1)	24(1)	4(1)
C(223)	4898(2)	3749(2)	5540(1)	92(1)	85(2)	119(2)	76(1)	42(1)	23(1)	37(1)
Si(23)	3806(1)	2141(1)	6565(1)	52(1)	33(1)	66(1)	57(1)	-15(1)	6(1)	-6(1)
C(231)	3147(1)	1391(2)	6085(1)	95(1)	46(1)	124(2)	114(2)	-58(2)	10(1)	-21(1)
C(232)	3673(2)	1725(2)	7203(1)	98(1)	67(1)	150(2)	84(2)	5(2)	34(1)	-14(1)

Atom	x	y	z	U(eq)	U11	U22	U33	U23	U13	U12
C(233)	3295(1)	3307(2)	6502(1)	92(1)	53(1)	86(2)	139(2)	-12(2)	16(1)	13(1)
C(31)	10770(10)	1731(14)	6381(6)	67(3)	47(3)	96(10)	58(4)	-7(5)	11(3)	12(5)
C(32)	10624(10)	2315(11)	5973(6)	65(3)	68(6)	87(4)	45(6)	-8(4)	24(4)	-19(4)
C(33)	9807(11)	2291(9)	5662(5)	64(3)	71(8)	71(6)	49(4)	7(4)	10(5)	7(6)
C(34)	9183(8)	1650(10)	5711(5)	60(3)	56(5)	69(9)	54(7)	-14(5)	9(4)	-4(5)
C(35)	9369(10)	1017(9)	6084(7)	64(3)	71(7)	45(3)	78(9)	-1(5)	21(5)	7(5)
C(36)	10147(11)	1064(11)	6427(6)	69(3)	66(7)	75(8)	71(6)	13(6)	25(5)	23(5)
C(31A)	10634(11)	1477(11)	6400(6)	70(3)	62(7)	73(7)	75(5)	-12(4)	7(5)	21(5)
C(32A)	10705(7)	2266(9)	6126(6)	60(3)	46(3)	83(5)	52(7)	-19(5)	14(4)	-8(3)
C(33A)	10056(11)	2477(10)	5730(5)	66(3)	66(6)	79(5)	59(5)	-5(4)	25(5)	-9(4)
C(34A)	9302(10)	1962(13)	5630(5)	73(4)	59(5)	104(10)	56(4)	-20(5)	10(4)	-7(6)
C(35A)	9193(8)	1228(11)	5923(6)	73(4)	63(5)	74(11)	85(12)	-33(7)	23(7)	-19(7)
C(36A)	9856(13)	967(8)	6308(6)	75(4)	100(12)	50(3)	81(9)	-7(5)	32(7)	0(7)
C(41)	10641(9)	7295(6)	8529(5)	77(3)	79(7)	56(3)	97(7)	-18(4)	12(5)	-1(4)
C(42)	11308(11)	6865(13)	8311(6)	79(3)	63(9)	98(7)	74(4)	2(4)	9(5)	-31(6)
C(43)	11715(7)	6079(10)	8517(6)	77(3)	47(3)	99(6)	86(7)	-20(4)	13(3)	-14(3)
C(44)	11500(10)	5769(10)	8969(6)	86(3)	55(7)	110(5)	84(5)	6(4)	-16(5)	3(4)
C(45)	10830(12)	6184(11)	9161(5)	86(4)	84(11)	113(9)	60(3)	-20(4)	13(6)	-15(7)
C(46)	10401(10)	6941(12)	8951(7)	94(5)	87(6)	110(12)	86(11)	-49(8)	17(7)	-7(8)
C(43A)	10551(12)	6439(15)	9128(7)	78(5)	63(9)	111(13)	62(6)	-10(7)	13(6)	-12(8)
C(44A)	11239(12)	5884(10)	9037(7)	74(4)	47(10)	78(7)	91(8)	21(6)	-6(6)	-6(6)
C(42A)	10325(12)	7165(14)	8806(8)	72(4)	57(4)	79(6)	81(10)	-16(6)	14(5)	-1(4)
C(46A)	11527(14)	6834(17)	8366(9)	74(4)	34(6)	93(7)	96(9)	-5(6)	15(6)	-7(5)
C(45A)	11740(10)	6110(12)	8681(7)	77(4)	56(4)	91(7)	80(10)	-11(6)	-3(5)	21(4)
C(41A)	10820(12)	7352(11)	8420(7)	76(4)	50(5)	95(7)	84(7)	18(5)	14(5)	-14(4)
C(61)	12084(12)	10331(8)	4982(5)	111(5)	123(11)	104(5)	92(7)	-36(5)	-28(8)	9(8)
C(62)	11357(11)	10169(10)	5233(7)	117(6)	104(10)	110(10)	121(15)	-59(8)	-25(9)	10(8)
C(63)	11340(7)	9445(11)	5543(5)	101(4)	96(7)	111(10)	96(7)	-41(7)	12(6)	-3(6)
C(64)	12085(9)	8869(8)	5619(5)	102(3)	97(9)	103(6)	102(5)	-30(4)	0(6)	-6(6)
C(65)	12805(7)	9034(7)	5379(4)	83(2)	93(5)	74(4)	80(5)	-24(3)	5(3)	-4(4)
C(66)	12829(6)	9747(9)	5051(3)	91(2)	118(6)	88(6)	66(4)	-23(4)	7(3)	-18(5)
C(61A)	12404(14)	10201(18)	4946(10)	94(5)	85(10)	98(10)	98(7)	-41(7)	13(8)	-7(8)
C(62A)	11568(15)	10449(14)	5064(7)	94(4)	91(10)	113(10)	77(7)	-39(6)	11(7)	-6(8)
C(63A)	11225(15)	9891(18)	5390(8)	93(6)	101(8)	99(16)	77(12)	-43(10)	13(8)	-7(11)
C(64A)	11683(17)	9116(14)	5595(7)	109(7)	111(18)	120(16)	89(7)	-42(10)	-3(13)	-1(11)
C(65A)	12510(16)	8863(13)	5490(9)	111(7)	104(15)	115(10)	103(13)	-27(9)	-11(9)	-5(11)
C(66A)	12793(11)	9436(15)	5175(7)	87(4)						
C(51)	3399(2)	-848(2)	7491(2)	119(1)	110(2)	107(2)	141(3)	18(2)	25(2)	-14(2)
C(52)	3081(2)	-836(2)	7944(1)	112(1)	136(3)	94(2)	102(2)	14(2)	6(2)	-17(2)
C(56)	2809(3)	-832(2)	7052(1)	110(1)	141(3)	95(2)	98(2)	3(2)	31(2)	0(2)

7.2.3 Bond lengths [Å].

Atoms	Bond length	Atoms	Bond length	Atoms	Bond length
P(1)-P(2)	2.1937(5)	K(2)-C(31A)	3.33(2)	Si(21)-C(212)	1.867(3)
P(1)-Si(1)	2.2142(6)	C(31)-C(36)	1.377(11)	Si(22)-C(223)	1.872(2)
P(1)-K(2)	3.1852(6)	C(31)-C(32)	1.382(10)	Si(22)-C(222)	1.8741(18)
P(1)-K(1)	3.2070(6)	C(32)-C(33)	1.377(10)	Si(22)-C(221)	1.877(2)
P(2)-P(3)	2.2599(6)	C(33)-C(34)	1.354(9)	Si(23)-C(231)	1.862(2)
P(2)-P(2)#1	2.2680(8)	C(34)-C(35)	1.363(10)	Si(23)-C(232)	1.864(2)
P(2)-K(1)#1	3.2167(6)	C(35)-C(36)	1.377(11)	Si(23)-C(233)	1.872(2)
P(3)-P(4)	2.1862(5)	C(31A)-C(36A)	1.383(10)	C(43)-C(44)	1.388(15)
P(3)-P(3)#1	2.2648(8)	C(31A)-C(32A)	1.386(10)	C(44)-C(45)	1.356(13)
P(3)-K(2)	3.2307(5)	C(32A)-C(33A)	1.366(10)	C(45)-C(46)	1.361(15)
P(4)-Si(2)	2.2156(6)	C(33A)-C(34A)	1.358(10)	C(43A)-C(44A)	1.373(15)
P(4)-K(1)#1	3.1843(7)	C(34A)-C(35A)	1.361(9)	C(43A)-C(42A)	1.38(2)
P(4)-K(2)#1	3.2120(6)	C(35A)-C(36A)	1.377(10)	C(44A)-C(45A)	1.356(18)
K(1)-P(4)#1	3.1843(7)	C(41)-C(46)	1.353(15)	C(42A)-C(41A)	1.41(2)
K(1)-P(2)#1	3.2167(6)	C(41)-C(42)	1.398(16)	C(46A)-C(41A)	1.34(2)

K(1)-C(43)	3.290(11)	C(42)-C(43)	1.379(17)	C(46A)-C(45A)	1.37(2)
K(1)-C(42)	3.293(19)	Si(1)-Si(12)	2.3341(7)	C(61)-C(62)	1.403(12)
K(1)-C(44A)	3.310(18)	Si(1)-Si(11)	2.3369(7)	C(61)-C(66)	1.404(12)
K(1)-C(41)	3.339(11)	Si(1)-Si(13)	2.3455(6)	C(62)-C(63)	1.354(15)
K(1)-C(43A)	3.345(19)	Si(11)-C(113)	1.868(3)	C(63)-C(64)	1.396(10)
K(1)-C(42A)	3.36(2)	Si(11)-C(112)	1.873(2)	C(64)-C(65)	1.376(11)
K(1)-C(46)	3.380(15)	Si(11)-C(111)	1.881(2)	C(65)-C(66)	1.373(12)
K(1)-C(45)	3.392(15)	Si(12)-C(122)	1.872(3)	C(61A)-C(66A)	1.37(2)
K(1)-C(44)	3.412(14)	Si(12)-C(121)	1.873(2)	C(61A)-C(62A)	1.403(16)
K(2)-P(4)#1	3.2120(6)	Si(12)-C(123)	1.879(3)	C(62A)-C(63A)	1.36(2)
K(2)-C(36)	3.259(17)	Si(13)-C(133)	1.867(2)	C(63A)-C(64A)	1.398(17)
K(2)-C(35A)	3.269(12)	Si(13)-C(131)	1.867(2)	C(64A)-C(65A)	1.377(14)
K(2)-C(32A)	3.275(13)	Si(13)-C(132)	1.869(2)	C(65A)-C(66A)	1.31(2)
K(2)-C(36A)	3.288(15)	Si(2)-Si(21)	2.3333(7)	C(51)-C(56)	1.364(4)
K(2)-C(35)	3.290(15)	Si(2)-Si(22)	2.3353(6)	C(51)-C(52)	1.382(4)
K(2)-C(31)	3.30(2)	Si(2)-Si(23)	2.3483(6)	C(52)-C(56)#2	1.349(4)
K(2)-C(34)	3.309(13)	Si(21)-C(211)	1.858(2)	C(56)-C(52)#2	1.349(4)
K(2)-C(34A)	3.326(15)	Si(21)-C(213)	1.860(3)		

7.2.4 Bond angles [deg].

Atoms	Angle	Atoms	Angle
P(2)-P(1)-Si(1)	105.35(2)	Si(2)-P(4)-K(1)#1	123.11(2)
P(2)-P(1)-K(2)	98.478(19)	P(3)-P(4)-K(2)#1	96.212(19)
Si(1)-P(1)-K(2)	125.34(2)	Si(2)-P(4)-K(2)#1	123.29(2)
P(2)-P(1)-K(1)	95.206(19)	K(1)#1-P(4)-K(2)#1	105.629(16)
Si(1)-P(1)-K(1)	119.82(2)	P(4)#1-K(1)-P(1)	70.416(14)
K(2)-P(1)-K(1)	105.726(17)	P(4)#1-K(1)-P(2)#1	66.364(13)
P(1)-P(2)-P(3)	100.63(2)	P(1)-K(1)-P(2)#1	66.348(12)
P(1)-P(2)-P(2)#1	103.95(3)	P(4)#1-K(1)-C(43)	122.3(2)
P(3)-P(2)-P(2)#1	88.793(14)	P(1)-K(1)-C(43)	128.9(3)
P(1)-P(2)-K(1)#1	157.73(2)	P(2)#1-K(1)-C(43)	163.3(2)
P(3)-P(2)-K(1)#1	93.398(17)	P(4)#1-K(1)-C(42)	145.1(3)
P(2)#1-P(2)-K(1)#1	93.47(2)	P(1)-K(1)-C(42)	119.1(3)
P(4)-P(3)-P(2)	103.98(2)	P(2)#1-K(1)-C(42)	148.3(3)
P(4)-P(3)-P(3)#1	103.27(3)	C(43)-K(1)-C(42)	24.2(3)
P(2)-P(3)-P(3)#1	88.873(14)	P(4)#1-K(1)-C(44A)	116.2(2)
P(4)-P(3)-K(2)	153.74(2)	P(1)-K(1)-C(44A)	158.7(3)
P(2)-P(3)-K(2)	95.790(17)	P(2)#1-K(1)-C(44A)	134.9(4)
P(3)#1-P(3)-K(2)	94.11(2)	C(43)-K(1)-C(44A)	29.9(3)
P(3)-P(4)-Si(2)	105.11(2)	C(42)-K(1)-C(44A)	43.4(3)
P(3)-P(4)-K(1)#1	95.755(19)	P(4)#1-K(1)-C(41)	161.53(18)
C(43)-K(1)-C(41)	42.7(3)	P(1)-K(1)-C(41)	126.2(2)
C(42)-K(1)-C(41)	24.3(3)	P(2)#1-K(1)-C(41)	125.1(2)
C(44A)-K(1)-C(41)	45.3(3)	P(4)#1-K(1)-C(45)	122.0(3)
P(4)#1-K(1)-C(43A)	128.2(4)	P(1)-K(1)-C(45)	166.3(2)
P(1)-K(1)-C(43A)	161.3(4)	P(2)#1-K(1)-C(45)	122.2(3)
P(2)#1-K(1)-C(43A)	116.2(3)	C(43)-K(1)-C(45)	41.4(2)
C(43)-K(1)-C(43A)	47.1(4)	C(42)-K(1)-C(45)	47.7(3)
C(42)-K(1)-C(43A)	48.3(4)	C(44A)-K(1)-C(45)	14.8(3)
C(44A)-K(1)-C(43A)	23.8(3)	C(41)-K(1)-C(45)	40.7(3)
C(41)-K(1)-C(43A)	36.0(4)	C(43A)-K(1)-C(45)	9.5(3)
P(4)#1-K(1)-C(42A)	151.4(4)	C(42A)-K(1)-C(45)	31.3(4)
P(1)-K(1)-C(42A)	137.5(4)	C(46)-K(1)-C(45)	23.2(3)
P(2)#1-K(1)-C(42A)	114.3(3)	P(4)#1-K(1)-C(44)	113.5(2)
C(43)-K(1)-C(42A)	50.6(4)	P(1)-K(1)-C(44)	151.3(3)
C(42)-K(1)-C(42A)	38.5(5)	P(2)#1-K(1)-C(44)	142.2(3)
C(44A)-K(1)-C(42A)	41.3(3)	C(43)-K(1)-C(44)	23.8(2)
C(41)-K(1)-C(42A)	16.6(4)	C(42)-K(1)-C(44)	41.4(3)
C(43A)-K(1)-C(42A)	23.7(3)	C(44A)-K(1)-C(44)	8.2(5)

Atoms	Angle	Atoms	Angle
P(4)#1-K(1)-C(46)	142.9(4)	C(41)-K(1)-C(44)	48.2(3)
P(1)-K(1)-C(46)	146.2(4)	C(43A)-K(1)-C(44)	31.7(4)
P(2)#1-K(1)-C(46)	114.8(2)	C(42A)-K(1)-C(44)	47.0(4)
C(43)-K(1)-C(46)	49.1(3)	C(46)-K(1)-C(44)	41.1(3)
C(42)-K(1)-C(46)	41.7(3)	C(45)-K(1)-C(44)	23.0(2)
C(44A)-K(1)-C(46)	34.6(3)	P(1)-K(2)-P(4)#1	70.341(13)
C(41)-K(1)-C(46)	23.2(3)	P(1)-K(2)-P(3)	64.578(12)
C(43A)-K(1)-C(46)	15.1(3)	P(4)#1-K(2)-P(3)	65.602(12)
C(42A)-K(1)-C(46)	8.7(4)	P(1)-K(2)-C(36)	156.1(3)
C(36)-K(2)-C(35A)	32.6(3)	P(4)#1-K(2)-C(36)	116.0(2)
P(1)-K(2)-C(32A)	118.2(2)	P(3)-K(2)-C(36)	139.3(3)
P(4)#1-K(2)-C(32A)	127.8(2)	P(1)-K(2)-C(35A)	147.4(4)
P(3)-K(2)-C(32A)	166.6(2)	P(4)#1-K(2)-C(35A)	142.2(4)
C(36)-K(2)-C(32A)	38.7(4)	P(3)-K(2)-C(35A)	120.61(19)
C(35A)-K(2)-C(32A)	49.3(2)	C(36)-K(2)-C(31)	24.2(2)
P(1)-K(2)-C(36A)	160.7(2)	C(35A)-K(2)-C(31)	46.8(3)
P(4)#1-K(2)-C(36A)	121.6(3)	C(32A)-K(2)-C(31)	18.1(4)
P(3)-K(2)-C(36A)	132.8(3)	C(36A)-K(2)-C(31)	31.1(4)
C(36)-K(2)-C(36A)	9.1(3)	C(35)-K(2)-C(31)	42.4(3)
C(35A)-K(2)-C(36A)	24.23(18)	P(1)-K(2)-C(34)	132.9(2)
C(32A)-K(2)-C(36A)	42.7(3)	P(4)#1-K(2)-C(34)	156.6(2)
P(1)-K(2)-C(35)	156.7(3)	P(3)-K(2)-C(34)	121.9(2)
P(4)#1-K(2)-C(35)	132.8(3)	C(36)-K(2)-C(34)	42.6(3)
P(3)-K(2)-C(35)	123.1(2)	C(35A)-K(2)-C(34)	14.6(2)
C(36)-K(2)-C(35)	24.3(2)	C(32A)-K(2)-C(34)	45.7(3)
C(35A)-K(2)-C(35)	9.9(3)	C(36A)-K(2)-C(34)	35.7(3)
C(32A)-K(2)-C(35)	48.9(3)	C(35)-K(2)-C(34)	23.84(19)
C(36A)-K(2)-C(35)	15.3(3)	C(31)-K(2)-C(34)	49.4(3)
P(1)-K(2)-C(31)	131.9(3)	P(1)-K(2)-C(34A)	124.4(3)
P(4)#1-K(2)-C(31)	116.6(2)	P(4)#1-K(2)-C(34A)	163.7(3)
P(3)-K(2)-C(31)	163.6(3)	P(3)-K(2)-C(34A)	124.9(2)
C(36)-K(2)-C(34A)	47.7(3)	C(113)-Si(11)-C(112)	107.66(14)
C(35A)-K(2)-C(34A)	23.79(18)	C(113)-Si(11)-C(111)	108.42(12)
C(32A)-K(2)-C(34A)	42.0(3)	C(112)-Si(11)-C(111)	107.72(12)
C(36A)-K(2)-C(34A)	42.2(3)	C(113)-Si(11)-Si(1)	108.85(8)
C(35)-K(2)-C(34A)	32.3(3)	C(112)-Si(11)-Si(1)	113.44(9)
C(31)-K(2)-C(34A)	49.5(4)	C(111)-Si(11)-Si(1)	110.60(8)
C(34)-K(2)-C(34A)	9.5(2)	C(122)-Si(12)-C(121)	107.49(12)
P(1)-K(2)-C(31A)	139.3(3)	C(122)-Si(12)-C(123)	108.31(14)
P(4)#1-K(2)-C(31A)	116.2(2)	C(121)-Si(12)-C(123)	108.21(11)
P(3)-K(2)-C(31A)	156.1(3)	C(122)-Si(12)-Si(1)	110.12(8)
C(36)-K(2)-C(31A)	16.8(3)	C(121)-Si(12)-Si(1)	109.77(7)
C(35A)-K(2)-C(31A)	42.2(3)	C(123)-Si(12)-Si(1)	112.80(10)
C(32A)-K(2)-C(31A)	24.2(2)	C(133)-Si(13)-C(131)	107.51(12)
C(36A)-K(2)-C(31A)	24.1(2)	C(133)-Si(13)-C(132)	106.75(12)
C(35)-K(2)-C(31A)	36.6(3)	C(131)-Si(13)-C(132)	109.09(14)
C(31)-K(2)-C(31A)	7.5(4)	C(133)-Si(13)-Si(1)	110.61(6)
C(34)-K(2)-C(31A)	47.1(3)	C(131)-Si(13)-Si(1)	109.65(7)
C(34A)-K(2)-C(31A)	48.7(3)	C(132)-Si(13)-Si(1)	113.04(9)
P(1)-Si(1)-Si(12)	114.78(3)	C(36)-C(31)-C(32)	119.2(10)
P(1)-Si(1)-Si(11)	114.51(3)	C(36)-C(31)-K(2)	76.1(11)
Si(12)-Si(1)-Si(11)	110.37(3)	C(32)-C(31)-K(2)	83.6(10)
P(1)-Si(1)-Si(13)	99.75(2)	C(33)-C(32)-C(31)	118.7(9)
Si(12)-Si(1)-Si(13)	108.84(2)	C(33)-C(32)-K(2)	75.2(9)
Si(11)-Si(1)-Si(13)	107.74(2)	C(31)-C(32)-K(2)	72.8(10)
P(4)-Si(2)-Si(21)	115.34(2)	C(34)-C(33)-C(32)	122.0(8)
P(4)-Si(2)-Si(22)	114.99(3)	C(34)-C(33)-K(2)	76.2(8)
Si(21)-Si(2)-Si(22)	109.47(2)	C(32)-C(33)-K(2)	81.5(9)
P(4)-Si(2)-Si(23)	99.01(2)	C(33)-C(34)-C(35)	118.7(9)
Si(21)-Si(2)-Si(23)	108.51(2)	C(33)-C(34)-K(2)	80.3(8)
Si(22)-Si(2)-Si(23)	108.71(2)	C(35)-C(34)-K(2)	77.3(8)

Atoms	Angle	Atoms	Angle
C(211)-Si(21)-C(213)	107.38(14)	C(34)-C(35)-C(36)	120.8(10)
C(211)-Si(21)-C(212)	107.74(14)	C(34)-C(35)-K(2)	78.8(8)
C(213)-Si(21)-C(212)	107.28(19)	C(36)-C(35)-K(2)	76.6(10)
C(211)-Si(21)-Si(2)	110.92(8)	C(35)-C(36)-C(31)	119.9(10)
C(213)-Si(21)-Si(2)	109.70(10)	C(35)-C(36)-K(2)	79.1(9)
C(212)-Si(21)-Si(2)	113.57(9)	C(31)-C(36)-K(2)	79.7(11)
C(223)-Si(22)-C(222)	107.90(10)	C(36A)-C(31A)-C(32A)	119.5(9)
C(223)-Si(22)-C(221)	108.38(13)	C(36A)-C(31A)-K(2)	76.4(10)
C(222)-Si(22)-C(221)	108.50(10)	C(32A)-C(31A)-K(2)	75.8(9)
C(223)-Si(22)-Si(2)	108.47(7)	C(33A)-C(32A)-C(31A)	119.8(9)
C(222)-Si(22)-Si(2)	111.18(6)	C(33A)-C(32A)-K(2)	80.3(8)
C(221)-Si(22)-Si(2)	112.29(8)	C(41)-C(42)-K(1)	79.7(8)
C(231)-Si(23)-C(232)	108.89(12)	C(42)-C(43)-C(44)	118.3(11)
C(231)-Si(23)-C(233)	107.90(12)	C(42)-C(43)-K(1)	78.1(8)
C(232)-Si(23)-C(233)	106.18(12)	C(44)-C(43)-K(1)	83.0(7)
C(231)-Si(23)-Si(2)	112.92(7)	C(45)-C(44)-C(43)	119.0(10)
C(232)-Si(23)-Si(2)	109.71(7)	C(45)-C(44)-K(1)	77.7(8)
C(233)-Si(23)-Si(2)	111.00(7)	C(43)-C(44)-K(1)	73.2(7)
C(31A)-C(32A)-K(2)	80.0(9)	C(44)-C(45)-C(46)	122.9(12)
C(34A)-C(33A)-C(32A)	120.4(10)	C(44)-C(45)-K(1)	79.3(9)
C(34A)-C(33A)-K(2)	78.0(9)	C(46)-C(45)-K(1)	77.9(8)
C(32A)-C(33A)-K(2)	75.8(8)	C(41)-C(46)-C(45)	119.1(11)
C(33A)-C(34A)-C(35A)	120.0(11)	C(41)-C(46)-K(1)	76.7(8)
C(33A)-C(34A)-K(2)	78.4(9)	C(45)-C(46)-K(1)	78.9(9)
C(35A)-C(34A)-K(2)	75.8(8)	C(44A)-C(43A)-C(42A)	117.5(15)
C(34A)-C(35A)-C(36A)	121.1(9)	C(44A)-C(43A)-K(1)	76.7(11)
C(34A)-C(35A)-K(2)	80.4(8)	C(42A)-C(43A)-K(1)	78.9(12)
C(36A)-C(35A)-K(2)	78.7(8)	C(45A)-C(44A)-C(43A)	120.6(9)
C(35A)-C(36A)-C(31A)	118.7(9)	C(45A)-C(44A)-K(1)	84.6(11)
C(35A)-C(36A)-K(2)	77.1(8)	C(43A)-C(44A)-K(1)	79.5(11)
C(31A)-C(36A)-K(2)	79.5(10)	C(43A)-C(42A)-C(41A)	120.5(15)
C(46)-C(41)-C(42)	119.5(7)	C(43A)-C(42A)-K(1)	77.3(12)
C(46)-C(41)-K(1)	80.1(8)	C(41A)-C(42A)-K(1)	81.6(11)
C(42)-C(41)-K(1)	76.0(9)	C(41A)-C(46A)-C(45A)	119.0(15)
C(43)-C(42)-C(41)	120.9(11)	C(41A)-C(46A)-K(1)	76.0(14)
C(43)-C(42)-K(1)	77.8(8)	C(45A)-C(46A)-K(1)	76.1(11)
C(46A)-C(45A)-K(1)	81.3(11)	C(44A)-C(45A)-C(46A)	121.8(13)
C(46A)-C(41A)-C(42A)	120.1(11)	C(44A)-C(45A)-K(1)	72.4(10)
C(46A)-C(41A)-K(1)	81.9(15)	C(63A)-C(62A)-C(61A)	116(2)
C(42A)-C(41A)-K(1)	74.7(11)	C(62A)-C(63A)-C(64A)	122(2)
C(62)-C(61)-C(66)	120.6(10)	C(65A)-C(64A)-C(63A)	123.2(18)
C(63)-C(62)-C(61)	121.6(12)	C(66A)-C(65A)-C(64A)	111.2(16)
C(62)-C(63)-C(64)	118.0(14)	C(65A)-C(66A)-C(61A)	130.9(15)
C(65)-C(64)-C(63)	120.5(13)	C(56)-C(51)-C(52)	119.6(3)
C(66)-C(65)-C(64)	122.8(10)	C(56)#2-C(52)-C(51)	119.9(3)
C(65)-C(66)-C(61)	116.4(9)	C(52)#2-C(56)-C(51)	120.4(3)
C(66A)-C(61A)-C(62A)	116.6(18)		

Symmetry transformations used to generate equivalent atoms:
#1 -x+3/2,y,-z+3/2   #2 -x+1/2,y,-z+3/2

7.3 Crystallographic data for Hyp$_3$P$_5$K$_2$·2C$_6$H$_6$

7.3.1 Crystal data and structure refinement

Empirical formula	Hyp$_3$P$_3$K$_2$·1.5benzene
Formula weight	1093.21
Temperature	193(2) K

Wavelength	0.71073 Å
Crystal system, space group	triclinic; $P\bar{1}$
Unit cell dimensions	a = 14.7289(14) Å alpha = 97.292(7)deg.
	b = 17.2007(15) Å beta = 93.032(7)deg.
	c = 27.467(2) Å gamma=105.980(7) deg.
Volume	6607.5(10) Å^3
Z, Calculated density	4, 1.099 g/cm^3
Absorption coefficient	0.505 mm^{-1}
F(000)	2348
Theta range for data collection	1.36 to 26.37 deg.
Limiting indices	-18<=h<=18, -21<=k<=21, -31<=l<=34
Reflections collected / unique	63967 / 26523 [R(int) = 0.0813]
Completeness to theta = 26.37	98.2 %
Refinement method	Full-matrix least-squares on F^2
Data / restraints / parameters	26523 / 352 / 1155
Goodness-of-fit on F^2	0.904
Final R indices [I>2sigma(I)]	R1 = 0.0573, wR2 = 0.1314
R indices (all data)	R1 = 0.1050, wR2 = 0.1455
Largest diff. peak and hole	0.638 and -0.504 e.Å^{-3}

7.3.2 Atomic coordinates (x 10^4), equivalent isotropic displacement parameters (Å^2 x 10^3) and Anisotropic displacement parameters (Å^2 x 10^3). U(eq) is defined as one third of the trace of the orthogonalized Uij tensor. The anisotropic displacement factor exponent takes the form: $-2\pi^2[h^2a^{*2}U11 + ... + 2hka^*b^*U12]$

Atom	x	y	z	U(eq)	U11	U22	U33	U23	U13	U12
P(1)	4173(1)	6134(1)	280(1)	38(1)	36(1)	36(1)	42(1)	8(1)	8(1)	8(1)
P(2)	4810(1)	6362(1)	-915(1)	43(1)	44(1)	46(1)	40(1)	10(1)	5(1)	13(1)
P(3)	6575(1)	7157(1)	205(1)	42(1)	34(1)	37(1)	53(1)	6(1)	4(1)	6(1)
P(4)	5218(1)	7367(1)	345(1)	39(1)	35(1)	36(1)	43(1)	4(1)	4(1)	7(1)
P(5)	4155(1)	6902(1)	-321(1)	40(1)	38(1)	42(1)	41(1)	7(1)	2(1)	11(1)
K(1)	6064(1)	5440(1)	625(1)	56(1)	64(1)	42(1)	63(1)	11(1)	9(1)	15(1)
K(2)	6982(1)	7291(1)	-932(1)	61(1)	57(1)	54(1)	65(1)	11(1)	11(1)	4(1)
C(21)	8196(6)	7214(6)	-1981(3)	111(2)	105(6)	131(7)	72(5)	11(5)	5(4)	-3(5)
C(22)	8424(7)	8000(6)	-1793(3)	118(3)	123(7)	117(7)	119(7)	53(6)	44(5)	18(5)
C(23)	9265(8)	8353(6)	-1535(4)	141(4)	103(7)	107(6)	179(9)	-16(6)	53(7)	-15(6)
C(24)	9872(7)	7922(9)	-1453(4)	172(5)	70(5)	192(11)	210(12)	-75(9)	7(6)	12(7)
C(25)	9677(8)	7142(8)	-1652(4)	140(3)	111(7)	161(9)	165(9)	28(8)	42(7)	61(7)
C(26)	8813(8)	6764(6)	-1931(4)	130(3)	140(8)	102(6)	126(7)	1(5)	50(6)	-3(6)
Si(1)	3116(1)	6385(1)	807(1)	41(1)	37(1)	37(1)	48(1)	8(1)	9(1)	8(1)
Si(11)	1904(1)	5152(1)	745(1)	54(1)	41(1)	44(1)	72(1)	9(1)	12(1)	1(1)
C(111)	2433(4)	4353(3)	950(2)	64(1)	64(3)	44(2)	78(3)	8(2)	21(3)	5(2)
C(112)	1360(4)	4755(4)	95(2)	89(2)	78(4)	79(4)	88(4)	5(3)	-11(3)	-7(3)
C(113)	931(4)	5250(3)	1138(3)	85(2)	49(3)	71(4)	134(5)	26(3)	30(3)	5(3)
Si(12)	3918(1)	6617(1)	1601(1)	48(1)	53(1)	46(1)	43(1)	8(1)	11(1)	13(1)
C(121)	4938(3)	6154(3)	1555(2)	60(1)	69(3)	62(3)	50(3)	9(2)	-3(2)	22(2)
C(122)	4410(4)	7735(3)	1824(2)	63(1)	67(3)	58(3)	61(3)	4(2)	9(2)	17(2)
C(123)	3149(4)	6149(3)	2068(2)	76(2)	90(4)	73(3)	53(3)	11(3)	22(3)	3(3)
Si(13)	2447(1)	7442(1)	680(1)	50(1)	44(1)	48(1)	62(1)	11(1)	10(1)	18(1)
C(131)	3336(3)	8411(3)	583(2)	60(1)	66(3)	48(3)	73(3)	11(2)	19(2)	23(2)
C(132)	1539(4)	7098(3)	138(2)	70(1)	54(3)	77(3)	83(4)	10(3)	0(3)	25(3)

Atom	x	y	z	U(eq)	U11	U22	U33	U23	U13	U12
C(133)	1843(4)	7661(3)	1243(2)	68(1)	60(3)	73(3)	81(4)	16(3)	17(3)	30(3)
Si(2)	3892(1)	6569(1)	-1537(1)	44(1)	48(1)	43(1)	41(1)	5(1)	1(1)	12(1)
Si(21)	2446(1)	5540(1)	-1696(1)	62(1)	45(1)	61(1)	70(1)	-7(1)	-6(1)	8(1)
C(211)	2665(4)	4542(3)	-1941(3)	85(2)	70(4)	54(3)	115(5)	-13(3)	-2(3)	3(3)
C(212)	1882(4)	5398(4)	-1104(2)	94(2)	61(3)	99(5)	102(5)	3(4)	10(3)	-6(3)
C(213)	1575(4)	5771(4)	-2148(3)	99(2)	78(4)	104(5)	102(5)	-28(4)	-41(4)	32(4)
Si(22)	3608(1)	7855(1)	-1456(1)	57(1)	73(1)	53(1)	51(1)	5(1)	-3(1)	29(1)
C(221)	2594(5)	7891(4)	-1081(2)	89(2)	103(5)	98(4)	84(4)	6(3)	10(3)	65(4)
C(222)	3303(5)	8122(3)	-2080(2)	83(2)	120(5)	74(4)	66(4)	15(3)	-12(3)	47(4)
C(223)	4681(4)	8650(3)	-1148(2)	77(2)	98(4)	55(3)	68(4)	3(3)	-10(3)	9(3)
Si(23)	4773(1)	6505(1)	-2219(1)	57(1)	75(1)	54(1)	47(1)	14(1)	14(1)	24(1)
C(231)	5410(4)	5700(3)	-2198(2)	63(1)	75(3)	60(3)	60(3)	16(2)	23(2)	25(3)
C(232)	5691(4)	7502(3)	-2218(2)	83(2)	96(4)	72(4)	97(4)	34(3)	39(3)	32(3)
C(233)	4010(5)	6267(4)	-2822(2)	87(2)	127(5)	93(4)	51(3)	11(3)	8(3)	52(4)
Si(3)	7502(1)	8402(1)	532(1)	40(1)	35(1)	39(1)	45(1)	7(1)	2(1)	5(1)
Si(31)	7404(1)	8862(1)	1367(1)	53(1)	49(1)	58(1)	44(1)	5(1)	0(1)	5(1)
C(311)	6465(4)	9400(3)	1444(2)	69(1)	75(3)	73(3)	56(3)	0(2)	8(2)	22(3)
C(312)	8550(4)	9596(4)	1661(2)	86(2)	64(3)	110(5)	55(3)	-11(3)	-5(3)	-14(3)
C(313)	7128(4)	7988(4)	1726(2)	81(2)	82(4)	100(4)	65(4)	36(3)	13(3)	21(3)
Si(32)	9005(1)	8188(1)	488(1)	54(1)	36(1)	57(1)	66(1)	10(1)	1(1)	8(1)
C(321)	9104(4)	7405(4)	888(2)	82(2)	58(3)	102(4)	101(5)	37(4)	3(3)	39(3)
C(322)	10038(4)	9119(4)	677(2)	86(2)	53(3)	80(4)	107(5)	-5(3)	13(3)	-4(3)
C(323)	9138(4)	7782(4)	-159(2)	79(2)	57(3)	96(4)	87(4)	1(3)	8(3)	31(3)
Si(33)	7359(1)	9468(1)	102(1)	47(1)	51(1)	38(1)	51(1)	9(1)	5(1)	8(1)
C(331)	7524(4)	9273(3)	-574(2)	61(1)	77(3)	53(3)	54(3)	9(2)	5(2)	18(2)
C(332)	8289(4)	10439(3)	370(2)	66(1)	71(3)	42(2)	75(3)	5(2)	5(3)	5(2)
C(333)	6150(3)	9635(3)	137(2)	62(1)	61(3)	64(3)	71(3)	26(2)	10(2)	24(2)
P(8)	-49(1)	8131(1)	-5886(1)	44(1)	42(1)	50(1)	38(1)	1(1)	2(1)	14(1)
P(7)	-1530(1)	8015(1)	-4828(1)	45(1)	38(1)	40(1)	56(1)	10(1)	6(1)	7(1)
P(6)	932(1)	9010(1)	-4668(1)	40(1)	39(1)	37(1)	41(1)	4(1)	-2(1)	8(1)
P(9)	755(1)	7925(1)	-5249(1)	41(1)	39(1)	43(1)	40(1)	3(1)	4(1)	12(1)
P(10)	-159(1)	7840(1)	-4619(1)	41(1)	40(1)	40(1)	43(1)	9(1)	5(1)	8(1)
K(3)	798(1)	10088(1)	-5636(1)	59(1)	64(1)	46(1)	68(1)	4(1)	7(1)	18(1)
K(4)	-2308(1)	7375(1)	-5969(1)	63(1)	55(1)	61(1)	63(1)	5(1)	-4(1)	2(1)
C(41A)	-3960(19)	6076(14)	-6843(9)	82(6)	93(14)	73(13)	68(13)	-9(9)	-11(9)	17(11)
C(42A)	-3841(12)	6797(18)	-7046(8)	76(6)	65(8)	77(15)	73(9)	2(10)	-13(6)	5(9)
C(43A)	-4399(18)	7308(13)	-6948(10)	90(7)	76(14)	101(10)	82(12)	4(10)	-25(10)	19(9)
C(44A)	-5142(17)	7070(16)	-6673(11)	99(6)	78(12)	122(14)	100(11)	8(11)	5(10)	40(10)
C(45A)	-5298(15)	6360(20)	-6467(9)	93(6)	72(9)	111(16)	86(10)	-1(12)	19(8)	14(10)
C(46A)	-4700(20)	5887(11)	-6551(9)	82(6)	75(15)	81(9)	76(13)	3(9)	6(10)	5(10)
C(41B)	-4260(20)	5857(15)	-6678(12)	80(7)	67(14)	79(11)	82(16)	-13(10)	17(10)	10(11)
C(42B)	-3834(16)	6450(20)	-6966(10)	76(8)	68(9)	80(20)	64(14)	-28(13)	1(9)	18(14)
C(43B)	-4090(20)	7149(19)	-6986(12)	88(9)	80(17)	94(16)	74(11)	5(12)	-5(13)	4(13)
C(44B)	-4820(30)	7265(17)	-6723(14)	101(8)	82(18)	114(13)	106(15)	8(13)	-15(14)	36(13)
C(45B)	-5250(20)	6710(20)	-6433(12)	98(8)	88(12)	115(18)	91(13)	-13(14)	1(11)	42(12)
C(46B)	-4990(20)	5999(16)	-6423(10)	80(6)	74(14)	87(12)	79(12)	3(10)	24(10)	23(9)
Si(6)	2119(1)	8936(1)	-4125(1)	42(1)	39(1)	42(1)	43(1)	3(1)	-3(1)	10(1)
Si(61)	3382(1)	10038(1)	-4257(1)	58(1)	45(1)	60(1)	59(1)	12(1)	-5(1)	-3(1)
C(611)	3026(4)	10997(3)	-4072(2)	76(2)	77(4)	51(3)	88(4)	12(3)	-9(3)	-1(3)
C(612)	4529(4)	10115(4)	-3895(2)	85(2)	45(3)	90(4)	108(5)	28(3)	-13(3)	-5(3)
C(613)	3584(5)	10000(4)	-4923(2)	93(2)	88(4)	106(5)	76(4)	24(3)	21(3)	3(4)
Si(62)	1719(1)	9265(1)	-3323(1)	54(1)	56(1)	59(1)	44(1)	2(1)	1(1)	16(1)
C(621)	1151(4)	8342(4)	-3037(2)	75(2)	70(3)	90(4)	66(3)	26(3)	13(3)	20(3)
C(622)	2813(4)	9879(4)	-2909(2)	83(2)	86(4)	89(4)	51(3)	-8(3)	-6(3)	-1(3)
C(623)	851(5)	9893(4)	-3338(2)	89(2)	108(5)	100(5)	76(4)	10(3)	21(3)	57(4)
Si(63)	2590(1)	7729(1)	-4162(1)	55(1)	56(1)	55(1)	58(1)	8(1)	-1(1)	25(1)
C(631)	3223(5)	7557(4)	-4714(2)	89(2)	102(5)	118(5)	64(4)	5(3)	2(3)	68(4)
C(632)	3446(4)	7880(4)	-3604(2)	75(2)	79(4)	90(4)	65(3)	16(3)	-5(3)	43(3)
C(633)	1602(4)	6777(3)	-4148(3)	89(2)	77(4)	52(3)	137(6)	17(3)	-8(4)	17(3)
Si(7)	-2369(1)	6967(1)	-4482(1)	45(1)	39(1)	41(1)	51(1)	6(1)	9(1)	3(1)
Si(71)	-1951(1)	6976(1)	-3642(1)	60(1)	55(1)	67(1)	49(1)	7(1)	9(1)	3(1)

Atom	x	y	z	U(eq)	U11	U22	U33	U23	U13	U12
C(711)	-2996(4)	6400(5)	-3338(2)	101(2)	74(4)	148(6)	62(4)	25(4)	13(3)	-5(4)
C(712)	-999(4)	6473(3)	-3547(2)	79(2)	87(4)	77(4)	66(4)	20(3)	-2(3)	10(3)
C(713)	-1553(4)	8048(4)	-3321(2)	87(2)	81(4)	93(4)	76(4)	-23(3)	-7(3)	23(3)
Si(72)	-3900(1)	7128(1)	-4529(1)	55(1)	41(1)	54(1)	67(1)	7(1)	12(1)	6(1)
C(721)	-4826(4)	6224(3)	-4382(2)	81(2)	45(3)	77(4)	110(5)	24(3)	7(3)	-3(3)
C(722)	-3938(4)	8037(4)	-4094(3)	89(2)	66(4)	83(4)	108(5)	-16(3)	9(3)	19(3)
C(723)	-4251(4)	7292(4)	-5167(2)	83(2)	65(3)	107(5)	87(4)	30(3)	9(3)	36(3)
Si(73)	-2379(1)	5681(1)	-4895(1)	53(1)	53(1)	40(1)	59(1)	6(1)	9(1)	4(1)
C(731)	-3043(4)	4837(3)	-4565(2)	71(1)	66(3)	49(3)	92(4)	15(3)	11(3)	2(2)
C(732)	-2959(4)	5482(3)	-5553(2)	75(2)	90(4)	57(3)	65(3)	0(2)	-3(3)	6(3)
C(733)	-1139(4)	5624(3)	-4948(2)	67(1)	64(3)	50(3)	84(4)	-1(2)	15(3)	12(2)
Si(8)	716(1)	7600(1)	-6468(1)	42(1)	45(1)	42(1)	37(1)	3(1)	6(1)	10(1)
Si(81)	500(1)	6198(1)	-6473(1)	62(1)	84(1)	43(1)	58(1)	5(1)	22(1)	16(1)
C(811)	1107(5)	5740(4)	-6969(2)	95(2)	146(6)	71(4)	86(4)	15(3)	50(4)	53(4)
C(812)	949(5)	5969(3)	-5870(2)	84(2)	127(5)	59(3)	77(4)	21(3)	23(4)	37(3)
C(813)	-801(5)	5663(3)	-6569(2)	96(2)	110(5)	57(3)	95(5)	3(3)	26(4)	-16(3)
Si(82)	-35(1)	7747(1)	-7212(1)	56(1)	53(1)	69(1)	41(1)	10(1)	3(1)	11(1)
C(821)	-1325(3)	7609(4)	-7136(2)	78(2)	50(3)	117(5)	57(3)	13(3)	-5(2)	10(3)
C(822)	65(4)	6972(4)	-7737(2)	81(2)	87(4)	100(4)	44(3)	0(3)	6(3)	14(3)
C(823)	469(4)	8788(3)	-7396(2)	76(2)	78(4)	80(4)	79(4)	34(3)	10(3)	28(3)
Si(83)	2327(1)	8295(1)	-6471(1)	51(1)	44(1)	55(1)	52(1)	7(1)	10(1)	11(1)
C(831)	2786(4)	8145(3)	-7090(2)	73(1)	68(3)	79(4)	71(4)	5(3)	25(3)	21(3)
C(832)	2511(4)	9418(3)	-6273(2)	68(1)	55(3)	61(3)	77(4)	0(3)	10(2)	3(2)
C(833)	3060(4)	7946(4)	-6008(2)	79(2)	52(3)	105(4)	86(4)	32(3)	8(3)	22(3)
C(31A)	7374(13)	9828(18)	-2133(12)	70(6)	73(8)	72(14)	63(17)	18(13)	27(12)	12(8)
C(32A)	7040(20)	9500(16)	-2608(12)	77(7)	91(17)	62(11)	71(17)	12(12)	25(13)	6(13)
C(33A)	6130(20)	9474(18)	-2780(8)	75(7)	79(17)	76(10)	70(11)	15(9)	12(12)	18(12)
C(34A)	5575(14)	9790(18)	-2454(11)	79(7)	83(10)	78(15)	78(18)	16(13)	13(12)	24(9)
C(35A)	5940(20)	10124(14)	-1970(10)	69(5)	101(15)	50(10)	56(13)	6(9)	7(10)	25(11)
C(36A)	6840(30)	10107(19)	-1806(8)	73(6)	109(17)	54(9)	57(10)	1(7)	25(11)	24(13)
C(31B)	7266(16)	9951(13)	-1935(8)	82(5)	96(11)	71(9)	67(12)	-6(9)	32(9)	8(8)
C(32B)	7373(13)	9590(12)	-2391(10)	81(5)	96(10)	74(10)	64(14)	13(10)	24(10)	5(8)
C(33B)	6620(20)	9367(12)	-2749(6)	80(6)	105(17)	60(8)	64(9)	9(6)	13(11)	7(11)
C(34B)	5777(17)	9553(14)	-2648(9)	89(7)	101(14)	72(11)	86(16)	24(11)	1(11)	10(11)
C(35B)	5706(13)	9950(12)	-2182(12)	90(6)	105(11)	67(10)	87(17)	-2(12)	16(12)	10(8)
C(36B)	6460(20)	10152(16)	-1827(8)	89(6)	111(16)	78(9)	77(11)	5(8)	19(11)	26(14)

7.3.3 Bond lengths [Å].

Atoms	Bond length	Atoms	Bond length	Atoms	Bond length
P(1)-P(4)	2.2303(14)	Si(3)-Si(31)	2.3544(17)	Si(33)-C(331)	1.887(5)
P(1)-P(5)	2.2442(14)	P(8)-P(9)	2.1819(14)	Si(63)-C(633)	1.873(6)
P(1)-Si(1)	2.2708(15)	P(8)-Si(8)	2.2448(16)	Si(63)-C(632)	1.875(5)
P(2)-P(5)	2.1757(15)	P(7)-P(10)	2.1814(14)	Si(7)-Si(72)	2.3454(17)
P(2)-Si(2)	2.2477(15)	P(7)-Si(7)	2.2404(16)	Si(7)-Si(73)	2.3503(17)
P(3)-P(4)	2.1724(14)	P(6)-P(10)	2.2273(15)	Si(7)-Si(71)	2.3517(18)
P(3)-Si(3)	2.2431(15)	P(6)-P(9)	2.2437(14)	Si(71)-C(713)	1.861(6)
P(4)-P(5)	2.2515(14)	P(6)-Si(6)	2.2770(14)	Si(71)-C(712)	1.862(6)
C(21)-C(22)	1.328(11)	P(9)-P(10)	2.2426(15)	Si(71)-C(711)	1.886(6)
C(21)-C(26)	1.358(12)	C(41A)-C(46A)	1.382(16)	Si(72)-C(722)	1.859(6)
C(22)-C(23)	1.338(12)	C(41A)-C(42A)	1.395(16)	Si(72)-C(721)	1.868(5)
C(23)-C(24)	1.338(14)	C(42A)-C(43A)	1.370(16)	Si(72)-C(723)	1.879(6)
C(24)-C(25)	1.329(13)	C(43A)-C(44A)	1.362(17)	Si(73)-C(733)	1.869(5)
C(25)-C(26)	1.395(13)	C(44A)-C(45A)	1.371(17)	Si(73)-C(731)	1.879(5)
Si(1)-Si(11)	2.3455(16)	C(45A)-C(46A)	1.365(16)	Si(73)-C(732)	1.906(5)
Si(1)-Si(13)	2.3476(15)	C(41B)-C(46B)	1.384(16)	Si(8)-Si(81)	2.3433(17)
Si(1)-Si(12)	2.3572(16)	C(41B)-C(42B)	1.399(17)	Si(8)-Si(83)	2.3464(17)
Si(11)-C(113)	1.871(6)	C(42B)-C(43B)	1.366(17)	Si(8)-Si(82)	2.3469(16)
Si(11)-C(112)	1.879(6)	C(43B)-C(44B)	1.364(17)	Si(81)-C(813)	1.870(6)

Atoms	Bond length	Atoms	Bond length	Atoms	Bond length
Si(11)-C(111)	1.884(5)	C(44B)-C(45B)	1.366(18)	Si(81)-C(811)	1.877(6)
Si(12)-C(122)	1.867(5)	C(45B)-C(46B)	1.368(17)	Si(81)-C(812)	1.879(6)
Si(12)-C(123)	1.867(5)	Si(6)-Si(61)	2.3431(17)	Si(82)-C(821)	1.875(5)
Si(12)-C(121)	1.887(5)	Si(6)-Si(62)	2.3497(18)	Si(82)-C(822)	1.876(6)
Si(13)-C(132)	1.868(5)	Si(6)-Si(63)	2.3553(16)	Si(82)-C(823)	1.886(5)
Si(13)-C(133)	1.872(5)	Si(61)-C(613)	1.866(6)	Si(83)-C(831)	1.877(5)
Si(13)-C(131)	1.873(5)	Si(61)-C(612)	1.877(5)	Si(83)-C(832)	1.879(5)
Si(2)-Si(23)	2.3416(18)	Si(61)-C(611)	1.882(6)	Si(83)-C(833)	1.882(5)
Si(2)-Si(21)	2.3426(18)	Si(62)-C(621)	1.869(5)	C(31A)-C(36A)	1.353(16)
Si(2)-Si(22)	2.3477(16)	Si(62)-C(622)	1.890(5)	C(31A)-C(32A)	1.361(16)
Si(21)-C(212)	1.877(7)	Si(62)-C(623)	1.891(6)	C(32A)-C(33A)	1.388(17)
Si(21)-C(211)	1.882(5)	Si(63)-C(631)	1.856(6)	C(33A)-C(34A)	1.398(17)
Si(21)-C(213)	1.892(6)	Si(31)-C(313)	1.866(5)	C(34A)-C(35A)	1.395(17)
Si(22)-C(223)	1.860(5)	Si(31)-C(311)	1.869(5)	C(35A)-C(36A)	1.387(17)
Si(22)-C(221)	1.869(6)	Si(31)-C(312)	1.876(5)	C(31B)-C(36B)	1.360(16)
Si(22)-C(222)	1.894(5)	Si(32)-C(323)	1.865(6)	C(31B)-C(32B)	1.362(15)
Si(23)-C(232)	1.870(6)	Si(32)-C(322)	1.874(5)	C(32B)-C(33B)	1.384(15)
Si(23)-C(231)	1.879(5)	Si(32)-C(321)	1.874(5)	C(33B)-C(34B)	1.392(16)
Si(23)-C(233)	1.884(6)	Si(33)-C(332)	1.879(5)	C(34B)-C(35B)	1.395(16)
Si(3)-Si(32)	2.3485(16)	Si(33)-C(333)	1.886(5)	C(35B)-C(36B)	1.377(16)
Si(3)-Si(33)	2.3528(15)				

7.3.4 Bond angles [deg].

Atoms	Angle	Atoms	Angle
P(4)-P(1)-P(5)	60.42(4)	P(7)-P(10)-P(9)	111.28(6)
P(4)-P(1)-Si(1)	101.43(5)	P(6)-P(10)-P(9)	60.26(5)
P(5)-P(1)-Si(1)	107.07(5)	C(46A)-C(41A)-C(42A)	115.9(18)
P(5)-P(2)-Si(2)	96.51(6)	C(43A)-C(42A)-C(41A)	122.4(19)
P(4)-P(3)-Si(3)	97.60(6)	C(44A)-C(43A)-C(42A)	118.6(18)
P(3)-P(4)-P(1)	106.19(5)	C(43A)-C(44A)-C(45A)	121.3(18)
P(3)-P(4)-P(5)	111.81(6)	C(46A)-C(45A)-C(44A)	118.7(14)
P(1)-P(4)-P(5)	60.09(4)	C(45A)-C(46A)-C(41A)	122.8(15)
P(2)-P(5)-P(1)	104.78(5)	C(46B)-C(41B)-C(42B)	116(2)
P(2)-P(5)-P(4)	109.11(6)	C(43B)-C(42B)-C(41B)	123.3(17)
P(1)-P(5)-P(4)	59.48(4)	C(44B)-C(43B)-C(42B)	118.3(17)
C(22)-C(21)-C(26)	121.3(9)	C(43B)-C(44B)-C(45B)	120.5(19)
C(21)-C(22)-C(23)	119.7(9)	C(44B)-C(45B)-C(46B)	120.7(18)
C(24)-C(23)-C(22)	121.0(9)	C(45B)-C(46B)-C(41B)	121(2)
C(25)-C(24)-C(23)	120.6(10)	P(6)-Si(6)-Si(61)	102.44(6)
C(24)-C(25)-C(26)	119.4(10)	P(6)-Si(6)-Si(62)	108.06(6)
C(21)-C(26)-C(25)	117.9(9)	Si(61)-Si(6)-Si(62)	106.16(6)
P(1)-Si(1)-Si(11)	105.73(6)	P(6)-Si(6)-Si(63)	120.21(6)
P(1)-Si(1)-Si(13)	117.21(6)	Si(61)-Si(6)-Si(63)	110.74(7)
Si(11)-Si(1)-Si(13)	109.29(6)	Si(62)-Si(6)-Si(63)	108.34(6)
P(1)-Si(1)-Si(12)	105.34(6)	C(613)-Si(61)-C(612)	108.6(3)
Si(11)-Si(1)-Si(12)	107.13(6)	C(613)-Si(61)-C(611)	106.7(3)
Si(13)-Si(1)-Si(12)	111.55(6)	C(612)-Si(61)-C(611)	108.9(3)
C(113)-Si(11)-C(112)	107.9(3)	C(613)-Si(61)-Si(6)	111.3(2)
C(113)-Si(11)-C(111)	109.0(3)	C(612)-Si(61)-Si(6)	113.99(19)
C(112)-Si(11)-C(111)	106.6(3)	C(611)-Si(61)-Si(6)	107.00(19)
C(113)-Si(11)-Si(1)	112.04(19)	C(621)-Si(62)-C(622)	107.8(3)
C(112)-Si(11)-Si(1)	112.8(2)	C(621)-Si(62)-C(623)	107.3(3)
C(111)-Si(11)-Si(1)	108.30(16)	C(622)-Si(62)-C(623)	108.6(3)
C(122)-Si(12)-C(123)	108.2(2)	C(621)-Si(62)-Si(6)	112.9(2)
C(122)-Si(12)-C(121)	108.3(2)	C(622)-Si(62)-Si(6)	110.4(2)
C(123)-Si(12)-C(121)	108.7(3)	C(623)-Si(62)-Si(6)	109.7(2)
C(122)-Si(12)-Si(1)	110.86(16)	C(631)-Si(63)-C(633)	107.7(3)
C(123)-Si(12)-Si(1)	113.15(19)	C(631)-Si(63)-C(632)	107.6(3)

Atoms	Angle	Atoms	Angle
C(121)-Si(12)-Si(1)	107.48(15)	C(633)-Si(63)-C(632)	108.2(3)
C(132)-Si(13)-C(133)	108.6(2)	C(631)-Si(63)-Si(6)	112.3(2)
C(132)-Si(13)-C(131)	108.9(2)	C(633)-Si(63)-Si(6)	114.74(19)
C(133)-Si(13)-C(131)	108.5(2)	C(632)-Si(63)-Si(6)	105.93(18)
C(132)-Si(13)-Si(1)	109.79(17)	P(7)-Si(7)-Si(72)	102.95(6)
C(133)-Si(13)-Si(1)	107.08(16)	P(7)-Si(7)-Si(73)	113.52(7)
C(131)-Si(13)-Si(1)	113.83(15)	Si(72)-Si(7)-Si(73)	110.55(6)
P(2)-Si(2)-Si(23)	104.07(6)	P(7)-Si(7)-Si(71)	116.64(6)
P(2)-Si(2)-Si(21)	111.83(7)	Si(72)-Si(7)-Si(71)	106.02(7)
Si(23)-Si(2)-Si(21)	109.07(7)	Si(73)-Si(7)-Si(71)	106.83(7)
P(2)-Si(2)-Si(22)	115.63(6)	C(713)-Si(71)-C(712)	109.5(3)
Si(23)-Si(2)-Si(22)	106.21(6)	C(713)-Si(71)-C(711)	108.1(3)
Si(21)-Si(2)-Si(22)	109.58(7)	C(712)-Si(71)-C(711)	106.3(3)
C(212)-Si(21)-C(211)	107.1(3)	C(713)-Si(71)-Si(7)	109.6(2)
C(212)-Si(21)-C(213)	108.2(3)	C(712)-Si(71)-Si(7)	112.34(19)
C(211)-Si(21)-C(213)	109.1(3)	C(711)-Si(71)-Si(7)	111.0(2)
C(212)-Si(21)-Si(2)	109.38(19)	C(722)-Si(72)-C(721)	107.8(3)
C(211)-Si(21)-Si(2)	109.61(19)	C(722)-Si(72)-C(723)	107.7(3)
C(213)-Si(21)-Si(2)	113.3(2)	C(721)-Si(72)-C(723)	107.1(3)
C(223)-Si(22)-C(221)	108.0(3)	C(722)-Si(72)-Si(7)	110.22(19)
C(223)-Si(22)-C(222)	109.1(3)	C(721)-Si(72)-Si(7)	113.27(19)
C(221)-Si(22)-C(222)	106.8(3)	C(723)-Si(72)-Si(7)	110.47(19)
C(223)-Si(22)-Si(2)	109.73(19)	C(733)-Si(73)-C(731)	109.7(2)
C(221)-Si(22)-Si(2)	112.2(2)	C(733)-Si(73)-C(732)	105.9(3)
C(222)-Si(22)-Si(2)	110.83(18)	C(731)-Si(73)-C(732)	107.7(3)
C(232)-Si(23)-C(231)	107.4(3)	C(733)-Si(73)-Si(7)	110.24(16)
C(232)-Si(23)-C(233)	107.5(3)	C(731)-Si(73)-Si(7)	110.99(19)
C(231)-Si(23)-C(233)	108.2(2)	C(732)-Si(73)-Si(7)	112.17(18)
C(232)-Si(23)-Si(2)	110.5(2)	P(8)-Si(8)-Si(81)	112.59(6)
C(231)-Si(23)-Si(2)	110.62(16)	P(8)-Si(8)-Si(83)	115.46(6)
C(233)-Si(23)-Si(2)	112.4(2)	Si(81)-Si(8)-Si(83)	110.83(7)
P(3)-Si(3)-Si(32)	100.24(6)	P(8)-Si(8)-Si(82)	104.02(6)
P(3)-Si(3)-Si(33)	114.87(6)	Si(81)-Si(8)-Si(82)	106.88(7)
Si(32)-Si(3)-Si(33)	111.48(6)	Si(83)-Si(8)-Si(82)	106.25(6)
P(3)-Si(3)-Si(31)	117.95(6)	C(813)-Si(81)-C(811)	108.8(3)
Si(32)-Si(3)-Si(31)	106.18(6)	C(813)-Si(81)-C(812)	107.0(3)
Si(33)-Si(3)-Si(31)	105.76(6)	C(811)-Si(81)-C(812)	107.2(3)
C(313)-Si(31)-C(311)	108.2(3)	C(813)-Si(81)-Si(8)	108.5(2)
C(313)-Si(31)-C(312)	107.0(3)	C(811)-Si(81)-Si(8)	113.1(2)
C(311)-Si(31)-C(312)	107.2(3)	C(812)-Si(81)-Si(8)	112.07(18)
C(313)-Si(31)-Si(3)	110.7(2)	C(821)-Si(82)-C(822)	108.3(3)
C(311)-Si(31)-Si(3)	111.75(17)	C(821)-Si(82)-C(823)	107.7(3)
C(312)-Si(31)-Si(3)	111.78(19)	C(822)-Si(82)-C(823)	107.2(3)
C(323)-Si(32)-C(322)	106.5(3)	C(821)-Si(82)-Si(8)	108.76(17)
C(323)-Si(32)-C(321)	108.1(3)	C(822)-Si(82)-Si(8)	112.26(19)
C(322)-Si(32)-C(321)	108.1(3)	C(823)-Si(82)-Si(8)	112.48(18)
C(323)-Si(32)-Si(3)	109.61(17)	C(831)-Si(83)-C(832)	108.9(3)
C(322)-Si(32)-Si(3)	115.5(2)	C(831)-Si(83)-C(833)	108.5(3)
C(321)-Si(32)-Si(3)	108.85(18)	C(832)-Si(83)-C(833)	106.9(3)
C(332)-Si(33)-C(333)	109.2(2)	C(831)-Si(83)-Si(8)	113.07(18)
C(332)-Si(33)-C(331)	106.8(2)	C(832)-Si(83)-Si(8)	109.16(17)
C(333)-Si(33)-C(331)	106.2(2)	C(833)-Si(83)-Si(8)	110.13(18)
C(332)-Si(33)-Si(3)	109.63(17)	C(36A)-C(31A)-C(32A)	122.9(17)
C(333)-Si(33)-Si(3)	111.36(15)	C(31A)-C(32A)-C(33A)	119.9(17)
C(331)-Si(33)-Si(3)	113.44(15)	C(32A)-C(33A)-C(34A)	118(2)
P(9)-P(8)-Si(8)	97.07(6)	C(35A)-C(34A)-C(33A)	120(2)
P(10)-P(7)-Si(7)	94.69(6)	C(36A)-C(35A)-C(34A)	119.6(18)
P(10)-P(6)-P(9)	60.21(5)	C(31A)-C(36A)-C(35A)	118.7(16)
P(10)-P(6)-Si(6)	100.70(5)	C(36B)-C(31B)-C(32B)	122.6(18)
P(9)-P(6)-Si(6)	103.72(5)	C(31B)-C(32B)-C(33B)	119.1(17)
P(8)-P(9)-P(10)	108.23(6)	C(32B)-C(33B)-C(34B)	119.7(17)

Atoms	Angle	Atoms	Angle
P(8)-P(9)-P(6)	106.52(6)	C(33B)-C(34B)-C(35B)	119.5(18)
P(10)-P(9)-P(6)	59.53(5)	C(36B)-C(35B)-C(34B)	120.0(16)
P(7)-P(10)-P(6)	106.60(5)	C(31B)-C(36B)-C(35B)	119.1(15)

7.4 Crystallographic data for Hyp$_3$P$_8$K$_3$·2C$_6$H$_6$

7.4.1 Crystal data and structure refinement

Empirical formula	Hyp$_3$P$_8$K$_3$·3benzene
Formula weight	1419.48
Temperature	173(2) K
Wavelength	0.71073 Å
Crystal system, space group	triclinic; P$\overline{1}$
Unit cell dimensions	a = 14.920(3) Å alpha = 72.961(13) deg. b = 16.401(3) Å beta = 77.152(12) deg. c = 18.743(4) Å gamma = 80.088(12) deg.
Volume	4247.2(14) Å^3
Z, Calculated density	2, 1.110 g/cm^3
Absorption coefficient	0.509 mm^{-1}
F(000)	1510
Theta range for data collection	2.29 to 25.00 deg.
Limiting indices	0<=h<=17, -18<=k<=18, -21<=l<=22
Reflections collected / unique	15225 / 14620 [R(int) = 0.0589]
Completeness to theta = 25.00	97.7 %
Refinement method	Full-matrix least-squares on F^2
Data / restraints / parameters	14620 / 49 / 729
Goodness-of-fit on F^2	0.861
Final R indices [I>2sigma(I)]	R1 = 0.0447, wR2 = 0.0927
R indices (all data)	R1 = 0.0868, wR2 = 0.1003
Largest diff. peak and hole	0.651 and -0.327 e.Å^{-3}

7.4.2 Atomic coordinates (x 10^4), equivalent isotropic displacement parameters (Å^2 x 10^3) and Anisotropic displacement parameters (Å^2 x 10^3). U(eq) is defined as one third of the trace of the orthogonalized Uij tensor. The anisotropic displacement factor exponent takes the form: $-2\pi^2[h^2a^{*2}U11 + ... + 2hka^*b^*U12]$

Atom	x	y	z	U(eq)	U11	U22	U33	U23	U13	U12
K(1)	-1262(1)	577(1)	474(1)	38(1)	44(1)	35(1)	23(1)	2(1)	3(1)	3(1)
P(1)	1225(1)	-3224(1)	2128(1)	28(1)	30(1)	22(1)	26(1)	-3(1)	-1(1)	0(1)
P(2)	1057(1)	150(1)	1147(1)	25(1)	31(1)	21(1)	23(1)	-4(1)	-3(1)	-6(1)
P(3)	-1289(1)	-1910(1)	3029(1)	27(1)	27(1)	28(1)	21(1)	-2(1)	3(1)	-3(1)
P(4)	-889(1)	-932(1)	1969(1)	23(1)	23(1)	24(1)	20(1)	-4(1)	1(1)	-2(1)
P(5)	-161(1)	-1420(1)	1006(1)	24(1)	27(1)	27(1)	17(1)	-5(1)	-3(1)	-1(1)
P(6)	1209(1)	-1985(1)	1256(1)	24(1)	25(1)	22(1)	21(1)	-5(1)	0(1)	0(1)
P(7)	1557(1)	-1122(1)	1846(1)	26(1)	27(1)	23(1)	26(1)	-4(1)	-6(1)	-4(1)
P(8)	208(1)	-409(1)	2269(1)	27(1)	31(1)	28(1)	21(1)	-9(1)	1(1)	-7(1)

Atom	x	y	z	U(eq)	U11	U22	U33	U23	U13	U12
Si(1)	2589(1)	-3815(1)	1592(1)	30(1)	31(1)	30(1)	26(1)	-7(1)	-5(1)	6(1)
Si(11)	2834(5)	-3737(4)	278(2)	37(1)	42(3)	40(2)	24(2)	-9(1)	-1(1)	5(2)
C(111)	2629(16)	-2643(10)	-387(14)	49(5)	52(9)	53(9)	19(6)	5(7)	1(6)	20(7)
C(112)	1970(12)	-4365(7)	166(6)	72(5)	132(14)	58(7)	46(7)	-13(6)	-40(8)	-34(9)
C(113)	4043(9)	-4211(10)	-67(6)	87(6)	80(10)	108(11)	49(7)	-26(7)	3(6)	48(8)
Si(1A)	2476(5)	-3901(3)	365(2)	38(1)	50(3)	33(2)	24(1)	-5(1)	-1(2)	7(2)
C(114)	3270(11)	-4783(7)	19(5)	94(6)	149(15)	77(8)	46(6)	-35(6)	-18(7)	44(9)
C(115)	2814(14)	-2877(10)	-358(13)	56(5)	65(11)	55(9)	42(7)	-8(7)	-16(8)	8(9)
C(116)	1255(8)	-4063(8)	352(6)	68(3)	70(8)	88(9)	57(7)	-12(6)	-25(6)	-35(7)
Si(12)	3842(1)	-3168(1)	1682(1)	49(1)	29(1)	43(1)	61(1)	1(1)	-4(1)	-2(1)
C(121)	4988(3)	-3873(3)	1582(3)	83(2)	30(3)	62(3)	130(5)	1(3)	-6(3)	8(2)
C(122)	3607(3)	-2940(3)	2641(3)	68(2)	71(4)	69(3)	73(3)	-10(3)	-34(3)	-24(3)
C(123)	3994(3)	-2107(3)	948(3)	67(2)	37(3)	51(3)	91(4)	1(3)	8(3)	-6(2)
Si(13)	2760(1)	-5256(1)	2336(1)	37(1)	39(1)	28(1)	42(1)	-8(1)	-14(1)	5(1)
C(131)	3648(3)	-5979(3)	1833(3)	65(1)	63(3)	42(3)	86(4)	-22(3)	-17(3)	19(2)
C(132)	3124(3)	-5319(3)	3254(2)	54(1)	60(3)	52(3)	43(3)	6(2)	-20(2)	-11(2)
C(133)	1629(3)	-5732(3)	2589(3)	55(1)	58(3)	39(3)	70(3)	-14(2)	-17(3)	-10(2)
Si(2)	1796(1)	1108(1)	1423(1)	25(1)	29(1)	23(1)	24(1)	-5(1)	-3(1)	-7(1)
Si(21)	2950(1)	1492(1)	332(1)	37(1)	29(1)	42(1)	38(1)	-14(1)	6(1)	-10(1)
C(211)	3716(3)	509(3)	171(3)	76(2)	54(3)	86(4)	78(4)	-34(3)	10(3)	12(3)
C(212)	2419(3)	2007(3)	-537(2)	51(1)	58(3)	63(3)	29(2)	-12(2)	8(2)	-18(2)
C(213)	3667(3)	2274(3)	435(3)	70(2)	62(3)	99(4)	58(3)	-30(3)	12(3)	-50(3)
Si(22)	2474(1)	666(1)	2520(1)	49(1)	70(1)	38(1)	46(1)	-2(1)	-33(1)	-15(1)
C(221)	3451(4)	-220(3)	2454(4)	92(2)	111(5)	54(3)	142(6)	-27(3)	-98(4)	12(3)
C(222)	1602(4)	313(3)	3406(2)	88(2)	139(5)	99(4)	33(3)	18(3)	-36(3)	-71(4)
C(223)	2965(3)	1614(3)	2604(2)	57(1)	76(4)	57(3)	50(3)	-13(2)	-25(3)	-21(3)
Si(23)	634(1)	2278(1)	1477(1)	34(1)	39(1)	28(1)	32(1)	-12(1)	2(1)	-1(1)
C(231)	146(3)	2329(3)	2478(2)	58(1)	54(3)	68(3)	48(3)	-29(2)	7(2)	3(3)
C(232)	1094(3)	3327(2)	920(3)	66(2)	84(4)	26(2)	69(3)	-13(2)	18(3)	-1(2)
C(233)	-351(3)	2162(3)	1053(3)	59(1)	53(3)	61(3)	69(3)	-30(3)	-22(3)	13(2)
Si(3)	-2652(1)	-1229(1)	3482(1)	28(1)	28(1)	32(1)	22(1)	-7(1)	4(1)	-6(1)
Si(31)	-3722(1)	-2244(1)	3788(1)	44(1)	33(1)	44(1)	48(1)	-9(1)	7(1)	-13(1)
C(311)	-3888(4)	-2442(3)	2889(3)	79(2)	75(4)	86(4)	96(4)	-38(3)	-22(3)	-32(3)
C(312)	-4917(3)	-1892(3)	4277(4)	96(2)	49(3)	84(4)	133(5)	-32(4)	49(3)	-27(3)
C(313)	-3225(4)	-3288(3)	4383(3)	73(2)	81(4)	48(3)	82(4)	10(3)	-20(3)	-27(3)
Si(32)	-2450(1)	-913(1)	4576(1)	44(1)	46(1)	59(1)	30(1)	-22(1)	-2(1)	-1(1)
C(321)	-2111(4)	-1953(3)	5284(3)	74(2)	98(4)	87(4)	39(3)	-18(3)	-24(3)	3(3)
C(322)	-1474(4)	-218(3)	4311(3)	75(2)	93(4)	89(4)	58(3)	-40(3)	-1(3)	-37(3)
C(323)	-3493(4)	-325(3)	5062(3)	78(2)	76(4)	107(4)	57(3)	-55(3)	-5(3)	24(3)
Si(33)	-3246(1)	46(1)	2659(1)	39(1)	35(1)	39(1)	36(1)	-8(1)	-2(1)	1(1)
C(331)	-2516(3)	944(3)	2451(3)	55(1)	57(3)	39(3)	61(3)	-10(2)	2(2)	-5(2)
C(332)	-4434(3)	434(3)	3135(3)	62(1)	41(3)	67(3)	68(3)	-17(3)	-5(2)	13(2)
C(333)	-3400(3)	-123(3)	1742(2)	57(1)	56(3)	63(3)	46(3)	-3(2)	-18(2)	-4(2)
C(011)	-4297(6)	3112(7)	2847(6)	154(4)	109(7)	216(11)	150(9)	-67(8)	-84(7)	62(7)
C(012)	-3528(8)	3430(4)	2365(4)	122(3)	193(10)	80(5)	82(5)	-10(4)	-59(6)	38(6)
C(013)	-2694(5)	3259(3)	2618(4)	91(2)	134(6)	48(3)	87(5)	-7(3)	-11(4)	-30(4)
C(014)	-2660(4)	2774(3)	3345(3)	71(2)	72(4)	75(4)	79(4)	-34(3)	-17(3)	-16(3)
C(015)	-3435(4)	2446(4)	3820(3)	76(2)	77(4)	99(4)	60(3)	-34(3)	-10(3)	-9(4)
C(016)	-4241(5)	2602(6)	3565(5)	121(3)	64(5)	193(9)	116(6)	-62(6)	-8(4)	-18(5)
C(021)	549(4)	-2648(7)	5447(3)	97(2)	62(4)	201(8)	39(3)	-53(5)	-11(3)	-3(5)
C(022)	927(6)	-1882(5)	5158(5)	110(3)	130(7)	107(6)	125(7)	-83(6)	-78(6)	62(5)
C(023)	1790(6)	-1877(4)	4748(4)	87(2)	138(7)	53(4)	89(5)	2(3)	-75(5)	-23(4)
C(024)	2282(4)	-2611(5)	4611(3)	77(2)	63(4)	115(5)	59(3)	-10(4)	-28(3)	-21(4)
C(025)	1909(4)	-3358(4)	4891(3)	72(2)	88(5)	60(4)	83(4)	-19(3)	-59(4)	10(3)
C(026)	1045(5)	-3379(4)	5300(3)	77(2)	107(5)	87(4)	40(3)	16(3)	-34(3)	-52(4)
C(031)	-815(3)	-5148(3)	1954(3)	61(1)	57(3)	43(3)	82(4)	-25(3)	-7(3)	5(2)
C(032)	-1373(5)	-4789(3)	1437(3)	67(2)	104(5)	58(3)	49(3)	-18(3)	-12(3)	-35(3)
C(033)	-2268(5)	-4467(3)	1651(4)	79(2)	87(5)	47(3)	112(5)	8(3)	-63(4)	-25(3)
C(034)	-2604(4)	-4511(3)	2413(5)	87(2)	39(3)	52(3)	158(7)	-24(4)	4(4)	-10(3)
C(035)	-2026(5)	-4881(3)	2933(3)	76(2)	102(5)	63(4)	62(4)	-21(3)	15(4)	-40(4)
C(036)	-1144(4)	-5191(3)	2704(3)	65(1)	79(4)	45(3)	73(4)	-1(3)	-36(3)	-11(3)

Atom	x	y	z	U(eq)	U11	U22	U33	U23	U13	U12
C(041)	-4876(4)	-5036(4)	4265(3)	77(2)	68(4)	113(5)	58(3)	-21(4)	-21(3)	-23(4)
C(042)	-5527(4)	-4428(4)	4524(3)	86(2)	71(4)	98(5)	72(4)	4(4)	-30(3)	12(4)
C(043)	-5639(4)	-4399(3)	5257(4)	73(2)	63(4)	66(4)	93(5)	-29(3)	-17(3)	-1(3)
C(051)	-859(3)	-4611(3)	5242(3)	61(1)	60(3)	43(3)	66(3)	-10(2)	7(3)	-3(2)
C(052)	-431(3)	-4318(3)	4485(3)	55(1)	63(3)	48(3)	49(3)	-4(2)	-7(2)	-18(3)
C(053)	431(4)	-4713(3)	4258(2)	56(1)	87(4)	45(3)	29(2)	-1(2)	4(2)	-23(3)
K(2)	686(1)	-2399(1)	3578(1)	40(1)	46(1)	48(1)	24(1)	-5(1)	-11(1)	-3(1)
K(3)	-926(1)	-3187(1)	1953(1)	41(1)	46(1)	36(1)	44(1)	-13(1)	-4(1)	-15(1)

7.4.3 Bond lengths[Å].

Atoms	Bond length	Atoms	Bond length	Atoms	Bond length
K(1)-P(5)#1	3.2021(13)	Si(11)-C(113)	1.888(9)	C(013)-C(014)	1.368(7)
K(1)-P(4)	3.2319(13)	Si(1A)-C(114)	1.880(9)	C(014)-C(015)	1.376(7)
K(1)-P(5)	3.3743(13)	Si(1A)-C(115)	1.889(12)	C(015)-C(016)	1.348(8)
K(1)-P(6)#1	3.3777(13)	Si(1A)-C(116)	1.892(9)	C(021)-C(026)	1.362(8)
K(1)-P(2)#1	3.5119(14)	Si(12)-C(122)	1.886(5)	C(021)-C(022)	1.380(9)
K(1)-P(2)	3.8265(15)	Si(12)-C(123)	1.888(4)	C(021)-K(2)	3.369(5)
K(1)-K(1)#1	4.1777(18)	Si(12)-C(121)	1.897(4)	C(022)-C(023)	1.345(9)
P(1)-P(6)	2.2039(13)	Si(13)-C(132)	1.887(4)	C(022)-K(2)	3.416(6)
P(1)-Si(1)	2.2510(14)	Si(13)-C(133)	1.887(4)	C(023)-C(024)	1.359(8)
P(1)-K(2)	3.2687(14)	Si(13)-C(131)	1.900(4)	C(023)-K(2)	3.382(5)
P(1)-K(3)	3.2857(15)	Si(2)-Si(22)	2.3612(16)	C(024)-C(025)	1.347(7)
P(2)-P(7)	2.2183(13)	Si(2)-Si(21)	2.3644(15)	C(024)-K(2)	3.303(5)
P(2)-P(8)	2.2251(13)	Si(2)-Si(23)	2.3650(15)	C(025)-C(026)	1.346(7)
P(2)-Si(2)	2.2965(13)	Si(21)-C(211)	1.871(4)	C(025)-K(2)	3.256(5)
P(2)-K(1)#1	3.5119(14)	Si(21)-C(213)	1.879(4)	C(026)-K(2)	3.273(5)
P(3)-P(4)	2.1930(13)	Si(21)-C(212)	1.881(4)	C(031)-C(032)	1.354(7)
P(3)-Si(3)	2.2610(14)	Si(22)-C(222)	1.876(5)	C(031)-C(036)	1.368(7)
P(3)-K(3)	3.2174(14)	Si(22)-C(221)	1.884(5)	C(031)-K(3)	3.191(4)
P(3)-K(2)	3.2301(14)	Si(22)-C(223)	1.888(4)	C(032)-C(033)	1.366(7)
P(4)-P(5)	2.1802(13)	Si(23)-C(231)	1.876(4)	C(032)-K(3)	3.265(5)
P(4)-P(8)	2.2146(14)	Si(23)-C(233)	1.879(4)	C(033)-C(034)	1.390(8)
P(4)-K(3)	3.7169(14)	Si(23)-C(232)	1.885(4)	C(033)-K(3)	3.374(5)
P(5)-P(6)	2.1838(14)	Si(3)-Si(32)	2.3482(16)	C(034)-C(035)	1.381(8)
P(5)-K(3)	3.1738(13)	Si(3)-Si(31)	2.3650(16)	C(034)-K(3)	3.398(5)
P(5)-K(1)#1	3.2021(13)	Si(3)-Si(33)	2.3700(15)	C(035)-C(036)	1.349(7)
P(6)-P(7)	2.2191(13)	Si(31)-C(313)	1.881(5)	C(035)-K(3)	3.320(5)
P(6)-K(1)#1	3.3777(13)	Si(31)-C(311)	1.881(5)	C(036)-K(3)	3.216(5)
P(6)-K(3)	3.8127(14)	Si(31)-C(312)	1.892(5)	C(041)-C(043)#2	1.351(7)
P(7)-P(8)	2.2524(14)	Si(32)-C(323)	1.885(4)	C(041)-C(042)	1.384(7)
P(7)-K(2)	3.4199(14)	Si(32)-C(322)	1.893(5)	C(042)-C(043)	1.360(7)
P(8)-K(2)	3.5318(14)	Si(32)-C(321)	1.898(5)	C(043)-C(041)#2	1.351(7)
Si(1)-Si(12)	2.3623(17)	Si(33)-C(331)	1.879(4)	C(051)-C(053)#3	1.388(6)
Si(1)-Si(13)	2.3698(15)	Si(33)-C(333)	1.887(4)	C(051)-C(052)	1.398(6)
Si(1)-Si(11)	2.376(3)	Si(33)-C(332)	1.893(4)	C(052)-C(053)	1.374(6)
Si(1)-Si(1A)	2.389(3)	C(011)-C(012)	1.370(11)	C(053)-C(051)#3	1.388(6)
Si(11)-C(112)	1.864(10)	C(011)-C(016)	1.373(10)	K(2)-K(3)	4.8346(14)
Si(11)-C(111)	1.881(13)	C(012)-C(013)	1.384(9)		

7.4.3 Bond angles [deg].

Atoms	Angle	Atoms	Angle
P(5)#1-K(1)-P(4)	130.07(4)	C(011)-C(012)-C(013)	119.3(7)
P(5)#1-K(1)-P(5)	101.17(3)	C(014)-C(013)-C(012)	119.1(7)
P(4)-K(1)-P(5)	38.46(2)	C(013)-C(014)-C(015)	121.1(6)

Atoms	Angle	Atoms	Angle
P(5)#1-K(1)-P(6)#1	38.65(3)	C(016)-C(015)-C(014)	119.6(6)
P(4)-K(1)-P(6)#1	167.90(4)	C(015)-C(016)-C(011)	120.3(7)
P(5)-K(1)-P(6)#1	130.75(3)	C(026)-C(021)-C(022)	119.7(6)
P(5)#1-K(1)-P(2)#1	62.58(3)	C(026)-C(021)-K(2)	74.3(3)
P(4)-K(1)-P(2)#1	113.90(3)	C(022)-C(021)-K(2)	80.2(4)
P(5)-K(1)-P(2)#1	78.35(3)	C(023)-C(022)-C(021)	118.9(6)
P(6)#1-K(1)-P(2)#1	59.46(3)	C(023)-C(022)-K(2)	77.2(4)
P(5)#1-K(1)-P(2)	75.92(3)	C(021)-C(022)-K(2)	76.3(3)
P(4)-K(1)-P(2)	58.43(3)	C(022)-C(023)-C(024)	120.9(6)
P(5)-K(1)-P(2)	57.70(3)	C(022)-C(023)-K(2)	80.0(4)
P(6)#1-K(1)-P(2)	112.86(3)	C(024)-C(023)-K(2)	75.0(3)
P(2)#1-K(1)-P(2)	110.75(3)	C(025)-C(024)-C(023)	120.0(6)
P(5)#1-K(1)-K(1)#1	52.41(3)	C(025)-C(024)-K(2)	76.2(3)
P(4)-K(1)-K(1)#1	82.01(3)	C(023)-C(024)-K(2)	81.6(3)
P(5)-K(1)-K(1)#1	48.76(3)	C(026)-C(025)-C(024)	120.2(6)
P(6)#1-K(1)-K(1)#1	85.91(3)	C(026)-C(025)-K(2)	78.8(3)
P(2)#1-K(1)-K(1)#1	58.93(3)	C(024)-C(025)-K(2)	80.1(3)
P(2)-K(1)-K(1)#1	51.82(3)	C(025)-C(026)-C(021)	120.3(6)
P(6)-P(1)-Si(1)	96.11(5)	C(025)-C(026)-K(2)	77.4(3)
P(6)-P(1)-K(2)	95.67(4)	C(021)-C(026)-K(2)	82.1(3)
Si(1)-P(1)-K(2)	131.00(5)	C(032)-C(031)-C(036)	120.0(5)
P(6)-P(1)-K(3)	85.58(4)	C(032)-C(031)-K(3)	81.0(3)
Si(1)-P(1)-K(3)	133.18(5)	C(036)-C(031)-K(3)	78.7(3)
K(2)-P(1)-K(3)	95.06(3)	C(031)-C(032)-C(033)	121.1(5)
P(7)-P(2)-P(8)	60.92(4)	C(031)-C(032)-K(3)	74.8(3)
P(7)-P(2)-Si(2)	104.53(5)	C(033)-C(032)-K(3)	82.6(3)
P(8)-P(2)-Si(2)	102.07(5)	C(032)-C(033)-C(034)	119.0(5)
P(7)-P(2)-K(1)#1	93.98(4)	C(032)-C(033)-K(3)	73.7(3)
P(8)-P(2)-K(1)#1	124.16(4)	C(034)-C(033)-K(3)	79.1(3)
Si(2)-P(2)-K(1)#1	133.38(4)	C(035)-C(034)-C(033)	119.2(5)
P(7)-P(2)-K(1)	122.31(4)	C(035)-C(034)-K(3)	75.0(3)
P(8)-P(2)-K(1)	83.30(4)	C(033)-C(034)-K(3)	77.2(3)
Si(2)-P(2)-K(1)	127.52(4)	C(036)-C(035)-C(034)	120.5(5)
K(1)#1-P(2)-K(1)	69.25(3)	C(036)-C(035)-K(3)	73.8(3)
P(4)-P(3)-Si(3)	99.26(5)	C(034)-C(035)-K(3)	81.3(3)
P(4)-P(3)-K(3)	84.53(4)	C(035)-C(036)-C(031)	120.2(5)
Si(3)-P(3)-K(3)	128.02(5)	C(035)-C(036)-K(3)	82.5(3)
P(4)-P(3)-K(2)	98.58(4)	C(031)-C(036)-K(3)	76.7(3)
Si(3)-P(3)-K(2)	132.57(5)	C(043)#2-C(041)-C(042)	119.7(5)
K(3)-P(3)-K(2)	97.15(4)	C(043)-C(042)-C(041)	119.8(5)
P(5)-P(4)-P(3)	115.63(5)	C(041)#2-C(043)-C(042)	120.5(5)
P(5)-P(4)-P(8)	103.12(5)	C(053)#3-C(051)-C(052)	121.0(4)
P(3)-P(4)-P(8)	100.60(5)	C(053)-C(052)-C(051)	117.7(4)
P(5)-P(4)-K(1)	74.30(4)	C(052)-C(053)-C(051)#3	121.3(4)
P(3)-P(4)-K(1)	154.96(5)	P(3)-K(2)-C(025)	149.91(13)
P(8)-P(4)-K(1)	99.07(4)	P(3)-K(2)-P(1)	81.79(3)
P(5)-P(4)-K(3)	58.38(4)	C(025)-K(2)-P(1)	112.81(11)
P(3)-P(4)-K(3)	59.50(4)	P(3)-K(2)-C(026)	126.53(13)
P(8)-P(4)-K(3)	127.13(4)	C(025)-K(2)-C(026)	23.79(13)
K(1)-P(4)-K(3)	118.08(4)	P(1)-K(2)-C(026)	125.82(14)
P(4)-P(5)-P(6)	106.28(5)	P(3)-K(2)-C(024)	160.17(12)
P(4)-P(5)-K(3)	85.81(4)	C(025)-K(2)-C(024)	23.69(13)
P(6)-P(5)-K(3)	88.74(4)	P(1)-K(2)-C(024)	117.98(12)
P(4)-P(5)-K(1)#1	130.87(5)	C(026)-K(2)-C(024)	41.59(14)
P(6)-P(5)-K(1)#1	75.02(4)	P(3)-K(2)-C(021)	114.16(11)
K(3)-P(5)-K(1)#1	142.53(4)	C(025)-K(2)-C(021)	41.48(15)
P(4)-P(5)-K(1)	67.23(4)	P(1)-K(2)-C(021)	149.20(17)
P(6)-P(5)-K(1)	136.51(5)	C(026)-K(2)-C(021)	23.62(15)
K(3)-P(5)-K(1)	131.21(4)	C(024)-K(2)-C(021)	47.93(14)
K(1)#1-P(5)-K(1)	78.83(3)	P(3)-K(2)-C(023)	138.53(15)
P(5)-P(6)-P(1)	114.56(5)	C(025)-K(2)-C(023)	41.29(13)

Atoms	Angle	Atoms	Angle
P(5)-P(6)-P(7)	103.53(5)	P(1)-K(2)-C(023)	137.98(16)
P(1)-P(6)-P(7)	102.02(5)	C(026)-K(2)-C(023)	47.91(13)
P(5)-P(6)-K(1)#1	66.32(4)	C(024)-K(2)-C(023)	23.41(14)
P(1)-P(6)-K(1)#1	159.23(5)	C(021)-K(2)-C(023)	40.68(16)
P(7)-P(6)-K(1)#1	97.68(4)	P(3)-K(2)-C(022)	119.25(14)
P(5)-P(6)-K(3)	56.33(4)	C(025)-K(2)-C(022)	48.11(14)
P(1)-P(6)-K(3)	59.23(4)	P(1)-K(2)-C(022)	158.89(13)
P(7)-P(6)-K(3)	123.60(4)	C(026)-K(2)-C(022)	41.45(16)
K(1)#1-P(6)-K(3)	114.09(3)	C(024)-K(2)-C(022)	40.94(16)
P(2)-P(7)-P(6)	100.77(5)	C(021)-K(2)-C(022)	23.45(16)
P(2)-P(7)-P(8)	59.69(4)	C(023)-K(2)-C(022)	22.82(15)
P(6)-P(7)-P(8)	106.33(5)	P(3)-K(2)-P(7)	86.12(3)
P(2)-P(7)-K(2)	133.50(5)	C(025)-K(2)-P(7)	123.88(13)
P(6)-P(7)-K(2)	91.30(4)	P(1)-K(2)-P(7)	61.81(3)
P(8)-P(7)-K(2)	73.81(4)	C(026)-K(2)-P(7)	145.81(11)
P(4)-P(8)-P(2)	103.39(5)	C(024)-K(2)-P(7)	104.23(11)
P(4)-P(8)-P(7)	106.08(5)	C(021)-K(2)-P(7)	141.08(16)
P(2)-P(8)-P(7)	59.39(4)	C(023)-K(2)-P(7)	102.09(12)
P(4)-P(8)-K(2)	89.92(4)	C(022)-K(2)-P(7)	117.78(19)
P(2)-P(8)-K(2)	127.81(5)	P(3)-K(2)-P(8)	60.00(3)
P(7)-P(8)-K(2)	68.42(4)	C(025)-K(2)-P(8)	142.80(11)
P(1)-Si(1)-Si(12)	111.73(6)	P(1)-K(2)-P(8)	86.69(3)
P(1)-Si(1)-Si(13)	105.35(6)	C(026)-K(2)-P(8)	146.25(13)
Si(12)-Si(1)-Si(13)	106.65(6)	C(024)-K(2)-P(8)	119.30(13)
P(1)-Si(1)-Si(11)	118.39(16)	C(021)-K(2)-P(8)	123.99(17)
Si(12)-Si(1)-Si(11)	102.9(2)	C(023)-K(2)-P(8)	103.09(10)
Si(13)-Si(1)-Si(11)	111.36(16)	C(022)-K(2)-P(8)	104.90(14)
P(1)-Si(1)-Si(1A)	109.26(16)	P(7)-K(2)-P(8)	37.77(3)
Si(12)-Si(1)-Si(1A)	117.58(18)	P(3)-K(2)-K(3)	41.32(2)
Si(13)-Si(1)-Si(1A)	105.33(14)	C(025)-K(2)-K(3)	137.96(10)
Si(11)-Si(1)-Si(1A)	14.65(11)	P(1)-K(2)-K(3)	42.61(2)
C(112)-Si(11)-C(111)	104.8(9)	C(026)-K(2)-K(3)	130.95(10)
C(112)-Si(11)-C(113)	109.8(6)	C(024)-K(2)-K(3)	156.39(13)
C(111)-Si(11)-C(113)	107.3(7)	C(021)-K(2)-K(3)	138.16(14)
C(112)-Si(11)-Si(1)	106.3(4)	C(023)-K(2)-K(3)	178.80(12)
C(111)-Si(11)-Si(1)	116.8(9)	C(022)-K(2)-K(3)	156.31(18)
C(113)-Si(11)-Si(1)	111.5(4)	P(7)-K(2)-K(3)	79.12(3)
C(114)-Si(1A)-C(115)	104.9(8)	P(8)-K(2)-K(3)	77.85(3)
C(114)-Si(1A)-C(116)	107.0(5)	P(5)-K(3)-C(031)	142.86(10)
C(115)-Si(1A)-C(116)	110.4(8)	P(5)-K(3)-C(036)	164.00(12)
C(114)-Si(1A)-Si(1)	115.5(4)	C(031)-K(3)-C(036)	24.66(12)
C(115)-Si(1A)-Si(1)	108.7(9)	P(5)-K(3)-P(3)	70.77(3)
C(116)-Si(1A)-Si(1)	110.2(4)	C(031)-K(3)-P(3)	143.84(11)
C(122)-Si(12)-C(123)	106.8(2)	C(036)-K(3)-P(3)	119.35(11)
C(122)-Si(12)-C(121)	108.3(2)	P(5)-K(3)-C(032)	132.07(9)
C(123)-Si(12)-C(121)	107.3(2)	C(031)-K(3)-C(032)	24.18(12)
C(122)-Si(12)-Si(1)	108.46(15)	C(036)-K(3)-C(032)	42.67(13)
C(123)-Si(12)-Si(1)	112.83(17)	P(3)-K(3)-C(032)	153.72(10)
C(121)-Si(12)-Si(1)	112.93(17)	P(5)-K(3)-P(1)	69.69(3)
C(132)-Si(13)-C(133)	107.3(2)	C(031)-K(3)-P(1)	97.37(10)
C(132)-Si(13)-C(131)	107.7(2)	C(036)-K(3)-P(1)	98.45(10)
C(133)-Si(13)-C(131)	107.0(2)	P(3)-K(3)-P(1)	81.71(3)
C(132)-Si(13)-Si(1)	110.80(14)	C(032)-K(3)-P(1)	116.06(12)
C(133)-Si(13)-Si(1)	110.73(14)	P(5)-K(3)-C(035)	171.78(13)
C(131)-Si(13)-Si(1)	113.06(16)	C(031)-K(3)-C(035)	42.36(13)
P(2)-Si(2)-Si(22)	119.04(5)	C(036)-K(3)-C(035)	23.76(13)
P(2)-Si(2)-Si(21)	103.52(5)	P(3)-K(3)-C(035)	106.48(10)
Si(22)-Si(2)-Si(21)	109.73(6)	C(032)-K(3)-C(035)	48.88(13)
P(2)-Si(2)-Si(23)	102.91(5)	P(1)-K(3)-C(035)	118.00(13)
Si(22)-Si(2)-Si(23)	111.20(6)	P(5)-K(3)-C(033)	134.59(10)
Si(21)-Si(2)-Si(23)	109.90(5)	C(031)-K(3)-C(033)	42.18(13)

Atoms	Angle	Atoms	Angle
C(211)-Si(21)-C(213)	109.5(2)	C(036)-K(3)-C(033)	49.16(13)
C(211)-Si(21)-C(212)	107.4(2)	P(3)-K(3)-C(033)	132.99(14)
C(213)-Si(21)-C(212)	107.9(2)	C(032)-K(3)-C(033)	23.67(13)
C(211)-Si(21)-Si(2)	109.69(16)	P(1)-K(3)-C(033)	138.95(12)
C(213)-Si(21)-Si(2)	111.21(15)	C(035)-K(3)-C(033)	41.82(14)
C(212)-Si(21)-Si(2)	111.00(14)	P(5)-K(3)-C(034)	149.48(13)
C(222)-Si(22)-C(221)	109.8(3)	C(031)-K(3)-C(034)	49.00(13)
C(222)-Si(22)-C(223)	107.4(2)	C(036)-K(3)-C(034)	41.90(14)
C(221)-Si(22)-C(223)	108.0(2)	P(3)-K(3)-C(034)	112.23(13)
C(222)-Si(22)-Si(2)	111.96(17)	C(032)-K(3)-C(034)	41.69(14)
C(221)-Si(22)-Si(2)	111.43(18)	P(1)-K(3)-C(034)	140.25(12)
C(223)-Si(22)-Si(2)	108.15(14)	C(035)-K(3)-C(034)	23.69(14)
C(231)-Si(23)-C(233)	107.2(2)	C(033)-K(3)-C(034)	23.69(14)
C(231)-Si(23)-C(232)	108.9(2)	P(5)-K(3)-P(4)	35.80(2)
C(233)-Si(23)-C(232)	107.8(2)	C(031)-K(3)-P(4)	176.11(10)
C(231)-Si(23)-Si(2)	112.05(15)	C(036)-K(3)-P(4)	155.24(11)
C(233)-Si(23)-Si(2)	109.65(14)	P(3)-K(3)-P(4)	35.97(2)
C(232)-Si(23)-Si(2)	111.07(15)	C(032)-K(3)-P(4)	158.85(11)
P(3)-Si(3)-Si(32)	106.53(6)	P(1)-K(3)-P(4)	78.74(3)
P(3)-Si(3)-Si(31)	104.79(6)	C(035)-K(3)-P(4)	139.62(10)
Si(32)-Si(3)-Si(31)	111.11(6)	C(033)-K(3)-P(4)	141.68(11)
P(3)-Si(3)-Si(33)	117.47(5)	C(034)-K(3)-P(4)	134.49(10)
Si(32)-Si(3)-Si(33)	108.85(6)	P(5)-K(3)-P(6)	34.94(2)
Si(31)-Si(3)-Si(33)	108.04(6)	C(031)-K(3)-P(6)	121.38(10)
C(313)-Si(31)-C(311)	107.6(2)	C(036)-K(3)-P(6)	131.37(11)
C(313)-Si(31)-C(312)	110.6(3)	P(3)-K(3)-P(6)	77.37(3)
C(311)-Si(31)-C(312)	105.8(3)	C(032)-K(3)-P(6)	128.49(11)
C(313)-Si(31)-Si(3)	108.80(16)	P(1)-K(3)-P(6)	35.19(2)
C(311)-Si(31)-Si(3)	109.18(16)	C(035)-K(3)-P(6)	153.03(13)
C(312)-Si(31)-Si(3)	114.55(17)	C(033)-K(3)-P(6)	148.32(14)
C(323)-Si(32)-C(322)	107.2(2)	C(034)-K(3)-P(6)	169.93(11)
C(323)-Si(32)-C(321)	108.2(2)	P(4)-K(3)-P(6)	55.24(2)
C(322)-Si(32)-C(321)	108.3(2)	P(5)-K(3)-K(2)	73.81(3)
C(323)-Si(32)-Si(3)	115.12(17)	C(031)-K(3)-K(2)	120.39(10)
C(322)-Si(32)-Si(3)	108.93(15)	C(036)-K(3)-K(2)	105.06(9)
C(321)-Si(32)-Si(3)	108.86(16)	P(3)-K(3)-K(2)	41.52(2)
C(331)-Si(33)-C(333)	109.8(2)	C(032)-K(3)-K(2)	144.57(11)
C(331)-Si(33)-C(332)	106.2(2)	P(1)-K(3)-K(2)	42.34(2)
C(333)-Si(33)-C(332)	106.3(2)	C(035)-K(3)-K(2)	109.55(11)
C(331)-Si(33)-Si(3)	112.24(15)	C(033)-K(3)-K(2)	151.36(11)
C(333)-Si(33)-Si(3)	112.66(15)	C(034)-K(3)-K(2)	129.75(15)
C(332)-Si(33)-Si(3)	109.28(15)	P(4)-K(3)-K(2)	56.51(2)
C(012)-C(011)-C(016)	120.7(8)	P(6)-K(3)-K(2)	55.38(2)

Symmetry transformations used to generate equivalent atoms:
#1 -x,-y,-z   #2 -x-1,-y-1,-z+1   #3 -x,-y-1,-z+1

7.5 Crystallographic data for $Hyp_2P_4Li_2 \cdot 4THF$

7.5.1 Crystal data and structure refinement

Empirical formula	$Hyp_2P_4Li_2 \cdot 4THF$
Formula weight	921.51
Temperature	293(2) K
Wavelength	0.71073 Å
Crystal system, space group	monoclinic, P2/c

Unit cell dimensions	a = 23.723(3) Å alpha = 90 deg. b = 9.9065(15)Å beta = 92.734(9) deg. c = 24.352(3) Å gamma = 90 deg.
Volume	5716.4(13) Å^3
Z, Calculated density	4, 1.071 g/cm^3
Absorption coefficient	0.329 mm^{-1}
F(000)	2000
Theta range for data collection	2.06 to 26.54 deg.
Limiting indices	-29<=h<=28, -12<=k<=12, -30<=l<=30
Reflections collected / unique	56355 / 11688 [R(int) = 0.1100]
Completeness to theta = 26.54	98.1 %
Refinement method	Full-matrix least-squares on F^2
Data / restraints / parameters	11688 / 238 / 571
Goodness-of-fit on F^2	0.650
Final R indices [I>2sigma(I)]	R1 = 0.0419, wR2 = 0.0936
R indices (all data)	R1 = 0.1552, wR2 = 0.1303
Largest diff. peak and hole	0.136 and -0.141 e.Å^{-3}

7.5.2 Atomic coordinates (x 10^4), equivalent isotropic displacement parameters (Å^2 x 10^3) and Anisotropic displacement parameters (Å^2 x 10^3). U(eq) is defined as one third of the trace of the orthogonalized Uij tensor. The anisotropic displacement factor exponent takes the form: $-2\pi^2[h^2a^{*2}U11 + ... + 2hka^*b^*U12]$

Atom	x	y	z	U(eq)	U11	U22	U33	U23	U13	U12
P(1)	496(1)	3132(1)	8018(1)	71(1)	79(1)	62(1)	70(1)	1(1)	-8(1)	1(1)
Si(1)	1165(1)	2773(1)	8686(1)	66(1)	75(1)	61(1)	60(1)	-1(1)	-3(1)	-2(1)
P(2)	302(1)	1075(1)	7819(1)	89(1)	102(1)	63(1)	97(1)	5(1)	-33(1)	-2(1)
Si(11)	2010(1)	1973(1)	8350(1)	80(1)	81(1)	79(1)	80(1)	-6(1)	2(1)	4(1)
Si(12)	875(1)	1354(1)	9393(1)	78(1)	89(1)	72(1)	71(1)	8(1)	3(1)	5(1)
Si(13)	1329(1)	4907(1)	9081(1)	78(1)	93(1)	64(1)	77(1)	-6(1)	-2(1)	-5(1)
O(1)	1087(1)	3467(4)	6570(1)	111(1)	121(3)	131(3)	80(2)	28(2)	4(2)	14(2)
C(121)	984(2)	-454(4)	9217(2)	101(1)	126(4)	68(3)	110(3)	17(2)	14(3)	8(3)
C(131)	1979(2)	4978(5)	9554(2)	105(2)	105(3)	106(3)	104(3)	-20(3)	-7(3)	-29(3)
C(122)	110(2)	1648(5)	9514(2)	112(2)	96(3)	118(4)	121(4)	24(3)	16(3)	9(3)
C(11)	1287(3)	2107(7)	6647(2)	182(3)	270(9)	185(7)	96(4)	45(4)	47(5)	120(6)
C(132)	704(2)	5401(4)	9482(2)	97(1)	129(4)	81(3)	82(3)	-13(2)	3(3)	1(3)
C(111)	1911(2)	353(4)	7969(2)	91(1)	99(3)	89(3)	84(3)	-6(2)	2(2)	17(2)
C(112)	2539(2)	1635(5)	8925(2)	127(2)	90(3)	143(4)	146(5)	-60(4)	-23(3)	48(3)
C(12)	1454(3)	1573(6)	6136(3)	145(2)	147(5)	155(6)	131(5)	16(5)	-2(4)	31(4)
C(133)	1436(2)	6170(4)	8522(2)	98(1)	123(4)	61(2)	109(3)	2(2)	1(3)	-5(2)
C(123)	1301(2)	1703(5)	10048(2)	112(2)	128(4)	117(4)	88(3)	24(3)	-6(3)	11(3)
C(113)	2299(2)	3279(4)	7862(2)	114(2)	116(4)	99(3)	131(4)	-3(3)	48(3)	-5(3)
C(14)	1166(2)	3827(6)	6011(2)	123(2)	141(5)	123(4)	104(4)	35(3)	1(3)	-26(4)
C(13)	1528(3)	2693(7)	5770(2)	149(2)	206(7)	143(5)	100(4)	18(4)	34(4)	-14(5)
Si(2)	6165(1)	2090(1)	3690(1)	67(1)	73(1)	61(1)	66(1)	-1(1)	-2(1)	1(1)
P(3)	5506(1)	1685(1)	3014(1)	70(1)	77(1)	62(1)	72(1)	-5(1)	-5(1)	2(1)
Si(21)	5763(1)	3009(1)	4469(1)	77(1)	91(1)	73(1)	67(1)	-7(1)	1(1)	2(1)
Si(22)	6896(1)	3490(1)	3412(1)	86(1)	87(1)	86(1)	85(1)	-5(1)	2(1)	-18(1)
Si(23)	6565(1)	-14(1)	3924(1)	87(1)	97(1)	71(1)	92(1)	-2(1)	-14(1)	13(1)
P(4A)	5437(2)	3673(4)	2709(2)	83(1)	93(3)	63(2)	91(3)	-8(2)	-19(2)	2(2)
P(4B)	4817(2)	3703(4)	2084(2)	80(1)	94(3)	58(1)	87(2)	6(2)	-20(2)	2(2)
C(221)	7175(2)	2904(5)	2758(2)	123(2)	122(4)	139(4)	112(4)	5(3)	31(3)	-17(3)
C(211)	5181(2)	1949(5)	4683(2)	111(2)	137(4)	95(3)	105(3)	-19(3)	33(3)	-7(3)

Atom	x	y	z	U(eq)	U11	U22	U33	U23	U13	U12
C(212)	6301(2)	3172(7)	5052(2)	148(2)	123(4)	238(7)	81(3)	-47(4)	-15(3)	-3(4)
C(231)	7053(3)	46(6)	4542(3)	210(4)	278(9)	148(6)	188(7)	-50(5)	-145(6)	91(6)
C(222)	7507(2)	3387(9)	3926(2)	202(4)	128(5)	349(11)	127(5)	27(6)	-15(4)	-106(6)
C(213)	5480(2)	4733(4)	4303(2)	126(2)	167(5)	80(3)	137(4)	6(3)	62(4)	29(3)
C(232)	6000(2)	-1307(5)	4042(3)	146(2)	168(5)	80(3)	193(6)	32(3)	43(5)	0(3)
C(233)	6981(2)	-659(5)	3347(2)	126(2)	124(4)	88(3)	167(5)	-15(3)	7(4)	25(3)
C(223)	6667(3)	5231(5)	3315(3)	197(4)	184(6)	66(3)	351(10)	13(4)	136(7)	-18(4)
O(2)	605(1)	6112(3)	6955(2)	123(1)	99(2)	102(2)	165(3)	63(2)	-33(2)	-20(2)
C(23)	480(3)	8001(6)	6423(3)	135(2)	112(5)	141(5)	153(5)	50(4)	14(4)	20(4)
C(21)	1113(2)	6862(7)	7033(2)	156(3)	121(4)	204(7)	139(5)	68(5)	-39(4)	-82(5)
Li(1)	538(3)	4178(7)	7033(3)	91(2)	90(5)	79(5)	102(5)	28(4)	-18(4)	-13(4)
C(24)	198(2)	7033(5)	6729(3)	130(2)	116(4)	96(4)	174(6)	22(4)	-23(4)	-4(3)
C(22)	1037(3)	8079(5)	6675(3)	148(2)	171(6)	86(4)	187(6)	25(4)	8(5)	-29(4)
Li(2)	4404(3)	1232(8)	3045(3)	95(2)	105(6)	91(5)	89(5)	19(4)	1(4)	-5(4)
O(3)	3923(8)	2138(14)	3502(10)	100(7)	128(14)	50(8)	124(14)	-15(8)	36(10)	23(8)
C(31)	3877(8)	3592(13)	3500(11)	130(7)	175(14)	74(9)	140(15)	3(8)	-10(11)	-5(9)
C(32)	3329(7)	3909(11)	3730(9)	123(5)	130(10)	67(7)	172(13)	5(8)	-3(10)	24(7)
C(33)	3231(10)	2760(20)	4128(9)	154(7)	147(15)	131(13)	187(14)	-34(12)	34(13)	-3(12)
C(34)	3543(9)	1625(15)	3908(10)	116(6)	122(13)	83(9)	147(14)	-6(8)	51(11)	-8(9)
O(3A)	3905(7)	2080(14)	3548(9)	97(6)	99(10)	87(9)	108(10)	23(7)	13(8)	-31(6)
C(31A)	3897(7)	3462(15)	3734(9)	129(6)	129(10)	88(8)	166(15)	33(9)	-28(9)	-29(8)
C(32A)	3443(7)	3585(19)	4122(10)	159(6)	145(12)	117(11)	218(15)	-30(12)	18(12)	-11(9)
C(33A)	3030(6)	2474(16)	3950(8)	140(6)	108(9)	130(10)	182(13)	-47(9)	12(9)	-19(7)
C(34A)	3379(7)	1445(12)	3701(8)	106(5)	101(9)	78(7)	139(12)	-11(7)	12(8)	-23(6)
O(4)	4293(7)	-582(9)	3176(3)	88(4)	112(9)	68(4)	82(5)	20(3)	-8(4)	-25(5)
C(41)	4482(7)	-1178(12)	3657(4)	127(5)	160(11)	101(9)	119(8)	25(7)	-18(7)	-4(8)
C(42)	4541(5)	-2660(11)	3541(4)	125(5)	160(10)	85(8)	128(8)	7(6)	-28(7)	27(7)
C(43)	4094(5)	-2928(9)	3125(5)	125(4)	159(9)	47(4)	166(10)	4(6)	-21(8)	15(5)
C(44)	4012(6)	-1678(8)	2810(4)	134(4)	183(11)	85(6)	130(8)	29(5)	-41(7)	-68(6)
O(4A)	4157(11)	-810(15)	3172(7)	96(6)	92(10)	66(8)	130(11)	25(7)	12(8)	-22(8)
C(41A)	4265(11)	-1533(18)	3646(6)	113(7)	169(16)	61(9)	111(11)	26(8)	34(10)	-14(10)
C(42A)	4353(12)	-2973(19)	3468(7)	137(8)	186(17)	64(10)	161(16)	0(12)	5(15)	29(13)
C(43A)	4651(7)	-2826(13)	2963(5)	124(5)	157(13)	94(9)	120(11)	-1(8)	-17(9)	18(9)
C(44A)	4461(9)	-1557(12)	2718(5)	130(6)	165(14)	75(9)	151(12)	10(9)	19(11)	-32(10)

7.5.3 Bond length (Å)

Atoms	Bond length	Atoms	Bond length	Atoms	Bond length
P(1)-P(2)	2.1389(15)	P(3)-P(4A)	2.110(4)	Li(2)-O(4)	1.846(12)
P(1)-Si(1)	2.2456(15)	P(3)-P(4B)#2	2.150(4)	Li(2)-O(3A)	1.936(14)
P(1)-Li(1)	2.620(7)	P(3)-Li(2)#2	2.637(7)	Li(2)-O(4A)	2.13(2)
P(1)-Li(1)#1	2.659(7)	P(3)-Li(2)	2.657(8)	Li(2)-P(3)#2	2.637(7)
Si(1)-Si(11)	2.3392(15)	Si(21)-C(211)	1.829(4)	Li(2)-P(4A)#2	3.069(8)
Si(1)-Si(13)	2.3473(15)	Si(21)-C(213)	1.872(4)	Li(2)-P(4B)#2	3.092(8)
Si(1)-Si(12)	2.3513(15)	Si(21)-C(212)	1.870(5)	O(3)-C(31)	1.445(9)
P(2)-P(2)#1	2.065(2)	Si(22)-C(223)	1.821(5)	O(3)-C(34)	1.460(10)
Si(11)-C(111)	1.864(4)	Si(22)-C(221)	1.846(5)	C(31)-C(32)	1.475(12)
Si(11)-C(112)	1.866(5)	Si(22)-C(222)	1.873(6)	C(32)-C(33)	1.516(14)
Si(11)-C(113)	1.906(4)	Si(23)-C(231)	1.856(6)	C(33)-C(34)	1.465(10)
Si(12)-C(121)	1.863(4)	Si(23)-C(233)	1.869(5)	O(3A)-C(31A)	1.442(9)
Si(12)-C(123)	1.878(5)	Si(23)-C(232)	1.885(5)	O(3A)-C(34A)	1.460(10)
Si(12)-C(122)	1.877(4)	P(4A)-P(4B)	2.065(3)	C(31A)-C(32A)	1.470(12)
Si(13)-C(133)	1.874(4)	P(4A)-Li(2)#2	3.069(8)	C(32A)-C(33A)	1.519(14)
Si(13)-C(131)	1.881(5)	P(4B)-P(3)#2	2.150(4)	C(33A)-C(34A)	1.463(10)
Si(13)-C(132)	1.879(4)	P(4B)-Li(2)#2	3.092(8)	O(4)-C(41)	1.369(7)
O(1)-C(14)	1.428(5)	O(2)-C(21)	1.421(5)	O(4)-C(44)	1.537(11)
O(1)-C(11)	1.437(6)	O(2)-C(24)	1.420(5)	C(41)-C(42)	1.503(10)
O(1)-Li(1)	1.899(9)	O(2)-Li(1)	1.932(7)	C(42)-C(43)	1.455(12)
C(11)-C(12)	1.425(7)	C(23)-C(24)	1.405(6)	C(43)-C(44)	1.465(9)

C(12)-C(13)	1.439(7)	C(23)-C(22)	1.430(7)	O(4A)-C(41A)	1.372(9)
C(14)-C(13)	1.545(7)	C(21)-C(22)	1.494(7)	O(4A)-C(44A)	1.536(13)
Si(2)-P(3)	2.2505(15)	Li(1)-P(1)#1	2.659(7)	C(41A)-C(42A)	1.509(11)
Si(2)-Si(22)	2.3449(16)	Li(1)-Li(1)#1	3.498(15)	C(42A)-C(43A)	1.455(14)
Si(2)-Si(21)	2.3488(15)	Li(2)-O(3)	1.862(14)	C(43A)-C(44A)	1.454(10)
Si(2)-Si(23)	2.3485(15)				

7.5.4 Bond Angle (deg).

Atoms	Angle	Atoms	Angle
P(2)-P(1)-Si(1)	98.62(6)	P(4A)-P(4B)-Li(2)#2	69.8(2)
P(2)-P(1)-Li(1)	100.74(17)	P(3)#2-P(4B)-Li(2)#2	57.60(17)
Si(1)-P(1)-Li(1)	131.99(16)	C(21)-O(2)-C(24)	105.8(4)
P(2)-P(1)-Li(1)#1	99.99(16)	C(21)-O(2)-Li(1)	125.4(4)
Si(1)-P(1)-Li(1)#1	135.56(17)	C(24)-O(2)-Li(1)	128.1(4)
Li(1)-P(1)-Li(1)#1	83.0(3)	C(24)-C(23)-C(22)	105.2(5)
P(1)-Si(1)-Si(11)	112.84(6)	O(2)-C(21)-C(22)	105.4(5)
P(1)-Si(1)-Si(13)	104.59(6)	O(1)-Li(1)-O(2)	104.3(4)
Si(11)-Si(1)-Si(13)	108.66(6)	O(1)-Li(1)-P(1)	117.1(3)
P(1)-Si(1)-Si(12)	113.83(6)	O(2)-Li(1)-P(1)	119.3(4)
Si(11)-Si(1)-Si(12)	109.79(6)	O(1)-Li(1)-P(1)#1	119.0(4)
Si(13)-Si(1)-Si(12)	106.69(6)	O(2)-Li(1)-P(1)#1	117.5(3)
P(2)#1-P(2)-P(1)	107.72(4)	P(1)-Li(1)-P(1)#1	79.25(19)
C(111)-Si(11)-C(112)	106.5(2)	O(1)-Li(1)-Li(1)#1	158.2(2)
C(111)-Si(11)-C(113)	108.3(2)	O(2)-Li(1)-Li(1)#1	97.5(3)
C(112)-Si(11)-C(113)	109.9(2)	P(1)-Li(1)-Li(1)#1	48.97(19)
C(111)-Si(11)-Si(1)	112.16(14)	P(1)#1-Li(1)-Li(1)#1	48.02(18)
C(112)-Si(11)-Si(1)	110.80(15)	C(23)-C(24)-O(2)	108.1(4)
C(113)-Si(11)-Si(1)	109.15(15)	C(23)-C(22)-C(21)	106.9(5)
C(121)-Si(12)-C(123)	107.4(2)	O(3)-Li(2)-O(4)	105.6(7)
C(121)-Si(12)-C(122)	109.3(2)	O(3)-Li(2)-O(3A)	3.4(12)
C(123)-Si(12)-C(122)	108.9(2)	O(4)-Li(2)-O(3A)	102.5(6)
C(121)-Si(12)-Si(1)	110.92(14)	O(3)-Li(2)-O(4A)	101.0(7)
C(123)-Si(12)-Si(1)	110.35(15)	O(4)-Li(2)-O(4A)	7.8(11)
C(122)-Si(12)-Si(1)	109.87(15)	O(3A)-Li(2)-O(4A)	98.0(6)
C(133)-Si(13)-C(131)	106.6(2)	O(3)-Li(2)-P(3)#2	125.7(9)
C(133)-Si(13)-C(132)	109.9(2)	O(4)-Li(2)-P(3)#2	110.7(4)
C(131)-Si(13)-C(132)	108.4(2)	O(3A)-Li(2)-P(3)#2	128.7(8)
C(133)-Si(13)-Si(1)	109.24(14)	O(4A)-Li(2)-P(3)#2	109.8(5)
C(131)-Si(13)-Si(1)	113.57(15)	O(3)-Li(2)-P(3)	124.6(8)
C(132)-Si(13)-Si(1)	109.10(14)	O(4)-Li(2)-P(3)	108.5(6)
C(14)-O(1)-C(11)	107.5(4)	O(3A)-Li(2)-P(3)	125.3(7)
C(14)-O(1)-Li(1)	126.8(4)	O(4A)-Li(2)-P(3)	116.2(7)
C(11)-O(1)-Li(1)	120.1(4)	P(3)#2-Li(2)-P(3)	79.6(2)
C(12)-C(11)-O(1)	109.7(5)	O(3)-Li(2)-P(4A)#2	94.2(7)
C(11)-C(12)-C(13)	107.5(6)	O(4)-Li(2)-P(4A)#2	153.2(4)
O(1)-C(14)-C(13)	106.3(4)	O(3A)-Li(2)-P(4A)#2	97.6(6)
C(12)-C(13)-C(14)	103.9(5)	O(4A)-Li(2)-P(4A)#2	151.2(6)
P(3)-Si(2)-Si(22)	113.08(6)	P(3)#2-Li(2)-P(4A)#2	42.56(13)
P(3)-Si(2)-Si(21)	111.40(6)	P(3)-Li(2)-P(4A)#2	72.63(18)
Si(22)-Si(2)-Si(21)	109.79(6)	O(3)-Li(2)-P(4B)#2	93.8(6)
P(3)-Si(2)-Si(23)	106.10(6)	O(4)-Li(2)-P(4B)#2	151.5(6)
Si(22)-Si(2)-Si(23)	107.46(6)	O(3A)-Li(2)-P(4B)#2	96.2(5)
Si(21)-Si(2)-Si(23)	108.80(6)	O(4A)-Li(2)-P(4B)#2	159.3(7)
P(4A)-P(3)-P(4B)#2	21.72(9)	P(3)#2-Li(2)-P(4B)#2	71.91(18)
P(4A)-P(3)-Si(2)	97.55(12)	P(3)-Li(2)-P(4B)#2	43.11(13)
P(4B)#2-P(3)-Si(2)	98.46(11)	P(4A)#2-Li(2)-P(4B)#2	39.16(10)
P(4A)-P(3)-Li(2)#2	79.74(19)	C(31)-O(3)-C(34)	107.5(7)
P(4B)#2-P(3)-Li(2)#2	95.36(19)	C(31)-O(3)-Li(2)	121.7(12)

Atoms	Angle	Atoms	Angle
Si(2)-P(3)-Li(2)#2	131.29(18)	C(34)-O(3)-Li(2)	130.7(10)
P(4A)-P(3)-Li(2)	96.14(19)	O(3)-C(31)-C(32)	106.1(8)
P(4B)#2-P(3)-Li(2)	79.29(19)	C(31)-C(32)-C(33)	104.4(10)
Si(2)-P(3)-Li(2)	131.27(17)	C(34)-C(33)-C(32)	104.3(9)
Li(2)#2-P(3)-Li(2)	97.1(2)	O(3)-C(34)-C(33)	108.6(8)
C(211)-Si(21)-C(213)	108.5(2)	C(31A)-O(3A)-C(34A)	107.7(7)
C(211)-Si(21)-C(212)	109.3(3)	C(31A)-O(3A)-Li(2)	128.9(10)
C(213)-Si(21)-C(212)	108.1(3)	C(34A)-O(3A)-Li(2)	122.0(11)
C(211)-Si(21)-Si(2)	110.39(14)	O(3A)-C(31A)-C(32A)	107.5(8)
C(213)-Si(21)-Si(2)	109.51(15)	C(31A)-C(32A)-C(33A)	104.3(10)
C(212)-Si(21)-Si(2)	111.00(17)	C(34A)-C(33A)-C(32A)	104.3(9)
C(223)-Si(22)-C(221)	107.6(3)	O(3A)-C(34A)-C(33A)	108.3(7)
C(223)-Si(22)-C(222)	110.8(4)	C(41)-O(4)-C(44)	107.9(7)
C(221)-Si(22)-C(222)	105.1(3)	C(41)-O(4)-Li(2)	121.6(10)
C(223)-Si(22)-Si(2)	112.22(18)	C(44)-O(4)-Li(2)	130.5(7)
C(221)-Si(22)-Si(2)	111.29(17)	O(4)-C(41)-C(42)	106.8(7)
C(222)-Si(22)-Si(2)	109.6(2)	C(43)-C(42)-C(41)	103.8(8)
C(231)-Si(23)-C(233)	106.8(3)	C(42)-C(43)-C(44)	106.5(7)
C(231)-Si(23)-C(232)	108.6(3)	C(43)-C(44)-O(4)	104.5(6)
C(233)-Si(23)-C(232)	106.7(2)	C(41A)-O(4A)-C(44A)	106.2(9)
C(231)-Si(23)-Si(2)	113.43(19)	C(41A)-O(4A)-Li(2)	125.1(15)
C(233)-Si(23)-Si(2)	110.00(17)	C(44A)-O(4A)-Li(2)	102.2(10)
C(232)-Si(23)-Si(2)	111.01(17)	O(4A)-C(41A)-C(42A)	105.9(9)
P(4B)-P(4A)-P(3)	108.3(3)	C(43A)-C(42A)-C(41A)	103.2(11)
P(4B)-P(4A)-Li(2)#2	71.0(2)	C(44A)-C(43A)-C(42A)	106.2(10)
P(3)-P(4A)-Li(2)#2	57.71(17)	C(43A)-C(44A)-O(4A)	105.6(8)
P(4A)-P(4B)-P(3)#2	107.9(2)		

Symmetry transformations used to generate equivalent atoms:
#1 -x,y,-z+3/2   #2 -x+1,y,-z+1/2

7.6 Crystallographic data for $Hyp_2P_3Li\cdot 2(MeNCH_2)_3$

7.6.1 Crystal data and structure refinement

Empirical formula	$Hyp_2P_3Li\cdot$3triazine(toluene)
Formula weight	945.74
Temperature	173(2) K
Wavelength	0.71073 Å
Crystal system, space group	monoclinic, P2(1)/n
Unit cell dimensions	a = 15.3307(10) Å alpha = 90 deg. b = 16.4357(10) Å beta = 98.311(3) deg. c = 24.0715(15) Å gamma = 90 deg.
Volume	6001.6(7) $Å^3$
Z, Calculated density	4, 1.047 g/cm^3
Absorption coefficient	0.287 mm^{-1}
F(000)	2064
Theta range for data collection	2.37 to 28.46 deg.
Limiting indices	-20<=h<=20, -21<=k<=21, -31<=l<=32
Reflections collected / unique	106062 / 14990 [R(int) = 0.0983]
Completeness to theta = 28.46	98.9 %
Refinement method	Full-matrix least-squares on F^2
Data / restraints / parameters	14990 / 177 / 596

Goodness-of-fit on F^2	1.006
Final R indices [I>2sigma(I)]	R1 = 0.0459, wR2 = 0.1004
R indices (all data)	R1 = 0.1065, wR2 = 0.1243
Largest diff. peak and hole	0.363 and -0.254 e.Å^{-3}

7.6.2 Atomic coordinates (x 10^4), equivalent isotropic displacement parameters (Å^2 x 10^3) and Anisotropic displacement parameters (Å^2 x 10^3). U(eq) is defined as one third of the trace of the orthogonalized Uij tensor. The anisotropic displacement factor exponent takes the form: $-2\pi^2[h^2a^{*2}U11 + ... + 2hka^*b^*U12]$

Atom	x	y	z	U(eq)	U11	U22	U33	U23	U13	U12
P(2)	9268(1)	1564(1)	1544(1)	31(1)	26(1)	34(1)	33(1)	-6(1)	7(1)	1(1)
Si(13)	12790(1)	1569(1)	2035(1)	36(1)	26(1)	39(1)	42(1)	-4(1)	2(1)	1(1)
P(3)	8417(1)	1257(1)	826(1)	33(1)	26(1)	43(1)	32(1)	-8(1)	6(1)	1(1)
P(1)	10528(1)	1369(1)	1349(1)	34(1)	25(1)	41(1)	37(1)	-9(1)	7(1)	0(1)
Si(1)	11312(1)	1672(1)	2185(1)	32(1)	27(1)	31(1)	39(1)	-6(1)	5(1)	-1(1)
Si(2)	7116(1)	1531(1)	1110(1)	32(1)	25(1)	36(1)	35(1)	-2(1)	8(1)	1(1)
Si(23)	6091(1)	1604(1)	288(1)	43(1)	26(1)	57(1)	44(1)	0(1)	2(1)	-2(1)
Si(22)	6663(1)	473(1)	1654(1)	41(1)	35(1)	44(1)	49(1)	3(1)	16(1)	-3(1)
Si(21)	7127(1)	2756(1)	1608(1)	40(1)	39(1)	40(1)	45(1)	-6(1)	14(1)	6(1)
Si(12)	11059(1)	2953(1)	2556(1)	44(1)	40(1)	38(1)	54(1)	-17(1)	5(1)	0(1)
Si(11)	11133(1)	716(1)	2879(1)	46(1)	48(1)	44(1)	44(1)	2(1)	5(1)	-8(1)
N(43)	9596(1)	1241(1)	-766(1)	34(1)	39(1)	35(1)	31(1)	-3(1)	11(1)	-2(1)
C(231)	4939(2)	1431(2)	437(1)	55(1)	30(1)	67(2)	68(2)	8(2)	4(1)	-3(1)
C(131)	13566(2)	1448(2)	2705(1)	59(1)	39(2)	82(2)	51(2)	-1(2)	-5(1)	3(1)
C(232)	6126(2)	2620(2)	-61(1)	64(1)	44(2)	86(2)	60(2)	27(2)	3(1)	-7(2)
C(221)	5680(2)	768(2)	1992(1)	62(1)	49(2)	74(2)	69(2)	4(2)	33(2)	-2(1)
C(132)	12929(2)	657(2)	1592(1)	61(1)	41(2)	60(2)	81(2)	-23(2)	8(2)	7(1)
C(211)	7555(2)	2574(2)	2365(1)	54(1)	47(2)	67(2)	48(2)	-17(1)	9(1)	6(1)
C(133)	13180(2)	2470(2)	1672(1)	61(1)	44(2)	61(2)	80(2)	12(2)	17(2)	-4(1)
C(121)	12032(2)	3249(2)	3081(1)	56(1)	64(2)	47(2)	54(2)	-15(1)	-5(2)	-11(1)
C(212)	5986(2)	3194(2)	1559(1)	58(1)	54(2)	66(2)	57(2)	-1(2)	17(1)	21(1)
C(222)	7568(2)	184(2)	2226(1)	58(1)	62(2)	56(2)	55(2)	15(1)	10(2)	-1(1)
C(223)	6360(2)	-452(2)	1216(1)	57(1)	54(2)	47(2)	74(2)	-3(1)	19(2)	-11(1)
C(111)	9950(2)	539(2)	2936(2)	74(1)	59(2)	78(2)	89(3)	20(2)	21(2)	-14(2)
C(213)	7854(2)	3525(2)	1333(1)	59(1)	65(2)	39(2)	77(2)	-9(1)	27(2)	-3(1)
C(112)	11618(2)	-287(2)	2726(2)	75(1)	85(2)	47(2)	90(3)	13(2)	2(2)	7(2)
C(122)	10884(2)	3749(2)	2002(1)	71(1)	83(2)	42(2)	80(2)	-10(2)	-18(2)	14(2)
C(113)	11716(3)	1055(2)	3579(1)	82(1)	108(3)	92(3)	43(2)	5(2)	5(2)	-31(2)
C(233)	6334(2)	802(2)	-221(1)	69(1)	47(2)	101(3)	55(2)	-23(2)	-3(1)	0(2)
C(123)	10077(2)	2951(2)	2934(2)	90(1)	65(2)	87(2)	126(3)	-60(2)	42(2)	-9(2)
N(41)	11118(1)	1344(1)	-490(1)	41(1)	39(1)	38(1)	46(1)	1(1)	8(1)	0(1)
N(31)	9412(1)	3262(1)	-330(1)	41(1)	41(1)	39(1)	42(1)	3(1)	8(1)	0(1)
N(33)	10462(1)	3800(1)	-844(1)	42(1)	47(1)	41(1)	38(1)	3(1)	8(1)	-4(1)
N(42)	10497(1)	1697(1)	-1401(1)	44(1)	52(1)	43(1)	42(1)	7(1)	23(1)	4(1)
N(32)	10894(1)	3261(1)	53(1)	44(1)	41(1)	48(1)	40(1)	8(1)	-1(1)	1(1)
C(43)	9719(2)	1217(2)	-1350(1)	39(1)	50(2)	35(1)	35(2)	-2(1)	14(1)	2(1)
C(42)	10345(2)	855(2)	-429(1)	39(1)	45(1)	34(1)	39(2)	-1(1)	11(1)	-3(1)
C(413)	8767(2)	841(2)	-687(1)	47(1)	44(1)	54(2)	47(2)	-2(1)	15(1)	-9(1)
C(33)	10010(2)	3359(2)	187(1)	44(1)	53(2)	44(2)	38(2)	-4(1)	9(1)	3(1)
C(32)	9571(2)	3906(2)	-721(1)	43(1)	50(2)	38(1)	42(2)	3(1)	6(1)	5(1)
C(41)	11258(2)	1314(2)	-1075(1)	49(1)	46(2)	42(2)	63(2)	1(1)	24(1)	-1(1)
C(331)	10652(2)	4372(2)	-1274(1)	63(1)	67(2)	75(2)	46(2)	15(2)	10(2)	-11(2)
C(31)	11082(2)	3895(2)	-330(1)	46(1)	46(2)	45(2)	47(2)	-1(1)	4(1)	-5(1)
C(311)	8494(2)	3236(2)	-239(1)	63(1)	48(2)	77(2)	66(2)	17(2)	13(2)	2(2)
C(412)	10607(2)	1783(2)	-1991(1)	70(1)	85(2)	79(2)	54(2)	22(2)	38(2)	9(2)
C(411)	11891(2)	1085(2)	-104(1)	61(1)	48(2)	60(2)	71(2)	2(2)	-2(2)	-2(1)

Atom	x	y	z	U(eq)	U11	U22	U33	U23	U13	U12
C(321)	11555(2)	3250(2)	552(1)	76(1)	60(2)	108(3)	55(2)	25(2)	-13(2)	-12(2)
Li	10315(3)	2419(2)	-642(2)	44(1)	47(2)	34(2)	53(3)	-6(2)	15(2)	3(2)
C(01)	3687(4)	4053(4)	-104(3)	86(2)	71(3)	95(3)	95(4)	-14(3)	17(3)	12(3)
C(011)	3930(8)	4382(6)	474(4)	143(4)	181(10)	114(8)	128(8)	-45(6)	3(7)	2(7)
C(02)	3486(6)	4573(5)	-559(4)	89(2)	79(4)	79(4)	113(4)	0(4)	26(4)	3(3)
C(03)	3316(5)	4275(5)	-1068(3)	91(2)	76(4)	102(4)	99(4)	26(4)	25(3)	1(3)
C(04)	3290(5)	3495(5)	-1186(3)	87(2)	74(3)	113(5)	79(4)	-11(4)	30(3)	-9(4)
C(05)	3494(5)	2935(5)	-733(3)	82(2)	70(3)	80(4)	96(4)	-19(4)	18(4)	-1(3)
C(06)	3658(7)	3240(4)	-220(3)	71(2)	62(3)	68(4)	83(4)	16(3)	17(4)	18(3)
C(07)	3523(7)	3643(7)	-641(5)	79(2)	68(3)	83(4)	91(4)	-2(3)	32(3)	3(3)
C(071)	3249(12)	3030(9)	-1093(7)	105(6)	112(12)	94(11)	110(14)	-8(12)	14(10)	-39(10)
C(08)	3741(16)	3438(11)	-58(7)	84(3)	68(5)	84(5)	103(6)	9(5)	22(5)	15(5)
C(09)	3934(10)	3959(9)	334(7)	103(3)	72(5)	125(6)	112(6)	-3(6)	14(6)	12(5)
C(0A)	4031(10)	4798(9)	182(7)	110(3)	101(6)	115(6)	115(6)	-25(6)	21(6)	4(5)
C(0B)	3813(9)	4977(9)	-347(6)	109(3)	100(5)	99(5)	126(6)	-7(5)	14(5)	5(5)
C(0C)	3602(13)	4447(9)	-755(7)	93(3)	86(5)	92(5)	105(5)	5(5)	27(5)	4(4)

7.6.3 Bond lengths [Å].

Atoms	Bond length	Atoms	Bond length	Atoms	Bond length
P(2)-P(3)	2.0730(8)	Si(12)-C(121)	1.874(3)	N(32)-C(33)	1.445(3)
P(2)-P(1)	2.0774(8)	Si(11)-C(111)	1.862(3)	N(32)-C(31)	1.447(3)
Si(13)-C(133)	1.862(3)	Si(11)-C(112)	1.865(3)	N(32)-C(321)	1.456(3)
Si(13)-C(132)	1.869(3)	Si(11)-C(113)	1.875(3)	N(32)-Li	2.252(5)
Si(13)-C(131)	1.870(3)	N(43)-C(43)	1.447(3)	C(43)-Li	2.682(5)
Si(13)-Si(1)	2.3509(9)	N(43)-C(42)	1.452(3)	C(42)-Li	2.619(5)
P(3)-Si(2)	2.2459(8)	N(43)-C(413)	1.468(3)	C(33)-Li	2.617(5)
P(1)-Si(1)	2.2454(9)	N(43)-Li	2.227(4)	C(32)-Li	2.693(5)
Si(1)-Si(11)	2.3385(10)	N(41)-C(41)	1.455(3)	C(41)-Li	2.628(5)
Si(1)-Si(12)	2.3415(9)	N(41)-C(42)	1.456(3)	C(31)-Li	2.752(5)
Si(2)-Si(21)	2.3414(9)	N(41)-C(411)	1.459(3)	C(01)-C(06)	1.365(10)
Si(2)-Si(22)	2.3420(9)	N(41)-Li	2.153(4)	C(01)-C(02)	1.388(10)
Si(2)-Si(23)	2.3446(10)	N(31)-C(33)	1.443(3)	C(01)-C(011)	1.487(10)
Si(23)-C(233)	1.873(3)	N(31)-C(311)	1.455(3)	C(02)-C(03)	1.310(10)
Si(23)-C(232)	1.872(3)	N(31)-C(32)	1.460(3)	C(03)-C(04)	1.312(10)
Si(23)-C(231)	1.874(2)	N(31)-Li	2.170(4)	C(04)-C(05)	1.428(10)
Si(22)-C(222)	1.869(3)	N(33)-C(32)	1.449(3)	C(05)-C(06)	1.321(9)
Si(22)-C(223)	1.870(3)	N(33)-C(31)	1.454(3)	C(07)-C(0C)	1.360(16)
Si(22)-C(221)	1.879(3)	N(33)-C(331)	1.458(3)	C(07)-C(08)	1.434(16)
Si(21)-C(213)	1.868(3)	N(33)-Li	2.340(4)	C(07)-C(071)	1.499(15)
Si(21)-C(211)	1.871(3)	N(42)-C(43)	1.449(3)	C(08)-C(09)	1.277(16)
Si(21)-C(212)	1.879(3)	N(42)-C(41)	1.452(3)	C(09)-C(0A)	1.439(17)
Si(12)-C(122)	1.860(3)	N(42)-C(412)	1.461(3)	C(0A)-C(0B)	1.303(15)
Si(12)-C(123)	1.867(3)	N(42)-Li	2.230(5)	C(0B)-C(0C)	1.317(15)

7.6.4 Bond Angles (deg).

Atoms	Angle	Atoms	Angle
P(3)-P(2)-P(1)	105.52(3)	N(31)-C(33)-Li	55.99(15)
C(133)-Si(13)-C(132)	107.40(14)	N(32)-C(33)-Li	59.26(15)
C(133)-Si(13)-C(131)	106.42(14)	N(33)-C(32)-N(31)	107.2(2)
C(132)-Si(13)-C(131)	107.17(14)	N(33)-C(32)-Li	60.22(14)
C(133)-Si(13)-Si(1)	113.36(9)	N(31)-C(32)-Li	53.51(14)
C(132)-Si(13)-Si(1)	109.67(9)	N(42)-C(41)-N(41)	106.8(2)
C(131)-Si(13)-Si(1)	112.51(9)	N(42)-C(41)-Li	58.03(16)

Atoms	Angle	Atoms	Angle
P(2)-P(3)-Si(2)	100.20(3)	N(41)-C(41)-Li	54.97(15)
P(2)-P(1)-Si(1)	99.10(3)	N(32)-C(31)-N(33)	107.4(2)
P(1)-Si(1)-Si(11)	112.82(3)	N(32)-C(31)-Li	54.76(15)
P(1)-Si(1)-Si(12)	116.39(4)	N(33)-C(31)-Li	58.23(15)
Si(11)-Si(1)-Si(12)	106.79(4)	N(41)-Li-N(31)	147.5(2)
P(1)-Si(1)-Si(13)	104.46(3)	N(41)-Li-N(43)	64.49(13)
Si(11)-Si(1)-Si(13)	106.04(3)	N(31)-Li-N(43)	105.88(18)
Si(12)-Si(1)-Si(13)	109.89(3)	N(41)-Li-N(42)	64.30(13)
P(3)-Si(2)-Si(21)	112.76(3)	N(31)-Li-N(42)	141.8(2)
P(3)-Si(2)-Si(22)	111.68(3)	N(43)-Li-N(42)	62.96(13)
Si(21)-Si(2)-Si(22)	109.43(4)	N(41)-Li-N(32)	103.0(2)
P(3)-Si(2)-Si(23)	105.65(3)	N(31)-Li-N(32)	63.42(13)
Si(21)-Si(2)-Si(23)	110.01(3)	N(43)-Li-N(32)	140.2(2)
Si(22)-Si(2)-Si(23)	107.10(3)	N(42)-Li-N(32)	148.6(2)
C(233)-Si(23)-C(232)	108.32(16)	N(41)-Li-N(33)	139.6(2)
C(233)-Si(23)-C(231)	107.43(13)	N(31)-Li-N(33)	62.41(12)
C(232)-Si(23)-C(231)	108.06(13)	N(43)-Li-N(33)	151.2(2)
C(233)-Si(23)-Si(2)	110.05(10)	N(42)-Li-N(33)	108.60(19)
C(232)-Si(23)-Si(2)	111.38(10)	N(32)-Li-N(33)	61.19(12)
C(231)-Si(23)-Si(2)	111.45(10)	N(41)-Li-C(33)	121.0(2)
C(222)-Si(22)-C(223)	107.83(14)	N(31)-Li-C(33)	33.46(10)
C(222)-Si(22)-C(221)	107.63(14)	N(43)-Li-C(33)	118.43(18)
C(223)-Si(22)-C(221)	107.72(13)	N(42)-Li-C(33)	174.7(2)
C(222)-Si(22)-Si(2)	110.69(9)	N(32)-Li-C(33)	33.47(10)
C(223)-Si(22)-Si(2)	110.96(10)	N(33)-Li-C(33)	67.58(13)
C(221)-Si(22)-Si(2)	111.83(10)	N(41)-Li-C(42)	33.77(9)
C(213)-Si(21)-C(211)	107.99(14)	N(31)-Li-C(42)	123.61(19)
C(213)-Si(21)-C(212)	108.44(13)	N(43)-Li-C(42)	33.65(9)
C(211)-Si(21)-C(212)	108.31(12)	N(42)-Li-C(42)	68.73(13)
C(213)-Si(21)-Si(2)	111.19(9)	N(32)-Li-C(42)	117.7(2)
C(211)-Si(21)-Si(2)	109.75(9)	N(33)-Li-C(42)	173.3(2)
C(212)-Si(21)-Si(2)	111.07(10)	C(33)-Li-C(42)	115.49(18)
C(122)-Si(12)-C(123)	107.94(18)	N(41)-Li-C(41)	33.61(10)
C(122)-Si(12)-C(121)	108.60(14)	N(31)-Li-C(41)	173.8(2)
C(123)-Si(12)-C(121)	106.95(15)	N(43)-Li-C(41)	68.68(13)
C(122)-Si(12)-Si(1)	111.92(10)	N(42)-Li-C(41)	33.51(10)
C(123)-Si(12)-Si(1)	111.98(11)	N(32)-Li-C(41)	122.6(2)
C(121)-Si(12)-Si(1)	109.28(9)	N(33)-Li-C(41)	120.86(18)
C(111)-Si(11)-C(112)	107.31(15)	C(33)-Li-C(41)	151.5(2)
C(111)-Si(11)-C(113)	108.87(17)	C(42)-Li-C(41)	53.47(11)
C(112)-Si(11)-C(113)	106.73(17)	N(41)-Li-C(43)	68.76(13)
C(111)-Si(11)-Si(1)	111.90(11)	N(31)-Li-C(43)	121.0(2)
C(112)-Si(11)-Si(1)	111.20(11)	N(43)-Li-C(43)	32.64(9)
C(113)-Si(11)-Si(1)	110.63(11)	N(42)-Li-C(43)	32.70(9)
C(43)-N(43)-C(42)	109.10(19)	N(32)-Li-C(43)	170.5(2)
C(43)-N(43)-C(413)	110.56(19)	N(33)-Li-C(43)	128.0(2)
C(42)-N(43)-C(413)	111.25(18)	C(33)-Li-C(43)	146.84(19)
C(43)-N(43)-Li	91.27(17)	C(42)-Li-C(43)	52.89(11)
C(42)-N(43)-Li	88.18(17)	C(41)-Li-C(43)	52.81(11)
C(413)-N(43)-Li	142.48(18)	N(41)-Li-C(32)	169.3(2)
C(41)-N(41)-C(42)	108.4(2)	N(31)-Li-C(32)	32.75(9)
C(41)-N(41)-C(411)	112.7(2)	N(43)-Li-C(32)	125.69(19)
C(42)-N(41)-C(411)	111.8(2)	N(42)-Li-C(32)	121.8(2)
C(41)-N(41)-Li	91.41(19)	N(32)-Li-C(32)	67.12(13)
C(42)-N(41)-Li	90.96(17)	N(33)-Li-C(32)	32.50(9)
C(411)-N(41)-Li	137.7(2)	C(33)-Li-C(32)	52.94(11)
C(33)-N(31)-C(311)	112.4(2)	C(42)-Li-C(32)	154.13(19)
C(33)-N(31)-C(32)	109.3(2)	C(41)-Li-C(32)	148.3(2)
C(311)-N(31)-C(32)	112.0(2)	C(43)-Li-C(32)	121.44(19)
C(33)-N(31)-Li	90.54(18)	N(41)-Li-C(31)	117.77(19)
C(311)-N(31)-Li	135.5(2)	N(31)-Li-C(31)	67.12(13)

Atoms	Angle	Atoms	Angle
C(32)-N(31)-Li	93.73(18)	N(43)-Li-C(31)	170.7(2)
C(32)-N(33)-C(31)	109.4(2)	N(42)-Li-C(31)	126.38(19)
C(32)-N(33)-C(331)	111.0(2)	N(32)-Li-C(31)	31.66(9)
C(31)-N(33)-C(331)	111.2(2)	N(33)-Li-C(31)	31.90(9)
C(32)-N(33)-Li	87.28(17)	C(33)-Li-C(31)	52.30(11)
C(31)-N(33)-Li	89.87(18)	C(42)-Li-C(31)	144.8(2)
C(331)-N(33)-Li	143.9(2)	C(41)-Li-C(31)	118.63(17)
C(43)-N(42)-C(41)	109.0(2)	C(43)-Li-C(31)	156.20(19)
C(43)-N(42)-C(412)	110.2(2)	C(32)-Li-C(31)	51.59(11)
C(41)-N(42)-C(412)	111.8(2)	C(06)-C(01)-C(02)	116.3(7)
C(43)-N(42)-Li	91.07(17)	C(06)-C(01)-C(011)	122.9(8)
C(41)-N(42)-Li	88.46(19)	C(02)-C(01)-C(011)	120.8(8)
C(412)-N(42)-Li	142.3(2)	C(03)-C(02)-C(01)	120.0(8)
C(33)-N(32)-C(31)	110.0(2)	C(02)-C(03)-C(04)	124.2(7)
C(33)-N(32)-C(321)	112.4(2)	C(03)-C(04)-C(05)	117.9(7)
C(31)-N(32)-C(321)	110.9(2)	C(06)-C(05)-C(04)	117.5(7)
C(33)-N(32)-Li	87.26(18)	C(05)-C(06)-C(01)	124.0(8)
C(31)-N(32)-Li	93.58(19)	C(0C)-C(07)-C(08)	114.3(12)
C(321)-N(32)-Li	139.2(2)	C(0C)-C(07)-C(071)	122.0(13)
N(43)-C(43)-N(42)	107.0(2)	C(08)-C(07)-C(071)	123.7(13)
N(43)-C(43)-Li	56.09(14)	C(09)-C(08)-C(07)	124.1(17)
N(42)-C(43)-Li	56.24(14)	C(08)-C(09)-C(0A)	118.4(16)
N(43)-C(42)-N(41)	106.97(19)	C(0B)-C(0A)-C(09)	116.3(14)
N(43)-C(42)-Li	58.17(14)	C(0A)-C(0B)-C(0C)	125.5(15)
N(41)-C(42)-Li	55.27(14)	C(0B)-C(0C)-C(07)	120.7(15)
N(31)-C(33)-N(32)	107.2(2)		

7.7 Crystallographic data for $Hyp_3P_5Na_2$

7.7.1 Crystal data and structure refinement

Empirical formula	$Hyp_3P_5Na_2 \cdot 1/3C_5H_{12}$
Formula weight	967.88
Temperature	293(2) K
Wavelength	0.71073 Å
Crystal system, space group	monoclinic, P2(1)/n
Unit cell dimensions	a = 45.543(2) Å alpha = 90 deg. b = 25.3055(9) Å beta = 106.608(3) deg. c = 48.6244(19) Å gamma = 90 deg.
Volume	53701(4) Å^3
Z, Calculated density	36, 1.077 g/cm^3
Absorption coefficient	0.428 mm^{-1}
F(000)	18792
Theta range for data collection	1.56 to 21.00 deg.
Limiting indices	-45<=h<=0, -25<=k<=0, -43<=l<=48
Reflections collected / unique	55236 / 55236 [R(int) = 0.0000]
Completeness to theta = 21.00	95.8 %
Refinement method	Full-matrix least-squares on F^2
Data / restraints / parameters	55236 / 180 / 3929
Goodness-of-fit on F^2	0.688
Final R indices [I>2sigma(I)]	R1 = 0.0722, wR2 = 0.1602
R indices (all data)	R1 = 0.1679, wR2 = 0.1830
Largest diff. peak and hole	0.753 and -0.418 e.Å^{-3}

7.7.2 Atomic coordinates (x 10^4), equivalent isotropic displacement parameters (Å ^{2} x 10^3). U(eq) is defined as one third of the trace of the orthogonalized Uij tensor.

Atom	x	y	z	U(eq)
SiDA	11090(1)	11581(1)	2393(1)	85(1)
SiDB	10579(1)	11302(2)	2391(2)	120(3)
C(0D1)	10466(4)	11591(10)	2690(4)	248(17)
C(0D2)	10599(5)	10570(7)	2451(6)	288(19)
C(0D3)	10294(3)	11526(7)	2051(4)	114(7)
SiDC	11124(1)	12473(2)	2491(2)	97(2)
C(0D4)	11502(5)	12730(9)	2503(6)	227(12)
C(0D5)	11085(5)	12597(8)	2864(5)	189(10)
C(0D6)	10840(5)	12874(8)	2208(5)	160(10)
SiDD	11142(2)	11380(3)	1948(1)	166(4)
C(0D7)	10870(3)	11741(6)	1633(4)	122(6)
C(0D8)	11531(4)	11709(10)	1946(6)	273(16)
C(0D9)	11160(5)	10729(8)	1871(6)	306(17)
SiDE	10685(4)	11053(8)	2150(5)	150(6)
C(0DA)	10360(10)	11390(20)	1902(13)	180(40)
C(0DB)	10858(8)	10569(13)	1931(8)	39(13)
C(0DC)	10522(16)	10690(20)	2416(13)	200(40)
SiDF	10975(6)	12371(7)	2563(5)	123(6)
C(0DD)	10758(11)	12828(16)	2293(10)	63(19)
C(0DE)	10753(15)	12290(20)	2835(12)	200(40)
C(0DF)	11355(10)	12724(18)	2752(13)	130(20)
SiDG	11375(7)	11770(11)	2067(6)	228(8)
C(0DG)	11752(11)	12140(20)	2216(14)	240(50)
C(0DH)	11137(16)	12280(20)	1804(13)	550(150)
C(0DI)	11431(10)	11225(15)	1878(9)	56(15)
SiPA	7076(1)	3353(1)	1764(1)	86(1)
SiPB	7512(1)	2952(3)	1684(2)	78(2)
C(0P1)	7670(7)	3415(11)	1466(6)	106(16)
C(0P2)	7805(6)	2752(10)	2007(5)	106(11)
C(0P3)	7381(4)	2329(7)	1491(5)	107(8)
SiPC	7277(1)	4021(2)	2128(1)	70(2)
C(0P4)	7575(4)	4445(7)	2033(4)	77(6)
C(0P5)	6955(5)	4493(8)	2125(5)	89(8)
C(0P6)	7440(4)	3720(7)	2484(4)	87(7)
SiPD	6809(1)	2744(2)	1937(2)	85(2)
C(0P7)	6542(5)	2329(8)	1642(5)	73(8)
C(0P8)	7084(4)	2226(7)	2175(4)	93(7)
C(0P9)	6599(5)	3041(9)	2177(5)	89(9)
SiPE	6923(2)	3577(4)	2162(2)	99(4)
C(0PA)	7250(7)	3393(13)	2479(6)	140(15)
C(0PB)	6863(7)	4296(10)	2147(8)	98(13)
C(0PC)	6572(6)	3254(12)	2183(8)	97(15)
SiPF	7571(2)	3389(5)	1816(3)	110(4)
C(0PD)	7694(8)	3299(15)	1480(6)	58(15)
C(0PE)	7821(8)	2921(13)	2086(8)	116(17)
C(0PF)	7679(7)	4086(10)	1954(8)	149(16)
SiPG	6877(3)	2417(3)	1658(3)	116(4)
C(0PG)	6447(5)	2411(15)	1590(11)	150(30)
C(0PH)	7053(6)	1969(10)	1978(6)	108(12)
C(0PI)	6999(8)	2163(12)	1353(7)	155(16)
SiWA	8092(1)	10019(1)	1632(1)	94(1)
SiWB	8314(1)	9199(2)	1850(2)	88(2)
C(0W1)	8102(6)	8631(9)	1647(7)	116(15)

Atom	x	y	z	U(eq)
C(0W2)	8717(4)	9160(8)	1831(5)	122(8)
C(0W3)	8275(4)	9107(7)	2212(4)	95(7)
SiWC	8381(2)	10710(3)	1888(2)	103(2)
C(0W4)	8571(6)	10613(10)	2274(5)	130(9)
C(0W5)	8117(5)	11305(7)	1868(5)	136(9)
C(0W6)	8679(6)	10914(10)	1713(6)	117(8)
SiWD	7593(2)	10051(3)	1653(2)	116(3)
C(0W7)	7412(6)	10749(10)	1516(6)	124(11)
C(0W8)	7559(7)	9984(12)	2018(6)	197(12)
C(0W9)	7378(7)	9428(12)	1455(7)	184(13)
SiWE	8566(2)	10247(5)	1934(2)	123(4)
C(0WA)	8825(7)	9661(11)	1979(8)	139(10)
C(0WB)	8751(8)	10783(12)	1781(9)	111(9)
C(0WC)	8577(8)	10356(15)	2308(6)	136(11)
SiWF	7709(3)	10643(5)	1694(3)	137(4)
C(0WD)	7645(9)	10562(16)	2053(7)	197(14)
C(0WE)	7838(9)	11334(10)	1646(10)	200(20)
C(0WF)	7332(5)	10552(12)	1418(6)	78(11)
SiWG	7910(7)	9214(5)	1735(4)	338(6)
C(0WG)	7860(30)	9220(30)	2126(12)	2000(600)
C(0WH)	7526(10)	9090(20)	1490(13)	290(40)
C(0WI)	8148(14)	8626(18)	1644(19)	310(70)
P(1J)	7009(1)	5281(1)	789(1)	66(1)
P(4E)	12225(1)	9704(1)	2836(1)	62(1)
P(1I)	6391(1)	3787(1)	1396(1)	77(1)
P(4D)	11571(1)	8925(1)	2677(1)	63(1)
P(4C)	12033(1)	8938(1)	2633(1)	66(1)
P(9E)	9566(1)	4586(1)	153(1)	70(1)
P(3C)	11280(1)	11147(1)	3067(1)	69(1)
P(9D)	10208(1)	3801(1)	364(1)	71(1)
P(3E)	12108(1)	11201(1)	3412(1)	73(1)
P(2E)	5023(1)	1091(1)	2448(1)	64(1)
P(1H)	6180(1)	4540(1)	1188(1)	70(1)
P(1G)	6922(1)	6025(1)	1355(1)	73(1)
P(4B)	12378(1)	8949(1)	3069(1)	70(1)
P(1F)	6775(1)	6009(1)	572(1)	74(1)
P(2D)	4675(1)	1097(1)	2006(1)	67(1)
P(2C)	4829(1)	339(1)	2234(1)	60(1)
P(1D)	6314(1)	6003(1)	619(1)	70(1)
P(1C)	6294(1)	3773(1)	626(1)	74(1)
P(5E)	5772(1)	-1104(1)	2091(1)	72(1)
P(1B)	7130(1)	6065(1)	1001(1)	76(1)
P(5D)	4979(1)	-1097(1)	1631(1)	71(1)
P(2B)	5493(1)	1121(1)	2420(1)	66(1)
P(2A)	4906(1)	1131(1)	1672(1)	65(1)
P(1E)	6855(1)	3795(1)	1359(1)	69(1)
P(5C)	5647(1)	-340(1)	1856(1)	65(1)
P(5B)	5459(1)	-1093(1)	1637(1)	69(1)
P(3B)	11454(1)	10404(1)	3297(1)	64(1)
P(3D)	11467(1)	11125(1)	2701(1)	72(1)
Si(4A)	7412(1)	5121(1)	608(1)	69(1)
P(5A)	5510(1)	-1121(1)	2405(1)	72(1)
P(3A)	11656(1)	11173(1)	3482(1)	69(1)
Si(9A)	5688(1)	1675(1)	2793(1)	67(1)
P(4A)	12158(1)	8926(1)	3411(1)	70(1)
P(9C)	9744(1)	3946(1)	-422(1)	74(1)
SiHA	12634(1)	9888(1)	2671(1)	72(1)
SiNA	6076(1)	-166(1)	1718(1)	71(1)
SiIA	9107(1)	4724(1)	248(1)	82(1)
P(1A)	6055(1)	3774(1)	956(1)	76(1)
Si(7B)	7298(1)	4277(1)	408(1)	81(1)

Atom	x	y	z	U(eq)
SiQA	7175(1)	6681(1)	1634(1)	82(1)
SiZA	8391(1)	8188(1)	417(1)	76(1)
P(9B)	9719(1)	3781(1)	314(1)	82(1)
SiCA	11151(1)	10209(1)	3584(1)	71(1)
P(8E)	8098(1)	9925(1)	1172(1)	86(1)
SiHD	12510(1)	10675(1)	2405(1)	84(1)
P(6D)	8505(1)	9059(1)	461(1)	77(1)
SiRA	6092(1)	6472(1)	220(1)	84(1)
P(8D)	8135(1)	10817(1)	645(1)	83(1)
P(6C)	9005(1)	9117(1)	517(1)	86(1)
P(8C)	7528(1)	9940(1)	421(1)	82(1)
SiFA	11361(1)	8421(1)	2291(1)	69(1)
SiGA	12467(1)	8332(1)	3705(1)	76(1)
SiTA	5758(1)	4686(1)	1344(1)	75(1)
SiKA	5813(1)	-1669(1)	2734(1)	80(1)
Si(8A)	4551(1)	1586(1)	1339(1)	68(1)
P(6B)	8670(1)	9188(1)	77(1)	82(1)
SiTE	5851(1)	5513(1)	1571(1)	83(1)
SiYA	9608(1)	9712(1)	964(1)	92(1)
SiLA	4822(1)	-1633(1)	1249(1)	77(1)
SiAC	4092(1)	812(1)	2423(1)	86(1)
P(6A)	9123(1)	9904(1)	706(1)	85(1)
SiND	6204(1)	-798(2)	1417(1)	87(1)
SiHC	12753(1)	9234(1)	2375(1)	83(1)
SiAA	4463(1)	155(1)	2451(1)	68(1)
SiGD	12138(1)	7882(1)	3922(1)	88(1)
P(8B)	7635(1)	10745(1)	583(1)	84(1)
Si(9D)	5341(1)	2297(1)	2882(1)	82(1)
P(6E)	8548(1)	10005(1)	-46(1)	85(1)
SiEA	12328(1)	11795(1)	3758(1)	82(1)
SiTD	5664(1)	4082(2)	1677(1)	95(1)
SiUA	8199(1)	11696(1)	597(1)	91(1)
Na(1)	6292(1)	4888(2)	618(1)	93(2)
SiNC	5962(1)	638(1)	1465(1)	83(1)
SiIC	9203(1)	5428(2)	569(1)	97(1)
P(9A)	9447(1)	3892(1)	-144(1)	81(1)
SiSA	6025(1)	3128(2)	342(1)	90(1)
SiCD	10788(1)	10830(1)	3635(1)	93(1)
SiKD	6162(1)	-1210(2)	3115(1)	93(1)
Na(16)	11533(1)	10029(2)	2703(1)	80(1)
Na(2)	4973(1)	18(2)	1656(1)	78(1)
SiJA	9460(1)	3506(1)	-810(1)	86(1)
SiNB	6470(1)	-46(1)	2142(1)	84(1)
Na(13)	6895(1)	4906(2)	1355(1)	91(2)
SiHB	13033(1)	10053(2)	3094(1)	83(1)
Si(4C)	7470(1)	5691(2)	249(1)	90(1)
SiGB	12844(1)	8751(1)	4080(1)	87(1)
Si(1D)	10118(1)	3280(2)	1085(1)	95(1)
SiVA	8584(1)	9987(2)	-498(1)	96(1)
SiFD	11383(1)	8790(2)	1857(1)	92(1)
P(8A)	7966(1)	10727(1)	1029(1)	96(1)
Si(1A)	10332(1)	3162(1)	698(1)	84(1)
Si(1C)	10194(1)	2312(2)	505(1)	101(1)
Si(1B)	10867(1)	3235(2)	860(1)	97(1)
SiCC	10902(1)	9426(1)	3400(1)	87(1)
SiRD	5869(1)	5887(2)	-154(1)	96(1)
Si(4B)	7855(1)	5107(1)	1004(1)	78(1)
SiLC	4292(1)	-1696(2)	1181(1)	92(1)
SiFC	11565(1)	7562(1)	2349(1)	82(1)
SiAB	4241(1)	-600(1)	2209(1)	90(1)
Na(3)	5019(1)	-1740(2)	2099(1)	92(2)

Atom	x	y	z	U(eq)
SiTB	5339(1)	4731(2)	934(1)	95(1)
SiYC	9629(1)	9086(2)	1328(1)	97(1)
Si(9C)	6053(1)	2150(1)	2639(1)	83(1)
SiSB	6328(1)	2841(2)	50(1)	90(1)
SiKC	5477(1)	-2127(2)	2938(1)	102(1)
Si(9B)	5941(1)	1239(1)	3222(1)	85(1)
Na(14)	5522(1)	0(2)	2428(1)	78(1)
Si(8C)	4333(1)	2318(1)	1501(1)	86(1)
SiRC	6416(1)	7061(2)	69(1)	95(1)
SiJC	9195(1)	4108(2)	-1167(1)	100(1)
SiLD	5037(1)	-2483(1)	1350(1)	101(1)
SiXA	7027(1)	10038(1)	188(1)	90(1)
SiRB	5710(1)	6969(2)	338(1)	107(2)
SiYB	9796(1)	10506(2)	1189(1)	119(2)
SiCB	11507(1)	10020(2)	4035(1)	98(1)
Na(4)	12152(1)	10061(2)	3432(1)	82(1)
SiZB	8235(1)	8000(1)	825(1)	88(1)
Si(8B)	4167(1)	1028(1)	1058(1)	89(1)
SiFB	10845(1)	8413(1)	2298(1)	80(1)
Na(12)	10225(1)	3314(2)	-134(1)	99(2)
Si(8D)	4843(1)	1919(2)	1048(1)	93(1)
Na(6)	5387(1)	1775(2)	1944(1)	115(2)
SiUB	8738(1)	11770(2)	738(1)	109(2)
Na(9)	11657(1)	8289(2)	3146(1)	95(2)
SiJB	9817(1)	3069(2)	-994(1)	94(1)
SiAD	4721(1)	-52(1)	2927(1)	90(1)
SiYD	9933(1)	9423(2)	696(1)	105(1)
SiIB	8786(1)	5005(2)	-205(1)	104(1)
Na(5)	6816(1)	3178(2)	884(1)	94(2)
Na(8)	11975(1)	11765(2)	2905(1)	103(2)
Na(10)	8607(1)	9924(2)	930(1)	98(2)
SiXD	6831(1)	9166(2)	188(1)	110(2)
SiZD	7988(1)	8156(2)	-10(1)	98(1)
SiLB	4906(1)	-1285(2)	827(1)	99(1)
Na(7)	6380(1)	6561(2)	1115(1)	102(2)
SiGC	12711(1)	7702(1)	3490(1)	90(1)
Na(11)	8030(1)	9972(2)	173(1)	90(2)
SiVC	8934(1)	9377(2)	-589(1)	117(2)
SiZC	8764(1)	7558(2)	396(1)	99(1)
SiXC	6732(1)	10554(2)	407(1)	127(2)
SiKB	6074(1)	-2315(2)	2552(1)	102(1)
SiQD	7702(1)	6631(2)	1840(1)	115(2)
SiJD	9128(1)	2841(2)	-749(1)	110(2)
SiVD	8109(1)	9910(2)	-855(1)	121(2)
SiUD	7951(1)	11878(2)	116(1)	132(2)
Na(17)	9757(1)	5070(2)	-392(1)	89(2)
SiID	8882(1)	4013(2)	413(1)	113(2)
SiVB	8783(1)	10831(2)	-545(1)	117(2)
SiXB	6943(1)	10311(2)	-286(1)	120(2)
SiUC	8017(1)	12251(2)	899(1)	121(2)
SiED	12705(1)	12194(2)	3592(2)	164(3)
SiSC	5985(2)	2355(2)	615(2)	215(4)
SiQC	6931(1)	6733(3)	1993(1)	173(3)
SiQB	7088(1)	7515(2)	1396(1)	150(2)
SiEC	12021(1)	12462(2)	3844(2)	174(3)
SiEB	12576(2)	11366(3)	4191(1)	208(3)
Na(15)	7561(1)	9409(2)	919(1)	137(2)
SiSD	5562(1)	3407(4)	38(2)	229(4)
Na(18)	9118(1)	10439(3)	223(1)	145(2)
C(1)	11196(2)	8914(4)	3401(3)	84(4)
C(2)	6301(3)	132(5)	2436(3)	99(4)

Atom	x	y	z	U(eq)
C(3)	12864(2)	10175(4)	3398(2)	86(4)
C(4)	11566(3)	7279(4)	2705(3)	90(4)
C(5)	5012(3)	-572(4)	890(3)	94(4)
C(6)	7317(2)	3808(4)	708(3)	83(4)
C(7)	5872(3)	6022(4)	1297(3)	96(4)
C(8)	11340(3)	7116(4)	2050(3)	100(5)
C(9)	10919(3)	11524(4)	3652(3)	104(5)
C(10)	9328(2)	6008(4)	394(3)	106(5)
C(11)	9001(3)	7744(5)	153(3)	116(5)
C(12)	6307(2)	1679(4)	2508(3)	91(4)
C(13)	4072(3)	2131(5)	1730(3)	117(5)
C(14)	5905(3)	1156(4)	1711(3)	107(5)
C(15)	5471(2)	4908(5)	626(3)	102(4)
C(16)	13252(3)	10664(5)	3061(3)	124(5)
C(17)	13301(3)	9478(5)	3180(3)	113(5)
C(18)	5486(3)	6547(5)	520(3)	109(5)
C(19)	11510(3)	9488(4)	1914(3)	112(5)
C(20)	12451(3)	9174(5)	2018(3)	104(5)
C(21)	5941(3)	4188(5)	2047(3)	103(4)
C(22)	8534(3)	8195(5)	1144(3)	101(4)
C(23)	4097(3)	2705(4)	1185(3)	105(5)
C(24)	10814(3)	8166(5)	2649(3)	98(4)
C(25)	4257(2)	1463(4)	2558(3)	79(4)
C(26)	4531(2)	-1145(4)	2304(3)	80(4)
C(27)	5932(3)	-786(5)	1056(3)	125(5)
C(28)	6229(2)	-1477(4)	1563(3)	98(5)
C(29)	10584(2)	7986(5)	2013(3)	101(5)
C(30)	6379(3)	-2047(5)	2397(3)	122(5)
C(31)	7168(3)	5539(5)	-105(2)	98(4)
C(32)	13033(3)	8004(5)	3372(3)	126(6)
C(34)	7746(3)	5002(5)	1336(3)	109(5)
C(35)	4124(3)	-479(4)	1809(3)	111(5)
C(36)	13028(3)	8279(5)	4371(3)	143(6)
C(37)	12428(3)	7390(6)	3176(3)	156(7)
C(38)	8896(3)	11349(5)	1058(3)	119(5)
C(39)	5060(3)	5260(6)	965(3)	133(6)
C(41)	6683(3)	7399(4)	365(3)	120(5)
C(42)	6699(2)	-657(4)	2241(3)	100(4)
C(43)	4989(3)	-2725(5)	1696(3)	117(5)
C(44)	4206(3)	-1906(5)	1522(3)	104(5)
C(46)	12813(3)	8564(4)	2538(3)	100(5)
C(47)	4756(3)	525(4)	3164(3)	104(5)
C(48)	4117(3)	-1053(5)	1074(3)	132(6)
C(50)	3829(2)	869(5)	2048(3)	104(5)
C(51)	6732(3)	498(5)	2105(3)	126(5)
C(52)	7790(3)	8813(4)	-76(3)	108(5)
C(53)	7912(3)	6555(6)	1562(3)	144(6)
C(54)	8260(3)	12133(5)	1296(3)	124(5)
C(55)	8538(3)	5579(5)	-148(3)	128(6)
C(56)	8066(3)	5751(4)	1020(3)	99(4)
C(57)	12256(3)	12993(5)	4070(3)	129(6)
C(58)	8890(3)	3364(4)	217(3)	118(5)
C(59)	11016(3)	3240(5)	551(3)	123(6)
C(60)	6629(3)	6735(5)	-160(3)	103(5)
C(61)	8119(2)	4558(4)	976(3)	99(4)
C(62)	7870(3)	8402(5)	793(3)	114(5)
C(63)	9642(3)	2559(5)	-1277(3)	124(5)
C(64)	12317(3)	7292(5)	4147(3)	122(5)
C(65)	13120(3)	9458(5)	2304(3)	116(5)
C(66)	5668(3)	3374(4)	1564(3)	101(4)
C(67)	7460(2)	6395(4)	346(3)	92(4)

Atom	x	y	z	U(eq)
C(68)	11654(3)	8428(5)	1707(3)	108(5)
C(69)	5849(3)	2589(5)	2322(3)	125(6)
C(70)	9034(3)	5234(5)	-441(3)	122(5)
C(71)	5608(3)	582(5)	1166(3)	150(7)
C(73)	10387(3)	3048(6)	1427(3)	132(6)
C(74)	12385(3)	11179(5)	2624(3)	108(5)
C(75)	6234(3)	5505(5)	1852(3)	132(6)
C(76)	7594(3)	12177(5)	852(3)	134(6)
C(77)	7903(3)	11246(5)	-94(3)	132(5)
C(78)	4853(3)	-2980(5)	1073(3)	141(6)
C(79)	5267(3)	4227(5)	1703(3)	122(5)
C(80)	11889(3)	9887(5)	3975(3)	119(5)
C(81)	8159(3)	8038(5)	-333(3)	108(5)
C(82)	5516(3)	5576(5)	-92(3)	114(5)
C(83)	8870(3)	11547(6)	411(3)	138(6)
C(84)	9283(3)	9327(6)	-274(3)	143(6)
C(85)	5056(2)	2532(4)	2540(3)	91(4)
C(87)	6249(2)	815(5)	3160(3)	99(4)
C(88)	6590(2)	-609(5)	1386(3)	110(5)
C(90)	10696(3)	10661(5)	3982(3)	115(5)
C(91)	5805(3)	-2715(6)	2262(4)	195(9)
C(92)	13149(3)	9042(6)	3946(3)	139(6)
C(93)	12672(3)	9284(6)	4235(3)	147(7)
C(94)	5446(3)	7270(5)	20(3)	133(6)
C(95)	10349(4)	2193(5)	194(3)	165(7)
C(96)	6563(3)	10061(6)	-535(3)	171(7)
C(97)	9022(3)	7402(5)	767(3)	125(5)
C(99)	7570(3)	4059(4)	208(3)	96(4)
C(011)	6877(3)	11242(5)	481(4)	161(8)
C(012)	10672(3)	9537(5)	3023(3)	105(5)
C(013)	11974(2)	7538(4)	2338(3)	89(4)
C(015)	10115(2)	2735(5)	-696(3)	104(5)
C(016)	12843(3)	10947(5)	2299(3)	121(5)
C(017)	9207(3)	10891(6)	-296(4)	155(7)
C(018)	5556(3)	5716(5)	1734(3)	124(6)
C(019)	5555(3)	2900(4)	3057(3)	116(5)
C(110)	8071(3)	12948(4)	794(3)	134(6)
C(111)	3858(3)	586(5)	2663(3)	114(5)
C(112)	8144(3)	7270(4)	849(3)	117(5)
C(113)	6281(4)	-2773(6)	2851(4)	192(9)
C(114)	6289(3)	3288(5)	-245(3)	134(6)
C(115)	11792(3)	7626(5)	3645(3)	115(5)
C(116)	4637(3)	2740(5)	1726(3)	116(5)
C(117)	6897(2)	4278(5)	151(3)	103(5)
C(118)	6226(3)	2149(5)	-91(3)	117(5)
C(119)	10700(2)	9116(4)	2258(3)	87(4)
C(120)	9286(3)	9192(6)	1459(3)	144(6)
C(121)	5465(3)	-2492(5)	1389(4)	137(6)
C(122)	5741(3)	6231(5)	-506(3)	117(5)
C(123)	12897(3)	7156(5)	3741(3)	139(6)
C(124)	6323(3)	10601(6)	140(5)	214(11)
C(125)	3895(3)	-803(5)	2321(4)	160(8)
C(127)	8544(3)	6943(5)	249(3)	125(5)
C(128)	10944(3)	3894(5)	1077(3)	130(6)
C(129)	10355(3)	1784(5)	780(3)	124(6)
C(130)	8873(3)	12448(5)	841(3)	143(6)
C(131)	4104(3)	-2184(5)	896(3)	119(5)
C(132)	5131(3)	2025(5)	3136(3)	105(5)
C(133)	6275(3)	853(5)	1316(3)	114(5)
C(134)	11067(3)	2685(5)	1086(3)	127(6)
C(135)	6168(3)	7593(5)	-155(3)	141(7)

Atom	x	y	z	U(eq)
C(136)	9625(3)	8395(4)	1196(3)	122(5)
C(137)	10042(3)	4010(5)	1123(3)	118(5)
C(138)	4513(3)	-591(5)	3061(3)	134(6)
C(139)	10656(3)	9185(5)	3624(3)	104(5)
C(142)	8199(4)	12328(8)	-19(4)	219(10)
C(143)	10429(3)	10760(5)	3328(3)	144(6)
C(144)	12201(3)	10571(5)	2074(3)	158(7)
C(145)	5977(3)	-600(5)	3199(3)	128(6)
C(146)	9076(3)	3978(5)	804(3)	108(5)
C(147)	8856(3)	5620(5)	680(3)	119(5)
C(148)	10992(3)	8770(8)	1577(3)	179(8)
C(149)	6317(3)	2571(5)	2931(3)	114(5)
C(150)	6506(3)	6918(6)	1816(4)	164(8)
C(151)	6682(3)	7569(6)	1145(4)	150(7)
C(152)	9687(3)	11046(5)	928(3)	150(7)
C(153)	5238(4)	-1652(5)	739(4)	164(8)
C(154)	9524(3)	5201(5)	907(3)	124(5)
C(155)	7899(3)	9289(5)	-795(3)	134(6)
C(156)	6400(2)	9159(5)	83(3)	133(6)
C(157)	9436(3)	4727(4)	-1160(3)	112(5)
C(158)	9758(3)	2912(5)	1033(3)	117(5)
C(160)	7704(3)	7634(5)	6(3)	121(5)
C(161)	6973(3)	8866(5)	568(3)	128(6)
C(163)	6746(2)	2810(5)	268(3)	110(5)
C(164)	4568(3)	-1347(6)	506(3)	175(8)
C(165)	5652(3)	-2719(5)	3167(3)	136(6)
C(166)	8819(3)	3075(6)	-592(3)	152(7)
C(167)	9048(4)	9597(6)	-913(4)	170(7)
C(168)	5116(3)	-267(5)	2941(3)	112(5)
C(169)	6148(3)	5325(5)	-154(3)	113(5)
C(170)	9120(3)	3800(5)	-1543(3)	117(5)
C(171)	11389(3)	9395(5)	4197(3)	127(6)
C(172)	5665(3)	809(5)	3347(3)	114(5)
C(173)	6120(3)	1734(5)	3520(3)	136(6)
C(174)	9371(3)	2325(5)	-491(4)	172(8)
C(175)	7841(3)	7267(6)	2044(4)	164(8)
C(176)	6961(3)	11027(5)	-307(3)	128(5)
C(177)	5887(3)	7473(6)	589(4)	158(7)
C(178)	10045(3)	3559(5)	-1143(3)	112(5)
C(179)	8904(3)	2592(6)	-1120(3)	149(7)
C(180)	8553(3)	11371(5)	-447(3)	136(6)
C(181)	11792(6)	12133(10)	4123(7)	420(30)
C(183)	10323(3)	9223(5)	953(3)	126(6)
C(185)	9760(3)	2222(5)	353(3)	135(6)
C(186)	8819(3)	4261(6)	-1103(3)	135(6)
C(187)	8468(3)	4181(5)	354(3)	136(6)
C(188)	12953(3)	11760(6)	3503(4)	191(9)
C(189)	11999(3)	8336(5)	4169(3)	152(7)
C(190)	7855(2)	5553(5)	188(3)	120(5)
C(191)	5769(5)	2438(7)	871(5)	273(14)
C(192)	5128(3)	4092(5)	872(3)	125(5)
C(193)	9780(3)	8862(6)	469(3)	127(6)
C(194)	7756(4)	6034(5)	2053(3)	160(7)
C(195)	3903(4)	1387(6)	755(4)	290(17)
C(197)	9630(3)	10626(5)	1502(3)	127(5)
C(199)	4933(4)	1424(6)	825(4)	181(8)
C(200)	11551(3)	10593(6)	4290(3)	136(6)
C(03B)	5345(6)	5028(8)	2535(6)	208(12)
C(234)	7567(3)	12200(5)	87(4)	158(7)
C(238)	9994(3)	9968(6)	461(3)	152(7)
C(217)	5141(3)	-2377(5)	2641(3)	132(6)

Atom	x	y	z	U(eq)
C(237)	10238(3)	10514(6)	1324(4)	193(9)
C(240)	8773(4)	10985(6)	-921(3)	156(7)
C(01B)	5450(5)	5974(8)	2533(5)	204(10)
C(221)	3937(4)	786(7)	1290(4)	207(10)
C(233)	8536(3)	4443(5)	-403(3)	140(6)
C(242)	6955(3)	8728(5)	-69(3)	131(6)
C(235)	7873(3)	10533(6)	-878(4)	182(8)
C(219)	4683(5)	2482(8)	834(5)	307(18)
C(241)	8761(3)	8692(5)	-652(3)	136(6)
C(215)	6515(3)	-1009(6)	3012(3)	132(6)
C(201)	7358(3)	7586(8)	1174(5)	258(13)
C(216)	6290(4)	-1616(5)	3450(3)	165(7)
C(222)	4343(3)	461(5)	922(4)	177(9)
C(243)	6679(4)	10223(7)	729(4)	203(9)
C(239)	9984(3)	9170(6)	1651(3)	146(6)
C(236)	8154(4)	9808(8)	-1230(3)	229(11)
C(220)	5243(4)	2106(7)	1305(4)	203(9)
C(203)	6971(4)	6038(11)	2171(4)	311(18)
C(218)	5318(4)	-1686(6)	3164(4)	177(8)
C(244)	7257(3)	10020(6)	-435(3)	166(7)
C(230)	12602(9)	10804(9)	4189(6)	770(60)
C(228)	12485(5)	12552(8)	3213(5)	276(14)
C(05B)	5227(7)	4062(8)	2547(5)	247(15)
C(02)	5524(7)	9424(12)	-16(8)	282(17)
C(229)	12938(3)	12707(7)	3836(4)	217(11)
C(04B)	5254(6)	4551(11)	2625(5)	226(12)
C(03)	5503(6)	9754(15)	206(6)	242(14)
C(205)	5406(3)	2874(9)	-235(5)	328(19)
C(223)	11764(5)	12712(8)	3531(5)	360(20)
C(208)	6456(4)	2220(8)	885(5)	235(11)
C(204)	7098(4)	7199(13)	2270(6)	440(30)
C(04)	5432(6)	10343(14)	148(9)	380(40)
C(202)	7107(4)	8048(7)	1690(6)	319(19)
C(05)	5371(15)	10610(20)	344(12)	720(40)
C(206)	5294(3)	3512(12)	248(6)	450(30)
C(209)	5821(8)	1780(9)	411(7)	470(30)
C(207)	5601(6)	4000(9)	-123(4)	310(20)
C(231)	12861(6)	11789(8)	4438(6)	420(30)
C(01)	5532(7)	8820(10)	42(5)	297(17)
C(02B)	5375(6)	5524(12)	2640(6)	247(14)
C(01A)	3258(5)	-655(8)	1329(7)	320(20)
C(02A)	3104(12)	-230(30)	1372(10)	530(70)
C(03A)	3087(16)	340(40)	1353(15)	670(110)
C(04A)	2951(7)	381(17)	1506(6)	260(14)
C(05A)	2945(5)	1026(9)	1468(6)	227(13)

7.8 Crystallographic data for Hyp_3P_4SnK

7.8.1 Crystal data and structure refinement

Empirical formula	Hyp_3P_4SnK
Formula weight	1024.67
Temperature	293(2) K
Wavelength	0.71073 Å
Crystal system, space group	monoclinic, P2(1)/c

Unit cell dimensions	a = 14.057(3) Å alpha = 90 deg. b = 24.037(4) Å beta = 103.135(13) deg. c = 17.628(3) Å gamma = 90 deg.
Volume	5800.3(18) Å^3
Z, Calculated density	4, 1.173 g/cm^3
Absorption coefficient	0.888 mm^{-1}
F(000)	2160
Theta range for data collection	2.27 to 30.00 deg.
Limiting indices	-5<=h<=18, -7<=k<=31, -23<=l<=23
Reflections collected / unique	13722 / 13302 [R(int) = 0.0287]
Completeness to theta = 30.00	78.7 %
Refinement method	Full-matrix least-squares on F^2
Data / restraints / parameters	13302 / 0 / 433
Goodness-of-fit on F^2	1.161
Final R indices [I>2sigma(I)]	R1 = 0.0475, wR2 = 0.1110
R indices (all data)	R1 = 0.0763, wR2 = 0.1210
Largest diff. peak and hole	1.765 and -0.824 e.Å^{-3}

7.8.2 Atomic coordinates (x 10^4), equivalent isotropic displacement parameters (Å^2 x 10^3) and Anisotropic displacement parameters (Å^2 x 10^3). U(eq) is defined as one third of the trace of the orthogonalized Uij tensor. The anisotropic displacement factor exponent takes the form: $-2\pi^2[h^2a^{*2}U11 + ... + 2hka^*b^*U12]$

Atom	x	y	z	U(eq)	U11	U22	U33	U23	U13	U12
Sn(1)	3449(1)	2715(1)	7597(1)	28(1)	29(1)	29(1)	25(1)	-6(1)	8(1)	1(1)
P(4)	4390(1)	1867(1)	7173(1)	24(1)	21(1)	26(1)	25(1)	1(1)	6(1)	1(1)
P(1)	2599(1)	3022(1)	6205(1)	24(1)	28(1)	19(1)	29(1)	-1(1)	11(1)	3(1)
Si(33)	762(1)	887(1)	6256(1)	29(1)	28(1)	27(1)	31(1)	-1(1)	4(1)	-7(1)
Si(1)	1418(1)	3590(1)	6474(1)	23(1)	26(1)	17(1)	26(1)	-2(1)	8(1)	1(1)
P(3)	3085(1)	1666(1)	6223(1)	22(1)	23(1)	18(1)	25(1)	-1(1)	6(1)	1(1)
Si(3)	2498(1)	867(1)	6675(1)	24(1)	28(1)	17(1)	25(1)	-1(1)	4(1)	-2(1)
P(2)	2006(1)	2236(1)	6577(1)	26(1)	21(1)	20(1)	37(1)	-3(1)	9(1)	0(1)
K(1)	2672(1)	2350(1)	4551(1)	50(1)	73(1)	48(1)	29(1)	-3(1)	13(1)	-5(1)
Si(13)	2065(1)	4495(1)	6477(1)	32(1)	40(1)	18(1)	42(1)	-5(1)	14(1)	-2(1)
Si(32)	2904(1)	721(1)	8041(1)	33(1)	44(1)	27(1)	25(1)	2(1)	3(1)	-8(1)
Si(2)	5688(1)	2209(1)	6740(1)	24(1)	20(1)	28(1)	26(1)	1(1)	6(1)	2(1)
Si(31)	3085(1)	95(1)	6084(1)	33(1)	42(1)	20(1)	35(1)	-3(1)	2(1)	7(1)
Si(12)	899(1)	3487(1)	7654(1)	30(1)	36(1)	27(1)	32(1)	-3(1)	16(1)	4(1)
Si(23)	5665(1)	3078(1)	6106(1)	36(1)	26(1)	29(1)	54(1)	7(1)	12(1)	-2(1)
Si(22)	6273(1)	1515(1)	6024(1)	39(1)	43(1)	34(1)	46(1)	-2(1)	24(1)	6(1)
Si(21)	6804(1)	2268(1)	7962(1)	52(1)	31(1)	86(1)	34(1)	4(1)	-3(1)	-11(1)
Si(11)	45(1)	3477(1)	5429(1)	34(1)	27(1)	39(1)	36(1)	-10(1)	4(1)	2(1)
C(321)	2089(4)	146(2)	8255(3)	59(1)	92(4)	48(3)	36(2)	1(2)	16(2)	-29(3)
C(331)	355(3)	1215(2)	5267(2)	41(1)	39(2)	42(2)	38(2)	3(2)	-1(2)	-1(2)
C(121)	1786(3)	3834(2)	8478(2)	43(1)	58(3)	42(3)	33(2)	-12(2)	16(2)	3(2)
C(131)	1191(3)	5042(2)	6685(3)	50(1)	61(3)	24(2)	66(3)	-3(2)	16(2)	12(2)
C(132)	2333(4)	4632(2)	5500(3)	64(2)	101(4)	37(3)	65(3)	4(2)	46(3)	-7(3)
C(322)	2685(3)	1356(2)	8600(2)	42(1)	56(2)	41(2)	28(2)	-3(2)	12(2)	-11(2)
C(122)	-315(3)	3849(2)	7528(3)	44(1)	47(2)	41(3)	51(2)	-4(2)	25(2)	8(2)
C(332)	147(3)	1253(2)	6967(3)	46(1)	36(2)	51(3)	53(3)	-9(2)	18(2)	-7(2)
C(333)	277(3)	155(2)	6173(3)	49(1)	49(2)	36(2)	57(3)	-3(2)	2(2)	-16(2)
C(111)	-824(3)	4073(2)	5331(3)	52(1)	42(2)	51(3)	55(3)	6(2)	-8(2)	12(2)
C(123)	699(3)	2759(2)	7970(2)	39(1)	42(2)	34(2)	49(2)	5(2)	26(2)	4(2)
C(311)	2663(5)	-575(2)	6411(4)	81(2)	106(5)	29(3)	111(5)	5(3)	30(4)	4(3)
C(323)	4212(3)	499(2)	8419(3)	56(1)	61(3)	54(3)	42(2)	13(2)	-6(2)	12(2)
C(221)	5301(4)	1328(3)	5149(3)	65(2)	67(3)	71(4)	60(3)	-29(3)	20(2)	2(3)

Atom	x	y	z	U(eq)	U11	U22	U33	U23	U13	U12
C(133)	3232(3)	4564(2)	7224(3)	54(1)	45(2)	36(3)	78(3)	-22(2)	9(2)	-6(2)
C(312)	2673(5)	141(3)	5004(3)	83(2)	133(5)	75(4)	35(2)	-11(3)	9(3)	51(4)
C(231)	5283(4)	3673(2)	6658(4)	69(2)	70(3)	32(3)	110(5)	-11(3)	32(3)	-6(2)
C(222)	6664(4)	894(2)	6677(3)	69(2)	83(4)	46(3)	80(4)	10(3)	24(3)	20(3)
C(223)	7384(3)	1732(3)	5683(3)	61(1)	47(3)	82(4)	64(3)	-4(3)	32(2)	2(3)
C(211)	6823(5)	1615(3)	8557(3)	96(2)	99(5)	120(7)	55(3)	36(4)	-8(3)	17(4)
C(112)	-619(3)	2823(2)	5558(3)	58(1)	31(2)	40(3)	94(4)	-13(3)	0(2)	-4(2)
C(113)	454(4)	3416(3)	4490(3)	77(2)	52(3)	133(6)	44(3)	-36(3)	7(2)	-5(3)
C(232)	4815(4)	3068(3)	5114(3)	62(1)	57(3)	71(4)	55(3)	27(3)	8(2)	-2(3)
C(313)	4446(4)	78(3)	6335(4)	76(2)	54(3)	71(4)	100(5)	-27(4)	13(3)	14(3)
C(212)	6384(7)	2812(4)	8554(4)	155(5)	203(10)	167(10)	60(4)	-64(6)	-43(5)	39(8)
C(233)	6922(3)	3251(2)	5981(4)	72(2)	39(2)	64(4)	121(5)	29(4)	33(3)	-4(2)
C(213)	8063(5)	2410(6)	7861(4)	186(6)	50(4)	419(18)	75(4)	61(7)	-17(3)	-106(7)

7.8.3 Bond lengths [Å].

Atoms	Bond length	Atoms	Bond length	Atoms	Bond length
Sn(1)-P(1)	2.5795(10)	P(3)-Si(3)	2.3027(13)	Si(12)-C(121)	1.881(4)
Sn(1)-P(4)	2.6286(10)	Si(3)-Si(31)	2.3656(14)	Si(12)-C(123)	1.878(4)
Sn(1)-P(2)	2.6492(10)	Si(3)-Si(32)	2.3705(14)	Si(12)-C(122)	1.884(4)
P(4)-P(3)	2.2380(12)	Si(13)-C(133)	1.863(5)	Si(23)-C(233)	1.876(4)
P(4)-Si(2)	2.2843(13)	Si(13)-C(132)	1.874(5)	Si(23)-C(231)	1.875(5)
P(1)-P(2)	2.2233(13)	Si(13)-C(131)	1.890(4)	Si(23)-C(232)	1.881(5)
P(1)-Si(1)	2.2805(12)	Si(32)-C(322)	1.881(4)	Si(22)-C(223)	1.871(4)
Si(33)-C(333)	1.882(4)	Si(32)-C(323)	1.884(5)	Si(22)-C(221)	1.867(5)
Si(33)-C(331)	1.880(4)	Si(32)-C(321)	1.887(5)	Si(22)-C(222)	1.888(5)
Si(33)-C(332)	1.893(4)	Si(2)-Si(22)	2.3508(15)	Si(21)-C(213)	1.850(6)
Si(33)-Si(3)	2.3837(14)	Si(2)-Si(21)	2.3627(15)	Si(21)-C(212)	1.852(8)
Si(1)-Si(13)	2.3588(14)	Si(2)-Si(23)	2.3659(15)	Si(21)-C(211)	1.885(7)
Si(1)-Si(11)	2.3608(14)	Si(31)-C(312)	1.863(5)	Si(11)-C(111)	1.865(5)
Si(1)-Si(12)	2.3680(14)	Si(31)-C(313)	1.864(5)	Si(11)-C(112)	1.869(5)
P(3)-P(2)	2.2349(12)	Si(31)-C(311)	1.854(6)	Si(11)-C(113)	1.877(5)

7.8.4 Bond angles [deg].

Atoms	Angle	Atoms	Angle
P(1)-Sn(1)-P(4)	96.06(3)	C(321)-Si(32)-Si(3)	107.14(15)
P(1)-Sn(1)-P(2)	50.31(3)	P(4)-Si(2)-Si(22)	109.14(6)
P(4)-Sn(1)-P(2)	80.05(3)	P(4)-Si(2)-Si(21)	97.62(5)
P(3)-P(4)-Si(2)	114.13(5)	Si(22)-Si(2)-Si(21)	106.93(6)
P(3)-P(4)-Sn(1)	90.01(4)	P(4)-Si(2)-Si(23)	123.33(5)
Si(2)-P(4)-Sn(1)	107.93(4)	Si(22)-Si(2)-Si(23)	109.97(6)
P(2)-P(1)-Si(1)	96.21(5)	Si(21)-Si(2)-Si(23)	108.18(6)
P(2)-P(1)-Sn(1)	66.47(3)	C(312)-Si(31)-C(313)	107.9(3)
Si(1)-P(1)-Sn(1)	100.10(4)	C(312)-Si(31)-C(311)	108.8(3)
C(333)-Si(33)-C(331)	106.9(2)	C(313)-Si(31)-C(311)	106.9(3)
C(333)-Si(33)-C(332)	106.0(2)	C(312)-Si(31)-Si(3)	110.22(18)
C(331)-Si(33)-C(332)	109.3(2)	C(313)-Si(31)-Si(3)	110.81(19)
C(333)-Si(33)-Si(3)	109.40(15)	C(311)-Si(31)-Si(3)	112.0(2)
C(331)-Si(33)-Si(3)	111.71(13)	C(121)-Si(12)-C(123)	107.5(2)
C(332)-Si(33)-Si(3)	113.20(14)	C(121)-Si(12)-C(122)	108.1(2)
P(1)-Si(1)-Si(13)	104.78(5)	C(123)-Si(12)-C(122)	105.78(19)
P(1)-Si(1)-Si(11)	105.92(5)	C(121)-Si(12)-Si(1)	110.49(14)
Si(13)-Si(1)-Si(11)	110.73(6)	C(123)-Si(12)-Si(1)	117.06(13)
P(1)-Si(1)-Si(12)	120.26(5)	C(122)-Si(12)-Si(1)	107.51(14)
Si(13)-Si(1)-Si(12)	106.80(5)	C(233)-Si(23)-C(231)	106.3(3)
Si(11)-Si(1)-Si(12)	108.22(5)	C(233)-Si(23)-C(232)	108.0(3)

Atoms	Angle	Atoms	Angle
P(2)-P(3)-P(4)	98.72(5)	C(231)-Si(23)-C(232)	107.2(3)
P(2)-P(3)-Si(3)	95.46(5)	C(233)-Si(23)-Si(2)	109.85(18)
P(4)-P(3)-Si(3)	102.65(5)	C(231)-Si(23)-Si(2)	113.76(19)
P(3)-Si(3)-Si(31)	108.24(5)	C(232)-Si(23)-Si(2)	111.44(18)
P(3)-Si(3)-Si(32)	116.86(5)	C(223)-Si(22)-C(221)	108.0(2)
Si(31)-Si(3)-Si(32)	107.67(5)	C(223)-Si(22)-C(222)	105.5(3)
P(3)-Si(3)-Si(33)	107.33(5)	C(221)-Si(22)-C(222)	111.7(3)
Si(31)-Si(3)-Si(33)	108.37(5)	C(223)-Si(22)-Si(2)	113.16(19)
Si(32)-Si(3)-Si(33)	108.12(5)	C(221)-Si(22)-Si(2)	109.56(17)
P(1)-P(2)-P(3)	96.56(5)	C(222)-Si(22)-Si(2)	108.81(19)
P(1)-P(2)-Sn(1)	63.22(3)	C(213)-Si(21)-C(212)	111.0(6)
P(3)-P(2)-Sn(1)	89.55(4)	C(213)-Si(21)-C(211)	108.3(4)
C(133)-Si(13)-C(132)	107.7(3)	C(212)-Si(21)-C(211)	103.9(4)
C(133)-Si(13)-C(131)	108.0(2)	C(213)-Si(21)-Si(2)	112.0(2)
C(132)-Si(13)-C(131)	109.4(2)	C(212)-Si(21)-Si(2)	109.0(2)
C(133)-Si(13)-Si(1)	111.13(17)	C(211)-Si(21)-Si(2)	112.3(2)
C(132)-Si(13)-Si(1)	108.48(17)	C(111)-Si(11)-C(112)	108.8(2)
C(131)-Si(13)-Si(1)	112.02(16)	C(111)-Si(11)-C(113)	107.7(3)
C(322)-Si(32)-C(323)	107.9(2)	C(112)-Si(11)-C(113)	107.6(3)
C(322)-Si(32)-C(321)	108.0(2)	C(111)-Si(11)-Si(1)	112.75(16)
C(323)-Si(32)-C(321)	108.0(3)	C(112)-Si(11)-Si(1)	110.13(17)
C(322)-Si(32)-Si(3)	112.46(14)	C(113)-Si(11)-Si(1)	109.68(16)
C(323)-Si(32)-Si(3)	113.10(16)		

7.9 Crystallographic data for $Hyp_4P_4Pb_4$

7.9.1 Crystal data and structure refinement

Empirical formula	$Hyp_4P_4Pb_4 \cdot 1.5$Cyclo-pentane
Formula weight	2048.50
Temperature	293(2) K
Wavelength	0.71073 Å
Crystal system, space group	hexagonal, $P\bar{3}c1$
Unit cell dimensions	a = 16.201(2) Å alpha = 90 deg. b = 16.201(2) Å beta = 90 deg. c = 37.756(8) Å gamma = 120 deg.
Volume	8582(2) Å^3
Z, Calculated density	4, 1.585 g/cm^3
Absorption coefficient	8.146 mm^{-1}
F(000)	3984
Theta range for data collection	2.16 to 22.50 deg.
Limiting indices	0<=h<=15, 0<=k<=15, -40<=l<=40
Reflections collected / unique	7522 / 3770 [R(int) = 0.1147]
Completeness to theta = 22.50	99.9 %
Refinement method	Full-matrix least-squares on F^2
Data / restraints / parameters	3770 / 30 / 213
Goodness-of-fit on F^2	1.101
Final R indices [I>2sigma(I)]	R1 = 0.0718, wR2 = 0.1449
R indices (all data)	R1 = 0.1397, wR2 = 0.1709
Largest diff. peak and hole	2.565 and -1.452 e.Å^{-3}

7.9.2 Atomic coordinates (x 10^4), equivalent isotropic displacement parameters (Å^2 x 10^3) and Anisotropic displacement parameters (Å^2 x 10^3). U(eq) is defined as one third of the trace of the orthogonalized Uij tensor. The anisotropic displacement factor exponent takes the form: $-2\pi^2[h^2a^{*2}U11 + ... + 2hka^*b^*U12]$

Atom	x	y	z	U(eq)	U11	U22	U33	U23	U13	U12
Pb(1)	3333	6667	3282(1)	35(1)	39(1)	39(1)	27(1)	0	0	20(1)
Pb(2)	4325(1)	5974(1)	4184(1)	38(1)	39(1)	40(1)	40(1)	3(1)	-1(1)	23(1)
P(1)	2729(4)	5223(3)	3763(1)	26(1)	31(3)	20(3)	27(3)	-4(2)	1(3)	12(2)
P(2)	3333	6667	4543(2)	25(2)	28(3)	28(3)	18(4)	0	0	14(2)
Si(2)	3333	6667	5147(2)	22(2)	28(3)	28(3)	10(4)	0	0	14(2)
Si(21)	2190(4)	7056(4)	5343(2)	40(2)	37(3)	48(4)	39(4)	-15(3)	-1(3)	26(3)
Si(1)	2124(4)	3712(4)	3565(2)	27(1)	37(3)	21(3)	27(3)	-3(3)	2(3)	16(3)
Si(11)	1586(5)	2695(4)	4057(2)	41(2)	59(4)	26(3)	34(4)	6(3)	2(3)	19(3)
Si(12)	885(4)	3306(4)	3164(2)	39(2)	34(3)	44(4)	28(4)	-7(3)	-7(3)	10(3)
Si(13)	3398(4)	3647(4)	3287(2)	42(2)	42(4)	43(4)	47(5)	-1(3)	9(3)	27(3)
C(131)	4013(15)	4657(16)	2982(6)	53(7)	39(14)	70(17)	42(16)	-4(14)	14(12)	22(13)
C(211)	968(14)	6149(14)	5202(7)	46(7)	30(12)	46(14)	70(18)	-29(13)	-5(12)	25(11)
C(121)	-57(15)	3500(18)	3351(6)	55(7)	43(14)	84(19)	33(16)	20(14)	18(12)	28(14)
C(122)	330(16)	2062(18)	3056(8)	74(9)	35(14)	80(20)	90(20)	-22(18)	-40(15)	12(14)
C(132)	2990(20)	2504(19)	3042(9)	88(10)	100(20)	90(20)	100(30)	-30(20)	0(20)	58(19)
C(123)	1358(15)	4034(18)	2751(6)	51(7)	42(13)	90(19)	25(14)	-1(13)	-13(11)	36(14)
C(111)	460(15)	2610(16)	4221(6)	42(6)	67(16)	56(15)	15(12)	1(11)	15(12)	39(13)
C(212)	2506(17)	8250(17)	5160(7)	63(8)	76(18)	70(17)	70(20)	-27(15)	-3(15)	56(15)
C(112)	1304(18)	1483(14)	3912(8)	76(10)	70(19)	17(12)	120(30)	0(15)	18(19)	5(13)
C(113)	2532(18)	3162(17)	4404(8)	81(10)	58(17)	47(16)	100(30)	24(17)	-6(18)	0(14)
C(213)	2140(20)	7010(30)	5850(7)	107(13)	110(30)	190(40)	60(20)	-90(20)	-30(19)	110(30)
C(133)	4300(19)	3810(20)	3646(7)	78(10)	100(20)	130(30)	70(20)	23(19)	37(18)	110(20)
C(021)	2920(40)	7240(30)	6950(20)	57(11)						
C(022)	2400(30)	6170(30)	6920(17)	57(11)						
C(023)	3130(50)	5850(40)	6960(30)	57(11)						
C(024)	4020(40)	6680(50)	7120(20)	57(11)						
C(025)	3920(40)	7560(30)	7088(19)	57(11)						
C(031)	600(60)	-60(50)	4930(20)	40(15)						
C(032)	-460(50)	-780(70)	4967(19)	40(15)						
C(033)	-590(40)	-1330(60)	5310(20)	40(15)						
C(034)	380(50)	-940(60)	5481(18)	40(15)						
C(035)	1120(40)	-320(70)	5200(20)	40(15)						

7.9.3 Bond lengths [Å].

Atoms	Bond length	Atoms	Bond length	Atoms	Bond length
Pb(1)-P(1)#1	2.729(5)	Si(2)-Si(21)#2	2.354(6)	Si(13)-C(131)	1.84(2)
Pb(1)-P(1)#2	2.729(5)	Si(21)-C(211)	1.86(2)	Si(13)-C(132)	1.87(3)
Pb(1)-P(1)	2.729(5)	Si(21)-C(212)	1.87(3)	Si(13)-C(133)	1.91(3)
Pb(2)-P(1)#2	2.720(5)	Si(21)-C(213)	1.91(3)	C(021)-C(025)	1.518(5)
Pb(2)-P(2)	2.734(4)	Si(1)-Si(12)	2.330(8)	C(021)-C(022)	1.519(5)
Pb(2)-P(1)	2.746(5)	Si(1)-Si(11)	2.344(8)	C(022)-C(023)	1.521(5)
P(1)-Si(1)	2.261(7)	Si(1)-Si(13)	2.363(8)	C(023)-C(024)	1.520(5)
P(1)-Pb(2)#1	2.720(5)	Si(11)-C(112)	1.86(2)	C(024)-C(025)	1.518(5)
P(2)-Si(2)	2.282(12)	Si(11)-C(111)	1.86(2)	C(031)-C(032)	1.519(5)
P(2)-Pb(2)#1	2.734(4)	Si(11)-C(113)	1.87(3)	C(031)-C(035)	1.520(5)
P(2)-Pb(2)#2	2.734(4)	Si(12)-C(122)	1.79(2)	C(032)-C(033)	1.517(5)
Si(2)-Si(21)	2.354(6)	Si(12)-C(121)	1.85(2)	C(033)-C(034)	1.519(5)
Si(2)-Si(21)#1	2.354(6)	Si(12)-C(123)	1.87(2)	C(034)-C(035)	1.522(5)

7.9.4 Bond angles [deg].

Atoms	Angle	Atoms	Angle
P(1)#1-Pb(1)-P(1)#2	80.46(15)	Si(12)-Si(1)-Si(11)	110.5(3)
P(1)#1-Pb(1)-P(1)	80.46(15)	P(1)-Si(1)-Si(13)	106.3(3)
P(1)#2-Pb(1)-P(1)	80.46(15)	Si(12)-Si(1)-Si(13)	110.4(3)
P(1)#2-Pb(2)-P(2)	82.01(16)	Si(11)-Si(1)-Si(13)	110.2(3)
P(1)#2-Pb(2)-P(1)	80.3(2)	C(112)-Si(11)-C(111)	107.8(11)
P(2)-Pb(2)-P(1)	81.54(16)	C(112)-Si(11)-C(113)	110.7(13)
Si(1)-P(1)-Pb(2)#1	119.8(2)	C(111)-Si(11)-C(113)	111.8(12)
Si(1)-P(1)-Pb(1)	118.9(2)	C(112)-Si(11)-Si(1)	108.5(10)
Pb(2)#1-P(1)-Pb(1)	99.29(16)	C(111)-Si(11)-Si(1)	108.8(7)
Si(1)-P(1)-Pb(2)	118.3(2)	C(113)-Si(11)-Si(1)	109.3(9)
Pb(2)#1-P(1)-Pb(2)	97.59(16)	C(122)-Si(12)-C(121)	106.6(12)
Pb(1)-P(1)-Pb(2)	98.66(15)	C(122)-Si(12)-C(123)	109.6(12)
Si(2)-P(2)-Pb(2)#1	119.72(16)	C(121)-Si(12)-C(123)	108.9(11)
Si(2)-P(2)-Pb(2)#2	119.72(16)	C(122)-Si(12)-Si(1)	110.0(8)
Pb(2)#1-P(2)-Pb(2)#2	97.5(2)	C(121)-Si(12)-Si(1)	111.9(8)
Si(2)-P(2)-Pb(2)	119.72(16)	C(123)-Si(12)-Si(1)	109.8(7)
Pb(2)#1-P(2)-Pb(2)	97.5(2)	C(131)-Si(13)-C(132)	109.7(14)
Pb(2)#2-P(2)-Pb(2)	97.5(2)	C(131)-Si(13)-C(133)	106.6(12)
P(2)-Si(2)-Si(21)	108.3(3)	C(132)-Si(13)-C(133)	110.8(12)
P(2)-Si(2)-Si(21)#1	108.3(3)	C(131)-Si(13)-Si(1)	109.6(8)
Si(21)-Si(2)-Si(21)#1	110.6(2)	C(132)-Si(13)-Si(1)	112.2(9)
P(2)-Si(2)-Si(21)#2	108.3(3)	C(133)-Si(13)-Si(1)	107.8(8)
Si(21)-Si(2)-Si(21)#2	110.6(2)	C(025)-C(021)-C(022)	107.7(4)
Si(21)#1-Si(2)-Si(21)#2	110.6(2)	C(021)-C(022)-C(023)	107.3(6)
C(211)-Si(21)-C(212)	110.1(11)	C(024)-C(023)-C(022)	107.1(7)
C(211)-Si(21)-C(213)	104.3(13)	C(025)-C(024)-C(023)	107.5(6)
C(212)-Si(21)-C(213)	113.1(13)	C(021)-C(025)-C(024)	107.8(4)
C(211)-Si(21)-Si(2)	111.6(7)	C(032)-C(031)-C(035)	107.0(8)
C(212)-Si(21)-Si(2)	108.5(8)	C(033)-C(032)-C(031)	107.6(4)
C(213)-Si(21)-Si(2)	109.3(9)	C(034)-C(033)-C(032)	107.7(5)
P(1)-Si(1)-Si(12)	111.5(3)	C(033)-C(034)-C(035)	106.9(7)
P(1)-Si(1)-Si(11)	107.8(3)	C(031)-C(035)-C(034)	106.6(9)

Symmetry transformations used to generate equivalent atoms:
#1 -x+y,-x+1,z   #2 -y+1,x-y+1,z

7.10 Crystallographic data for $Hyp_4P_4Sn_4$

7.10.1 Crystal data and structure refinement

Empirical formula	$Hyp_4P_4Sn_4 \cdot 1.5$benzene
Formula weight	1706.47
Temperature	293(2) K
Wavelength	0.71073 Å
Crystal system, space group	hexagonal, $P32_1$
Unit cell dimensions	a = 16.2775(3) Å alpha = 90 deg. b = 16.2775(3) Å beta = 90 deg. c = 18.5675(4) Å gamma = 120 deg.
Volume	4260.49(14) $Å^3$
Z, Calculated density	2, 1.330 g/cm^3
Absorption coefficient	1.485 mm^{-1}
F(000)	1742
Theta range for data collection	2.50 to 28.31 deg.

Limiting indices	-21<=h<=21, -20<=k<=21, -24<=l<=22
Reflections collected / unique	31724 / 7064 [R(int) = 0.0328]
Completeness to theta = 28.31	99.6 %
Refinement method	Full-matrix least-squares on F^2
Data / restraints / parameters	7064 / 22 / 230
Goodness-of-fit on F^2	1.100
Final R indices [I>2sigma(I)]	R1 = 0.0213, wR2 = 0.0541
R indices (all data)	R1 = 0.0237, wR2 = 0.0561
Absolute structure parameter	-0.032(11)
Largest diff. peak and hole	0.735 and -0.303 e.Å^{-3}

7.10.2 Atomic coordinates (x 10^4), equivalent isotropic displacement parameters (Å^2 x 10^3) and Anisotropic displacement parameters (Å^2 x 10^3). U(eq) is defined as one third of the trace of the orthogonalized Uij tensor. The anisotropic displacement factor exponent takes the form: $-2\pi^2[h^2a^{*2}U11 + ... + 2hka^*b^*U12]$

Atom	x	y	z	U(eq)	U11	U22	U33	U23	U13	U12
Sn(1)	3333	6667	1570(1)	34(1)	36(1)	36(1)	30(1)	0	0	18(1)
Sn(2)	1723(1)	5741(1)	3341(1)	32(1)	29(1)	32(1)	35(1)	1(1)	1(1)	14(1)
P(1)	3333	6667	4078(1)	28(1)	30(1)	30(1)	24(1)	0	0	15(1)
P(2)	2729(1)	5252(1)	2512(1)	30(1)	31(1)	26(1)	32(1)	-3(1)	-1(1)	14(1)
Si(1)	3333	6667	5299(1)	26(1)	27(1)	27(1)	25(1)	0	0	13(1)
Si(1A)	3609(1)	8139(1)	5731(1)	39(1)	51(1)	34(1)	34(1)	-8(1)	-4(1)	22(1)
C(111)	3294(5)	8048(4)	6711(2)	58(1)	69(4)	65(3)	40(2)	-17(2)	0(2)	33(3)
C(112)	2915(6)	8580(4)	5231(3)	61(1)	93(4)	58(2)	57(3)	-6(2)	-8(2)	56(3)
C(113)	4900(3)	9013(3)	5637(2)	63(1)	62(2)	37(2)	66(2)	-9(2)	1(2)	7(2)
Si(1B)	2726(5)	7613(5)	5728(3)	37(2)	48(4)	49(4)	26(3)	8(3)	12(3)	34(4)
C(114)	3000(30)	7910(30)	6708(11)	40(11)						
C(115)	3170(40)	8740(20)	5230(30)	80(20)						
C(116)	1400(12)	6900(20)	5675(16)	52(7)						
Si(2)	2126(1)	3735(1)	2150(1)	30(1)	30(1)	27(1)	33(1)	-5(1)	-2(1)	14(1)
Si(21)	1579(1)	2751(1)	3169(1)	39(1)	40(1)	33(1)	42(1)	2(1)	3(1)	17(1)
C(211)	423(2)	2626(2)	3476(2)	54(1)	44(2)	56(2)	57(2)	10(1)	14(1)	21(1)
C(212)	1397(3)	1544(2)	2953(2)	66(1)	93(3)	40(2)	72(2)	10(2)	14(2)	39(2)
C(213)	2475(2)	3294(3)	3909(2)	62(1)	51(2)	76(2)	44(2)	6(2)	-2(1)	20(2)
Si(22)	3379(1)	3647(1)	1598(1)	39(1)	40(1)	42(1)	40(1)	-8(1)	0(1)	24(1)
C(221)	4005(3)	4671(3)	956(2)	64(1)	51(2)	74(2)	68(2)	14(2)	20(2)	32(2)
C(222)	2928(3)	2516(3)	1084(2)	69(1)	71(2)	66(2)	76(2)	-32(2)	-1(2)	39(2)
C(223)	4227(2)	3700(3)	2299(2)	59(1)	56(2)	85(2)	55(2)	-10(2)	-8(1)	49(2)
Si(23)	876(1)	3325(1)	1335(1)	42(1)	34(1)	46(1)	41(1)	-9(1)	-7(1)	17(1)
C(231)	-51(3)	3547(3)	1730(2)	68(1)	54(2)	106(3)	61(2)	9(2)	3(2)	52(2)
C(232)	1354(2)	4028(3)	486(2)	58(1)	52(2)	74(2)	44(2)	-3(1)	-9(1)	29(2)
C(233)	284(3)	2023(3)	1117(2)	73(1)	55(2)	52(2)	88(3)	-22(2)	-24(2)	9(2)
C(01)	487(3)	971(3)	5001(2)	73(1)	92(3)	62(2)	55(2)	2(2)	7(2)	32(2)
C(02)	2923(5)	5726(4)	-979(4)	121(2)	95(4)	58(3)	207(7)	9(3)	34(4)	37(3)
C(03)	6251(5)	3863(4)	958(4)	114(2)	91(4)	79(3)	191(6)	-1(4)	-4(4)	57(3)

7.10.3 Bond lengths [Å].

Atoms	Bond length	Atoms	Bond length	Atoms	Bond length
Sn(1)-P(2)#1	2.6565(6)	Si(1)-Si(1A)	2.3471(8)	Si(21)-C(212)	1.878(3)
Sn(1)-P(2)#2	2.6565(6)	Si(1)-Si(1A)#2	2.3471(8)	Si(22)-C(222)	1.867(3)
Sn(1)-P(2)	2.6565(6)	Si(1)-Si(1A)#1	2.3471(8)	Si(22)-C(223)	1.868(3)
Sn(2)-P(2)	2.6446(6)	Si(1A)-C(112)	1.863(5)	Si(22)-C(221)	1.881(4)

Sn(2)-P(2)#1	2.6508(6)	Si(1A)-C(113)	1.865(4)	Si(23)-C(231)	1.870(4)
Sn(2)-P(1)	2.6576(5)	Si(1A)-C(111)	1.876(4)	Si(23)-C(232)	1.873(3)
P(1)-Si(1)	2.2676(12)	Si(1B)-C(115)	1.848(18)	Si(23)-C(233)	1.882(4)
P(1)-Sn(2)#1	2.6576(5)	Si(1B)-C(116)	1.874(16)	C(01)-C(01)#3	1.363(9)
P(1)-Sn(2)#2	2.6576(5)	Si(1B)-C(114)	1.877(16)	C(01)-C(01)#4	1.374(10)
P(2)-Si(2)	2.2565(8)	Si(2)-Si(23)	2.3479(9)	C(02)-C(03)#5	1.329(8)
P(2)-Sn(2)#2	2.6508(6)	Si(2)-Si(21)	2.3489(9)	C(02)-C(03)#6	1.337(8)
Si(1)-Si(1B)	2.346(6)	Si(2)-Si(22)	2.3500(9)	C(03)-C(02)#5	1.329(8)
Si(1)-Si(1B)#2	2.346(6)	Si(21)-C(213)	1.872(3)	C(03)-C(02)#7	1.337(8)
Si(1)-Si(1B)#1	2.346(6)	Si(21)-C(211)	1.876(3)		

7.10.4 Bond angles [deg].

Atoms	Angle	Atoms	Angle
P(2)#1-Sn(1)-P(2)#2	81.427(18)	C(112)-Si(1A)-C(113)	109.2(3)
P(2)#1-Sn(1)-P(2)	81.427(18)	C(112)-Si(1A)-C(111)	108.6(2)
P(2)#2-Sn(1)-P(2)	81.427(18)	C(113)-Si(1A)-C(111)	108.1(2)
P(2)-Sn(2)-P(2)#1	81.75(3)	C(112)-Si(1A)-Si(1)	112.33(18)
P(2)-Sn(2)-P(1)	83.487(17)	C(113)-Si(1A)-Si(1)	108.32(13)
P(2)#1-Sn(2)-P(1)	83.369(17)	C(111)-Si(1A)-Si(1)	110.24(16)
Si(1)-P(1)-Sn(2)	120.973(16)	C(115)-Si(1B)-C(116)	110.3(18)
Si(1)-P(1)-Sn(2)#1	120.973(16)	C(115)-Si(1B)-C(114)	108.2(17)
Sn(2)-P(1)-Sn(2)#1	95.90(2)	C(116)-Si(1B)-C(114)	105.2(13)
Si(1)-P(1)-Sn(2)#2	120.973(16)	C(115)-Si(1B)-Si(1)	113.1(16)
Sn(2)-P(1)-Sn(2)#2	95.90(2)	C(116)-Si(1B)-Si(1)	107.9(9)
Sn(2)#1-P(1)-Sn(2)#2	95.90(2)	C(114)-Si(1B)-Si(1)	111.8(12)
Si(2)-P(2)-Sn(2)	120.43(3)	P(2)-Si(2)-Si(23)	110.13(4)
Si(2)-P(2)-Sn(2)#2	117.45(3)	P(2)-Si(2)-Si(21)	108.39(3)
Sn(2)-P(2)-Sn(2)#2	96.372(18)	Si(23)-Si(2)-Si(21)	110.30(4)
Si(2)-P(2)-Sn(1)	121.51(3)	P(2)-Si(2)-Si(22)	106.28(3)
Sn(2)-P(2)-Sn(1)	97.993(19)	Si(23)-Si(2)-Si(22)	110.90(4)
Sn(2)#2-P(2)-Sn(1)	97.84(2)	Si(21)-Si(2)-Si(22)	110.73(4)
P(1)-Si(1)-Si(1B)	109.84(15)	C(213)-Si(21)-C(211)	109.36(17)
P(1)-Si(1)-Si(1B)#2	109.84(15)	C(213)-Si(21)-C(212)	109.19(19)
Si(1B)-Si(1)-Si(1B)#2	109.10(15)	C(211)-Si(21)-C(212)	109.05(18)
P(1)-Si(1)-Si(1B)#1	109.84(15)	C(213)-Si(21)-Si(2)	109.20(11)
Si(1B)-Si(1)-Si(1B)#1	109.10(15)	C(211)-Si(21)-Si(2)	109.63(11)
Si(1B)#2-Si(1)-Si(1B)#1	109.10(15)	C(212)-Si(21)-Si(2)	110.40(12)
P(1)-Si(1)-Si(1A)	109.98(3)	C(222)-Si(22)-C(223)	108.62(18)
Si(1B)-Si(1)-Si(1A)	30.95(19)	C(222)-Si(22)-C(221)	108.74(19)
Si(1B)#2-Si(1)-Si(1A)	132.18(18)	C(223)-Si(22)-C(221)	109.83(18)
Si(1B)#1-Si(1)-Si(1A)	80.68(18)	C(222)-Si(22)-Si(2)	110.96(13)
P(1)-Si(1)-Si(1A)#2	109.98(3)	C(223)-Si(22)-Si(2)	109.75(11)
Si(1B)-Si(1)-Si(1A)#2	80.68(18)	C(221)-Si(22)-Si(2)	108.93(12)
Si(1B)#2-Si(1)-Si(1A)#2	30.95(19)	C(231)-Si(23)-C(232)	109.98(17)
Si(1B)#1-Si(1)-Si(1A)#2	132.18(18)	C(231)-Si(23)-C(233)	107.1(2)
Si(1A)-Si(1)-Si(1A)#2	108.96(3)	C(232)-Si(23)-C(233)	109.22(18)
P(1)-Si(1)-Si(1A)#1	109.98(3)	C(231)-Si(23)-Si(2)	111.13(13)
Si(1B)-Si(1)-Si(1A)#1	132.18(18)	C(232)-Si(23)-Si(2)	109.43(11)
Si(1B)#2-Si(1)-Si(1A)#1	80.68(18)	C(233)-Si(23)-Si(2)	109.96(13)
Si(1B)#1-Si(1)-Si(1A)#1	30.95(19)	C(01)#3-C(01)-C(01)#4	120.000(4)
Si(1A)-Si(1)-Si(1A)#1	108.96(3)	C(03)#5-C(02)-C(03)#6	120.5(6)
Si(1A)#2-Si(1)-Si(1A)#1	108.96(3)	C(02)#5-C(03)-C(02)#7	119.4(6)

Symmetry transformations used to generate equivalent toms:
#1 -x+y,-x+1,z #2 -y+1,x-y+1,z #3 y,x,-z+1
#4 -x,-x+y,-z+1 #5 y,x,-z #6 x-y,-y+1,-z
#7 x-y+1,-y+1,-z

7.11 Crystallographic data for (Hyp$_2$Pb·PH$_2$)Li·Et$_2$O(DME)

7.11.1 Crystal data and structure refinement

Empirical formula	Hyp$_2$PbP(H$_2$)Li·Et$_2$O(DME)
Formula weight	906.69
Temperature	173(2) K
Wavelength	0.71073 Å
Crystal system, space group	triclinic, P$\overline{1}$
Unit cell dimensions	a = 13.084(2) Å alpha = 88.150(17) deg. b = 13.334(3) Å beta = 79.516(12) deg. c = 15.404(3) Å gamma = 68.553(15) deg.
Volume	2457.8(9) Å^3
Z, Calculated density	2, 1.225 g/cm^3
Absorption coefficient	3.681 mm^{-1}
F(000)	936
Theta range for data collection	2.08 to 25.00 deg.
Limiting indices	-7<=h<=15, -15<=k<=15, -18<=l<=18
Reflections collected / unique	8968 / 8565 [R(int) = 0.0532]
Completeness to theta = 25.00	98.9 %
Refinement method	Full-matrix least-squares on F^2
Data / restraints / parameters	8565 / 42 / 409
Goodness-of-fit on F^2	0.733
Final R indices [I>2sigma(I)]	R1 = 0.0333, wR2 = 0.0587
R indices (all data)	R1 = 0.0594, wR2 = 0.0624
Largest diff. peak and hole	0.865 and -0.666 e.Å^{-3}

7.11.2 Atomic coordinates (x 10^4), equivalent isotropic displacement parameters (Å^2 x 10^3) and Anisotropic displacement parameters (Å^2 x 10^3). U(eq) is defined as one third of the trace of the orthogonalized Uij tensor. The anisotropic displacement factor exponent takes the form: $-2\pi^2[h^2a^{*2}U11 + \ldots + 2hka^*b^*U12]$

Atom	x	y	z	U(eq)	U11	U22	U33	U23	U13	U12
Pb	7822(1)	6721(1)	6714(1)	27(1)	28(1)	27(1)	26(1)	1(1)	-4(1)	-10(1)
Si(1)	5876(1)	6374(1)	7392(1)	25(1)	25(1)	27(1)	24(1)	5(1)	-8(1)	-10(1)
Si(2)	7788(1)	8736(1)	7110(1)	27(1)	30(1)	26(1)	27(1)	3(1)	-6(1)	-13(1)
P	8906(1)	5744(1)	8067(1)	40(1)	40(1)	34(1)	50(1)	9(1)	-22(1)	-12(1)
Si(13)	4758(1)	6983(1)	8778(1)	36(1)	38(1)	45(1)	25(1)	0(1)	-2(1)	-16(1)
Si(23)	6986(1)	9830(1)	6002(1)	38(1)	46(1)	28(1)	43(1)	10(1)	-19(1)	-14(1)
Si(12)	4676(1)	6931(1)	6352(1)	36(1)	31(1)	45(1)	31(1)	5(1)	-11(1)	-11(1)
Si(22)	9707(1)	8474(1)	6784(1)	38(1)	32(1)	50(1)	37(1)	5(1)	-7(1)	-21(1)
Si(21)	7065(1)	9734(1)	8459(1)	38(1)	46(1)	36(1)	33(1)	-4(1)	1(1)	-21(1)
Si(11)	6503(1)	4486(1)	7286(1)	33(1)	31(1)	29(1)	43(1)	3(1)	-10(1)	-14(1)
O(3)	11007(4)	3525(3)	6757(3)	58(1)	46(3)	72(3)	47(3)	-1(2)	-6(2)	-11(3)
O(1)	11948(4)	3818(4)	8074(3)	62(1)	49(3)	85(3)	63(3)	9(3)	-16(3)	-33(3)
C(213)	5577(5)	10689(5)	8534(4)	53(2)	54(5)	37(4)	55(4)	-9(3)	7(4)	-7(3)
C(123)	3577(5)	8301(4)	6634(4)	49(2)	34(4)	54(4)	53(4)	15(3)	-11(3)	-10(3)
C(232)	7175(5)	11174(4)	5952(4)	56(2)	71(5)	35(4)	68(4)	19(3)	-24(4)	-22(4)
C(113)	5369(5)	3928(5)	7608(4)	52(2)	44(4)	53(4)	64(4)	6(3)	-7(3)	-26(3)
C(212)	7150(5)	8810(5)	9413(3)	54(2)	66(5)	57(4)	31(3)	3(3)	-4(3)	-19(4)
C(122)	3879(5)	6022(5)	6245(4)	54(2)	47(4)	71(5)	53(4)	1(3)	-30(3)	-23(4)
C(121)	5512(5)	6944(5)	5223(3)	52(2)	46(4)	70(5)	32(3)	13(3)	-12(3)	-11(4)
C(112)	7172(5)	4028(5)	6104(4)	58(2)	58(5)	43(4)	69(5)	-16(3)	6(4)	-23(4)

Atom	x	y	z	U(eq)	U11	U22	U33	U23	U13	U12
C(222)	10429(6)	7996(6)	7755(4)	69(2)	59(5)	95(6)	70(5)	30(4)	-31(4)	-41(5)
C(133)	4297(6)	8484(5)	8896(4)	62(2)	65(5)	60(5)	58(4)	-12(4)	-6(4)	-22(4)
C(111)	7558(6)	3791(5)	7993(5)	69(2)	68(5)	44(4)	105(6)	20(4)	-45(5)	-21(4)
C(132)	5536(6)	6387(5)	9699(4)	64(2)	77(5)	88(6)	33(4)	14(4)	-13(4)	-37(5)
C(131)	3447(5)	6661(5)	8978(4)	57(2)	45(4)	72(5)	54(4)	2(4)	4(3)	-28(4)
C(231)	7611(6)	9120(5)	4891(4)	59(2)	94(6)	41(4)	46(4)	18(3)	-26(4)	-24(4)
C(221)	9994(5)	9721(5)	6430(4)	62(2)	56(5)	83(5)	61(4)	24(4)	-12(4)	-43(4)
C(211)	7865(6)	10617(5)	8631(4)	71(2)	95(6)	79(5)	58(4)	-21(4)	9(4)	-61(5)
C(41)	9678(6)	2608(6)	9542(4)	65(2)	57(5)	86(6)	51(4)	24(4)	-15(4)	-24(4)
C(223)	10472(5)	7462(5)	5859(4)	73(2)	45(5)	77(5)	95(6)	-23(4)	-6(4)	-20(4)
C(233)	5446(5)	10123(6)	6169(4)	67(2)	55(5)	88(6)	71(5)	20(4)	-37(4)	-32(4)
C(72)	10319(6)	3734(6)	6086(4)	83(3)	76(6)	102(6)	40(4)	-11(4)	-14(4)	4(5)
C(42)	9366(6)	3669(6)	10016(4)	76(2)	80(6)	104(7)	57(5)	19(5)	-17(4)	-47(5)
C(62)	12581(6)	3489(7)	8753(5)	92(3)	74(6)	135(8)	90(6)	23(6)	-43(5)	-55(6)
C(71)	11870(7)	3917(8)	6556(5)	102(3)	101(7)	180(10)	54(5)	11(6)	2(5)	-95(8)
C(61)	12624(7)	3503(9)	7221(6)	120(4)	63(6)	229(12)	97(7)	-4(8)	-6(6)	-89(8)
Li	10434(8)	3810(9)	8063(6)	46(3)	30(6)	66(7)	38(6)	2(5)	-6(5)	-15(5)
O(2)	10276(4)	2610(3)	8673(3)	60(1)	49(3)	51(3)	81(3)	7(3)	-14(3)	-19(2)
C(51A)	10547(8)	1687(7)	8108(7)	54(3)	55(7)	36(6)	73(7)	4(5)	-27(6)	-14(5)
C(52A)	11483(13)	758(9)	8367(11)	125(7)	124(13)	54(8)	169(16)	-22(9)	-62(12)	22(9)
C(51B)	10790(40)	1475(8)	8500(30)	100(14)	80(20)	26(18)	170(30)	10(20)	-50(30)	22(18)
C(52B)	11740(30)	1170(30)	7730(30)	111(14)	110(30)	70(20)	150(30)	50(20)	-60(30)	-10(20)

7.11.3 Bond lengths [Å].

Atoms	Bond length	Atoms	Bond length	Atoms	Bond length
Pb-Si(2)	2.7566(15)	Si(23)-C(233)	1.877(6)	O(3)-C(72)	1.448(7)
Pb-P	2.7573(17)	Si(23)-C(232)	1.895(5)	O(3)-Li	2.010(10)
Pb-Si(1)	2.7660(15)	Si(12)-C(123)	1.869(6)	O(1)-C(62)	1.412(8)
Si(1)-Si(13)	2.337(2)	Si(12)-C(121)	1.883(5)	O(1)-C(61)	1.424(8)
Si(1)-Si(11)	2.347(2)	Si(12)-C(122)	1.893(6)	O(1)-Li	1.988(11)
Si(1)-Si(12)	2.360(2)	Si(22)-C(223)	1.862(6)	C(41)-O(2)	1.423(5)
Si(2)-Si(23)	2.348(2)	Si(22)-C(221)	1.879(6)	C(41)-C(42)	1.496(7)
Si(2)-Si(21)	2.351(2)	Si(22)-C(222)	1.884(6)	C(71)-C(61)	1.503(11)
Si(2)-Si(22)	2.364(2)	Si(21)-C(212)	1.880(5)	C(71)-Li	2.743(11)
P-Li	2.622(11)	Si(21)-C(213)	1.882(6)	Li-O(2)	1.886(11)
P-H(1)	1.26(7)	Si(21)-C(211)	1.891(6)	Li-C(51A)	2.779(14)
P-H(2)	1.18(7)	Si(11)-C(111)	1.870(6)	O(2)-C(51B)	1.425(6)
Si(13)-C(133)	1.872(6)	Si(11)-C(113)	1.875(5)	O(2)-C(51A)	1.427(6)
Si(13)-C(132)	1.881(6)	Si(11)-C(112)	1.885(6)	C(51A)-C(52A)	1.493(8)
Si(13)-C(131)	1.887(6)	O(3)-C(71)	1.392(8)	C(51B)-C(52B)	1.494(8)
Si(23)-C(231)	1.875(6)				

7.11.4 Bond angles [deg].

Atoms	Angle	Atoms	Angle
Si(2)-Pb-P	94.37(5)	C(213)-Si(21)-C(211)	104.9(3)
Si(2)-Pb-Si(1)	114.79(4)	C(212)-Si(21)-Si(2)	110.68(19)
P-Pb-Si(1)	94.75(5)	C(213)-Si(21)-Si(2)	112.9(2)
Si(13)-Si(1)-Si(11)	109.37(8)	C(211)-Si(21)-Si(2)	112.1(2)
Si(13)-Si(1)-Si(12)	106.41(8)	C(111)-Si(11)-C(113)	104.9(3)
Si(11)-Si(1)-Si(12)	103.50(8)	C(111)-Si(11)-C(112)	107.6(3)
Si(13)-Si(1)-Pb	125.98(7)	C(113)-Si(11)-C(112)	107.3(3)
Si(11)-Si(1)-Pb	101.19(6)	C(111)-Si(11)-Si(1)	113.9(2)
Si(12)-Si(1)-Pb	108.29(6)	C(113)-Si(11)-Si(1)	114.1(2)
Si(23)-Si(2)-Si(21)	108.02(8)	C(112)-Si(11)-Si(1)	108.7(2)

Atoms	Angle	Atoms	Angle
Si(23)-Si(2)-Si(22)	105.71(8)	C(71)-O(3)-C(72)	113.1(6)
Si(21)-Si(2)-Si(22)	106.20(8)	C(71)-O(3)-Li	106.0(5)
Si(23)-Si(2)-Pb	104.74(7)	C(72)-O(3)-Li	125.3(5)
Si(21)-Si(2)-Pb	128.31(7)	C(62)-O(1)-C(61)	112.0(6)
Si(22)-Si(2)-Pb	101.94(7)	C(62)-O(1)-Li	127.8(5)
Li-P-Pb	128.3(2)	C(61)-O(1)-Li	109.6(5)
Li-P-H(1)	117(3)	O(2)-C(41)-C(42)	110.5(5)
Pb-P-H(1)	102(3)	O(3)-C(71)-C(61)	108.0(6)
Li-P-H(2)	112(3)	O(3)-C(71)-Li	44.8(3)
Pb-P-H(2)	104(3)	C(61)-C(71)-Li	76.7(5)
H(1)-P-H(2)	83(4)	O(1)-C(61)-C(71)	107.2(7)
C(133)-Si(13)-C(132)	107.6(3)	O(2)-Li-O(1)	109.2(5)
C(133)-Si(13)-C(131)	106.5(3)	O(2)-Li-O(3)	114.1(5)
C(132)-Si(13)-C(131)	107.1(3)	O(1)-Li-O(3)	83.5(4)
C(133)-Si(13)-Si(1)	110.1(2)	O(2)-Li-P	127.3(4)
C(132)-Si(13)-Si(1)	111.6(2)	O(1)-Li-P	113.4(5)
C(131)-Si(13)-Si(1)	113.6(2)	O(3)-Li-P	100.3(4)
C(231)-Si(23)-C(233)	106.7(3)	O(2)-Li-C(71)	130.7(5)
C(231)-Si(23)-C(232)	108.0(3)	O(1)-Li-C(71)	57.1(3)
C(233)-Si(23)-C(232)	107.1(3)	O(3)-Li-C(71)	29.2(2)
C(231)-Si(23)-Si(2)	110.2(2)	P-Li-C(71)	98.6(4)
C(233)-Si(23)-Si(2)	111.1(2)	O(2)-Li-C(51A)	28.1(3)
C(232)-Si(23)-Si(2)	113.4(2)	O(1)-Li-C(51A)	108.6(5)
C(123)-Si(12)-C(121)	108.8(3)	O(3)-Li-C(51A)	86.0(4)
C(123)-Si(12)-C(122)	105.0(3)	P-Li-C(51A)	137.9(4)
C(121)-Si(12)-C(122)	106.3(3)	C(71)-Li-C(51A)	105.6(4)
C(123)-Si(12)-Si(1)	112.5(2)	C(41)-O(2)-C(51B)	98.7(16)
C(121)-Si(12)-Si(1)	109.8(2)	C(41)-O(2)-C(51A)	117.2(6)
C(122)-Si(12)-Si(1)	114.1(2)	C(51B)-O(2)-C(51A)	30(2)
C(223)-Si(22)-C(221)	105.2(3)	C(41)-O(2)-Li	127.4(5)
C(223)-Si(22)-C(222)	107.1(3)	C(51B)-O(2)-Li	133.4(16)
C(221)-Si(22)-C(222)	105.3(3)	C(51A)-O(2)-Li	113.3(6)
C(223)-Si(22)-Si(2)	111.7(2)	O(2)-C(51A)-C(52A)	110.7(8)
C(221)-Si(22)-Si(2)	114.1(2)	O(2)-C(51A)-Li	38.6(4)
C(222)-Si(22)-Si(2)	112.8(2)	C(52A)-C(51A)-Li	124.8(8)
C(212)-Si(21)-C(213)	109.0(3)	O(2)-C(51B)-C(52B)	113(3)
C(212)-Si(21)-C(211)	107.0(3)		

7.12 Crystallographic data for $(Hyp_2Pb{\cdot}PH_2)K{\cdot}2(MeNCH_2)_3$

7.12.1 Crystal data and structure refinement

Empirical formula	$Hyp_2PbP(H_2)K{\cdot}2$triazine
Formula weight	1020.93
Temperature	193(2) K
Wavelength	0.71073 Å
Crystal system, space group	triclinic, $P\bar{1}$
Unit cell dimensions	a = 12.5404(10) Å alpha = 86.5800(10) deg.
	b = 13.0367(11) Å beta = 82.5140(10) deg.
	c = 17.4872(14) Å gamma = 76.9430(10) deg.
Volume	2759.9(4) Å^3
Z, Calculated density	2, 1.229 g/cm^3
Absorption coefficient	3.359 mm^{-1}
F(000)	1048

Theta range for data collection	1.60 to 28.33 deg.
Limiting indices	-16<=h<=16, -16<=k<=16, -23<=l<=23
Reflections collected / unique	32172 / 12902 [R(int) = 0.0844]
Completeness to theta = 28.33	93.7 %
Refinement method	Full-matrix least-squares on F^2
Data / restraints / parameters	12902 / 307 / 750
Goodness-of-fit on F^2	0.942
Final R indices [I>2sigma(I)]	R1 = 0.0400, wR2 = 0.0810
R indices (all data)	R1 = 0.0635, wR2 = 0.0881
Extinction coefficient	0.00062(15)
Largest diff. peak and hole	0.900 and -0.966 e.Å^{-3}

7.12.2 Atomic coordinates (x 10^4), equivalent isotropic displacement parameters (Å^2 x 10^3) and Anisotropic displacement parameters (Å^2 x 10^3). U(eq) is defined as one third of the trace of the orthogonalized Uij tensor. The anisotropic displacement factor exponent takes the form: $-2\pi^2[h^2a^{*2}U11 + \ldots + 2hka^*b^*U12]$

Atom	x	y	z	U(eq)	U11	U22	U33	U23	U13	U12
Pb(1)	7707(1)	7214(1)	6902(1)	45(1)	35(1)	42(1)	60(1)	-13(1)	4(1)	-12(1)
P(1)	8753(2)	6212(2)	8075(2)	107(1)	73(1)	77(1)	177(2)	60(1)	-55(1)	-21(1)
Pb(1A)	7239(3)	7618(3)	6612(2)	48(1)	40(1)	64(2)	42(1)	-21(1)	11(1)	-18(1)
P(1A)	5736(14)	8961(16)	5868(10)	105(6)	109(13)	139(16)	74(11)	20(11)	-35(10)	-33(12)
Pb(1B)	7351(5)	7247(5)	7956(4)	82(3)						
P(1B)	9097(15)	5841(16)	8106(13)	18(5)						
Si(1A)	7573(15)	9182(16)	7399(12)	118(12)						
Si(14)	7843(11)	10609(10)	6583(7)	66(4)						
C(141)	6550(30)	11640(30)	6480(40)	60(20)						
C(142)	8480(30)	10180(30)	5585(14)	32(11)						
C(143)	8790(30)	11390(30)	6950(20)	57(11)						
Si(15)	9334(10)	8504(9)	7767(7)	59(3)						
C(151)	10370(30)	8350(50)	6900(20)	70(30)						
C(152)	9760(40)	9270(30)	8500(20)	60(18)						
C(153)	9440(30)	7156(19)	8230(20)	62(12)						
Si(16)	6451(15)	9995(13)	8483(10)	11(3)						
C(161)	6850(70)	11190(40)	8790(40)	120(60)						
C(162)	4960(20)	10390(70)	8350(40)	100(50)						
C(163)	6560(50)	9000(30)	9313(19)	24(11)						
Si(1)	7564(1)	9250(1)	7329(1)	38(1)	39(1)	35(1)	44(1)	-2(1)	-11(1)	-10(1)
Si(11)	9389(1)	9338(1)	7421(1)	45(1)	46(1)	46(1)	47(1)	3(1)	-12(1)	-19(1)
C(113)	9620(4)	10727(3)	7314(3)	61(1)	70(3)	59(3)	67(3)	7(2)	-21(2)	-36(2)
C(112)	10383(4)	8544(6)	6664(5)	68(2)	42(3)	81(4)	82(4)	-4(4)	-4(3)	-17(2)
C(111)	9814(5)	8836(5)	8389(3)	63(1)	69(3)	65(4)	65(3)	12(3)	-28(3)	-28(3)
Si(12)	6530(3)	10020(3)	8437(2)	63(1)	57(1)	74(1)	58(1)	-14(1)	-6(1)	-12(1)
C(122)	5053(5)	10603(9)	8285(4)	76(3)	59(4)	83(4)	79(5)	-14(3)	-2(3)	-2(3)
C(121)	6531(9)	9003(8)	9225(5)	98(4)	82(5)	144(7)	65(4)	19(4)	-10(4)	-20(4)
C(123)	7022(10)	11130(7)	8799(5)	88(4)	88(5)	96(6)	84(6)	-51(4)	2(3)	-26(4)
Si(13)	7098(1)	10332(1)	6244(1)	55(1)	64(1)	47(1)	50(1)	-1(1)	-18(1)	-2(1)
C(131)	6833(8)	11779(5)	6417(5)	99(3)	150(7)	52(3)	88(5)	5(3)	-27(5)	1(4)
C(132)	8227(6)	10083(6)	5419(3)	84(2)	102(5)	95(5)	55(4)	2(3)	-13(4)	-18(4)
C(133)	5851(5)	10055(5)	5888(4)	102(2)	83(4)	117(5)	108(5)	23(4)	-50(4)	-13(4)
Si(2)	5768(10)	6557(9)	7397(9)	31(2)	21(3)	24(3)	47(4)	-2(2)	8(3)	-11(2)
Si(21)	3982(3)	7519(4)	7827(3)	32(2)	17(2)	25(3)	55(4)	0(2)	-5(2)	-6(2)
C(211)	3820(20)	7900(20)	8850(10)	75(8)	58(13)	66(14)	89(17)	1(10)	8(10)	-2(10)
C(212)	3660(20)	8740(16)	7189(15)	58(7)	57(14)	43(8)	75(15)	-7(8)	-20(10)	-2(8)
C(213)	2888(18)	6780(20)	7723(17)	88(9)	39(9)	56(9)	170(30)	-23(14)	-7(12)	-6(7)

Atom	x	y	z	U(eq)	U11	U22	U33	U23	U13	U12
Si(22)	6056(5)	5202(5)	8370(3)	66(2)	61(2)	68(3)	62(3)	5(2)	-12(2)	2(2)
C(221)	7243(14)	4128(13)	7994(13)	82(6)	86(12)	56(10)	116(14)	6(8)	-37(12)	-28(9)
C(222)	6371(14)	5635(14)	9295(8)	93(6)	94(12)	114(14)	58(9)	-12(9)	-33(8)	18(9)
C(223)	4866(11)	4535(13)	8644(9)	106(6)	110(11)	116(13)	90(11)	42(10)	1(9)	-42(10)
Si(23)	5600(5)	5677(5)	6311(3)	59(1)	69(2)	50(3)	61(3)	-14(2)	-12(2)	-17(2)
C(231)	7009(14)	4945(19)	5887(12)	85(7)	93(17)	107(15)	55(9)	-48(9)	5(10)	-18(12)
C(232)	4718(10)	4683(11)	6461(10)	89(6)	53(8)	95(13)	128(14)	-65(10)	8(8)	-31(8)
C(233)	5020(20)	6665(15)	5565(11)	161(14)	240(30)	133(19)	94(14)	-8(13)	-103(18)	43(19)
Si(2A)	5777(13)	6682(13)	7340(10)	67(7)	85(11)	46(12)	58(11)	0(7)	1(8)	7(7)
Si(24)	6215(4)	4916(4)	7006(4)	76(2)	47(3)	46(3)	132(6)	-22(3)	13(3)	-16(2)
C(241)	5019(16)	4328(16)	6890(20)	95(13)	53(15)	24(10)	210(40)	-6(17)	-26(19)	-1(9)
C(242)	7110(30)	4810(30)	6051(15)	180(40)	90(30)	100(30)	340(80)	-160(40)	140(40)	-80(20)
C(243)	7070(30)	4100(20)	7720(20)	190(40)	180(50)	35(19)	390(100)	-40(30)	-180(50)	-20(20)
Si(25)	4452(5)	7453(4)	6500(5)	83(2)	52(3)	58(4)	145(7)	-19(4)	-42(4)	-5(3)
C(251)	5130(30)	7390(30)	5485(12)	130(30)	100(30)	200(60)	40(20)	-30(30)	-10(20)	50(30)
C(252)	3810(30)	8866(13)	6702(15)	91(11)	100(20)	64(16)	90(20)	-19(16)	-30(20)	29(16)
C(253)	3264(19)	6784(19)	6530(30)	230(30)	110(30)	69(18)	560(90)	20(30)	-220(50)	-30(18)
Si(26)	4859(6)	6740(5)	8578(4)	87(2)	84(5)	81(4)	92(5)	-16(4)	45(4)	-37(4)
C(261)	4020(30)	8094(19)	8810(20)	110(20)	35(17)	180(50)	120(40)	20(30)	-22(19)	-30(20)
C(262)	5860(20)	6320(20)	9318(12)	117(11)	160(30)	150(30)	44(15)	-16(19)	0(18)	-40(30)
C(263)	3870(30)	5830(30)	8720(17)	200(30)	240(40)	250(40)	160(30)	-120(30)	140(30)	-220(40)
Si(2B)	5691(11)	6573(10)	7375(8)	57(5)	29(6)	81(9)	64(9)	-26(6)	-5(5)	-15(5)
Si(27)	5997(5)	4948(5)	8049(7)	73(3)	44(2)	42(3)	121(7)	22(3)	16(3)	-9(2)
C(271)	4986(12)	4121(10)	7890(19)	152(15)	54(9)	34(8)	360(50)	35(16)	4(17)	-15(7)
C(272)	5895(19)	5200(20)	9090(8)	138(13)	120(20)	200(30)	42(13)	38(14)	35(12)	44(19)
C(273)	7421(15)	4140(20)	7750(20)	149(18)	88(16)	150(30)	140(30)	42(18)	12(15)	90(17)
Si(28)	5466(5)	6130(8)	6118(5)	66(2)	52(3)	80(5)	70(5)	-32(4)	16(3)	-28(3)
C(281)	4126(12)	5780(20)	6032(11)	122(10)	74(12)	210(30)	103(14)	-79(16)	-5(10)	-64(16)
C(282)	6584(14)	5015(16)	5720(14)	69(6)	74(13)	69(11)	65(13)	-24(9)	4(10)	-22(10)
C(283)	5520(30)	7271(18)	5413(13)	101(9)	90(17)	130(20)	58(13)	-27(14)	7(10)	21(15)
Si(29)	3978(8)	7522(8)	7864(7)	85(4)	90(7)	73(7)	84(8)	-26(6)	12(5)	-13(5)
C(291)	2920(20)	6680(30)	7982(19)	61(7)	42(11)	70(14)	70(13)	-15(9)	15(8)	-22(10)
C(292)	3950(30)	8050(30)	8843(12)	74(11)	130(30)	45(11)	43(13)	-32(9)	52(13)	-30(13)
C(293)	3410(30)	8670(20)	7210(20)	62(9)	37(11)	66(14)	84(19)	-2(11)	-16(8)	-10(8)
K(1)	9952(1)	3160(1)	7624(1)	54(1)	48(1)	73(1)	41(1)	-3(1)	-2(1)	-17(1)
N(31)	11183(3)	1772(2)	8774(2)	53(1)	57(2)	48(2)	57(2)	-9(2)	-15(2)	-8(2)
N(32)	9550(3)	2929(3)	9293(2)	53(1)	56(2)	61(2)	41(2)	-8(2)	1(2)	-16(2)
N(33)	11119(3)	3591(2)	8812(2)	54(1)	58(2)	52(2)	59(2)	-7(2)	-8(2)	-22(2)
C(31)	10253(4)	1883(3)	9364(2)	61(1)	77(3)	57(3)	54(3)	5(2)	-17(2)	-22(2)
C(32)	10179(4)	3705(3)	9407(2)	60(1)	76(3)	53(2)	53(3)	-14(2)	-9(2)	-11(2)
C(33)	11816(3)	2547(3)	8882(3)	61(1)	57(2)	66(3)	65(3)	-8(2)	-17(2)	-17(2)
C(321)	8576(4)	3038(4)	9870(3)	84(2)	75(3)	112(4)	62(3)	-9(3)	16(2)	-29(3)
C(331)	11750(4)	4395(4)	8879(3)	88(2)	104(4)	72(3)	104(4)	-15(3)	-17(3)	-49(3)
C(311)	11884(4)	702(3)	8808(3)	83(2)	91(4)	58(3)	102(4)	-16(3)	-34(3)	-6(3)
C(341)	9786(4)	2762(5)	5327(3)	89(2)	97(4)	130(5)	54(3)	-15(3)	-17(3)	-48(4)
C(351)	11140(5)	5446(4)	6399(4)	93(2)	98(4)	58(3)	128(5)	1(3)	-4(3)	-31(3)
N(34)	10366(3)	3021(3)	5942(2)	53(1)	60(2)	62(2)	40(2)	1(2)	-8(2)	-20(2)
N(35)	11040(3)	4337(2)	6472(2)	56(1)	57(2)	46(2)	67(2)	2(2)	-14(2)	-14(2)
N(36)	11978(3)	2563(3)	6567(2)	61(1)	53(2)	61(2)	57(2)	5(2)	-7(2)	9(2)
C(34)	10513(3)	4096(3)	5839(2)	58(1)	56(2)	59(3)	55(3)	15(2)	-7(2)	-6(2)
C(35)	12106(3)	3642(3)	6462(3)	64(1)	50(2)	74(3)	65(3)	0(2)	-3(2)	-13(2)
C(36)	11437(4)	2308(3)	5937(2)	63(1)	77(3)	57(2)	46(2)	-5(2)	12(2)	-8(2)
C(361)	13054(4)	1833(5)	6599(3)	104(2)	77(4)	109(4)	99(4)	10(4)	-7(3)	34(3)

7.12.3 Bond lengths [Å].

Atoms	Bond length	Atoms	Bond length	Atoms	Bond length
Pb(1)-P(1)	2.6915(19)	Si(2)-Si(23)	2.334(15)	Si(27)-C(272)	1.853(13)

Pb(1A)-P(1A)	2.680(13)	Si(2)-Si(21)	2.358(12)	Si(27)-C(273)	1.885(14)
Pb(1B)-P(1B)	2.550(15)	Si(2)-Si(22)	2.379(15)	Si(27)-C(271)	1.896(12)
Si(1A)-Si(14)	2.334(16)	Si(21)-C(211)	1.859(14)	Si(28)-C(281)	1.864(11)
Si(1A)-Si(15)	2.344(17)	Si(21)-C(213)	1.879(13)	Si(28)-C(282)	1.873(13)
Si(1A)-Si(16)	2.359(18)	Si(21)-C(212)	1.886(13)	Si(28)-C(283)	1.882(14)
Si(14)-C(141)	1.873(19)	Si(22)-C(222)	1.862(11)	Si(29)-C(292)	1.874(14)
Si(14)-C(142)	1.885(18)	Si(22)-C(221)	1.877(13)	Si(29)-C(293)	1.884(15)
Si(14)-C(143)	1.915(17)	Si(22)-C(223)	1.888(11)	Si(29)-C(291)	1.892(15)
Si(15)-C(151)	1.853(19)	Si(23)-C(232)	1.872(11)	N(31)-C(31)	1.440(5)
Si(15)-C(152)	1.874(18)	Si(23)-C(233)	1.873(13)	N(31)-C(33)	1.453(5)
Si(15)-C(153)	1.876(18)	Si(23)-C(231)	1.887(14)	N(31)-C(311)	1.474(5)
Si(16)-C(162)	1.86(2)	Si(2A)-Si(26)	2.312(16)	N(32)-C(32)	1.452(5)
Si(16)-C(161)	1.87(2)	Si(2A)-Si(24)	2.334(16)	N(32)-C(31)	1.456(5)
Si(16)-C(163)	1.887(19)	Si(2A)-Si(25)	2.373(18)	N(32)-C(321)	1.465(5)
Si(1)-Si(12)	2.331(3)	Si(24)-C(241)	1.867(14)	N(33)-C(33)	1.450(5)
Si(1)-Si(11)	2.3429(17)	Si(24)-C(243)	1.877(16)	N(33)-C(32)	1.454(5)
Si(1)-Si(13)	2.3523(19)	Si(24)-C(242)	1.883(16)	N(33)-C(331)	1.467(5)
Si(11)-C(111)	1.877(5)	Si(25)-C(251)	1.866(15)	C(341)-N(34)	1.469(5)
Si(11)-C(112)	1.879(6)	Si(25)-C(252)	1.871(13)	C(351)-N(35)	1.476(5)
Si(11)-C(113)	1.893(4)	Si(25)-C(253)	1.883(14)	N(34)-C(36)	1.449(5)
Si(12)-C(121)	1.855(7)	Si(26)-C(261)	1.875(16)	N(34)-C(34)	1.452(5)
Si(12)-C(123)	1.868(6)	Si(26)-C(263)	1.886(14)	N(35)-C(35)	1.434(5)
Si(12)-C(122)	1.882(5)	Si(26)-C(262)	1.888(15)	N(35)-C(34)	1.445(5)
Si(13)-C(133)	1.871(6)	Si(2B)-Si(29)	2.307(14)	N(36)-C(35)	1.450(5)
Si(13)-C(132)	1.872(6)	Si(2B)-Si(27)	2.340(13)	N(36)-C(36)	1.458(5)
Si(13)-C(131)	1.877(7)	Si(2B)-Si(28)	2.372(16)	N(36)-C(361)	1.471(5)

7.12.4 Bond angles [deg].

Atoms	Angle	Atoms	Angle
Si(14)-Si(1A)-Si(15)	102.6(8)	Si(24)-Si(2A)-Si(25)	102.4(6)
Si(14)-Si(1A)-Si(16)	103.2(9)	C(241)-Si(24)-C(243)	109.6(12)
Si(15)-Si(1A)-Si(16)	107.3(10)	C(241)-Si(24)-C(242)	107.2(12)
C(141)-Si(14)-C(142)	107.9(18)	C(243)-Si(24)-C(242)	106.2(13)
C(141)-Si(14)-C(143)	102.8(17)	C(241)-Si(24)-Si(2A)	115.7(8)
C(142)-Si(14)-C(143)	106.6(15)	C(243)-Si(24)-Si(2A)	110.1(11)
C(141)-Si(14)-Si(1A)	113.9(16)	C(242)-Si(24)-Si(2A)	107.6(10)
C(142)-Si(14)-Si(1A)	112.0(14)	C(251)-Si(25)-C(252)	107.9(13)
C(143)-Si(14)-Si(1A)	113.0(12)	C(251)-Si(25)-C(253)	106.3(13)
C(151)-Si(15)-C(152)	109.8(19)	C(252)-Si(25)-C(253)	105.4(11)
C(151)-Si(15)-C(153)	106.2(18)	C(251)-Si(25)-Si(2A)	109.2(12)
C(152)-Si(15)-C(153)	103.5(16)	C(252)-Si(25)-Si(2A)	113.0(10)
C(151)-Si(15)-Si(1A)	109.7(16)	C(253)-Si(25)-Si(2A)	114.6(10)
C(152)-Si(15)-Si(1A)	115.6(15)	C(261)-Si(26)-C(263)	106.5(13)
C(153)-Si(15)-Si(1A)	111.5(13)	C(261)-Si(26)-C(262)	108.3(12)
C(162)-Si(16)-C(161)	107(2)	C(263)-Si(26)-C(262)	106.9(12)
C(162)-Si(16)-C(163)	106(2)	C(261)-Si(26)-Si(2A)	111.8(13)
C(161)-Si(16)-C(163)	108(2)	C(263)-Si(26)-Si(2A)	111.9(9)
C(162)-Si(16)-Si(1A)	113.5(19)	C(262)-Si(26)-Si(2A)	111.2(10)
C(161)-Si(16)-Si(1A)	114(2)	Si(29)-Si(2B)-Si(27)	107.4(6)
C(163)-Si(16)-Si(1A)	107.6(14)	Si(29)-Si(2B)-Si(28)	104.7(6)
Si(12)-Si(1)-Si(11)	105.76(11)	Si(27)-Si(2B)-Si(28)	103.6(6)
Si(12)-Si(1)-Si(13)	109.47(11)	C(272)-Si(27)-C(273)	107.8(11)
Si(11)-Si(1)-Si(13)	104.11(7)	C(272)-Si(27)-C(271)	109.6(10)
C(111)-Si(11)-C(112)	107.8(3)	C(273)-Si(27)-C(271)	106.8(10)
C(111)-Si(11)-C(113)	105.2(2)	C(272)-Si(27)-Si(2B)	108.2(8)
C(112)-Si(11)-C(113)	106.9(3)	C(273)-Si(27)-Si(2B)	111.3(10)
C(111)-Si(11)-Si(1)	111.53(18)	C(271)-Si(27)-Si(2B)	113.0(7)
C(112)-Si(11)-Si(1)	111.73(19)	C(281)-Si(28)-C(282)	107.1(9)

Atoms	Angle	Atoms	Angle
C(113)-Si(11)-Si(1)	113.27(15)	C(281)-Si(28)-C(283)	104.8(10)
C(121)-Si(12)-C(123)	107.6(4)	C(282)-Si(28)-C(283)	105.5(10)
C(121)-Si(12)-C(122)	107.9(4)	C(281)-Si(28)-Si(2B)	115.0(6)
C(123)-Si(12)-C(122)	104.5(4)	C(282)-Si(28)-Si(2B)	112.8(8)
C(121)-Si(12)-Si(1)	109.2(3)	C(283)-Si(28)-Si(2B)	111.0(9)
C(123)-Si(12)-Si(1)	115.1(3)	C(292)-Si(29)-C(293)	107.7(12)
C(122)-Si(12)-Si(1)	112.2(2)	C(292)-Si(29)-C(291)	105.6(12)
C(133)-Si(13)-C(132)	106.2(3)	C(293)-Si(29)-C(291)	105.1(12)
C(133)-Si(13)-C(131)	108.3(4)	C(292)-Si(29)-Si(2B)	113.4(10)
C(132)-Si(13)-C(131)	105.6(4)	C(293)-Si(29)-Si(2B)	113.3(12)
C(133)-Si(13)-Si(1)	110.7(2)	C(291)-Si(29)-Si(2B)	111.2(11)
C(132)-Si(13)-Si(1)	111.6(2)	C(31)-N(31)-C(33)	109.1(3)
C(131)-Si(13)-Si(1)	114.0(3)	C(31)-N(31)-C(311)	110.5(4)
Si(23)-Si(2)-Si(21)	106.2(6)	C(33)-N(31)-C(311)	110.0(3)
Si(23)-Si(2)-Si(22)	104.0(5)	C(32)-N(32)-C(31)	108.6(3)
Si(21)-Si(2)-Si(22)	102.0(5)	C(32)-N(32)-C(321)	110.3(3)
C(211)-Si(21)-C(213)	107.7(10)	C(31)-N(32)-C(321)	109.9(3)
C(211)-Si(21)-C(212)	109.3(9)	C(33)-N(33)-C(32)	109.3(3)
C(213)-Si(21)-C(212)	105.3(9)	C(33)-N(33)-C(331)	110.2(3)
C(211)-Si(21)-Si(2)	113.3(8)	C(32)-N(33)-C(331)	110.7(3)
C(213)-Si(21)-Si(2)	112.4(9)	N(31)-C(31)-N(32)	109.2(3)
C(212)-Si(21)-Si(2)	108.5(9)	N(32)-C(32)-N(33)	108.6(3)
C(222)-Si(22)-C(221)	108.0(8)	N(33)-C(33)-N(31)	108.7(3)
C(222)-Si(22)-C(223)	105.4(8)	C(36)-N(34)-C(34)	109.1(3)
C(221)-Si(22)-C(223)	105.1(8)	C(36)-N(34)-C(341)	110.1(4)
C(222)-Si(22)-Si(2)	114.5(7)	C(34)-N(34)-C(341)	110.6(3)
C(221)-Si(22)-Si(2)	108.4(8)	C(35)-N(35)-C(34)	108.9(3)
C(223)-Si(22)-Si(2)	114.9(5)	C(35)-N(35)-C(351)	110.6(3)
C(232)-Si(23)-C(233)	107.2(9)	C(34)-N(35)-C(351)	109.8(3)
C(232)-Si(23)-C(231)	106.1(8)	C(35)-N(36)-C(36)	109.2(3)
C(233)-Si(23)-C(231)	107.9(10)	C(35)-N(36)-C(361)	110.7(4)
C(232)-Si(23)-Si(2)	116.7(6)	C(36)-N(36)-C(361)	110.5(4)
C(233)-Si(23)-Si(2)	109.2(7)	N(35)-C(34)-N(34)	109.1(3)
C(231)-Si(23)-Si(2)	109.4(7)	N(35)-C(35)-N(36)	109.4(3)
Si(26)-Si(2A)-Si(24)	106.4(7)	N(34)-C(36)-N(36)	108.8(3)
Si(26)-Si(2A)-Si(25)	107.0(7)		

7.13 Crystallographic data for $[\{(MeNCH_2)_3\}_3K]$ $[(Hyp_2Pb)_2 \cdot PH_2]$

7.13.1 Crystal data and structure refinement

Empirical formula	$Hyp_4Pb_2PK \cdot 3triazine(Et_2O)$
Formula weight	1936.86
Temperature	173(2) K
Wavelength	1.54178 Å
Crystal system, space group	triclinic, $P\bar{1}$
Unit cell dimensions	a = 16.460(5) Å alpha = 95.48(3) deg.
	b = 16.906(6) Å beta = 100.81(3) deg.
	c = 19.253(6) Å gamma = 100.62(3) deg.
Volume	5125(3) $Å^3$
Z, Calculated density	2, 1.255 g/cm^3
Absorption coefficient	8.881 mm^{-1}
F(000)	2008
Theta range for data collection	2.68 to 73.89 deg.

Limiting indices	-20<=h<=20, -20<=k<=21, -23<=l<=0
Reflections collected / unique	21220 / 20580 [R(int) = 0.0906]
Completeness to theta = 73.89	99.0 %
Max. and min. transmission	0.2697 and 0.0408
Refinement method	Full-matrix least-squares on F^2
Data / restraints / parameters	20580 / 311 / 914
Goodness-of-fit on F^2	1.021
Final R indices [I>2sigma(I)]	R1 = 0.0743, wR2 = 0.1928
R indices (all data)	R1 = 0.0945, wR2 = 0.2081
Extinction coefficient	0.00007(4)
Largest diff. peak and hole	4.631 and -3.168 e.Å^{-3}

7.13.2 Atomic coordinates (x 10^4), equivalent isotropic displacement parameters (Å^2 x 10^3) and Anisotropic displacement parameters (Å^2 x 10^3). U(eq) is defined as one third of the trace of the orthogonalized Uij tensor. The anisotropic displacement factor exponent takes the form: $-2\pi^2[h^2a^{*2}U11 + \ldots + 2hka^*b^*U12]$

Atom	x	y	z	U(eq)	U11	U22	U33	U23	U13	U12
Pb(1)	1643(1)	8003(1)	3510(1)	32(1)	30(1)	32(1)	34(1)	3(1)	6(1)	7(1)
Pb(1A)	1594(2)	8146(2)	2219(2)	44(1)	27(1)	50(2)	51(2)	-13(1)	13(1)	5(1)
P(1)	13(1)	7579(1)	2607(1)	38(1)	29(1)	38(1)	43(1)	-1(1)	5(1)	0(1)
Si(11)	1966(1)	9591(1)	3208(1)	38(1)	33(1)	31(1)	46(1)	-1(1)	7(1)	1(1)
Si(12)	1009(2)	10112(2)	3799(2)	57(1)	49(2)	47(2)	81(2)	7(1)	25(2)	16(1)
C(123)	1346(10)	11220(8)	4159(8)	83(4)	108(11)	57(8)	98(10)	-3(7)	51(9)	29(7)
C(122)	-29(7)	10013(8)	3201(10)	90(5)	37(6)	58(8)	174(16)	22(9)	10(8)	16(5)
C(121)	867(11)	9567(10)	4578(9)	99(5)	125(13)	97(11)	114(12)	38(9)	87(11)	51(10)
Si(13)	3296(2)	10202(2)	3905(1)	48(1)	38(1)	53(2)	46(1)	9(1)	2(1)	-3(1)
C(133)	4142(8)	9789(9)	3575(8)	79(4)	52(6)	80(9)	107(11)	25(8)	21(7)	12(6)
C(132)	3565(8)	11324(7)	3921(7)	71(3)	55(6)	55(7)	83(8)	-2(6)	-1(6)	-14(5)
C(131)	3350(9)	10012(10)	4838(7)	82(4)	87(9)	93(11)	57(7)	23(7)	-3(7)	9(8)
Si(14)	1881(2)	10111(2)	2133(2)	64(1)	72(2)	70(2)	44(2)	14(1)	1(1)	9(2)
C(143)	963(12)	9521(11)	1434(8)	109(6)	139(16)	88(12)	71(9)	8(8)	-22(10)	-4(11)
C(142)	1752(10)	11185(9)	2239(9)	87(4)	91(10)	68(9)	111(11)	48(8)	10(9)	28(8)
C(141)	2881(11)	10156(10)	1795(7)	92(5)	127(13)	107(12)	60(8)	21(8)	54(9)	26(10)
Si(15)	2469(2)	7030(2)	2806(1)	41(1)	35(1)	41(1)	49(1)	-3(1)	9(1)	14(1)
Si(16)	3079(2)	7258(2)	1819(2)	66(1)	55(2)	80(2)	61(2)	-7(2)	22(2)	3(2)
C(163)	3322(12)	6338(10)	1373(11)	121(7)	140(16)	84(11)	148(16)	-37(11)	91(14)	11(11)
C(162)	4062(8)	8067(9)	2043(8)	77(4)	56(7)	83(9)	92(9)	5(7)	28(7)	5(6)
C(161)	2292(10)	7599(13)	1133(8)	105(6)	95(11)	163(18)	61(8)	38(10)	22(8)	23(11)
Si(17)	3520(2)	6800(2)	3727(2)	60(1)	48(2)	58(2)	70(2)	5(1)	0(1)	16(1)
C(173)	4252(8)	6222(9)	3369(10)	89(5)	46(6)	75(9)	144(14)	2(9)	4(8)	29(6)
C(172)	3008(9)	6174(9)	4353(8)	86(4)	83(9)	84(10)	79(9)	26(8)	-9(7)	4(8)
C(171)	4179(9)	7756(8)	4249(8)	77(4)	72(8)	62(8)	82(9)	-2(6)	-16(7)	14(6)
Si(18)	1538(2)	5763(2)	2507(2)	51(1)	42(1)	41(1)	69(2)	-8(1)	12(1)	10(1)
C(183)	2094(9)	4885(7)	2470(9)	82(4)	72(8)	44(7)	129(12)	-11(7)	21(8)	22(6)
C(182)	832(7)	5688(8)	1621(6)	64(3)	48(6)	71(8)	61(6)	-27(6)	7(5)	3(5)
C(181)	838(7)	5594(7)	3164(7)	61(3)	60(6)	46(6)	74(7)	1(5)	15(6)	8(5)
Pb(2)	-1346(1)	6243(1)	2066(1)	31(1)	30(1)	33(1)	30(1)	4(1)	6(1)	7(1)
Si(21)	-2097(1)	6923(1)	908(1)	36(1)	37(1)	34(1)	34(1)	6(1)	4(1)	4(1)
Si(22)	-3400(2)	6035(2)	404(1)	44(1)	40(1)	46(1)	39(1)	11(1)	-4(1)	1(1)
C(223)	-3718(8)	5946(8)	-592(6)	69(3)	72(8)	63(8)	52(6)	9(5)	-17(5)	-10(6)
C(222)	-3329(7)	4986(6)	612(6)	57(3)	70(7)	41(6)	52(6)	14(4)	0(5)	3(5)
C(221)	-4299(7)	6358(9)	756(7)	70(3)	40(5)	87(9)	82(8)	25(7)	8(5)	8(6)
Si(23)	-2235(2)	8264(2)	818(2)	52(1)	63(2)	38(1)	50(1)	10(1)	-4(1)	10(1)
C(231)	-3030(30)	8310(20)	20(20)	109(16)	150(30)	60(20)	90(20)	3(18)	-50(20)	40(20)
C(232)	-2400(30)	8850(20)	1634(18)	96(12)	130(30)	60(20)	85(17)	-22(17)	9(19)	20(30)

Atom	x	y	z	U(eq)	U11	U22	U33	U23	U13	U12
C(233)	-1200(20)	8863(19)	690(30)	107(15)	108(19)	21(13)	190(40)	0(20)	50(20)	-11(16)
C(234)	-1660(30)	8779(16)	196(15)	109(11)	220(30)	50(15)	81(15)	34(13)	70(20)	32(19)
C(235)	-3388(14)	8327(14)	590(20)	113(12)	77(9)	37(11)	200(30)	8(16)	-56(13)	24(11)
C(236)	-1858(17)	8919(14)	1700(10)	65(6)	81(14)	48(11)	56(8)	5(7)	8(9)	-6(12)
Si(24)	-1221(2)	6646(2)	124(1)	44(1)	46(1)	53(2)	31(1)	6(1)	6(1)	6(1)
C(243)	-1566(8)	6871(9)	-807(6)	72(4)	81(8)	95(10)	38(5)	11(6)	17(5)	5(7)
C(242)	-101(7)	7234(8)	466(6)	64(3)	51(6)	85(9)	52(6)	10(6)	14(5)	0(6)
C(241)	-1172(8)	5558(7)	51(6)	60(3)	74(7)	61(7)	49(6)	0(5)	20(5)	18(6)
Si(25)	-2211(1)	6355(2)	3158(1)	38(1)	35(1)	46(1)	34(1)	3(1)	12(1)	5(1)
Si(26)	-1304(2)	6243(3)	4219(2)	69(1)	47(2)	117(3)	38(1)	17(2)	7(1)	7(2)
C(263)	-1791(8)	6325(11)	5033(6)	86(5)	73(8)	142(14)	39(6)	20(7)	20(6)	-3(8)
C(262)	-328(9)	7102(15)	4434(8)	132(9)	58(8)	240(30)	63(9)	24(12)	-3(7)	-35(12)
C(261)	-975(12)	5238(14)	4163(9)	116(7)	110(13)	190(20)	82(10)	59(12)	23(9)	81(14)
Si(27)	-3233(2)	5135(2)	2977(1)	43(1)	49(1)	39(1)	43(1)	7(1)	21(1)	5(1)
C(273)	-4228(6)	5167(7)	2334(7)	62(3)	42(5)	61(7)	78(8)	1(6)	12(5)	2(5)
C(272)	-3576(9)	4862(7)	3815(6)	66(3)	94(9)	53(6)	56(6)	7(5)	44(6)	1(6)
C(271)	-2808(8)	4260(6)	2622(6)	60(3)	87(8)	45(6)	62(6)	15(5)	36(6)	23(6)
Si(28)	-2812(2)	7459(2)	3408(2)	49(1)	47(1)	44(2)	57(2)	0(1)	23(1)	4(1)
C(283)	-1949(8)	8393(7)	3680(7)	70(3)	78(8)	54(7)	69(7)	3(6)	20(6)	-10(6)
C(282)	-3575(8)	7605(8)	2607(8)	75(3)	68(8)	65(8)	95(10)	14(7)	15(7)	18(6)
C(281)	-3396(9)	7359(9)	4145(8)	81(4)	95(9)	77(9)	87(9)	2(7)	62(8)	20(7)
K(1)	7477(2)	2124(2)	2152(1)	70(1)	50(1)	99(2)	64(1)	33(1)	15(1)	9(1)
N(51)	8998(7)	1843(6)	1602(6)	70(3)	84(7)	47(6)	82(7)	16(5)	13(6)	26(5)
C(51)	8925(9)	2473(7)	1135(7)	66(3)	92(9)	41(6)	68(7)	8(5)	21(6)	17(6)
C(511)	9237(14)	1145(10)	1247(11)	121(7)	157(18)	63(10)	143(17)	-1(10)	10(14)	56(11)
N(52)	8668(5)	3139(5)	1481(5)	50(2)	58(5)	41(4)	56(5)	17(4)	16(4)	16(4)
C(52)	9304(7)	3469(7)	2128(6)	59(3)	58(6)	55(7)	66(7)	17(5)	19(5)	11(5)
C(521)	8589(8)	3760(7)	1020(7)	65(3)	87(8)	43(6)	74(7)	24(5)	22(6)	22(6)
N(53)	9379(7)	2849(7)	2589(6)	69(3)	74(7)	68(7)	70(6)	26(5)	14(5)	15(5)
C(53)	9605(10)	2189(9)	2247(8)	81(4)	84(9)	73(9)	88(10)	33(8)	8(8)	20(8)
C(531)	9971(12)	3185(12)	3262(9)	110(6)	126(15)	108(14)	79(10)	13(9)	-11(10)	14(12)
N(41A)	6407(9)	2005(9)	3309(10)	62(5)	61(9)	66(10)	75(10)	20(8)	34(8)	30(8)
C(41A)	6582(13)	1206(12)	3389(13)	94(7)	114(15)	92(13)	105(14)	46(11)	54(12)	44(12)
C(411)	5575(14)	2110(20)	3392(17)	105(10)	56(14)	150(30)	120(20)	0(20)	38(15)	28(16)
N(42A)	7867(11)	2463(13)	3804(11)	100(7)	74(11)	152(17)	83(12)	57(12)	17(10)	23(12)
C(42A)	6993(13)	2493(15)	3916(12)	81(6)	66(11)	116(16)	75(12)	27(11)	30(10)	33(11)
C(421)	8490(20)	3110(20)	4362(19)	158(17)	90(20)	210(40)	130(30)	10(30)	-30(20)	-20(30)
N(43A)	7403(16)	1174(13)	3255(13)	92(6)	121(14)	93(14)	103(14)	55(11)	65(12)	61(11)
C(43A)	7920(20)	1700(20)	3819(17)	118(9)	113(16)	157(19)	101(17)	48(16)	49(14)	25(16)
C(431)	7600(30)	430(20)	3320(20)	141(12)	200(30)	130(30)	130(20)	30(20)	80(20)	100(20)
N(41B)	6483(13)	1988(13)	3197(16)	83(8)	74(13)	87(15)	101(15)	29(13)	43(12)	13(13)
C(41B)	6211(17)	1119(15)	3168(16)	88(8)	90(16)	74(15)	115(18)	15(15)	68(14)	8(14)
C(412)	5910(20)	2470(20)	3410(20)	116(15)	80(30)	110(30)	140(30)	10(30)	30(30)	0(20)
N(42B)	7856(17)	1730(20)	3538(17)	127(10)	127(16)	148(19)	117(18)	55(17)	45(16)	15(16)
C(42B)	7214(18)	2160(20)	3776(16)	99(8)	86(15)	130(18)	95(16)	34(15)	49(13)	22(15)
C(422)	8690(20)	2040(40)	4080(30)	180(20)	150(40)	230(40)	150(40)	50(40)	30(30)	10(40)
N(43B)	6810(20)	712(16)	2916(15)	104(8)	122(17)	89(16)	124(17)	42(14)	70(14)	22(14)
C(43B)	7510(20)	960(20)	3470(20)	108(9)	122(17)	122(19)	114(18)	43(17)	76(15)	47(17)
C(432)	6590(40)	-110(20)	2870(30)	164(19)	240(50)	100(30)	180(40)	50(30)	60(40)	70(30)
N(31)	6684(13)	1106(13)	632(11)	145(7)	160(17)	129(16)	164(18)	17(13)	91(15)	19(13)
C(31)	6031(19)	569(15)	799(14)	169(13)	210(30)	130(20)	150(20)	-41(16)	100(20)	-46(18)
C(311)	7015(19)	788(17)	63(16)	193(14)	200(30)	160(30)	220(30)	-70(20)	90(20)	30(20)
N(32)	6081(9)	2172(10)	1043(9)	108(5)	82(9)	96(11)	133(13)	17(9)	1(9)	11(8)
C(32)	5416(13)	1540(20)	1227(14)	159(11)	77(13)	220(30)	150(20)	-20(20)	7(13)	8(17)
C(321)	5731(15)	2848(14)	927(14)	161(11)	150(20)	127(19)	180(20)	31(17)	-58(17)	66(17)
N(33)	5793(14)	844(13)	1407(11)	138(7)	146(17)	119(15)	142(16)	9(12)	47(14)	-2(13)
C(33)	6402(13)	1852(11)	503(10)	99(5)	114(13)	82(12)	96(12)	11(9)	21(10)	6(10)
C(331)	5160(20)	200(20)	1586(17)	280(30)	350(50)	260(40)	180(30)	-10(30)	140(30)	-160(40)
C(64)	3814(16)	2720(14)	2106(9)	130(8)	190(20)	134(18)	73(10)	49(11)	20(12)	32(16)
C(63)	3540(13)	3281(12)	2602(11)	111(6)	106(13)	101(14)	128(16)	41(12)	-1(12)	39(11)
O(6)	4092(7)	3347(7)	3285(6)	92(3)	101(7)	86(7)	111(8)	41(6)	46(7)	37(6)

Atom	x	y	z	U(eq)	U11	U22	U33	U23	U13	U12
C(62)	3862(14)	3787(12)	3804(13)	119(7)	126(16)	83(12)	170(20)	20(13)	65(16)	47(11)
C(61)	4430(14)	3833(13)	4508(10)	123(7)	138(17)	141(18)	100(13)	18(12)	71(13)	4(14)

7.13.3 Bond lengths [Å].

Atoms	Bond length	Atoms	Bond length	Atoms	Bond length
Pb(1)-Si(15)	2.735(2)	Si(22)-C(222)	1.875(10)	C(51)-N(52)	1.424(14)
Pb(1)-Si(11)	2.777(3)	Si(22)-C(221)	1.886(12)	N(52)-C(521)	1.447(12)
Pb(1)-P(1)	2.836(2)	Si(23)-C(231)	1.84(2)	N(52)-C(52)	1.457(14)
Pb(1A)-Si(15)	2.776(4)	Si(23)-C(234)	1.85(2)	C(52)-N(53)	1.444(14)
Pb(1A)-Si(11)	2.844(4)	Si(23)-C(236)	1.866(19)	N(53)-C(53)	1.386(18)
Pb(1A)-P(1)	2.864(3)	Si(23)-C(232)	1.87(2)	N(53)-C(531)	1.460(19)
Pb(1A)-Si(16)	3.264(4)	Si(23)-C(233)	1.88(2)	N(41A)-C(42A)	1.44(2)
P(1)-Pb(2)	2.828(2)	Si(23)-C(235)	1.89(2)	N(41A)-C(41A)	1.45(2)
Si(11)-Si(14)	2.314(4)	Si(24)-C(241)	1.849(12)	N(41A)-C(411)	1.45(2)
Si(11)-Si(13)	2.338(4)	Si(24)-C(243)	1.872(11)	C(41A)-N(43A)	1.43(2)
Si(11)-Si(12)	2.355(4)	Si(24)-C(242)	1.888(11)	N(42A)-C(43A)	1.31(4)
Si(12)-C(122)	1.841(14)	Si(25)-Si(28)	2.321(4)	N(42A)-C(42A)	1.50(3)
Si(12)-C(121)	1.864(14)	Si(25)-Si(26)	2.340(4)	N(42A)-C(421)	1.53(3)
Si(12)-C(123)	1.876(13)	Si(25)-Si(27)	2.360(4)	N(43A)-C(43A)	1.37(4)
Si(13)-C(131)	1.843(12)	Si(26)-C(261)	1.88(2)	N(43A)-C(431)	1.37(3)
Si(13)-C(133)	1.854(13)	Si(26)-C(263)	1.894(11)	N(41B)-C(42B)	1.44(2)
Si(13)-C(132)	1.862(13)	Si(26)-C(262)	1.908(17)	N(41B)-C(41B)	1.45(2)
Si(14)-C(142)	1.863(14)	Si(27)-C(273)	1.870(12)	N(41B)-C(412)	1.45(2)
Si(14)-C(141)	1.873(14)	Si(27)-C(271)	1.874(10)	C(41B)-N(43B)	1.43(2)
Si(14)-C(143)	1.876(16)	Si(27)-C(272)	1.877(10)	N(42B)-C(43B)	1.31(4)
Si(15)-Si(16)	2.341(4)	Si(28)-C(281)	1.861(11)	N(42B)-C(42B)	1.50(3)
Si(15)-Si(18)	2.343(4)	Si(28)-C(282)	1.864(14)	N(42B)-C(422)	1.53(3)
Si(15)-Si(17)	2.348(4)	Si(28)-C(283)	1.877(12)	N(43B)-C(43B)	1.37(4)
Si(16)-C(163)	1.848(14)	K(1)-N(43A)	2.789(18)	N(43B)-C(432)	1.37(3)
Si(16)-C(162)	1.867(13)	K(1)-N(32)	2.848(15)	N(31)-C(31)	1.38(3)
Si(16)-C(161)	1.879(16)	K(1)-N(41B)	2.82(3)	N(31)-C(311)	1.42(3)
Si(17)-C(171)	1.853(13)	K(1)-N(42B)	2.80(3)	N(31)-C(33)	1.45(3)
Si(17)-C(173)	1.870(13)	K(1)-N(52)	2.932(8)	C(31)-N(33)	1.37(3)
Si(17)-C(172)	1.894(14)	K(1)-N(51)	2.993(11)	N(32)-C(33)	1.36(2)
Si(18)-C(182)	1.855(12)	K(1)-N(43B)	3.06(3)	N(32)-C(321)	1.39(2)
Si(18)-C(181)	1.870(11)	K(1)-N(53)	3.068(11)	N(32)-C(32)	1.51(3)
Si(18)-C(183)	1.885(12)	K(1)-N(41A)	3.086(18)	C(32)-N(33)	1.46(3)
Pb(2)-Si(25)	2.763(2)	K(1)-N(42A)	3.10(2)	N(33)-C(331)	1.48(3)
Pb(2)-Si(21)	2.792(2)	K(1)-N(31)	3.16(2)	C(64)-C(63)	1.47(3)
Si(21)-Si(23)	2.340(4)	K(1)-N(33)	3.18(2)	C(63)-O(6)	1.43(2)
Si(21)-Si(24)	2.347(3)	N(51)-C(53)	1.437(18)	O(6)-C(62)	1.34(2)
Si(21)-Si(22)	2.356(3)	N(51)-C(511)	1.461(17)	C(62)-C(61)	1.48(3)
Si(22)-C(223)	1.874(11)	N(51)-C(51)	1.465(14)		

7.13.4 Bond angles [deg].

Atoms	Angle	Atoms	Angle
Si(15)-Pb(1)-Si(11)	112.24(8)	N(42B)-K(1)-N(43B)	45.0(7)
Si(15)-Pb(1)-P(1)	100.03(8)	N(52)-K(1)-N(43B)	157.3(6)
Si(11)-Pb(1)-P(1)	94.75(7)	N(51)-K(1)-N(43B)	110.8(5)
Si(15)-Pb(1A)-Si(11)	109.05(12)	N(43A)-K(1)-N(53)	96.4(6)
Si(15)-Pb(1A)-P(1)	98.40(12)	N(32)-K(1)-N(53)	138.6(4)
Si(11)-Pb(1A)-P(1)	92.72(10)	N(41B)-K(1)-N(53)	120.2(6)
Si(15)-Pb(1A)-Si(16)	44.71(9)	N(42B)-K(1)-N(53)	78.6(6)
Si(11)-Pb(1A)-Si(16)	121.88(12)	N(52)-K(1)-N(53)	46.5(3)

Atoms	Angle	Atoms	Angle
P(1)-Pb(1A)-Si(16)	133.80(13)	N(51)-K(1)-N(53)	45.2(3)
Pb(2)-P(1)-Pb(1)	142.00(9)	N(43B)-K(1)-N(53)	116.3(7)
Pb(2)-P(1)-Pb(1A)	133.69(10)	N(43A)-K(1)-N(41A)	47.0(5)
Pb(1)-P(1)-Pb(1A)	52.20(7)	N(32)-K(1)-N(41A)	93.9(5)
Si(14)-Si(11)-Si(13)	106.37(14)	N(41B)-K(1)-N(41A)	1.0(6)
Si(14)-Si(11)-Si(12)	106.88(16)	N(42B)-K(1)-N(41A)	49.6(7)
Si(13)-Si(11)-Si(12)	104.30(15)	N(52)-K(1)-N(41A)	148.1(3)
Si(14)-Si(11)-Pb(1)	131.36(13)	N(51)-K(1)-N(41A)	150.6(3)
Si(13)-Si(11)-Pb(1)	105.98(12)	N(43B)-K(1)-N(41A)	47.8(6)
Si(12)-Si(11)-Pb(1)	99.09(11)	N(53)-K(1)-N(41A)	119.4(4)
Si(14)-Si(11)-Pb(1A)	78.64(13)	N(43A)-K(1)-N(42A)	44.7(6)
Si(13)-Si(11)-Pb(1A)	125.71(13)	N(32)-K(1)-N(42A)	135.3(5)
Si(12)-Si(11)-Pb(1A)	126.39(13)	N(41B)-K(1)-N(42A)	45.7(6)
Pb(1)-Si(11)-Pb(1A)	52.98(8)	N(42B)-K(1)-N(42A)	24.6(6)
C(122)-Si(12)-C(121)	109.0(8)	N(52)-K(1)-N(42A)	114.3(4)
C(122)-Si(12)-C(123)	105.0(7)	N(51)-K(1)-N(42A)	111.5(4)
C(121)-Si(12)-C(123)	106.2(7)	N(43B)-K(1)-N(42A)	64.2(7)
C(122)-Si(12)-Si(11)	111.7(6)	N(53)-K(1)-N(42A)	74.6(4)
C(121)-Si(12)-Si(11)	110.0(4)	N(41A)-K(1)-N(42A)	45.0(4)
C(123)-Si(12)-Si(11)	114.7(4)	N(43A)-K(1)-N(31)	112.4(7)
C(131)-Si(13)-C(133)	108.1(7)	N(32)-K(1)-N(31)	45.8(5)
C(131)-Si(13)-C(132)	106.8(7)	N(41B)-K(1)-N(31)	117.1(6)
C(133)-Si(13)-C(132)	106.7(6)	N(42B)-K(1)-N(31)	134.4(8)
C(131)-Si(13)-Si(11)	110.2(5)	N(52)-K(1)-N(31)	87.9(4)
C(133)-Si(13)-Si(11)	111.0(5)	N(51)-K(1)-N(31)	76.9(4)
C(132)-Si(13)-Si(11)	113.7(4)	N(43B)-K(1)-N(31)	92.1(7)
C(142)-Si(14)-C(141)	104.4(7)	N(53)-K(1)-N(31)	120.7(4)
C(142)-Si(14)-C(143)	107.3(8)	N(41A)-K(1)-N(31)	118.1(4)
C(141)-Si(14)-C(143)	109.7(8)	N(42A)-K(1)-N(31)	156.3(5)
C(142)-Si(14)-Si(11)	111.1(5)	N(43A)-K(1)-N(33)	82.3(7)
C(141)-Si(14)-Si(11)	111.8(5)	N(32)-K(1)-N(33)	46.6(5)
C(143)-Si(14)-Si(11)	112.1(6)	N(41B)-K(1)-N(33)	74.7(6)
Si(16)-Si(15)-Si(18)	106.62(15)	N(42B)-K(1)-N(33)	104.3(7)
Si(16)-Si(15)-Si(17)	107.88(15)	N(52)-K(1)-N(33)	128.5(4)
Si(18)-Si(15)-Si(17)	102.89(16)	N(51)-K(1)-N(33)	113.5(5)
Si(16)-Si(15)-Pb(1)	128.74(15)	N(43B)-K(1)-N(33)	60.0(8)
Si(18)-Si(15)-Pb(1)	105.21(11)	N(53)-K(1)-N(33)	157.8(5)
Si(17)-Si(15)-Pb(1)	102.81(12)	N(41A)-K(1)-N(33)	75.7(5)
Si(16)-Si(15)-Pb(1A)	78.78(14)	N(42A)-K(1)-N(33)	117.0(5)
Si(18)-Si(15)-Pb(1A)	106.30(13)	N(31)-K(1)-N(33)	42.5(5)
Si(17)-Si(15)-Pb(1A)	146.69(15)	C(53)-N(51)-C(511)	111.1(12)
Pb(1)-Si(15)-Pb(1A)	54.13(7)	C(53)-N(51)-C(51)	108.8(10)
C(163)-Si(16)-C(162)	108.3(7)	C(511)-N(51)-C(51)	111.2(12)
C(163)-Si(16)-C(161)	106.0(10)	C(53)-N(51)-K(1)	96.1(8)
C(162)-Si(16)-C(161)	107.8(8)	C(511)-N(51)-K(1)	135.1(11)
C(163)-Si(16)-Si(15)	113.8(6)	C(51)-N(51)-K(1)	91.5(7)
C(162)-Si(16)-Si(15)	112.7(5)	N(52)-C(51)-N(51)	110.5(9)
C(161)-Si(16)-Si(15)	108.0(5)	N(52)-C(51)-K(1)	60.2(5)
C(163)-Si(16)-Pb(1A)	145.9(6)	N(51)-C(51)-K(1)	62.7(6)
C(162)-Si(16)-Pb(1A)	105.2(5)	C(51)-N(52)-C(521)	110.7(9)
C(161)-Si(16)-Pb(1A)	56.8(5)	C(51)-N(52)-C(52)	108.0(9)
Si(15)-Si(16)-Pb(1A)	56.51(11)	C(521)-N(52)-C(52)	109.9(9)
C(171)-Si(17)-C(173)	107.0(7)	C(51)-N(52)-K(1)	94.8(6)
C(171)-Si(17)-C(172)	108.6(7)	C(521)-N(52)-K(1)	133.6(7)
C(173)-Si(17)-C(172)	107.5(8)	C(52)-N(52)-K(1)	97.1(5)
C(171)-Si(17)-Si(15)	112.6(4)	N(53)-C(52)-N(52)	109.8(9)
C(173)-Si(17)-Si(15)	111.4(5)	N(53)-C(52)-K(1)	63.3(6)
C(172)-Si(17)-Si(15)	109.5(5)	N(52)-C(52)-K(1)	58.0(5)
C(182)-Si(18)-C(181)	106.6(5)	C(53)-N(53)-C(52)	110.8(10)
C(182)-Si(18)-C(183)	106.9(6)	C(53)-N(53)-C(531)	112.0(13)
C(181)-Si(18)-C(183)	107.2(6)	C(52)-N(53)-C(531)	110.5(12)

Atoms	Angle	Atoms	Angle
C(182)-Si(18)-Si(15)	111.2(4)	C(53)-N(53)-K(1)	94.0(8)
C(181)-Si(18)-Si(15)	111.4(4)	C(52)-N(53)-K(1)	91.8(7)
C(183)-Si(18)-Si(15)	113.2(4)	C(531)-N(53)-K(1)	135.1(10)
Si(25)-Pb(2)-Si(21)	110.18(7)	N(53)-C(53)-N(51)	111.4(12)
Si(25)-Pb(2)-P(1)	98.28(7)	N(53)-C(53)-K(1)	62.4(7)
Si(21)-Pb(2)-P(1)	96.62(7)	N(51)-C(53)-K(1)	59.5(7)
Si(23)-Si(21)-Si(24)	105.28(13)	C(42A)-N(41A)-C(41A)	101.4(15)
Si(23)-Si(21)-Si(22)	109.53(14)	C(42A)-N(41A)-C(411)	105.9(17)
Si(24)-Si(21)-Si(22)	103.75(13)	C(41A)-N(41A)-C(411)	115.7(17)
Si(23)-Si(21)-Pb(2)	130.05(12)	C(42A)-N(41A)-K(1)	101.3(10)
Si(24)-Si(21)-Pb(2)	98.34(10)	C(41A)-N(41A)-K(1)	88.8(9)
Si(22)-Si(21)-Pb(2)	106.50(10)	C(411)-N(41A)-K(1)	138.1(13)
C(223)-Si(22)-C(222)	106.0(5)	N(43A)-C(41A)-N(41A)	109.8(14)
C(223)-Si(22)-C(221)	105.7(6)	N(43A)-C(41A)-K(1)	54.0(9)
C(222)-Si(22)-C(221)	109.4(6)	N(41A)-C(41A)-K(1)	65.9(8)
C(223)-Si(22)-Si(21)	114.8(4)	C(43A)-N(42A)-C(42A)	105(2)
C(222)-Si(22)-Si(21)	108.9(4)	C(43A)-N(42A)-C(421)	118(2)
C(221)-Si(22)-Si(21)	111.8(4)	C(42A)-N(42A)-C(421)	107(2)
C(231)-Si(23)-C(234)	73.2(16)	C(43A)-N(42A)-K(1)	88.4(18)
C(231)-Si(23)-C(236)	132.9(14)	C(42A)-N(42A)-K(1)	99.2(12)
C(234)-Si(23)-C(236)	106.0(11)	C(421)-N(42A)-K(1)	134.6(16)
C(231)-Si(23)-C(232)	112.2(17)	N(41A)-C(42A)-N(42A)	106.8(18)
C(234)-Si(23)-C(232)	120.7(16)	C(43A)-N(43A)-C(431)	107(3)
C(236)-Si(23)-C(232)	26.8(14)	C(43A)-N(43A)-C(41A)	102(2)
C(231)-Si(23)-C(233)	105.8(17)	C(431)-N(43A)-C(41A)	113(2)
C(234)-Si(23)-C(233)	33.1(16)	C(43A)-N(43A)-K(1)	100.7(17)
C(236)-Si(23)-C(233)	79.7(14)	C(431)-N(43A)-K(1)	130.0(17)
C(232)-Si(23)-C(233)	102.5(15)	C(41A)-N(43A)-K(1)	101.5(12)
C(231)-Si(23)-C(235)	42.1(17)	N(43A)-C(43A)-N(42A)	115(3)
C(234)-Si(23)-C(235)	110.0(13)	N(43A)-C(43A)-K(1)	55.4(12)
C(236)-Si(23)-C(235)	102.3(11)	N(42A)-C(43A)-K(1)	68.5(16)
C(232)-Si(23)-C(235)	76.2(14)	C(42B)-N(41B)-C(41B)	101.4(15)
C(233)-Si(23)-C(235)	136.5(15)	C(42B)-N(41B)-C(412)	105.9(17)
C(231)-Si(23)-Si(21)	110.6(11)	C(41B)-N(41B)-C(412)	115.6(17)
C(234)-Si(23)-Si(21)	115.4(9)	C(42B)-N(41B)-K(1)	92.9(12)
C(236)-Si(23)-Si(21)	111.6(8)	C(41B)-N(41B)-K(1)	103.2(12)
C(232)-Si(23)-Si(21)	116.3(14)	C(412)-N(41B)-K(1)	131.6(15)
C(233)-Si(23)-Si(21)	108.6(12)	N(43B)-C(41B)-N(41B)	109.8(14)
C(235)-Si(23)-Si(21)	110.7(7)	N(43B)-C(41B)-K(1)	62.3(11)
C(241)-Si(24)-C(243)	106.6(6)	N(41B)-C(41B)-K(1)	52.7(10)
C(241)-Si(24)-C(242)	106.5(6)	C(43B)-N(42B)-C(42B)	105(2)
C(243)-Si(24)-C(242)	107.1(5)	C(43B)-N(42B)-C(422)	118(2)
C(241)-Si(24)-Si(21)	109.8(4)	C(42B)-N(42B)-C(422)	107(2)
C(243)-Si(24)-Si(21)	115.0(4)	C(43B)-N(42B)-K(1)	103(2)
C(242)-Si(24)-Si(21)	111.3(4)	C(42B)-N(42B)-K(1)	92.5(14)
Si(28)-Si(25)-Si(26)	106.08(16)	C(422)-N(42B)-K(1)	126.0(18)
Si(28)-Si(25)-Si(27)	110.38(13)	N(41B)-C(42B)-N(42B)	106.8(18)
Si(26)-Si(25)-Si(27)	102.40(15)	N(41B)-C(42B)-K(1)	60.7(11)
Si(28)-Si(25)-Pb(2)	122.40(12)	N(42B)-C(42B)-K(1)	59.8(12)
Si(26)-Si(25)-Pb(2)	107.96(11)	C(43B)-N(43B)-C(432)	107(3)
Si(27)-Si(25)-Pb(2)	105.86(10)	C(43B)-N(43B)-C(41B)	102(2)
C(261)-Si(26)-C(263)	106.8(8)	C(432)-N(43B)-C(41B)	113(2)
C(261)-Si(26)-C(262)	109.8(10)	C(43B)-N(43B)-K(1)	89.6(17)
C(263)-Si(26)-C(262)	104.4(7)	C(432)-N(43B)-K(1)	145.2(18)
C(261)-Si(26)-Si(25)	110.6(6)	C(41B)-N(43B)-K(1)	93.2(12)
C(263)-Si(26)-Si(25)	113.8(5)	N(43B)-C(43B)-N(42B)	115(3)
C(262)-Si(26)-Si(25)	111.2(6)	N(43B)-C(43B)-K(1)	66.1(14)
C(273)-Si(27)-C(271)	107.5(6)	N(42B)-C(43B)-K(1)	54.4(16)
C(273)-Si(27)-C(272)	105.3(6)	C(31)-N(31)-C(311)	114(2)
C(271)-Si(27)-C(272)	106.5(5)	C(31)-N(31)-C(33)	109(2)
C(273)-Si(27)-Si(25)	113.1(4)	C(311)-N(31)-C(33)	112(2)

Atoms	Angle	Atoms	Angle
C(271)-Si(27)-Si(25)	110.7(4)	C(31)-N(31)-K(1)	100.0(15)
C(272)-Si(27)-Si(25)	113.3(4)	C(311)-N(31)-K(1)	135.0(18)
C(281)-Si(28)-C(282)	107.1(7)	C(33)-N(31)-K(1)	81.4(12)
C(281)-Si(28)-C(283)	107.6(6)	N(33)-C(31)-N(31)	113(2)
C(282)-Si(28)-C(283)	109.1(6)	C(33)-N(32)-C(321)	117(2)
C(281)-Si(28)-Si(25)	113.5(5)	C(33)-N(32)-C(32)	110.1(17)
C(282)-Si(28)-Si(25)	110.7(5)	C(321)-N(32)-C(32)	108(2)
C(283)-Si(28)-Si(25)	108.7(5)	C(33)-N(32)-K(1)	95.7(11)
N(43A)-K(1)-N(32)	124.9(6)	C(321)-N(32)-K(1)	125.4(13)
N(43A)-K(1)-N(41B)	46.7(7)	C(32)-N(32)-K(1)	99.7(13)
N(32)-K(1)-N(41B)	93.4(6)	N(33)-C(32)-N(32)	108.4(17)
N(43A)-K(1)-N(42B)	22.9(8)	N(33)-C(32)-K(1)	67.6(12)
N(32)-K(1)-N(42B)	141.6(7)	N(32)-C(32)-K(1)	54.7(10)
N(41B)-K(1)-N(42B)	49.8(5)	C(31)-N(33)-C(32)	105(2)
N(43A)-K(1)-N(52)	142.4(5)	C(31)-N(33)-C(331)	110(2)
N(32)-K(1)-N(52)	92.2(4)	C(32)-N(33)-C(331)	110(3)
N(41B)-K(1)-N(52)	149.1(5)	C(31)-N(33)-K(1)	99.4(15)
N(42B)-K(1)-N(52)	124.8(6)	C(32)-N(33)-K(1)	87.3(13)
N(43A)-K(1)-N(51)	104.9(5)	C(331)-N(33)-K(1)	140.1(19)
N(32)-K(1)-N(51)	112.8(4)	N(32)-C(33)-N(31)	113.7(16)
N(41B)-K(1)-N(51)	150.6(5)	N(32)-C(33)-K(1)	59.9(10)
N(42B)-K(1)-N(51)	101.5(6)	N(31)-C(33)-K(1)	72.6(12)
N(52)-K(1)-N(51)	47.2(2)	O(6)-C(63)-C(64)	107.1(15)
N(43A)-K(1)-N(43B)	22.4(5)	C(62)-O(6)-C(63)	113.2(15)
N(32)-K(1)-N(43B)	104.1(7)	O(6)-C(62)-C(61)	112.3(16)
N(41B)-K(1)-N(43B)	47.0(5)		

7.14 Crystallographic data for [(Hyp$_2$Pb·P(H)Hyp]$_2$

7.14.1 Crystal data and structure refinement

Empirical formula	$Hyp_4P_2(H)_2Pb_2\cdot Et_2O$
Formula weight	1541.10
Temperature	188(2) K
Wavelength	0.71073 Å
Crystal system, space group	monoclinic, P2(1)/n
Unit cell dimensions	a = 14.4402(4) Å alpha = 90 deg. b = 24.4936(6) Å beta = 94.287(2) deg. c = 22.2942(6) Å gamma = 90 deg.
Volume	7863.2(4) Å^3
Z, Calculated density	4, 1.302 g/cm^3
Absorption coefficient	4.586 mm^{-1}
F(000)	3136
Theta range for data collection	3.43 to 28.31 deg.
Limiting indices	-19<=h<=17, -32<=k<=31, -29<=l<=27
Reflections collected / unique	71278 / 19355 [R(int) = 0.0738]
Completeness to theta = 28.31	98.9 %
Refinement method	Full-matrix least-squares on F^2
Data / restraints / parameters	19355 / 167 / 745
Goodness-of-fit on F^2	1.036
Final R indices [I>2sigma(I)]	R1 = 0.0460, wR2 = 0.0995
R indices (all data)	R1 = 0.0835, wR2 = 0.1197
Largest diff. peak and hole	1.917 and -0.791 e.Å^{-3}

7.14.2 Anisotropic displacement parameters (Å^2 x 10^3). The anisotropic displacement factor exponent takes the form: $-2\pi^2[h^2a^{*2}U11 + \ldots + 2hka^*b^*U12]$

Atom	U11	U22	U33	U23	U13	U12
Pb(1)	44(1)	35(1)	45(1)	1(1)	4(1)	3(1)
Pb(2)	39(1)	36(1)	42(1)	4(1)	2(1)	2(1)
P(2)	34(1)	36(1)	50(1)	4(1)	4(1)	-1(1)
P(1)	37(1)	38(1)	46(1)	5(1)	8(1)	-1(1)
Pb(1A)	54(2)	43(2)	55(2)	1(1)	9(1)	-4(1)
Pb(2A)	51(2)	49(2)	56(2)	2(1)	9(1)	1(1)
P(1B)	54(10)	31(8)	81(13)	-43(8)	-47(9)	-9(7)
P(2B)	58(11)	0(5)	90(14)	3(8)	-24(9)	-7(6)
Si(2)	36(1)	38(1)	39(1)	5(1)	3(1)	1(1)
Si(21)	44(1)	48(1)	47(1)	7(1)	12(1)	1(1)
Si(22)	49(1)	42(1)	54(1)	11(1)	7(1)	11(1)
Si(23)	46(1)	62(2)	45(1)	0(1)	4(1)	-12(1)
Si(4)	34(1)	40(1)	39(1)	6(1)	2(1)	-3(1)
Si(41)	36(1)	60(1)	48(1)	11(1)	4(1)	-7(1)
Si(42)	47(1)	40(1)	62(1)	0(1)	-3(1)	-4(1)
Si(43)	57(1)	60(1)	45(1)	16(1)	-3(1)	0(1)
Si(3)	41(1)	42(1)	50(1)	13(1)	12(1)	4(1)
Si(31)	56(1)	52(1)	50(1)	5(1)	10(1)	11(1)
Si(32)	61(1)	74(2)	64(1)	29(1)	15(1)	23(1)
Si(33)	51(1)	60(1)	78(2)	8(1)	17(1)	-15(1)
Si(1)	54(1)	34(1)	53(1)	-1(1)	4(1)	8(1)
Si(11)	63(1)	58(1)	79(2)	-11(1)	19(1)	2(1)
Si(12)	68(1)	57(1)	81(2)	-16(1)	-3(1)	5(1)
Si(13)	117(2)	48(1)	61(1)	6(1)	9(1)	25(1)
C(111)	91(7)	72(6)	86(6)	5(5)	34(5)	-6(5)
C(112)	64(6)	76(7)	146(10)	-9(6)	-9(6)	10(5)
C(113)	114(8)	81(7)	104(8)	-34(6)	54(7)	-11(6)
C(121)	115(9)	133(10)	73(7)	27(7)	-13(6)	-4(8)
C(122)	75(6)	72(6)	142(11)	-22(6)	-3(7)	-12(5)
C(123)	98(8)	109(9)	161(12)	-88(9)	-31(8)	18(7)
C(131)	147(9)	68(6)	41(4)	4(4)	-16(5)	28(6)
C(132)	133(10)	51(5)	80(6)	3(5)	5(6)	39(6)
C(133)	203(14)	50(5)	112(9)	12(6)	61(9)	-19(7)
C(211)	93(7)	64(6)	109(8)	1(5)	60(7)	14(5)
C(212)	61(5)	96(8)	78(6)	3(5)	17(5)	-29(5)
C(213)	77(6)	133(9)	46(4)	27(5)	11(4)	14(6)
C(231)	97(7)	53(5)	82(6)	-11(4)	6(5)	-17(5)
C(232)	58(5)	84(7)	112(8)	-20(6)	26(5)	-27(5)
C(233)	88(7)	122(9)	63(5)	19(6)	-31(5)	-29(6)
C(221)	107(8)	88(7)	73(6)	30(5)	10(5)	48(6)
C(222)	92(6)	54(5)	65(5)	4(4)	24(4)	17(4)
C(223)	84(7)	44(5)	151(10)	-7(5)	17(6)	-2(4)
C(311)	90(7)	60(5)	73(7)	-16(5)	-7(5)	1(4)
C(313)	108(9)	90(7)	86(7)	19(6)	53(7)	37(6)
C(312)	65(5)	49(4)	74(5)	10(4)	2(4)	9(4)
C(321)	94(7)	120(8)	78(6)	61(6)	43(5)	45(6)
C(322)	88(6)	69(6)	113(8)	43(5)	44(6)	35(5)
C(323)	109(10)	134(11)	98(8)	19(8)	-29(7)	26(8)
C(331)	53(5)	135(10)	95(7)	8(7)	18(5)	-21(6)
C(332)	60(5)	105(8)	84(6)	2(6)	-2(5)	-20(5)
C(333)	134(10)	53(6)	145(12)	14(6)	13(8)	-19(6)
C(411)	63(5)	110(7)	53(5)	19(5)	8(4)	-20(5)
C(413)	42(4)	77(5)	70(5)	18(4)	4(3)	-15(4)

Atom	U11	U22	U33	U23	U13	U12
C(412)	56(5)	67(5)	89(6)	3(4)	20(4)	6(4)
C(421)	67(6)	62(5)	123(9)	-27(6)	-1(6)	-22(4)
C(422)	115(8)	52(5)	89(7)	20(5)	-7(6)	12(5)
C(423)	59(5)	71(6)	89(6)	-17(5)	13(4)	-7(4)
C(431)	100(8)	140(11)	72(6)	27(7)	-39(6)	-33(7)
C(432)	65(5)	69(6)	101(8)	30(6)	-2(5)	8(4)
C(433)	130(9)	110(9)	65(6)	27(6)	31(6)	24(7)
C(01)	290(30)	370(40)	154(18)	40(20)	22(19)	-70(30)
C(02)	180(20)	280(30)	560(60)	-220(40)	-90(30)	-40(20)
O(03)	320(20)	720(50)	261(19)	340(30)	156(18)	290(30)
C(04)	820(110)	650(90)	890(110)	260(80)	100(80)	-240(80)
C(05)	220(20)	310(30)	210(20)	70(20)	-21(17)	10(20)

7.14.3 Bond lengths [Å].

Atoms	Bond length	Atoms	Bond length	Atoms	Bond length
Pb(1)-P(1)	2.7762(17)	Si(26)-C(263)	1.90(2)	Si(3B)-Si(34)	2.360(5)
Pb(1)-Si(1)	2.785(2)	Si(4)-Si(43)	2.355(3)	Si(34)-C(342)	1.864(10)
Pb(1)-P(2)	2.7943(16)	Si(4)-Si(41)	2.356(3)	Si(34)-C(341)	1.868(11)
Pb(2)-Si(2)	2.771(3)	Si(4)-Si(42)	2.362(3)	Si(34)-C(343)	1.881(11)
Pb(2)-P(1)	2.7921(17)	Si(41)-C(411)	1.858(8)	Si(35)-C(352)	1.882(10)
Pb(2)-P(2)	2.7965(17)	Si(41)-C(412)	1.873(8)	Si(35)-C(351)	1.885(10)
P(2)-Si(4)	2.282(2)	Si(41)-C(413)	1.879(8)	Si(35)-C(353)	1.886(15)
P(1)-Si(3)	2.286(3)	Si(42)-C(423)	1.852(9)	Si(36)-C(362)	1.853(11)
Pb(1A)-P(2B)	2.707(14)	Si(42)-C(422)	1.855(11)	Si(36)-C(363)	1.853(12)
Pb(1A)-P(1B)	2.767(18)	Si(42)-C(421)	1.894(8)	Si(36)-C(361)	1.884(11)
Pb(1A)-Si(3B)	2.80(3)	Si(43)-C(432)	1.850(10)	Si(1)-Si(12)	2.330(3)
Pb(2A)-P(2B)	2.81(2)	Si(43)-C(433)	1.858(10)	Si(1)-Si(13)	2.349(3)
Pb(2A)-P(1B)	2.84(2)	Si(43)-C(431)	1.859(10)	Si(1)-Si(11)	2.371(3)
Pb(2A)-Si(4B)	3.138(19)	Si(4B)-Si(45)	2.329(16)	Si(11)-C(111)	1.860(10)
P(1B)-Si(1B)	2.11(2)	Si(4B)-Si(44)	2.349(16)	Si(11)-C(112)	1.860(11)
P(2B)-Si(2A)	2.30(4)	Si(4B)-Si(46)	2.397(16)	Si(11)-C(113)	1.882(9)
Si(2)-Si(23)	2.348(3)	Si(44)-C(441)	1.87(2)	Si(12)-C(121)	1.870(11)
Si(2)-Si(21)	2.353(3)	Si(44)-C(442)	1.88(2)	Si(12)-C(123)	1.885(10)
Si(2)-Si(22)	2.354(3)	Si(44)-C(443)	1.88(2)	Si(12)-C(122)	1.896(11)
Si(21)-C(213)	1.851(8)	Si(45)-C(453)	1.85(2)	Si(13)-C(132)	1.871(9)
Si(21)-C(212)	1.862(9)	Si(45)-C(452)	1.86(2)	Si(13)-C(131)	1.889(9)
Si(21)-C(211)	1.870(9)	Si(45)-C(451)	1.900(19)	Si(13)-C(133)	1.938(14)
Si(22)-C(223)	1.863(10)	Si(46)-C(462)	1.84(2)	Si(1B)-Si(15)	2.329(6)
Si(22)-C(221)	1.867(9)	Si(46)-C(461)	1.85(2)	Si(1B)-Si(16)	2.349(5)
Si(22)-C(222)	1.877(8)	Si(46)-C(463)	1.86(2)	Si(1B)-Si(14)	2.371(6)
Si(23)-C(231)	1.866(10)	Si(3)-Si(32)	2.359(3)	Si(14)-C(142)	1.860(12)
Si(23)-C(232)	1.883(9)	Si(3)-Si(33)	2.359(3)	Si(14)-C(141)	1.861(11)
Si(23)-C(233)	1.890(9)	Si(3)-Si(31)	2.361(3)	Si(14)-C(143)	1.881(10)
Si(2A)-Si(24)	2.354(17)	Si(31)-C(312)	1.859(8)	Si(15)-C(151)	1.871(12)
Si(2A)-Si(26)	2.355(17)	Si(31)-C(311)	1.866(9)	Si(15)-C(153)	1.885(11)
Si(2A)-Si(25)	2.364(17)	Si(31)-C(313)	1.878(9)	Si(15)-C(152)	1.896(12)
Si(24)-C(243)	1.85(2)	Si(32)-C(322)	1.882(9)	Si(16)-C(162)	1.871(11)
Si(24)-C(242)	1.85(2)	Si(32)-C(321)	1.884(9)	Si(16)-C(161)	1.890(11)
Si(24)-C(241)	1.88(2)	Si(32)-C(323)	1.887(14)	Si(16)-C(163)	1.938(14)
Si(25)-C(253)	1.85(2)	Si(33)-C(332)	1.852(10)	C(01)-C(02)	1.51(3)
Si(25)-C(252)	1.87(2)	Si(33)-C(333)	1.852(11)	C(02)-O(03)	1.08(4)
Si(25)-C(251)	1.87(2)	Si(33)-C(331)	1.884(10)	C(02)-C(04)	1.93(8)
Si(26)-C(261)	1.86(2)	Si(3B)-Si(35)	2.359(5)	O(03)-C(04)	1.10(4)
Si(26)-C(262)	1.87(2)	Si(3B)-Si(36)	2.359(6)	C(04)-C(05)	1.54(3)

7.14.4 Bond angles [deg].

Atoms	Angle	Atoms	Angle
P(1)-Pb(1)-Si(1)	106.38(6)	C(452)-Si(45)-Si(4B)	109.5(19)
P(1)-Pb(1)-P(2)	79.56(5)	C(451)-Si(45)-Si(4B)	112.6(18)
Si(1)-Pb(1)-P(2)	106.36(6)	C(462)-Si(46)-C(461)	106.2(19)
Si(2)-Pb(2)-P(1)	106.21(7)	C(462)-Si(46)-C(463)	110(2)
Si(2)-Pb(2)-P(2)	105.43(7)	C(461)-Si(46)-C(463)	111(2)
P(1)-Pb(2)-P(2)	79.25(5)	C(462)-Si(46)-Si(4B)	114.5(17)
Si(4)-P(2)-Pb(1)	112.71(8)	C(461)-Si(46)-Si(4B)	106.6(16)
Si(4)-P(2)-Pb(2)	117.14(9)	C(463)-Si(46)-Si(4B)	108.5(17)
Pb(1)-P(2)-Pb(2)	98.46(5)	P(1)-Si(3)-Si(32)	112.76(11)
Si(3)-P(1)-Pb(1)	114.11(8)	P(1)-Si(3)-Si(33)	108.00(14)
Si(3)-P(1)-Pb(2)	115.93(9)	Si(32)-Si(3)-Si(33)	107.10(13)
Pb(1)-P(1)-Pb(2)	98.99(5)	P(1)-Si(3)-Si(31)	109.26(16)
P(2B)-Pb(1A)-P(1B)	82.5(5)	Si(32)-Si(3)-Si(31)	107.98(13)
P(2B)-Pb(1A)-Si(3B)	102.6(7)	Si(33)-Si(3)-Si(31)	111.78(13)
P(1B)-Pb(1A)-Si(3B)	100.4(6)	C(312)-Si(31)-C(311)	108.9(4)
P(2B)-Pb(2A)-P(1B)	79.3(5)	C(312)-Si(31)-C(313)	108.9(5)
P(2B)-Pb(2A)-Si(4B)	97.2(5)	C(311)-Si(31)-C(313)	107.6(5)
P(1B)-Pb(2A)-Si(4B)	101.0(4)	C(312)-Si(31)-Si(3)	109.5(3)
Si(1B)-P(1B)-Pb(1A)	111.3(6)	C(311)-Si(31)-Si(3)	112.1(3)
Si(1B)-P(1B)-Pb(2A)	121.6(11)	C(313)-Si(31)-Si(3)	109.8(3)
Pb(1A)-P(1B)-Pb(2A)	95.9(6)	C(322)-Si(32)-C(321)	109.1(4)
Si(2A)-P(2B)-Pb(1A)	114.5(10)	C(322)-Si(32)-C(323)	106.5(6)
Si(2A)-P(2B)-Pb(2A)	112.8(12)	C(321)-Si(32)-C(323)	110.5(6)
Pb(1A)-P(2B)-Pb(2A)	97.9(5)	C(322)-Si(32)-Si(3)	112.2(4)
Si(23)-Si(2)-Si(21)	107.93(12)	C(321)-Si(32)-Si(3)	107.0(3)
Si(23)-Si(2)-Si(22)	106.68(13)	C(323)-Si(32)-Si(3)	111.5(4)
Si(21)-Si(2)-Si(22)	107.98(12)	C(332)-Si(33)-C(333)	108.2(6)
Si(23)-Si(2)-Pb(2)	117.12(13)	C(332)-Si(33)-C(331)	107.1(5)
Si(21)-Si(2)-Pb(2)	117.69(13)	C(333)-Si(33)-C(331)	108.6(6)
Si(22)-Si(2)-Pb(2)	98.09(10)	C(332)-Si(33)-Si(3)	111.6(3)
C(213)-Si(21)-C(212)	107.3(5)	C(333)-Si(33)-Si(3)	111.0(5)
C(213)-Si(21)-C(211)	108.1(5)	C(331)-Si(33)-Si(3)	110.2(4)
C(212)-Si(21)-C(211)	107.5(5)	Si(35)-Si(3B)-Si(36)	107.0(5)
C(213)-Si(21)-Si(2)	112.3(3)	Si(35)-Si(3B)-Si(34)	107.9(5)
C(212)-Si(21)-Si(2)	111.4(3)	Si(36)-Si(3B)-Si(34)	112.0(5)
C(211)-Si(21)-Si(2)	110.1(3)	Si(35)-Si(3B)-Pb(1A)	97.8(9)
C(223)-Si(22)-C(221)	107.1(5)	Si(36)-Si(3B)-Pb(1A)	117.0(14)
C(223)-Si(22)-C(222)	106.4(5)	Si(34)-Si(3B)-Pb(1A)	113.4(10)
C(221)-Si(22)-C(222)	107.7(5)	C(342)-Si(34)-C(341)	108.9(7)
C(223)-Si(22)-Si(2)	111.9(3)	C(342)-Si(34)-C(343)	108.6(7)
C(221)-Si(22)-Si(2)	112.3(3)	C(341)-Si(34)-C(343)	107.7(7)
C(222)-Si(22)-Si(2)	111.2(3)	C(342)-Si(34)-Si(3B)	109.4(6)
C(231)-Si(23)-C(232)	109.9(5)	C(341)-Si(34)-Si(3B)	112.3(6)
C(231)-Si(23)-C(233)	106.0(5)	C(343)-Si(34)-Si(3B)	109.8(6)
C(232)-Si(23)-C(233)	106.0(5)	C(352)-Si(35)-C(351)	109.1(7)
C(231)-Si(23)-Si(2)	110.8(3)	C(352)-Si(35)-C(353)	106.6(8)
C(232)-Si(23)-Si(2)	111.7(3)	C(351)-Si(35)-C(353)	110.5(8)
C(233)-Si(23)-Si(2)	112.3(3)	C(352)-Si(35)-Si(3B)	112.2(6)
P(2B)-Si(2A)-Si(24)	114.4(16)	C(351)-Si(35)-Si(3B)	106.9(6)
P(2B)-Si(2A)-Si(26)	110.6(16)	C(353)-Si(35)-Si(3B)	111.5(6)
Si(24)-Si(2A)-Si(26)	106.9(13)	C(362)-Si(36)-C(363)	108.1(8)
P(2B)-Si(2A)-Si(25)	110.6(15)	C(362)-Si(36)-C(361)	107.2(7)
Si(24)-Si(2A)-Si(25)	107.8(13)	C(363)-Si(36)-C(361)	108.6(8)
Si(26)-Si(2A)-Si(25)	106.2(13)	C(362)-Si(36)-Si(3B)	111.6(6)
C(243)-Si(24)-C(242)	108(2)	C(363)-Si(36)-Si(3B)	111.0(7)
C(243)-Si(24)-C(241)	108(2)	C(361)-Si(36)-Si(3B)	110.3(6)
C(242)-Si(24)-C(241)	107(2)	Si(12)-Si(1)-Si(13)	106.35(13)

Atoms	Angle	Atoms	Angle
C(243)-Si(24)-Si(2A)	112(2)	Si(12)-Si(1)-Si(11)	108.22(12)
C(242)-Si(24)-Si(2A)	112.2(19)	Si(13)-Si(1)-Si(11)	105.42(12)
C(241)-Si(24)-Si(2A)	109.1(17)	Si(12)-Si(1)-Pb(1)	120.86(10)
C(253)-Si(25)-C(252)	109(2)	Si(13)-Si(1)-Pb(1)	102.54(9)
C(253)-Si(25)-C(251)	108(2)	Si(11)-Si(1)-Pb(1)	112.07(9)
C(252)-Si(25)-C(251)	107(2)	C(111)-Si(11)-C(112)	109.9(5)
C(253)-Si(25)-Si(2A)	112.3(19)	C(111)-Si(11)-C(113)	105.1(5)
C(252)-Si(25)-Si(2A)	110.3(17)	C(112)-Si(11)-C(113)	108.8(6)
C(251)-Si(25)-Si(2A)	109.8(17)	C(111)-Si(11)-Si(1)	111.6(3)
C(261)-Si(26)-C(262)	111(2)	C(112)-Si(11)-Si(1)	110.1(4)
C(261)-Si(26)-C(263)	106(2)	C(113)-Si(11)-Si(1)	111.1(4)
C(262)-Si(26)-C(263)	106(2)	C(121)-Si(12)-C(123)	109.8(7)
C(261)-Si(26)-Si(2A)	111.8(18)	C(121)-Si(12)-C(122)	108.7(6)
C(262)-Si(26)-Si(2A)	112.0(18)	C(123)-Si(12)-C(122)	106.5(5)
C(263)-Si(26)-Si(2A)	110.0(18)	C(121)-Si(12)-Si(1)	109.8(4)
P(2)-Si(4)-Si(43)	111.45(10)	C(123)-Si(12)-Si(1)	110.4(4)
P(2)-Si(4)-Si(41)	110.78(10)	C(122)-Si(12)-Si(1)	111.5(4)
Si(43)-Si(4)-Si(41)	107.52(10)	C(132)-Si(13)-C(131)	106.9(5)
P(2)-Si(4)-Si(42)	108.19(9)	C(132)-Si(13)-C(133)	106.8(6)
Si(43)-Si(4)-Si(42)	108.74(10)	C(131)-Si(13)-C(133)	108.7(6)
Si(41)-Si(4)-Si(42)	110.15(10)	C(132)-Si(13)-Si(1)	112.3(4)
C(411)-Si(41)-C(412)	109.1(5)	C(131)-Si(13)-Si(1)	112.2(4)
C(411)-Si(41)-C(413)	106.7(4)	C(133)-Si(13)-Si(1)	109.6(4)
C(412)-Si(41)-C(413)	107.8(4)	P(1B)-Si(1B)-Si(15)	115.8(9)
C(411)-Si(41)-Si(4)	111.7(3)	P(1B)-Si(1B)-Si(16)	117.0(8)
C(412)-Si(41)-Si(4)	110.2(3)	Si(15)-Si(1B)-Si(16)	106.5(4)
C(413)-Si(41)-Si(4)	111.2(3)	P(1B)-Si(1B)-Si(14)	103.3(9)
C(423)-Si(42)-C(422)	109.5(6)	Si(15)-Si(1B)-Si(14)	107.8(4)
C(423)-Si(42)-C(421)	107.5(4)	Si(16)-Si(1B)-Si(14)	105.7(4)
C(422)-Si(42)-C(421)	106.9(5)	C(142)-Si(14)-C(141)	109.8(7)
C(423)-Si(42)-Si(4)	111.8(3)	C(142)-Si(14)-C(143)	108.9(8)
C(422)-Si(42)-Si(4)	108.3(4)	C(141)-Si(14)-C(143)	105.1(7)
C(421)-Si(42)-Si(4)	112.6(3)	C(142)-Si(14)-Si(1B)	110.2(6)
C(432)-Si(43)-C(433)	108.3(5)	C(141)-Si(14)-Si(1B)	111.3(6)
C(432)-Si(43)-C(431)	105.3(5)	C(143)-Si(14)-Si(1B)	111.3(6)
C(433)-Si(43)-C(431)	110.2(6)	C(151)-Si(15)-C(153)	109.7(9)
C(432)-Si(43)-Si(4)	114.5(3)	C(151)-Si(15)-C(152)	108.7(8)
C(433)-Si(43)-Si(4)	111.0(4)	C(153)-Si(15)-C(152)	106.4(7)
C(431)-Si(43)-Si(4)	107.4(3)	C(151)-Si(15)-Si(1B)	110.0(6)
Si(45)-Si(4B)-Si(44)	112.0(9)	C(153)-Si(15)-Si(1B)	110.4(6)
Si(45)-Si(4B)-Si(46)	105.6(9)	C(152)-Si(15)-Si(1B)	111.5(6)
Si(44)-Si(4B)-Si(46)	107.4(9)	C(162)-Si(16)-C(161)	106.9(7)
Si(45)-Si(4B)-Pb(2A)	98.4(7)	C(162)-Si(16)-C(163)	106.9(8)
Si(44)-Si(4B)-Pb(2A)	102.0(7)	C(161)-Si(16)-C(163)	108.7(8)
Si(46)-Si(4B)-Pb(2A)	130.9(8)	C(162)-Si(16)-Si(1B)	112.4(6)
C(441)-Si(44)-C(442)	108(2)	C(161)-Si(16)-Si(1B)	112.2(6)
C(441)-Si(44)-C(443)	106(2)	C(163)-Si(16)-Si(1B)	109.6(6)
C(442)-Si(44)-C(443)	109(2)	O(03)-C(02)-C(01)	118(3)
C(441)-Si(44)-Si(4B)	110.7(17)	O(03)-C(02)-C(04)	28(3)
C(442)-Si(44)-Si(4B)	110.9(17)	C(01)-C(02)-C(04)	131(4)
C(443)-Si(44)-Si(4B)	112.2(19)	C(02)-O(03)-C(04)	125(5)
C(453)-Si(45)-C(452)	109(2)	O(03)-C(04)-C(05)	108(3)
C(453)-Si(45)-C(451)	108(2)	O(03)-C(04)-C(02)	27(3)
C(452)-Si(45)-C(451)	106(2)	C(05)-C(04)-C(02)	129(3)
C(453)-Si(45)-Si(4B)	111.7(17)		

7.15 Crystallographic data for Hyp_6Pb_{12}

7.15.1 Crystal data and structure refinement

Empirical formula	Hyp_6Pb_{12}·pentane
Formula weight	4044.42
Temperature	293(2) K
Wavelength	0.71073 Å
Crystal system, space group	hexagonal, $R\bar{3}$
Unit cell dimensions	a = 16.1051(3) Å alpha = 90 deg. b = 16.1051(3) Å beta = 90 deg. c = 41.6827(10) Å gamma = 120 deg.
Volume	9363.0(3) $Å^3$
Z, Calculated density	3, 2.152 g/cm^3
Absorption coefficient	16.374 mm^{-1}
F(000)	5544
Theta range for data collection	2.44 to 28.31 deg.
Limiting indices	-12<=h<=21, -21<=k<=18, -55<=l<=54
Reflections collected / unique	23561 / 5183 [R(int) = 0.0798]
Completeness to theta = 28.31	99.6 %
Refinement method	Full-matrix least-squares on F^2
Data / restraints / parameters	5183 / 13 / 192
Goodness-of-fit on F^2	1.044
Final R indices [I>2sigma(I)]	R1 = 0.0459, wR2 = 0.1093
R indices (all data)	R1 = 0.0756, wR2 = 0.1242
Largest diff. peak and hole	1.332 and -0.780 e.$Å^{-3}$

7.15.2 Atomic coordinates (x 10^4), equivalent isotropic displacement parameters ($Å^2$ x 10^3) and Anisotropic displacement parameters ($Å^2$ x 10^3). U(eq) is defined as one third of the trace of the orthogonalized Uij tensor. The anisotropic displacement factor exponent takes the form: $-2\pi^2[h^2a^{*2}U11 + \dots + 2hka^*b^*U12]$

Atom	x	y	z	U(eq)	U11	U22	U33	U23	U13	U12
Pb(1)	4785(1)	6228(1)	1375(1)	39(1)	35(1)	38(1)	38(1)	0(1)	4(1)	13(1)
Pb(2)	5237(1)	7484(1)	2062(1)	44(1)	32(1)	51(1)	36(1)	-1(1)	-3(1)	10(1)
Pb(3)	3463(1)	5162(1)	2020(1)	37(1)	41(1)	31(1)	36(1)	2(1)	3(1)	15(1)
Pb(4)	3494(2)	6670(8)	936(1)	41(1)	41(2)	39(1)	32(1)	-8(1)	-1(1)	11(2)
Pb(5)	5199(1)	8334(1)	1372(1)	41(1)	37(1)	37(1)	36(1)	0(1)	4(1)	9(1)
Pb(6)	2430(1)	4667(1)	1326(1)	47(1)	52(1)	34(1)	37(1)	-6(1)	5(1)	9(1)
Si(1)	6099(1)	6529(1)	921(1)	38(1)	37(1)	35(1)	43(1)	-2(1)	0(1)	18(1)
Si(13)	7579(1)	7485(1)	1174(1)	47(1)	35(1)	40(1)	64(1)	-8(1)	-2(1)	17(1)
Si(12)	5895(1)	4991(1)	853(1)	42(1)	36(1)	37(1)	56(1)	-5(1)	2(1)	20(1)
Si(11)	6034(2)	7185(2)	426(1)	48(1)	60(1)	52(1)	39(1)	3(1)	9(1)	32(1)
C(121)	4642(5)	4082(5)	753(2)	55(2)	46(4)	43(4)	75(5)	-10(4)	2(4)	21(3)
C(111)	6011(7)	8312(6)	481(2)	59(2)	73(6)	49(4)	59(5)	13(4)	11(4)	34(4)
C(122)	6688(6)	4992(6)	517(2)	60(2)	48(4)	62(5)	74(5)	-16(4)	6(4)	30(4)
C(131)	7513(6)	7192(7)	1606(2)	62(2)	52(5)	76(6)	68(5)	-12(4)	-15(4)	41(4)
C(123)	6244(7)	4614(6)	1229(2)	63(2)	66(5)	46(4)	80(6)	8(4)	-1(4)	30(4)
C(132)	8531(6)	7281(7)	990(2)	66(2)	37(4)	76(6)	84(6)	-10(5)	5(4)	26(4)
C(133)	7949(6)	8775(6)	1143(3)	70(3)	56(5)	38(4)	105(8)	-9(4)	-10(5)	15(4)
C(112)	4946(8)	6302(7)	197(2)	76(3)	98(7)	73(6)	52(5)	-7(4)	-17(5)	38(6)
C(113)	7131(9)	7475(9)	183(3)	91(4)	104(8)	113(9)	80(7)	34(6)	54(6)	72(7)
C(01)	10080(170)	9910(160)	536(14)	110(30)						
C(02)	9990(80)	9340(70)	240(20)	140(30)						
C(03)	9520(50)	9540(60)	-36(17)	100(20)						

C(04)	10200(80)	10380(50)	-240(20)	110(30)
C(05)	10580(100)	10110(120)	-520(30)	200(50)

7.15.2 Bond lengths [Å].

Atoms	Bond length	Atoms	Bond length	Atoms	Bond length
Pb(1)-Pb(3)#1	0.8500(10)	Pb(3)-Si(1)#2	2.638(2)	Pb(6)-Pb(5)#4	1.0615(12)
Pb(1)-Pb(2)#2	1.1210(12)	Pb(3)-Pb(5)#4	2.7576(11)	Pb(6)-Pb(3)#2	1.3625(14)
Pb(1)-Pb(6)#3	2.1794(15)	Pb(3)-Pb(4)#2	2.769(3)	Pb(6)-Pb(1)#4	2.1794(15)
Pb(1)-Pb(5)#2	2.4683(11)	Pb(3)-Pb(4)#1	3.090(7)	Pb(6)-Pb(2)#2	2.4119(13)
Pb(1)-Pb(5)#4	2.4985(12)	Pb(3)-Pb(5)#5	3.1013(13)	Pb(6)-Pb(1)#2	2.7205(12)
Pb(1)-Si(1)	2.697(2)	Pb(3)-Pb(4)#5	3.110(9)	Pb(6)-Pb(4)#4	3.049(4)
Pb(1)-Pb(6)#1	2.7206(12)	Pb(3)-Pb(6)	3.2335(13)	Pb(6)-Pb(2)#5	3.0558(14)
Pb(1)-Pb(4)	3.110(5)	Pb(3)-Pb(2)#2	3.2690(11)	Pb(6)-Pb(2)#4	3.0955(11)
Pb(1)-Pb(5)	3.1118(13)	Pb(4)-Pb(4)#3	0.443(6)	Pb(6)-Pb(5)#5	3.2452(11)
Pb(1)-Pb(3)	3.3241(10)	Pb(4)-Pb(4)#4	0.443(6)	Si(1)-Si(11)	2.343(3)
Pb(1)-Pb(6)	3.3492(12)	Pb(4)-Pb(3)#1	2.769(3)	Si(1)-Si(13)	2.344(3)
Pb(1)-Pb(2)	3.3682(11)	Pb(4)-Pb(2)#2	2.829(8)	Si(1)-Si(12)	2.347(3)
Pb(2)-Pb(1)#1	1.1211(12)	Pb(4)-Pb(2)#1	2.996(9)	Si(1)-Pb(3)#1	2.638(2)
Pb(2)-Pb(5)#2	1.5420(13)	Pb(4)-Pb(6)#3	3.049(4)	Si(1)-Pb(2)#2	3.085(2)
Pb(2)-Pb(3)#3	1.7378(13)	Pb(4)-Pb(3)#2	3.090(7)	Si(13)-C(131)	1.854(9)
Pb(2)-Pb(6)#1	2.4119(13)	Pb(4)-Pb(3)#5	3.110(9)	Si(13)-C(133)	1.857(8)
Pb(2)-Pb(4)#1	2.829(8)	Pb(4)-Pb(2)#5	3.217(2)	Si(13)-C(132)	1.883(8)
Pb(2)-Pb(4)#2	2.996(10)	Pb(4)-Pb(6)	3.233(9)	Si(12)-C(121)	1.854(8)
Pb(2)-Pb(6)#5	3.0558(14)	Pb(4)-Pb(5)	3.267(6)	Si(12)-C(123)	1.866(9)
Pb(2)-Si(1)#1	3.085(2)	Pb(5)-Pb(6)#3	1.0616(12)	Si(12)-C(122)	1.893(8)
Pb(2)-Pb(6)#3	3.0955(11)	Pb(5)-Pb(2)#1	1.5421(13)	Si(11)-C(111)	1.848(8)
Pb(2)-Pb(5)	3.1988(11)	Pb(5)-Pb(3)#1	2.3252(13)	Si(11)-C(112)	1.873(10)
Pb(2)-Pb(4)#5	3.217(2)	Pb(5)-Pb(1)#1	2.4683(11)	Si(11)-C(113)	1.882(9)
Pb(2)-Pb(3)#1	3.2690(11)	Pb(5)-Pb(1)#3	2.4985(12)	C(01)-C(02)	1.50(5)
Pb(3)-Pb(1)#2	0.8499(10)	Pb(5)-Pb(3)#3	2.7576(11)	C(02)-C(03)	1.50(5)
Pb(3)-Pb(6)#1	1.3624(15)	Pb(5)-Pb(3)#5	3.1013(13)	C(03)-C(04)	1.50(5)
Pb(3)-Pb(2)#4	1.7378(13)	Pb(5)-Pb(6)#5	3.2452(11)	C(04)-C(05)	1.50(5)
Pb(3)-Pb(5)#2	2.3253(13)	Pb(5)-Pb(4)#3	3.311(9)		

7.15.3 Bond angles [deg].

Atoms	Angle	Atoms	Angle
Pb(3)#1-Pb(1)-Pb(2)#2	123.10(12)	Pb(2)#2-Pb(4)-Pb(3)#2	69.73(19)
Pb(3)#1-Pb(1)-Pb(6)#3	12.55(6)	Pb(2)#1-Pb(4)-Pb(3)#2	114.25(9)
Pb(2)#2-Pb(1)-Pb(6)#3	132.98(8)	Pb(6)#3-Pb(4)-Pb(3)#2	113.55(10)
Pb(3)#1-Pb(1)-Pb(5)#2	100.84(8)	Pb(4)#3-Pb(4)-Pb(3)#5	37.0(13)
Pb(2)#2-Pb(1)-Pb(5)#2	121.39(7)	Pb(4)#4-Pb(4)-Pb(3)#5	83(2)
Pb(6)#3-Pb(1)-Pb(5)#2	88.34(4)	Pb(3)#1-Pb(4)-Pb(3)#5	96.44(16)
Pb(3)#1-Pb(1)-Pb(5)#4	128.65(9)	Pb(2)#2-Pb(4)-Pb(3)#5	118.73(5)
Pb(2)#2-Pb(1)-Pb(5)#4	23.90(5)	Pb(2)#1-Pb(4)-Pb(3)#5	33.00(10)
Pb(6)#3-Pb(1)-Pb(5)#4	133.14(5)	Pb(6)#3-Pb(4)-Pb(3)#5	76.22(18)
Pb(5)#2-Pb(1)-Pb(5)#4	98.66(4)	Pb(3)#2-Pb(4)-Pb(3)#5	90.15(6)
Pb(3)#1-Pb(1)-Si(1)	76.94(8)	Pb(4)#3-Pb(4)-Pb(1)	141.3(9)
Pb(2)#2-Pb(1)-Si(1)	99.38(7)	Pb(4)#4-Pb(4)-Pb(1)	124.8(18)
Pb(6)#3-Pb(1)-Si(1)	83.86(5)	Pb(3)#1-Pb(4)-Pb(1)	15.25(4)
Pb(5)#2-Pb(1)-Si(1)	129.10(5)	Pb(2)#2-Pb(4)-Pb(1)	21.08(4)
Pb(5)#4-Pb(1)-Si(1)	122.67(5)	Pb(2)#1-Pb(4)-Pb(1)	84.88(9)
Pb(3)#1-Pb(1)-Pb(6)#1	120.27(9)	Pb(6)#3-Pb(4)-Pb(1)	41.43(4)
Pb(2)#2-Pb(1)-Pb(6)#1	98.71(7)	Pb(3)#2-Pb(4)-Pb(1)	84.23(19)
Pb(6)#3-Pb(1)-Pb(6)#1	108.31(4)	Pb(3)#5-Pb(4)-Pb(1)	104.94(11)
Pb(5)#2-Pb(1)-Pb(6)#1	22.95(3)	Pb(4)#3-Pb(4)-Pb(2)#5	56.6(19)
Pb(5)#4-Pb(1)-Pb(6)#1	76.77(4)	Pb(4)#4-Pb(4)-Pb(2)#5	26.8(6)

Atoms	Angle	Atoms	Angle
Si(1)-Pb(1)-Pb(6)#1	140.21(6)	Pb(3)#1-Pb(4)-Pb(2)#5	117.09(10)
Pb(3)#1-Pb(1)-Pb(4)	58.94(19)	Pb(2)#2-Pb(4)-Pb(2)#5	99.3(2)
Pb(2)#2-Pb(1)-Pb(4)	65.19(19)	Pb(2)#1-Pb(4)-Pb(2)#5	95.81(17)
Pb(6)#3-Pb(1)-Pb(4)	67.80(19)	Pb(6)#3-Pb(4)-Pb(2)#5	120.76(7)
Pb(5)#2-Pb(1)-Pb(4)	127.19(10)	Pb(3)#2-Pb(4)-Pb(2)#5	31.90(4)
Pb(5)#4-Pb(1)-Pb(4)	71.42(16)	Pb(3)#5-Pb(4)-Pb(2)#5	64.77(9)
Si(1)-Pb(1)-Pb(4)	95.68(5)	Pb(1)-Pb(4)-Pb(2)#5	108.80(15)
Pb(6)#1-Pb(1)-Pb(4)	124.09(4)	Pb(4)#3-Pb(4)-Pb(6)	113.1(19)
Pb(3)#1-Pb(1)-Pb(5)	19.09(7)	Pb(4)#4-Pb(4)-Pb(6)	61.9(19)
Pb(2)#2-Pb(1)-Pb(5)	127.65(7)	Pb(3)#1-Pb(4)-Pb(6)	78.18(19)
Pb(6)#3-Pb(1)-Pb(5)	11.18(3)	Pb(2)#2-Pb(4)-Pb(6)	46.30(14)
Pb(5)#2-Pb(1)-Pb(5)	84.08(4)	Pb(2)#1-Pb(4)-Pb(6)	121.97(3)
Pb(5)#4-Pb(1)-Pb(5)	123.51(4)	Pb(6)#3-Pb(4)-Pb(6)	100.68(14)
Si(1)-Pb(1)-Pb(5)	94.57(5)	Pb(3)#2-Pb(4)-Pb(6)	24.76(7)
Pb(6)#1-Pb(1)-Pb(5)	101.82(3)	Pb(3)#5-Pb(4)-Pb(6)	108.12(4)
Pb(4)-Pb(1)-Pb(5)	63.36(19)	Pb(1)-Pb(4)-Pb(6)	63.71(16)
Pb(3)#1-Pb(1)-Pb(3)	126.19(9)	Pb(2)#5-Pb(4)-Pb(6)	56.56(10)
Pb(2)#2-Pb(1)-Pb(3)	77.44(6)	Pb(4)#3-Pb(4)-Pb(5)	92(2)
Pb(6)#3-Pb(1)-Pb(3)	117.00(4)	Pb(4)#4-Pb(4)-Pb(5)	137.3(14)
Pb(5)#2-Pb(1)-Pb(3)	44.34(3)	Pb(3)#1-Pb(4)-Pb(5)	44.37(7)
Pb(5)#4-Pb(1)-Pb(3)	54.32(2)	Pb(2)#2-Pb(4)-Pb(5)	79.17(4)
Si(1)-Pb(1)-Pb(3)	154.59(6)	Pb(2)#1-Pb(4)-Pb(5)	28.08(7)
Pb(6)#1-Pb(1)-Pb(3)	23.43(3)	Pb(6)#3-Pb(4)-Pb(5)	18.95(5)
Pb(4)-Pb(1)-Pb(3)	105.39(6)	Pb(3)#2-Pb(4)-Pb(5)	115.58(3)
Pb(5)-Pb(1)-Pb(3)	107.41(3)	Pb(3)#5-Pb(4)-Pb(5)	58.14(15)
Pb(3)#1-Pb(1)-Pb(6)	116.16(9)	Pb(1)-Pb(4)-Pb(5)	58.35(4)
Pb(2)#2-Pb(1)-Pb(6)	27.57(5)	Pb(2)#5-Pb(4)-Pb(5)	111.55(14)
Pb(6)#3-Pb(1)-Pb(6)	120.62(4)	Pb(6)-Pb(4)-Pb(5)	110.32(8)
Pb(5)#2-Pb(1)-Pb(6)	101.31(3)	Pb(6)#3-Pb(5)-Pb(2)#1	134.94(8)
Pb(5)#4-Pb(1)-Pb(6)	12.60(2)	Pb(6)#3-Pb(5)-Pb(3)#1	18.65(5)
Si(1)-Pb(1)-Pb(6)	125.71(5)	Pb(2)#1-Pb(5)-Pb(3)#1	121.13(5)
Pb(6)#1-Pb(1)-Pb(6)	81.35(3)	Pb(6)#3-Pb(5)-Pb(1)#1	91.99(7)
Pb(4)-Pb(1)-Pb(6)	59.93(15)	Pb(2)#1-Pb(5)-Pb(1)#1	112.18(6)
Pb(5)-Pb(1)-Pb(6)	111.27(3)	Pb(3)#1-Pb(5)-Pb(1)#1	87.76(4)
Pb(3)-Pb(1)-Pb(6)	57.96(2)	Pb(6)#3-Pb(5)-Pb(1)#3	136.49(7)
Pb(3)#1-Pb(1)-Pb(2)	76.04(7)	Pb(2)#1-Pb(5)-Pb(1)#3	17.13(4)
Pb(2)#2-Pb(1)-Pb(2)	135.35(6)	Pb(3)#1-Pb(5)-Pb(1)#3	119.00(4)
Pb(6)#3-Pb(1)-Pb(2)	63.67(3)	Pb(1)#1-Pb(5)-Pb(1)#3	95.48(4)
Pb(5)#2-Pb(1)-Pb(2)	25.08(3)	Pb(6)#3-Pb(5)-Pb(3)#3	107.13(7)
Pb(5)#4-Pb(1)-Pb(2)	111.58(3)	Pb(2)#1-Pb(5)-Pb(3)#3	94.75(5)
Si(1)-Pb(1)-Pb(2)	125.09(5)	Pb(3)#1-Pb(5)-Pb(3)#3	99.41(4)
Pb(6)#1-Pb(1)-Pb(2)	45.13(3)	Pb(1)#1-Pb(5)-Pb(3)#3	17.62(2)
Pb(4)-Pb(1)-Pb(2)	109.37(15)	Pb(1)#3-Pb(5)-Pb(3)#3	78.29(3)
Pb(5)-Pb(1)-Pb(2)	59.00(2)	Pb(6)#3-Pb(5)-Pb(3)#5	124.24(7)
Pb(3)-Pb(1)-Pb(2)	60.86(2)	Pb(2)#1-Pb(5)-Pb(3)#5	20.21(4)
Pb(6)-Pb(1)-Pb(2)	109.06(3)	Pb(3)#1-Pb(5)-Pb(3)#5	107.10(4)
Pb(1)#1-Pb(2)-Pb(5)#2	138.96(8)	Pb(1)#1-Pb(5)-Pb(3)#5	98.95(4)
Pb(1)#1-Pb(2)-Pb(3)#3	24.18(5)	Pb(1)#3-Pb(5)-Pb(3)#5	12.36(2)
Pb(5)#2-Pb(2)-Pb(3)#3	141.94(6)	Pb(3)#3-Pb(5)-Pb(3)#5	82.90(3)
Pb(1)#1-Pb(2)-Pb(6)#1	140.00(7)	Pb(6)#3-Pb(5)-Pb(1)	23.47(5)
Pb(5)#2-Pb(2)-Pb(6)#1	18.15(4)	Pb(2)#1-Pb(5)-Pb(1)	120.87(5)
Pb(3)#3-Pb(2)-Pb(6)#1	132.02(5)	Pb(3)#1-Pb(5)-Pb(1)	6.87(2)
Pb(1)#1-Pb(2)-Pb(4)#1	93.72(17)	Pb(1)#1-Pb(5)-Pb(1)	81.53(3)
Pb(5)#2-Pb(2)-Pb(4)#1	93.82(11)	Pb(1)#3-Pb(5)-Pb(1)	116.48(4)
Pb(3)#3-Pb(2)-Pb(4)#1	70.04(16)	Pb(3)#3-Pb(5)-Pb(1)	92.68(3)
Pb(6)#1-Pb(2)-Pb(4)#1	75.71(11)	Pb(3)#5-Pb(5)-Pb(1)	105.09(3)
Pb(1)#1-Pb(2)-Pb(4)#2	100.32(8)	Pb(6)#3-Pb(5)-Pb(2)	74.83(6)
Pb(5)#2-Pb(2)-Pb(4)#2	85.77(10)	Pb(2)#1-Pb(5)-Pb(2)	122.93(5)
Pb(3)#3-Pb(2)-Pb(4)#2	77.08(6)	Pb(3)#1-Pb(5)-Pb(2)	70.55(3)
Pb(6)#1-Pb(2)-Pb(4)#2	67.65(10)	Pb(1)#1-Pb(5)-Pb(2)	17.41(3)
Pb(4)#1-Pb(2)-Pb(4)#2	8.08(7)	Pb(1)#3-Pb(5)-Pb(2)	105.81(3)

Atoms	Angle	Atoms	Angle
Pb(1)#1-Pb(2)-Pb(6)#5	31.45(6)	Pb(3)#3-Pb(5)-Pb(2)	32.88(3)
Pb(5)#2-Pb(2)-Pb(6)#5	135.51(5)	Pb(3)#5-Pb(5)-Pb(2)	106.02(3)
Pb(3)#3-Pb(2)-Pb(6)#5	8.58(3)	Pb(1)-Pb(5)-Pb(2)	64.50(3)
Pb(6)#1-Pb(2)-Pb(6)#5	124.02(4)	Pb(6)#3-Pb(5)-Pb(6)#5	127.75(7)
Pb(4)#1-Pb(2)-Pb(6)#5	62.28(16)	Pb(2)#1-Pb(5)-Pb(6)#5	70.58(4)
Pb(4)#2-Pb(2)-Pb(6)#5	69.07(5)	Pb(3)#1-Pb(5)-Pb(6)#5	115.26(4)
Pb(1)#1-Pb(2)-Si(1)#1	59.61(6)	Pb(1)#1-Pb(5)-Pb(6)#5	42.17(3)
Pb(5)#2-Pb(2)-Si(1)#1	159.28(6)	Pb(1)#3-Pb(5)-Pb(6)#5	54.69(3)
Pb(3)#3-Pb(2)-Si(1)#1	58.66(5)	Pb(3)#3-Pb(5)-Pb(6)#5	24.55(3)
Pb(6)#1-Pb(2)-Si(1)#1	157.03(5)	Pb(3)#5-Pb(5)-Pb(6)#5	61.21(3)
Pb(4)#1-Pb(2)-Si(1)#1	93.57(8)	Pb(1)-Pb(5)-Pb(6)#5	108.46(3)
Pb(4)#2-Pb(2)-Si(1)#1	100.90(12)	Pb(2)-Pb(5)-Pb(6)#5	56.61(3)
Pb(6)#5-Pb(2)-Si(1)#1	64.60(4)	Pb(6)#3-Pb(5)-Pb(4)	68.85(16)
Pb(1)#1-Pb(2)-Pb(6)#3	60.31(6)	Pb(2)#1-Pb(5)-Pb(4)	66.15(16)
Pb(5)#2-Pb(2)-Pb(6)#3	81.40(4)	Pb(3)#1-Pb(5)-Pb(4)	56.36(16)
Pb(3)#3-Pb(2)-Pb(6)#3	78.49(4)	Pb(1)#1-Pb(5)-Pb(4)	120.09(10)
Pb(6)#1-Pb(2)-Pb(6)#3	91.83(3)	Pb(1)#3-Pb(5)-Pb(4)	70.40(13)
Pb(4)#1-Pb(2)-Pb(6)#3	120.81(11)	Pb(3)#3-Pb(5)-Pb(4)	116.54(6)
Pb(4)#2-Pb(2)-Pb(6)#3	120.15(9)	Pb(3)#5-Pb(5)-Pb(4)	58.39(12)
Pb(6)#5-Pb(2)-Pb(6)#3	80.74(3)	Pb(1)-Pb(5)-Pb(4)	58.29(16)
Si(1)#1-Pb(2)-Pb(6)#3	111.03(5)	Pb(2)-Pb(5)-Pb(4)	109.73(13)
Pb(1)#1-Pb(2)-Pb(5)	41.20(5)	Pb(6)#5-Pb(5)-Pb(4)	108.33(5)
Pb(5)#2-Pb(2)-Pb(5)	99.23(4)	Pb(6)#3-Pb(5)-Pb(4)#3	76.53(7)
Pb(3)#3-Pb(2)-Pb(5)	59.47(4)	Pb(2)#1-Pb(5)-Pb(4)#3	58.49(5)
Pb(6)#1-Pb(2)-Pb(5)	106.97(3)	Pb(3)#1-Pb(5)-Pb(4)#3	63.70(4)
Pb(4)#1-Pb(2)-Pb(5)	112.09(14)	Pb(1)#1-Pb(5)-Pb(4)#3	120.85(11)
Pb(4)#2-Pb(2)-Pb(5)	114.23(7)	Pb(1)#3-Pb(5)-Pb(4)#3	62.91(6)
Pb(6)#5-Pb(2)-Pb(5)	62.46(3)	Pb(3)#3-Pb(5)-Pb(4)#3	114.74(11)
Si(1)#1-Pb(2)-Pb(5)	95.86(4)	Pb(3)#5-Pb(5)-Pb(4)#3	51.03(6)
Pb(6)#3-Pb(2)-Pb(5)	19.33(2)	Pb(1)-Pb(5)-Pb(4)#3	65.26(5)
Pb(1)#1-Pb(2)-Pb(4)#5	93.26(19)	Pb(2)-Pb(5)-Pb(4)#3	112.61(10)
Pb(5)#2-Pb(2)-Pb(4)#5	91.5(2)	Pb(6)#5-Pb(5)-Pb(4)#3	103.63(10)
Pb(3)#3-Pb(2)-Pb(4)#5	69.99(19)	Pb(4)-Pb(5)-Pb(4)#3	7.69(14)
Pb(6)#1-Pb(2)-Pb(4)#5	73.5(2)	Pb(5)#4-Pb(6)-Pb(3)#2	146.93(9)
Pb(4)#1-Pb(2)-Pb(4)#5	4.05(4)	Pb(5)#4-Pb(6)-Pb(1)#4	145.35(7)
Pb(4)#2-Pb(2)-Pb(4)#5	7.1(2)	Pb(3)#2-Pb(6)-Pb(1)#4	7.79(4)
Pb(6)#5-Pb(2)-Pb(4)#5	61.98(18)	Pb(5)#4-Pb(6)-Pb(2)#2	26.91(5)
Si(1)#1-Pb(2)-Pb(4)#5	96.81(17)	Pb(3)#2-Pb(6)-Pb(2)#2	125.52(6)
Pb(6)#3-Pb(2)-Pb(4)#5	117.17(4)	Pb(1)#4-Pb(6)-Pb(2)#2	127.61(4)
Pb(5)-Pb(2)-Pb(4)#5	109.23(9)	Pb(5)#4-Pb(6)-Pb(1)#2	65.06(6)
Pb(1)#1-Pb(2)-Pb(3)#1	83.00(5)	Pb(3)#2-Pb(6)-Pb(1)#2	103.99(5)
Pb(5)#2-Pb(2)-Pb(3)#1	57.21(4)	Pb(1)#4-Pb(6)-Pb(1)#2	96.59(4)
Pb(3)#3-Pb(2)-Pb(3)#1	97.09(4)	Pb(2)#2-Pb(6)-Pb(1)#2	81.79(4)
Pb(6)#1-Pb(2)-Pb(3)#1	67.45(3)	Pb(5)#4-Pb(6)-Pb(4)#4	92.2(2)
Pb(4)#1-Pb(2)-Pb(3)#1	113.98(6)	Pb(3)#2-Pb(6)-Pb(4)#4	65.2(2)
Pb(4)#2-Pb(2)-Pb(3)#1	109.89(11)	Pb(1)#4-Pb(6)-Pb(4)#4	70.8(2)
Pb(6)#5-Pb(2)-Pb(3)#1	96.76(3)	Pb(2)#2-Pb(6)-Pb(4)#4	65.34(19)
Si(1)#1-Pb(2)-Pb(3)#1	135.23(5)	Pb(1)#2-Pb(6)-Pb(4)#4	119.44(5)
Pb(6)#3-Pb(2)-Pb(3)#1	24.53(3)	Pb(5)#4-Pb(6)-Pb(2)#5	136.90(7)
Pb(5)-Pb(2)-Pb(3)#1	42.12(2)	Pb(3)#2-Pb(6)-Pb(2)#5	10.98(4)
Pb(4)#5-Pb(2)-Pb(3)#1	109.93(8)	Pb(1)#4-Pb(6)-Pb(2)#5	15.57(3)
Pb(1)#2-Pb(3)-Pb(6)#1	159.66(10)	Pb(2)#2-Pb(6)-Pb(2)#5	114.56(4)
Pb(1)#2-Pb(3)-Pb(2)#4	32.70(7)	Pb(1)#2-Pb(6)-Pb(2)#5	104.24(3)
Pb(6)#1-Pb(3)-Pb(2)#4	160.44(7)	Pb(4)#4-Pb(6)-Pb(2)#5	55.2(2)
Pb(1)#2-Pb(3)-Pb(5)#2	154.04(9)	Pb(5)#4-Pb(6)-Pb(2)#4	85.84(6)
Pb(6)#1-Pb(3)-Pb(5)#2	14.42(4)	Pb(3)#2-Pb(6)-Pb(2)#4	84.89(5)
Pb(2)#4-Pb(3)-Pb(5)#2	146.96(5)	Pb(1)#4-Pb(6)-Pb(2)#4	77.21(3)
Pb(1)#2-Pb(3)-Si(1)#2	84.78(8)	Pb(2)#2-Pb(6)-Pb(2)#4	99.93(4)
Pb(6)#1-Pb(3)-Si(1)#2	105.75(7)	Pb(1)#2-Pb(6)-Pb(2)#4	20.97(2)
Pb(2)#4-Pb(3)-Si(1)#2	87.10(5)	Pb(4)#4-Pb(6)-Pb(2)#4	118.76(7)
Pb(5)#2-Pb(3)-Si(1)#2	118.89(6)	Pb(2)#5-Pb(6)-Pb(2)#4	87.13(3)

Atoms	Angle	Atoms	Angle
Pb(1)#2-Pb(3)-Pb(5)#4	61.54(7)	Pb(5)#4-Pb(6)-Pb(4)	84.84(8)
Pb(6)#1-Pb(3)-Pb(5)#4	98.20(5)	Pb(3)#2-Pb(6)-Pb(4)	71.73(10)
Pb(2)#4-Pb(3)-Pb(5)#4	87.66(5)	Pb(1)#4-Pb(6)-Pb(4)	76.95(10)
Pb(5)#2-Pb(3)-Pb(5)#4	95.29(3)	Pb(2)#2-Pb(6)-Pb(4)	57.99(6)
Si(1)#2-Pb(3)-Pb(5)#4	119.66(5)	Pb(1)#2-Pb(6)-Pb(4)	115.54(8)
Pb(1)#2-Pb(3)-Pb(4)#2	105.8(2)	Pb(4)#4-Pb(6)-Pb(4)	7.4(2)
Pb(6)#1-Pb(3)-Pb(4)#2	88.3(2)	Pb(2)#5-Pb(6)-Pb(4)	61.47(9)
Pb(2)#4-Pb(3)-Pb(4)#2	73.8(2)	Pb(2)#4-Pb(6)-Pb(4)	117.70(11)
Pb(5)#2-Pb(3)-Pb(4)#2	79.3(2)	Pb(5)#4-Pb(6)-Pb(3)	54.59(6)
Si(1)#2-Pb(3)-Pb(4)#2	105.81(9)	Pb(3)#2-Pb(6)-Pb(3)	108.51(5)
Pb(5)#4-Pb(3)-Pb(4)#2	129.79(5)	Pb(1)#4-Pb(6)-Pb(3)	101.82(4)
Pb(1)#2-Pb(3)-Pb(4)#1	109.47(19)	Pb(2)#2-Pb(6)-Pb(3)	69.01(3)
Pb(6)#1-Pb(3)-Pb(4)#1	83.51(15)	Pb(1)#2-Pb(6)-Pb(3)	13.12(2)
Pb(2)#4-Pb(3)-Pb(4)#1	78.10(16)	Pb(4)#4-Pb(6)-Pb(3)	109.48(6)
Pb(5)#2-Pb(3)-Pb(4)#1	73.87(13)	Pb(2)#5-Pb(6)-Pb(3)	106.25(3)
Si(1)#2-Pb(3)-Pb(4)#1	110.53(7)	Pb(2)#4-Pb(6)-Pb(3)	31.78(2)
Pb(5)#4-Pb(3)-Pb(4)#1	126.83(11)	Pb(4)-Pb(6)-Pb(3)	104.68(7)
Pb(4)#2-Pb(3)-Pb(4)#1	6.0(3)	Pb(5)#4-Pb(6)-Pb(5)#5	111.58(6)
Pb(1)#2-Pb(3)-Pb(5)#5	38.98(7)	Pb(3)#2-Pb(6)-Pb(5)#5	57.25(4)
Pb(6)#1-Pb(3)-Pb(5)#5	145.51(6)	Pb(1)#4-Pb(6)-Pb(5)#5	49.49(3)
Pb(2)#4-Pb(3)-Pb(5)#5	17.85(3)	Pb(2)#2-Pb(6)-Pb(5)#5	118.33(4)
Pb(5)#2-Pb(3)-Pb(5)#5	131.12(4)	Pb(1)#2-Pb(6)-Pb(5)#5	48.54(3)
Si(1)#2-Pb(3)-Pb(5)#5	104.93(5)	Pb(4)#4-Pb(6)-Pb(5)#5	105.26(14)
Pb(5)#4-Pb(3)-Pb(5)#5	79.80(3)	Pb(2)#5-Pb(6)-Pb(5)#5	60.93(3)
Pb(4)#2-Pb(3)-Pb(5)#5	68.4(2)	Pb(2)#4-Pb(6)-Pb(5)#5	28.02(2)
Pb(4)#1-Pb(3)-Pb(5)#5	71.23(17)	Pb(4)-Pb(6)-Pb(5)#5	107.71(12)
Pb(1)#2-Pb(3)-Pb(4)#5	101.41(10)	Pb(3)-Pb(6)-Pb(5)#5	57.20(2)
Pb(6)#1-Pb(3)-Pb(4)#5	91.67(10)	Pb(5)#4-Pb(6)-Pb(1)	30.90(5)
Pb(2)#4-Pb(3)-Pb(4)#5	69.91(8)	Pb(3)#2-Pb(6)-Pb(1)	117.47(5)
Pb(5)#2-Pb(3)-Pb(4)#5	81.73(10)	Pb(1)#4-Pb(6)-Pb(1)	118.18(4)
Si(1)#2-Pb(3)-Pb(4)#5	109.06(12)	Pb(2)#2-Pb(6)-Pb(1)	12.42(2)
Pb(5)#4-Pb(3)-Pb(4)#5	124.87(9)	Pb(1)#2-Pb(6)-Pb(1)	73.73(3)
Pb(4)#2-Pb(3)-Pb(4)#5	5.53(11)	Pb(4)#4-Pb(6)-Pb(1)	63.62(17)
Pb(4)#1-Pb(3)-Pb(4)#5	8.19(10)	Pb(2)#5-Pb(6)-Pb(1)	106.80(3)
Pb(5)#5-Pb(3)-Pb(4)#5	63.48(5)	Pb(2)#4-Pb(6)-Pb(1)	90.08(3)
Pb(1)#2-Pb(3)-Pb(6)	46.60(7)	Pb(4)-Pb(6)-Pb(1)	56.35(4)
Pb(6)#1-Pb(3)-Pb(6)	113.87(5)	Pb(3)-Pb(6)-Pb(1)	60.63(2)
Pb(2)#4-Pb(3)-Pb(6)	69.73(4)	Pb(5)#5-Pb(6)-Pb(1)	106.32(3)
Pb(5)#2-Pb(3)-Pb(6)	108.17(3)	Si(11)-Si(1)-Si(13)	111.04(11)
Si(1)#2-Pb(3)-Pb(6)	120.02(5)	Si(11)-Si(1)-Si(12)	110.79(10)
Pb(5)#4-Pb(3)-Pb(6)	18.28(2)	Si(13)-Si(1)-Si(12)	107.88(10)
Pb(4)#2-Pb(3)-Pb(6)	118.10(10)	Si(11)-Si(1)-Pb(3)#1	106.41(9)
Pb(4)#1-Pb(3)-Pb(6)	116.86(14)	Si(13)-Si(1)-Pb(3)#1	99.96(8)
Pb(5)#5-Pb(3)-Pb(6)	61.59(3)	Si(12)-Si(1)-Pb(3)#1	120.21(9)
Pb(4)#5-Pb(3)-Pb(6)	112.67(6)	Si(11)-Si(1)-Pb(1)	119.49(9)
Pb(1)#2-Pb(3)-Pb(2)#2	89.34(8)	Si(13)-Si(1)-Pb(1)	104.55(9)
Pb(6)#1-Pb(3)-Pb(2)#2	70.59(5)	Si(12)-Si(1)-Pb(1)	102.22(8)
Pb(2)#4-Pb(3)-Pb(2)#2	112.06(5)	Pb(3)#1-Si(1)-Pb(1)	18.29(2)
Pb(5)#2-Pb(3)-Pb(2)#2	67.32(3)	Si(11)-Si(1)-Pb(2)#2	112.12(9)
Si(1)#2-Pb(3)-Pb(2)#2	131.45(5)	Si(13)-Si(1)-Pb(2)#2	124.16(9)
Pb(5)#4-Pb(3)-Pb(2)#2	28.04(3)	Si(12)-Si(1)-Pb(2)#2	87.91(7)
Pb(4)#2-Pb(3)-Pb(2)#2	122.07(11)	Pb(3)#1-Si(1)-Pb(2)#2	34.24(3)
Pb(4)#1-Pb(3)-Pb(2)#2	116.79(4)	Pb(1)-Si(1)-Pb(2)#2	21.01(3)
Pb(5)#5-Pb(3)-Pb(2)#2	99.86(3)	C(131)-Si(13)-C(133)	107.2(5)
Pb(4)#5-Pb(3)-Pb(2)#2	119.32(12)	C(131)-Si(13)-C(132)	107.4(4)
Pb(6)-Pb(3)-Pb(2)#2	43.54(2)	C(133)-Si(13)-C(132)	109.5(4)
Pb(4)#3-Pb(4)-Pb(4)#4	60.000(3)	C(131)-Si(13)-Si(1)	111.1(3)
Pb(4)#3-Pb(4)-Pb(3)#1	133.3(17)	C(133)-Si(13)-Si(1)	110.9(3)
Pb(4)#4-Pb(4)-Pb(3)#1	137.5(14)	C(132)-Si(13)-Si(1)	110.6(3)
Pb(4)#3-Pb(4)-Pb(2)#2	149.2(6)	C(121)-Si(12)-C(123)	108.5(4)
Pb(4)#4-Pb(4)-Pb(2)#2	108(2)	C(121)-Si(12)-C(122)	107.5(4)

Atoms	Angle	Atoms	Angle
Pb(3)#1-Pb(4)-Pb(2)#2	36.16(8)	C(123)-Si(12)-C(122)	107.9(4)
Pb(4)#3-Pb(4)-Pb(2)#1	64(2)	C(121)-Si(12)-Si(1)	112.6(3)
Pb(4)#4-Pb(4)-Pb(2)#1	116(2)	C(123)-Si(12)-Si(1)	109.7(3)
Pb(3)#1-Pb(4)-Pb(2)#1	71.91(13)	C(122)-Si(12)-Si(1)	110.5(3)
Pb(2)#2-Pb(4)-Pb(2)#1	104.70(6)	C(111)-Si(11)-C(112)	109.7(5)
Pb(4)#3-Pb(4)-Pb(6)#3	111(2)	C(111)-Si(11)-C(113)	107.5(5)
Pb(4)#4-Pb(4)-Pb(6)#3	147.4(4)	C(112)-Si(11)-C(113)	108.6(6)
Pb(3)#1-Pb(4)-Pb(6)#3	26.52(4)	C(111)-Si(11)-Si(1)	111.1(3)
Pb(2)#2-Pb(4)-Pb(6)#3	62.51(6)	C(112)-Si(11)-Si(1)	110.0(3)
Pb(2)#1-Pb(4)-Pb(6)#3	47.02(11)	C(113)-Si(11)-Si(1)	109.8(4)
Pb(4)#3-Pb(4)-Pb(3)#2	88.5(19)	C(03)-C(02)-C(01)	114(5)
Pb(4)#4-Pb(4)-Pb(3)#2	40.7(14)	C(02)-C(03)-C(04)	114(5)
Pb(3)#1-Pb(4)-Pb(3)#2	96.90(19)	C(05)-C(04)-C(03)	114(5)

Symmetry transformations used to generate equivalent atoms:
#1 x-y+2/3,x+1/3,-z+1/3 #2 y-1/3,-x+y+1/3,-z+1/3 #3 -y+1,x-y+1,z #4 -x+y,-x+1,z #5 -x+2/3,-y+4/3,-z+1/3

7.16 Crystallographic data for Hyp_6Pb_{10}

7.16.1 Crystal data and structure refinement

Empirical formula	$Hyp_6Pb_{10}\cdot$2benzene
Formula weight	3714.11
Temperature	186(2) K
Wavelength	0.71073 Å
Crystal system, space group	orthorhombic, $P\bar{3}c1$
Unit cell dimensions	a = 15.597(2) Å alpha = 90 deg. b = 24.943(4) Å beta = 90.042(6) deg. c = 33.873(5) Å gamma = 90 deg.
Volume	13178(3) $Å^3$
Z, Calculated density	4, 1.872 g/cm^3
Absorption coefficient	12.971 mm^{-1}
F(000)	6904
Theta range for data collection	2.76 to 25.00 deg.
Limiting indices	-18<=h<=17, -29<=k<=29, -40<=l<=26
Reflections collected / unique	62117 / 22869 [R(int) = 0.3679]
Completeness to theta = 25.00	98.4 %
Refinement method	Full-matrix least-squares on F^2
Data / restraints / parameters	22869 / 522 / 609
Goodness-of-fit on F^2	0.932
Final R indices [I>2sigma(I)]	R1 = 0.0783, wR2 = 0.1639
R indices (all data)	R1 = 0.2867, wR2 = 0.2781
Extinction coefficient	0.00163(2)
Largest diff. peak and hole	2.289 and -2.101 e.$Å^{-3}$

7.16.2 Atomic coordinates (x 10^4), equivalent isotropic displacement parameters ($Å^2$ x 10^3) and Anisotropic displacement parameters ($Å^2$ x 10^3). U(eq) is defined as one third of the trace of the orthogonalized Uij tensor. The anisotropic displacement factor exponent takes the form: $-2\pi^2[h^2a^{*2}U11 + \ldots + 2hka^*b^*U12]$

Atom	x	y	z	U(eq)	U11	U22	U33	U23	U13	U12

Atom	x	y	z	U(eq)	U11	U22	U33	U23	U13	U12	
Pb(1)	7103(1)	7501(2)	1661(1)	31(1)	Pb(1)	24(1)	27(1)	40(1)	-6(3)	-1(1)	1(3)
Pb(2)	10004(1)	7499(2)	650(1)	31(1)	Pb(2)	27(1)	28(1)	37(1)	6(3)	1(1)	-3(3)
Pb(3)	7892(1)	8320(1)	1059(1)	30(1)	Pb(3)	26(1)	20(1)	43(1)	2(1)	-9(1)	4(1)
Pb(4)	7893(1)	6681(1)	1057(1)	30(1)	Pb(4)	27(1)	20(1)	42(2)	-2(1)	-8(1)	-3(1)
Pb(5)	9860(1)	6422(1)	1122(1)	32(1)	Pb(5)	30(1)	22(1)	42(1)	-1(1)	-5(1)	6(1)
Pb(6)	9858(2)	8580(1)	1122(1)	31(1)	Pb(6)	28(1)	23(1)	44(2)	-1(1)	-7(1)	-6(1)
Pb(7)	8147(1)	7502(2)	426(1)	33(1)	Pb(7)	34(1)	27(1)	38(1)	11(3)	-12(1)	5(3)
Pb(8)	10446(1)	7499(2)	1549(1)	33(1)	Pb(8)	23(1)	30(1)	45(1)	-1(4)	-12(1)	0(3)
Pb(9)	8813(1)	8142(1)	1860(1)	31(1)	Pb(9)	30(1)	25(1)	36(1)	-5(1)	-6(1)	-1(1)
Pb(10)	8815(2)	6859(1)	1860(1)	31(1)	Pb(10)	32(1)	24(1)	37(2)	4(1)	-6(1)	0(1)
Si(1)	6795(3)	7501(2)	2465(2)	35(2)	Si(1)	30(5)	39(5)	35(5)	1(19)	5(4)	7(19)
Si(11)	7794(4)	7764(2)	2936(2)	61(4)	Si(11)	74(10)	55(8)	54(9)	-12(8)	4(8)	-4(7)
C(111)	8881(6)	7519(8)	2735(5)	190(30)							
C(112)	7429(12)	7400(6)	3410(3)	83(17)							
C(113)	7686(14)	8533(3)	2961(6)	360(100)							
Si(12)	5627(5)	8074(3)	2518(2)	88(6)	Si(12)	89(12)	103(13)	71(12)	13(11)	24(10)	54(10)
C(121)	5479(12)	8175(8)	3078(3)	230(60)							
C(122)	5962(12)	8715(4)	2241(5)	100(20)							
C(123)	4699(7)	7688(7)	2270(6)	170(40)							
Si(13)	6321(4)	6649(3)	2634(2)	70(5)	Si(13)	92(12)	68(10)	52(9)	1(9)	18(9)	-5(9)
C(132)	7351(7)	6258(6)	2760(6)	170(40)							
C(133)	5740(11)	6390(7)	2168(4)	110(20)							
C(131)	5568(9)	6759(8)	3078(4)	68(18)							
Si(2)	11073(3)	7495(2)	35(2)	36(2)	Si(2)	37(5)	31(4)	39(5)	0(20)	1(4)	4(19)
Si(21)	10667(5)	6742(3)	-327(2)	59(6)	Si(21)	112(15)	26(9)	38(10)	-13(9)	17(10)	-8(10)
C(211)	10596(17)	6165(5)	-22(5)	140(40)							
C(212)	9506(7)	6836(10)	-509(7)	110(30)							
C(213)	11282(12)	6655(10)	-788(5)	180(50)							
Si(22)	10669(5)	8269(3)	-303(2)	61(7)	Si(22)	71(13)	39(11)	72(14)	25(11)	33(11)	-2(10)
C(221)	10765(17)	8845(5)	1(6)	120(30)							
C(222)	9456(7)	8239(11)	-409(8)	170(40)							
C(223)	11150(14)	8325(10)	-799(5)	90(20)							
Si(23)	12544(5)	7493(4)	153(3)	98(5)	Si(23)	33(6)	150(14)	111(11)	20(40)	17(7)	20(30)
C(231)	12775(13)	7447(15)	666(4)	94(16)							
C(232)	13004(15)	8185(7)	14(11)	100(20)							
C(233)	13146(14)	7027(11)	-166(9)	250(70)							
Si(3)	6881(4)	9159(3)	875(2)	39(5)	Si(3)	24(8)	27(8)	67(12)	3(9)	-19(8)	-2(7)
Si(31)	7513(5)	9490(3)	302(2)	48(5)	Si(31)	43(9)	35(9)	65(12)	23(9)	14(9)	2(7)
C(311)	8598(7)	9709(9)	376(6)	64(16)							
C(312)	7543(17)	9034(6)	-91(5)	70(17)							
C(313)	6924(11)	10080(6)	107(6)	29(10)							
Si(32)	5566(5)	8764(3)	732(2)	70(8)	Si(32)	33(10)	17(7)	160(20)	-6(10)	-29(12)	0(7)
C(321)	4806(10)	9234(7)	533(7)	130(30)							
C(322)	5062(12)	8454(9)	1132(5)	130(40)							
C(323)	5675(15)	8230(6)	354(6)	69(16)							
Si(33)	6753(6)	9823(4)	1355(3)	71(7)	Si(33)	35(9)	46(9)	131(17)	-58(10)	-23(10)	26(7)
C(331)	7293(17)	9657(10)	1807(5)	80(20)							
C(332)	5697(10)	9985(10)	1481(8)	68(17)							
C(333)	7230(18)	10465(7)	1186(8)	80(20)							
Si(4)	6913(4)	5849(3)	867(2)	30(5)	Si(4)	25(9)	21(8)	45(11)	-12(8)	-4(8)	6(7)
Si(41)	7580(5)	5501(3)	301(2)	57(7)	Si(41)	66(13)	31(10)	73(16)	-7(11)	1(12)	-9(9)
C(412)	8658(6)	5215(7)	442(6)	70(20)							
C(411)	7756(14)	6059(5)	-67(4)	67(17)							
C(413)	6731(11)	4926(7)	104(7)	170(50)							
Si(42)	5587(5)	6237(3)	704(2)	47(6)	Si(42)	26(10)	56(12)	60(11)	5(10)	-18(8)	-1(9)
C(421)	4892(8)	5706(5)	467(5)	27(10)							
C(422)	5045(10)	6472(8)	1171(4)	100(30)							
C(423)	5905(16)	6852(6)	326(6)	210(60)							
Si(43)	6780(4)	5200(3)	1366(3)	54(6)	Si(43)	87(15)	31(9)	44(10)	-15(9)	-16(10)	-5(9)
C(431)	7444(12)	5411(8)	1805(4)	42(13)							

Atom	x	y	z	U(eq)	U11	U22	U33	U23	U13	U12	
C(432)	5619(7)	5158(9)	1520(6)	50(14)							
C(433)	7218(16)	4506(7)	1103(8)	150(40)							
Si(5)	10874(4)	5846(2)	1634(2)	36(5)	Si(5)	32(8)	37(9)	39(9)	9(8)	-6(7)	1(7)
Si(51)	10616(4)	4975(3)	1425(2)	150(15)	Si(51)	92(16)	30(9)	330(40)	16(16)	40(20)	4(10)
C(513)	11038(12)	4942(7)	891(3)	81(18)							
C(511)	9558(6)	4714(6)	1473(7)	140(30)							
C(512)	11248(10)	4461(5)	1752(5)	56(14)							
Si(52)	10686(5)	5893(3)	2311(2)	194(14)	Si(52)	180(20)	190(20)	210(30)	70(20)	-50(20)	141(17)
C(521)	10690(13)	6537(4)	2541(4)	54(13)							
C(522)	11658(7)	5560(7)	2586(4)	110(20)							
C(523)	9660(7)	5491(7)	2422(5)	290(80)							
Si(53)	12290(4)	6049(3)	1486(2)	124(11)	Si(53)	67(13)	121(17)	190(30)	52(18)	-28(15)	29(12)
C(532)	12597(11)	6071(9)	979(3)	320(90)							
C(533)	13055(8)	5480(5)	1675(7)	420(130)							
C(531)	12543(11)	6704(5)	1762(6)	90(20)							
Si(6)	10923(2)	9151(1)	1618(1)	56(7)	Si(6)	51(12)	36(10)	81(16)	-8(11)	-25(11)	-17(9)
Si(61)	11650(3)	8703(2)	2119(1)	60(7)	Si(61)	61(10)	61(10)	59(10)	-2(8)	-9(7)	1(7)
C(611)	12099(7)	9255(3)	2459(3)	81(8)							
C(613)	12430(5)	8215(4)	1985(4)	81(8)							
C(612)	10852(6)	8255(4)	2421(3)	81(8)							
Si(62)	10171(3)	9850(2)	1907(1)	36(6)	Si(62)	32(9)	37(9)	39(9)	-10(7)	-3(7)	-9(7)
C(621)	9348(4)	10171(4)	1629(3)	81(8)							
C(622)	10931(5)	10462(3)	2007(4)	81(8)							
C(623)	9766(8)	9575(5)	2405(2)	81(8)							
Si(63)	11920(3)	9504(2)	1183(1)	62(8)	Si(63)	60(10)	68(10)	58(10)	3(8)	4(7)	-9(7)
C(631)	12967(4)	9650(5)	1366(3)	81(8)							
C(632)	11573(8)	10221(3)	1008(4)	81(8)							
C(633)	11933(10)	9027(4)	736(2)	81(8)							
Si(64)	10706(4)	10021(2)	1391(2)	24(5)	Si(64)	23(8)	18(8)	30(8)	7(6)	-11(6)	-9(6)
C(641)	9517(5)	10177(6)	1490(6)	81(8)							
C(642)	11412(9)	10534(4)	1558(5)	81(8)							
C(643)	10917(15)	10056(7)	820(3)	81(8)							
Si(65)	12337(4)	8933(3)	1477(2)	61(8)	Si(65)	59(10)	59(10)	65(11)	5(8)	1(7)	-8(7)
C(651)	12820(8)	8389(5)	1735(5)	81(8)							
C(652)	13105(7)	9519(5)	1631(6)	81(8)							
C(653)	12381(11)	8846(10)	912(3)	81(8)							
Si(66)	10731(4)	9138(3)	2296(2)	36(5)	Si(66)	44(8)	36(8)	28(8)	4(7)	0(7)	-7(7)
C(661)	11374(9)	9575(6)	2589(4)	81(8)							
C(662)	9586(6)	9402(8)	2436(5)	81(8)							
C(663)	10830(16)	8398(4)	2451(4)	81(8)							
C(07)	5095(5)	3228(2)	1015(2)	180(20)							
C(08)	5187(5)	3607(2)	709(2)	180(20)							
C(09)	4692(5)	4079(3)	711(2)	180(20)							
C(010)	4110(6)	4176(3)	1022(3)	180(20)							
C(011)	4013(6)	3796(3)	1326(3)	180(20)							
C(012)	4505(7)	3322(3)	1323(3)	180(20)							
C(06)	4805(4)	11465(3)	1367(2)	163(17)							
C(05)	4157(4)	11071(3)	1363(2)	163(17)							
C(04)	4039(5)	10748(3)	1025(2)	163(17)							
C(03)	4571(5)	10819(4)	693(2)	163(17)							
C(02)	5215(6)	11215(4)	697(2)	163(17)							
C(01)	5333(6)	11538(5)	1034(2)	163(17)							

7.16.3 Bond lengths [Å].

Atoms	Bond length	Atoms	Bond length	Atoms	Bond length
Pb(1)-Si(1)	2.768(7)	Si(2)-Si(21)	2.331(7)	Si(52)-C(523)	1.926(8)
Pb(1)-Pb(3)	3.139(4)	Si(21)-C(211)	1.775(13)	Si(52)-C(522)	1.963(8)

Atoms	Bond length	Atoms	Bond length	Atoms	Bond length
Pb(1)-Pb(4)	3.145(4)	Si(21)-C(213)	1.845(16)	Si(53)-C(532)	1.783(8)
Pb(1)-Pb(9)	3.181(3)	Si(21)-C(212)	1.926(13)	Si(53)-C(531)	1.924(8)
Pb(1)-Pb(10)	3.185(4)	Si(22)-C(221)	1.775(13)	Si(53)-C(533)	1.961(8)
Pb(2)-Si(2)	2.670(7)	Si(22)-C(223)	1.844(16)	Si(6)-Si(66)	2.316(5)
Pb(2)-Pb(7)	2.9933(16)	Si(22)-C(222)	1.927(13)	Si(6)-Si(63)	2.317(4)
Pb(2)-Pb(8)	3.1220(18)	Si(23)-C(231)	1.776(14)	Si(6)-Si(62)	2.319(4)
Pb(2)-Pb(5)	3.134(5)	Si(23)-C(233)	1.845(17)	Si(6)-Si(65)	2.321(5)
Pb(2)-Pb(6)	3.143(5)	Si(23)-C(232)	1.928(14)	Si(6)-Si(61)	2.325(4)
Pb(3)-Si(3)	2.694(7)	Si(3)-Si(32)	2.325(7)	Si(6)-Si(64)	2.327(5)
Pb(3)-Pb(7)	2.983(4)	Si(3)-Si(31)	2.329(7)	Si(61)-C(613)	1.780(7)
Pb(3)-Pb(9)	3.103(3)	Si(3)-Si(33)	2.330(8)	Si(61)-C(611)	1.925(7)
Pb(3)-Pb(6)	3.141(3)	Si(31)-C(312)	1.752(14)	Si(61)-C(612)	1.962(7)
Pb(4)-Si(4)	2.657(7)	Si(31)-C(311)	1.796(13)	Si(62)-C(621)	1.782(7)
Pb(4)-Pb(7)	2.986(4)	Si(31)-C(313)	1.856(15)	Si(62)-C(623)	1.927(7)
Pb(4)-Pb(10)	3.108(4)	Si(32)-C(322)	1.750(15)	Si(62)-C(622)	1.961(7)
Pb(4)-Pb(5)	3.143(3)	Si(32)-C(321)	1.798(14)	Si(63)-C(631)	1.783(6)
Pb(5)-Si(5)	2.752(7)	Si(32)-C(323)	1.856(15)	Si(63)-C(633)	1.925(7)
Pb(5)-Pb(10)	3.180(3)	Si(33)-C(332)	1.750(15)	Si(63)-C(632)	1.962(7)
Pb(5)-Pb(8)	3.186(5)	Si(33)-C(331)	1.795(14)	Si(64)-C(642)	1.779(8)
Pb(6)-Si(6)	2.759(4)	Si(33)-C(333)	1.857(15)	Si(64)-C(641)	1.924(8)
Pb(6)-Pb(9)	3.179(3)	Si(4)-Si(42)	2.348(7)	Si(64)-C(643)	1.962(8)
Pb(6)-Pb(8)	3.193(5)	Si(4)-Si(41)	2.349(7)	Si(65)-C(651)	1.781(8)
Pb(8)-Pb(10)	3.182(4)	Si(4)-Si(43)	2.350(8)	Si(65)-C(653)	1.927(8)
Pb(8)-Pb(9)	3.190(4)	Si(41)-C(412)	1.888(10)	Si(65)-C(652)	1.961(8)
Pb(9)-Pb(10)	3.1984(17)	Si(41)-C(411)	1.888(10)	Si(66)-C(661)	1.784(8)
Si(1)-Si(13)	2.321(8)	Si(41)-C(413)	2.063(16)	Si(66)-C(663)	1.925(8)
Si(1)-Si(12)	2.322(7)	Si(42)-C(422)	1.888(10)	Si(66)-C(662)	1.962(8)
Si(1)-Si(11)	2.323(7)	Si(42)-C(421)	1.890(10)	C(07)-C(012)	1.410(5)
Si(11)-C(111)	1.927(8)	Si(42)-C(423)	2.060(16)	C(07)-C(08)	1.410(4)
Si(11)-C(113)	1.927(8)	Si(43)-C(431)	1.887(10)	C(08)-C(09)	1.410(4)
Si(11)-C(112)	1.929(8)	Si(43)-C(432)	1.888(10)	C(09)-C(010)	1.410(4)
Si(12)-C(122)	1.926(8)	Si(43)-C(433)	2.062(16)	C(010)-C(011)	1.410(4)
Si(12)-C(121)	1.929(8)	Si(5)-Si(52)	2.316(6)	C(011)-C(012)	1.410(5)
Si(12)-C(123)	1.929(9)	Si(5)-Si(51)	2.320(6)	C(06)-C(05)	1.410(4)
Si(13)-C(132)	1.927(8)	Si(5)-Si(53)	2.321(6)	C(06)-C(01)	1.410(4)
Si(13)-C(131)	1.928(8)	Si(51)-C(511)	1.782(8)	C(05)-C(04)	1.410(4)
Si(13)-C(133)	1.930(8)	Si(51)-C(513)	1.927(8)	C(04)-C(03)	1.410(4)
Si(2)-Si(23)	2.329(7)	Si(51)-C(512)	1.960(8)	C(03)-C(02)	1.410(5)
Si(2)-Si(22)	2.330(7)	Si(52)-C(521)	1.784(8)	C(02)-C(01)	1.409(5)

7.16.4 Bond angles [deg].

Atoms	Angle	Atoms	Angle
Si(1)-Pb(1)-Pb(3)	135.1(2)	Si(32)-Si(3)-Si(31)	110.5(3)
Si(1)-Pb(1)-Pb(4)	135.2(2)	Si(32)-Si(3)-Si(33)	111.8(3)
Pb(3)-Pb(1)-Pb(4)	81.15(4)	Si(31)-Si(3)-Si(33)	111.5(4)
Si(1)-Pb(1)-Pb(9)	86.39(12)	Si(32)-Si(3)-Pb(3)	103.6(3)
Pb(3)-Pb(1)-Pb(9)	58.80(8)	Si(31)-Si(3)-Pb(3)	102.7(3)
Pb(4)-Pb(1)-Pb(9)	97.81(7)	Si(33)-Si(3)-Pb(3)	116.2(3)
Si(1)-Pb(1)-Pb(10)	86.44(12)	C(312)-Si(31)-C(311)	106.2(10)
Pb(3)-Pb(1)-Pb(10)	97.79(7)	C(312)-Si(31)-C(313)	104.9(9)
Pb(4)-Pb(1)-Pb(10)	58.82(9)	C(311)-Si(31)-C(313)	105.9(9)
Pb(9)-Pb(1)-Pb(10)	60.32(4)	C(312)-Si(31)-Si(3)	114.6(7)
Si(2)-Pb(2)-Pb(7)	114.03(13)	C(311)-Si(31)-Si(3)	113.0(7)
Si(2)-Pb(2)-Pb(8)	128.61(13)	C(313)-Si(31)-Si(3)	111.5(7)
Pb(7)-Pb(2)-Pb(8)	117.36(5)	C(322)-Si(32)-C(321)	106.3(10)
Si(2)-Pb(2)-Pb(5)	116.11(19)	C(322)-Si(32)-C(323)	105.0(9)
Pb(7)-Pb(2)-Pb(5)	93.54(13)	C(321)-Si(32)-C(323)	105.8(9)

Atoms	Angle	Atoms	Angle
Pb(8)-Pb(2)-Pb(5)	61.23(12)	C(322)-Si(32)-Si(3)	115.0(7)
Si(2)-Pb(2)-Pb(6)	116.47(19)	C(321)-Si(32)-Si(3)	112.5(6)
Pb(7)-Pb(2)-Pb(6)	93.19(13)	C(323)-Si(32)-Si(3)	111.5(8)
Pb(8)-Pb(2)-Pb(6)	61.28(12)	C(332)-Si(33)-C(331)	106.7(11)
Pb(5)-Pb(2)-Pb(6)	118.07(5)	C(332)-Si(33)-C(333)	104.6(10)
Si(3)-Pb(3)-Pb(7)	116.33(15)	C(331)-Si(33)-C(333)	105.9(10)
Si(3)-Pb(3)-Pb(9)	125.73(14)	C(332)-Si(33)-Si(3)	114.6(8)
Pb(7)-Pb(3)-Pb(9)	117.93(9)	C(331)-Si(33)-Si(3)	113.0(8)
Si(3)-Pb(3)-Pb(1)	115.23(14)	C(333)-Si(33)-Si(3)	111.3(8)
Pb(7)-Pb(3)-Pb(1)	94.26(11)	Si(42)-Si(4)-Si(41)	110.6(3)
Pb(9)-Pb(3)-Pb(1)	61.28(6)	Si(42)-Si(4)-Si(43)	112.0(3)
Si(3)-Pb(3)-Pb(6)	115.26(14)	Si(41)-Si(4)-Si(43)	111.8(3)
Pb(7)-Pb(3)-Pb(6)	93.42(8)	Si(42)-Si(4)-Pb(4)	104.0(3)
Pb(9)-Pb(3)-Pb(6)	61.21(7)	Si(41)-Si(4)-Pb(4)	103.4(3)
Pb(1)-Pb(3)-Pb(6)	118.22(8)	Si(43)-Si(4)-Pb(4)	114.5(3)
Si(4)-Pb(4)-Pb(7)	116.04(15)	C(412)-Si(41)-C(411)	108.5(8)
Si(4)-Pb(4)-Pb(10)	126.15(15)	C(412)-Si(41)-C(413)	113.0(7)
Pb(7)-Pb(4)-Pb(10)	117.80(10)	C(411)-Si(41)-C(413)	113.2(7)
Si(4)-Pb(4)-Pb(5)	114.68(14)	C(412)-Si(41)-Si(4)	109.1(6)
Pb(7)-Pb(4)-Pb(5)	93.51(8)	C(411)-Si(41)-Si(4)	109.3(5)
Pb(10)-Pb(4)-Pb(5)	61.14(7)	C(413)-Si(41)-Si(4)	103.6(6)
Si(4)-Pb(4)-Pb(1)	116.10(15)	C(422)-Si(42)-C(421)	108.4(8)
Pb(7)-Pb(4)-Pb(1)	94.10(12)	C(422)-Si(42)-C(423)	113.4(7)
Pb(10)-Pb(4)-Pb(1)	61.24(7)	C(421)-Si(42)-C(423)	113.3(7)
Pb(5)-Pb(4)-Pb(1)	118.13(9)	C(422)-Si(42)-Si(4)	109.1(6)
Si(5)-Pb(5)-Pb(2)	136.68(13)	C(421)-Si(42)-Si(4)	108.4(5)
Si(5)-Pb(5)-Pb(4)	135.40(14)	C(423)-Si(42)-Si(4)	103.9(7)
Pb(2)-Pb(5)-Pb(4)	81.85(7)	C(431)-Si(43)-C(432)	108.8(8)
Si(5)-Pb(5)-Pb(10)	88.71(13)	C(431)-Si(43)-C(433)	113.1(8)
Pb(2)-Pb(5)-Pb(10)	98.26(8)	C(432)-Si(43)-C(433)	113.0(8)
Pb(4)-Pb(5)-Pb(10)	58.90(7)	C(431)-Si(43)-Si(4)	109.1(6)
Si(5)-Pb(5)-Pb(8)	89.37(14)	C(432)-Si(43)-Si(4)	108.8(6)
Pb(2)-Pb(5)-Pb(8)	59.19(8)	C(433)-Si(43)-Si(4)	103.8(7)
Pb(4)-Pb(5)-Pb(8)	97.91(8)	Si(52)-Si(5)-Si(51)	109.2(3)
Pb(10)-Pb(5)-Pb(8)	59.99(6)	Si(52)-Si(5)-Si(53)	109.0(3)
Si(6)-Pb(6)-Pb(3)	137.40(11)	Si(51)-Si(5)-Si(53)	107.7(3)
Si(6)-Pb(6)-Pb(2)	135.16(10)	Si(52)-Si(5)-Pb(5)	121.6(3)
Pb(3)-Pb(6)-Pb(2)	81.90(7)	Si(51)-Si(5)-Pb(5)	101.3(3)
Si(6)-Pb(6)-Pb(9)	90.46(10)	Si(53)-Si(5)-Pb(5)	107.2(3)
Pb(3)-Pb(6)-Pb(9)	58.79(7)	C(511)-Si(51)-C(513)	112.8(7)
Pb(2)-Pb(6)-Pb(9)	98.21(9)	C(511)-Si(51)-C(512)	100.1(7)
Si(6)-Pb(6)-Pb(8)	89.31(10)	C(513)-Si(51)-C(512)	109.4(7)
Pb(3)-Pb(6)-Pb(8)	97.86(8)	C(511)-Si(51)-Si(5)	118.4(6)
Pb(2)-Pb(6)-Pb(8)	59.03(8)	C(513)-Si(51)-Si(5)	105.5(6)
Pb(9)-Pb(6)-Pb(8)	60.07(6)	C(512)-Si(51)-Si(5)	110.6(5)
Pb(3)-Pb(7)-Pb(4)	86.43(5)	C(521)-Si(52)-C(523)	112.8(7)
Pb(3)-Pb(7)-Pb(2)	87.14(10)	C(521)-Si(52)-C(522)	99.9(7)
Pb(4)-Pb(7)-Pb(2)	86.90(11)	C(523)-Si(52)-C(522)	109.1(7)
Pb(2)-Pb(8)-Pb(10)	98.45(9)	C(521)-Si(52)-Si(5)	118.5(6)
Pb(2)-Pb(8)-Pb(5)	59.57(12)	C(523)-Si(52)-Si(5)	105.8(6)
Pb(10)-Pb(8)-Pb(5)	59.90(9)	C(522)-Si(52)-Si(5)	110.5(5)
Pb(2)-Pb(8)-Pb(9)	98.43(9)	C(532)-Si(53)-C(531)	112.8(7)
Pb(10)-Pb(8)-Pb(9)	60.26(4)	C(532)-Si(53)-C(533)	100.0(7)
Pb(5)-Pb(8)-Pb(9)	110.19(8)	C(531)-Si(53)-C(533)	109.3(7)
Pb(2)-Pb(8)-Pb(6)	59.69(12)	C(532)-Si(53)-Si(5)	118.1(6)
Pb(10)-Pb(8)-Pb(6)	110.11(8)	C(531)-Si(53)-Si(5)	105.9(6)
Pb(5)-Pb(8)-Pb(6)	115.10(5)	C(533)-Si(53)-Si(5)	110.5(5)
Pb(9)-Pb(8)-Pb(6)	59.74(9)	Si(66)-Si(6)-Si(63)	136.4(3)
Pb(3)-Pb(9)-Pb(6)	60.00(7)	Si(66)-Si(6)-Si(62)	61.7(2)
Pb(3)-Pb(9)-Pb(1)	59.93(7)	Si(63)-Si(6)-Si(62)	108.87(18)
Pb(6)-Pb(9)-Pb(1)	115.87(9)	Si(66)-Si(6)-Si(65)	108.9(2)

Atoms	Angle	Atoms	Angle
Pb(3)-Pb(9)-Pb(8)	98.75(8)	Si(63)-Si(6)-Si(65)	47.2(2)
Pb(6)-Pb(9)-Pb(8)	60.18(9)	Si(62)-Si(6)-Si(65)	138.1(3)
Pb(1)-Pb(9)-Pb(8)	110.30(11)	Si(66)-Si(6)-Si(61)	48.2(2)
Pb(3)-Pb(9)-Pb(10)	98.26(10)	Si(63)-Si(6)-Si(61)	108.64(18)
Pb(6)-Pb(9)-Pb(10)	110.06(10)	Si(62)-Si(6)-Si(61)	107.46(17)
Pb(1)-Pb(9)-Pb(10)	59.90(10)	Si(65)-Si(6)-Si(61)	64.8(2)
Pb(8)-Pb(9)-Pb(10)	59.76(10)	Si(66)-Si(6)-Si(64)	108.9(2)
Pb(4)-Pb(10)-Pb(5)	59.96(7)	Si(63)-Si(6)-Si(64)	62.1(2)
Pb(4)-Pb(10)-Pb(8)	98.70(9)	Si(62)-Si(6)-Si(64)	50.6(2)
Pb(5)-Pb(10)-Pb(8)	60.11(9)	Si(65)-Si(6)-Si(64)	106.8(2)
Pb(4)-Pb(10)-Pb(1)	59.94(8)	Si(61)-Si(6)-Si(64)	139.5(2)
Pb(5)-Pb(10)-Pb(1)	115.85(9)	Si(66)-Si(6)-Pb(6)	121.2(2)
Pb(8)-Pb(10)-Pb(1)	110.38(12)	Si(63)-Si(6)-Pb(6)	102.30(15)
Pb(4)-Pb(10)-Pb(9)	98.19(10)	Si(62)-Si(6)-Pb(6)	109.93(15)
Pb(5)-Pb(10)-Pb(9)	110.13(11)	Si(65)-Si(6)-Pb(6)	109.0(2)
Pb(8)-Pb(10)-Pb(9)	59.98(10)	Si(61)-Si(6)-Pb(6)	119.25(16)
Pb(1)-Pb(10)-Pb(9)	59.78(10)	Si(64)-Si(6)-Pb(6)	101.10(19)
Si(13)-Si(1)-Si(12)	107.1(3)	C(613)-Si(61)-C(611)	113.2(5)
Si(13)-Si(1)-Si(11)	107.6(3)	C(613)-Si(61)-C(612)	100.2(4)
Si(12)-Si(1)-Si(11)	107.5(3)	C(611)-Si(61)-C(612)	109.0(5)
Si(13)-Si(1)-Pb(1)	107.3(3)	C(613)-Si(61)-Si(6)	118.4(4)
Si(12)-Si(1)-Pb(1)	102.2(3)	C(611)-Si(61)-Si(6)	105.6(3)
Si(11)-Si(1)-Pb(1)	124.0(3)	C(612)-Si(61)-Si(6)	110.2(4)
C(111)-Si(11)-C(113)	114.0(7)	C(621)-Si(62)-C(623)	112.7(5)
C(111)-Si(11)-C(112)	113.9(6)	C(621)-Si(62)-C(622)	100.2(4)
C(113)-Si(11)-C(112)	113.9(7)	C(623)-Si(62)-C(622)	109.0(5)
C(111)-Si(11)-Si(1)	105.0(5)	C(621)-Si(62)-Si(6)	118.6(4)
C(113)-Si(11)-Si(1)	104.6(6)	C(623)-Si(62)-Si(6)	105.5(4)
C(112)-Si(11)-Si(1)	103.9(5)	C(622)-Si(62)-Si(6)	110.6(3)
C(122)-Si(12)-C(121)	113.7(6)	C(631)-Si(63)-C(633)	112.9(5)
C(122)-Si(12)-C(123)	114.0(7)	C(631)-Si(63)-C(632)	99.9(5)
C(121)-Si(12)-C(123)	113.8(7)	C(633)-Si(63)-C(632)	109.2(5)
C(122)-Si(12)-Si(1)	105.1(5)	C(631)-Si(63)-Si(6)	118.1(4)
C(121)-Si(12)-Si(1)	104.5(6)	C(633)-Si(63)-Si(6)	105.9(4)
C(123)-Si(12)-Si(1)	104.4(5)	C(632)-Si(63)-Si(6)	110.7(4)
C(132)-Si(13)-C(131)	114.1(6)	C(642)-Si(64)-C(641)	113.3(6)
C(132)-Si(13)-C(133)	113.7(7)	C(642)-Si(64)-C(643)	100.3(6)
C(131)-Si(13)-C(133)	113.5(6)	C(641)-Si(64)-C(643)	109.0(6)
C(132)-Si(13)-Si(1)	104.6(5)	C(642)-Si(64)-Si(6)	118.3(5)
C(131)-Si(13)-Si(1)	104.8(6)	C(641)-Si(64)-Si(6)	105.7(5)
C(133)-Si(13)-Si(1)	104.7(6)	C(643)-Si(64)-Si(6)	110.1(5)
Si(23)-Si(2)-Si(22)	110.7(4)	C(651)-Si(65)-C(653)	112.7(7)
Si(23)-Si(2)-Si(21)	110.9(4)	C(651)-Si(65)-C(652)	100.3(6)
Si(22)-Si(2)-Si(21)	109.6(4)	C(653)-Si(65)-C(652)	109.0(7)
Si(23)-Si(2)-Pb(2)	118.7(4)	C(651)-Si(65)-Si(6)	118.7(5)
Si(22)-Si(2)-Pb(2)	102.2(3)	C(653)-Si(65)-Si(6)	105.4(5)
Si(21)-Si(2)-Pb(2)	104.1(3)	C(652)-Si(65)-Si(6)	110.5(4)
C(211)-Si(21)-C(213)	115.5(10)	C(661)-Si(66)-C(663)	112.9(7)
C(211)-Si(21)-C(212)	103.0(10)	C(661)-Si(66)-C(662)	99.8(6)
C(213)-Si(21)-C(212)	103.5(9)	C(663)-Si(66)-C(662)	109.2(6)
C(211)-Si(21)-Si(2)	111.4(6)	C(661)-Si(66)-Si(6)	118.0(5)
C(213)-Si(21)-Si(2)	113.5(8)	C(663)-Si(66)-Si(6)	105.9(5)
C(212)-Si(21)-Si(2)	109.0(8)	C(662)-Si(66)-Si(6)	110.7(5)
C(221)-Si(22)-C(223)	115.7(10)	C(012)-C(07)-C(08)	120.0(4)
C(221)-Si(22)-C(222)	102.9(11)	C(07)-C(08)-C(09)	120.0(4)
C(223)-Si(22)-C(222)	103.5(10)	C(010)-C(09)-C(08)	120.0(4)
C(221)-Si(22)-Si(2)	111.2(7)	C(09)-C(010)-C(011)	120.0(4)
C(223)-Si(22)-Si(2)	113.6(8)	C(010)-C(011)-C(012)	120.0(4)
C(222)-Si(22)-Si(2)	108.9(8)	C(07)-C(012)-C(011)	120.0(4)
C(231)-Si(23)-C(233)	115.4(11)	C(05)-C(06)-C(01)	120.0(4)
C(231)-Si(23)-C(232)	102.8(11)	C(06)-C(05)-C(04)	120.0(4)

Atoms	Angle	Atoms	Angle
C(233)-Si(23)-C(232)	103.3(10)	C(05)-C(04)-C(03)	120.0(4)
C(231)-Si(23)-Si(2)	111.6(8)	C(04)-C(03)-C(02)	120.0(4)
C(233)-Si(23)-Si(2)	113.7(9)	C(01)-C(02)-C(03)	120.0(4)
C(232)-Si(23)-Si(2)	108.8(8)	C(02)-C(01)-C(06)	120.0(4)

8 List of Abbreviations

av.	averrage
i-B*u*	*iso*-butyl
t-Bu	*tert*-butyl
δ	chemical shift
calc.	calculated
d	doublet
dec.	decompose
DME	1,2-dimethoxyethane
e.g.	*exempli grati*a/ for example
EI	electron impact ionization
Et	ethyl
Et2O	diethyl ether
Eq.	equation
Fig.	figure
GooF	goodness-of-fit
η	hapto
h	hour(s)
Hyp	hypersilyl, -tris(trimethylsilyl)silyl
IR	infrared
Me	methyl
min	minute
MS	mass spectrometry
µ	bridging
m/*z*	mass/charge
mbar	millibar
NMR	nuclear magnetic resonance
ppm	parts per million
r.t.	room temperature
*ter*t	*t* tertiary
TMS	trimethylsilane
THF	tetrahydrofuran
Triazine	hxahydro-1,3,5-trimethyl-S-triazine
TMEDA	tetramethylethelenediamine
vs	versus
Z	number of molecules in the unit cell

9 Numbering List of the New Compounds

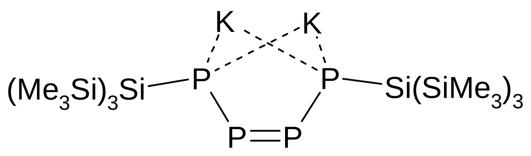

1

$[(Me_3Si)_3Si]_2P_4K_2 \cdot 4\,C_6H_6$ **1a**

$[(Me_3Si)_3Si]_2P_4K_2 \cdot 2\,C_7H_8$ **1b**

$[(Me_3Si)_3Si]_2P_4K_2 \cdot 2\,C_6H_6 \cdot 2\,(Me_3NCH_2)_3$ **1c**

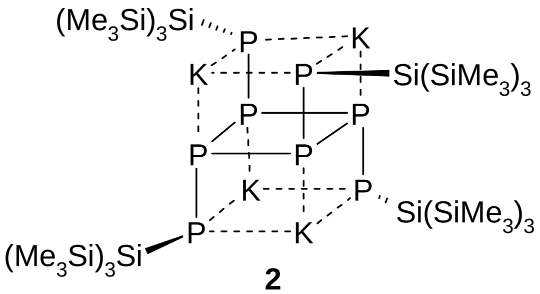

2

$[(Me_3Si)_3Si]_4P_8K_4 \cdot 4\,C_6H_6$ **2a**

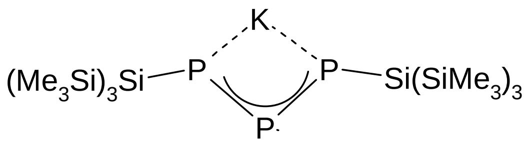

3

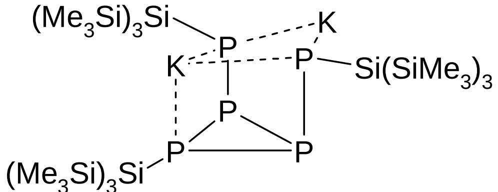

4

$[(Me_3Si)_3Si]_3P_5K_2 \cdot 2\,C_6H_6$ **4a**

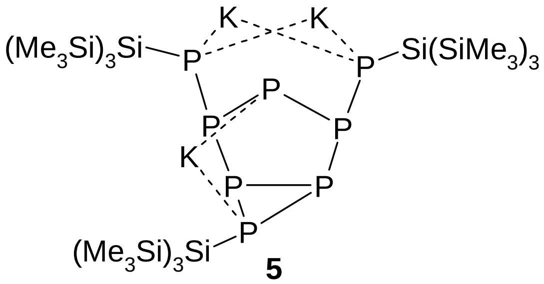

5

$[(Me_3Si)_3Si]_3P_8K_3 \cdot 2\,C_6H_6$ **5a**

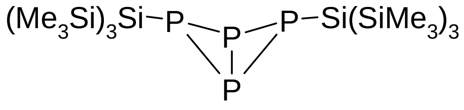

6

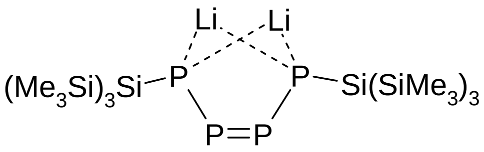

7

$[(Me_3Si)_3Si]_2P_4K_2 \cdot 4\,THF$ **7a**

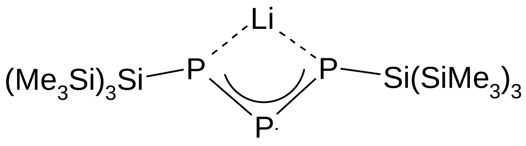

8

$[(Me_3Si)_3Si]_2P_4Li \cdot 2\,(Me_3NCH_2)_3$ **8a**

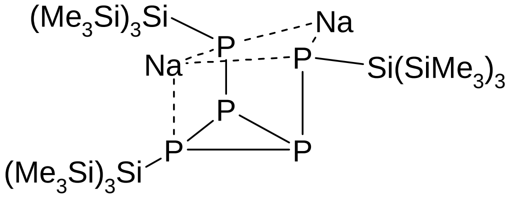

9

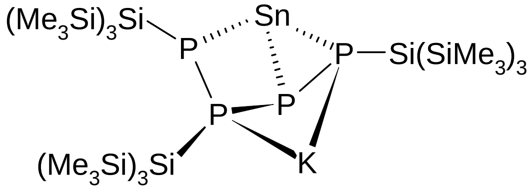

10

$[(Me_3Si)_3Si]_2[(Me_3Si)_2N]P_4SnK$ **11**

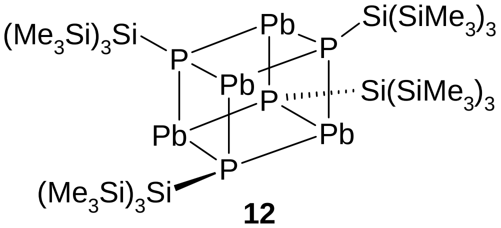

12

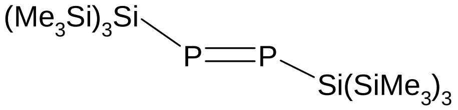

13

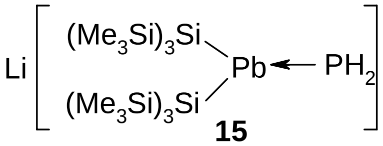

15

Li[Hyp$_2$Pb P(H)$_2$]· Et$_2$O ·DME **15a**

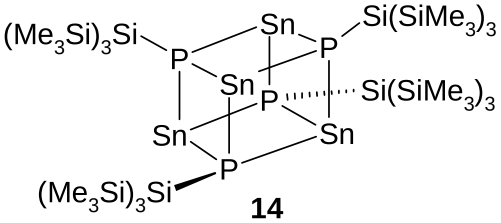

14

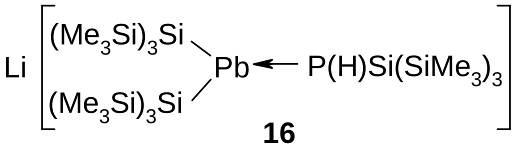

16

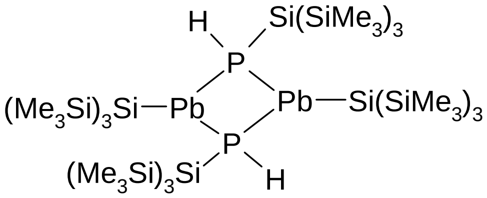

17

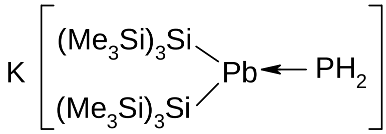

18

[((Me$_3$NCH$_2$)$_3$)K][Hyp$_2$Pb P(H)$_2$] **18a**

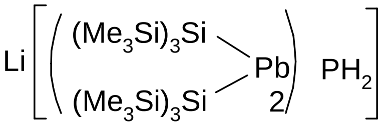

19

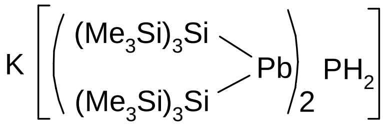

20

[((MeNCH$_2$)$_3$)$_3$K][(Hyp$_2$Pb)$_2$ P(H)$_2$] **20a**

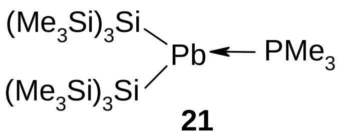

21

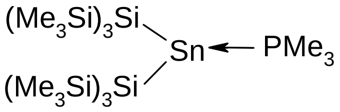

22

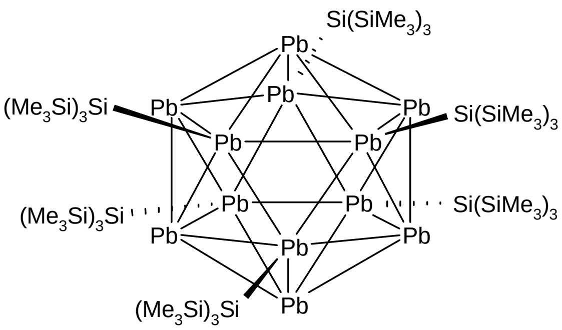

23

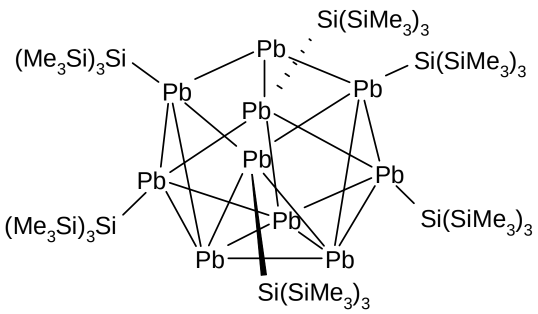

24

10 References

[1] P. J. Dacidson, M. F. Lappert, R. Pearce, *Chem. Rev*. **1976**, 76, 219.

[2] T. Tsmumuraya, S. A. Batcheller, S. Masamune, *Angew. Chem, Int. Ed. Engl*. **1991**, 30, 902.

[3] W. Uhl. *Angew. Chem. Int. Ed. Engl. **1993***, 32, 1386.

[4] A. Sekiguchi, H. Sakurai, *Adv. Organomet. Chem*. **1994**, 37, 1.

[5] M. Driess, H. Grützmacher, *Angew. Chem. Int. Ed. Engl.* **1996**, 35, 827.

[6] N. Wiberg, Coord. *Chem. Rev*. 163(**1997**)217.

[7] Hypersilane and supersilane were proposed as trivial names for trivial names for tris(trimethylsilyl)silane and tri-tert-butylsilane, respectively, by N. Wiberg dring the Xth International Symposium on Organosilicon Chemistry in Poznan (Poland).

[8] J. Frey, E. Schottland, Z. Rappopot, D. Bravo-Zhivotovskii, M. Nakash, M. Botoshansky, M. Kaftory, Y. Apeloig, *J. Chem. Soc. Perkin Trans,* 2 **1994**, 2555.

[9] H. Bock, J. Meuret, K. Ruppert, *J. Organomet. Chem*. **1993**, 446, 113.

[10] H. Bock, J. Meuret, K. Ruppert. *Angew. Chem. Int. Ed. Engl*. **1993**, 32, 414.

[11] Y. Apeloig, G. Korogodsky, D. Bravo-Zhivotovskii, D. Bläser, R. Boese, *Eur, J, Inorg. Chem*. **2000**, 1091.

[12] K. W. Klinkhammer, W. Schwarz, *Angew. Chem*. **1995**, 107, 1448; *Angew. Chem. INt. Ed. Engl*. **1995**. 34. 1334.

[13] A. M. Arif, A. H. Cowley, T. M. Elkins, R. A. Jones, *J. Chem. Soc. Chem. Commun*. **1986**, 1776.

[14] A. M. Arif, A. H. Cowley, T. M. Eklins, *J. Organomet. Chem*. **1987**, 325, C11.

[15] S. P. Mallela, R. A. Genanagel, *Inorg. Chem*. **1990**, 29, 3525.

[16] H. Piana, H. Wagner, U. Schubert, *Chem. Ber*. **1991**, 124, 63.

[17] J. Arnold, T. D. Tilley, A. L. Rheingold, S. Geib, *J. Inorg. Chem*. **1987**, 26, 2106……….

[18] J. Meyer, J. Willnecker, U. Schbert, *Chem. Ber*. **1989**, 122, 223.

[19] Gilman, H.; Smith, C.L. *J. Organomet. Chem*. **1967**, 8, 245

[20] H. Gilman, C. L. Smith, *J. Organomet. Chem*. **1968**, 14, 91

[21] A. Heine, R. Herbst-Irmer, G. M. Sheldrick, D. Stalke, *Inorg. Chem*. **1993**, 32, 2694.

[22] H. Dias, M. Olmstead, K. Ruhlandt-Senge, P. Power, *J. Organomet. Chem*. **1993**, 462, 1.

[23] A. Heine, L. Lameyer, D. Stalke in *Organosilicon Chemistry* III (Eds.: N. Auner, J. Weis), VCH, Weinheim, **1996**: P162.

[24] G. Becker, H. Hartmann, A. Münch, H. Riffel, *Z. Anorg. Allg. Chem*. **1985**, 530,29.

[25] H.-M. Hartmann, *Dissertation*, University of Stuttgart, **1988**.

---

[26] E. N. Gladyshev, E. A. Feodorova, L. O. Yuntila, G. A. Razuvaev, N. S. Vyazankin, *J. Organomet. Chem*. **1975,** 96, 169.

[27] A. H. Cowley, T. M. Elkins, R. A. Jones, *J. Chem. Soc. Chem. Commun*. **1986**, 1777.

[28] A. M. Arif, A. H. Cowley, T. M. Elkins, *J. Organomet. Chem*. **1987**. 325. C11.

[29] K. W. Klinkhammer, W. Scharz. *Z. Anorg. Allg. Chem.* **1993**, 619,177

[30] K. W. Klinkhammer, G. Becker, W. Scharz in *Organosilicon Chemistry* II (Eds. : N. Auner, J. Weis), VCH, Weinheim **1996**.

[31] K. W. Klinkhammer, *Chem. Eur. J*. **1997**, 3, 1418.

[32] F. Schaller, W. Schwarz, H. D. Hausen, K. W. Klinkhammer, J. Weidlein, *Z. Anorg. Allg. Chem*. **1997**, 623, 1455.

[33] R. E. Wochele, *Dissertation*, **2001**, P13.

[34] C. Marschner, *Eur. J. Inorg. Chem*. , **1998**, 221

[35] R. E. Benkeser, R. J. Severson, *J. Am. Chem. Soc*. **1951**, 73, 1424.

[36] H. Gilman, T. C. Wu, *J. Org. Chem*. **1953**, 18, 753.

[37] E. Wiberg, O. Stecher, H. J. Andrascheck, L. Kreuzbichler, E. Staude, *Angew. Chem*. **1963**, 75, 516. *Angew. Chem. Int. Ed. Engl.* **1963**, 2, 507.

[38] H. Sakurai, A. Okada, M. Kira, K. Yonezawa, *Tetrahedron Lett*. **1977**, 1511.

[39] H. Sakurai, M. Kira, H. Umino, *Chem. Lett*. **1977**, 1265.

[40] E. N. Gladyshev, E. A. Feodorova, L. O. Yuntila, G. A. Razuvaev, N. S. Vyazankin, *J. Organomet. Chem*. **1975**, 96, 169.

[41] R. Wochele, W. Schwarz, K. W. Klinkhammer, K. Locke, J. Weidlein, *Z. Anorg. Allg. Chem.* **2000**, 626, 1963.

[42] R. Wochele, K. W. Klinkhammer, J. Weidlein, *Z. Anorg. Allg. Chem*. **2001**, 627, 1420.

[43] R. Wochele, W. Schwarz, K. W. Klinkhammer, J. Weidlein, *Z. Anorg. Allg. Chem*. **2000**, 626, 833.

[44] S.P. Mallela, I. Bernal, R.A. Geanangel, *Inorg. Chem*. **1992**, 31, 1626.

[45] S. Henkel, K. W. Klinkhammer, W. Schwarz, *Angew. Chem*. **1994**, 106, 721; *Angew. Chem. Int. Ed. Engl*. **1994**, 33, 681.

[46] J. Klett, K. W. Klinkhammer, M. Niemeyer, *Chem. Eur. J*. **1999**, 5, 2531.

[47] K. W. Klinkhammer, *Z. Anorg. Allg. Chem*. **2000**, 626, 1217.

[48] K. W. Klinkhammer, J. Klett, Y. Xiong, S. Yao, *Eur. J. Inorg. Chem*. **2003**, 3417.

[49] C. Kayser, R. Fischer, J. Baumgartner, C. Marschner, *Organometallics*, **2002**, 21, 1023.

[50] C. Kayser, G. Kickelbick, C. Marschner, *Angew. Chem. Int. Ed. Engl.* **2002**, 41,989.

[51] Y. Xiong, *Dessertation*, University of Johnanes Gutenberg Mainz, **2004**.

---

[52] P. J. Davidson, M. F. Lappert, *J. Chem. Soc. Chem. Commun*. **1973**, 317.

[53] M. Kira, R. Yauchibara, R. Hurano, C. Kabuto, H. Sakurai, *J. Am. Chem. Soc*. 113(**1991**)7785.

[54] M. Kira, S. Ishida, T. Iwamoto, R. Yauchibara, H. Sakurai, *J. Organomet. Chem*. **2001**,636, 144.

[55] R.S. Simons, L. Pu, M.M. Olmstead, P.P. Power, *Organometallics*, **1997**,16,1920.

[56] M. Stürmann, M. Weidenbruch, K.W. Klinkhammer, F. Lissner, H. Marsmann, *Organometallics*, **1998**, 17, 4425.

[57] N. Tokitoh, R. Okazaki, Coord. *Chem. Rev*. **2000**, 210, 251.

[58] Y. Apeloig, in *The chemistry of Organic Silicon Compounds*, Part I(Eds, S. Patai, Z. Rappoport), Wiley, Chichester, U. K., **1989**, p. 57-225.

[59] H. Jacobsen, T. Ziegler, *J. Am. Chem. Soc*. **1994**, 116, 3667.

[60] W. Kutzelnigg, *Angew. Chem. Int. Ed. Engl*. **1984**, 23, 272.

[61] G. Trinquier, J. –P. Malrieu, *J. Am. Chem. Soc*. **1990**, 112, 2130.

[62] T. L. Windus, M. S. Grordon, *J. Am. Chem. Soc*. **1992**, 114, 9559.

[63] M. Driess, H. Grützmacher, *Angew. Chem. Int. Ed. Engl*. **1996**, 35, 827.

[64] K. W. Klinkhammer, *Angew. Chem. Int. Ed. Engl*. **1997**, 36, 2320.

[65] P. P. Power, *Chem. Rev.* **1999**, 99, 3463.

[66] H. Grützmacher, T. F. Fässler, *Chem. Eur. J*. **2000**, 6, 2317.

[67] E. A. Carter, W. A. Goddard, *J. Phys. Chem.* **1986**, 90, 998.

[68] G. Trinquier, J. –P. Malrieu, *J. Am. Chem. Soc*. **1987**, 109, 5303.

[69] G. Trinquier, J. –P. Malrieu, *J. Am. Chem. Soc*. **1989**, 111, 5916.

[70] G. Trinquier, J. –P. Malrieu, in *The Chemistry of Double Bonded Functional Groups*(Ed: S. Patai), vol. 2, Wiley, Chichester, **1989**, p. 1 Part 1.

[71] Y. Apeloig, M. Karni, *J. Chem. Soc., Chem. Commun*. **1985**, 1048.

[72] S. G. Bott, P. Marshall, P. E. Wagenseller, Y. Wong, R. T. Conlin, *J. Organomet. Chem*. **1995**, 499, 11.

[73] K. Klinkhammer, *Polyhedron*, **2002**, 21, 587.

[74] C. J. Cardin, D. J. Cardin, S.P. Constantine, A.K. Todd, S.J. Teat, S. Coles, *Organometallics*, **1988**, 17, 2144.

[75] K.W. Klinkhammer, T.F. Fässler, H. Grützmacher, *Angew. Chem., Int. Ed. Engl*. **1998**, 37, 124.

[76] S. Benet, C.J. Cardin, D.J. Cardin, S.P. Constantine, P. Heath, H. Rashid, S. Teixeira, J.H. Thorpe, A.K. Todd, *Organometallics*, **1999**, 18, 389.

---

[77] M. Stürmann, W. Saak, K.W. Klinkhammer, M. Weidenbruch, *Z. Anorg. Allg. Chem*. **1999**, 625, 1955.

[78] M. Stürmann, W. Saak, M. Weidenbruch, K.W. Klinkhammer, *Eur. J. Inorg. Chem*. **1999**, 579.

[79] C. Drost, B. Gehrhus, P.B. Hitchcock, M.F. Lappert, *Chem. Commun.* **1997**, 1845.

[80] J.J. Schneider, N. Czap, D. Bläser, R. Boese, *J. Am. Chem. Soc*. **1999**, 121, 1409.

[81] J.J. Schnerder, N. Czap, *J. Organomet. Chem*. **1999**, 584, 338.

[82] J.J. Schnerder, J. Hagen, D. Bläser, R. Boese, F.F. Biani, P. Zanello, C. Krüger, *Eur. J. Inorg. Chem*. **1999**, 1987.

[83] J.J. Schnerder, N. Czap, D. Bläser, R. Boese, J. Ensling, P. Gütlich, C. Janiak, *Chem. Eur. J.* **2000**, 6, No. 3, 469.

[84] K.W. Klinkhammer, in: *Silylderivate der schweren Alkalimetalle in der Synthese niedervalenter Hauptgruppenelementverbindungen* (Habilitation Thesis in German, U. Grauer, Stuttgart, **1998**.)

[85] M. Haag, K.W. Klinkhammer N. Schöne, unpublished results.

[86] H. Grützmacher, S. Freitag, R. Herbst-Irmer, G.S. Sheldrick, *Angew. Chem. Int. Ed. Engl.* **1992**, 31, 437.

[87] K. Klinkhammer, unpublished results.

[88] a) H.-P. Abicht, W. Hönle, H.G. v. Schnering, *Z. Anorg. Allg. Chem*. **1984**, 519,7; b) W. Schmettow, A. Lipka, H.G. v. Schnering, *Angew. Chem. Int. Ed. Engl*. **1974**, 13, 345;c) H.G. v. Schnering, T. Meyer, W. Hönle, W. Schmettow, U. Hinze, *Z. Anorg. Allg. Chem*. **1987**, 553, 261.

[89] a) T. Meyer, W. Hönle, H.G.v. Schnering, Z. Anorg. Allg. Chem. 1987, 552, 69. b) H.G.v. Schnering, W. Hönle, *Chem. Rev*. **1988**, 243.

[90] See for example: a) R.A. Bartlett, M.M. Olmstead, P.P. Power, G.A. Sigel, *Inorg. Chem*. **1987**, 26, 1941; b) E. Hey-Hawkins, E. Sattler, *J. Chem. Soc. Chem. Commun*. **1992**, 775; c) M. Drieß, G. Huttner, N. Knopf, H. Pritzkow, L Zsolnai, *Angew. Chem. Int. Ed. Engl*. **1995**, 34, 316; d) G. Becker, B. Eschbach, O. Mundt, N. Seidler, *Z. Anorg. Allg. Chem*. **1994**, 620,1381; R.E. Mulvey, *Chem. Soc. Rev*. **1991**, 20, 167.

[91] Holleman-Wiberg, *Lehrbuch der Anorganischen Chemie*, 101 Aufl., Verlag DeGruyter, Berlin, **1995**.

[92] M. Baudler, K. Glinka, *Chem, Rev*. **1993**, 93, 1623.

[93] M. Baudler, K. Glinka, *Chem, Rev*. **1994**, 94, 1273.

[94] P. Jutzi, U. Meyer. *Phosphorus and sulfur*, **1988**, 40,275

---

[95] V. Thelen, D. Schmidt, M. Nieger, E. Nieche, W. W. Schoeller, *Angew. Chem.* **1996**,108, 354; *Angew. Chem. Int. Ed. Engl.* **1996**, 35, 313.

[96] M. Baudler, J. Hahn, *Z. Naturforsch*. **1990**, 45b, 1139.

[97] G. Fritz, E. Layher, H. Krautscheid, B. Mayer, E. Matern, *Z. anorg. Allg. Chem*. **1992**,611, 56.

[98] N. Wiberg, A. Wörner, H. Nöth, K. Karaghiosoff, in: N. Auner, J. Weis(Eds), *Organosilicon Chemistry* II, VCH, Weinheim, **1996**, S. 195.

[99] I. Kovács, G. Baum, G. Fritz, D. Fenske, N. Wiberg, H. Schuster, K. Karaghiosoff, *Z. Anorg. Allg. Chem*. **1993**, 619, 453.

[100] N. Wiberg, A. Woerner, H.-W. Lerner, K. Karaghiosoff, D. Fenske, *Eur, J. Inorg. Chem.* **1998**, 833.

[101] N. Wiberg, A. Woener, K. Karaghiosoff, D. Fenske, *Chem. Ber*. /Recueil **1997**, 130, 125.

[102] N. Wiberg. A. Wörner, H. –W. Lerner, K. Karaghiosoff and H. Nöth, *Z. Naturforschung*, **1998**, 53B, 1004.

[103] H. –W. Lerner, M. Wagner, M. Bolte, *Chem. Commun*. **2003**, 990.

[104] Joachim Dautel, *Dissertation*, University Stuttgart, **1992**.

[105] H. Siegl, W. KrumLacher, K. Hassler, *Monatshefte für Chemie*, **1999**, 130, 139.

[106] M. Baudler, *Angew. Chem.* **1987**, 99, 429.

[107] M. Baudler, K. Glinka, *Chem. Rev*. **1993**,93, 1623.

[108] M.J. Gallagher in *Handbook of Phosphorus-31 Nuclear Magnetic Resonance Data* (Ed. J.C. Tebby), CRC Press, **1991**, S.45.

[109] K. Karaghiosoff in *Multiple Bonds and low coordination in Phosphorus Chemistry* (Eds. M. Regitz, O.J. Scherer), Thieme, **1990**, S.463.

[110] Peter H.M. Budzelaar, *gNMR* V4.1.2.

[111] J. Geier, J. Harmer, H. Grützmacher, *Angew. Chem*. **2004**, 116, 4185.

[112] G. W. Rabe, G. P. A. Yap and A. L. Rheigold, *Inorg. Chem*. , **1997**, 36, 1990.

[113] Harald Siegl, Werner Krumlacher, and Karl Hassler, *Monatshefte für Chemie* 130(**1999**)139-145

[114] J. Hahn, M. Baudler, C. Krüger, Y. –H. Tsay, *Z. Naturforsch*. 37b, 797(**1982**); M. Baudler, J. *Pure Appl. Chem.* 52, 755(**1980**).

[115] Y. Leroux, R. Burgada, S. G. Kleemann, E. Fluck in *Handbook of Phosphorus-31 Nuclear Magnetic Resonance Data*, (Ed. J. C. Tebby), CRC-press, Boca Raton, Chap. 5 (**1998**).

[116] K. Karaghiosoff in *Encyclopedia of Nuclear Magnetic Resonance* (Hrsg. D. M. Grant, R. K. Harris), Wiley, Chichester, 3612 (**1996**).

---

[117] R. J. Abraham, *Analysis of High Resolution NMR Spectra*, Elsevier, Amsterdam (**1971**).

[118] M. Andrianarison, D. Stalke, U. Klingebiel, *Chem. Ber*. **1990**, 123, 71.

[119] G.W. Rabe, G.P.A. Yap, A.L. Rheingold, *Inorg. Chem,* **1997**, 36, 1990.

[120] C. Frenzel, P, Joechel, E. Hey-Hawkins, *Chem, Commun*. **1998**, 1363.

[121] K. Karaghiosoff in *Multiple Bonds and Low Coordination in Phosphorus Chemistry*(Eds.: M. Regitz, O. J. Scherer), Thieme, Stuttgart, **1990**, p.463.

[122] M. Baudler, J. Hahn, *Z. Naturforsch.* **1990**, 45b, 1139.

[123] N. Maigrot, M. Sierra, C. Charrier, F. Mathey, *Bull. Soc. Chim. Fr.* **1994**, 131, 397.

[124] P. Jutzi, U. Meyer. *Phosphorus and sulfur*, **1988**, 40,275.

[125] E. Hey, P. B. Hitchcock, M. F. Lappert, A. K. Rai, *J. Organomet. Chem.* , **1987**, 325, 1.

[126] M. Yoshifuji, I. Shima, N. Inamoto, *J. Am. Chem. Soc*. 103(**1981**)4587.

[127] M. Baudler, K. Glinka, *Chem. Rev*. **1994**, 94, 1273.

[128] W. Uhl, F. Hannemann, W. Saak, R. Wartchow *Eur. J. Inorg. Chem.* **1998**, 921-926.

[129] K. Karaghiosoff in *Encyclopedia of Nuclear Magnetic Resonance* (Hrsg. D. M. Grant, R. K. Harris), Wiley, Chichester, 3612 (**1996**).

[130] U. Englich, K. Hassler, K. Ruhlandt-Senge, F. Uhlig, *Inorg. Chem*. **1998**, 37, 3532-3537.

[131] W.-W. du Mont, H.-J. Kroth, *Angew. Chem.* **1977**, *89*, 832.

[132] A.H. Cowley, D.M. Giolando, R.A. Jones, C.M. Nunn, J.M. Power, *Polyhedron*, **1988**, *7*, 1909.

[133] S.C. Goel, M.Y. Chiang, D.J. Raushcer, W.E. Buhro, *J. Am. Chem. Soc*. **1993**, *115*, 160.

[134] M. Driess, R. Janoschek, H. Pritzkow, S. Rell, U. Winkler, *Angew. Chem*. **1995**, *107*, 1746; *Angew. Chem. Int. Ed. Engl*. **1995**, *34*, 1614.

[135] M. Driess, S. Martin, K. Merz, V. Pintchouk, H. Pritzkow, H. Grützmacher, M. Kaupp, *Angew. Chem*. **1997**, *109*,1982; *Angew. Chem. Int. Ed. Engl*. **1997**, *36*, 1894.

[136] Matthias Westerhausen, Mathias Krofta, Nils Wiberg, Jörg Knizek, Heinrich Nöth, Arno Pfitzner, *Z. Naturforsch*. **1998**, *53b*,1489.

[137] C. von Hänisch D. Nikolova, *Z. Anorg. All. Chem*. **2004**, *630*, 345.

[138] A. L. Balch, D. E. Oram, *Inorg. Chem.* , **1987**, 26, 1906

[139] A.L. Seligson, J. Arnold, *J. Am. Chem. Soc.* **1993**, 115, 8214.

[140] G. Trinquier, *J. Am. Chem. Soc*. **1990**, *112*, 2130.

[141] J.D. Corbett, *Bonding*, **1997**, 87, 157.

[142] T.F. Fässler, In *Metal Cluster in Chemistry*, (Eds. P. Braunstein, L.A. Oro, P.R. Raithby), Wiley-VCH Verlag: Weiheim, **1998**.

[143] J.D. Corbett, *Angew. Chem. Int. Ed. Engl.* **2000**, 39, 670.

---

[144] C.R. Joannis, *Hebd. Sceances Acad. Sci*. **1891**, 113, 795.

[145] C.R. Joannis, *Hebd. Sceances Acad. Sci*. **1892**, 114, 587.

[146] C.A. Kraus, *J. Am. Chem. Soc.* **1907**, 29, 1571.

[147] E. Zintl, J. Goubeau, W.Z. Dullenkopf, *Phys. Chem*. Abt. B **1932**, 16, 183.

[148] D. Kummer, L. Diehl, *Angew. Chem. Int. Ed. Engl*. **1970**, 9, 895.

[149] P.A. Edwards, J.D. Corbett, *Inorg. Chem*. **1976**, 16, 903.

[150] L. Pu, B. Twanley, P.P. Power, *J. Am. Chem. Soc*. **2000**, 122, 3524.

[151] M. Stürmann, W. Saak, H. Marsmann, M. Weidenbruch. *Angew. Chem*. **1999**, 111, 145. *Angew. Chem. Int. Ed. Engl.* **1999**, 38, 187.

[152] F. Stabenow, W. Saak, H. Marsmann, M. Weidenbruch, *J. Am. Soc*. **2003**, 125, 10172.

[153] B.W. Eichhorn, R.C. Haushalter, *J. Chem. Soc.* , *Chem. Commun.* **1990**, 937.

[154] B.E. Eichler, P.P. Power, *Angew. Chem. Int. Ed. Engl*. **2001**. 40. 796.

[155] N. Wieberg, H.-W. Lerner, S. Wagner, H. Nöth, T. Seifert, *Z. Naturforsch*. B **1999**, 877.

[156] A. Schnepf, *Angew. Chem. Int. Ed. Engl*. **2003**, 42, 2624.

[157] A. Schnepf, R. Köppe, *Angew. Chem, Int. Ed. Engl*. **2003**, 42, 911.

[158] J. Campbell, D.A. Dixon, H.P.A. Mercier, G.J. Scrobilgen, *Inorg. Chem*. **1995**, 34, 5798.

[159] T.F. Fässler, R. Hoffmann, *J. Chem. Soc., Dalton Trans*., **1999**, 3339.

[160] S. Bobev, S.C. Sevov, *Polyhedron*, **2002**, 21, 641

[161] M. Schütze, *Angew. Chem*. **1958**, 70, 697.

[162] K.J.L.Paciorek, , J.H.Nakahara, L.Hoferkamp,C.George, J.L.Flippenanderson, R.Gilardi, W.R.Schmidt, *Chem Mater*. **1991**, 3, 82

[163] H. Hope, Progr. *Inorg. Chem*. **1995**, 41, 1.

[164] *SHELXLTL PC 5.03*; Siemens Analytical X-Ray Instruments Inc.: Madison, WI, **1994**.

[165] G. M. Sheldrick, *SHELXLTL-97*, Program for Crystal Structure Solution and Refinement; University of Göttingen, German, **1997**.

[166] T. Fjeldberg, H. Hope, M.F. Lappert, P.P. Power, A.J. Thorne, *J. Chem. Soc., Chem. Commun*. **1983**, 639.

[167] M.J.S. Gyname, D.H. Harris, M.F. Lappert, P.P. Power, P. Rivière, M. Rivière-Baudet, *J. Chem. Soc. Dalton*. **1977**, 2004.

[168] R.A. Kva, J.O. Calaway, C.H. van Dyke, N.D. Miro, *Inorg. Synth*. **1975**, 17, 6.

[169] Herrmann/Brauer, *Synthetic Methods of Organometallic and Inorganic Chemistry*,Ed.by W.A.Herrmann,Vol.2, N.Auner,U.Klingbiel, Groups 1,2,13 and 14.pp.186-193.

[170] R. E. Wochele, *Dissertation*, Universität Stuttgart, **2001**.